

**Biomimetic Approach towards  
Alkaloid Natural Product Synthesis  
and the  
Synthesis of Epicocconone Analogues  
with Near Infra-Red Fluorescence**

**Wendy L. Loa-Kum-Cheung**

*BMedScs (Hons 1<sup>st</sup> Class), Macquarie University, Australia*

This thesis is submitted in partial fulfilment of the requirements for the degree of

**Doctor of Philosophy**

Department of Chemistry and Biomolecular Sciences

Faculty of Science



**Macquarie University**

Sydney, Australia

June 2014

Supervisor: Prof Peter H. Karuso



## **DECLARATION OF ORIGINALITY**

I declare that the work described in this thesis was carried out by me and has not been submitted, in part or in full, to any other university or institution for any other degree.

To the best of my knowledge and belief, the thesis contains no material previously published or written by another person except where due references are made.

**Wendy L. Loa-Kum-Cheung**

2<sup>nd</sup> June 2014



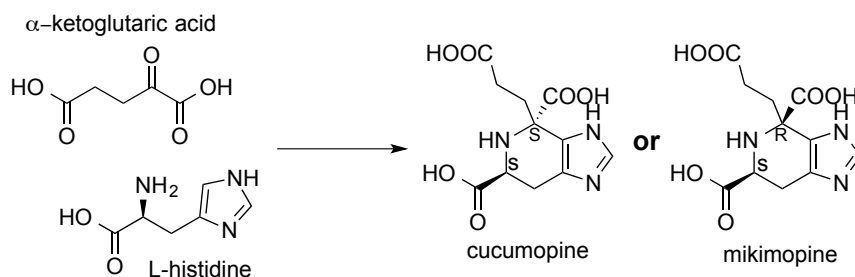


## ABSTRACT

Nature generates huge diversity in molecular frameworks by using the simplest route, starting from abundantly available precursors. The biogenesis of natural products provides valuable information for the design of efficient routes for complex natural products based on structural analysis and biosynthetic pathways. **Chapter 1** investigates the diastereoselective biomimetic synthesis of the natural products mikimopine and cucumopine, based on their biogenesis from the Pictet-Spengler reaction between the naturally abundant precursors  $\alpha$ -ketoglutaric acid and L-histidine. **Chapter 2** and **3** then focus on the structurally diverse and complex family of natural products, known as the oroidin alkaloids. In **Chapter 2**, a comprehensive review of the oroidin alkaloids isolated thus far, is first provided. The biogenesis of all the currently known oroidin alkaloids has been analysed and this has led, for the first time, to a unifying theory for their formation in Nature. Haloperoxidase enzymes are thought to play an important role in the biosynthesis of these marine natural products. Taking this into account, our proposed biogenesis explains the formation of every oroidin alkaloid from the reactive intermediate epoxide or bromonium ion of the precursor oroidin or dihydrooroidin, and forms the basis of a biomimetic approach towards the synthesis of these fascinating and biologically active alkaloids. Our efforts towards this, are described in **Chapter 3**, first by exploring the epoxide route and then the bromonium ion route, and have led to the synthesis of some natural and unnatural oroidin alkaloids. **Chapter 4** then moves away from the topic of biomimetic synthesis and describes the synthesis of hemicyanine hybrids of the fluorescent natural product epicocconone. The photophysical properties of these novel near infra-red dyes are reported and their potential in the detection of biomolecules demonstrated. Finally the experimental and appendices for the whole thesis are provided in **Chapter 5** and **6** respectively.

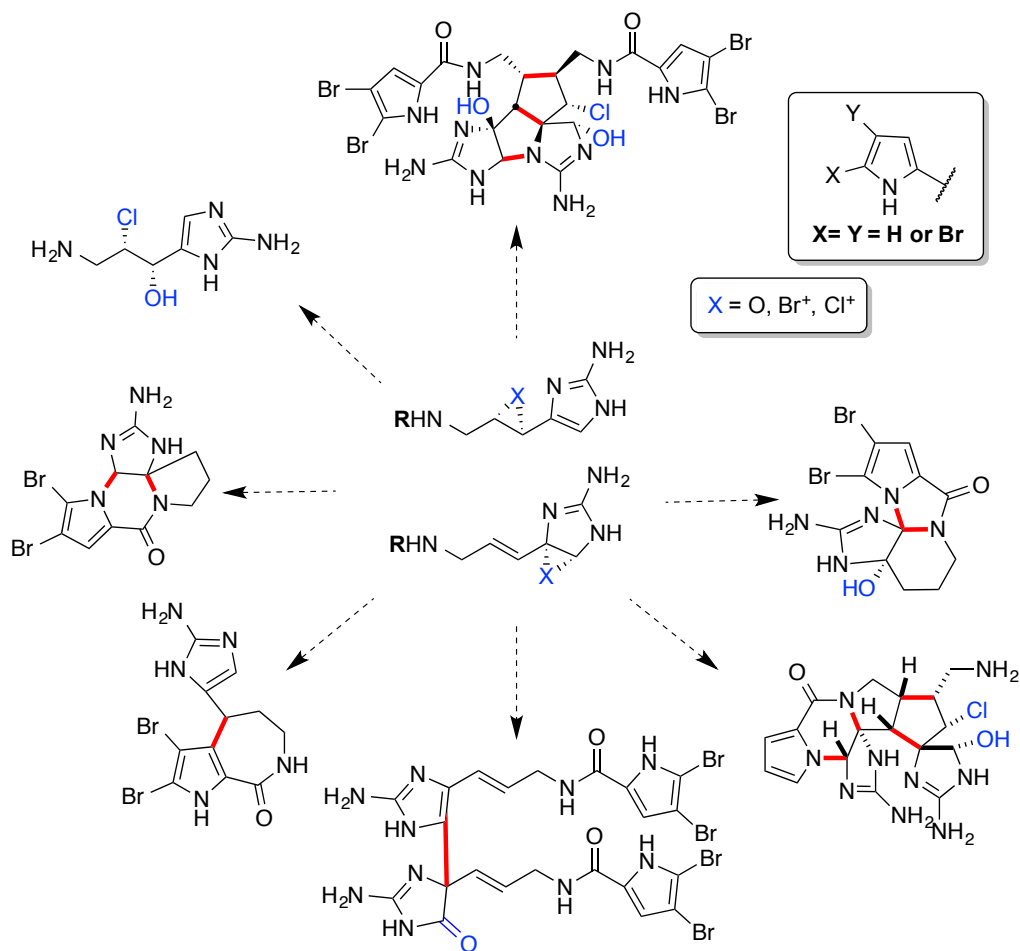
## GRAPHICAL ABSTRACTS

### Chapter 1: Diastereoselective biomimetic synthesis of natural products mikimopine and cucumopine

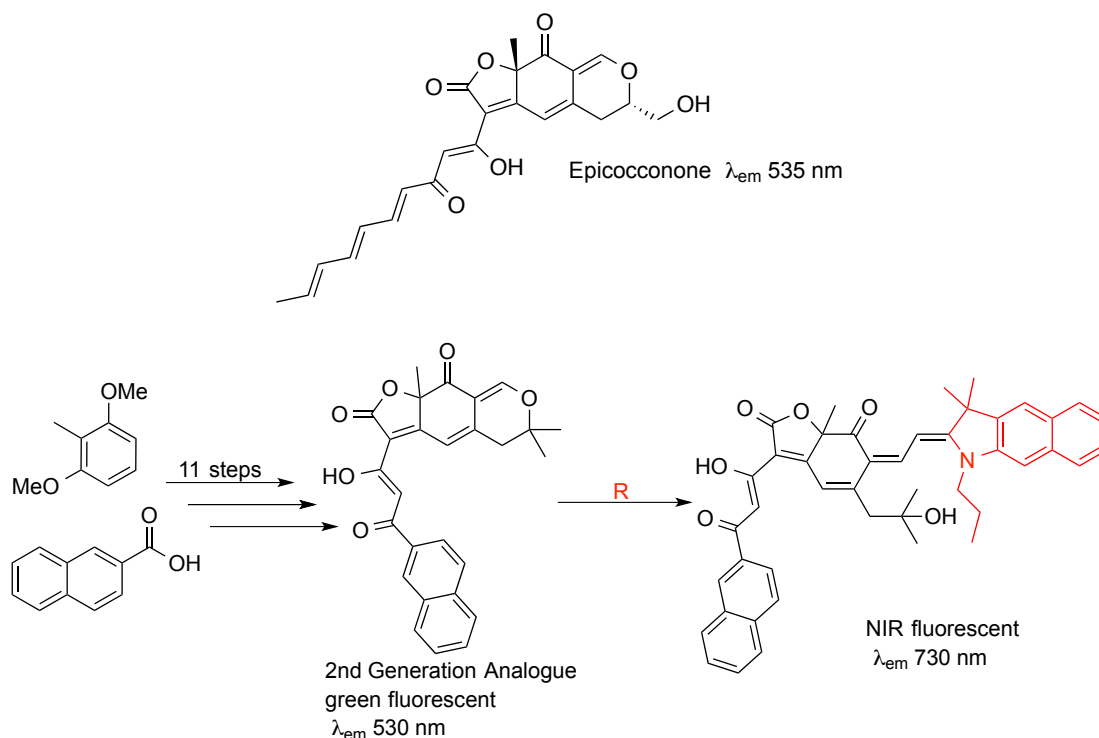


### Chapter 2: Biogenesis of the oroidin alkaloids AND

### Chapter 3: Biomimetic approach towards the synthesis of oroidin alkaloids from their biogenetic precursor(s)



## Chapter 4: Synthesis of epicocconone-hemicyanine hybrids for near infra-red fluorescence



A diastereoselective biomimetic synthesis for the natural products mikimopine and cucumopine, have been developed. Screening of solvents, bases and lewis acids showed the bases triethylamine and potassium carbonate to be responsible for the 80% diastereoselectivity achieved in the synthesis of mikimopine and cucumopine respectively.

We have proposed a unifying theory for the formation of the structurally diverse and complex family of oroidin alkaloids based on the enzymatic catalysis of haloperoxidases and have validated this proposal by synthesising 2 natural and 6 unnatural products from the oroidin family using the oxidant bromodiethylsulfide bromopentachloroantimonate (BDSB) as a source of bromonium ion with oroidin and dihydrooroidin.

Seven hemicyanine hybrids of the fluorescent natural product epicocconone have been synthesised. These are novel near infra-red (NIR) dyes with potential as molecular probes.



## TABLE OF CONTENTS

<b>DECLARATION OF ORIGINALITY</b>	<b>i</b>
<b>ABSTRACT</b>	<b>iii</b>
<b>GRAPHICAL ABSTRACTS</b>	<b>iv</b>
<b>TABLE OF CONTENTS</b>	<b>vii</b>
<b>ABBREVIATIONS</b>	<b>xii</b>
<b>ACKNOWLEDGEMENTS</b>	<b>xv</b>
<b>Chapter 1: Diastereoselective biomimetic synthesis of natural products mikimopine and cucumopine</b>	<b>1</b>
1.1. Introduction	2
1.1.1. The Pictet-Spengler Reaction	3
1.1.1.1. The Pictet–Spenglerases	4
1.1.1.2. P-S Reaction of Imidazoles	5
1.1.2. Previous Work	9
1.1.3. Cucumopine and Mikimopine	11
1.2. Results and Discussion	12
1.2.1. Screening of Bases	12
1.2.2. Screening of Solvents	14
1.2.3. Equivalence of the Base TEA	15
1.2.4. The Carbonates as Base	16
1.2.5. Thermodynamic Product versus Kinetic Product	18
1.2.6. Lewis Acids	20
1.2.7. Substrates Scope	21
1.2.8. Potential Siderophores	26
1.2.8.1. Fluorescence-based Assay to Assess the Fe(III) Chelating Ability of Mikimopine	27
1.3. Summary	29
1.4. References	30
<b>Chapter 2: Biogenesis of the oroidin alkaloids</b>	<b>35</b>
2.1. Introduction	36
2.1.1. The Oroidin Alkaloids	36
2.1.1.1. Oroidin	36

2.1.2. Linear Monomers	37
2.1.3. Cyclic Monomers	40
2.1.4. Bicyclic Monomers	43
2.1.5. Dimers	47
2.1.5.1. Acyclic Dimers	48
2.1.5.2. Monocyclic Dimers	51
2.1.5.3. Bicyclic Dimers	54
2.1.5.4. Tricyclic Dimers	56
2.1.6. Tetramers	58
2.1.7. Summary of the Oroidin Alkaloids	59
2.2. Biosynthetic Studies	60
2.3. Biogenesis of the Oroidin Alkaloids	62
2.4. Marine Haloperoxidases	69
2.5. Alkene Double Bond Character in the 2-Aminoimidazole Ring	71
2.6. Bromonium to Epoxide	73
2.7. Proposed Biogenesis of the Oroidin Alkaloids	73
2.7.1. Linear monomers	74
2.7.2. Monocyclic monomers	76
2.7.3. Bicyclic monomers	78
2.7.4. Acyclic Dimers	79
2.7.5. The More Complex Oroidin Alkaloids	80
2.8. Conclusions	86
2.9. References	86
 <b>Chapter 3: Biomimetic approach towards the synthesis of oroidin alkaloids from their biogenetic precursor(s)</b>	 <b>93</b>
<b>PART A: Investigation of the Epoxide Route</b>	
3.1. Introduction	94
3.1.1. Biomimetic Synthesis of the Oroidin Alkaloids	94
3.2. Results and Discussion	100
3.2.1. Epoxidation using DMDO	101
3.2.2. Other Epoxidation Conditions	103
3.2.3. Biomimetic synthesis of Dispacamide A and Unnatural Dihydrodispacamide A	106
3.3. Summary- Epoxidation Route	107

<b>PART B: Investigation of the Bromonium Ion Route</b>	<b>108</b>
3.4. Introduction	108
3.4.1. Biomimetic Cyclisation: Lessons from Terpene Chemistry	109
3.5. Results and Discussion	114
3.5.1. Initial Investigation into Bromonium-Induced Cyclisation of Pyrrole-Terpene Hybrids	114
3.5.1.1. Effect of an Acid Additive	118
3.5.1.2. Addition of bases	120
3.5.1.3. The Use of DMF as Solvent	121
3.5.1.3.1. Formylation of an Halohydrin or Bromoformyloxylation	121
3.5.2. Investigation with DHO	125
3.5.2.1. Temperature Screening	126
3.5.2.2. Acid/Base Screening	127
3.5.2.3. Spirocyclic Monomer	128
3.5.3. Application to Oroidin	132
3.5.4. Dimerisation of DHO	133
3.5.5. Dimerisation of Oroidin	138
3.6. Summary- Bromonium Ion Route	139
3.7. References	140
 <b>Chapter 4: Synthesis of epicocconone-hemicyanine hybrids for near infra-red fluorescence</b>	 <b>145</b>
4.1. Introduction	146
4.1.2. Fluorescence	147
4.1.3. Epicocconone	148
4.1.3.1. Epicocconone Analogues	150
4.1.4. Near Infra-Red (NIR) Fluorescence	152
4.1.4.1. Near Infra-Red Fluorophores	155
4.1.4.1.1. Cyanines	156
4.1.4.1.2. Porphyrins and Phthalocyanines	158
4.1.4.1.3. Squaraines	160
4.1.4.1.4. BODIPY Dyes	160
4.1.4.1.5. Xanthene/coumarin derivatives	161
4.1.4.1.6. Benzo[ <i>c</i> ]heterocycles	163
4.1.4.2. NIR Epicocconone Analogues	164
4.2. Results and Discussion	165
4.2.1. Hemicyanines	165

4.2.2. Synthesis of the Second Generation Naphthyl Epicocconone Analogue	166
4.2.3. Synthesis of the hemicyanine moieties	171
4.2.4. Synthesis of the Epicocconone-Hemicyanine Hybrid Dyes	172
4.2.5. Photophysical Properties of the Epicocconone-Hemicyanine Hybrid Dyes	177
4.2.6. Investigation of the Hybrid Dyes as Fluorescent Probes	180
4.2.6.1. Effect of pH on the Fluorescence of the Hybrid Dyes	181
4.2.6.2. Influence of SDS on the fluorescence of the hybrid dyes	184
4.2.6.3. Fluorescence of the Hybrid Dyes in the Presence of Biomolecules	186
4.2.7. Total Protein Stain in Gel Electrophoresis	188
4.2.8. The Hybrid Dyes in Fluorescence Microscopy	192
4.2.8.1. Live Cell Imaging using the NIR Hybrid Dyes	192
4.3. Conclusions	198
4.4. References	199
<b>Chapter 5: Experimental</b>	<b>205</b>
5.1. General	206
5.2. Experimental for Chapter 1	207
5.2.1. General Procedure for Conducting the Pictet-Spengler Reaction	207
5.2.2. Fluorescence-based Assay to Assess the Fe(III) Chelating Ability of Mikimopine	209
5.3. Experimental for Chapter 3	210
5.3.1. Synthesis of DHO (2.2) and oroidin (2.1)	210
5.3.2. Epoxidation Reactions	213
5.3.3. Reaction with Snyder's Reagent, BDSB (3.26)	215
5.3.4. Application of BDSB to DHO (2.2) and oroidin (2.1)	227
5.4. Experimental for Chapter 4	231
5.4.1. Synthesis of the Second Generation Epicocconone Analogue (4.2)	231
5.4.2. Synthesis of the Hemicyanine Moieties	236
5.4.3. Synthesis of the Epicocconone-Hemicyanine Hybrids	240
5.4.4. Determination of the Extinction Coefficient and Fluorescence Quantum Yield	246
5.4.5. Investigation of the Hybrid Dyes as Fluorescent Probes	247
5.4.6. Staining of 1D PAGE Gels	248
5.4.7. Live Cell Imaging Using the NIR Hybrids	249



5.5. References	250
<b>Chapter 6: Appendices</b>	<b>253</b>
6.1. NMR Spectra of Newly Synthesised Compounds	
6.1.1. NMR Spectroscopic Data- 2D Correlation for Selected Compounds	318
6.2. UV-Vis Absorbance and Fluorescence Spectra of the Epicocconone-hemicyanine Hybrid Dyes	331
6.3. Effect of pH on the UV-Vis Absorbance and Fluorescence of the Epicocconone-hemicyanine Hybrid Dyes	338
6.4. Response of Fluorescence of the Epicocconone-hemicyanine Hybrid Dyes to SDS	354
6.5. Response of the Epicocconone-hemicyanine Hybrid Dyes to dsDNA	364
6.6. Response of the Epicocconone-hemicyanine Hybrid Dyes to BSA	365
6.7. Protein Detection on Gel Electrophoresis	369
6.7.1. Typhoon Scans of the gel stained with the hybrid dyes <b>4.48-4.53</b>	369
6.7.2. Determination of Limit of Detection of BSA Detected on Gel in ng of the Hybrid Dyes <b>4.48-4.53</b>	371
6.8. Additional Live Cell Images with Hybrid Dye <b>4.49</b>	374

## LIST OF ABBREVIATIONS

ACN	Acetonitrile
BDSB	Bromodiethylsulfoniumbromopentachloroantimonate
br	broad
Boc	<i>tert</i> -butoxycarbonyl
BSA	Bovine Serum Albumin
COSY	Correlated Spectroscopy
DABCO	1,4-Diazabicyclo[2.2.2]octane
DBU	1,8-Diazabicycloundec-7-ene
DMDO	Dimethyldioxirane
<i>de</i>	diastereomeric excess
dec.	decomposition
DIB	(diacetoxyiodo)benzene
DHO	Dihydrooroidin
DIBAL-H	Diisobutylaluminium hydride
DIPEA	<i>N,N</i> -diisopropylethylamine
DNA	Deoxyribonucleic acid
DMAP	Dimethylaminopyridine
DMF	Dimethyl formamide
DMSO	Dimethylsulfoxide
$\epsilon$	Extinction coefficient
EDTA	Ethylenediaminetetraacetic acid
EtOAc	Ethyl acetate
equiv.	equivalent
ESI	Electrospray Ionization
EI	Electron Impact
F	Fluorescence
HEPES	4-(2-hydroxyethyl)-1-piperazineethanesulfonic acid
HMBC	Heteronuclear Multi Bond Coherence
HPLC	High Performance Liquid Chromatography
HRMS	High Resolution Mass Spectrometry
HSQC	Heteronuclear Single Quantum Coherence
I	Intensity

ICT	Internal Charge Transfer
IBX	2-Iodoxybenzoic acid
inc.	incomplete
iPrOH	isopropyl alcohol
<i>J</i>	coupling constant
LCMS	Liquid Chromatography Mass Spectrometry
m	Multiplet
Max	Maximum
MeNO <sub>2</sub>	Nitromethane
MeOH	Methanol
MOM-Cl	Chloromethyl methyl ether
<i>m</i> -CPBA	<i>m</i> -chloroperbenzoic acid
NBS	<i>N</i> -bromosuccinimide
<i>n</i> -BuLi	<i>n</i> -butyl lithium
NIR	Near Infra-Red
NMR	Nuclear Magnetic Resonance
NOESY	Nuclear Overhauser Effect Spectroscopy
NO <sub>2</sub> Me	Nitromethane
NR	No reaction
ON	Overnight
PAGE	Polyacrylamide Gel Electrophoresis
Pet ether	Petroleum ether
P-S	Pictet-Spengler
q	quartet
quint	quintet
quant	quantitative
ROE	Rotating-frame Overhauser Enhancement
r.t.	room temperature
s	Singlet
SDS	Sodium Dodecyl Sulfate
sp.	species
t	triplet
TBCO	2,4,4,6-tetrabromocyclohexa-2,5-dienone

TBDMS	<i>tert</i> -butyldimethylsilyltriflate
TIPS	triisopropylsilyltriflate
<i>t</i> -BuLi	<i>tert</i> -butyl lithium
<i>t</i> -BuOH	<i>tert</i> -butanol
TEA	Triethylamine
TFA	Trifluoroacetic Acid
TPA	Tripropylamine
THF	Tetrahydrofuran
TLC	Thin Layer Chromatography
UV	Ultraviolet
Vis	Visible
$\lambda_{\text{em}}$	emission wavelength
$\lambda_{\text{ex}}$	excitation wavelength
$\Phi_{\text{F}}$	Quantum yield

## ACKNOWLEDGEMENTS

First and foremost, I would like to express my deepest gratitude to Professor Peter Karuso for his guidance and support all through my studies and research. Your endless patience, knowledge and advice have been invaluable to me in many ways.

I am very grateful to Dr Fei Liu for my first “taste” of research by offering me the opportunity of working in her lab during my undergraduate years.

I wish to thank past and present members of the Karuso and Liu groups with whom I’ve had the chance to interact, in particular Dr Sudhir Shengule, Dr Michael Gotsbacher, Dr Alpesh Patel, Dr Shurook Saadedin, Ben, Soumit, Girish, Mark, André, Jérémie, Marie, Ryan, Harry, Calum, Alex, Ketan and Kavita for their much appreciated friendship, kind support, help, and the hard and happy days spent together in the lab.

I would like to thank Dr Chris McCrae, Mark Tran, Jason Smith and Tony Wang for technical support; Dr Andrew Try for lending a listening ear; Michelle Kang, Maria Hyland and Catherine Wong for their assistance during my time at Macquarie University. A special thank you to Dr Debra Birch for assisting with confocal laser microscopy and to Harish Cheruku for providing me with cells for staining.

I am very grateful to have had the opportunity to spend 6 months of research at l’IRCOF, Rouen in France. I am very thankful for the warm welcome I have received and would like to express my gratitude to my adjunct supervisor Dr Xavier Franck for his guidance and support during my time at l’IRCOF. Thanks to Dr Philip Peixoto, Dr Agathe Boulangé, Dr Stéphane Leleu, Dr Cyril Sabot, Dr Anthony Romieu for the chemistry advice and to ‘mes camarades de labo’: Marine, Caroline, Laurie-Anne, Emilia, Rob, Laëtitia, Inma and Theo for the good times spent together in and outside the lab.

A special thank you to ‘mes p’tits Français’: Jérémie, Marie et Eloïse for their help and support, and the memorable moments spent together, to ‘ma coach’ Aude for

her challenges and for lifting my spirit up when needed, and to Eric Brice for his infinite kindness, during my stay in France.

A special thank you also to Noorie, Saima, Simone, Yeewon and Hong for their much appreciated friendship and support, and to the Stephens family for such warm welcome into their home and for the time spent together.

I am grateful for the financial support from the Australian Government both for an Australian Postgraduate Award (APA) and an Endeavour Research Fellowship Award. The latter has made possible 6 months of research at l'IRCOF, Rouen, France.

These past 4 years have been a roller coaster ride for me with perhaps more lows than highs. I have lost people very dear to me: my grandfather, my aunt and most recently my dad.

I thank God for giving me the strength and resources to complete my thesis, despite all of the difficult times I have faced.

I am very grateful to be surrounded by amazing relatives that have been there for me during these hard times. I would especially like to express heartfelt thanks to my aunts: Denise and Joséphine, and uncles Camille, Cyril and John for their continuous support and invaluable help from the very first day I set foot in Australia, 9 years ago.

Last but not least, I would like to thank my loving parents, André and Danielle, and my brother and sister, Yannick and Jaimie, for their endless love, support, patience and understanding. Thank you for sharing over this past four years, the many uncertainties, challenges and sacrifices in the completion of this thesis. This would not have been possible without you all. Thank you mum for your incredible strength despite everything, thank you Yannick for sticking by me and for the laughs, and Jaimie for helping as you can. Thank you Dad for your hard work, sacrifices and your dedication to your family. Thank you for respecting my choices and for having faith in me. I hope to have made you proud during your time with us.

*To the memory of my beloved father,  
a hardworking, dedicated and incredibly patient man*





---

**CHAPTER 1**

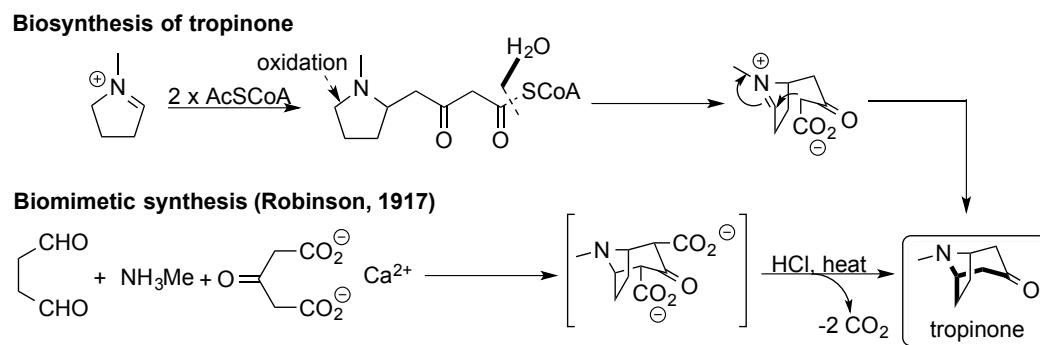
**DIASTEREOSELECTIVE BIOMIMETIC SYNTHESIS OF  
NATURAL PRODUCTS: CUCUMOPINE AND MIKIMOPINE**

---

## 1.1. Introduction

Nature generates a huge diversity of simple and complex molecular frameworks in natural products by using the simplest route, starting from abundantly available precursors. In so doing, it provides elegant solutions to the synthesis of natural products in the laboratory. The term *biomimetic* derives from the Greek “bios” meaning life, and mimetic, the adjective for “mimesis” or mimicry. Biomimetic synthesis is thus an attempt to assemble natural products along biosynthetic lines without having recourse to the full enzymatic machinery of nature.<sup>1</sup>

The concept of biomimetic synthesis was introduced by Sir Robert Robinson in 1917 when he prepared the alkaloid tropinone, using the simple starting materials, succinaldehyde, methylamine and acetone dicarboxylic acid, in a one-pot procedure (**Scheme 1.1**).<sup>2</sup> This landmark synthesis of organic chemistry follows closely the now well-established biosynthesis of the tropinone skeleton (**Scheme 1.1**).



**Scheme 1.1** Tropinone biosynthesis involving the enzyme Acetyl CoA synthase (AcSCoA) and the landmark biomimetic synthesis by Robinson.

Since then, many specific targets have been the focus of pivotal experiments undertaken in the field of biomimetic synthesis and have been the subject of recent reviews.<sup>3-8</sup> The biomimetic syntheses of oroidin alkaloids and any others of relevance are discussed in **Chapter 3**.

### 1.1.1. The Pictet-Spengler Reaction

Since its discovery over a century ago, the Pictet-Spengler (P-S) reaction, first reported by Pictet and Spengler in 1911, has been an important reaction for the simultaneous C-N and C-C bond formation leading to the formation of ring systems such as the tetrahydroisoquinolines and tetrahydro- $\beta$ -carboline (Figure 1.1).<sup>9</sup>

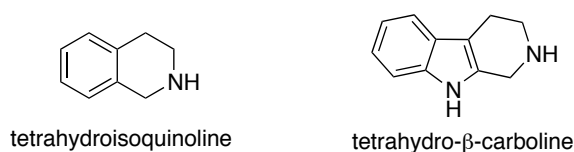
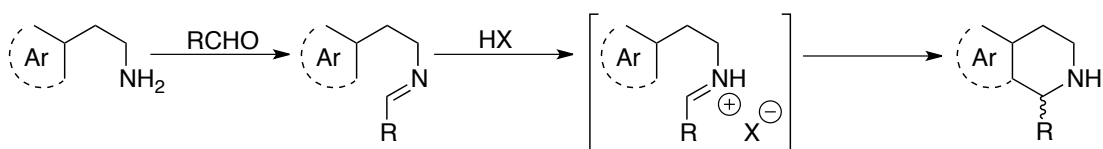


**Figure 1.1** The tetrahydroisoquinoline and tetrahydro- $\beta$ -carboline scaffolds.

A typical P-S reaction is a two-step process that involves the condensation of an aliphatic amine ( $\beta$ -arylethylamine or tryptamine) with an aldehyde to form an imine, which is most commonly activated by Brønsted acids. Final intramolecular cyclisation between a sufficiently reactive, electron-rich aromatic ring and the activated iminium ion results in an *N*-heterocyclic ring (Scheme 1.2).

Stereochemically, the reaction produces a racemic mixture since the imine can be attacked from the top or bottom face equally.



**Scheme 1.2** Typical P-S reaction catalysed by a Brønsted acid

Tetrahydroisoquinolines and tetrahydro- $\beta$ -carboline form the structural key elements of thousands of naturally occurring alkaloids, several of them being of enormous physiological and therapeutic significance. For examples: berberine is a quaternary ammonium salt isoquinoline plant alkaloid that has shown antifungal, anti-

bacterial and anti-viral activities; reserpine is an indole plant alkaloid that has been used as an antipsychotic and antihypertensive drug; manzamine is an indole marine alkaloid that exhibits broad biological activity, including cytotoxic, antibacterial, antimalarial, insecticidal, anti-inflammatory and anti-HIV (**Figure 1.2**).<sup>10-15</sup> As such, the P-S reaction has been extensively studied and continues to be a focus of research in areas that include its application to the total synthesis of natural and unnatural products, and the preparation of new heterocycles for combinatorial applications.<sup>16,17</sup>

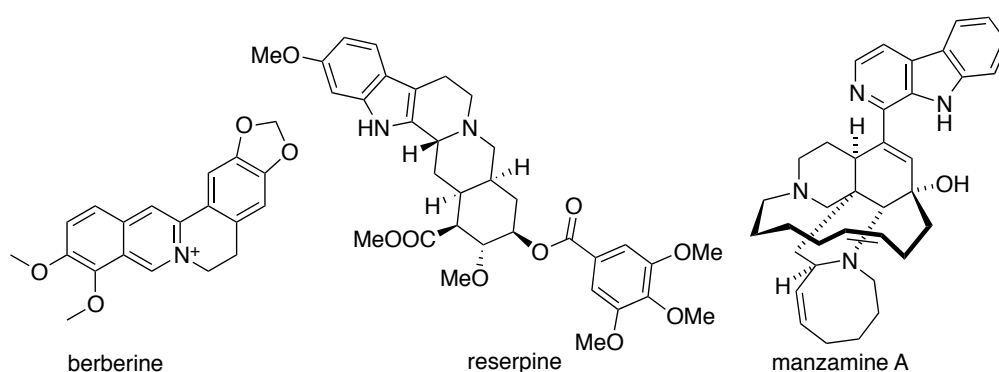


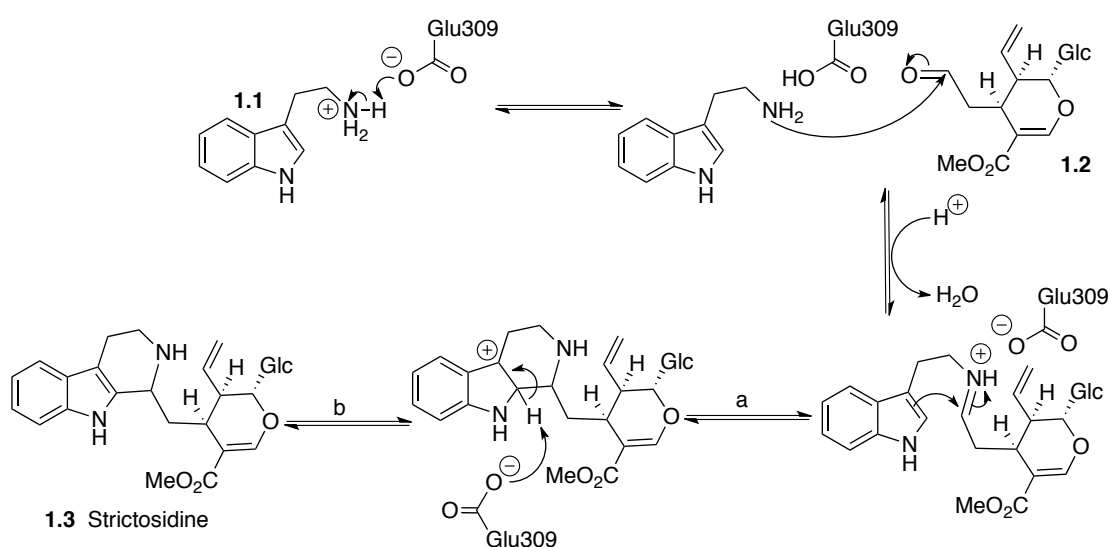
**Figure 1.2** Some examples of isoquinoline and indole alkaloids of enormous physiological and therapeutic significance.

The reaction has undergone continuous modification and found broader application to a wider variety of aromatic ethylamines, including *N*-alkylated, *N*-acylated or *N*-sulfonated amines, and also with the use of ketones instead of aldehydes which then generate quaternary centres adjacent to the aromatic ring.<sup>17</sup> There is also a variant of the reaction that uses alcohols rather than amines, termed the oxo-P-S reaction.<sup>18</sup>

#### 1.1.1.1. The Pictet–Spenglerases

Biosynthetically, the P-S reaction is carried out by so-called “Pictet-Spenglerase” enzymes and these have been isolated from several plant alkaloid

biosynthetic pathways.<sup>19-22</sup> Strictosidine synthase is the first “Pictet-Spenglerase” to be crystallised as a complex with its substrates tryptamine (**1.1**) and secologanin (**1.2**).<sup>23</sup> This has led to structural insights on the mechanism of the enantiospecific reaction.<sup>24</sup> Glu309 has been shown to be instrumental in the P-S reaction by acting as a catalyst. It does so by playing key role in both an acid-catalyzed step involved in iminium formation (**a**) and a base-catalysed step involved in the final deprotonation step (**b**) (**Scheme 1.3**) to form strictosidine (**1.3**).<sup>25</sup>



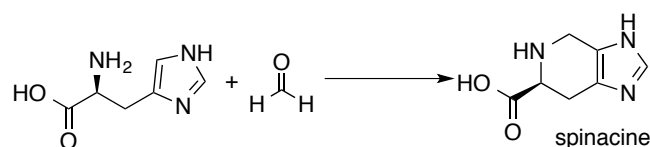
**Scheme 1.3** Suggested mechanism of the strictosidine synthase catalysed P-S reaction between **1.1** and **1.2** to form strictosidine (**1.3**).<sup>24</sup> A key Glu309 residue acts both as a proton donor and acceptor. Glc: glucose.

#### 1.1.1.2. P-S Reaction of Imidazoles

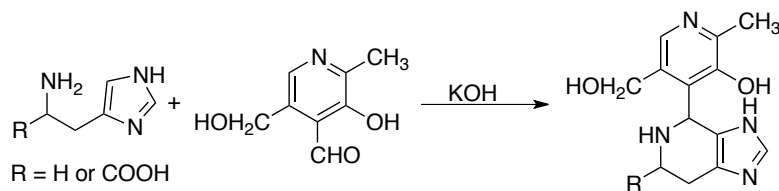
While the P-S reaction has been widely applied to the synthesis of tetrahydroisoquinolines and tetrahydro- $\beta$ -carboline, little investigation has been conducted with the imidazoles as substrates in the P-S reaction.

The first report of the P-S reaction of imidazole is from Wellish who in 1913 reported the synthesis of spinacine, (*S*)-4,5,6,7-tetrahydro-1*H*-imidazole[4,5-*c*]pyridine carboxylic acid, from the reaction of L-histidine and formaldehyde

(**Scheme 1.4**).<sup>26</sup> Spinacine is a natural product first isolated from extracts of green spinach leaves.<sup>27</sup> It is much later that Klutchko *et al.* described the synthesis of a large number of spinacine derivatives.<sup>28</sup> In 1948, Folkers and co-workers isolated 4-aryl-4,5,6,7-tetrahydroimidazol[4,5-*c*]pyridine from the reaction of pyridoxal with histamine or histidine in the presence of a base while synthesising amino acid derivatives of vitamin B<sub>6</sub> (**Scheme 1.5**).<sup>29</sup>



**Scheme 1.4** First reported example of the P-S reaction of the imidazole, L-histidine with acetaldehyde in the synthesis of the natural product spinacine.



**Scheme 1.5** P-S reaction of histamine/histidine with pyridoxal to make amino acid derivatives of vitamin B<sub>6</sub>.

Later Stocker *et al.* effected such condensations in the absence of a base and in organic solvents.<sup>30</sup> However, the reaction condition was not general and cyclisation failed to occur with aliphatic aldehydes or ketones as well as with alkyl/aryl ketones under similar conditions. Acid-catalysed P-S of histamine also failed to proceed to the cyclised product.<sup>30</sup> As proposed by Stocker, the presence of a base is crucial to promote cyclisation by making the C5 position of the imidazole more nucleophilic (**Figure 1.3**). However it is possible that base is simply required to avoid the non-nucleophilic imidazolium ion. The P-S reaction can lead to the formation of both tautomers where either nitrogen N1 or N3 of the imidazole is protonated. The proton is shown on N1 but both tautomers are present.

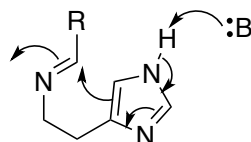
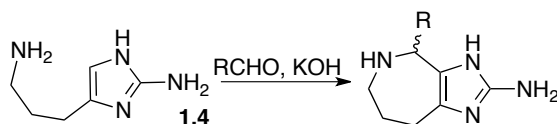


**Figure 1.3** Base catalysis in the P-S cyclisation of imidazoles.

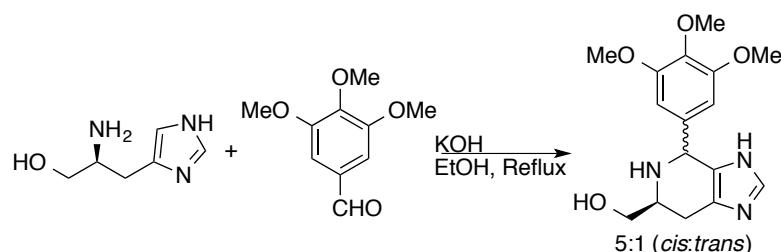
Horne and co-workers first reported the P-S reaction of 4-(3-aminopropyl)-1*H*-imidazol-2-amine (**1.4**), bearing a 2-aminoimidazole nucleus instead of imidazole, with various aromatic and aliphatic aldehydes in the presence of a base to form unusual seven membered analogues of 2-aminoimidazole (**Scheme 1.6**).<sup>31</sup> However there is no mention of the stereochemistry of the products.



**Scheme 1.6** P-S reaction of **1.4** by Horne and co-workers.

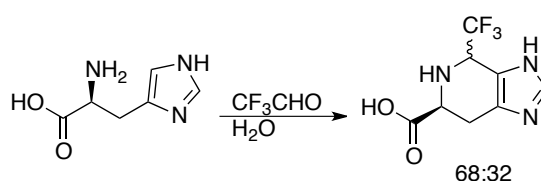
Most of the work done in the field of diastereoselective P-S reactions, has involved starting with an existing stereocentre (such as an amino acid) that will remain in the final product. Other methods include using a stereocentre in a chiral auxiliary that is removed afterwards, to direct the ring closure, or alternatively using a chiral Lewis acid or chiral catalyst to promote the reaction as well as direct stereoselectivity.<sup>32,33</sup> Enantioselective/diastereoselective P-S reaction of imidazoles has not been studied in detail. There are only a few reports where the stereochemistry of the product is determined when the reaction was carried out with histidine. Furthermore, the P-S reactions with ketones are even more sparse in the literature compared to the extensive examples with aldehydes.

In the synthesis of analogues of azotoxin, a hybrid anticancer molecule, Medarde and co-workers condensed L-histidinol with 3,4,5-trimethoxybenzaldehyde and observed formation of cyclised products in a *cis:trans* ratio of 5:1 (**Scheme 1.7**).<sup>34</sup>



**Scheme 1.7** P-S reaction of L-histidinol with 3,4,5-trimethoxybenzaldehyde, reported by Medarde and co-workers.

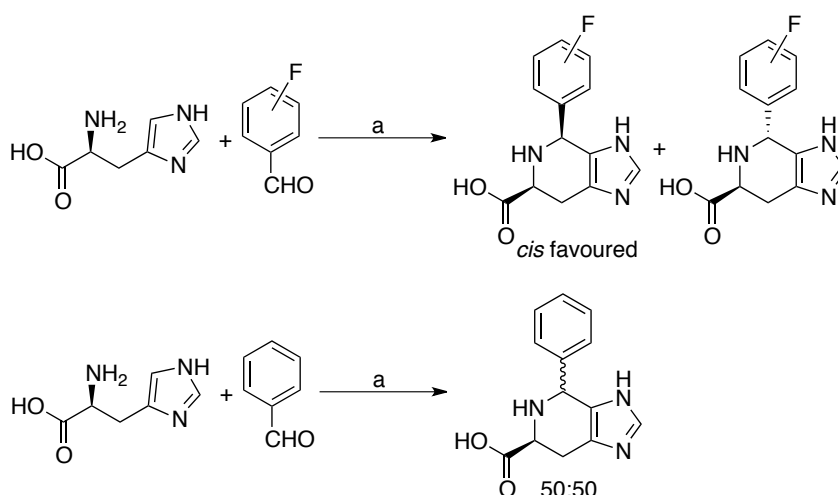
Fujii *et al.*, while synthesising analogues of the natural product spinaceamine, condensed L-histidine with trifluoroacetaldehyde in boiling water and observed formation of a cyclised product as a diastereomeric mixture (68:32) (**Scheme 1.8**).<sup>35</sup>



**Scheme 1.8** P-S reaction of L-histidine with trifluoroacetaldehyde, reported by Fujii *et al.*<sup>35</sup>

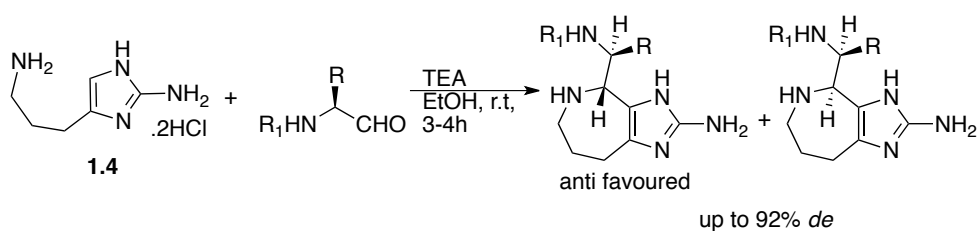
More recently, Smith *et al.* reported the synthesis of 4-phenylspinacine from the P-S reaction between L-histidine and benzaldehyde refluxing in an ethanol-water mixture in the presence of excess strong base (**Scheme 1.9**).<sup>36</sup> No diastereoselectivity was observed. Interestingly, when fluorobenzaldehydes were used, the P-S cyclization proceeded diastereoselectively, with predominant formation of the *cis*-spinacine products (**Scheme 1.9**).<sup>36</sup> The diastereoselectivity is likely due to an electronic effect of the fluorine atom on the imine in the electrophilic cyclisation step of the P-S reaction. However, no *de* values were reported.





**Scheme 1.9** P-S reaction of L-histidine with fluorinated benzaldehyde led to the observed diastereoselective for the *cis*-products as reported by Smith *et al.* while with benzaldehyde, no diastereoselectivity was observed.<sup>36</sup> Reaction conditions: **a.** KOH (3 equiv.), refluxing EtOH/H<sub>2</sub>O (2:1, v/v).

Karuso and co-workers have reported the diastereoselective P-S reaction of 4-(3-aminopropyl)-1*H*-imidazol-2-amine (**1.4**) with enantiopure amino acid-derived aldehydes where anti stereochemistry is favoured with up to 92% *de* observed (**Scheme 1.10**).<sup>37</sup> The diastereoselectivity was found to be a result of the steric bulk of the amino acid side chain R while the bulk of the protecting group R<sub>1</sub> had little to no effect on *de*.

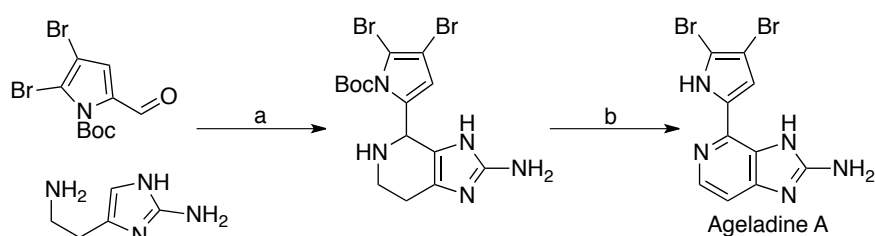


**Scheme 1.10** Diastereoselective P-S reaction of **1.4** with various enantiopure amino-derived aldehydes.

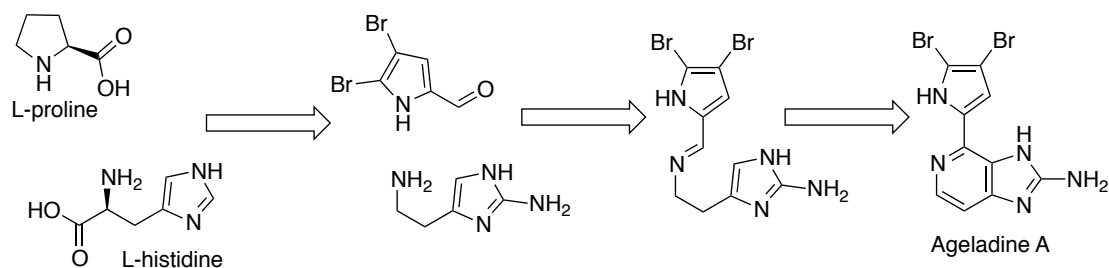
### 1.1.2. Previous Work

Previous work conducted in the Karuso lab, has led to the biomimetic synthesis of the marine natural product, ageladine A (**Scheme 1.11**).<sup>38</sup> The synthesis

follows the biogenesis proposal that ageladine A is likely to be derived from the amino acids proline and histidine (**Scheme 1.12**).<sup>39</sup> This pyrrole-imidazole alkaloid was first isolated from the marine sponge *Agelas nakamurai* by Fusetani in 2003 and has shown promising anticancer and antiangiogenic activity.<sup>39</sup> The first synthesis published in 2006 by Weinreb required 13 steps followed shortly by a 3-step biomimetic synthesis from our lab.<sup>40</sup> Weinreb soon after published a 10-step synthesis that avoided an end game that gave a very poor yield.<sup>41,42</sup> Concomitantly, we published a one pot synthesis of ageladine A from 2-aminohistamine.<sup>43</sup>



**Scheme 1.11** Biomimetic synthesis of ageladine A. **a.**  $\text{Sc}(\text{OTf})_3$ , EtOH, r.t, 5 h, 44%; **b.** chloranil,  $\text{CHCl}_3$ , reflux, 8h, 65%



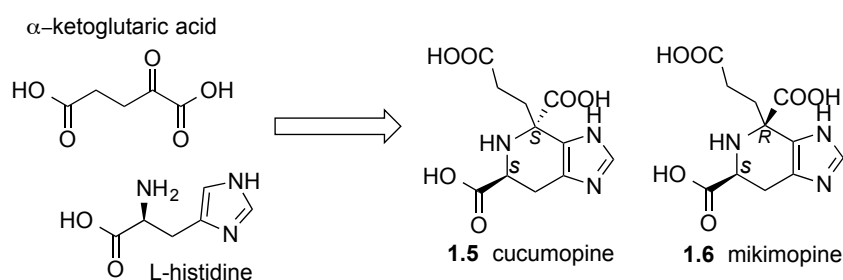
**Scheme 1.12** Biogenesis of marine natural product, ageladine A.

We have used this method to synthesise various analogues of ageladine A, either with different aldehydes or with imidazole variants such as histidine, histamine, or tryptophan.<sup>43</sup> Consequently, our aim has been to extend this approach to investigate a biomimetic approach to the synthesis of related natural products.

### 1.1.3. Cucumopine and Mikimopine

Cucumopine (**1.5**) and mikimopine (**1.6**) are natural products that have been isolated from the hairy roots of tobacco induced by two different strains of *Agrobacterium rhizogenes* (**Scheme 1.13**).<sup>44,45</sup> They are opines, small molecule metabolites, believed to act as nitrogen sources for the bacterium.<sup>46</sup> It was reported that roots were able to take up exogenously supplied opines and that the addition of opines to the culture medium of hairy root, replaced carbon or nitrogen sources of the media to some degree.<sup>47</sup> The addition of mikimopine was observed to enhance alkaloid production in hairy root and to have some insecticidal effect, reducing the growth of *Manduca sexta* larvae and exhibiting deterrent properties at higher concentrations.<sup>47</sup> In addition, mikimopine showed allelopathic properties and retarded the germination of *Lepidium sativum* seeds and growth of seedlings.<sup>47</sup> The structure suggests these compounds may also function as siderophores.

Compound **1.5** and **1.6** are diastereomers, bearing the same configuration at C2, indicating that they are likely to have been derived by the P-S reaction between the naturally occurring precursors  $\alpha$ -ketoglutaric acid and L-histidine (**Scheme 1.13**). Indeed, when  $\alpha$ -ketoglutaric acid and L-histidine were heated in water in the presence of lithium hydroxide as a base, a mixture of mikimopine and cucumopine was obtained.<sup>45</sup>



**Scheme 1.13** Biogenesis of the mikimopine and cucumopine is likely to involve the Pictet-Spengler cyclisation of abundantly available precursors  $\alpha$ -ketoglutaric acid and L-histidine.

We have investigated the diastereoselective biomimetic synthesis of mikimopine and cucumopine and the potential of these compounds as siderophores, using a novel fluorescence based assay.

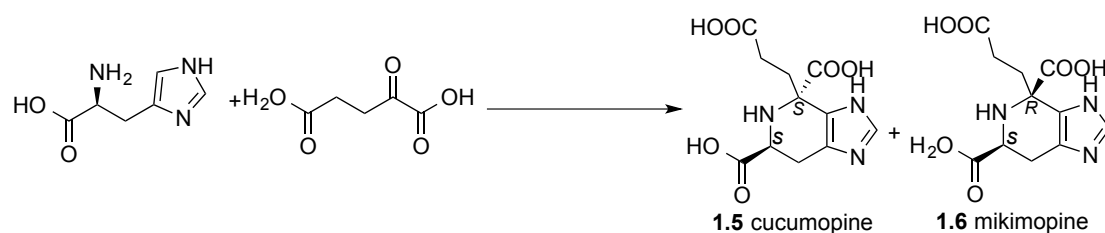
## 1.2. Results and Discussion

In our investigation into a diastereoselective biomimetic synthesis of the opines, enantiopure L-histidine was used as a chiral inductor. As reported in the literature, when L-histidine was stirred with  $\alpha$ -ketoglutaric acid in the presence of LiOH in water at 50 °C, a 50:50 mixture of the (*cis*)-*S,R*- and (*trans*)-*S,S*-diastereoisomers was obtained (**Table 1.1, Entry 1**). The absence of diastereoselectivity is not surprising since diastereocontrol is generally limited under aqueous conditions unless under the action of an enzyme.<sup>16</sup> When the reaction was conducted in methanol, no product was formed while decomposition was observed in DMSO (**Entry 2 and 4**). Changing the base from LiOH to KOH in refluxing methanol did not have any effect on the outcome of the reaction (**Entry 3**).

### 1.2.1. Screening of Bases

For histidine to undergo a Pictet–Spengler reaction it is essential that the side chain remain deprotonated for the addition of the intermediate imine because protonated imidazoles are deactivated towards electrophilic addition. Therefore we started by trialing different organic and inorganic bases. Indeed, in the absence of any base, no reaction was observed in water at 50 °C (**Entry 5**). As shown in **Table 1.1**, most of the organic bases proved to be ineffective in promoting the P-S reaction,

mostly resulting in no reaction or decomposition if allowed to proceed for a longer time. The use of DABCO led to the formation of products but no diastereoselectivity was observed (**Entry 8**). Triethylamine as base showed the most promising results when used in refluxing methanol leading to the preferential formation of cucumopine over mikimopine. No reaction was observed at room temperature in methanol with TEA (**Entry 13**).

**Table 1.1** Screening a variety of organic bases.

Entry	Base <sup>a</sup>	Solvent	Temp (°C)	Time (h)	Cucu:Miki <sup>b</sup>	Yield (%)
1 <sup>c</sup>	LiOH	H <sub>2</sub> O	50	24	50:50	quant. <sup>e</sup>
2 <sup>c</sup>	LiOH	MeOH	50	18	- <sup>d</sup>	NR
3	KOH	MeOH	64	24	-	NR
4 <sup>c</sup>	LiOH	DMSO	50	3.5	-	dec.
5	-	H <sub>2</sub> O	50	24	-	NR
6	DIPEA	MeOH	64	18	-	NR
7	Pyridine	MeOH	64	20	-	NR
8	DABCO	MeOH	64	20	47:53	inc. <sup>f</sup>
9	DBU	MeOH	64	24	-	dec. <sup>g</sup>
10	2,6-lutidine	MeOH	64	48	-	dec.
11	TPA	MeOH	64	24	-	dec.
12	TEA	MeOH	64	45	88:12	95
13	TEA	MeOH	r.t.	45	-	NR

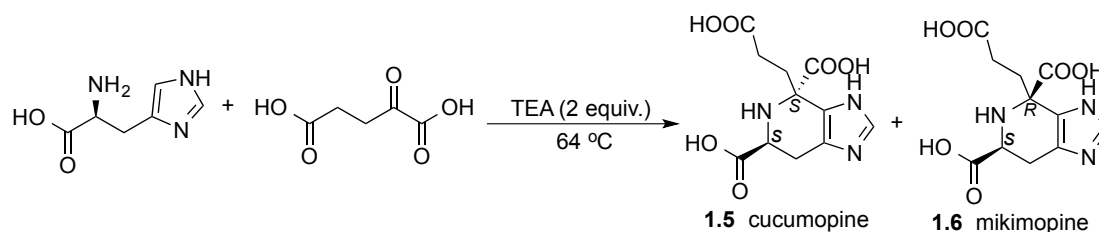
**a.** 2 equiv. used; **b.** diastereomeric ratio determined by <sup>1</sup>H NMR of crude reaction mixture; **c.** 9 equiv. as in literature; **d.** - = only starting materials are observed; **e.** quant. = quantitative; **f.** inc. = incomplete; **g.** dec. = decomposition observed; **h.** NR = no reaction.

### 1.2.2 Screening of Solvents

The effect of solvents on diastereoselectivity with TEA as base was next investigated (**Table 1.2**). When the same base was used in water, a reversal but

limited diastereoselectivity was noted (**Table 1.2; Entry 2**). The use of DMSO as solvent or conducting the reaction in neat TEA only led to decomposition (**Entry 2-3**). In other alcoholic solvents such as ethanol or isopropanol, a decrease in diastereoselectivity and yield was observed (**Entry 5-6**).

**Table 1.2** Solvent effects on the P-S reaction

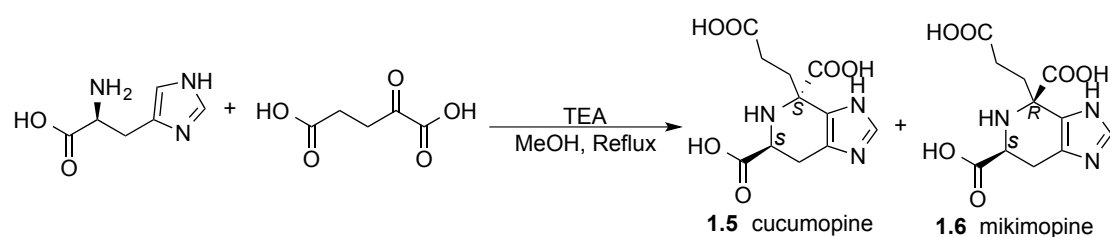


Entry	Solvent	Time (h)	Cucu:Miki <sup>a</sup>	Yield (%) <sup>b</sup>
1	H <sub>2</sub> O <sup>c</sup>	42	42:58	95
2	DMSO	3.5	-	dec. <sup>d</sup>
3	TEA	3.5	-	dec.
4	EtOH	45	75:25	85
5	iPrOH	45	60:40	65

**a.** diastereomeric ratio determined by <sup>1</sup>H NMR of crude reaction mixture; **b.** yield determined by <sup>1</sup>H NMR of crude reaction mixture; **c.** Temperature used is 50 °C; **d.** dec. = decomposition observed.

### 1.2.3. Equivalent of the Base TEA

Refluxing the reagents with excess base led to a Boltzmann distribution of products (91:9) suggesting a difference of 1.55 kcal/mol between **1.5** and **1.6** (**Table 1.3**).<sup>48</sup> The use of limited base led to poorer diastereoselectivity (**Entry 1**).

**Table 1.3** Effect of number of equivalents of TEA on the P-S reaction

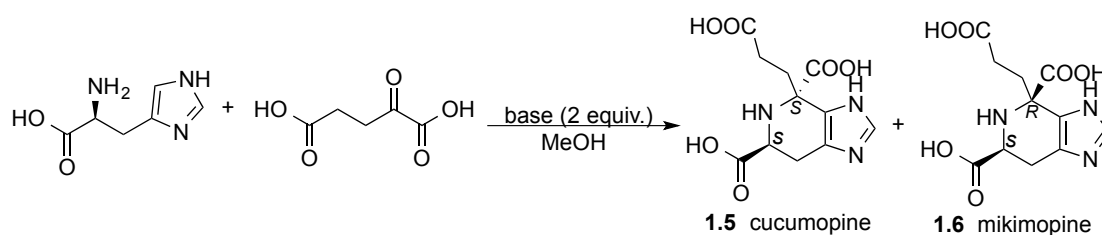
Entry	Equiv.	Time (h)	Cucu:Miki <sup>a</sup>	Yield (%)
1	2	45	88:12	95
2	16	17	91:9	95
3	32	12	91:9	95

a. diastereomeric ratio determined by <sup>1</sup>H NMR of crude reaction mixture

#### 1.2.4 The Carbonates as Base

A series of trials were conducted with metal carbonates to test whether complexation with cations can affect diastereoselectivity (**Table 1.4**). In refluxing methanol, diastereoselectivity was observed mainly with Li<sub>2</sub>CO<sub>3</sub> and Na<sub>2</sub>CO<sub>3</sub>, favouring the formation of mikimopine (**1.6**). As cucumopine seemed to be the thermodynamic product, this suggested that alkali earth metals could complex the transition state in a way to affect the diastereoselectivity. Despite solubility issues at room temperature, an improvement of the diastereoselectivity in favour of **1.6** was observed with Na<sub>2</sub>CO<sub>3</sub> and K<sub>2</sub>CO<sub>3</sub>. The use of a greater equivalent of the base led to a further improvement of the *de* with a much cleaner reaction mixture in the case of K<sub>2</sub>CO<sub>3</sub>.



**Table 1.4** The carbonates as base in the P-S cyclisation of  $\alpha$ -ketoglutaric acid and L-histidine in methanol.

Entry	Base <sup>a</sup>	Temp (°C)	Time (h)	Cucu:Miki <sup>b</sup>	Yield (%)
1	Li <sub>2</sub> CO <sub>3</sub>	64	24	29:71	95
2	Na <sub>2</sub> CO <sub>3</sub>	64	18	31:69	95
3	K <sub>2</sub> CO <sub>3</sub>	64	24	49:51	98
4	Cs <sub>2</sub> CO <sub>3</sub>	64	17	56:44	quant. <sup>c</sup>
5	Li <sub>2</sub> CO <sub>3</sub>	r.t.	48	-	NR <sup>d</sup>
6	Na <sub>2</sub> CO <sub>3</sub>	r.t.	72	15:85	70
7	Na <sub>2</sub> CO <sub>3</sub> (16 equiv.)	r.t.	72	10:90	60
8	K <sub>2</sub> CO <sub>3</sub>	r.t.	48	25:75	63
9	K <sub>2</sub> CO <sub>3</sub> (16 equiv.)	r.t.	120	10:90	90
10	Cs <sub>2</sub> CO <sub>3</sub>	r.t.	48	-	NR

a. 2 equiv. used unless otherwise specified; b. diastereomeric ratio determined by <sup>1</sup>H NMR of crude reaction mixture; c. quant. = quantitative; d. NR = no reaction

The cation is playing a role in the diastereoselectivity observed since even at high temperature, the formation of **1.6** is favoured with Na<sup>+</sup> and K<sup>+</sup> but not Cs<sup>+</sup> (**Table 1.4; Entry 1-2**). Therefore the diastereoselectivity cannot be solely due to the kinetic condition in use. This indicates the likely role of the metal cations in diastereocontrol. The metal cations are likely to help stabilise the imine intermediate

as shown in **Figure 1.4**. The imidazole would then preferentially attack the imine from the less hindered lower face which is also constrained by the interaction of the histidine carboxylate and imine via a cation. With caesium carbonate under heating (**Entry 4**), the diastereoselectivity becomes reversed. The involvement of metal complexation ( $M^+$ ) in the transition state would explain this reversal since  $Cs^+$  ion is bigger in size (167 pm compared to  $Li^+$ ,  $Na^+$  and  $K^+$  ions being 76, 102 and 138 pm respectively)<sup>49</sup> and might not be able to complex the imine as the other cations.

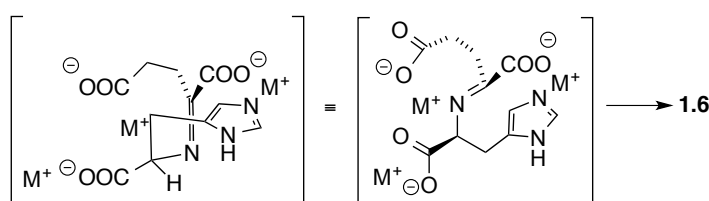


**Figure 1.4** Transition state needed for the formation of mikimopine (**1.6**) and stabilisation of the imine intermediate in the presence of metal cations, leading preferentially to **1.6**.

### 1.2.5. Thermodynamic Product versus Kinetic Product

The diastereomer formed was identified by the ROE between the  $\alpha$ -CH<sub>2</sub> of the  $\alpha$ -ketoglutaric acid moiety and the  $\alpha$ -hydrogen of the amino acid (**Figure 1.5A** and **B**). The presence of a strong ROE indicates these groups are on the same side of the ring (i.e mikimopine (**1.6**)). Alternatively, a weak ROE correlation would indicate the *trans*-diastereomer (i.e. cucumopine (**1.5**)).

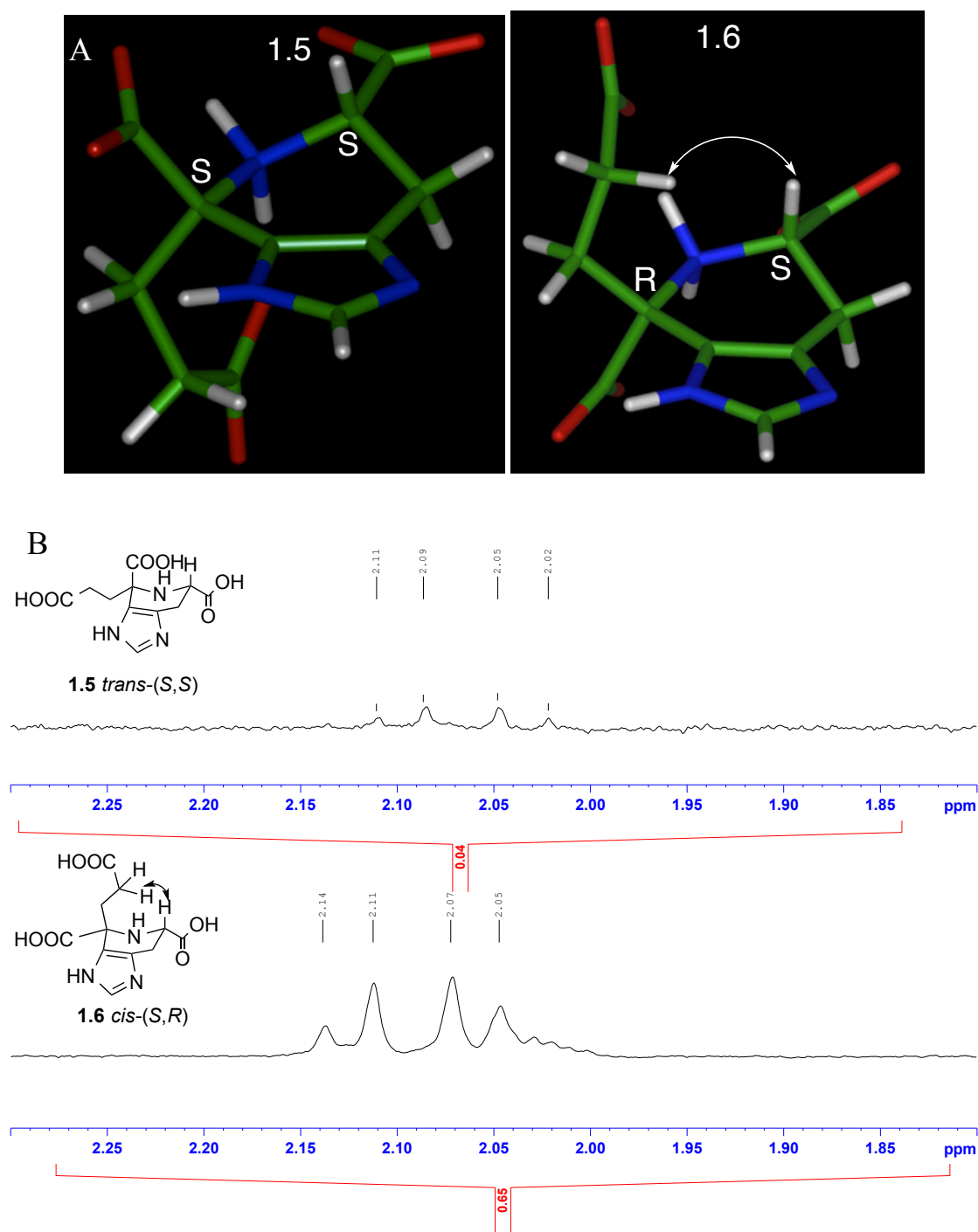
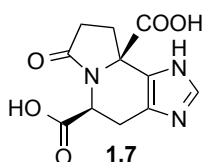


**Figure 1.5** A. 3D model of **1.5** and **1.6**. Arrow indicating the proximity of the glutarate CH<sub>2</sub> with the α-H of histidine used to differentiate between the two diastereomers; B. 1D ROE of **1.5** and **1.6** irradiation at H<sub>α</sub> of histidine showing ROE integration (red) relative to the irradiation frequency (-100).

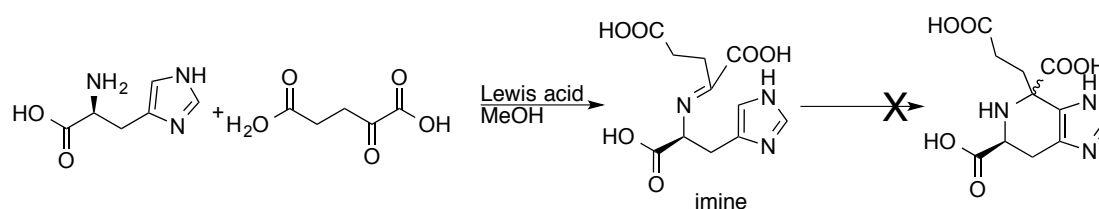
The formation of mikimopine at room temperature (**Table 1.4; Entry 9**) indicates the latter to be the kinetic product while cucumopine is favoured at high temperature and longer reaction times, and is therefore the thermodynamic product.

When mikimopine was heated in methanol in the presence or absence of TEA, conversion to its thermodynamically more stable *trans*-diastereomer **1.6** was not observed, indicating that the new bonds formed are not reversible. In the case of the P-S cyclisation between an aldehyde and tryptophan, the *cis* to *trans* epimerisation at the newly formed chiral centre is known to occur under acidic conditions.<sup>50</sup> However, heating mikimopine in the presence of acid leads to lactamisation (**1.7**) with preservation of stereochemistry as determined by 2D NMR spectroscopy.<sup>45</sup> Indeed the opines were converted to the lactams quantitatively with 0.5 N HCl in one hour at room temperature or during chromatography using an acid additive (e.g. acetic acid) in the eluent.<sup>51</sup>



#### 1.2.6. Lewis Acids

To avoid lactamisation, Lewis acids were investigated. In all cases, this led to the imine but no P-S cyclisation (**Table 1.5**).

**Table 1.5** Lewis acids in the P-S reaction between L-histidine and  $\alpha$ -ketoglutaric acid

Entry	Lewis acid <sup>a</sup>	Temp (°C)	Time (h)	Outcome <sup>b</sup>
1	Sc(OTf) <sub>3</sub>	r.t	1.5	NR <sup>e</sup>
2	Sc(OTf) <sub>3</sub>	64	3.5	25% imine
3	Sc(OTf) <sub>3</sub>	115 <sup>c</sup>	5	100% imine
4	Sc(OTf) <sub>3</sub>	115 <sup>c</sup>	24	60% imine
5	Sc(OTf) <sub>3</sub>	64 (μW) <sup>d</sup>	1	35% imine
6	Sc(OTf) <sub>3</sub>	160 (μW) <sup>d</sup>	1	100% imine
7	Ln(OTf) <sub>3</sub>	r.t	5 days	9% imine
8	Ln(OTf) <sub>3</sub>	64	15	100% imine

**a.** 1.2 equiv. used unless otherwise specified; **b.** determined by <sup>1</sup>H NMR of crude reaction mixture; **c.** heated to 115°C in a sealed tube; **d.** set at maximum power of 300 W and sealed tube used; **e.** NR = no reaction.

### 1.2.7. Substrates Scope

With a view of synthesising analogues of the opines, we applied our diastereoselective conditions to other ketones. A vast majority of the literature concerning the P-S reactions so far deals with aldehydes while ketones have been only sparsely studied.<sup>17,52</sup> This is presumably due to their poor reactivity, the imine intermediates being both more sterically hindered and less electrophilic than those derived from aldehydes.

Much to our disappointment, the diastereoselective reaction conditions developed for mikimopine did not prove to be general. Pyruvic acid was the only

ketone that provided the desired products in comparable *de* to  $\alpha$ -ketoglutaric acid under thermodynamic condition (**Table 1.6; Entry 1**). Compounds **1.8** and **1.9** are not known as a natural products but such a structure would be isolated in the future as pyruvic acid is at least as common as  $\alpha$ -ketoglutaric acid in Nature.

The stereochemistry of the product was proven by separation of the two diastereomers and 1D ROESY analysis. In the minor diastereomer **1.9**, the methyl group gave a strong ROE to  $\alpha$ -H which was weak in the major diastereomer **1.8** (**Figure 1.6A and B**).

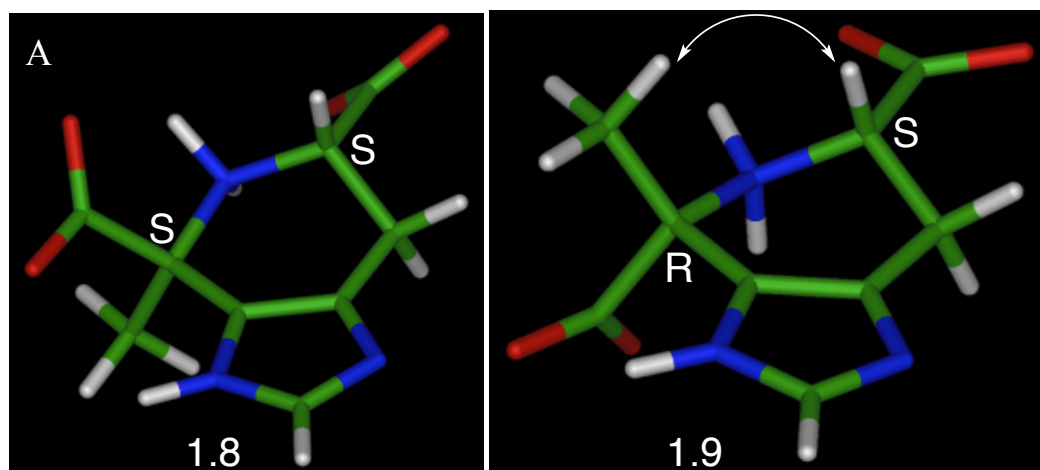


**Figure 1.6 A.** 3D model of **1.8** and **1.9**. Arrow indicating the proximity of the pyruvate CH<sub>3</sub> with the  $\alpha$ -H of hisitidine used to differentiate between the two diastereomers.

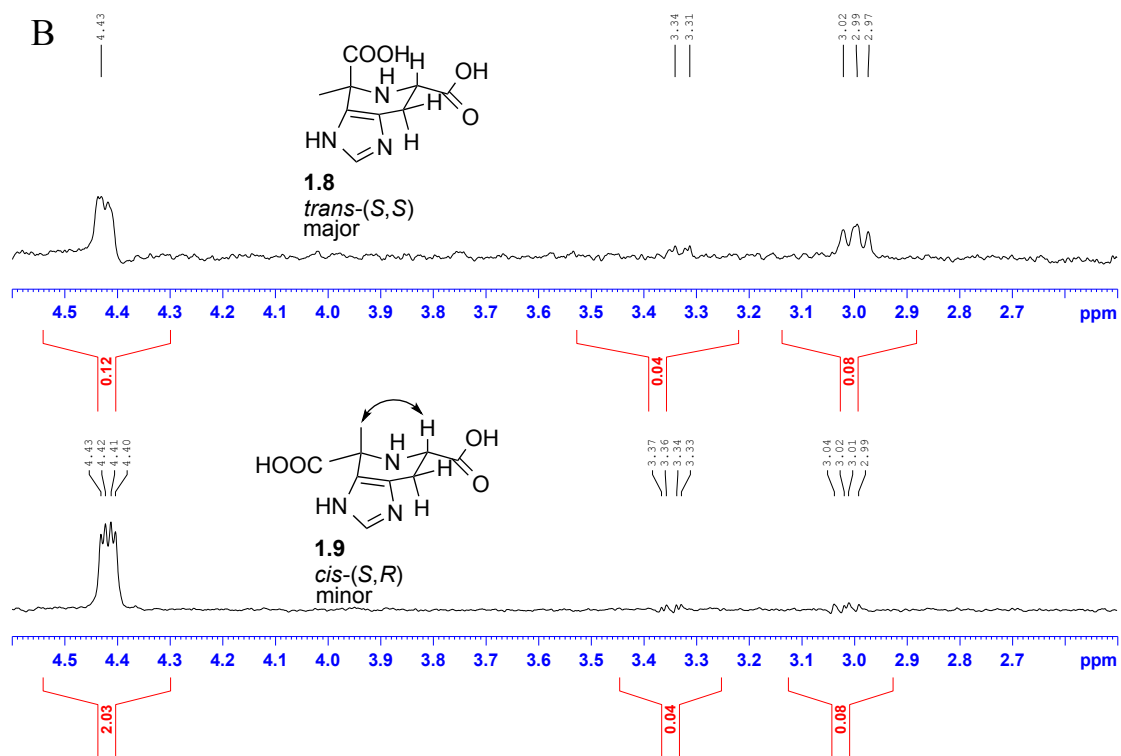


**Figure 1.6 B.** 1D ROE of **1.8** and **1.9** irradiation at the CH<sub>3</sub>.

**Table 1.6** Substrate scope under the thermodynamic condition developed for cucumopine.

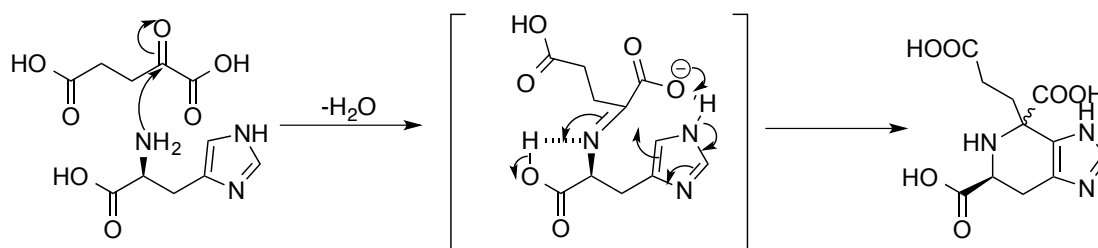
Reaction scheme: 2-amino-3-(1H-imidazol-2-yl)propanoic acid derivative + Ketone (R-C(=O)-R<sub>1</sub>)  $\xrightarrow[\text{MeOH, reflux, 24 h}]{\text{TEA (32 equiv.)}}$  Imine + Cucumopine derivative

Entry	ketone	product	Yield (%)
1		( <i>S,R</i> ):( <i>S,S</i> ) 91:9	80
2		Imine	-
3		Imine	-
4		Imine	-
5		dec.	-
6		Imine	-
7		dec.	-
8		dec.	-
9		Imine	-

The absence of cyclisation with the dimethyl ester of  $\alpha$ -ketoglutaric acid (**Entry 4**) indicates the key role of the carboxylic acid adjacent to the ketone in promoting the P-S cyclisation. Once the imine has formed, the adjacent carboxylic



must play a role in promoting the P-S cyclisation of the imidazole onto the imine by acting as an internal proton abstractor from the imidazole ring (**Scheme 1.14**).



**Scheme 1.14** Key role of the COOH groups adjacent to the imine in promoting the P-S cyclisation.

Moreover, when the other ketones (**Table 1.6; Entry 2-9**) were subjected to conventional heating or to microwave irradiation in the presence of either TEA,  $K_2CO_3$  or KOH in methanol, in most case, only the corresponding imines were formed, even with prolonged reaction time. Attempted purification on silica gel led to the recovery of starting materials only.

The low reactivity with ketones may be attributed to a slow imine formation or to steric hindrance (**Table 1.6; Entry 2-3 and 9**). The latter was observed in benzoyl formic acid, which only produced the imine despite bearing the  $\alpha$ -carboxylic acid, likely involved in the intramolecular catalysed P-S cyclisation (**Entry 2**). Under the kinetic condition developed for the formation of mikimopine (**Table 1.3; Entry 2**), none of the ketones reacted to give the desired P-S products.

When L-tyrosine and L-tryptophan were used as substrates with  $\alpha$ -ketoglutaric acid, no cyclisation occurred either under the thermodynamic or kinetic conditions. While the P-S reaction of imidazoles, is known to be base-catalysed<sup>36,37</sup>, the formation of tetrahydroisoquinolines and tetrahydro- $\beta$ -carboline is known to occur mainly under acidic conditions.<sup>17</sup> Both L-tyrosine and L-tryptophan formed the

corresponding imines with  $\alpha$ -ketoglutaric acid under our thermodynamic conditions but the P-S cyclisation did not occur even with prolonged reaction times.

### 1.2.8. Potential Siderophores

Siderophores are small, iron chelating compounds, secreted by microorganisms, fungi and plants.<sup>53</sup> They possess a high affinity and selectivity for Fe(III) to sequester and solubilise extracellular Fe(III) and then take up the complex via specific receptors on the cell membrane.<sup>53</sup> Siderophores have found applications in medicine in better targeting antibiotics and for iron overload therapy.<sup>54,55</sup> Their mode of action in the former application consists of designed siderophore-drug conjugates that will be taken in by specific membrane bound iron-siderophore receptors in the targeted pathogenic microorganisms or in the latter application by scavenging intracellular Fe(III) by complexation and egression of the complex.<sup>54,55</sup> The main ligands that are present in siderophores are catecholates, hydroxamates and carboxylates that include  $\alpha$ -aminocarboxylate and  $\alpha$ -hydroxycarboxylate, and the less common ligands such as  $\alpha$ -hydroxyimidazole (**Figure 1.7**).<sup>53</sup>

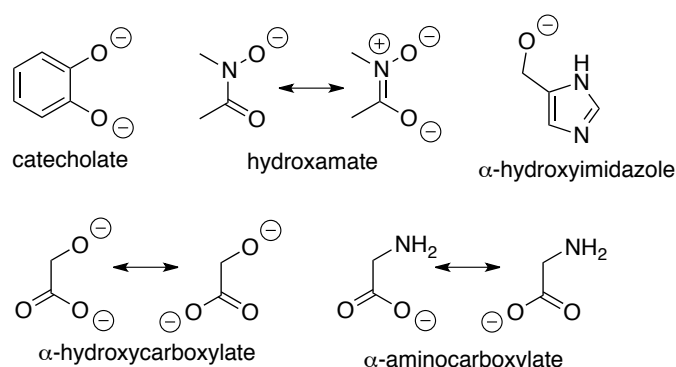


**Figure 1.7** Structural motifs of ligands present in siderophores.

The arrangement of carboxylates and nitrogens in mikimopine and cucumopine and the structural relationship to  $\alpha$ -hydroxyl imidazoles, suggested their potential as siderophores. More specifically, molecular modeling and DFT calculation (DFT//B88-P86/TZVPP) in continuum water (COSMO) model suggested the tetradentate diaqua complex was stable (**Figure 1.8**). However, siderophores are commonly hexadentate ligands in order to completely saturate all the binding sites of Fe(III) and bring it to the cell without ligand dissociation occurring.<sup>56</sup>

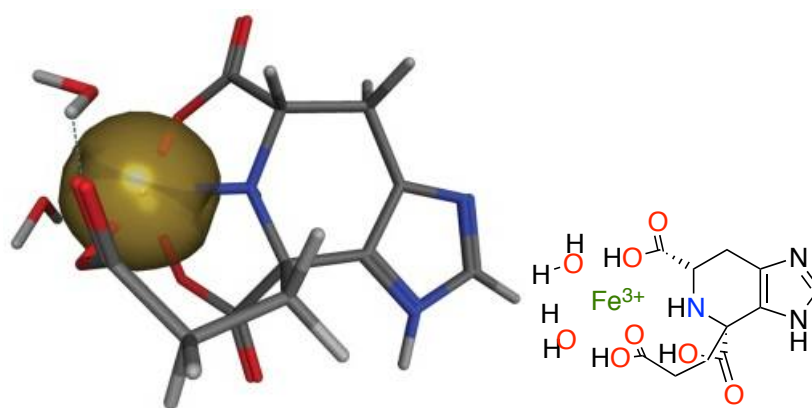


**Figure 1.8** Result of ab initio calculations (DFT//BP88/TZVP) structure optimisation. Mikimopine chelating an Fe(III) ion, assisted by two H<sub>2</sub>O molecules.

#### 1.2.8.1. Fluorescence-based Assay to Assess the Fe(III) Chelating Ability of Mikimopine

In order to assess the Fe(III) chelating ability of the opines, a fluorescence-based assay using the commercially available fluorescent probe, calcein (**1.9**) was developed. Calcein (**1.9**) carries two aminodiacetic chelating arms, and the combination of carboxylates and phenolate stabilises the Fe(III) adduct (**Figure 1.9**).<sup>57</sup> The fluorescence of **1.9** is quenched upon binding to iron.<sup>57</sup>

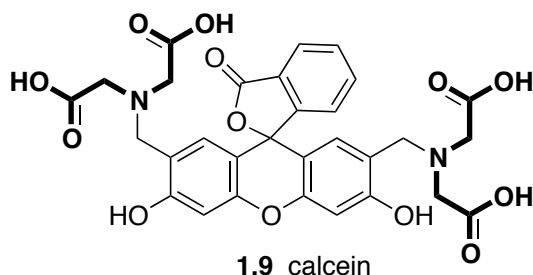
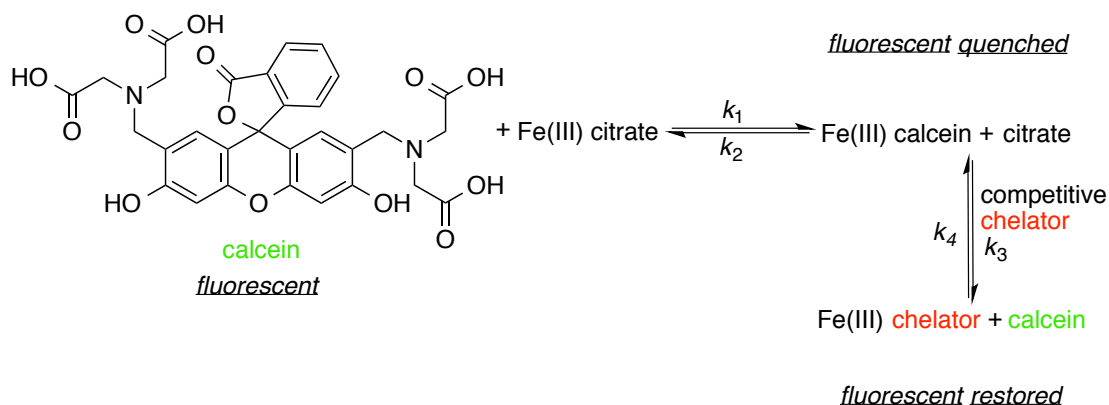


**Figure 1.9** Calcein, a fluorescein-based fluorescent probe with the diaminetetraacetic chelating arms (in bold).

When another Fe(III) chelator is added to a solution of **1.9**-Fe(III) complex, a chelator-Fe(III) complex is formed as a result of a ligand exchange reaction between **1.9** and the chelator which then allows the fluorescence from **1.9** to be recovered (**Scheme 1.15**). EDTA which was used as a positive control, was found to increase fluorescence in a concentration dependant manner (**Figure 1.10A**) while mikimopine did not show any effect on the fluorescence (**Figure 1.10B**). Fitting the data to a Gaddum/Schild plot gave a dissociation constants,  $K_D$  of EDTA and mikimopine for Fe(III) were determined as 0.72  $\mu\text{M}$  and 12.6 mM respectively, indicating that mikimopine is not a siderophore.



**Scheme 1.15** When calcein (shown as fluorescent in green and non-fluorescent in black) chelates Fe(III), its fluorescence becomes quenched.

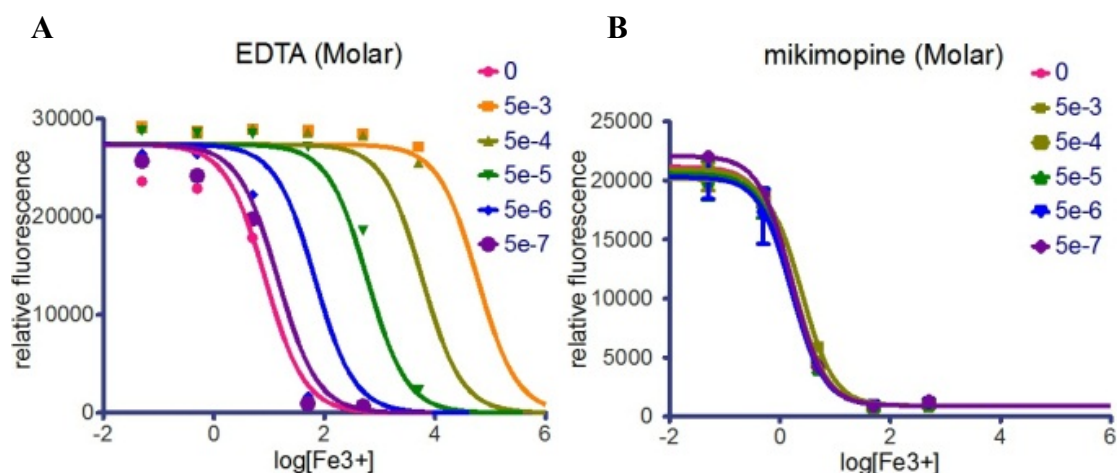


**Figure 1.10** Gaddum/Schild EC<sub>50</sub> shift plots showing relative fluorescence (y-axis) at different Fe(III) concentrations (x-axis) for different concentrations of **A.** EDTA and **B.** mikimopine in the presence of  $5 \times 10^{-6}$  M calcein.

### 1.3. Summary

Compared to  $\beta$ -arylethylamine or tryptamine, the P-S reaction of the imidazoles has been less extensively investigated. Moreover, the P-S cyclisation with ketones has received very little attention as compared to aldehydes. The biogenesis of the natural products mikimopine and cucumopine led us to investigate a possible biomimetic diastereoselective synthesis for these opine diastereomers. In order to do so, we exploited the P-S reaction between L-histidine and  $\alpha$ -ketoglutaric acid and screened a variety of different conditions (bases, Lewis acids, solvents, temperatures, time). Cucumopine, the *trans*-(S,S) diastereomer, was synthesised with a *de* of 82% under reflux in methanol in the presence of excess TEA. Mikimopine, the *cis*-(S,R) diastereomer, on the other hand was synthesised with a *de* of 80% at room temperature in methanol in the presence of excess K<sub>2</sub>CO<sub>3</sub>. While it might appear that the diastereoselectivity was achieved using thermodynamic or kinetic control, the bases were responsible for the observed diastereoselectivity. Lewis acids only led to the formation of imine and imine hydrolysis was observed over extended reaction

time. It is now well established that the P-S cyclisation of imidazoles is activated/catalysed by base.

Various ketones were investigated in the P-S reaction with L-histidine under the optimised diastereoselective conditions. However the diastereoselective conditions did not prove to be general for all ketones. Moreover a carboxylic acid adjacent to the imine appears to be important in the P-S cyclisation and possibly in the diastereoselectivity observed. L-Tyrosine and L-tryptophan, both known to undergo the P-S cyclisation under acidic conditions, failed to form the cyclised product with  $\alpha$ -ketoglutaric acid under the optimised base-catalysed diastereoselective conditions developed with L-histidine.

The three carboxylic acids and nitrogen rich nature of the opines led us to speculate that the opines could be potential siderophores. Molecular modeling showed that mikimopine is able to chelate an Fe(III) with the assistance of two water molecules. In order to investigate the potential Fe(III) chelating ability of the opines, a competitive fluorescence-based assay using calcein was developed. Much to our disappointment, mikimopine does not appear to possess any iron chelating ability.

#### 1.4. References

- (1) Breslow, R. *Chem. Soc. Rev.* **1972**, *1*, 553-580.
- (2) Robinson, R. *J. Chem. Soc., Trans.* **1917**, *111*, 762-768.
- (3) Beaudry, C. M.; Malerich, J. P.; Trauner, D. *Chem. Rev.* **2005**, *105*, 4757-4778.
- (4) Brunoldi, E.; Luparia, M.; Porta, A.; Zanoni, G.; Vidari, G. *Curr. Org. Chem.* **2006**, *10*, 2259-2282.
- (5) Bulger, P. G.; Bagal, S. K.; Marquez, R. *Nat. Prod. Rep.* **2008**, *25*, 254-297.
- (6) Scholz, U.; Winterfeldt, E. *Nat. Prod. Rep.* **2000**, *17*, 349-366.

- (7) Taylor, S. K. *Org. Prep. Proced. Int.* **1992**, 24, 245-&.
- (8) Yoder, R. A.; Johnston, J. N. *Chem. Rev.* **2005**, 105, 4730-4756.
- (9) Pictet, A.; Spengler, T. *Ber. Dtsch. Keram. Ges.* **1911**, 44, 2030.
- (10) In *The Alkaloids, Chemistry and Physiology*; Manske, R. H. F., Ed.; Academic Press, New York: 1981; Vol. XX.
- (11) Stork, G.; Tang, P. C.; Casey, M.; Goodman, B.; Toyota, M. *J. Am. Chem. Soc.* **2005**, 127, 16255-16262.
- (12) Wang, Y.-X.; Wang, Y.-P.; Zhang, H.; Kong, W.-J.; Li, Y.-H.; Liu, F.; Gao, R.-M.; Liu, T.; Jiang, J.-D.; Song, D.-Q. *Bioorg. Med. Chem. Lett.* **2009**, 19, 6004-6008.
- (13) Winkler, J. D.; Axten, J. M. *J. Am. Chem. Soc.* **1998**, 120, 6425-6426.
- (14) Doherty, G. J.; McMahon, H. T. *Annu. Rev. Biochem.* **2009**, 78, 857-902.
- (15) Dempster, D. N.; Morrow, T.; Rankin, R.; Thompson, G. F. *Chem. Phys. Lett.* **1973**, 18, 488-492.
- (16) Stöckigt, J.; Antonchick, A. P.; Wu, F.; Waldmann, H. *Angew. Chem. Int. Ed.* **2011**, 50, 8538-8564.
- (17) Youn, S. W. *Org. Prep. Proced. Int.* **2006**, 38, 505-591.
- (18) Larghi, E. L.; Kaufman, T. S. *Synthesis* **2006**, 187-220.
- (19) Barleben, L.; Panjikar, S.; Ruppert, M.; Koepke, J.; Stockigt, J. *Plant Cell* **2007**, 19, 2886-2897.
- (20) Berkner, H.; Schweimer, K.; Matecko, I.; Rosch, P. *Biochem. J.* **2008**, 413, 281-290.
- (21) Ma, X. Y.; Koepke, J.; Frittsch, G.; Diem, R.; Kutchan, T. M.; Michel, H.; Stockigt, J. *Biochim. Biophys. Acta, Proteins Proteomics* **2004**, 1702, 121-124.
- (22) Rueffer, M.; Elshagi, H.; Nagakura, N.; Zenk, M. H. *FEBS Lett.* **1981**, 129, 5-9.
- (23) Gorman, A.; Killoran, J.; O'Shea, C.; Kenna, T.; Gallagher, W. M.; O'Shea, D. F. *J. Am. Chem. Soc.* **2004**, 126, 10619-10631.
- (24) Maresh, J. J.; Giddings, L. A.; Friedrich, A.; Loris, E. A.; Panjikar, S.; Trout, B. L.; Stockigt, J.; Peters, B.; O'Connor, S. E. *J. Am. Chem. Soc.* **2008**, 130, 710-723.
- (25) Koepke, J.; Ma, X. Y.; Frittsch, U.; Michel, H.; Stockigt, J. *Acta Crystallogr., Sect. D: Biol. Crystallogr.* **2005**, 61, 690-693.

- (26) Wellisch, J. *Biochem. Z.* **1913**, *49*, 173-194.
- (27) Chibnall, A. *J. Biol. Chem.* **1924**, *61*, 303-308.
- (28) Klutchko, S.; Hodges, J. C.; Blankley, C. J.; Colbry, N. L. *J. Heterocycl. Chem.* **1991**, *28*, 97-108.
- (29) Heyl, D.; Harris, S. A.; Folkers, K. *J. Am. Chem. Soc.* **1948**, *70*, 3429-3431.
- (30) Stocker, F. B.; Fordice, M. W.; Larson, J. K.; Thorstenson, J. H. *J. Org. Chem.* **1966**, *31*, 2380-2383.
- (31) Devlin, R.; Dandliker, W. B.; Arrhenius, P. O. G. Patent US6060598, 2000.
- (32) Cox, E. D.; Cook, J. M. *Chem. Rev.* **1995**, *95*, 1797-1842.
- (33) Kawate, T.; Yamanaka, M.; Nakagawa, M. *Heterocycles* **1999**, *50*, 1033-1039.
- (34) Madrigal, B.; Puebla, P.; Caballero, E.; Pelaez, R.; Gravalos, D. G.; Medarde, M. *Arch. Pharm.* **2001**, *334*, 177-179.
- (35) Fujii, S.; Maki, Y.; Kimoto, H.; Cohen, L. A. *J. Fluorine Chem.* **1987**, *35*, 581-589.
- (36) Smith, D. D.; Gallagher, A. T.; Crowley, V. M.; Gergens, W. M.; Abel, P. W.; Hulce, M. *Synthesis* **2014**, *46*, 515-521.
- (37) Shengule, S. R.; Karuso, P. *Aust. J. Chem.* **2014**, *67*, 184-191.
- (38) Shengule, S. R.; Karuso, P. *Org. Lett.* **2006**, *8*, 4083-4084.
- (39) Fujita, M.; Nakao, Y.; Matsunaga, S.; Seiki, M.; Itoh, Y.; Yamashita, J.; van Soest, R. W. M.; Fusetani, N. *J. Am. Chem. Soc.* **2003**, *125*, 15700-15701.
- (40) Meketa, M. L.; Weinreb, S. M. *Org. Lett.* **2006**, *8*, 1443-1446.
- (41) Meketa, M. L.; Weinreb, S. M.; Nakao, Y.; Fusetani, N. *J. Org. Chem.* **2007**, *72*, 4892-4899.
- (42) Meketa, M. L.; Weinreb, S. M. *Org. Lett.* **2007**, *9*, 853-855.
- (43) Shengule, S. R.; Loa-Kum-Cheung, W. L.; Parish, C. R.; Blairvacq, M.; Meijer, L.; Nakao, Y.; Karuso, P. *J. Med. Chem.* **2011**, *54*, 2492-2503.
- (44) Davioud, E.; Petit, A.; Tate, M. E.; Ryder, M. H.; Tempé, J. *Phytochemistry* **1988**, *27*, 2429-2433.
- (45) Isogai, A.; Fukuchi, N.; Hayashi, M.; Kamada, H.; Harada, H.; Suzuki, A. *Phytochemistry* **1990**, *29*, 3131-3134.
- (46) Tempé, J. *Chemistry and Biochemistry of Amino Acids, Peptides and Proteins*; B. Weinstein ed.; Marcel Dekker: New York, 1983; Vol. 7.



- (47) Sauerwein, M.; Wink, M. *J. Plant Physiol.* **1993**, *142*, 446-451.
- (48) Goodman, J. M.; Kirby, P. D.; Haustedt, L. O. *Tetrahedron Lett.* **2000**, *41*, 9879-9882.
- (49) Shannon, R. D. *Acta Cryst.* **1976**, *A32*, 751-767.
- (50) Van Linn, J. M.; Cook, J. M. *J. Org. Chem.* **2010**, *75*, 3587-3599.
- (51) Isogai, A.; Fukuchi, N.; Hayashi, M.; Kamada, H.; Harada, H.; Suzuki, A. *Agric. Biol. Chem.* **1988**, *52*, 3235-3237.
- (52) Kuo, F.-M.; Tseng, M.-C.; Yen, Y.-H.; Chu, Y.-H. *Tetrahedron* **2004**, *60*, 12075-12084.
- (53) Hider, R. C.; Kong, X. *Nat. Prod. Rep.* **2010**, *27*, 637-657.
- (54) Braun, V.; Pramanik, A.; Gwinner, T.; Koberle, M.; Bohn, E. *BioMetals* **2009**, *22*, 3-13.
- (55) Evans, R. W.; Kong, X. L.; Hider, R. C. *Biochim. Biophys. Acta, Gen. Subj.* **2012**, *1820*, 282-290.
- (56) Albrecht-Gary, A. M.; Crumbliss, A. L. *Metal Ions in Biological Systems, Vol 35* **1998**, *35*, 239-327.
- (57) Thomas, F.; Serratrice, G.; Beguin, C.; Saint Aman, E.; Pierre, J. L.; Fontecave, M.; Laulhere, J. P. *J. Biol. Chem.* **1999**, *274*, 13375-13383.



---

**CHAPTER 2**  
 **BIOGENESIS OF THE OROIDIN ALKALOIDS**

---

## 2.1. Introduction

In the previous chapter the biogenetic hypothesis of the opines: cucumopine and mikimopine led to the application of the Pictet-Spengler reaction in a diastereoselective biomimetic approach towards the synthesis of these natural products which are relatively simple in structure. We now turned our attention to a structurally diverse and more complex family of natural products, known as the oroidin alkaloids.

### 2.1.1. The Oroidin Alkaloids

The oroidin alkaloids form part of a continuously growing family of natural products that have been isolated from marine sponges, with over 150 members reported so far.<sup>1</sup> All compounds can be considered to be closely related and seem to share a common biogenetic origin. The oroidin alkaloids demonstrate beautifully how nature generates structural complexity and biological activity from the diversification of a simple precursor.<sup>1</sup> As such this group of marine compounds have not only been the subject of numerous synthetic and biological investigations but also of biogenetic speculation.<sup>2-15</sup> The oroidin alkaloids have become an interesting and highly relevant group of targets for biomimetic synthesis.

#### 2.1.1.1. Oroidin

Oroidin (**2.1**), initially isolated from *Agelas oroides* in 1971 by Forenza *et al.*<sup>16</sup> and is the first member of this growing family of natural products (**Figure 2.1**). It has since been isolated from various other sponges.<sup>14,17-23</sup> The initial structure **2.1a** suggested for oroidin by Forenza *et al.* was revised to **2.1** by Garcia *et al.* two years

later.<sup>24</sup> Oroidin exhibits antifouling activity and anti-feedant activity.<sup>25-28</sup> Oroidin is considered to be the biogenetic precursor of all the oroidin alkaloids, which take the form of linear monomers, cyclic monomers and polycyclic dimers and tetramers.<sup>2</sup>

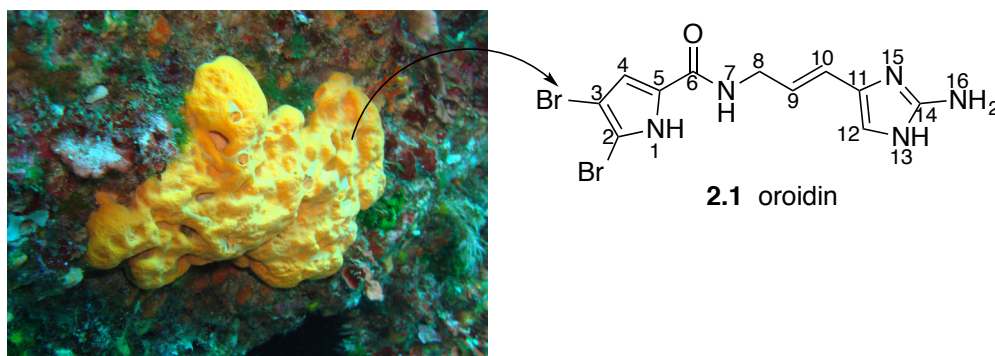
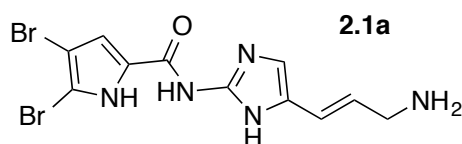


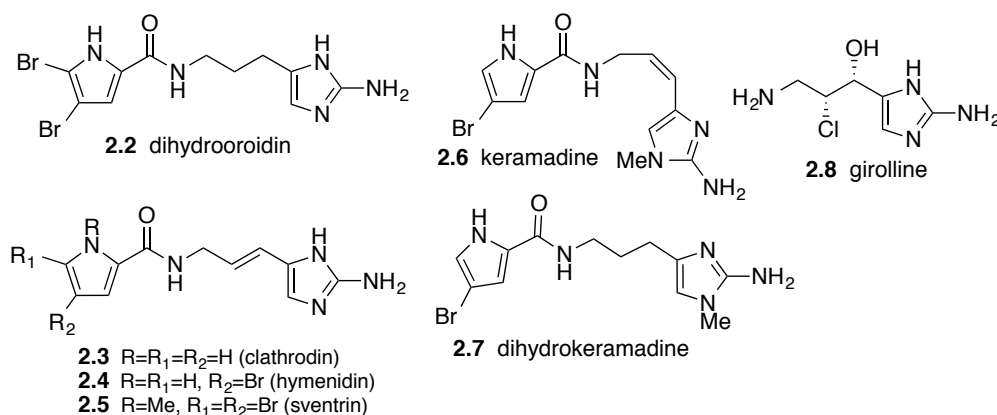
**Figure 2.1** Oroidin isolated from *Agelas oroides*, photo taken from ref. 29 (public domain).



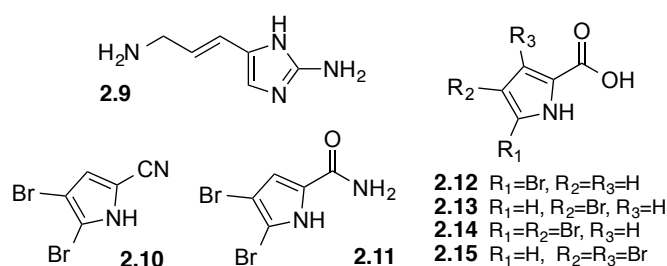
### 2.1.2. Linear Monomers

The oroidin alkaloids vary with regard to the oxidation, reduction, or hydrolysis state of the 2-amino-4(5)-vinylimidazole unit. Dihydrooroidin (DHO, **2.2**) is the reduced version of oroidin at the alkene double bond. The pyrrole-2-carboxamide moiety can be non-, mono-, or dibrominated in the 2- and 3-positions. Hymenidin (**2.4**) was initially isolated by Kobayashi *et al.* from the Okinawa marine sponge *Hymeniacidon* sp. and later by Köck and coworkers<sup>30</sup> from *Agelas sventrus*, and was found to be a potent antagonist of serotonergic receptors.<sup>31</sup> Clathrocin (**2.3**), isolated by Morales *et al.* from the sponge *Agelas clathrodes*, exhibits neurotoxic activity.<sup>32,33</sup> Methylated analogues **2.5-2.7** have been isolated from various marine sponge *Agelas* species.<sup>30,34-36</sup> Girolline (**2.8**), is the chlorohydrin of 3-amino-1-(2-aminoimidazolyl)-prop-1-ene which is one of the building block of oroidin alkaloids.

It has antitumour activity and was isolated from the sponge *Peudaxinyssa cantharella* by Potier and coworkers.<sup>37,38</sup>



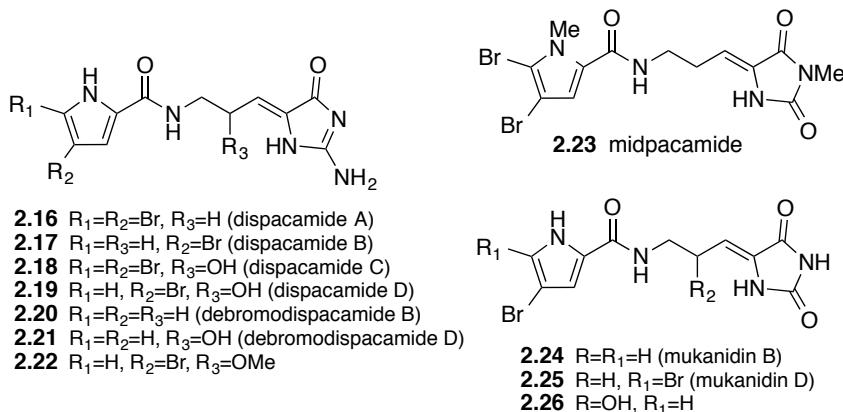
Biosynthetic precursors to the oroidin alkaloids have been isolated from various marine sponges. These include 3-amino-1-(2-aminoimidazolyl)-prop-1-ene (**2.9**), 4,5-dibromopyrrole-2-carbonitrile (**2.10**), 4,5-dibromopyrrole-2-carboxamide (**2.11**) and the bromopyrrole-2-carboxylic acids (**2.12-2.15**).<sup>14,16,39-42</sup>



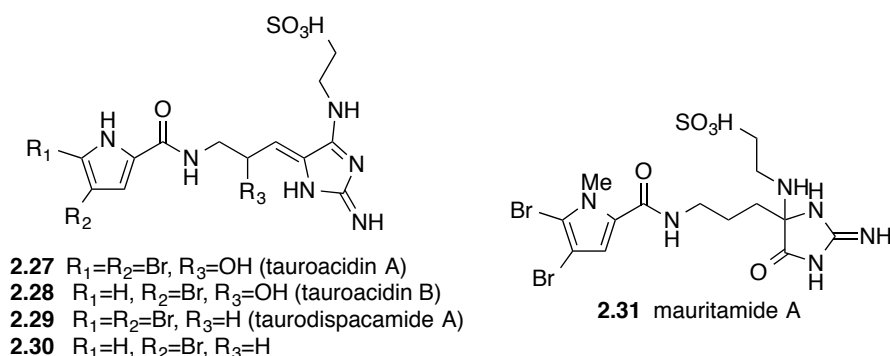
Oroidin (**2.1**) can be oxidised at the alkene double bond and/or at the 2-aminoimidazole. Indeed, the imidazolone is a common motif to many of the oroidin alkaloids. Dispacamides A-D (**2.16-2.19**) were isolated from four Caribbean *Agelas* sponges by Fattorusso and coworkers.<sup>43</sup> Dispacamide A (**2.16**) has shown potent and selective antagonistic activity against histaminergic receptors.<sup>17</sup>

Debromodispacamide B and D (**2.20-2.21**) have been isolated by Al-Mourabit and coworkers from the sponge *Agelas mauritiana*.<sup>44</sup> Midpacamide (**2.23**) and the

mukanadins **2.24-2.26** have their imidazolone ring further oxidised. Schroder and coworkers isolated **2.26** from an unidentified marine sponge and compound **2.22** and **2.26** from the sponge *Axinella verrucosa*.<sup>45,46</sup> Mukanidin B (**2.24**) and D (**2.25**) were isolated from the sponge *Didiscus oxeata* by Harmann and coworkers.<sup>47</sup>

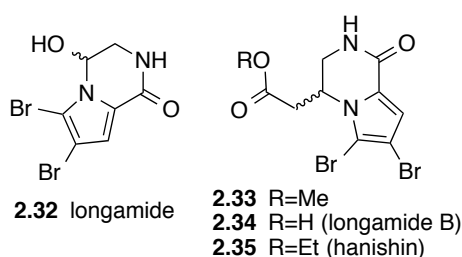


Several of the oroidin alkaloids have been formed by the oxidation of the imidazole double bond with substitution by taurine. The linear monomers include the tauroacidins (**2.27-2.28**)<sup>48</sup> and the taurodispacamides **2.29-2.30**<sup>45,49</sup> and in mauritamide A **2.31**<sup>50</sup>. Tauroacidin A and B (**2.27-2.28**) exhibit kinase inhibitory activity and were first isolated from a *Hymeniacidon* sp. by Kobayashi *et al.*<sup>48</sup> Taurodispacamide A (**2.29**), with antihistaminic activity, was first isolated from an unidentified Mediterranean sponge by Fattorusso *et al.*<sup>49</sup> Schroder and coworkers reported the isolation of **2.30** from the sponge *Axinella verrucosa*.<sup>45</sup> Mauritamide A **2.31**, where taurine has added onto the C4 of the 2-aminoimidazolone, was isolated from the Fijian marine sponge *Agelas mauritiana* by Crews *et al.*<sup>50</sup>



### 2.1.3. Cyclic Monomers

The cyclic monomers can be monocyclic or bicyclic. The bromopyrrole (+)-longamide (**2.32**) which possesses antibacterial activity, was initially isolated from the Caribbean sponge *Agelas longissimalis*<sup>51</sup> and more recently from a *Homaxinella* sp. from Japan.<sup>52</sup> Also isolated from a *Homaxinella* sp. is longamide B methyl ester **2.33** which has cytotoxic activity *in vitro* against a leukemia cell line. The corresponding acid **2.34**, which shows modest antibacterial activity against several Gram-positive bacteria, was isolated from the marine sponge *Agelas dispar*.<sup>34</sup> The ethyl ester of longamide B **2.35**, isolated from the extracts of the highly polymorphic sponge *Acanthella carteri* and shows cytotoxicity towards lung carcinoma.<sup>53</sup> All of these compounds have been isolated in their racemic forms suggesting that they could have been formed through non-enzymatic processes.



Cyclooroidin (**2.36**), which was isolated from the sponge *Agelas oroides* by Fattorusso *et al.*, is formed from the intramolecular cyclisation between the pyrrole



nitrogen (N1) and the alkene double bond at C9 (**Figure 2.2**).<sup>49</sup> Oxocyclostylidol (**2.37**) was isolated from the Caribbean sponge *Styllissa caribica* by Köck and Grube and is the first oroidin alkaloid containing an oxidised pyrrole moiety.<sup>54</sup> Agesamide A (**2.38**) and B (**2.39**) are racemates isolated from the marine sponge *Agelas* sp. by Kobayshi *et al.*<sup>55</sup> They differ from cyclooroidin by the presence of a fully oxidised imidazole. The slagenins **2.40-2.42**, isolated from the marine sponge *Agelas nakamurai*, bear a urea moiety in place of the guanidine and has an indirect C9-C12 bond connection via an ether from an intramolecular cyclisation.<sup>56</sup>

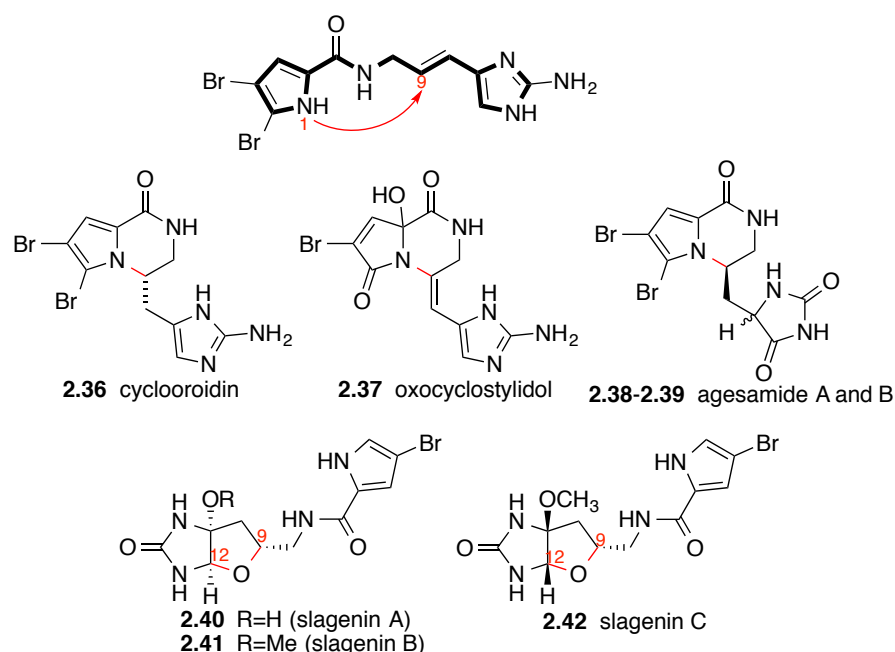


**Figure 2.2** Cyclic monomers with N1 to C9 bond connection and the slagenins with C9-O-C12 ether bond connection.

The cyclic monomers also include the azepine analogues, formed by the intramolecular cyclisation between the pyrrole carbon C4 and the alkene double bond at C10 (**Figure 2.3**). Stevensine (**2.43**) is a representative for a sub-family of cyclic alkaloids within the oroidin class possessing a pyrrolo[2,3-c]azepin-8-one fused bicycle system unique to these marine natural products. It was simultaneously isolated by Faulkner<sup>57</sup> from an unidentified Micronesian sponge and by De Nanteuil

*et al.*<sup>58</sup> as “odiline” from the New Calodenian sponge, *Pseudaxinyssa cantharella* and since then from various other sponges.<sup>35,45,59-61</sup> Hymenin (**2.44**) is the reduced version of stevensine which was first isolated from the marine sponge *Hymeniacidon* sp. by Kobayashi *et al.* and possesses potent  $\alpha$ -adrenoreceptor blocking activity.<sup>31</sup> From the same marine sponge, Kobayashi *et al.* also isolated the spongiacidines A-D.<sup>62</sup> The spongiacidines A (**2.45**) and B (**2.46**) and the aldisines **2.47-2.50** possess the 2-aminoimidazolone, with (7*E*)-geometry or (7*Z*)-geometry. Spongiacidines C and D **2.51-2.52** and axinohydantoin E (**2.53**)<sup>63</sup> on the other hand bear the fully oxidised imidazole, existing either as the (7*E*)-geometry or the (7*Z*)-geometry. While spongiacidines A (**2.34**) and B (**2.35**) have shown inhibitory activities against C-erbB-2 and cyclin-dependent kinase 4, spongiacidines C (**2.51**) and D (**2.52**) did not have any such activities.<sup>52</sup> (Z)-Debromohymenialdesine (**2.48**) was first isolated from the marine sponge *Phakellia flabellate* by Sharma *et al.*<sup>64</sup> while its *E*-isomer was isolated from the common shallow-water sponge *Stylotella aurantium*.<sup>65</sup> 3-Bromohymenialdesine (**2.50**) was isolated from the sponge *Axinella carteri* by Proksch *et al.*<sup>66</sup> and hymenialdesine (**2.38**) was isolated from various marine sponges of the genus *Hymeniacidon*.<sup>18,58,63,67</sup> Hymenialdesine (**2.38**) was found to be a potent inhibitor of kinases CDKs, Mek1, GSK3 $\beta$ , CK1 and Chk1.<sup>68,69</sup> Hymenin and aldesine compounds have been isolated from various sponges.<sup>60,61,70,71</sup>

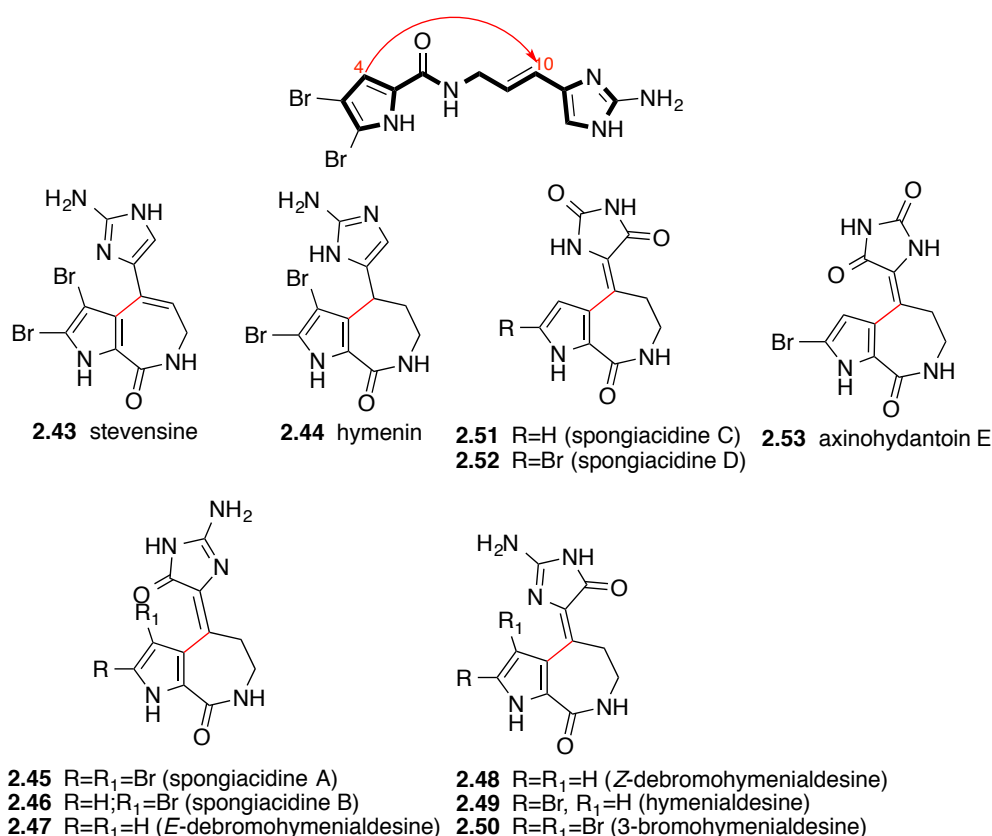


**Figure 2.3** Cyclic monomers with seven membered ring formed by a C4-C10 bond connection.

#### 2.1.4. Bicyclic Monomers

The bicyclic monomers consist of tetracyclic derivatives of oroidin (**Figure 2.4**). Two modes of intramolecular cyclisation have been observed in bicyclic monomers. These involve the bond formation between the imidazole carbons (C11 and 12) with the pyrrole nucleophiles (N1 or C4) and the amide nitrogen (N7). The phakellins **2.54-2.55** are of historical importance in marine natural product chemistry as being amongst the first complex, halogenated alkaloids to be described.<sup>72</sup> Oroidin is related to dibromophakellin (**2.54**) by a complex cyclisation that connects the pyrrole nitrogen (N1) to the unalkylated 2-aminoimidazole (C12) and the amide nitrogen (N7) to the alkylated 2-aminoimidazole (C11). Dibromophakellin (**2.54**) and monobromophakellin (**2.55**) were isolated from the marine sponge *Phakellia flabellate* by Sharma *et al.* in 1969.<sup>72</sup> (–)-7-*N*-methyldibromophakellin (**2.56**) and (–)-

7-*N*-methylmonobromophakellin (**2.57**) were isolated from the *Agelas* sp. by Crews and coworkers.<sup>73</sup> More recently, Hertiani *et al.* isolated the hydroxyl derivative of dibromophakellin **2.54a** from Indonesian marine sponges *Agelas linnaei* and *A. nakamurai*.<sup>74</sup>

As implied by the name, the isophakellins **2.58-2.60** are isomers to the phakellins and differ from the latter by the connection of the pyrrole through carbon C4 to the unalkylated 2-aminoimidazole (C12).<sup>75-77</sup> Dibromoisophakellin (**2.58**) was isolated from the marine sponge *Acanthella carteri* by Maximov *et al.*<sup>5</sup> *N*-methyldibromoisophakellin (**2.59**) was isolated from the sponge *Stylissa caribica* by Köck and coworkers<sup>30</sup> and was found to be active as a feeding deterrent against a common omnivorous reef fish. Monobromoisophakellin (**2.60**) was also isolated by Köck from *Agelas* sp.<sup>78</sup> Dibromocantharellin (**2.61**) is the racemate of dibromoisophakellin and was isolated from the New Caledonian sponge, *Pseudaxinyssa cantharella* by De Nanteuil *et al.*<sup>58</sup> The phakellstatins **2.62-2.63** differ from phakellin by the presence of urea instead of guanidine. Phakellstatin (**2.62**) and dibromophakellstatin (**2.63**) were isolated from *Phakellia mauritiana* by Pettit *et al.*<sup>63</sup> **2.63** and **2.54** have recently been found to inhibit the human 20S proteasome.<sup>79</sup>

In the dibromoagelaspongins (**2.64**), isolated from the marine sponge *Agelas* by Fedoreyev *et al.*<sup>5</sup>, both the pyrrole nitrogen (N1) and the amide nitrogen (N7) are connected to the unalkylated 2-aminoimidazole (C12) while the alkylated 2-aminoimidazole (C11) is oxidised. The agelastatins **2.65-2.70** possess a novel heterocyclic scaffold with bond connections of C8 to C12 and N1 to C9. Agelastatin A (**2.65**) together with agelastatin B (**2.66**) as a minor component, have been isolated from the deep water marine sponge *Agelas dendromorpha* collected from the coral sea.<sup>4,80</sup> Agelastatin A has shown significant *in vitro* cytotoxic activity against

leukemia and epithelial tumor lines as well as exhibiting potent activity against brine shrimp and insecticidal activity against larvae of beet army and corn worm.<sup>4,80</sup>

Agelastatins C (**2.67**) and D (**2.68**) along with agelastatin A were isolated from the Indian ocean sponge *Cymbastela* sp.<sup>81</sup> Agelastatins E (**2.69**) and F (**2.70**) are the two most recent bicyclic monomers to be isolated from the New Caledonia sponge *Agelas dendromorpha* by Al-Mourabit and coworkers.<sup>82</sup>

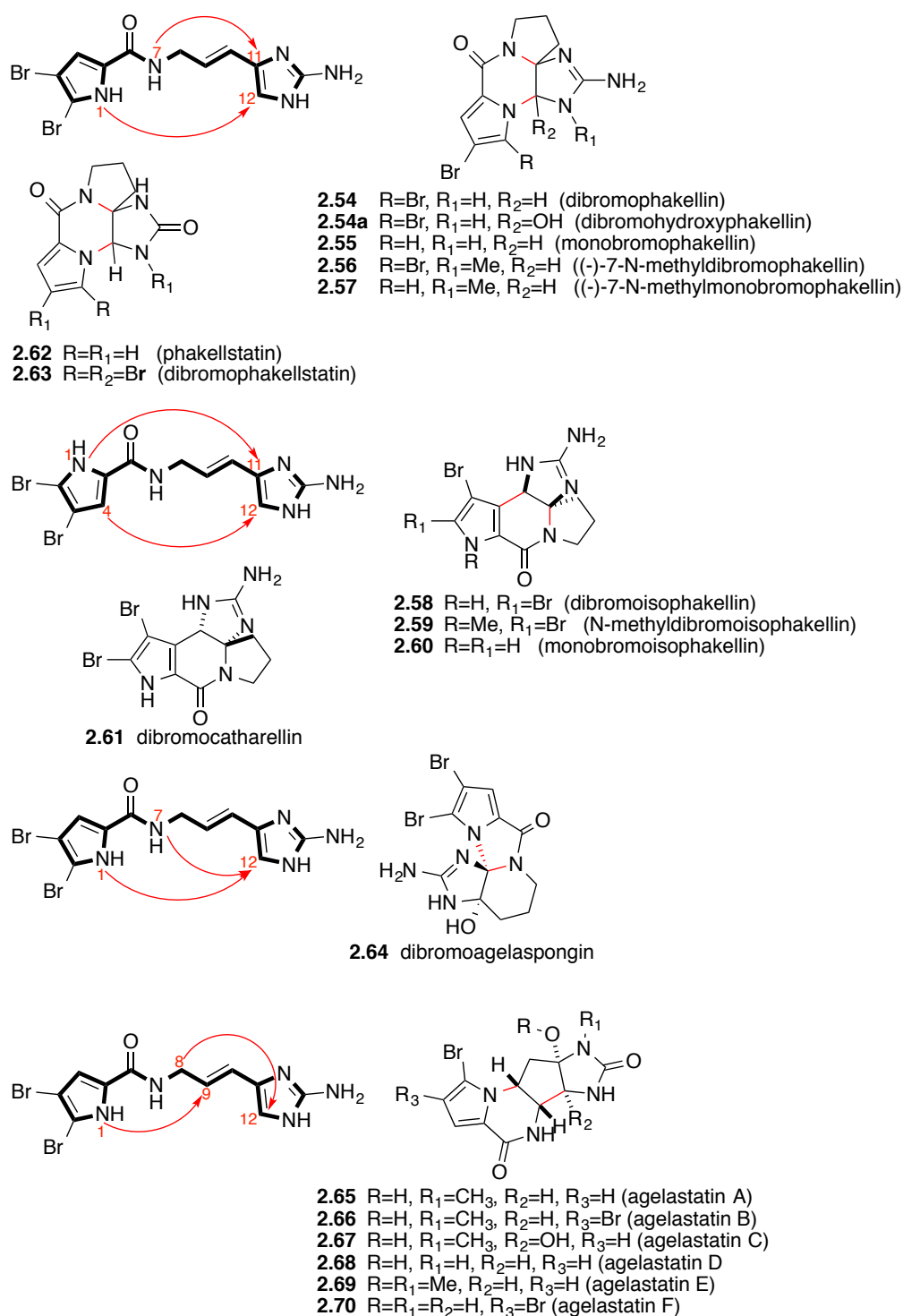
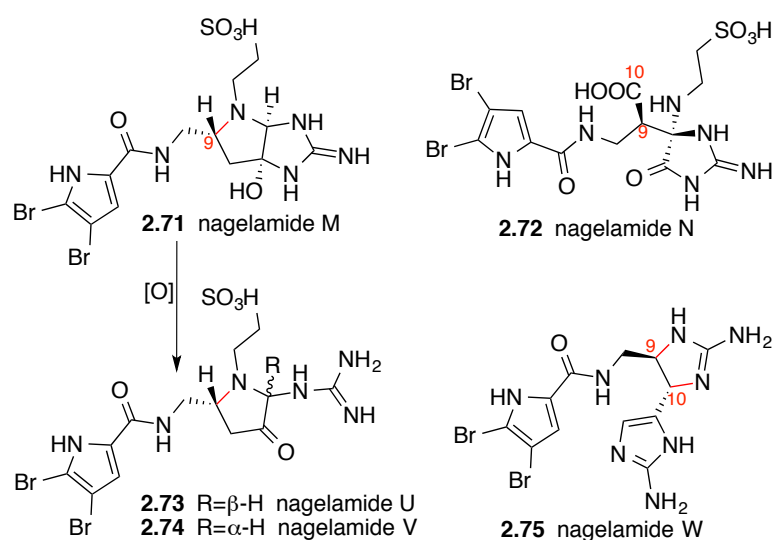


**Figure 2.4** Tetracyclic oroidin alkaloids.

Nagelamide M (**2.71**) bears a 2-amino-hexahydropyrrolo[2,3-*d*]imidazole ring with a taurine unit and is thought to be the product of the intramolecular cyclisation of the taurine nitrogen of taurodispacamide A (**2.29**) onto C-9 of the propyl chain.<sup>83</sup>

Nagelamide N (**2.72**) possesses a 2-amino-tetrahydroimidazole-4-one ring with a taurine unit and 3-(dibromopyrrole-2-carboxamido)propanoic acid moiety and is also thought to be derived from **2.29** through a series of transformations involving oxidation, cyclisation and hydrolysis.<sup>83</sup> They have both been isolated from an Okinawan marine sponge *Agelas* sp. by Kobayashi and coworkers and has shown antimicrobial activity.<sup>83</sup> Most recently, also from the same sponge, three new bromopyrrole alkaloids, nagelamides U-W (**2.73-2.75**) were isolated.<sup>84</sup> Nagelamides U (**2.73**) and V (**2.74**) possess a  $\beta$ -pyrrolidone ring with an *N*-ethanesulfonic acid and guanidino moieties, and could arise from the oxidative C-N bond cleavage of **2.71** (Scheme 2.1). Nagelamide W (**2.75**) has two aminoimidazole moieties in the molecule and could be generated by addition of a guanidine to oroidin. Nagelamides U (**2.73**) and W (**2.75**) possess antimicrobial activity against *Candida albicans*.



**Scheme 2.1** Oroidin alkaloids from cyclic ring formation and oxidation within acyclic monomer taurodispacamide A (**2.29**).

### 2.1.5. Dimers

Dimers can be divided into four sub groups: acyclic, monocyclic, bicyclic and tricyclic dimers.

### 2.1.5.1. Acyclic Dimers

Mauritiamine (**2.76**) is an oroidin dimer that has been isolated as a racemate from the marine sponge *Agelas mauritiana* by Fusetani and coworkers.<sup>14</sup> The two monomeric units are connected by a C12-C11' bond (**Figure 2.5**). It is similar to mauritamide A (**2.31**) and differs from the latter by the imidazole being connected to another oroidin unit instead of taurine. Nagelamides A-D, I, J, L, H, R and Z (**2.77-2.82**, **2.84-2.86**, **2.88** and **2.89**) were isolated from the Okinawan marine sponge *Agelas* sp. by Kobayashi and coworkers.<sup>85-89</sup> Nagelamides S (**2.83**) and T (**2.87**) were isolated from the Pacific marine sponges *Agelas cf. mauritiana* by Al-Mourabit and coworkers.<sup>90</sup> Nagelamide H (**2.77**) differs from mauritiamine, by having a 5-aurine-2-aminoimidazole instead of the 2-aminoimidazolone. Nagelamides A-D, I, J, L, R, T, S and Z (**2.78-2.89**) possess a C12 to C10' bond connecting the two linear monomeric units (**Figure 2.5**). Nagelamide Z (**2.85**) is the first dimeric bromopyrrole alkaloid involving the C8 position in dimerisation and has shown showed potent inhibitory activity against *Candida albicans*.<sup>89</sup>

Nagelamide R (**2.86**) is the first oroidin alkaloid containing an oxazoline ring.<sup>85</sup> Nagelamide T (**2.87**) is another example of an oroidin alkaloid with an oxazoline ring formed by the intramolecular cyclisation of the amide oxygen to the unalkylated 2-aminoimidazole C12.<sup>90</sup> Nagelamide L (**2.88**) is a new dimeric bromopyrrole alkaloid containing an ester linkage.<sup>86</sup> It is likely to be formed by the cleavage of the oxazoline ring at the imine bond in nagelamide R (**2.86**). Lindel and coworkers have reported that treatment of oroidin with DMSO/TFA yielded a compound containing an ester linkage.<sup>91</sup> However, when nagelamide C (**2.81**) was subjected to the same condition, **2.88** was not observed.<sup>86</sup> Nagelamide J (**2.89**) is the



first oroidin alkaloid possessing a cyclopentane ring fused to a 2-aminoimidazole ring formed by a C12-C8 intramolecular bond connection.<sup>87</sup>

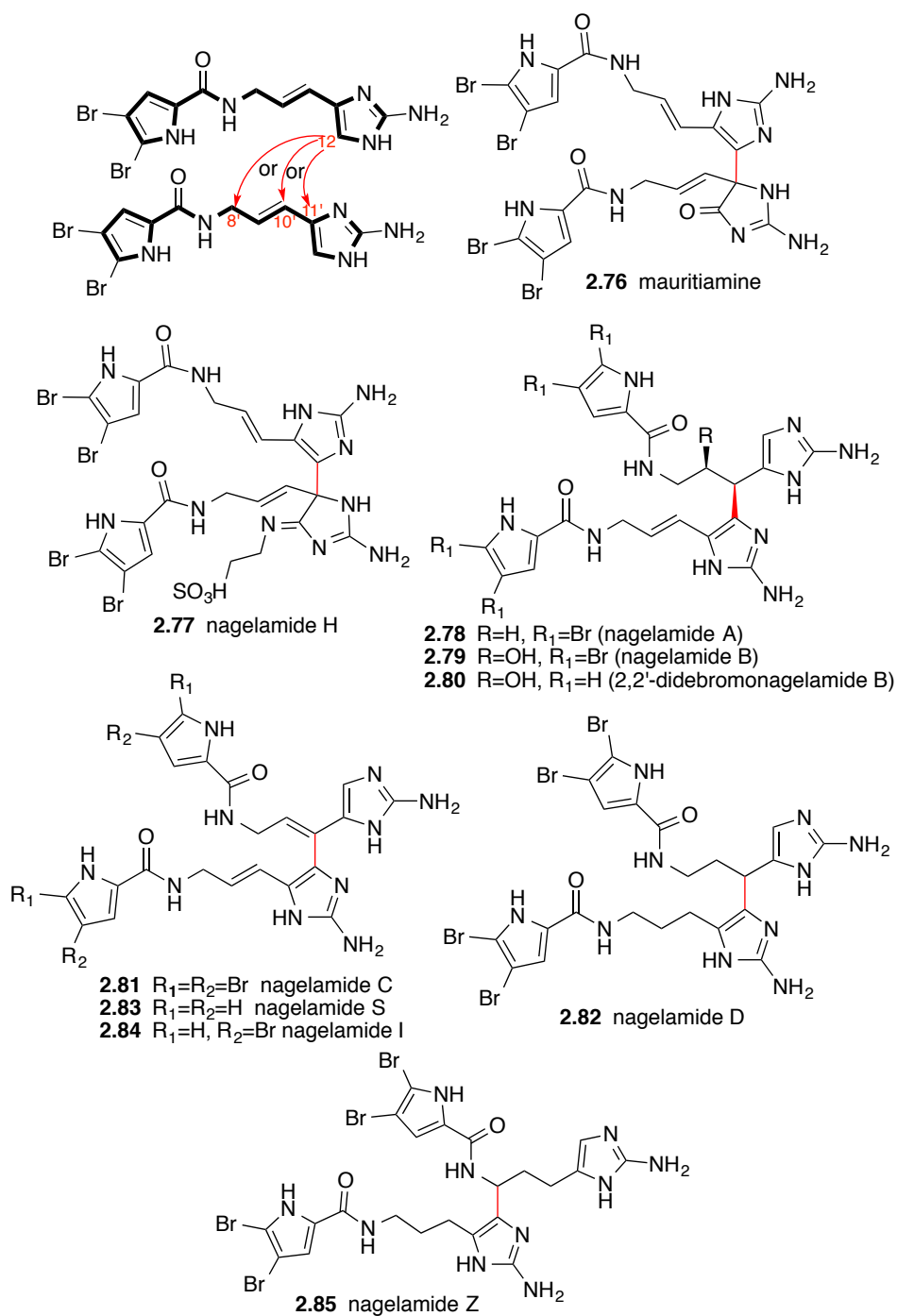


**Figure 2.5** Acyclic dimers

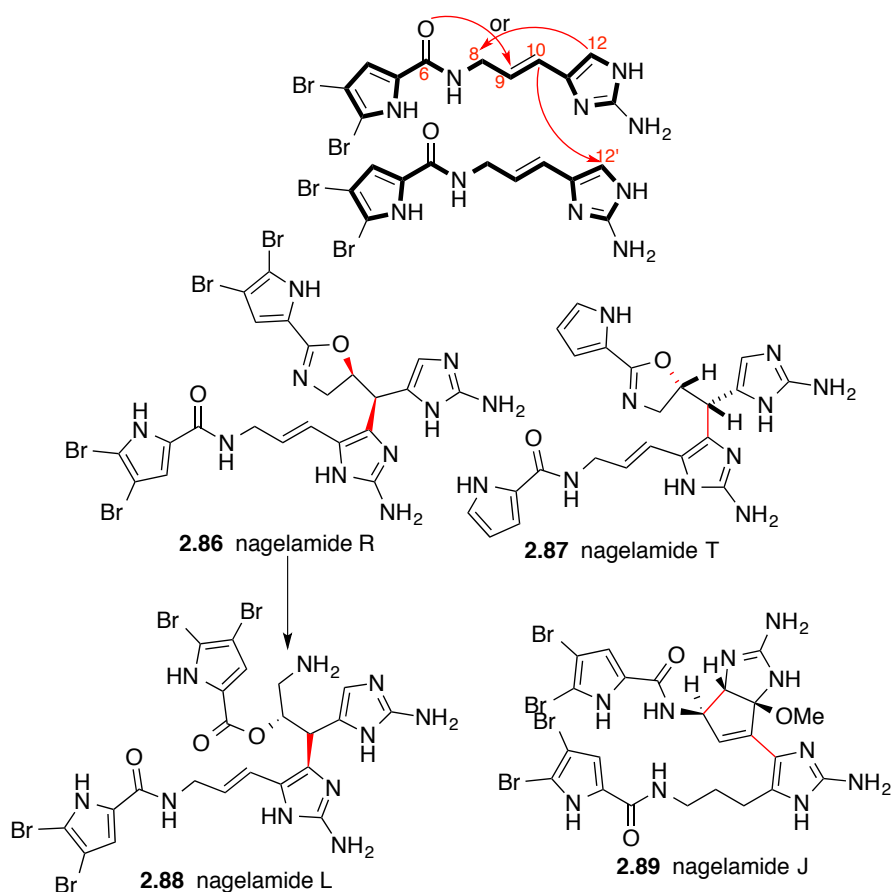


**Figure 2.5 cont'd** Acyclic dimers

The stylissazoles A-C (**2.90-2.92**) provide one of the first examples of dimerisation involving exclusively C-N bond formations between the 2-aminoimidazolone ring of *Z*-debromohymenialdisine **2.48** and hymenidin **2.4** (**Figure 2.6**).<sup>92</sup> They were isolated by Al-Mourabit and coworkers from *Stylissa carteri* collected in the Solomon Islands.<sup>92</sup> Stylissazoles A (**2.90**) and B (**2.91**) are acyclic dimers where the two oroidin alkaloids are linked via a N13'-C12 and a N13'-C9 bond respectively. Stylissazole C (**2.92**) is an example of a monocyclic dimer discussed in the next section, where C9-N13' and C10-N16' bond formations lead to the formation of a bicyclic ring between the two oroidin monomers.

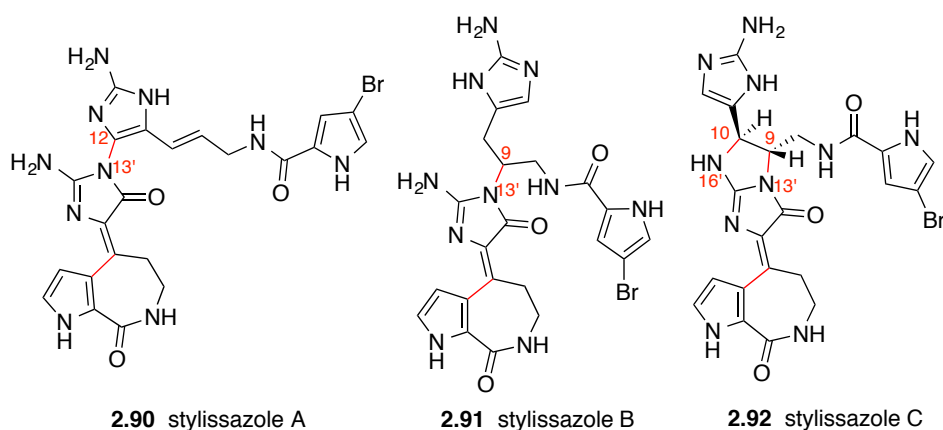


**Figure 2.6** Acyclic dimers and a bicyclic dimer formed via dimerisation of Z-debromohymenialdisine **2.48** and hymenidin **2.4**.

### 2.1.5.2. Monocyclic Dimers

The first of the monocyclic dimers to be isolated was sceptrin (**2.93**) from the sponge *Agelas sceptrum* by Faulkner and coworkers.<sup>93</sup> The sceptrins **2.93-2.97** can be thought of as [2+2] cycloaddition products of hymenidin (**2.4**) with a C9 to C9' and C10 to C10' bond connections (**Figure 2.7**). Several attempts of solid-state and solution photodimerisation reactions of oroidin (**2.1**) by Faulkner and coworkers, failed to synthesis any of the sceptrins.<sup>93</sup> The biosynthesis of the sceptrins is unlikely to be a chemical photodimerisation of oroidin or clathrocin as there is insufficient light at the depth where *Agelas sceptrum* is found and the sceptrins are optically active indicating the role of an enzyme in their syntheses. Sceptrin, in addition to its antibacterial, antiviral<sup>20</sup>, antimuscarinic<sup>23</sup>, and antihistaminic<sup>43</sup> properties, is also a somatostatin inhibitor in the sub- $\mu$ M range.<sup>94</sup> Debromosceptrin (**2.94**) and dibromosceptrin (**2.95**) were isolated from sponge *Agelas conifera* by Keifer *et al.*<sup>20</sup> whereas didebromosceptrin (**2.96**) was isolated from the same sponge by Shen *et al.*<sup>95</sup> Bromosceptrin (**4.97**) was isolated from the sponge *Agelas conifer* by Köck and coworkers.<sup>78</sup> Oxysceptrin (**2.98**) differs from sceptrin by having an oxidised 2-aminoimidazole. It displays antibacterial and antiviral activity and was isolated from

the *Agelas nemoechinata* and *Agelas conifer* by Kobayashi<sup>22</sup> and Rinehart<sup>20</sup>.

Nakamuric acid (**2.99**) and its corresponding methyl ester **2.100**, both with antibacterial activity, were isolated from the sponge *Agelas nakamurai* by Eder *et al.*<sup>59</sup>

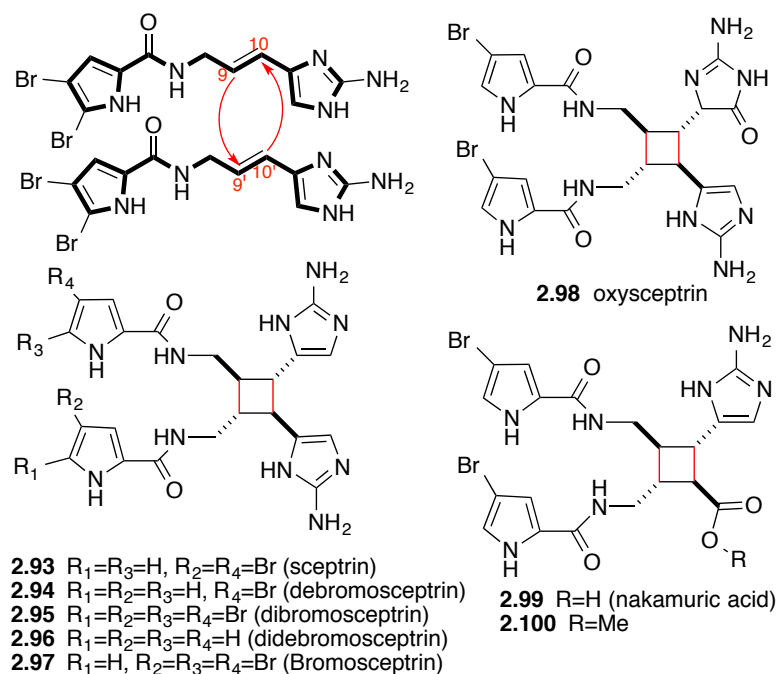


**Figure 2.7** Monocyclic dimers with a cyclobutane ring.

The agelifेरins **2.101-2.103** can be considered as Diels-Alder [4+2] cycloaddition products of the monomeric unit with a C9 to C9' and C10 to the C12' bond connections (**Figure 2.7**).<sup>96</sup> Ageliferin (**2.101**), an antiviral compound possessing unsymmetrical dimeric structure of hymenidin (**2.4**) along with monobromo **2.101** and dibromo **2.103** analogues, as isolated from *Agelas coniferin*<sup>97</sup> and *Agelas mauritiana*.<sup>96</sup>

The nagelamides (**Figure 2.7** and **2.8**) were isolated from Okinawan marine sponges *Agelas* spp. by Kobayashi and coworkers.<sup>35,85-87</sup> Nagelamide E-G (**2.104-2.106**) differ from the agelifेरins in the stereochemistry at C10. Nagelamide K (**2.107**) is a bromopyrrole alkaloid possessing a rare piperidinoiminoimidazolone ring with an aminoimidazole ring and a taurine unit.<sup>86</sup> It is likely to be formed from

oroidin (**2.1**) and taurodispacamide A (**2.29**) by a C9 to C9' bond connection and an imidazole N15' to C10 instead of the C12' to C10 bond connection as observed in ageliferin (**2.101**).

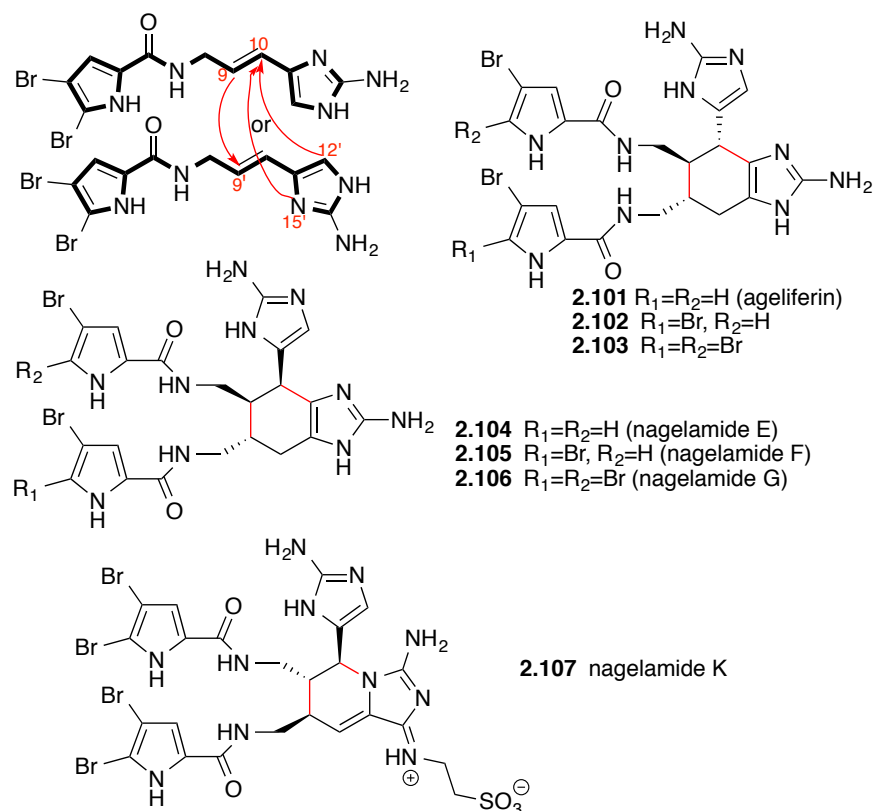


**Figure 2.7** Monocyclic dimers with a cyclohexane ring.

Like in nagelamide K (**2.107**), nagelamide Q, X and Y must be formed from oroidin (**2.1**) and taurodispacamide A (**2.29**). Nagelamide Q (**2.108**) is a rare dimeric oroidin alkaloid possessing a pyrrolidine ring, formed via a C10'-C9 and amide N7-C9' bond connections (**Figure 2.8**).<sup>85</sup> Nagelamides X (**2.109**) and Y (**2.110**) possess a novel tricyclic skeleton consisting of spiro-bonded tetrahydrobenzaminoimidazole and aminoimidazolidine moieties, formed via a C9-C11' and C12-C10' bond connections (**Figure 2.8**).<sup>89</sup> Donnazoles A (**2.111**) and B (**2.112**) were isolated from the sponge *Axinella donnani* collected from the island of Mauritius by Ali-Mourabit and coworkers.<sup>98</sup> Both natural products contain a cyclopentane ring, formed via a C9-

C9' and C10'-C11 bond (**Figure 2.8**), possible intermediates in the formation of some of the more complex bi- and tri-cyclic dimers (**Sections 2.1.5.3. and 2.1.5.4.**).

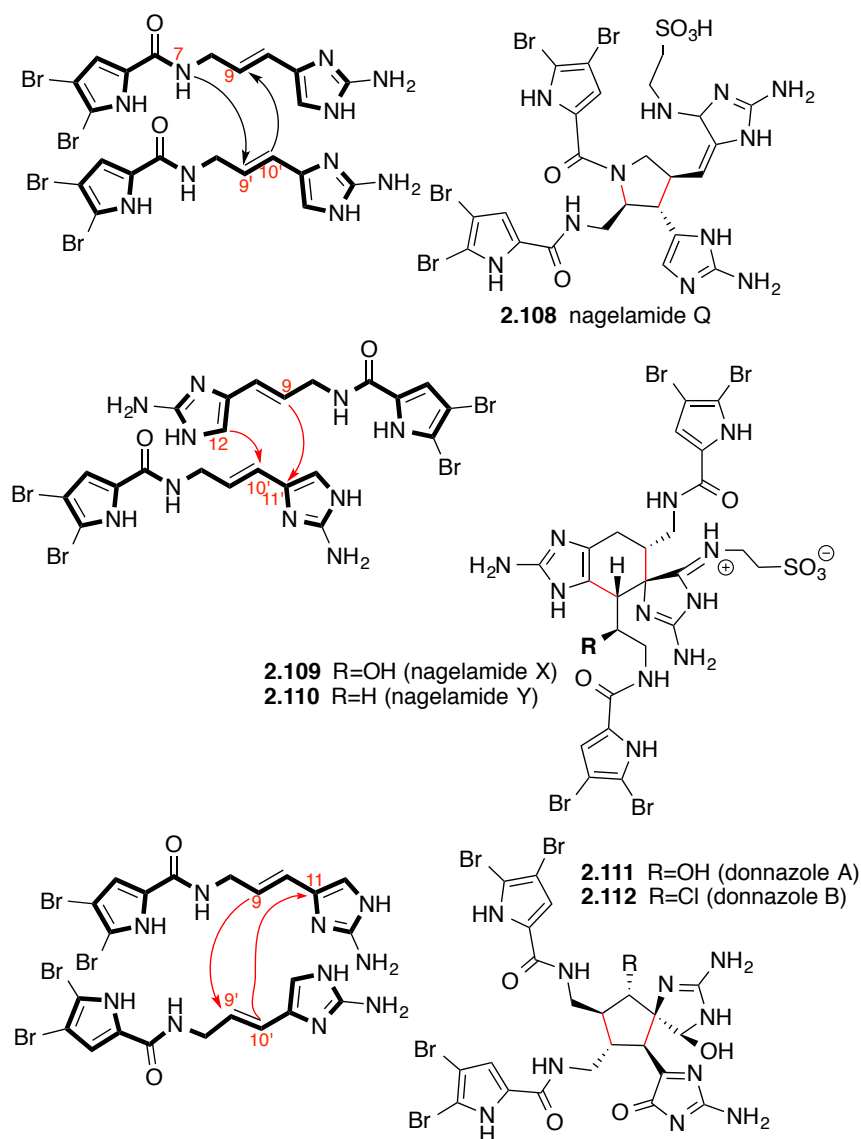


**Figure 2.8** Other monocyclic dimers.

### 2.1.5.3. Bicyclic Dimers

The bicyclic dimers include the axinellamines and the massadines.

Axinellamines A-D (**2.113-2.116**), isolated from an Australian marine sponge *Axinella* sp. by Urban *et al.*, have unique perhydrocyclopenta-imidazolazolo-imidazole carbon skeleton formed by three bond connections between two monomeric

units.<sup>99</sup> These include two C-C bonds: C9-C9' and C11-C10' and one C-N bond: C12'-N15 (**Figure 2.9**). Axinellamine B-D had shown low antibacterial activity against *Helicobacter pylori* at 1000  $\mu\text{M}$ .<sup>99</sup>

The massadines **2.117-2.121** have two monomeric units connected via two C-C bonds: C10-C11', C9-C9' and an ether linkage between the unalkylated C12(s) of the 2-aminoimidazoles (**Figure 2.9**).<sup>61,100,101</sup> Massadine (**2.117**) was first isolated from the marine sponge *Stylissa cf massa* as a geranylgeranyltransferase type I inhibitor by Fusetani *et al.*<sup>100</sup> Massadine chloride (**2.118**), a possible biosynthetic precursor for **2.117**, was isolated from the sponge *Stylissa caribica* by Köck and coworkers. Compounds **2.119-2.121** were isolated from a deep-water Great Australian Bight sponge *Axinella* sp. by Capon and coworkers.<sup>61</sup> **2.120** and **2.121** are likely to be artefacts of extraction (MeOH).

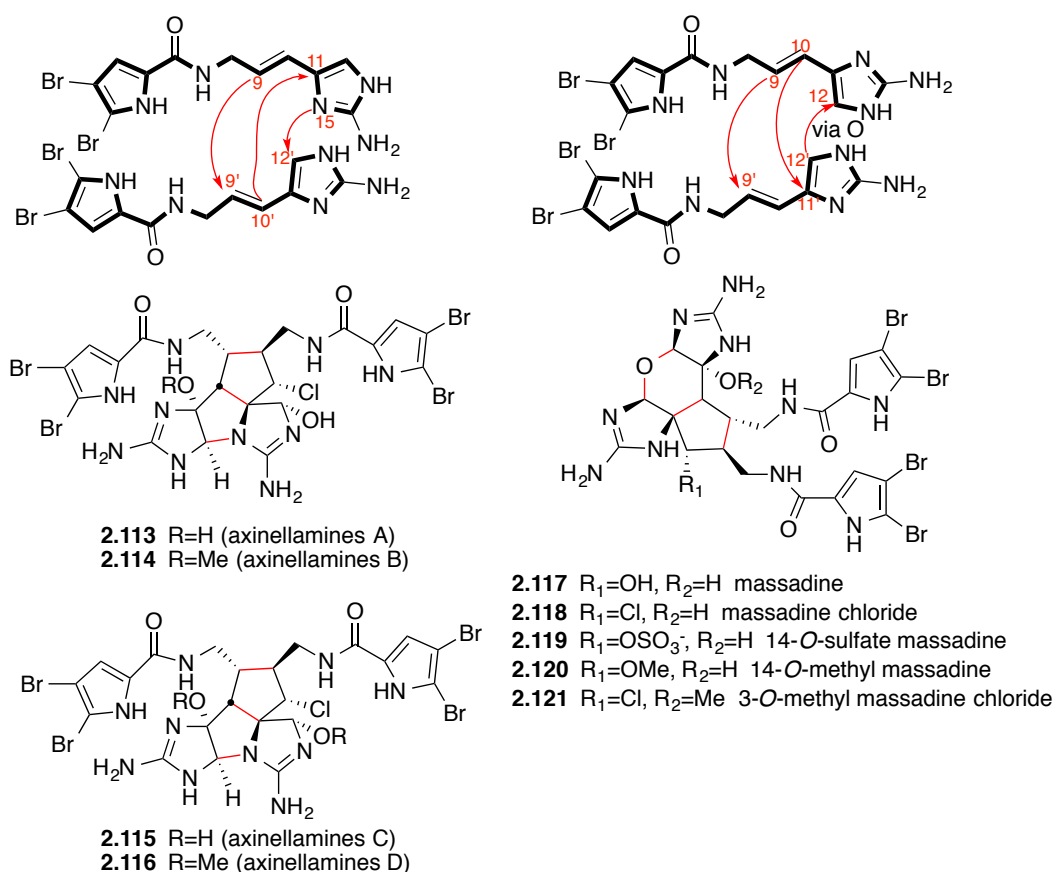


**Figure 2.9** Bicyclic dimers.

Recent isolation of oroidin alkaloids has revealed novel architecture in the benzosceptrin family **2.122-2.124** (Figure 2.10).<sup>82,90</sup> Benzosceptrins A-C (**2.122-2.124**) are sceptrins that have undergone further intramolecular cyclisation and dehydrogenation to form a highly strained benzocyclobutane ring through a C12-C12' bond connection. Benzosceptrin A (**2.122**) was isolated from the sponge *Agelas cf. mauritiana* from the Solomon Islands while benzosceptrins B (**2.123**) and C (**2.124**) were both isolated from *Phakellia* sp. from New Caledonia by Al-Mourabit and coworkers.<sup>82,90</sup>

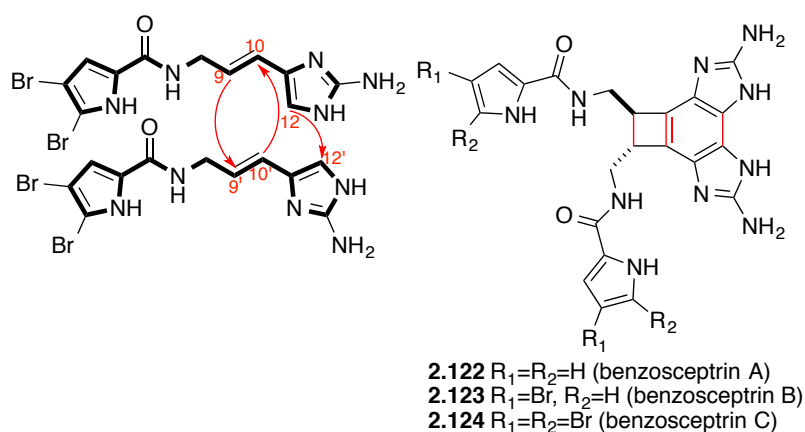


**Figure 2.10** The benzosceptrins.

#### 2.1.5.4. Tricyclic Dimers

Palau'amine (**2.125**) is probably the most important member of this family of alkaloids.<sup>102</sup> It is a bisguanidine alkaloid constructed from six contiguous rings with an unbroken chain of eight chiral centres and has thus also been an important synthetic target that was finally achieved in 2010 after a 20 year effort by Baran.<sup>103,104</sup> It has been isolated from the marine sponge *Stylotella agminata* by Scheuer *et al.*<sup>21</sup> and later on from the sponge *Stylotella aurantinum*<sup>7</sup> collected from Yap. Palau'amine (**2.125**) is reasonably non-toxic, exhibits cytotoxic, antibiotic, antifungal activities and shows particularly striking immunomodulatory activity.<sup>102</sup> Monobromo



**2.126** and dibromo **2.127** palau'amine derivatives were isolated from the marine sponge *Stylotella aurantium* by Scheuer and coworkers.<sup>7</sup> These bromo derivatives are less active than **2.125**. The structure of palau'amine (**2.125**) was revised from **2.125a** (with the opposite stereochemistry at C-12 and C-17) based on detailed NMR analysis by the Köck and Quinn groups simultaneously.<sup>102,105</sup> There are five different modes of inter- as well as intra-molecular cyclisations observed in the tricyclic dimers. These include the C9-C9', C10-C11', N7-C11 and N1-C12 or N4-C12 bond formations which are also accompanied by the incorporation of chlorine and oxygen (**Figure 2.11**). Konbu'acidin A (**2.128**) and B (**2.129**) with an amide dibromopyrrole instead of a free amine, were both first isolated by Kobayashi and coworkers from an Okinawan marine sponge *Hymeniacidon* sp.<sup>48</sup> Compound **2.128** has shown promising inhibitory activity against cyclin dependent kinase 4 (cdk4).<sup>106</sup>

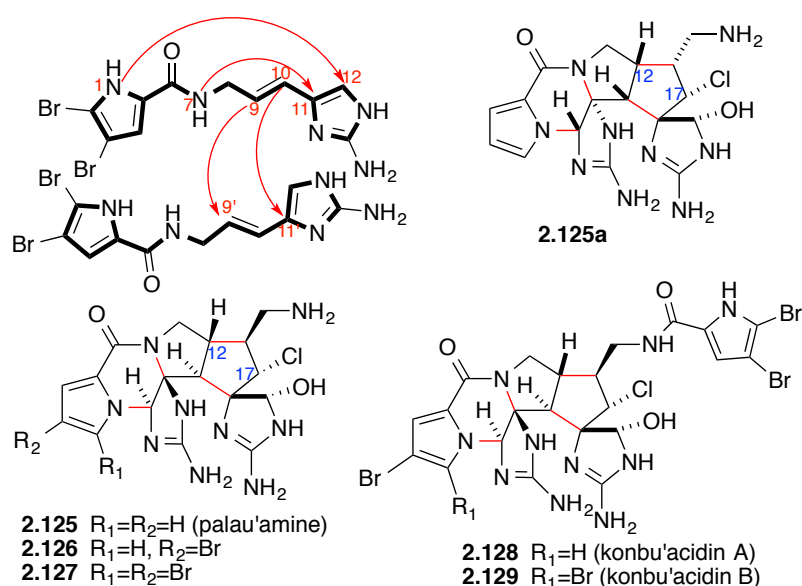


**Figure 2.11** Tricyclic dimers.

The styloguanidines **2.130-2.132** are pyrrole ring regio isomers of palau'amines **2.125-2.127** where the cyclisation is between N1 instead of C4 to the C12 (**Figure 2.12**).<sup>107</sup> They were initially isolated from a sponge *Stylotella*

*aurantinium* collected from Yap by Endo and coworkers<sup>107</sup>, later on by Scheuer *et al.*<sup>7</sup> from the sponge *Stylotella aurantium*. More recently Köck and coworkers reported the isolation of tetrabromostyloguanidine (**1.133**) from *Stylissa caribica*.<sup>102</sup> It is the regio isomers of konbu'acidin B (**2.129**).

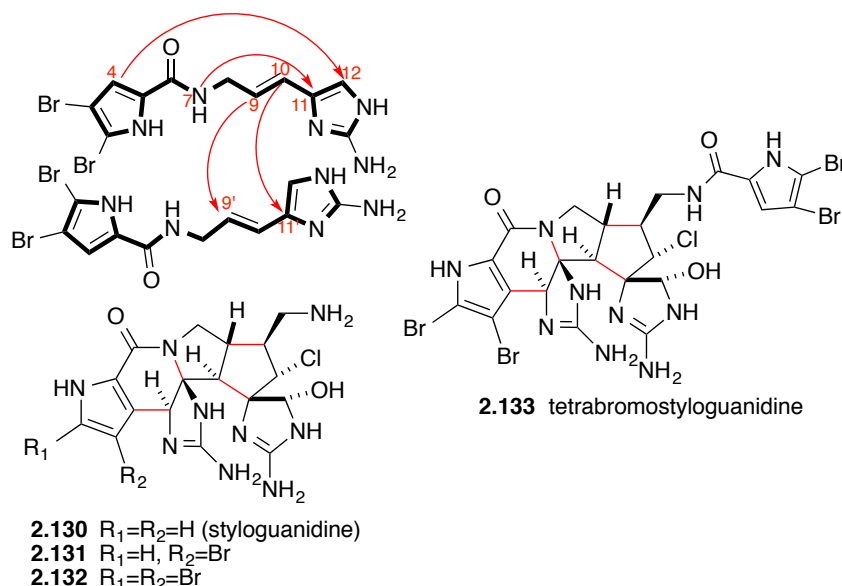
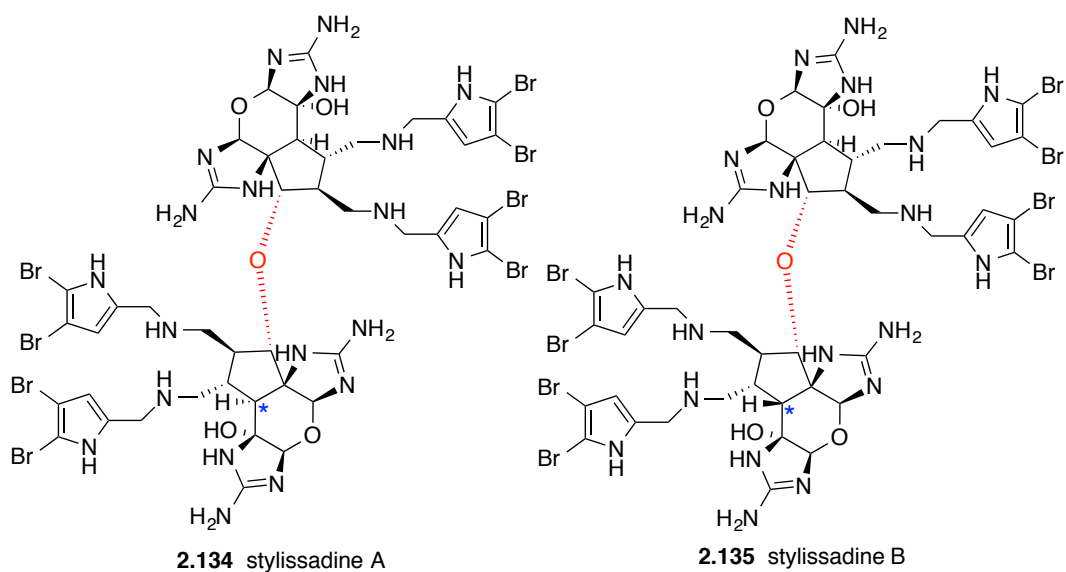


**Figure 2.12** Tricyclic dimers with N1 instead of C4 nucleophilicity for bond formation.

### 2.1.6. Tetramers

To date there has been only two tetramers reported so far. Stylissadine A (**2.134**) and B (**2.135**) were first reported to be isolated from the Caribbean sponge *Stylissa caribica* by Köck and coworkers.<sup>108</sup> Soon after, Quinn and coworkers reported the bioassay guided isolation of the same tetramers from the Australian marine sponge *Stylissa flabellate*.<sup>109</sup> They are the most potent natural P2X<sub>7</sub> antagonists to be isolated to date and provide a novel class of P2X<sub>7</sub> receptor inhibitors.<sup>109</sup> Stylissadine A (**2.134**) and B (**2.135**) are diastereomers and are formally dimers of massadine **2.117** connected via an ether bond.<sup>108,109</sup> While an ether connection is not common in the oroidin alkaloids it does occur in the slagenins **2.40-2.42** and in massadine (**2.117**) itself.



### 2.1.7. Summary of the Oroidin Alkaloids

A summary of some of the structural relationship that was found to exist within the oroidin alkaloids is given in **Figure 2.13**.

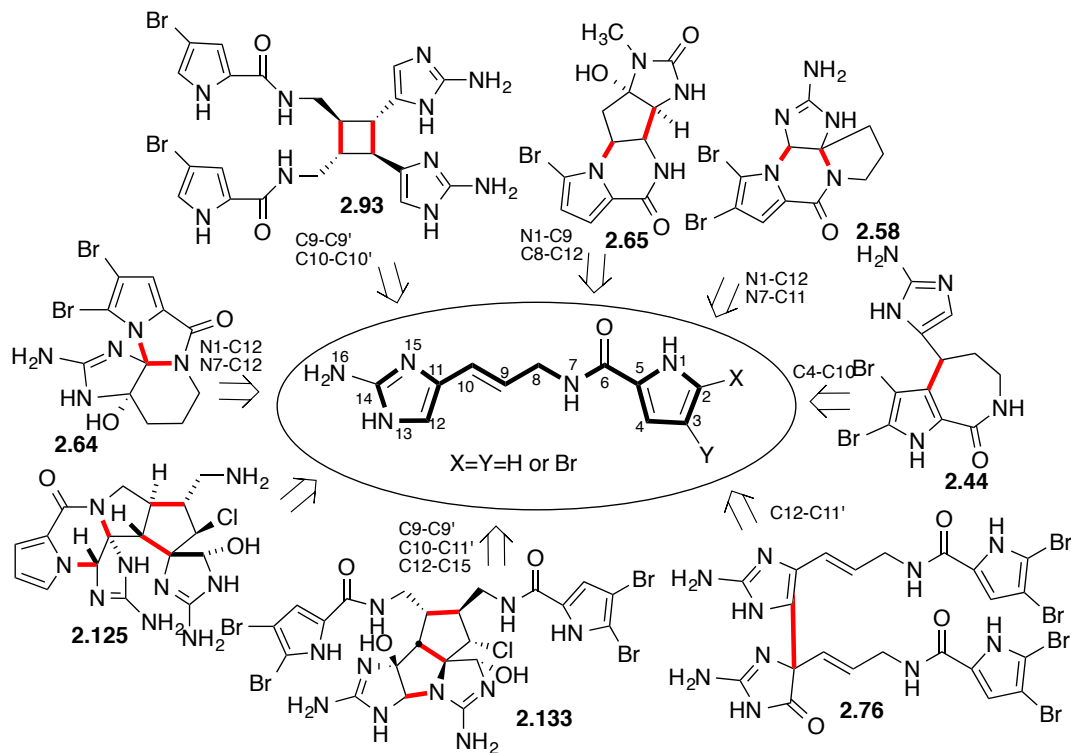
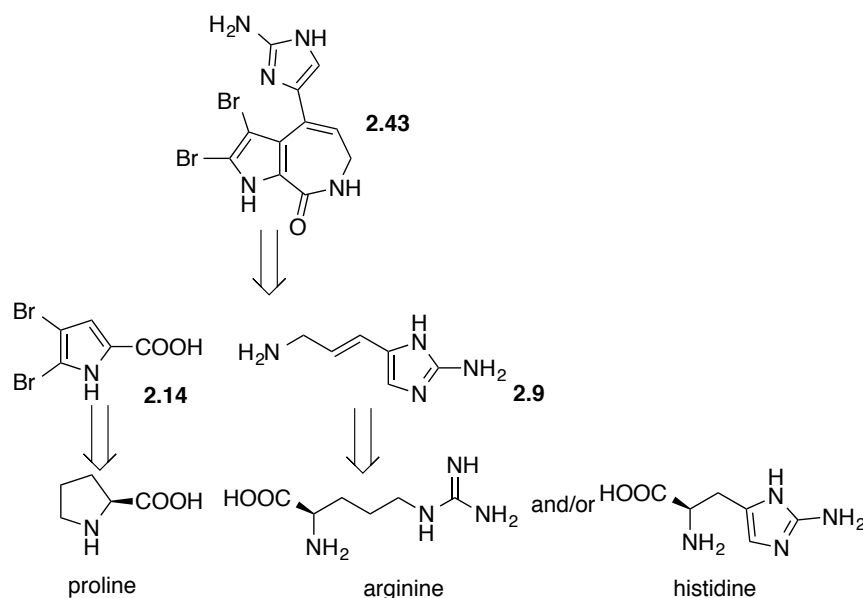


**Figure 2.13** Summary that include some of the bond connections observed in the oroidin alkaloids.

In order to investigate the biosynthetic origin of the oroidin alkaloids, a number of labelling studies have been conducted.

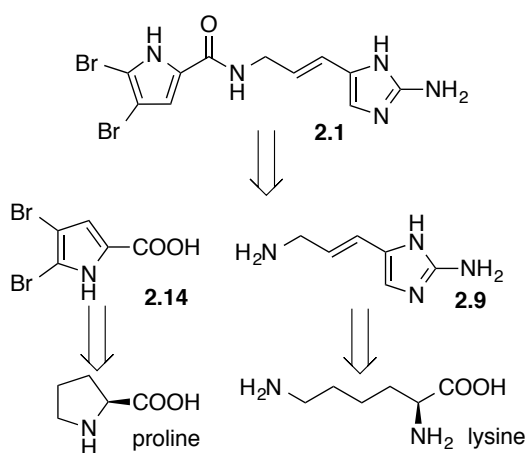
## 2.2. Biosynthetic Studies

In 1999, Kerr and co-workers reported the first biosynthetic study of the oroidin alkaloids.<sup>3</sup> They investigated stevensine (**2.43**), which was postulated to be a cyclised analogue of oroidin, itself thought to arise from the condensation product of 3-amino-1-(2-aminoimidazolyl)-prop-1-ene (**2.9**) and 4,5-dibromopyrrole carboxylic acid (**2.14**), both known natural products (**Scheme 2.2**). The study involved the incorporation of <sup>14</sup>C-labelled amino acids into *Teichaxinella morchella* cell culture and the subsequent extraction and isolation of stevensine (**2.43**) that was then analysed for radioactivity. Both histidine and arginine were found to be incorporated into **2.43** and proline, into the pyrrole carboxylic acid part of stevensine.<sup>3</sup>



**Scheme 2.2** First biosynthetic study of stevensine.

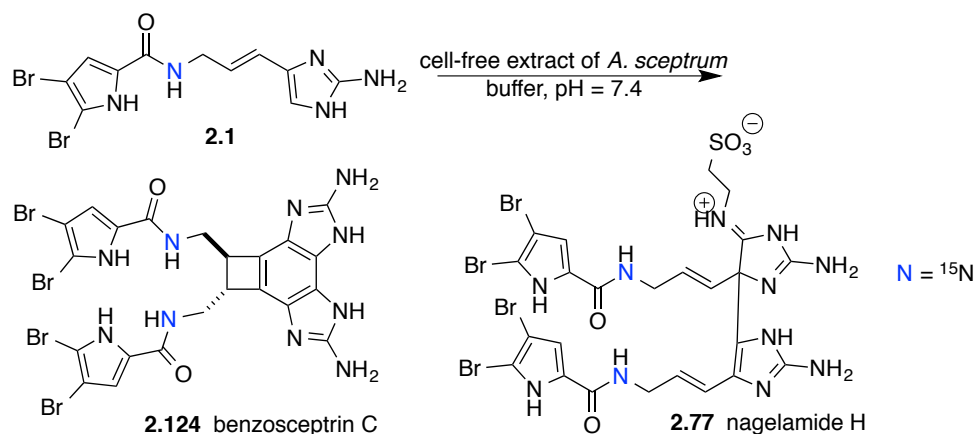
While proline is well accepted to be the precursor of the pyrrole moiety of oroidin, uncertainty still surrounded the 2-aminoimidazole part of the oroidin alkaloids. More than a decade later, Genta-Jouve and co-workers revisited the biosynthesis of oroidin by developing an improved feeding experiment on a sponge cell culture of *Axinella damicornis*.<sup>6</sup> The experiment involved the use of a more sensitive detection technique. Unlike in the experiment of Kerr and co-workers, incorporation of radioactivity from arginine and ornithine were low and no incorporation of histidine was detected at all. However, the incorporation of lysine was quite efficient and unexpected. These new findings bring evidence to a biosynthetic pathway, whereby proline can be generated from arginine or ornithine as part of the urea cycle, and following similar steps well known in the urea cycle for the guanidinylation of ornithine, lysine is converted to homoarginine and eventually to the 2-aminoimidazole part of the oroidin (**Scheme 2.3**).<sup>6</sup>



**Scheme 2.3** Revisited biosynthetic study of oroidin using a more sensitive radiolabelling technique.

While the above biosynthetic studies substantiate the origin of oroidin and monomeric unit of oroidin, such as **2.44**, they do not provide any concrete evidence for the biosynthesis of more complex oroidin alkaloids. Recently, Stout and co-workers reported the de novo synthesis of <sup>15</sup>N-labelled benzosceptrin C (**2.124**) and

nagelamide H (**2.77**) from 7-<sup>15</sup>N-oroidin (**Scheme 2.4**) using a cell-free enzyme preparations of *Agelas sceptrum* and *Stylissa caribica*, thus proving unequivocally that oroidin can be converted to **2.124** and **2.77**.<sup>110</sup> Biosynthetic pathways based on single-electron transfer by oxido-reductases were proposed as an explanation for this de novo synthesis.



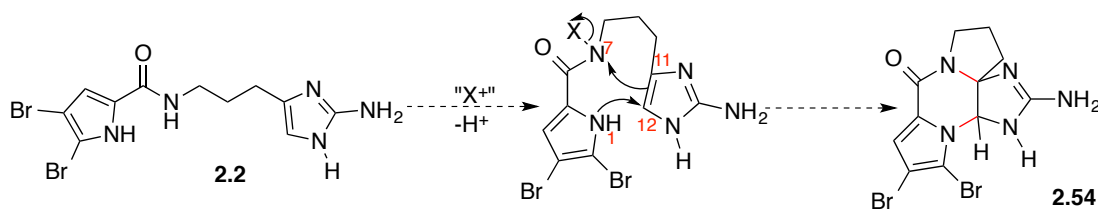
**Scheme 2.4** de novo synthesis of <sup>15</sup>N-labelled benzosceptrin C (**2.122**) and nagelamide H (**2.77**) from 7-<sup>15</sup>N-oroidin using cell-free enzyme preparations of *Agelas sceptrum* and *Stylissa caribica*.

### 2.3. Biogenesis of the Oroidin Alkaloids

The oroidin alkaloids have been postulated to arise from a linear intermediate, long before the de novo synthesis of benzosceptrin C (**2.124**) and nagelamide H (**2.77**) from oroidin was shown. Though it is easy to visualise their structural similarities (**Figure 2.13**), a logical chemical pathway is necessary to support a common biogenesis.

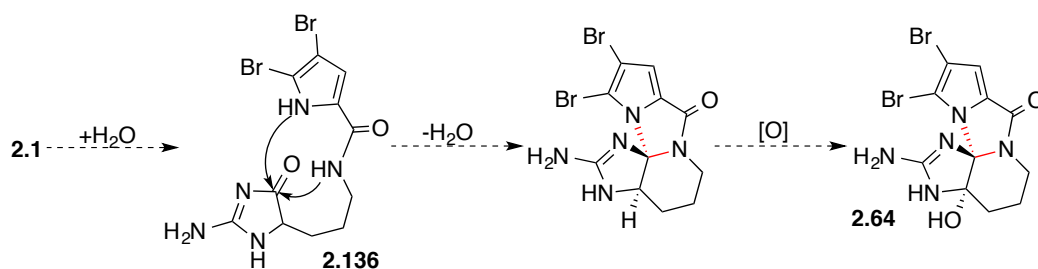
A biogenetic hypothesis that can explain the generation of the oroidin alkaloids from a common precursor or a small set of precursors can also point the way to a biomimetic synthesis.

The first biosynthesis proposal for the conversion of a linear precursor into a tetracyclic product was offered by Sharma and Magdoff-Fairchild, who in 1977 suggested that dibromophakellin was formed from DHO (**2.2**) via initial oxidation of the amide (N7) and then subsequent nucleophilic attack by C11 (**Scheme 2.5**).<sup>12</sup> Subsequently, an electrophilic C12 is trapped by the pyrrole (N1).



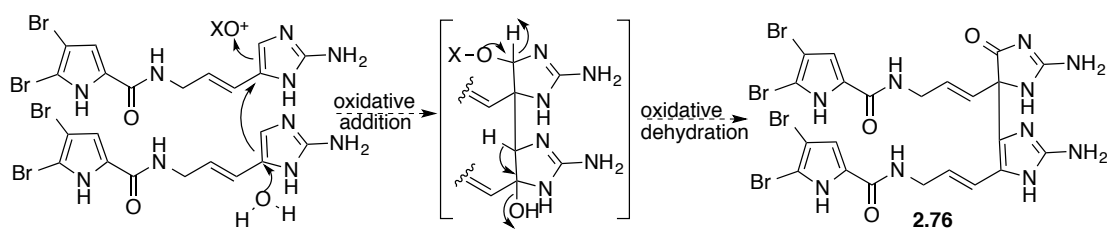
**Scheme 2.5** Biogenesis of dibromophakellin (**2.54**) as proposed by Sharma and Magdoff-Fairchild.

Maximov, who first isolated dibromoagelaspongin (**2.64**), proposed the formation of the latter from the initial dehydration of oroidin (**2.1**) to form dihydrodispacamide A (**2.136**) that upon dehydration with dual C-N bond formation gave **2.64** (**Scheme 2.6**).<sup>5</sup>



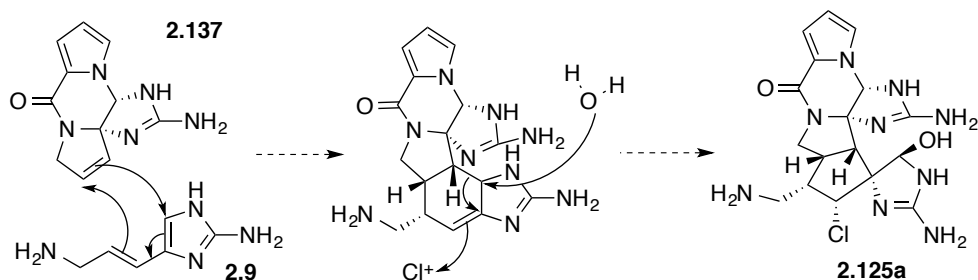
**Scheme 2.6** Biogenesis of dibromoagelaspongin (**2.64**) as proposed by Maximov.

Fusetani proposed a biogenetic pathway for the formation of mauritiamine (**2.76**) that involves an oxidation-dehydration process leading to the dimerisation of two oroidin molecules being connected by a C12-C11' bond (**Scheme 2.7**).<sup>14</sup>



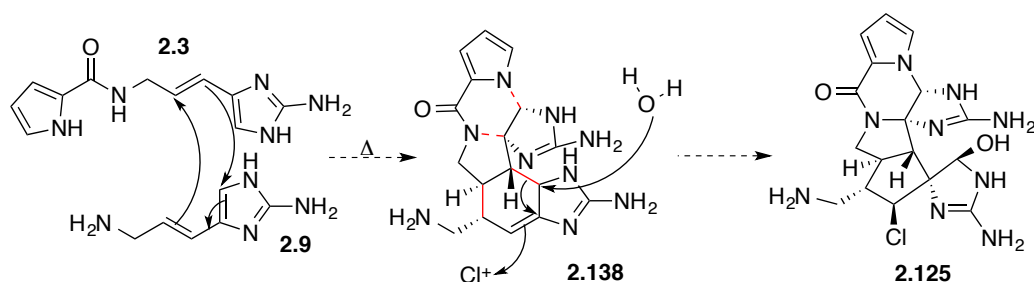
**Scheme 2.7** Biogenesis of mauritiamine (**2.76**) as proposed by Fusetani.

Scheuer and Kinnel proposed a biogenetic pathway for the formation of palau'amine (**Scheme 2.8**) from 11,12-dihydrophakellin (**2.137**) and 3-amino-1-(2-aminoimidazolyl)prop-1-ene (**2.9**), which can undergo a Diels-Alder reaction, followed by a chloroperoxidase-initiated chlorination and subsequent bond migration and reaction with water to form palau'amine (**2.125a**).<sup>7</sup> With the revision of the stereochemistry, the C-11/C-12 *anti* stereochemistry in **2.125** cannot easily be explained by this proposal since the thermal Diels-Alder reaction will result in a *syn* stereochemistry, and the photo Diels-Alder reaction pathway is not likely. With that in mind, Chen and coworkers has revisited the original Kinnel-Scheuer hypothesis and proposed **2.125** to be formed from a [4+2] cycloaddition reaction of **2.9** and clathrodin (**2.3**) that would give rise to **2.138**, and set the C-11/C-12 *anti* stereochemistry (**Scheme 2.9**).<sup>9</sup> An oxidative bicyclization would then provide the modified Kinnel-Scheuer intermediate **2.138**, which following a chlorinative ring contraction would afford **2.125**.



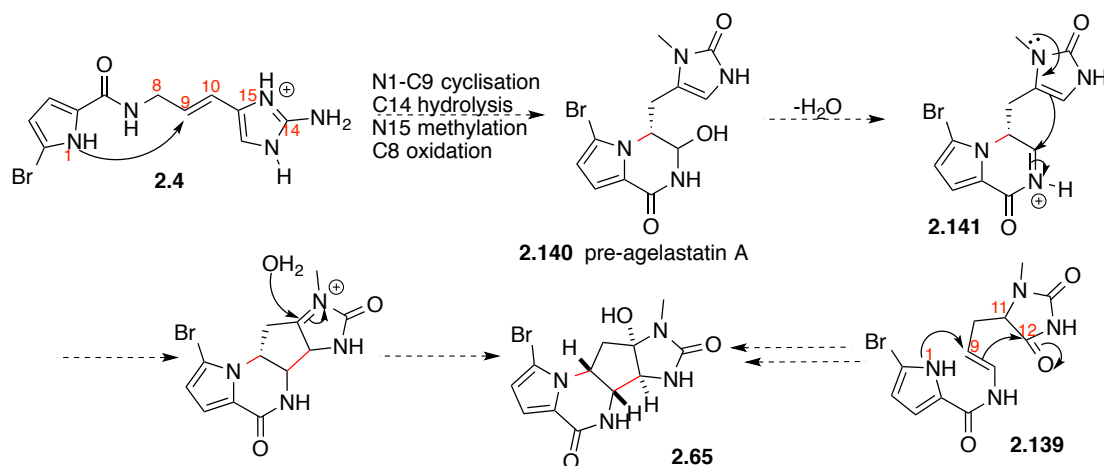
**Scheme 2.8** Biogenesis of palau'amine (**2.125a**) (before a revision in stereochemistry) proposed by Scheuer and Kinnel.<sup>7</sup>





**Scheme 2.9** Revised Scheuer and Kinnel biogenesis of palau'amine (**2.125**) by Chen and coworkers.<sup>9</sup>

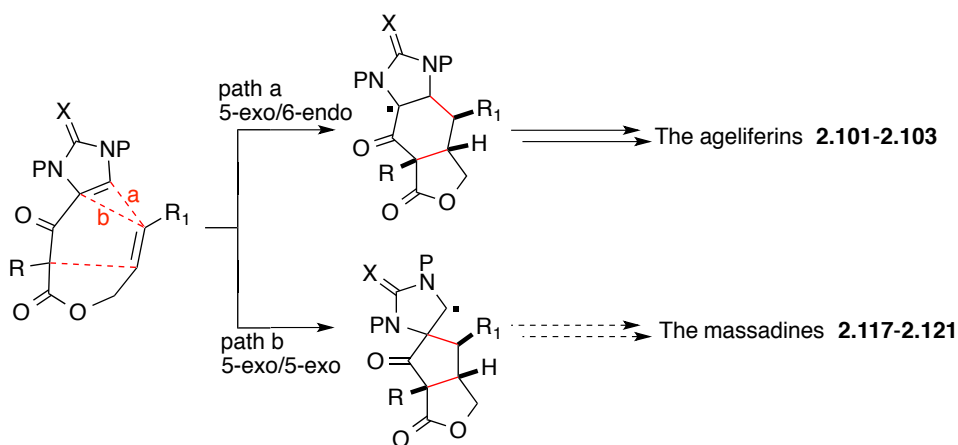
D'Ambrosio *et al.* proposed the biogenesis of agelastatin A (**2.65**) from an enzyme-driven C9 attack at C12 from the hymenidin-like precursor **2.139** and pyrrole N1 attack at the developing positive C9 followed by re-functionalisation at C11 and C12 (**Scheme 2.10**).<sup>4</sup> Movassaghi *et al.* provided a more detailed biogenesis of **2.65** starting from hymenidin (**2.4**) leading to the key intermediate pre-agelastatin A (**2.140**) that could be ionised to an acyliminium ion **2.141** and, following cyclisation and hydroxylation, provide **2.65** (**Scheme 2.10**).<sup>10</sup>



**Scheme 2.10** Proposed biogenesis of agelastatin (**2.65**).

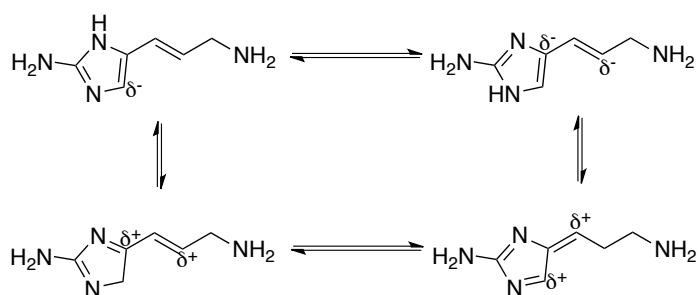
Chen and coworkers have proposed that the dimerisation of a monomeric unit (example clathrocin, **2.3**) proceeds through a radical mechanism, whereby a single-electron transfer (SET) oxidation of **2.3** would give a radical cation that is highly active toward cycloadditions and can lead to the ageliferin skeleton **2.101-2.103** or the

massadines **2.117-2.121** depending on the reaction pathway (**Scheme 2.11**).<sup>15</sup> They have successfully applied this strategy in the asymmetric synthesis of ageliferin (**2.101**).



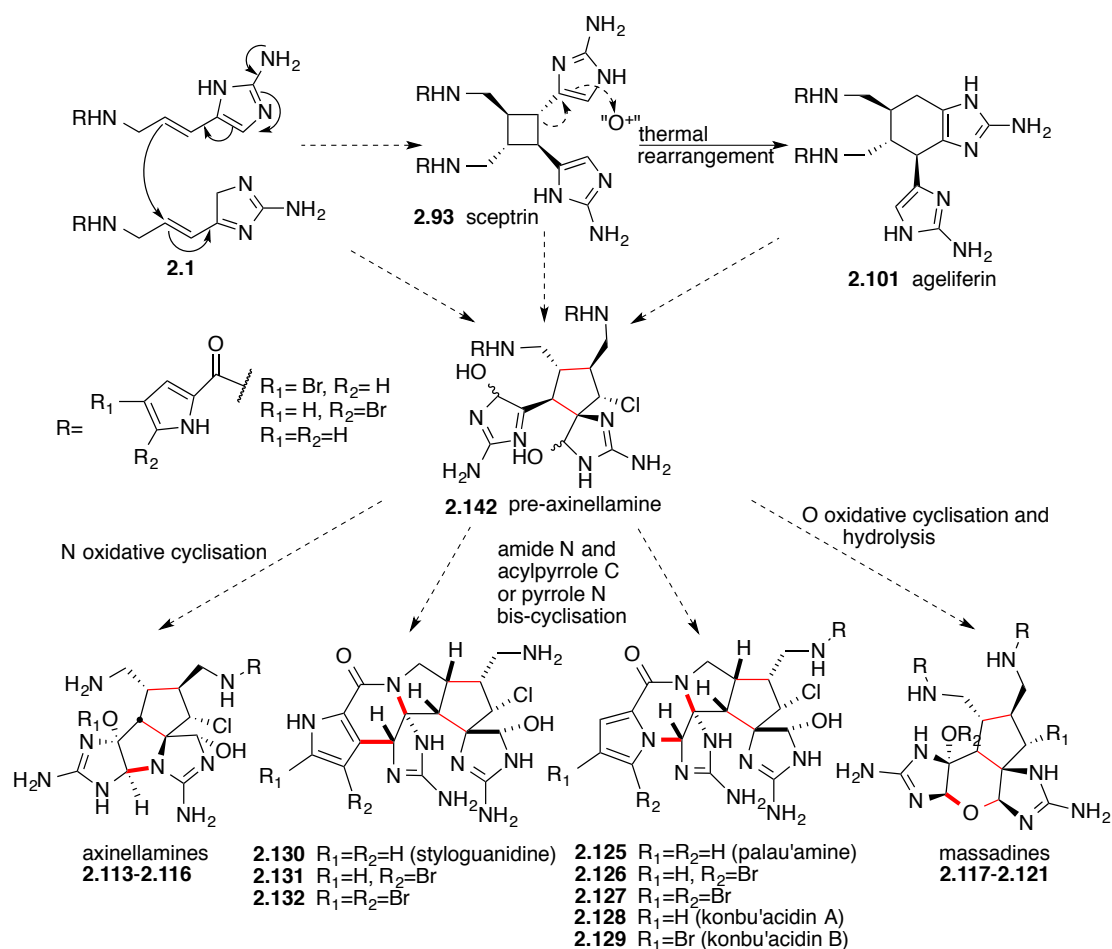
**Scheme 2.11** Biogenic dimerisation proceeding through a radical mechanism leading to the skeleton of ageliferin or massadine depending on the reaction pathway as proposed by Chen and coworkers.<sup>15</sup>

It was Potier and Al-Mourabit who, in a review presented in 2001, proposed biogenetic pathways for the formation of all the oroidin alkaloids from oroidin.<sup>2</sup> The pathways rely on the proposed ambivalent reactivity of 2-amino imidazole and its extended  $\pi$ -system. The four tautomeric forms lead to the proposed nucleophilic or electrophilic reactivity of the amino imidazole (**Scheme 2.12**). Potier and Al-Mourabit suggest that these tautomers can exist simultaneously, giving rise to polycyclic metabolites upon combination with pyrrolic building blocks through diverse modes of cyclisation and/or dimerisation (*vide infra*). However there is no explanation of the insertion of the various functional groups or the generation of chiral centres observed.



**Scheme 2.12** Amphiphilic nature of 2-amino-4(5)-vinylimidazole proposed as leading to the oroidin alkaloids by Poitier and Al-Mourabit.<sup>2</sup>

Baran and Köck have elaborated on Al-Mourabit's postulated biosynthetic intermediates to explain the formation of the more complex oroidin alkaloids. Their biogenetic pathway for axinellamines, styloguanidines, konbu'acidins, palau'amine, massadines and styllissadines starts from key intermediate "pre-axinellamine" (**1.142**) which itself could be formed from sceptrin or ageliferin, originating from the dimerisation of two oroidin molecules (**Scheme 2.13**).<sup>8</sup> They have proposed the biogenesis of nagelamide E (**2.104**) and ageliferin (**2.101**) from sceptrin (**2.93**), and have already demonstrated both conversions via a vinylcyclobutane-cyclohexene rearrangement under microwave condition at 200 °C.<sup>11</sup>



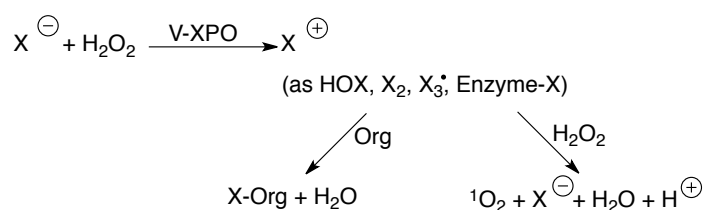
**Scheme 2.13** Summary of Baran and Köck's elaboration on Al-Mourabit's postulated biosynthetic intermediates to explain the formation of the more complex oroidin alkaloids.

While Köck and Baran have elaborated on Potier's hypothesis for the tricyclic dimers, they do not account for all the intramolecular cyclisations proposed on the unactivated imidazole ring and is restricted to the bicyclic and tricyclic dimers.

We believe that the structural diversity and complexity observed in the oroidin alkaloids originate from the action of haloperoxidases. These enzymes are known to play a significant role in the halogenation of natural products.<sup>111</sup>

## 2.4. Marine Haloperoxidases

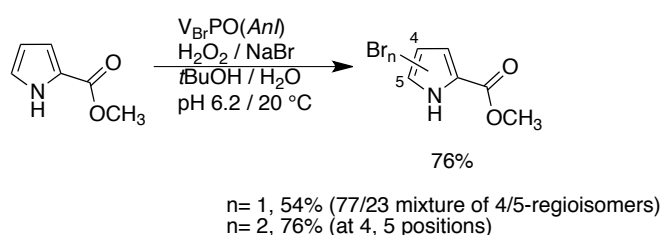
More than 4500 halogenated natural products have been inventoried and further still await discovery. Amongst those, 2300 are organochlorines, 2100 organobromines, 210 organoiodines and 30 organofluorines.<sup>112</sup> Haloperoxidase generate the carbon-halogen bonds in these halogenated organic molecules.<sup>111,113</sup> There are two types of haloperoxidase that have been isolated and identified from marine organisms: (1) vanadium haloperoxidase (V-XPO), a non-heme enzyme, and (2) FeHeme haloperoxidase (FeHeme-XPO).<sup>113</sup> While the active-metal centres differ, the two haloperoxidases function in a similar manner by generating high-valent metal-oxo species with hydrogen peroxide (H<sub>2</sub>O<sub>2</sub>) and catalysing the oxidation of a halide (i.e., Cl<sup>-</sup>, Br<sup>-</sup> or I<sup>-</sup>) to produce hydrohalous acid (HOCl, HOBr, or HOI) as the electrophilic source of halogens (Cl<sup>+</sup>, Br<sup>+</sup>, or I<sup>+</sup>) (**Scheme 2.14**).<sup>113,114</sup> In the presence of electron-rich substrates, electrophilic halogens are delivered regiospecifically and with varying degrees of stereoselectivity.<sup>111</sup>



**Scheme 2.14** Generation of electrophilic halogens by haloperoxidases.

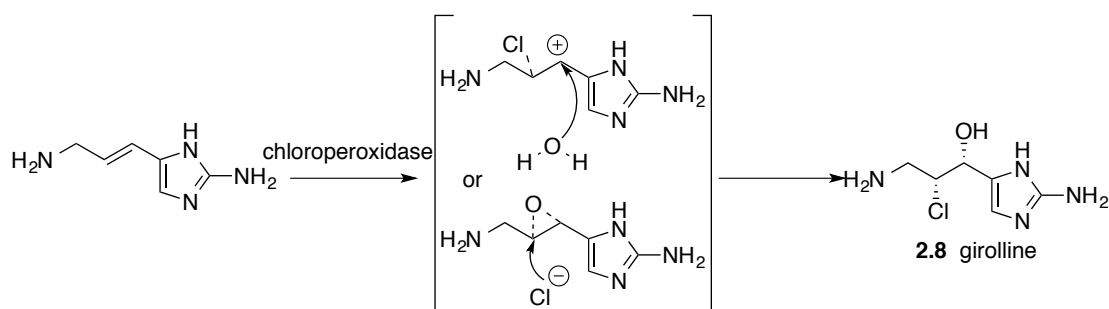
While the enzymes, or the corresponding genes by which sponges generates the oroidin alkaloids are not known, the haloperoxidase-mediated introduction of halogen(s) onto marine alkaloids are easily inferred. As observed in the family of the oroidin alkaloids, the brominated pyrrole-2-carboxylate occurs as a common structural motif and can also exists on their own as secondary metabolites in marine sponges.

Hartung and co-workers have successfully demonstrated the introduction of bromine into the heteroaromatic core of O-methyl-pyrrole-2-carboxylate *via* bromoperoxidase-catalysed oxidations.<sup>115</sup> Oxidations catalysed by vanadium-bound bromoperoxidases from the brown alga *Ascophyllum nodosum* ( $V_{Br}PO(AnI)$ ) afforded bromopyrrole-2-carboxylic acid methyl ester or the dibrominated ester depending on the ratio of the substrate to the bromination reagent used (**Scheme 2.15**).<sup>115</sup>



**Scheme 2.15** Synthesis of the mono and dibrominated o-methyl pyrrole-2-carboxylate, known secondary metabolites from the marine sponge of *Axinella tenuidigitata* and *agelas oroides* respectively. The use of 1.1 equiv. of NaBr and  $\text{H}_2\text{O}_2$ , led to the monobrominated products whilst 2.2 equiv. of NaBr and  $\text{H}_2\text{O}_2$ , led to the dibrominated product.

The organic transformation of haloperoxidase enzymes is not limited only to the halogenation of organic substrate. They have also been implicated in epoxidation reactions that could be of significance in the generation of the oroidin alkaloids. In the presence of both chloride and  $\text{H}_2\text{O}_2$ , chloroperoxidase lead to the formation of hypochlorous acid which is a chlorinating agent. Girolline (**2.8**) is likely to be formed by the action of a chloroperoxidase on 3-amino-1-(2-aminoimidazolyl)-prop-1-ene, an isolated natural product.<sup>7</sup> The formation of the halohydrin can proceed either by the initial formation of the chloronium ion and reaction with water or by the ring opening of an epoxide by a chloride ion (**Scheme 2.16**). In the absence of chloride, a chloroperoxidase has been shown to oxidise styrene stereospecifically to styrene epoxide.<sup>116</sup>



**Scheme 2.16** Biosynthesis of girolline through the action of a chloroperoxidase.

## 2.5. Alkene Double Bond Character in the 2-Aminoimidazole Ring

The carbon double bond of the 2-aminoimidazole ring is not a typical double bond in an aromatic system in that it possesses more alkene bond character. This is because the guanidinium forms a delocalised ion (**Figure 2.14**).<sup>12</sup> This can be seen by comparing the X-ray crystal structure of oroidin<sup>93</sup> to the X-ray structure of histidine<sup>117</sup> (**Figure 2.14**). In the former the C=C bond is 0.07 Å shorter than the same bond in histidine. The alkene character of the imidazole carbon double bond suggests the possibility of it forming an epoxide under the action of haloperoxidases.

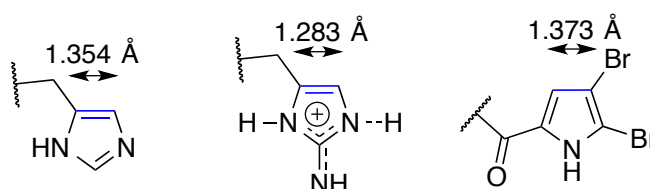
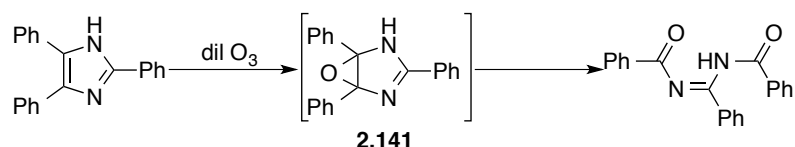


**Figure 2.14** Imidazole carbon double bond character due to the resonance of the guanidinium moiety of the 2-aminoimidazole ring.

Although there are no reports of isolated imidazole epoxides in the literature, there are now numerous accounts of imidazole epoxides as putative intermediates in chemical reactions. Wasserman and co-workers first proposed the formation of an epoxide intermediate **2.141** in the reaction of triphenylimidazole with dilute ozone (**Scheme 2.15**).<sup>118</sup>



**Scheme 2.15** Ozone catalysed epoxidation of imidazole.

Lovely proposed the intermediacy of an epoxide in the oxidation of tetrahydrobenzimidazoles with dimethyldioxirane (DMDO) (**Scheme 2.16**).<sup>119</sup> The 5-imidazolone is formed following ring contraction. This type of reaction has direct analogy to the formation of many oroidin alkaloids such as the axinellamines, palau'amines, styloguanidines and others with spiroimidazoles. Since then, there have been several examples where formation of a given product could only be explained by the formation of an imidazole epoxide.<sup>120</sup> In a biomimetic step in Baran's synthesis of the axinellamines, intramolecular cyclisation was effected by oxidation of the imidazole with DMDO to make the C12-N15' connection required. This would involve the intermediacy of an epoxide (**Scheme 2.17**).<sup>120</sup>

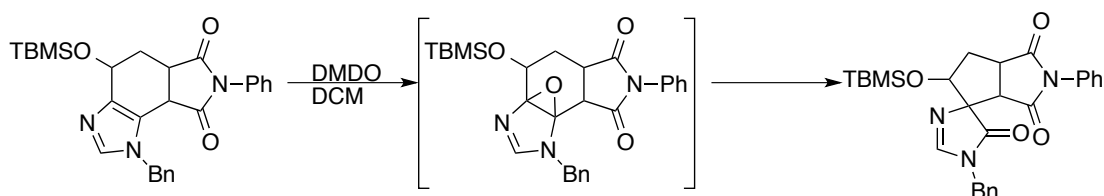
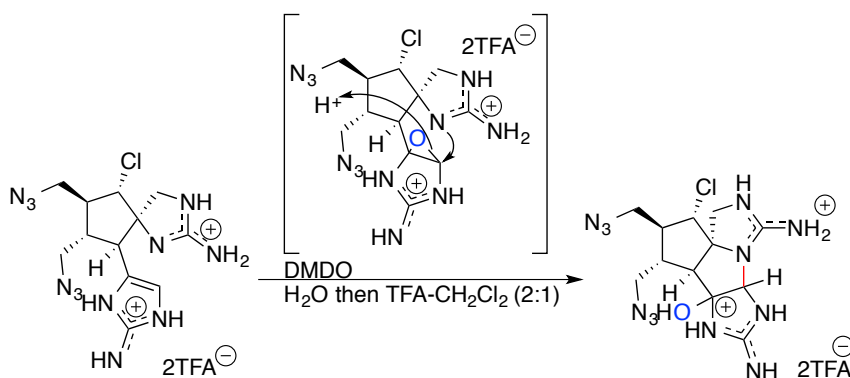


**Figure 2.16** Spirocyclic ring formation from a ring contraction mediated by the oxidation of the imidazole ring.

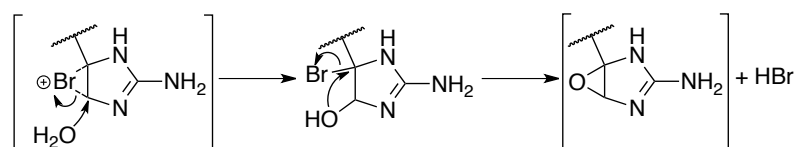


**Scheme 2.17** Intramolecular cyclisation via an imidazole epoxide intermediate leading to a C12-N15' bond connection and introduction of a hydroxyl group.

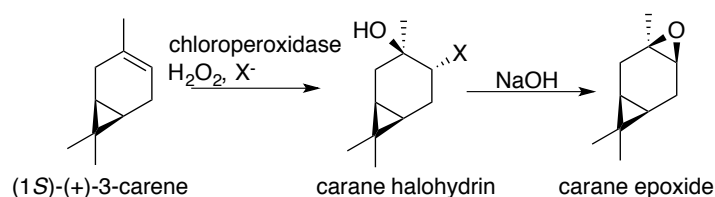


## 2.6. Bromonium to Epoxide

Of significance to the haloperoxidases, is the fact that a halonium ion is analogous to an epoxide. It can be easily converted to an epoxide with water via a halohydrin (**Scheme 2.18**). For example, Kaup *et al.* has reported the halohydrin formation of monoterpene hydrocarbon carene in the presence of chloroperoxidase and its conversion to its epoxide in the presence of sodium hydroxide (**Scheme 2.19**).<sup>121</sup>



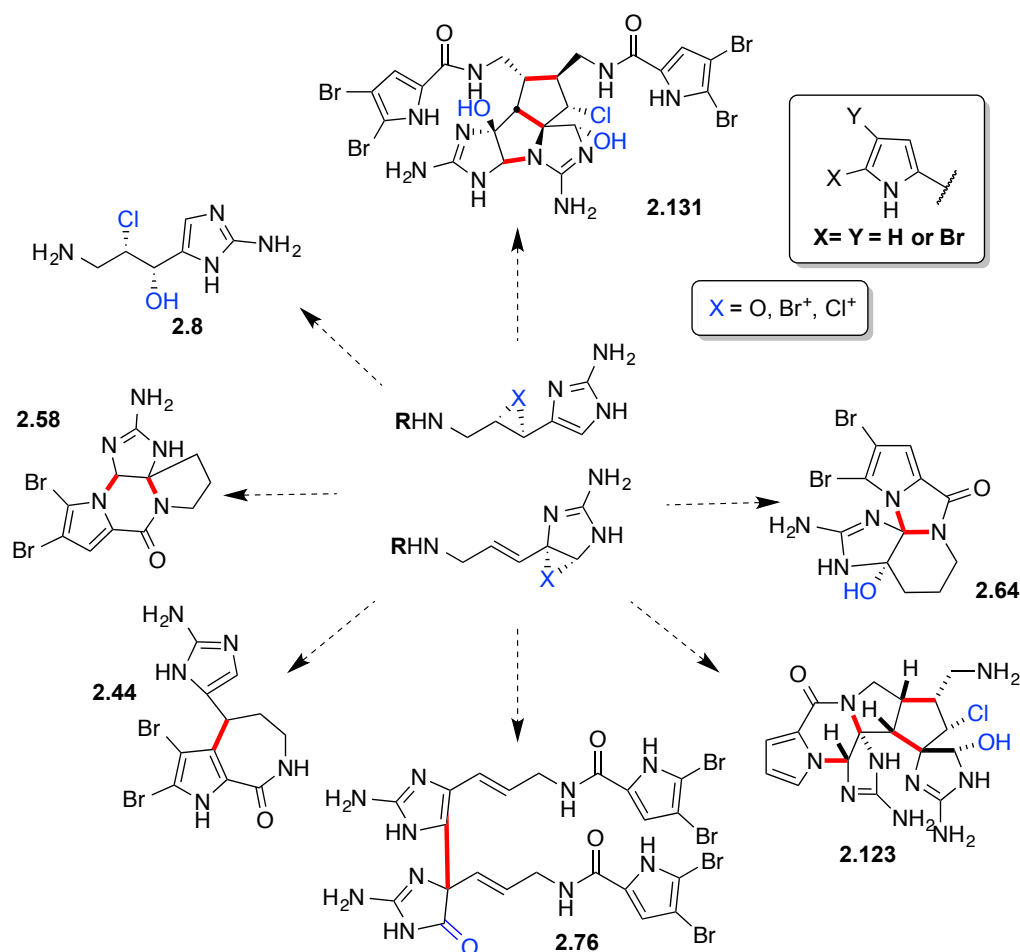
**Scheme 2.18** Conversion of a bromonium ion to an epoxide.



**Scheme 2.19** Halohydrin formation by a chloroperoxidase and its conversion to epoxide.

## 2.7. Proposed Biogenesis of the Oroidin Alkaloids

The putative role of haloperoxidases in the biosynthesis of the oroidin alkaloids suggests they may also be involved in the generation of the complexity observed in the family. Epoxidation (or halonium ion formation) of the C9-C10 and C11-C12 would lead to reactive intermediates that could cyclise and dimerise. This could also explain the observed incorporation of oxygen and halogen atoms (**Scheme 2.20**).



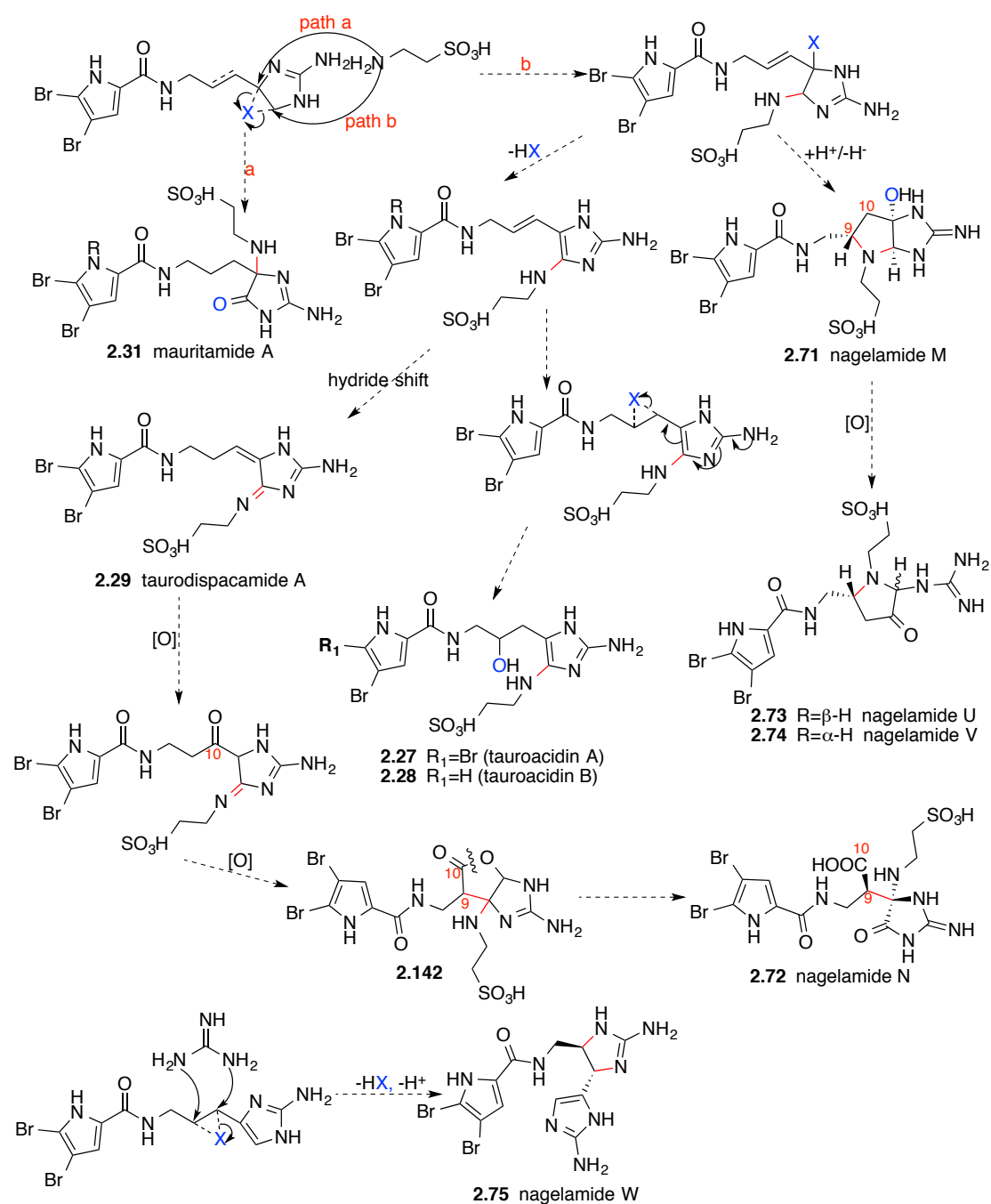
**Scheme 2.20** The Biomimetic generation of the oroidin alkaloids via key epoxide or halonium intermediates of the linear precursors can be deduced from the C-C bond formations (red) and residual OH/Cl (blue).

### 2.7.1. Linear monomers

The substitution observed on the linear monomer can be explained by the nucleophilic opening of the epoxide or halonium ion intermediate (e.g. see **Scheme 2.20**). Taurine can act as a nucleophile leading to mauritamide A (**2.31**) (**path a**) (**Scheme 2.21**). Ring opening from the opposite side (**path b**), followed by elimination and subsequent epoxidation (or bromonium ion formation) of C9-C10 double bond can lead to the tauroacidins **2.27-2.28**. Alternatively, intramolecular cyclisation of the amine of the taurine moiety onto C9 can lead to nagelamide M

(2.71). Oxidative C-N cleavage of the latter would provide nagelamides U and V

(2.73-2.74).



**Scheme 2.21** Examples of biogenesis of linear oroidin alkaloid from key bromonium or epoxide intermediate of the linear precursor.

As proposed by Kobayashi, nagelamide N (**2.72**) can be generated from hydrolysis and oxidation of intermediate **2.142**, which could be derived from

taurodispacamide A (**2.29**) through Baeyer–Villiger oxidation and cyclisation.<sup>83</sup>

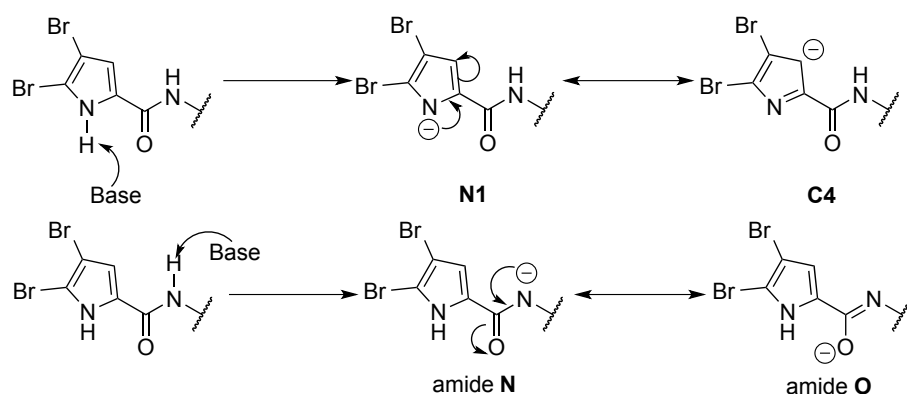
Nagelamide W (**2.75**) can be generated by ring opening of an epoxide (or bromonium ion) at C9-C10 by a guanidine. Similarly, Z-debromohymenialdesine (**2.48**) can be added onto hymenidin (**2.4**) in stylissazole C (**2.92**). Ring opening of an epoxide (or bromonium ion) at C9 or C12 of hymenidin (**2.4**) by nucleophilic imidazole N13 of Z-debromohymenialdesine (**2.48**) will lead to stylissazole B (**2.91**) and A (**2.90**) respectively.

### 2.7.2. Monocyclic monomers

The intramolecular cyclisations observed in the monocyclic monomers can be rationalised as the intramolecular quenching of the putative epoxide/bromonium ion.

The pyrrole nitrogen N1 (and C4 by resonance) can act as a internal nucleophiles.

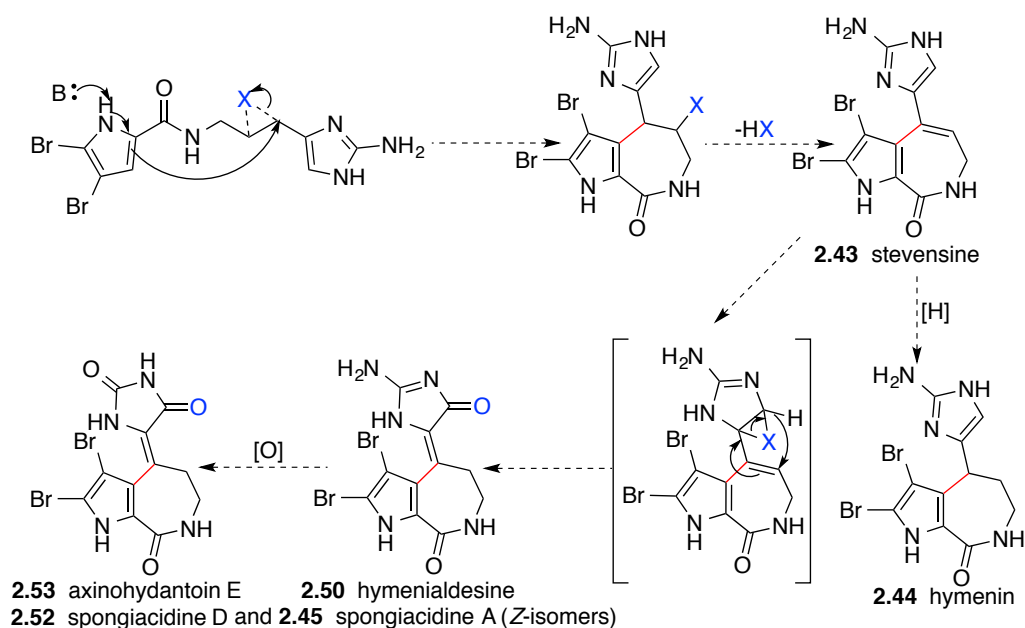
The amide nitrogen (or oxygen by resonance) can similarly do so (**Scheme 2.22**).



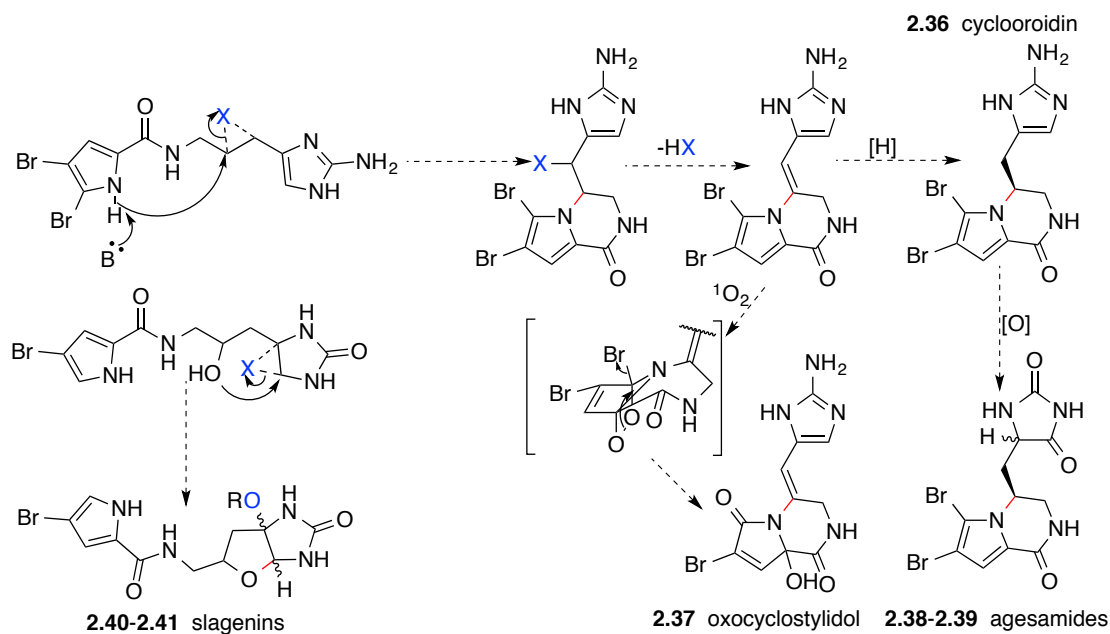
**Scheme 2.22** Presence of internal nucleophiles.

Ring opening of the C9-C10 epoxide by pyrrole C4 can lead to the azepine bicyclic oroidin alkaloids (**Scheme 2.23**) while ring opening by the pyrrole N1 will allow access to cyclooroidin and its oxidised derivatives (**Scheme 2.24**). The

intramolecular cyclisation of the alcohol intermediate onto the C11-C12 epoxide or bromonium ion will allow the formation of the slagenins (**Scheme 2.24**).

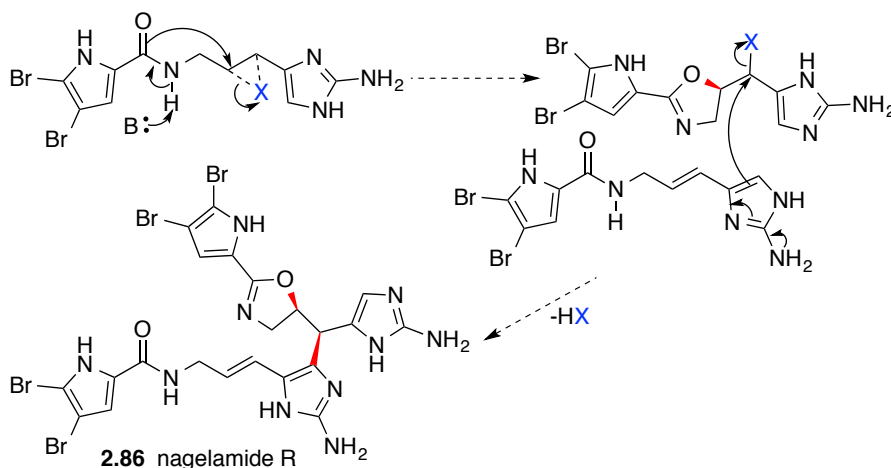


**Scheme 2.23** Some examples of the involved C4 nucleophilicity of the pyrrole ring in the formation of the cyclic monomers.



**Scheme 2.24** Some examples of the involved N1 nucleophilicity of the pyrrole ring in the formation of the cyclic monomers.

Ring opening of the C9-C10 epoxide by amide O can lead to the formation of an oxazoline ring. This is observed in Nagelamide R (**2.86**) where a subsequent nucleophilic substitution by another oroidin molecule leads to the dimer (**Scheme 2.25**).

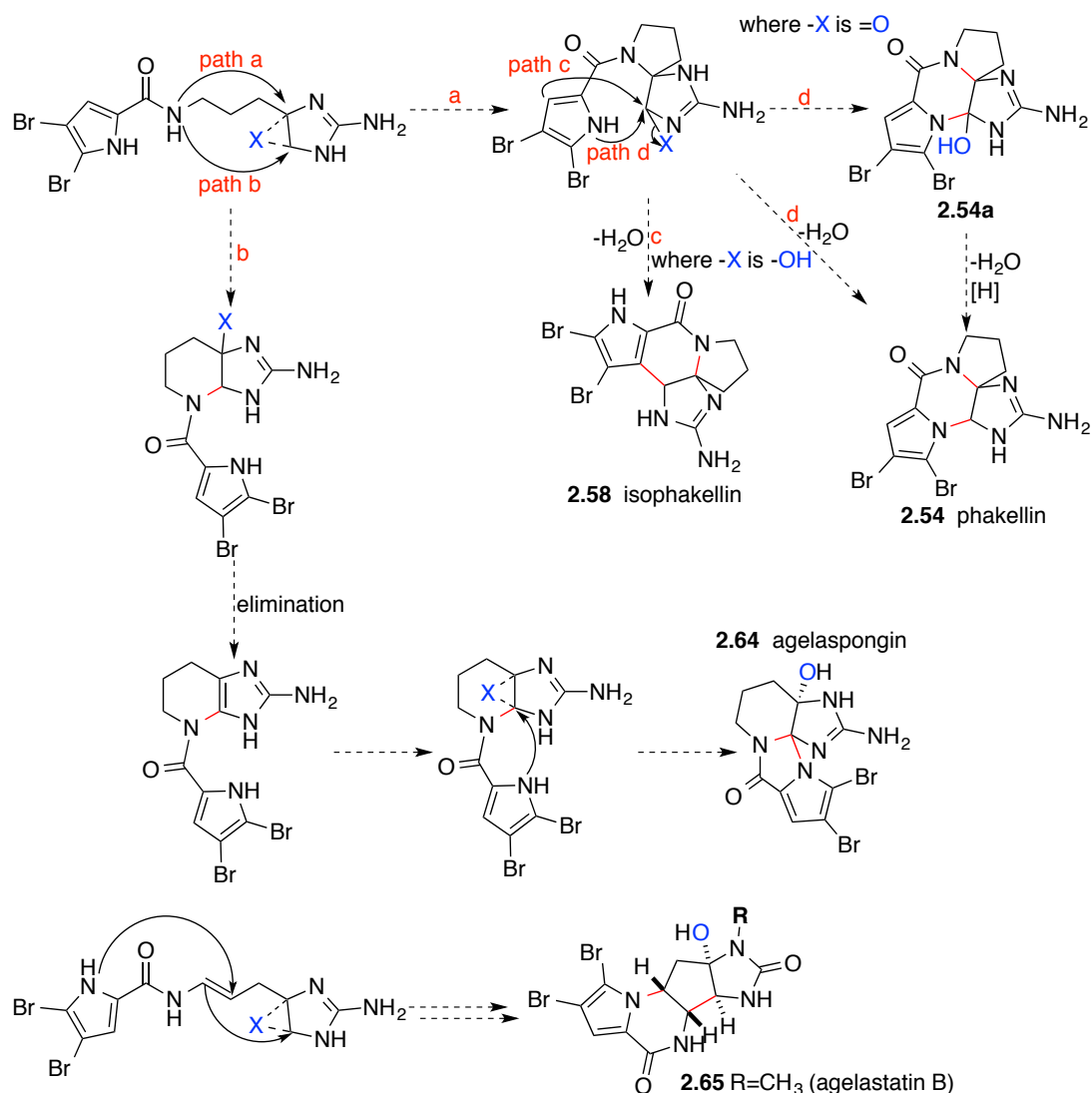


**Scheme 2.25** Example of amide O nucleophilicity in the formation of the oxazoline ring.

### 2.7.3. Bicyclic monomers

The bicyclic monomers can be thought of as arising from the attack of C4 or N1 on the C11-C12 epoxide of DHO (**2.2**) (**Scheme 2.26**). Nucleophilic attack of C4 (**path c**) will then provide phakellin (**2.54**) directly or its hydroxyl derivative **2.54a**, while nucleophilic attack of N1 (**path d**) on the imidazole C12 will afford isophakellin (**2.58**). **2.54a** can subsequently be reduced to phakellin (**2.54**). Ring opening through **path b** will lead to a tetrahydropyridine intermediate. Formation of an epoxide ion at the imidazole of the latter and subsequent nucleophilic attack by N1 will lead to the formation of agelaspongine (**2.64**) (**Scheme 2.26**). An epoxide (or bromonium ion) induced cascade reaction starting with the nucleophilic attack of the pyrrole onto the alkene carbon double bond and leading to the ring opening of an

epoxide (or bromonium ion) will lead to the formation of the agelastatin (**2.65**) after oxidation of the guanidine to a urea (**Scheme 2.26**).

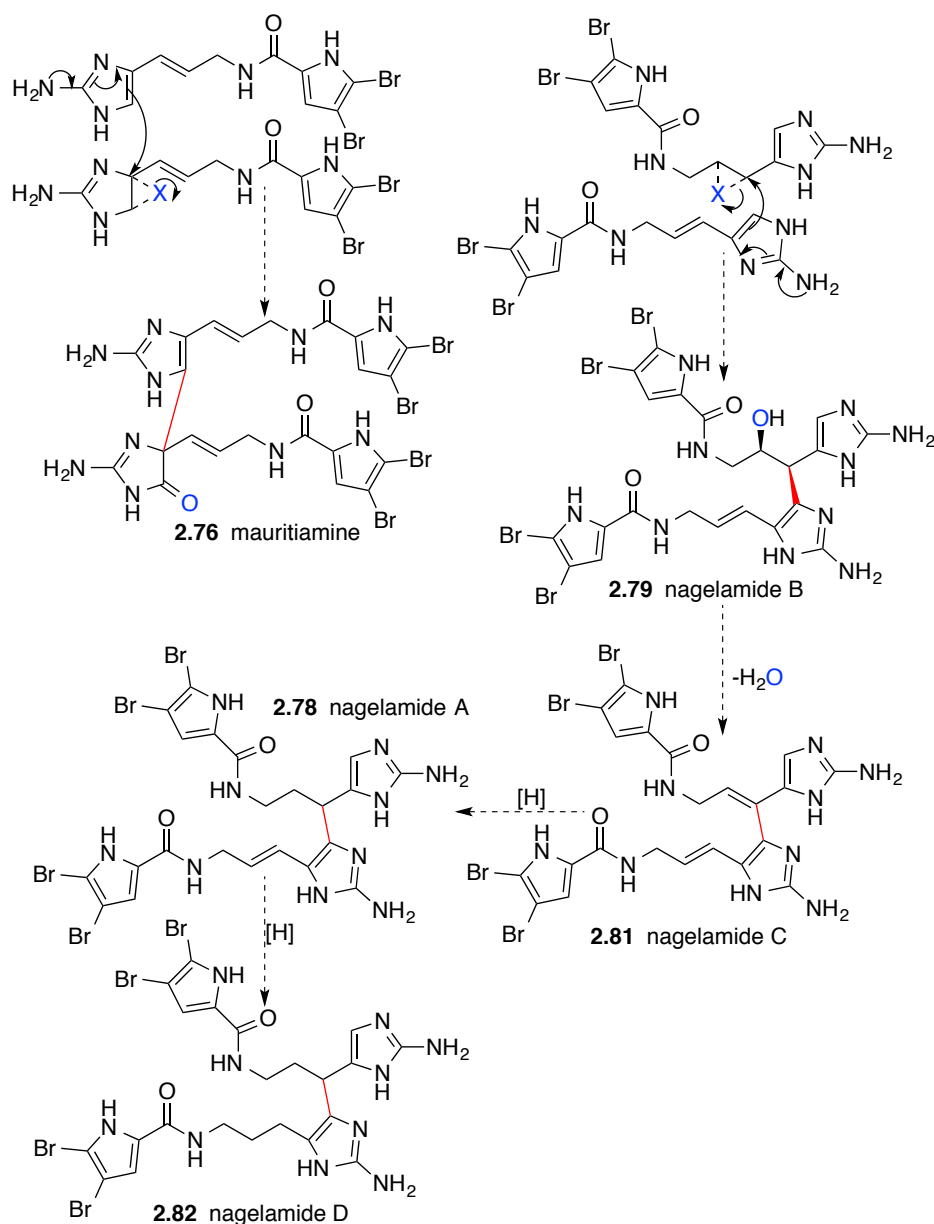


**Scheme 2.26** Biogenesis of the tetracyclic oroidin alkaloids from the key bromonium or epoxide intermediate of the linear precursor.

#### 2.7.4. Acyclic Dimers

Mauritiamine (**2.76**) could form by the nucleophilic addition of the imidazole of oroidin on the epoxide (or bromonium ion) of another unit of oroidin (**Scheme 2.27**). Similar attack of the epoxide (or bromonium ion) formed at the alkene double

bond can lead to the formation of the nagelamides A-D (**2.79-2.82**) through subsequent elimination and reduction reactions (**Scheme 2.27**).



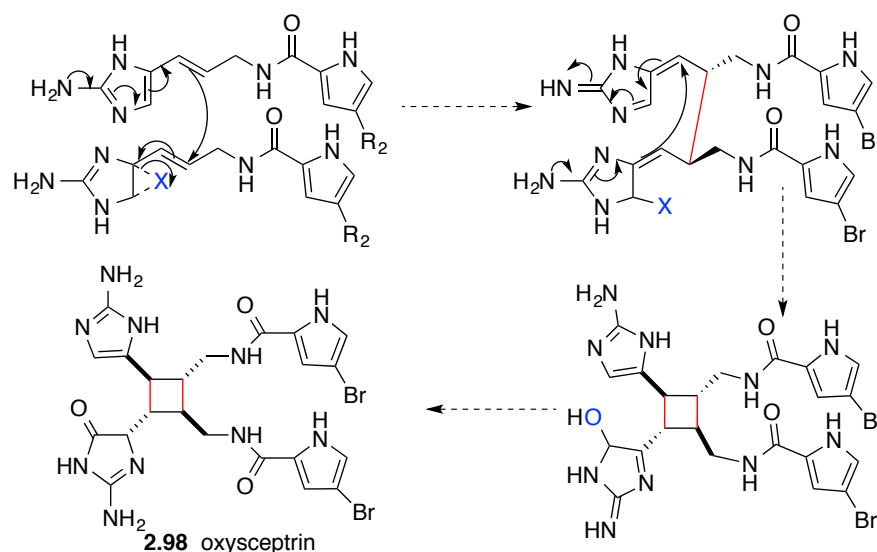
**Scheme 2.27** Biogenesis of the acyclic dimers from the key bromonium or epoxide intermediate of the linear precursor.

### 2.7.5. The More Complex Oroidin Alkaloids

The sceptrins have been proposed to be the result of a [2+2]-cycloaddition or/and ionic mechanism.<sup>93,122</sup> The synthetic strategy using [2+2]-cycloaddition has however been unsuccessful.<sup>93</sup> Taking note of the oxygen on oxysceptrin (**2.98**), it is



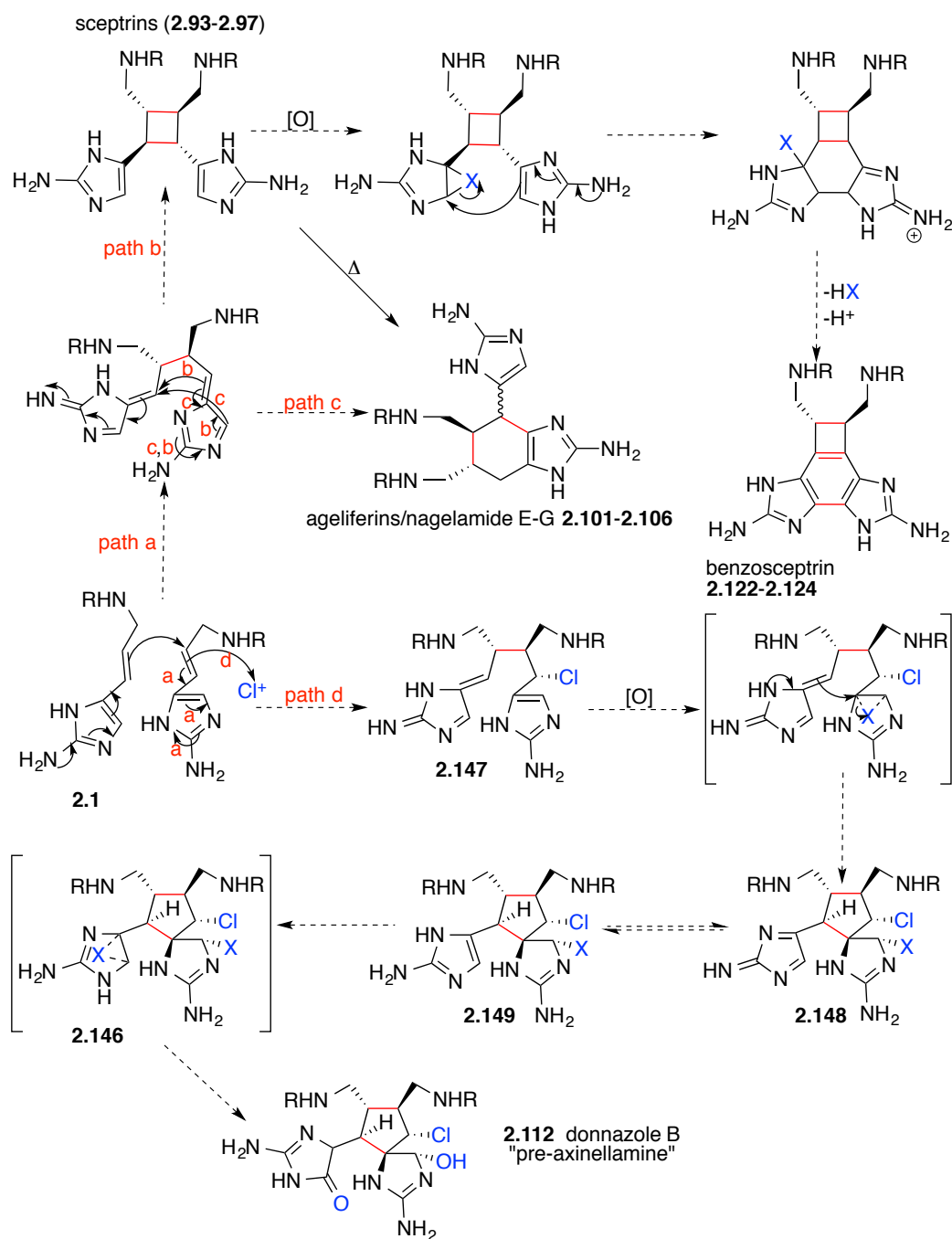
possible that two molecules of oroidin could couple, catalysed by epoxide ring opening (**Scheme 2.28**).



**Scheme 2.28** Biogenesis of the oxosceptrin (**2.98**).

Alternatively, the guanidine could stabilise an adjacent negative charge to couple two molecules of oroidin via C9-C9' (**2.143**) (**path a**) (**Scheme 2.29**). Formation of sceptrin (**2.93**) (C10-C10') (**path b**) or agelifेरins/nagelamides E-G **2.101-2.106** (**path c**) could then be readily accomplished via an intramolecular ene-type reaction. The benzosceptrins **2.122-2.124** could be formed from the ring opening of an epoxide (or bromonium ion) at one of the imidazole double bonds by the other imidazole ring, followed by aromatisation via elimination reactions. The formation of nagelamides X (**2.109**) and Y (**2.110**) would follow a similar path to the ageliferin, starting from oroidin and taurodispacamide (**2.29**). Baran has reported the thermal conversion of sceptrin (**2.93**) to ageliferin (**2.101**).<sup>123</sup> The epoxide (or bromonium ion) intermediate **2.146** could have derived from oroidin (**2.1**). Dimerisation of oroidin at C9-C9' followed by nucleophilic attack of double bond on the chloronium ion (**path d**) form **2.147**. This intermediate could further undergo epoxidation (or

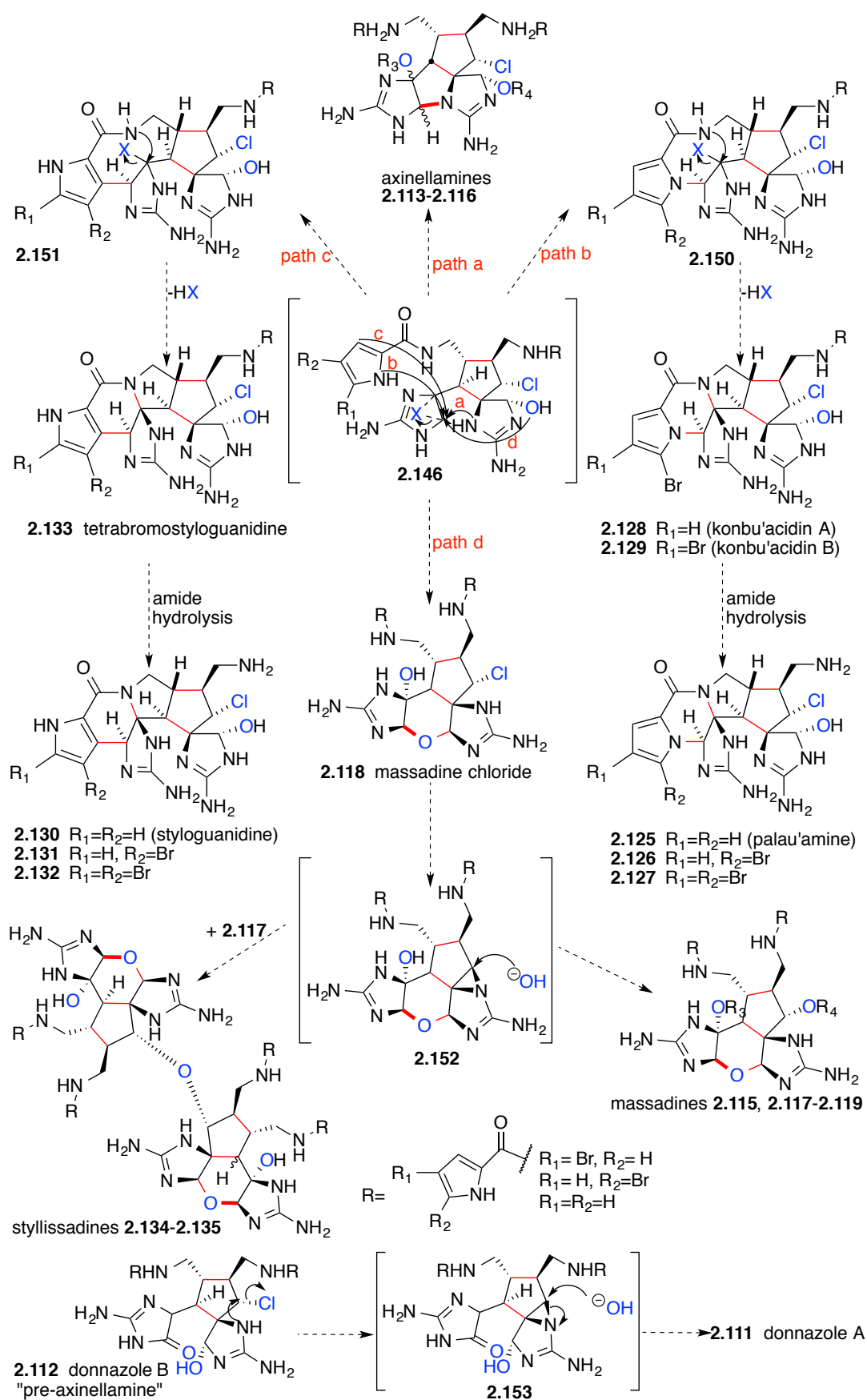
bromonium ion formation) at the second imidazole double bond to form the cyclopentane ring **2.148** after intramolecular cyclisation/epoxide ring opening. Compound **2.149** is a tautomer of **2.148**. A further epoxidation (or bromonium ion formation) at the first imidazole double bond would give key intermediate **2.146**, which can form donnazole B (**2.112**). The latter is the oxidised “pre-axinellamine” (**2.142**) proposed by Köck and Baran as the key intermediate to bicyclic and tricyclic dimers.<sup>8</sup>



**Scheme 2.29** Biogenesis of the sceptrin (2.93-2.97), benzosceptrins (2.122-2.124), ageliferins/nagelamide E-G 2.101-2.106, donnazole B (2.112) and key intermediate 2.146. R can be either an unbrominated, monobrominated or dibrominated acetylpyrrole or H.

Intermediate **2.146** can explain the formation of all the complex polycyclic oroidin alkaloids (Scheme 2.30). In **path a**, ring opening by N15 of imidazole leads to the formation of axinellamines (2.113-2.116). In **path b**, ring opening by N1 nucleophile leads to the formation of intermediate **2.150**, which upon dehydration

followed by intramolecular cyclisation, leads to the formation of the konbu'acidins **2.128-2.129**. Palau'amine is the amide hydrolysed product of the konbu'acidin A (**2.128**). Similarly ring opening by C4 nucleophile lead to the intermediate **2.151**, which upon dehydration followed by intramolecular cyclisation leads to the formation stylloguanidines **2.130-2.133 (path c)**. Ring opening by a hydroxyl nucleophile leads to the formation of massadine chloride (**2.118**) (**path d**). Romo<sup>124</sup> first, and later Baran<sup>101</sup>, have suggested the intermediacy of massadine aziridine (**2.152**) in the formation of massadine (**2.115**) on reaction with water, in order to explain the retention in the stereochemistry.<sup>124</sup> On reaction with massadine (**2.117**) itself, massadine aziridine (**2.152**) would lead to the formation of tetramers stylissadine A and B (**2.134-2.135**). Similarly, the intermediacy of aziridine **2.153** would lead to the conversion of donnazole B (**2.112**) to donnazole A (**2.111**).



Scheme 2.30 Biogenesis for bicyclic and tricyclic dimers.

## 2.8. Conclusions

The biological activities and unique structures of the oroidin alkaloids make them attractive targets for the synthetic chemist. The proposed biogenesis of the oroidin alkaloids provide a simple, logical, yet comprehensive explanation for the formation of the oroidin alkaloids that points the way to efficient biomimetic syntheses of these alkaloids. In the next chapter we explored the key reactive intermediates of our biogenesis.

## 2.9. References

- (1) Appenzeller, J.; Al-Mourabit, A. In *Biomimetic Organic Synthesis*; Wiley-VCH Verlag GmbH & Co. KGaA: 2011, p 225-269.
- (2) Al-Mourabit, A.; Potier, P. *Eur. J. Org. Chem.* **2001**, 237-243.
- (3) Andrade, P.; Willoughby, R.; Pomponi, S. A.; Kerr, R. G. *Tetrahedron Lett.* **1999**, 40, 4775-4778.
- (4) D'Ambrosio, M.; Guerriero, A.; Debitus, C.; Ribes, O.; Pusset, J.; Leroy, S.; Pietra, F. *Chem. Commun.* **1993**, 1305-1306.
- (5) Fedoreyev, S. A.; Ilyin, S. G.; Utkina, N. K.; Maximov, O. B.; Reshetnyak, M. V.; Antipin, M. Y.; Struchkov, Y. T. *Tetrahedron* **1989**, 45, 3487-3492.
- (6) Genta-Jouve, G.; Cachet, N.; Holderith, S.; Oberhansli, F.; Teyssie, J. L.; Jeffree, R.; Al Mourabit, A.; Thomas, O. P. *ChemBioChem* **2011**, 12, 2298-2301.
- (7) Kinnel, R. B.; Gehrken, H.-P.; Swali, R.; Skoropowski, G.; Scheuer, P. J. *J. Org. Chem.* **1998**, 63, 3281-3286.
- (8) Köck, M.; Grube, A.; Seiple, I. B.; Baran, P. S. *Angew. Chem. Int. Ed.* **2007**, 46, 6586-6594.
- (9) Ma, Z.; Lu, J.; Wang, X.; Chen, C. *Chem. Commun.* **2011**, 47, 427-429.
- (10) Movassaghi, M.; Siegel, D. S.; Han, S. *Chem. Sci.* **2010**, 1, 561-566.
- (11) Northrop, B. H.; O'Malley, D. P.; Zografos, A. L.; Baran, P. S.; Houk, K. N. *Angew. Chem., Int. Ed.* **2006**, 45, 4126-4130.
- (12) Sharma, G. M.; Magdoff-Fairchild, B. *J. Org. Chem.* **1977**, 42, 4118-4124.
- (13) Stout, E. P.; Morinaka, B. I.; Wang, Y.-G.; Romo, D.; Molinski, T. F. *J. Nat. Prod.* **2012**, 75, 527-530.

- (14) Tsukamoto, S.; Kato, H.; Hirota, H.; Fusetani, N. *J. Nat. Prod.* **1996**, *59*, 501-503.
- (15) Wang, X.; Wang, X.; Tan, X.; Lu, J.; Cormier, K. W.; Ma, Z.; Chen, C. *J. Am. Chem. Soc.* **2012**, *134*, 18834-18842.
- (16) Forenza, S.; Minale, L.; Riccio, R.; Fattorusso, E. *Chem. Commun.* **1971**, 1129-1130.
- (17) Cafieri, F.; Fattorusso, E.; Mangoni, A.; Taglialatela-Scafati, O. *Tetrahedron Lett.* **1996**, *37*, 3587-3590.
- (18) Cimino, G.; De Rosa, S.; De Stefano, S.; Mazzarella, L.; Puliti, R.; Sodano, G. *Tetrahedron Lett.* **1982**, *23*, 767-768.
- (19) Cimino, G.; de Stefano, S.; Minale, L.; Sodano, G. *Comp. Biochem. Physiol., Part B: Biochem. Mol. Biol.* **1975**, *50*, 279-285.
- (20) Keifer, P. A.; Schwartz, R. E.; Koker, M. E. S.; Hughes, R. G., Jr.; Rittschof, D.; Rinehart, K. L. *J. Org. Chem.* **1991**, *56*, 2965-2975.
- (21) Kinnel, R. B.; Gehrken, H. P.; Scheuer, P. J. *J. Am. Chem. Soc.* **1993**, *115*, 3376-3377.
- (22) Kobayashi, J.; Tsuda, M.; Ohizumi, Y. *Experientia* **1991**, *47*, 301-304.
- (23) Rosa, R.; Silva, W.; Escalona de Motta, G.; Rodriguez, A. D.; Morales, J. J.; Ortiz, M. *Experientia* **1992**, *48*, 885-887.
- (24) Garcia, E. E.; Benjamin, L. E.; Fryer, R. I. *J. Chem. Soc., Chem. Commun.* **1973**, 78-79.
- (25) Assmann, M.; Lichte, E.; Pawlik, J. R.; Kock, M. *Mar. Ecol.* **2000**, *207*, 255-262.
- (26) Chanas, B.; R. Pawlik, J.; Lindel, T.; Fenical, W. *J. Exp. Mar. Biol. Ecol.* **1997**, *208*, 185-196.
- (27) Lindel, T.; Hoffmann, H.; Hochgurtel, M.; Pawlik, J. R. *J. Chem. Ecol.* **2000**, *26*, 1477-1496.
- (28) Wilson, D. M.; Puyana, M.; Fenical, W.; Pawlik, J. R. *J. Chem. Ecol.* **1999**, *25*, 2811-2823.
- (29) [http://ceb.wikipedia.org/wiki/Payl:Agelas\\_oroide\\_Capo\\_Gallo\\_025.JPG](http://ceb.wikipedia.org/wiki/Payl:Agelas_oroide_Capo_Gallo_025.JPG);  
Accessed: 22/03/2014.
- (30) Assmann, M.; van Soest, R. W.; Köck, M. *J. Nat. Prod.* **2001**, *64*, 1345-1347.
- (31) Kobayashi, J.; Ohizumi, Y.; Nakamura, H.; Hirata, Y. *Experientia* **1986**, *42*, 1176-1177.

- (32) Morales, J. J.; Rodríguez, A. D. *J. Nat. Prod.* **1991**, *54*, 629-631.
- (33) Rentas, A. L. R.; Rosa, R.; Rodríguez, A. D.; De Motta, G. E. *Toxicon* **1995**, *33*, 491-497.
- (34) Cafieri, F.; Fattorusso, E.; Taglialatela-Scafati, O. *J. Nat. Prod.* **1998**, *61*, 122-125.
- (35) Endo, T.; Tsuda, M.; Okada, T.; Mitsunashi, S.; Shima, H.; Kikuchi, K.; Mikami, Y.; Fromont, J.; Kobayashi, J. *J. Nat. Prod.* **2004**, *67*, 1262-1267.
- (36) Nakamura, H.; Ohizumi, Y.; Kobayashi, J.; Hirata, Y. *Tetrahedron Lett.* **1984**, *25*, 2475-2478.
- (37) Ahond, A.; Zurita, M. B.; Colin, M.; Fizames, C.; Laboute, P.; Lavelle, F.; Laurent, D.; Poupat, C.; Pusset, J.; et al. *C. R. l'Academie. Sci., Ser. II Univers* **1988**, *307*, 145-148.
- (38) Lavelle, F.; Zerial, A.; Fizames, C.; Rabault, B.; Curaudeau, A. *Invest. New Drugs* **1991**, *9*, 233-244.
- (39) Wright, A. E.; Chiles, S. A.; Cross, S. S. *J. Nat. Prod.* **1991**, *54*, 1684-1686.
- (40) Regalado, E. L.; Laguna, A.; Mendiola, J.; Thomas, O. P.; Nogueiras, C. *Quim. Nova* **2011**, *34*, 289-291.
- (41) Barrow, R. A.; Capon, R. J. *Natural Product Letters* **1993**, *1*, 243-250.
- (42) Kuramoto, M.; Miyake, N.; Ishimaru, Y.; Ono, N.; Uno, H. *Org. Lett.* **2008**, *10*, 5465-5468.
- (43) Cafieri, F.; Carnuccio, R.; Fattorusso, E.; Taglialatela-Scafati, O.; Vallefucio, T. *Bioorg. Med. Chem. Lett.* **1997**, *7*, 2283-2288.
- (44) Vergne, C.; Appenzeller, J.; Ratinaud, C.; Martin, M.-T.; Debitus, C.; Zapparucha, A.; Al-Mourabit, A. *Org. Lett.* **2008**, *10*, 493-496.
- (45) Aiello, A.; D'Esposito, M.; Fattorusso, E.; Menna, M.; Müller, W. E. G.; Perović-Ottstadt, S.; Schröder, H. C. *Bioorg. Med. Chem.* **2006**, *14*, 17-24.
- (46) Chevolot, L.; Padua, S.; Ravi, B. N.; Blyth, P. C.; Scheuer, P. J. *Heterocycles* **1977**, *7*, 891-894.
- (47) Hu, J.-F.; Peng, J.; Kazi, A. B.; Kelly, M.; Hamann, M. T. *J. Chem. Res.* **2005**, 427-428.
- (48) Kobayashi, J.; Inaba, K.; Tsuda, M. *Tetrahedron* **1997**, *53*, 16679-16682.
- (49) Fattorusso, E.; Taglialatela-Scafati, O. *Tetrahedron Lett.* **2000**, *41*, 9917-9922.
- (50) Jiménez, C.; Crews, P. *Tetrahedron Lett.* **1994**, *35*, 1375-1378.



- (51) Cafieri, F.; Fattorusso, E.; Mangoni, A.; Taglialetela-Scafati, O. *Tetrahedron Lett.* **1995**, *36*, 7893-7896.
- (52) Umeyama, A.; Ito, S.; Yuasa, E.; Arihara, S.; Yamada, T. *J. Nat. Prod.* **1998**, *61*, 1433-1434.
- (53) Mancini, I.; Guella, G.; Amade, P.; Roussakis, C.; Pietra, F. *Tetrahedron Lett.* **1997**, *38*, 6271-6274.
- (54) Grube, A.; Köck, M. *J. Nat. Prod.* **2006**, *69*, 1212-1214.
- (55) Tsuda, M.; Yasuda, T.; Fukushi, E.; Kawabata, J.; Sekiguchi, M.; Fromont, J.; Kobayashi, J. *Org. Lett.* **2006**, *8*, 4235-4238.
- (56) Tsuda, M.; Uemoto, H.; Kobayashi, J. *Tetrahedron Lett.* **1999**, *40*, 5709-5712.
- (57) Albizati, K. F.; Faulkner, D. J. *J. Org. Chem.* **1985**, *50*, 4163-4164.
- (58) De Nanteuil, G.; Ahond, A.; Guilhem, J.; Poupat, C.; Tran Huu Dau, E.; Potier, P.; Pusset, M.; Pusset, J.; Laboute, P. *Tetrahedron* **1985**, *41*, 6019-6033.
- (59) Eder, C.; Proksch, P.; Wray, V.; Steube, K.; Bringmann, G.; Van Soest, R. W. M.; Sudarsono; Ferdinandus, E.; Pattisina, L. A.; Wiryowidagdo, S.; Moka, W. *J. Nat. Prod.* **1999**, *62*, 184-187.
- (60) Hassan, W.; Elkhayat, E. S.; Edrada, R. A.; Ebel, R.; Proksch, P. *Nat. Prod. Commun.* **2007**, *2*, 1149-1154.
- (61) Zhang, H.; Khalil, Z.; Conte, M. M.; Plisson, F.; Capon, R. J. *Tetrahedron Lett.* **2012**, *53*, 3784-3787.
- (62) Inaba, K.; Sato, H.; Tsuda, M.; Kobayashi, J. *J. Nat. Prod.* **1998**, *61*, 693-695.
- (63) Pettit, G. R.; Herald, C. L.; Leet, J. E.; Gupta, R.; Schaufelberger, D. E.; Bates, R. B.; Clewlow, P. J.; Doubek, D. L.; Manfredi, K. P.; et al. *Can. J. Chem.* **1990**, *68*, 1621-1624.
- (64) Sharma, G. M.; Buyer, J. S.; Pomerantz, M. W. *Chem. Commun.* **1980**, 435-435.
- (65) Williams, D. H.; Faulkner, D. J. *Nat. Prod. Lett.* **1996**, *9*, 57-64.
- (66) Supriyono, A.; Schwarz, B.; Wray, V.; Witte, L.; Mueller, W. E. G.; van Soest, R.; Sumaryono, W.; Proksch, P. *Z. Naturforsch., C* **1995**, *50*, 669-674.
- (67) Kitagawa, I.; Kobayashi, M.; Kitanaka, K.; Kido, M.; Kyogoku, Y. *Chem. Pharm. Bull.* **1983**, *31*, 2321-2328.
- (68) Wan, Y.; Hur, W.; Cho, C. Y.; Liu, Y.; Adrian, F. J.; Lozach, O.; Bach, S.; Mayer, T.; Fabbro, D.; Meijer, L.; Gray, N. S. *Chem. Biol.* **2004**, *11*, 247-259.

- (69) Meijer, L.; Thunnissen, A. M. W. H.; White, A. W.; Garnier, M.; Nikolic, M.; Tsai, L. H.; Walter, J.; Cleverley, K. E.; Salinas, P. C.; Wu, Y. Z.; Biernat, J.; Mandelkow, E. M.; Kim, S. H.; Pettit, G. R. *Chem. Biol.* **2000**, *7*, 51-63.
- (70) Eder, C.; Proksch, P.; Wray, V.; van Soest, R. W. M.; Ferdinandus, E.; Pattisina, L. A.; Sudarsono *J. Nat. Prod.* **1999**, *62*, 1295-1297.
- (71) Zhang, H.; Jin, Y.; Zhang, W. *Zhongyaocai* **2006**, *29*, 1299-1301.
- (72) Sharma, G. M.; Burkholder, P. R. *Chem. Commun.* **1971**, 151-152.
- (73) Gautschi, J. T.; Whitman, S.; Holman, T. R.; Crews, P. *J. Nat. Prod.* **2004**, *67*, 1256-1261.
- (74) Hertiani, T.; Edrada-Ebel, R.; Ortlepp, S.; van Soest, R. W. M.; de Voogd, N. J.; Wray, V.; Hentschel, U.; Kozytska, S.; Mueller, W. E. G.; Proksch, P. *Bioorg. Med. Chem.* **2010**, *18*, 1297-1311.
- (75) Goetz, G. H.; Harrigan, G. G.; Likos, J. *J. Nat. Prod.* **2001**, *64*, 1581-1582.
- (76) Fedoreyev, S. A.; Utkina, N. K.; Ilyin, S. G.; Reshetnyak, M. V.; Maximov, O. B. *Tetrahedron Lett.* **1986**, *27*, 3177-3180.
- (77) Assmann, M.; Kock, M. *Z. Naturforsch., C* **2002**, *57*, 153-156.
- (78) Assmann, M.; Kock, M. *Z. Naturforsch., C* **2002**, *57*, 157-160.
- (79) Lansdell, T. A.; Hewlett, N. M.; Skoumbourdis, A. P.; Fodor, M. D.; Seiple, I. B.; Su, S.; Baran, P. S.; Feldman, K. S.; Tepe, J. J. *J. Nat. Prod.* **2012**, *75*, 980-985.
- (80) D'Ambrosio, M.; Guerriero, A.; Chiasera, G.; Pietra, F. *Helv. Chim. Acta* **1994**, *77*, 1895-1902.
- (81) Hong, T. W.; Jimenez, D. R.; Molinski, T. F. *J. Nat. Prod.* **1998**, *61*, 158-161.
- (82) Tilvi, S.; Moriou, C.; Martin, M. T.; Gallard, J. F.; Sorres, J.; Patel, K.; Petek, S.; Debitus, C.; Ermolenko, L.; Al-Mourabit, A. *J. Nat. Prod.* **2010**, *73*, 720-723.
- (83) Kubota, T.; Araki, A.; Ito, J.; Mikami, Y.; Fromont, J.; Kobayashi, J. *Tetrahedron* **2008**, *64*, 10810-10813.
- (84) Tanaka, N.; Kusama, T.; Takahashi-Nakaguchi, A.; Gono, T.; Fromont, J.; Kobayashi, J. *Tetrahedron Lett.* **2013**, *54*, 3794-3796.
- (85) Araki, A.; Kubota, T.; Aoyama, K.; Mikami, Y.; Fromont, J.; Kobayashi, J. *Org. Lett.* **2009**, *11*, 1785-1788.
- (86) Araki, A.; Kubota, T.; Tsuda, M.; Mikami, Y.; Fromont, J.; Kobayashi, J. *Org. Lett.* **2008**, *10*, 2099-2102.

- (87) Araki, A.; Tsuda, M.; Kubota, T.; Mikami, Y.; Fromont, J.; Kobayashi, J. *Org. Lett.* **2007**, *9*, 2369-2371.
- (88) Iwai, T.; Kubota, T.; Fromont, J.; Kobayashi, J. *Chem. Pharm. Bull.* **2014**, *62*, 213-216.
- (89) Tanaka, N.; Kusama, T.; Takahashi-Nakaguchi, A.; Gono, T.; Fromont, J.; Kobayashi, J. *Org. Lett.* **2013**, *15*, 3262-3265.
- (90) Appenzeller, J.; Tilvi, S.; Martin, M.-T.; Gallard, J.-F.; El-bitar, H.; Dau, E. T. H.; Debitus, C.; Laurent, D.; Moriou, C.; Al-Mourabit, A. *Org. Lett.* **2009**, *11*, 4874-4877.
- (91) Lindel, T.; Breckle, G.; Hochgürtel, M.; Volk, C.; Grube, A.; Köck, M. *Tetrahedron Lett.* **2004**, *45*, 8149-8152.
- (92) Patel, K.; Laville, R.; Martin, M.-T.; Tilvi, S.; Moriou, C.; Gallard, J.-F.; Ermolenko, L.; Debitus, C.; Al-Mourabit, A. *Angew. Chem. Int. Ed.* **2010**, *49*, 4775-4779.
- (93) Walker, R. P.; Faulkner, D. J.; Van Engen, D.; Clardy, J. *J. Am. Chem. Soc.* **1981**, *103*, 6772-6773.
- (94) Vassas, A.; Bourdy, G.; Paillard, J. J.; Lavayre, J.; Pais, M.; Quirion, J. C.; Debitus, C. *Planta Med.* **1996**, *62*, 28-30.
- (95) Shen, X.; Perry, T. L.; Dunbar, C. D.; Kelly-Borges, M.; Hamann, M. T. *J. Nat. Prod.* **1998**, *61*, 1302-1303.
- (96) Kobayashi, J.; Tsuda, M.; Murayama, T.; Nakamura, H.; Ohizumi, Y.; Ishibashi, M.; Iwamura, M.; Ohta, T.; Nozoe, S. *Tetrahedron* **1990**, *46*, 5579-5586.
- (97) Rinehart, K. L. *Pure Appl. Chem.* **1989**, *61*, 525-528.
- (98) Muñoz, J.; Moriou, C.; Gallard, J.-F.; Marie, P. D.; Al-Mourabit, A. *Tetrahedron Lett.* **2012**, *53*, 5828-5832.
- (99) Urban, S.; de Almeida Leone, P.; Carroll, A. R.; Fechner, G. A.; Smith, J.; Hooper, J. N. A.; Quinn, R. J. *J. Org. Chem.* **1999**, *64*, 731-735.
- (100) Nishimura, S.; Matsunaga, S.; Shibasaki, M.; Suzuki, K.; Furihata, K.; van Soest, R. W. M.; Fusetani, N. *Org. Lett.* **2003**, *5*, 2255-2257.
- (101) Grube, A.; Immel, S.; Baran, P. S.; Köck, M. *Angew. Chem. Int. Ed.* **2007**, *46*, 6721-6724.
- (102) Grube, A.; Köck, M. *Angew. Chem., Int. Ed.* **2007**, *46*, 2320-2324.
- (103) Seiple, I. B.; Su, S.; Young, I. S.; Lewis, C. A.; Yamaguchi, J.; Baran, P. S. *Angew. Chem. Int. Ed.* **2010**, *49*, 1095-1098.

- (104) Gaich, T.; Baran, P. S. *J. Org. Chem.* **2010**, *75*, 4657-4673.
- (105) Buchanan, M. S.; Carroll, A. R.; Quinn, R. J. *Tetrahedron Lett.* **2007**, *48*, 4573-4574.
- (106) Kobayashi, J.; Suzuki, M.; Tsuda, M. *Tetrahedron* **1997**, *53*, 15681-15684.
- (107) Kato, T.; Shizuri, Y.; Izumida, H.; Yokoyama, A.; Endo, M. *Tetrahedron Lett.* **1995**, *36*, 2133-2136.
- (108) Grube, A.; Kock, M. *Org. Lett.* **2006**, *8*, 4675-4678.
- (109) Buchanan, M. S.; Carroll, A. R.; Addepalli, R.; Avery, V. M.; Hooper, J. N. A.; Quinn, R. J. *J. Org. Chem.* **2007**, *72*, 2309-2317.
- (110) Stout, E. P.; Morinaka, B. I.; Wang, Y.-G.; Romo, D.; Molinski, T. F. *J. Nat. Prod.* **2012**, *75*, 527-530.
- (111) Vaillancourt, F. H.; Yeh, E.; Vosburg, D. A.; Garneau-Tsodikova, S.; Walsh, C. T. *Chem. Rev.* **2006**, *106*, 3364-3378.
- (112) Gribble, G. W. J. *J. Chem. Educ.* **2004**, *81*, 1441-1449.
- (113) Butler, A.; Walker, J. V. *Chem. Rev.* **1993**, *93*, 1937-1944.
- (114) Butler, A.; Carter-Franklin, J. N. *Nat. Prod. Rep.* **2004**, *21*, 180-188.
- (115) Wischang, D.; Radlow, M.; Hartung, J. *Dalton Trans.* **2013**, *42*, 11926-11940.
- (116) Geigert, J.; Lee, T. D.; Dalietos, D. J.; Hirano, D. S.; Neidleman, S. L. *Biochem. Biophys. Res. Commun.* **1986**, *136*, 778-782.
- (117) Natarajan, S.; Moovendaran, K.; Sundar, J. K.; Ravikumar, K. *J. Amino Acids* **2012**, *2012*, 6.
- (118) Wasserman, H. H.; Yoo, J. U.; DeSimone, R. W. *J. Am. Chem. Soc.* **1995**, *117*, 9772-9773.
- (119) He, Y.; Du, H.; Lovely, C. J. *Org. Lett.* **2004**, *6*, 735-738.
- (120) O'Malley, D. P.; Yamaguchi, J.; Young, I. S.; Seiple, I. B.; Baran, P. S. *Angew. Chem. Int. Ed. Engl.* **2008**, *47*, 3581-3583.
- (121) Kaup, B.-A.; Piantini, U.; Wüst, M.; Schrader, J. *Appl. Microbiol. Biotechnol.* **2007**, *73*, 1087-1096.
- (122) Hao, E.; Fromont, J.; Jardine, D.; Karuso, P. *Molecules* **2001**, *6*, 130-141.
- (123) Baran, P. S.; O'Malley, D. P.; Zografos, A. L. *Angew. Chem., Int. Ed.* **2004**, *43*, 2674-2677.
- (124) Wang, S.; Dilley, A. S.; Poullennec, K. G.; Romo, D. *Tetrahedron* **2006**, *62*, 7155-7161

---

## **CHAPTER 3**

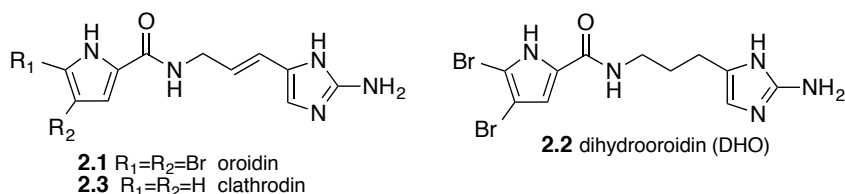
### **BIOMIMETIC APPROACH TO THE GENERATION OF OROIDIN ALKALOIDS FROM THEIR BIOGENESIS PRECURSOR(S)**

---

## PART A: Investigation of the Epoxide Route

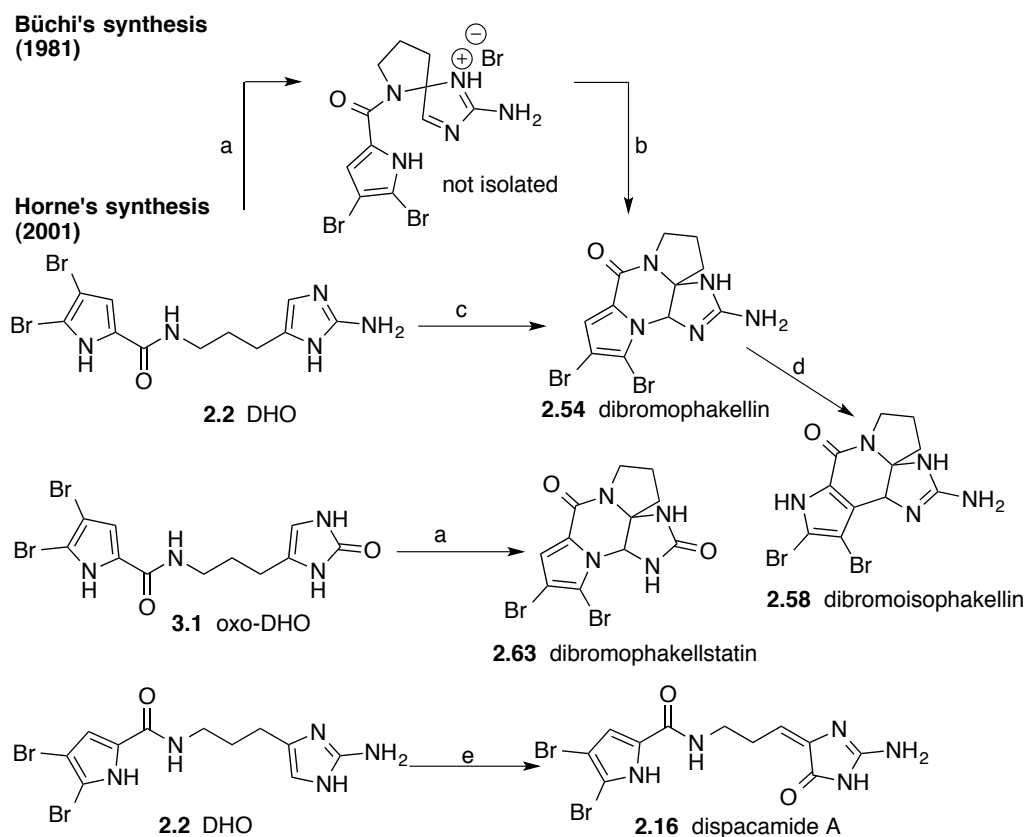
### 3.1. Introduction

Biomimetic natural product synthesis takes inspiration from Nature in as much that it tries to mimic the steps of natural product synthesis. The biomimetic synthesis of oroidin alkaloids generally starts with fully assembled C<sub>11</sub>N<sub>4</sub>-building blocks such as oroidin **2.1**, dihydrooroidin (DHO) **2.2** or clathrocin **2.3**. While the syntheses of the complex oroidin alkaloids have been mainly non-biomimetic, some of these syntheses have involved a few biomimetic step(s).



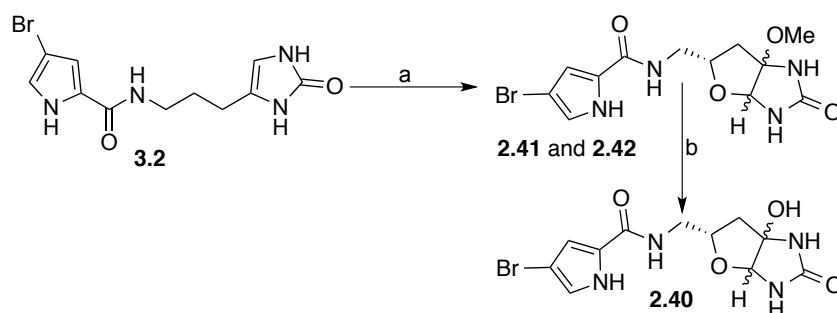
#### 3.1.1. Biomimetic Synthesis of the Oroidin Alkaloids

Büchi and co-workers were the first to report a biomimetic synthesis of an oroidin alkaloid, dibromophakellin (**2.54**).<sup>1</sup> The reaction of bromine with dihydrooroidin led to the postulated spirocyclic intermediate that provided racemic **2.54** upon treatment with potassium *t*-butoxide (**Scheme 3.1**).<sup>1</sup> Horne and co-workers reported the second biomimetic synthesis of dibromophakellin using similar conditions.<sup>2</sup> Treatment of DHO with NBS and TEA afforded the racemic **2.54** in excellent yield. Isomerisation of **2.54** to dibromoisophakellin (**2.58**) was achieved by heating **2.54** in the presence of potassium carbonate in chlorobenzene, via a N to C rearrangement (**Scheme 3.1**).<sup>2</sup> Dibromophakellstatin (**2.63**), an oxo analogue of dibromophakellin, was synthesised similarly from oxo-dihydrooroidin (**3.1**) (**Scheme 3.1**).<sup>2</sup>



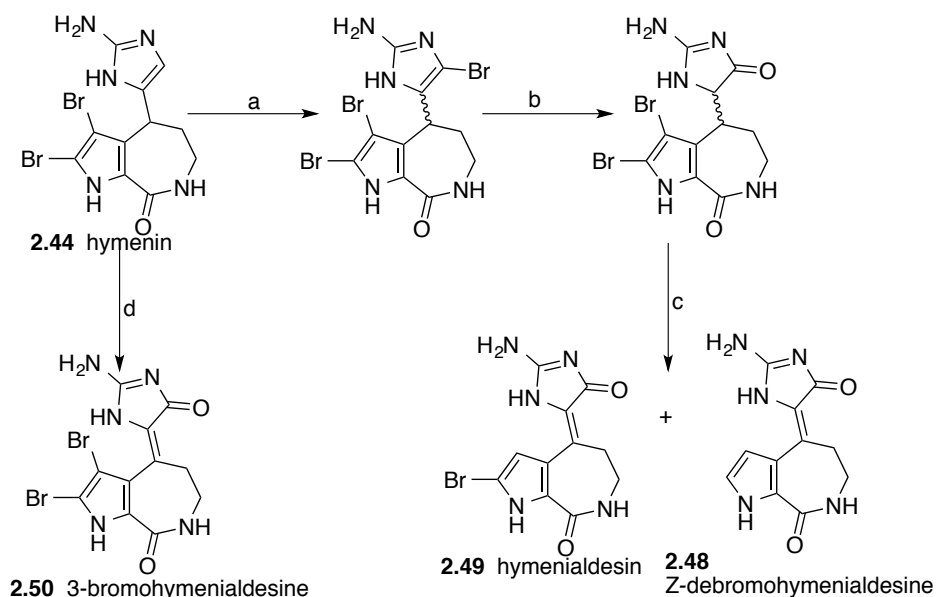
**Scheme 3.1** Reaction conditions: **a.** Br<sub>2</sub> (1 equiv.), acetic acid; **b.** *t*-BuOK, quantitative; **c.** 1. NBS, TFA, 5 min, 2. TEA:THF (1:1, v/v), 90%; **d.** K<sub>2</sub>CO<sub>3</sub>, PhCl, 130 °C, 40%; **e.** Br<sub>2</sub> (1 equiv.), DMSO, r.t., 1h, 60%.

Horne reported the conversion of DHO (**2.2**) to dispacamide A (**2.16**) under oxidative conditions using bromine in DMSO (**Scheme 3.1**).<sup>3</sup> Horne also conducted the biomimetic synthesis of slagenin A-C by treating **3.2** with NCS in methanol to afford slagenins B (**2.41**) and C (**2.42**), both of which under acidic condition led to the formation of slagenin A (**2.40**) (**Scheme 3.2**).<sup>4</sup>



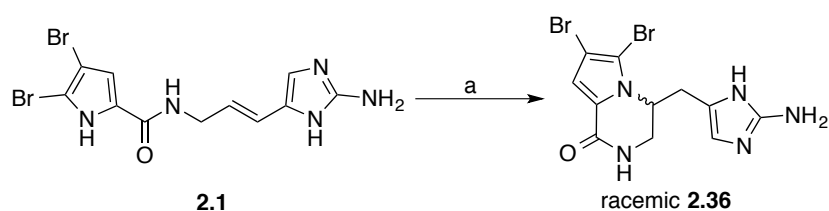
**Scheme 3.2** Horne's biomimetic synthesis of the slagenins. Reaction conditions: **a.** NCS, MeOH; **b.** H<sub>2</sub>O, H<sup>+</sup>.

Horne also took a biomimetic approach towards the synthesis of (*Z*)-hymenialdesine (**2.48**) and its brominated analogues starting from hymenin (**2.44**) (**Scheme 3.3**).



**Scheme 3.3** Biomimetic synthesis of the aldesines starting from hymenin. Reaction conditions: **a.** Br<sub>2</sub>, TFA, 95%; **b.** AcOH, H<sub>2</sub>O, reflux, 72%; **c.** MeSO<sub>3</sub>H, cat. HBr, sealed tube, 33% and 27% respectively; **d.** Br<sub>2</sub>, AcOH/NaOAc, 85%.

Lindel and co-workers reported the efficient conversion of oroidin into racemic cyclooroidin by heating oroidin in a protic medium (**Scheme 3.4**).<sup>5</sup>

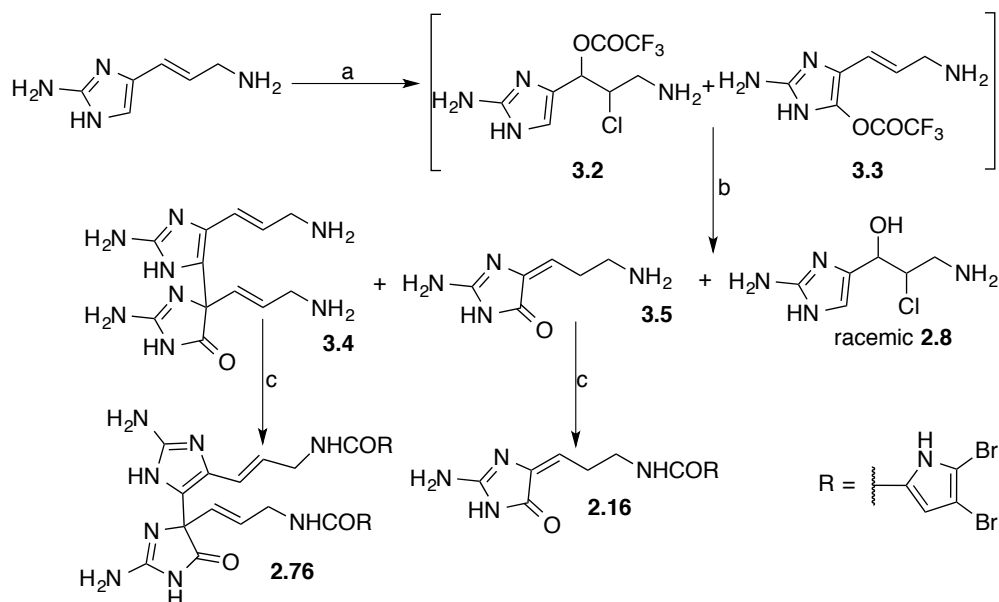


**Scheme 3.4** Lindel's conversion of oroidin into racemic cyclooroidin. **a.** H<sub>2</sub>O/EtOH (4:1), 95 °C, sealed tube, 45 h, 93%.

Horne's biomimetic strategy in the synthesis of the dimer mauritiamine involved joining the two pre-synthesised intermediates **3.2** and **3.3**, formed by the treatment of 3-amino-1-(2-aminoimidazolyl)-prop-1-ene with NCS in TFA. Heating

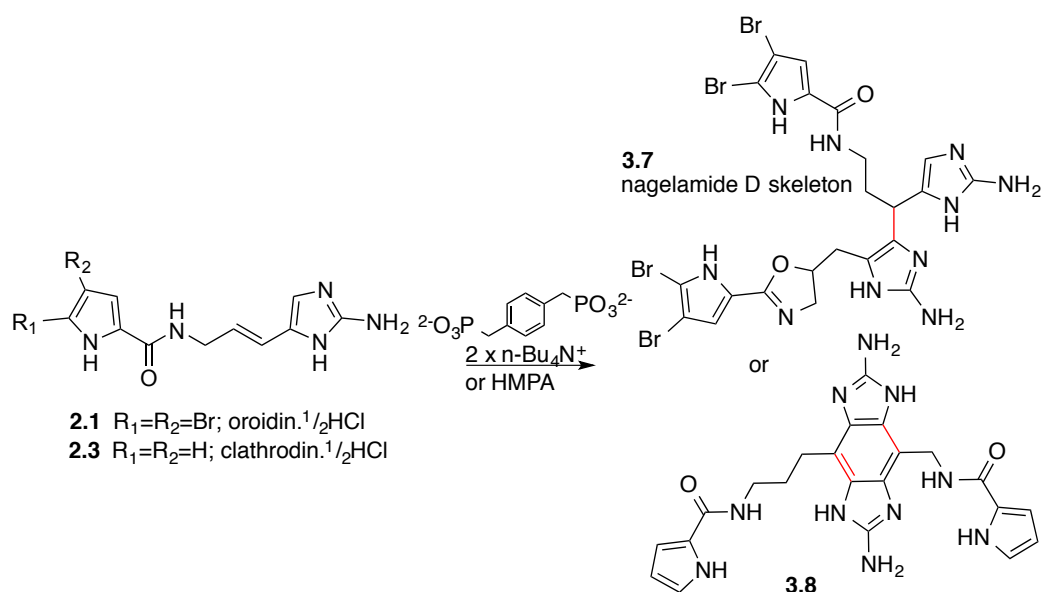


the two intermediates in a mixture of methanol/xylene also led to the formation of racemic girolline (**2.8**) and **3.5**. Condensation of **3.4** and **3.5** with 4,5-dibromotrichloroacetylpyrrole provided mauritiamine (**2.76**) and dispacamide A (**2.16**) respectively (**Scheme 3.5**).



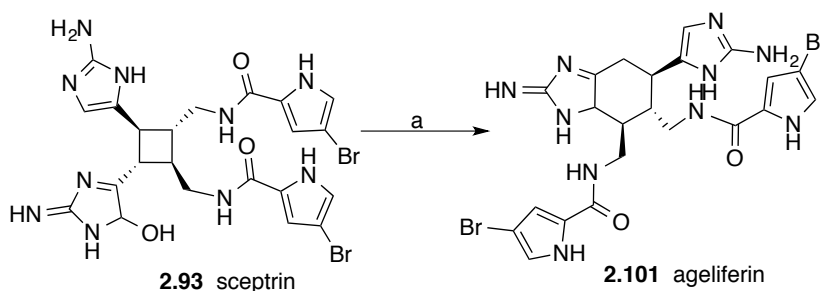
**Scheme 3.5** Biomimetic steps in the synthesis of mauritiamine, girolline and dispacamide A. Reaction conditions: **a.** NCS, TFA, r.t; **b.** MeOH/xylene, 135 °C, 23%; **c.** 4,5-dibromotrichloroacetylpyrrole (**3.6**), DMF, r.t, 65%.

Recently, the first example of the dimerisation of the biogenetic precursors oroidin and clathrocin without enzymatic catalysis, was reported by Al-Mourabit and co-workers using molecular tweezers to yield the nagelamide D skeleton **3.7**, however in low yields (**Scheme 3.6**).<sup>6</sup> They used hexamethylphosphoramide (HMPA) and diphosphonate salts as strong guanidinium and amide chelating agents to interfere with the intramolecular preorganisation to favour intermolecular reaction with kinetic preference for the dimerisation process.



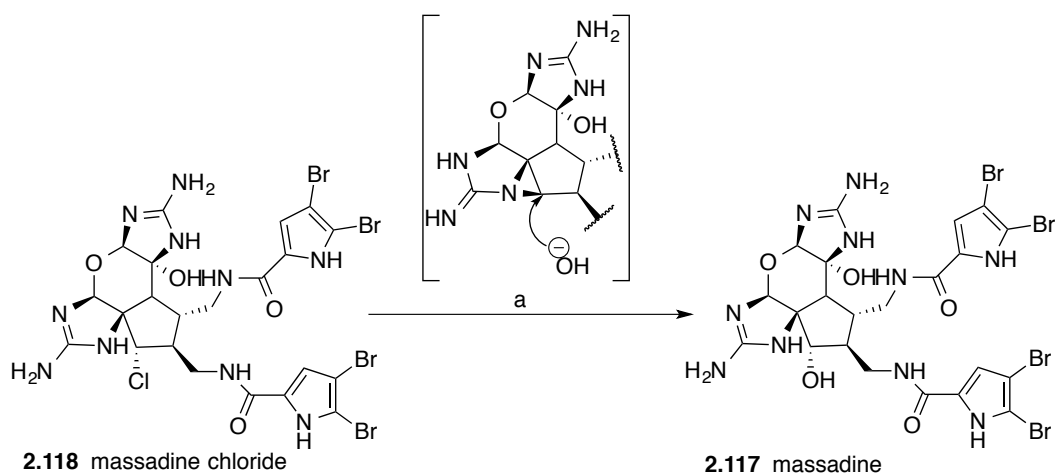
**Scheme 3.6** Oroidin and clathroдин homodimerisation. Reactions were conducted in DMSO at 130 °C for 6 h. Yields are 5% and 10% respectively for the nagelamide D **3.7** and benzene para-symmetrical structure **3.8**.

Baran has reported the remarkable conversion of sceptrin into ageliferin under microwave irradiation (**Scheme 3.7**).<sup>7</sup> The rearrangement could be via a radical or ionic mechanism.



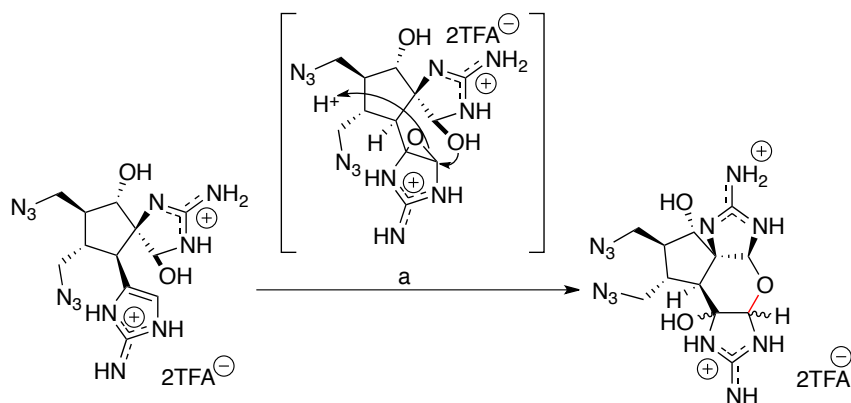
**Scheme 3.7** Conversion of sceptrin to ageliferin. Reaction conditions: **a.** H<sub>2</sub>O, 195 °C, 1 min, microwave, 40%.

Baran has also reported the rapid conversion of massadine chloride into massadine in aqueous media at 60 °C (**Scheme 3.8**).<sup>8</sup> The reaction is thought to proceed through an aziridinium intermediate for the retention of configuration.



**Scheme 3.8** Conversion of massadine chloride to massadine. Reaction conditions: **a.** H<sub>2</sub>O, 60 °C, 4h, quantitative.

In the quest for the synthesis of several complex oroidin alkaloids, Baran has made use of biomimetic steps that involved the formation of a putative imidazole epoxide in order to effect intramolecular cyclisation. One such example was provided earlier on in the synthesis of the axinellamine.<sup>9</sup> Intramolecular cyclisation was effected through the oxidation of the imidazole carbon double bond by DMDO to make the C12-N15' connection required in the axinellamines and at the same time introduce a hydroxyl group on C11' (**Scheme 2.17**).<sup>9</sup> In a similar example, the ether bond in massadine was formed through the oxidation of the imidazole carbon double bond by DMDO followed by addition of TFA (**Scheme 3.9**).<sup>10</sup>

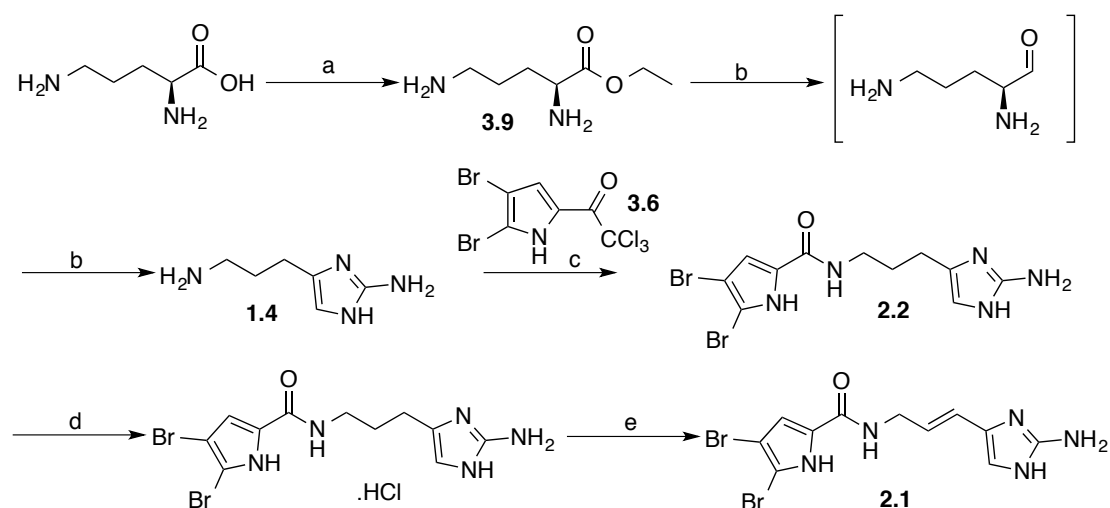


**Scheme 3.9** Formation of the ether bond in the massadine scaffold. Reaction conditions: **a.** 1. DMDO, H<sub>2</sub>O-TFA, 2. TFA, 65% over two steps.

Both of these intramolecular cyclisations suggest the intermediacy of an imidazole epoxide that induces a nucleophilic attack by an internal nucleophile to form the desired ring in the oroidin alkaloid. While there are few examples of imidazole epoxidation, looking at the biogenesis of oroidin alkaloids (see **Chapter 2**; **Section 2.7**), it is apparent that epoxidation could explain the biogenesis of almost all of the group of alkaloids. We set about to test this hypothesis.

### 3.2. Results and Discussion

To begin our investigation, dihydrooroidin was synthesised using literature methods (**Scheme 3.10**).<sup>3</sup> The direct conversion of DHO (**2.2**) to oroidin (**2.1**), reported by Lindel<sup>11</sup> was then undertaken by first forming the 5-chlorodihydrooroidin in the presence of NCS in DMF at r.t and then subsequent elimination of HCl to provide oroidin (**2.1**) (**Scheme 3.10**).

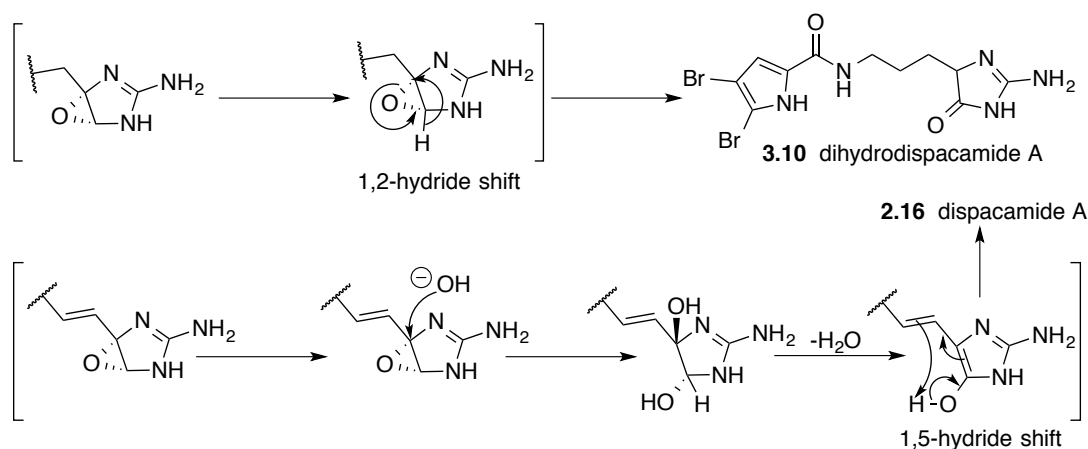


**Scheme 3.10** Synthesis of DHO and oroidin. Reaction conditions: **a.** thionyl chloride, EtOH, 0 °C to reflux, 24 h, quant; **b.** 1. NaHg, H<sub>2</sub>O, 0-7 °C, pH 1-2, 1 h, 2. cyanamide, pH 4.5, reflux, 3 h, 8%; **c.** K<sub>2</sub>CO<sub>3</sub>, DMF, r.t, ON, 80%; **d.** conc. HCl, MeOH, reflux, 12 min, quant; **e.** 1. NCS, DMF, r.t, 1 h, 2. 100 °C, 1 h, 20%.

### 3.2.1. Epoxidation using DMDO

DMDO is one of the most used dioxiranes and has allowed access to highly sensitive epoxides that are otherwise difficult to obtain with more classical oxygen atom transfer reagents.<sup>12,13</sup> DMDO has proven to be versatile, with various kinds of alkenes, either electron-rich or electron-poor, successfully epoxidised.<sup>14</sup> Moreover, the use of dioxiranes is preferred over peracids in epoxidation reactions due to the enhanced rates of reaction and of their performance under neutral and mild conditions.<sup>14</sup>

DMDO was generated *in situ* by adding acetone to an aqueous solution of potassium peroxymonosulfate (oxone) in the presence of NaHCO<sub>3</sub> as base.<sup>15</sup> When DHO was subjected to *in situ* formed DMDO, dihydrodispacamide A was isolated in 21% yield as the main product along with a mixture of unidentified products (**Table 3.1, Entry 1**). Similarly when oroidin was subjected to the same treatment, the natural product displacamide A was isolated in 12% yield from a complex reaction mixture (**Entry 2**). Both products obtained, point to the formation of an imidazole epoxide intermediate (**Scheme 3.11**).



**Scheme 3.11** Formation of dihydrodispacamide A and displacamide A via the an imidazole epoxide.

With the aim of trapping the imidazole epoxide intermediate with an external nucleophile, taurine was included in the reaction with DHO as substrate (**Table 3.1, Entry 3**). If taurine opened the imidazole epoxide, mauritamide A (**2.31**) would be formed (**Scheme 2.21**). Unfortunately LCMS analysis did not show any detectable presence of the mass corresponding to mauritamide A. Dihydrodispacamide A (**3.10**) was the main product, isolated in 18% yield.

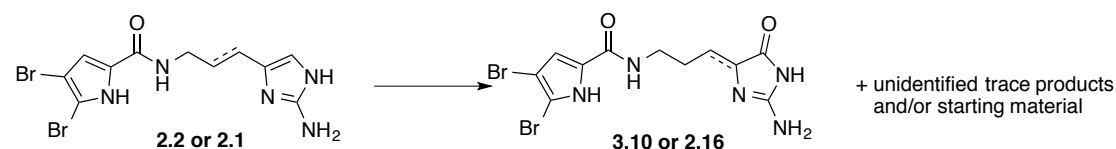
With the *in situ* generation of DMDO, water is always present and will compete with other nucleophiles for the ring opening of the epoxide. In order to overcome this problem, DMDO was also prepared as a solution in acetone and the distillate dried over anhydrous sodium sulfate.<sup>16</sup>

Unfortunately, DHO and oroidin were not soluble in acetone or ACN, only. Thus, a solution of DMDO in acetone was added to a solution of the substrate dissolved in DMF at 0 °C and led to an improvement in the yields of dihydrodispacamide A (56%) and displacamide A (60%) for DHO and oroidin respectively (**Table 3.1, Entry 4 and 5**).

An organic base (DBU) and an inorganic base (NaHCO<sub>3</sub>) were added to the reaction solution, in order to facilitate intramolecular cyclisation to pyrrole N1/C4 (**Scheme 2.22**). Much to our disappointment, only dihydrodispacamide A and displacamide A were obtained as the main products in their respective reaction along with decompositions (**Table 3.1; Entry 6, 7 and 8**). The same result was obtained when butylamine was added as a base/nucleophile, again with the isolation of dihydrodispacamide A only (**Entry 9**). All these reactions proceeded in low yield, mostly with decomposition. Similar results were obtained when methanol was used as solvent at very low temperatures (**Entry 10-12**). The low temperatures (as low as –

120 °C) and short reaction time used (**Table 3.1**), indicate that DMDO is very reactive, readily forming the imidazole epoxide which is short lived, before undergoing a hydride shift to give the imidazolones (**Scheme 3.11**).

**Table 3.1** Epoxidation reaction of DHO **2.2** or oroidin **2.1** with DMDO under different conditions.



Entry	Reagent <sup>a</sup>	Conditions	Yield (%) <sup>b</sup>
1	oxone, acetone, NaHCO <sub>3</sub>	H <sub>2</sub> O, 0°C, 1 h	21
2 <sup>c</sup>	oxone, acetone, NaHCO <sub>3</sub>	H <sub>2</sub> O, 0°C, 1 h	12 <sup>d</sup>
3	oxone, acetone, taurine	H <sub>2</sub> O, 0°C, 1 h	18
4	DMDO	DMF, 0°C to r.t, 1h	56
5 <sup>c</sup>	DMDO	DMF, 0°C to r.t, 1h	60 <sup>d</sup>
6	DMDO, DBU	DMF, 0°C to r.t, ON	39
7	DMDO, NaHCO <sub>3</sub>	DMF, 0°C to r.t, ON	35
8 <sup>c</sup>	DMDO, NaHCO <sub>3</sub>	DMF, 0°C to r.t, ON	29 <sup>d</sup>
9	DMDO, butylamine	DMF, -78°C to r.t, 1h	41
10	DMDO	MeOH, -78°C, 10 min	54
11	DMDO, Cs <sub>2</sub> CO <sub>3</sub>	MeOH, -120°C, 30 min	38
12	DMDO, butylamine	MeOH, -120°C, 30 min	35

DMDO was prepared as a solution in acetone. The concentration was determined using iodometric titration before use and ranged between 0.05-0.09 M. DMDO was used in 1.2 equiv. **a.** 1.1 equiv. of the base used for **entry 6-9 and 11-12**; **b.** isolated yield; **c.** oroidin used as substrate; **d.** % yield of dispacamide A.

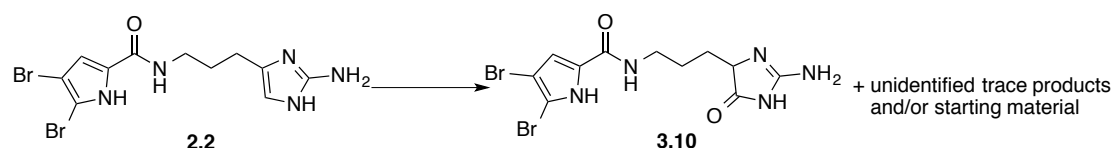
### 3.2.2. Other Epoxidation Conditions

The use of peracids<sup>17</sup>, perbenzoic acid and mCPBA, led to complex reaction mixtures of unidentifiable products, while the use of the hypervalent iodine reagent diacetoxyiodobenzene (DIB)<sup>18,19</sup> led to the isolation of the dihydrodispacamide A and

dispacamide A from DHO and oroidin respectively, along with starting material (**Table 3.2; Entry 1-3** and **Table 3.3; Entry 1-3**).

While DMDO provided the best result thus far, the difficulties faced with DMDO are its preparation, variable concentration and the presence of variable levels of water. *N*-sulfonyloxaziridines have similar characteristics to dioxiranes with the added benefit of being stable, crystalline and less reactive.<sup>20</sup> These reagents are readily accessible by oxidation of the corresponding *N*-sulfonylimines, which in turn can be obtained from aldehydes.<sup>20,21</sup> When DHO was used as substrate with two different *N*-sulfonyloxaziridines **3.11** and **3.12**, only dihydrodispacamide A (**3.10**) was isolated (**Table 3.2, Entry 4** and **Entry 6**). The use of 2 equivalents of *N*-sulfonyloxaziridine **3.11** on DHO, led to the isolation of displacamide A (**2.16**) from the double oxidation of the substrate (**Entry 5**).

**Table 3.2** Other epoxidation reagents tried on DHO as substrate.



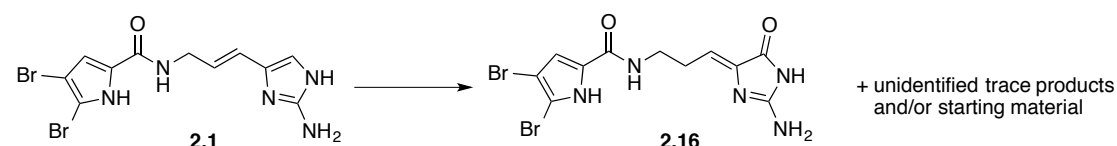
Entry	Reagent <sup>a</sup>	Conditions	Yield of <b>3.10</b> (%)
1	DIB, TFA	DMF/ACN, 0°C to r.t	11
2	peroxybenzoic acid	MeOH, 0°C-r.t, 1h	dec.
3	m-CPBA	MeOH, 0°C-r.t, ON	3
4	<b>3.11</b> , K <sub>2</sub> CO <sub>3</sub>	MeOH, r.t, 4 h	18
5	<b>3.11</b> (2 equiv.), K <sub>2</sub> CO <sub>3</sub>	MeOH, r.t, 4 h	9 <sup>b</sup>
6	<b>3.12</b> , K <sub>2</sub> CO <sub>3</sub>	MeOH, r.t, ON	8

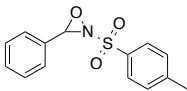
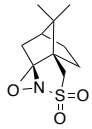
ON: overnight; **a.** All reagents used in 1 equivalent unless otherwise stated; **b.** Isolated yield of displacamide A (**2.16**)



*N*-sulfonyloxaziridines show preference for activated carbon double bond<sup>22</sup> such that enamines react faster than enols which react faster than alkenes. As the imidazole is formally a double enamine, the *N*-sulfonyloxaziridines were expected to react at the imidazole carbon double bond over the alkene in oroidin (**2.1**). However this selectivity was not observed and while the *N*-sulfonyloxaziridine **3.12** gave dispacamide A (**2.16**), **3.11** led to a complex mixture (Table 3.3; Entry 4-5).

**Table 3.3** Other epoxidation reagents tried on oroidin as substrate.

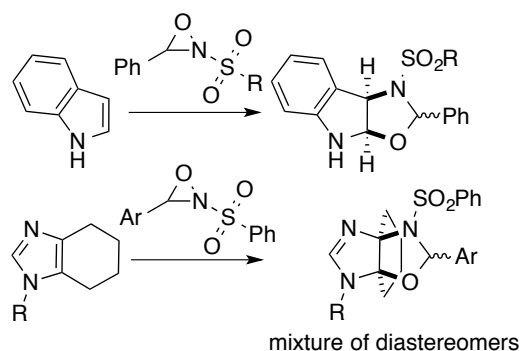


Entry	Reagent	Conditions	Yield of <b>2.16</b> (%)
1	DIB, TFA	DMF/ACN, 0°C to r.t	dec.
2	peroxybenzoic acid	MeOH, 0°C-r.t, 1 h	dec.
3	m-CPBA	MeOH, 0°C-r.t, ON	dec.
4	 <b>3.11</b> , K <sub>2</sub> CO <sub>3</sub>	MeOH, r.t, 1 h	dec.
5	 <b>3.12</b> , K <sub>2</sub> CO <sub>3</sub>	MeOH, r.t, ON	11

a. isolated yield; ON: overnight

There was evidence from DI-MS of the crude reaction mixture containing fragments derived from the oxaziridine, which were not isolated. There has been reported precedence of such occurrence. For example, Dmitrienko isolated oxaziridine–alkene cycloadducts formed by the addition of the oxaziridine across indole 2,3-bond as the major products when simple benzaldehyde-derived

oxaziridines were used (**Scheme 3.12**).<sup>23</sup> Lovely isolated adducts formed through the addition of the oxaziridine across the imidazole 4,5-bond (**Scheme 3.12**).<sup>24</sup>

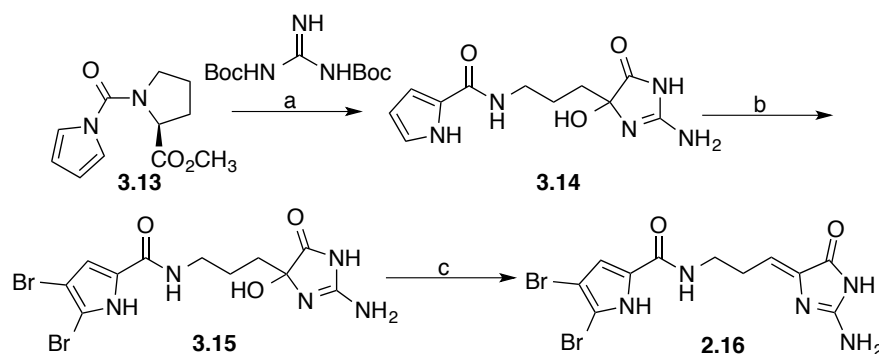


**Scheme 3.12** Evidence of oxaziridine-substrate adducts.

### 3.2.3. Biomimetic synthesis of Dispacamide A and Unnatural Dihydrodispacamide A

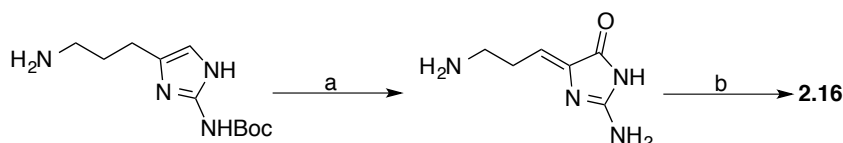
Dispacamide A, a potent, non-competitive, antihistaminic agent and a fish feeding deterrent, was been isolated in 1996 by Fattorusso and co-workers from the sponge *Agelas dispar*.<sup>25</sup> In displacamide A, the oroidin 2-aminoimidazole moiety has been oxidised to an alkylidene glycoxyamidine. Two years after its isolation, Horne reported the conversion of DHO (**2.2**) to displacamide A (**2.16**) in 60% yield under oxidative conditions using bromine in DMSO (**Scheme 3.2**).<sup>3</sup> Since then, several total syntheses of displacamide A have been reported and reviewed.<sup>3,26-29</sup>

Al-Mourabit's synthesis of displacamide A follows his proposed biogenesis hypothesis which involves the one-pot reaction of the pseudodipeptide pyrrole-proline methyl ester **3.13** in the presence of diBoc-guanidine and oxygen at reflux in THF.<sup>29,30</sup> This afforded the 5-hydroxy-2-aminoimidazole **3.14** which, following bromination of the pyrrole gave **3.15**. Removal of the Boc group and elimination of water led to the formation of displacamide A (**2.16**) (**Scheme 3.13**).<sup>29</sup>



**Scheme 3.13** Al-Mourabit's synthesis of dispacamide A. **a.** THF, O<sub>2</sub>, reflux, 3 h, 46%; **b.** 1. Br<sub>2</sub>, AcOH, r.t., 2. TFA, CH<sub>2</sub>Cl<sub>2</sub>, r.t., 74%; **c.** MeSO<sub>3</sub>H, 80 °C, 65%.

In Ando's strategy, tetra-*n*-butylammonium tribromide was employed to oxidise the imidazole ring in a 2-aminohomohistamine where the primary amino group of the imidazole ring was selectively Boc-protected (**Scheme 3.14**).<sup>28</sup> The pyrrole part of the natural product was introduced in the last step of the synthesis.



**Scheme 3.14** Ando's synthesis of dispacamide A. **a.** 1. Bu<sub>4</sub>N<sup>+</sup>Br<sub>3</sub><sup>-</sup>, DMSO, 2. Boc<sub>2</sub>O, MeOH, 40%; **b.** 1. HCl 20%, EtOH, 2. 4,5-dibromotrichloroacetylpyrrole, Na<sub>2</sub>CO<sub>3</sub>, DMF, r.t., 85%.

### 3.3. Summary- Epoxidation Route

Our approach has allowed the direct conversion of oroidin (**2.1**) to dispacamide A (**2.16**) via the formation of a putative epoxide intermediate, in the same yield as Horne's synthesis<sup>3</sup>. In a similar way, DHO (**2.2**) produced dihydrodispacamide A (**3.10**), an unnatural product in 56% yield. However, we were unsuccessful in trapping the putative epoxide either via intramolecular cyclisation or by external nucleophiles.

## PART B: Investigation of the Bromonium Ion Route

### 3.4. Introduction

A bromonium ion is isosteric with an epoxide and can be easily converted to the latter with water via a halohydrin (**Scheme 2.18**; **Section 2.6**). Such transformation can occur via haloperoxidases. Standard electrophilic bromine sources include Br<sub>2</sub>, *N*-bromosuccinimide (NBS) and 2,4,4,6-tetrabromocyclohexa-2,5-dienone (TBCO), and are briefly reviewed in the context of terpene chemistry which is of particular interest to our investigation of the oroidin alkaloids as it involves the initiation of cation- $\pi$ -cyclisations with electrophilic bromine.<sup>31-38</sup>

#### 3.4.1. Biomimetic Cyclisation: Lessons from Terpene Chemistry

Terpenes are a class of natural products currently spanning well over 55 000 members.<sup>39</sup> A seemingly endless number of enzyme (terpene synthase/cyclase)-mediated carbocation cyclisations leads to many different carbocyclic skeletons, which are often further oxidised and rearranged (e.g. Wagner-Meerwein).<sup>39</sup> Intramolecular cyclisation is initiated in terpenoid biosynthesis by protonation (e.g. in lupeol), epoxidation (e.g. in aplysin-20) or halogenation (e.g. in albicanol) (**Figure 3.1**).<sup>40-43</sup>

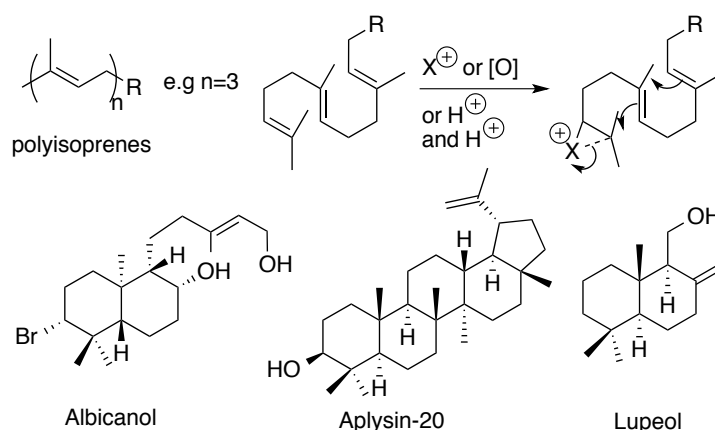


**Figure 3.1** Cationic or epoxide induced cyclisation of polyisoprenes.

Of particular interest in our oroidin alkaloids work, is the occurrence of brominated terpenes typically produced by marine microorganisms. Brominated terpenes have been isolated as secondary metabolites from numerous marine organisms and to date there are more than 135 bromine-containing members of this natural product family (**Figure 3.2**).<sup>44</sup> The biosynthesis of these natural products is thought to involve the action of vanadium bromoperoxidases whereby the formation of a key bromonium ion intermediate of the polyene would initiate the intramolecular domino cyclisation needed to form a number of new C-C bonds, rings and quaternary stereocentres stereoselectively to give complex molecules from linear substrates.<sup>45,46</sup>

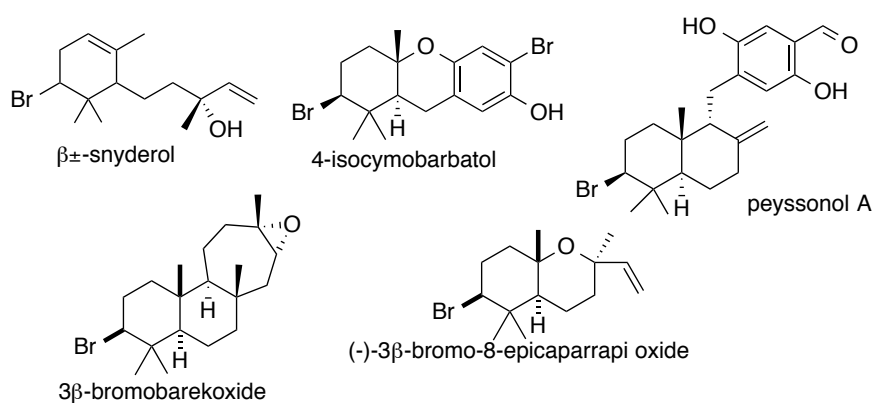
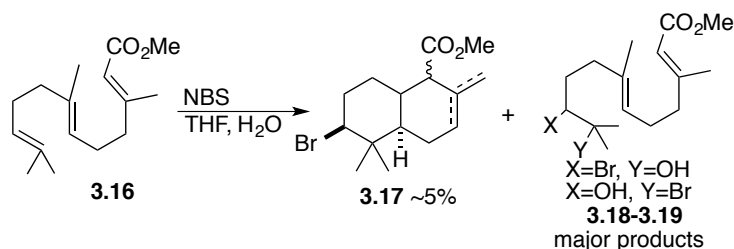


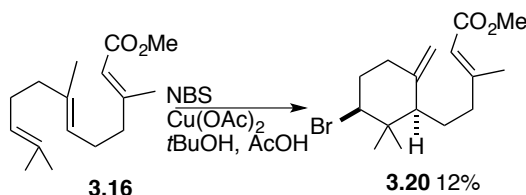
**Figure 3.2** Examples of brominated terpenoids isolated from *Laurencia* species.

The first bromonium-ion induced cation- $\pi$  cyclisation in the laboratory was reported in 1966 by van Tamelen and Hessler.<sup>36</sup> They found that the reaction of NBS with methyl farnesate (**3.16**) in water-ethylene glycol mixture or THF gave rise to bicycle **3.17** as a mixture of endo- and exocyclic alkenes in ~5% yield (**Scheme 3.15**). Mono-bromohydrins **3.18-3.19** of the terminus alkene represented the major product.



**Scheme 3.15** Brominative cyclisation of methyl farnesate **3.15** using NBS.

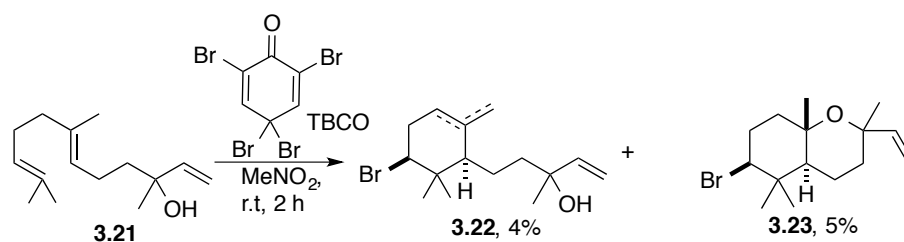
A decade later, copper (II) acetate was used as an additive in *t*-butanol and acetic acid to improve on van Tamelen's conditions.<sup>31</sup> Monocyclic adduct **3.20** was isolated in 12% yield (**Scheme 3.16**).



**Scheme 3.16** Brominative cyclisation of methyl farnesate **3.15** using NBS and Cu(OAc)<sub>2</sub>.

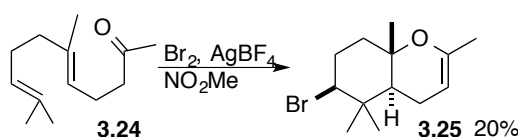
Kato and co-workers found 2,4,4,6-tetrabromocyclohexa-2,5-dienone (TBCO) to be a useful reagent for the brominative cyclisation of polyene precursors in the synthesis of up to three rings.<sup>32</sup> They have shown the utility of this reagent in presumed biomimetic syntheses of a number of natural products, albeit in low yields.<sup>33,34,38</sup> For example, when TBCO was used in the brominative cyclisation of nerolidol (**3.20**),  $\alpha$  and  $\beta$ -snyderol (**3.21**) and racemic 3-bromo-8-epicaparrapi oxide

(**3.22**) were formed (**Scheme 3.17**), which are marine natural products that have been isolated from *Laurencia* spp.<sup>32</sup>



**Scheme 3.17** Biomimetic syntheses of racemic snyderol and racemic 3-bromo-8-epicaparrapi oxide using TBCO.

Molecular bromine and silver tetrafluoroborate were also used to effect the bromonium-induced cyclisation of polyenes (**Scheme 3.18**).<sup>37</sup> Ketone **3.24** underwent bromonium ion induced cyclisation to form bicycle **3.25** in 20% yield. The purpose of AgBF<sub>4</sub> was to sequester the nucleophilic bromide ions as they were produced.

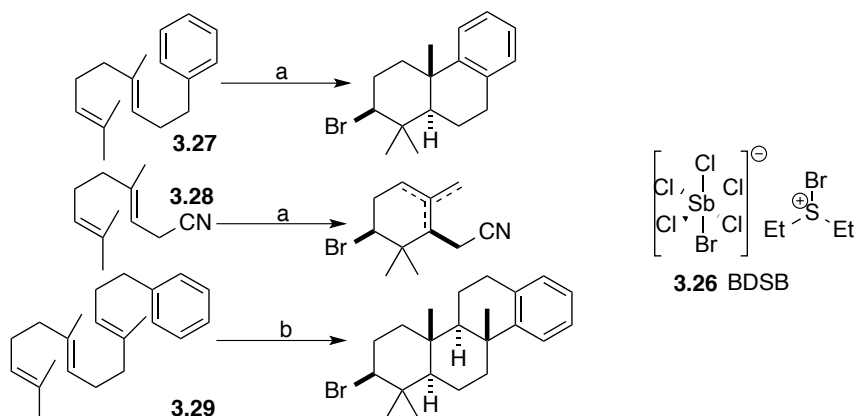


**Scheme 3.18** Brominative cyclisation of geranyl acetone **3.24** using molecular bromine and silver tetrafluoroborate.

All these methods produce electrophilic bromonium in the absence of an effective nucleophile to allow the organic bromonium ion time to cyclise. However, most methods of direct brominative cyclisation are low-yielding.

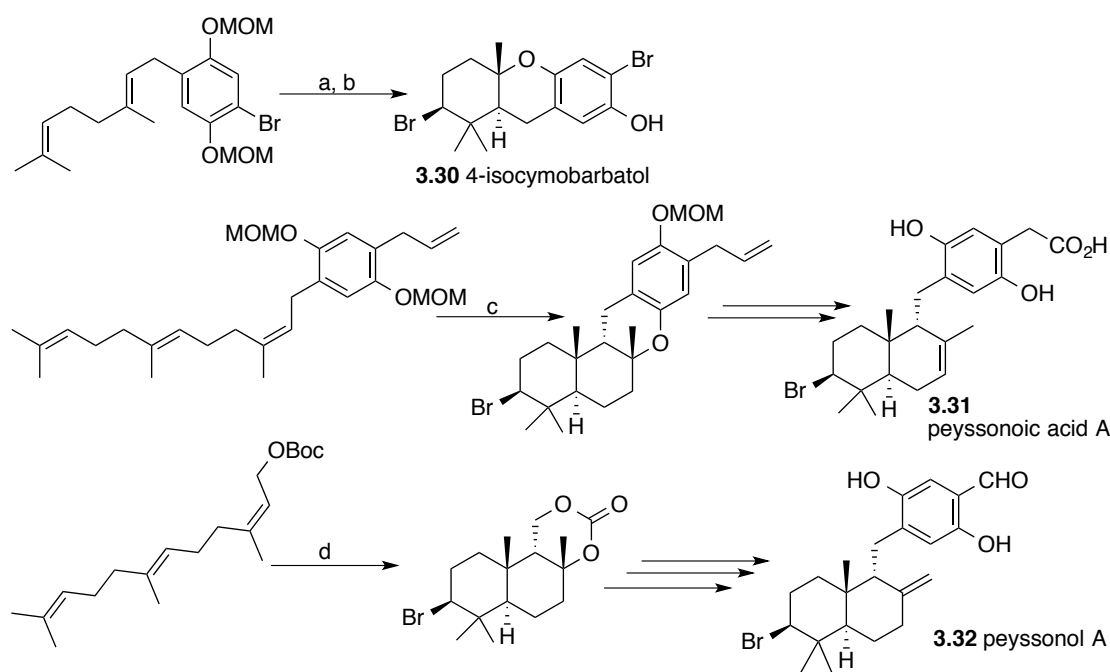
Bromodiethylsulfide bromopentachloroantimonate (BDSB) (**3.26**) was recently introduced by Snyder and Treitler in 2009. It is a source of electrophilic bromine, supposedly free from any additional nucleophilic species which allows for highly efficient bromonium ion induced cation- $\pi$  cyclisations of a diverse set of polyenes derived from geraniol (such as **3.27** and **3.28**) and farnesol (such as **3.29**), in

>55% yield, usually within 5 minutes (**Scheme 3.19**).<sup>35</sup> Larger polyenes derived from farnesol (such as **3.29**) require the addition of a strong acid (e.g. methanesulfonic acid) to effect full cyclisation.<sup>35</sup>



**Scheme 3.19** Bromonium ion induced cyclisations of polyenes using BDSB. Reaction conditions: a. BDSB, MeNO<sub>2</sub>, –25°C, 5 min, 73–75%; b. BDSB, MeNO<sub>2</sub>, –25°C, 5 min then MeSO<sub>3</sub>H, 58%.

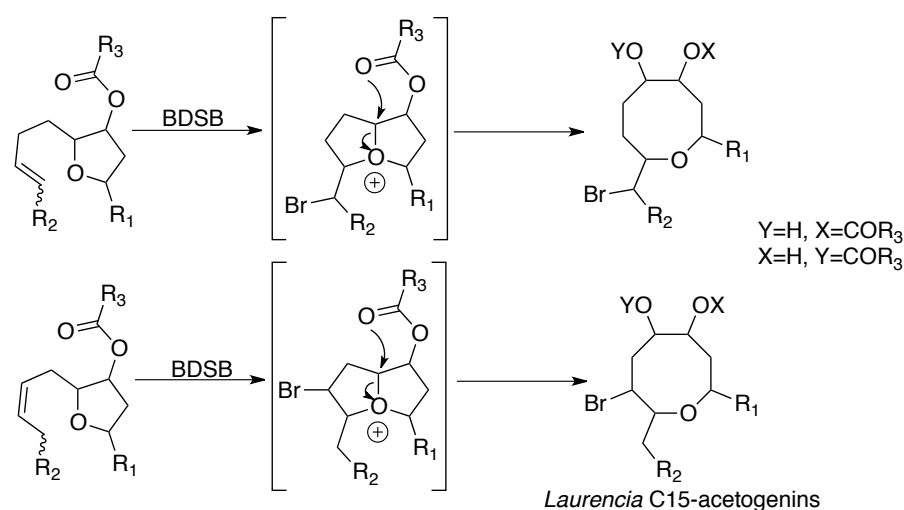
Bromonium ion-induced cyclisations using BDSB have been successfully applied in the biomimetic syntheses of brominated terpenoids: 4-isocymobarbatol (**3.30**), peyssonoic acid A (**3.31**) and peyssonal A (**3.32**) (**Scheme 3.20**).<sup>35,47</sup>



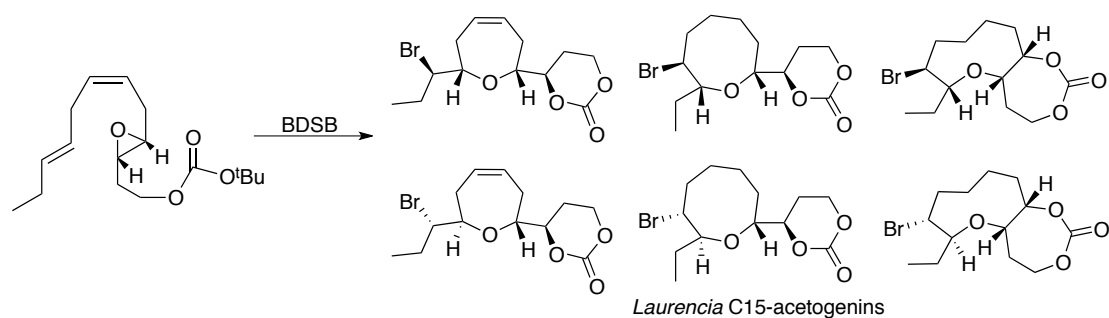
**Scheme 3.20** Total synthesis of 4-isocymobarbatol, peyssonoic acid A and peyssonal A. Reaction conditions: a. BDSB, MeNO<sub>2</sub>, –25 °C, 5 min, 74%; b. HCl (conc.), THF, 25 °C, 5 h, 97%; c. BDSB, MeNO<sub>2</sub>, –25 °C, 5 min, 31%; d. BDSB, MeNO<sub>2</sub>, –25 °C, 5 min then 25 °C, 60 min, 56%.



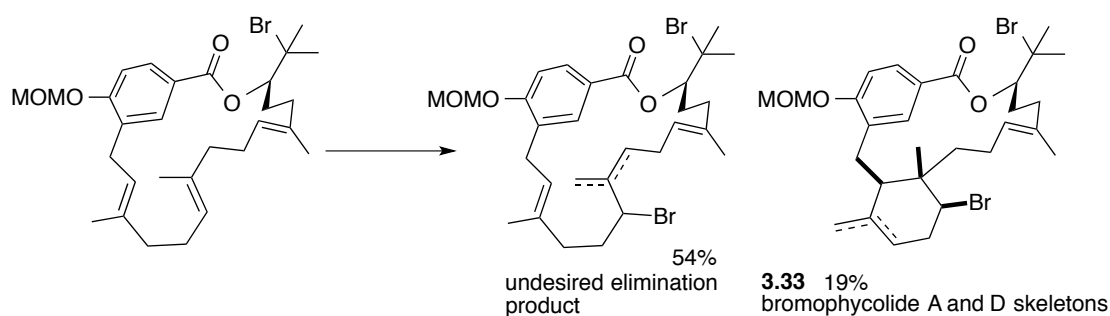
The groups of Snyder and Braddock made use of BDSB in order to access the *Laurencia* C15-acetogenins. Snyder used a ring-expanding bromoetherification of tetrahydrofurans (**Scheme 3.21**) while Braddock using an intramolecular bromonium ion assisted epoxide ring-opening reaction (**Scheme 3.22**).<sup>48,49</sup> Another example is the construction of alkenic regioisomers, bromophycolide A and D skeletons (**3.33**) that was achieved via a diastereoselective bromonium ion-induced cyclisation of a triene substrate, albeit in low yield with the competitive elimination product being the major product (**Scheme 3.23**).<sup>50</sup>



**Scheme 3.21** Ring-expanding bromoetherification using BDSB to access the *Laurencia* C15-acetogenin scaffolds from tetrahydrofurans.



**Scheme 3.22** Bromonium induced cyclisation with BDSB to access the *Laurencia* C15-acetogenin scaffolds starting from an epoxide.



**Scheme 3.23** The use of BDSB to access the bromophycolide A and D skeletons.

The advantages (mild, short reaction time and high yields) associated with BDSB prompted us to apply this reagent on oroidin and DHO. But first we wanted to investigate the utility of BDSB on pyrrole-terpene hybrids that would be considered oroidin analogues (**Figure 3.3**). The reactivity of BDSB in the presence of heterocyclic nitrogen atom as well as amide, have not been investigated before.

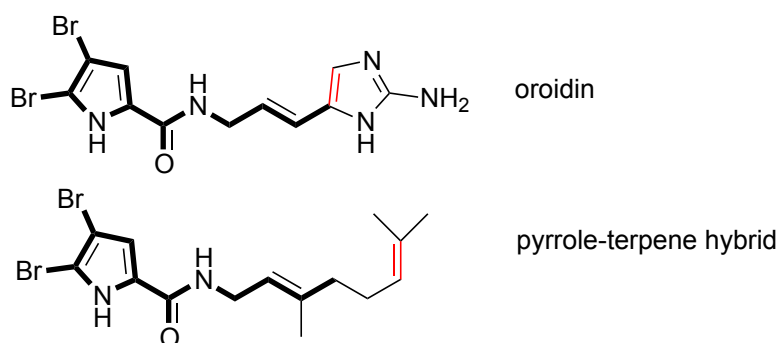


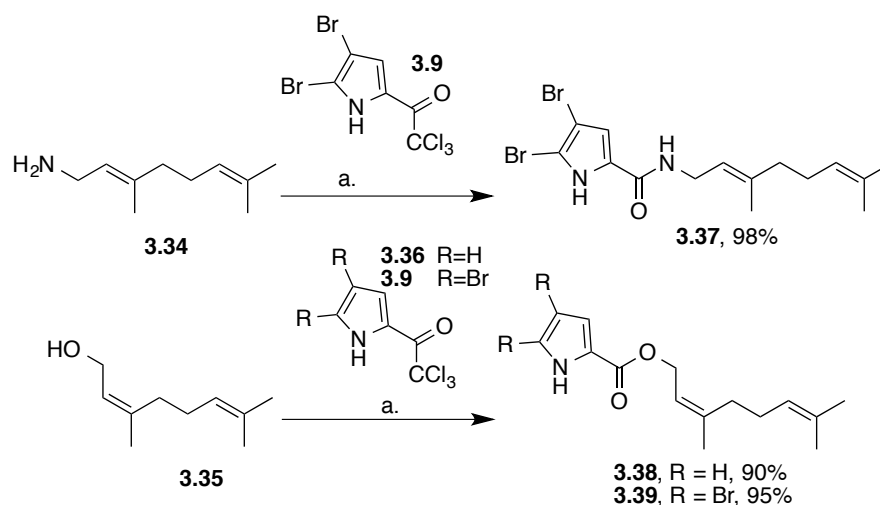
**Figure 3.3** Structural similarity between oroidin and the pyrrole-terpene hybrid

### 3.5. Results and Discussion

#### 3.5.1. Initial Investigation into Bromonium-Induced Cyclisation of Pyrrole-Terpene Hybrids

The hybrid pyrrole-terpene substrates were synthesised by the condensation of commercially available geranylamine (**3.34**) or nerol (**3.35**) to either

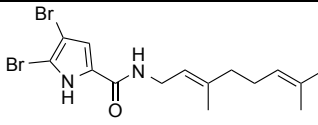
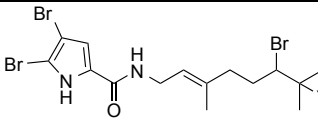
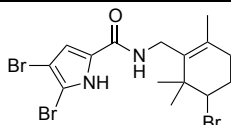
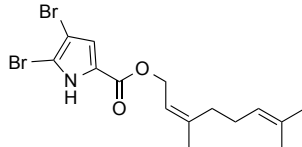
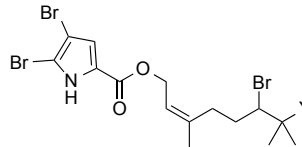
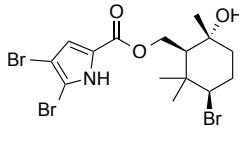
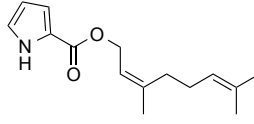
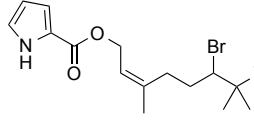
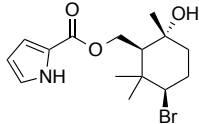
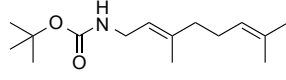
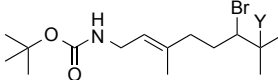
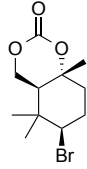
trichloroacetylpyrrole (**3.36**) or dibrominated trichloroacetylpyrrole (**3.9**) in DMF in the presence of  $K_2CO_3$  as base (**Scheme 3.24**).



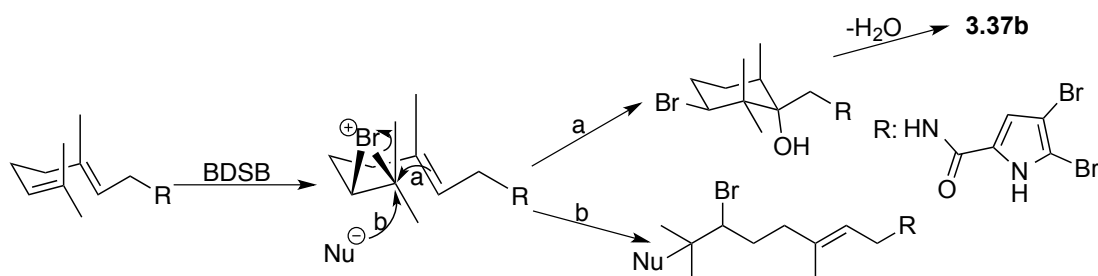
**Scheme 3.24** Synthesis of the pyrrole-terpene hybrids. *a*.  $K_2CO_3$  (3 equiv.), DMF, r.t, ON.

When the reaction was conducted at r.t. or at 0 °C with **3.37**, a complex reaction mixture was obtained. A 1.1 equivalents of BDSB in a reaction solution consisting of the solvent mixture of 1:1 (v/v) ratio MeNO<sub>2</sub>/dichloromethane at an overall concentration of 0.01 M was employed. Decreasing the temperature to −40 °C for the addition of BDSB and subsequent warming to −15 °C over an hour and allowing the reaction to stir at −15 °C for a further 30 min, led to the formation of a cyclised product along with three addition products (**Table 3.4; Entry 1**). The same reaction condition was applied to substrates **3.38-3.40** (**Entry 2-4**).

**Table 3.4** Reaction of the pyrrole-terpene hybrid substrates with BDSB.

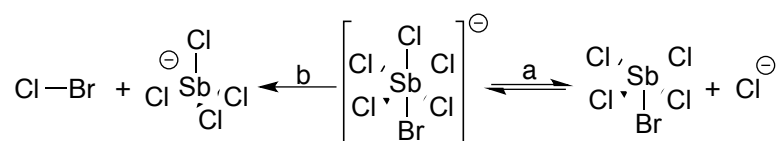
Entry	Substrate	Products (%)
1	 <p><b>3.37</b></p>	 <p><b>3.37a</b> Y=Br 42%  <b>3.37b</b> Y=Cl, 20%  <b>3.37c</b> Y=OH, 17%</p>  <p><b>3.37d</b>, 2%</p>
2	 <p><b>3.38</b></p>	 <p><b>3.38a</b> Y=Br, 43%  <b>3.38b</b> Y=Cl, 17%  <b>3.38c</b> Y=OH, 12%</p>  <p><b>3.38d</b>, 9%</p>
3	 <p><b>3.39</b></p>	 <p><b>3.39a</b> Y=Br, 42%  <b>3.39b</b> Y=Cl, 14%  <b>3.39c</b> Y=OH, 10%</p>  <p><b>3.39d</b>, 5%</p>
4	 <p><b>3.40</b></p>	 <p><b>3.40a</b> Y=Br, 55%  <b>3.40b</b> Y=Cl, trace  <b>3.40c</b> Y=OH, not isolated</p>  <p><b>3.40d</b> not isolated</p>

The products isolated suggest the intermediacy of a bromonium ion at the most activated terminal alkene during the reaction (**Scheme 3.25**), as previously reported with geraniol-derived substrates.<sup>35</sup> The cyclised product **3.37d** formed is a result of elimination of water after intramolecular cyclisation. All the products that failed to cyclise, are the results of the exogenous incorporation of nucleophiles such as water, which would compete with any internal nucleophile. This is likely due to the low rate of intramolecular cyclisation within the intermediate and/or due to the pyrrole amide or ester attached making the olefin electron-deficient.



**Scheme 3.25** Formation of the bromonium ion of the dibromopyrrole-geranylamine substrate leading to the products observed.

The isolation of Cl and Br addition products indicate that Snyder's reagent is not exactly nucleophile free (**Scheme 3.26**). Nucleophilic chloride ion can be produced either through equilibrium (**pathway a**) or disproportionation (**pathway b**). To our knowledge this is the first report of the occurrence of chlorination using the BDSB reagent. It is noted that antimony pentachloride can be used for chlorination and is converted, in the process, into its trichloride salt.<sup>51,52</sup>



**Scheme 3.26** Nucleophilic chloride ion from BDSB.

The stereochemistry for the pyrrole-nerol hybrid substrates **3.38d** and **3.39d**, where H8, CH<sub>3</sub>-10 and Br are on the same side of the molecule, were assigned by coupling constant analysis and NOESY correlations (**Figure 3.4**). Proton H11a ( $J = 13.9, 13.9, 4.1$  Hz), H12a ( $J = 14.7, 14.1, 3.7, 3.4$  Hz) and H12b ( $J = 14.9, 6.5, 3.5, 3.5$  Hz) were assigned axial or equatorial, based on coupling constants while H11b was assigned by default due to signals overlap. Proton H13 is equatorial based on its coupling constant with adjacent H12s ( $J_{13-12a}$  and  $J_{13-12b} = 4.30$  Hz) and on the absence of diaxial NOESY correlations to H11a and H8. Proton H8 has NOESY correlations to both CH<sub>3</sub>-16 and CH<sub>3</sub>-10, and diaxial NOESY correlation to H11a.

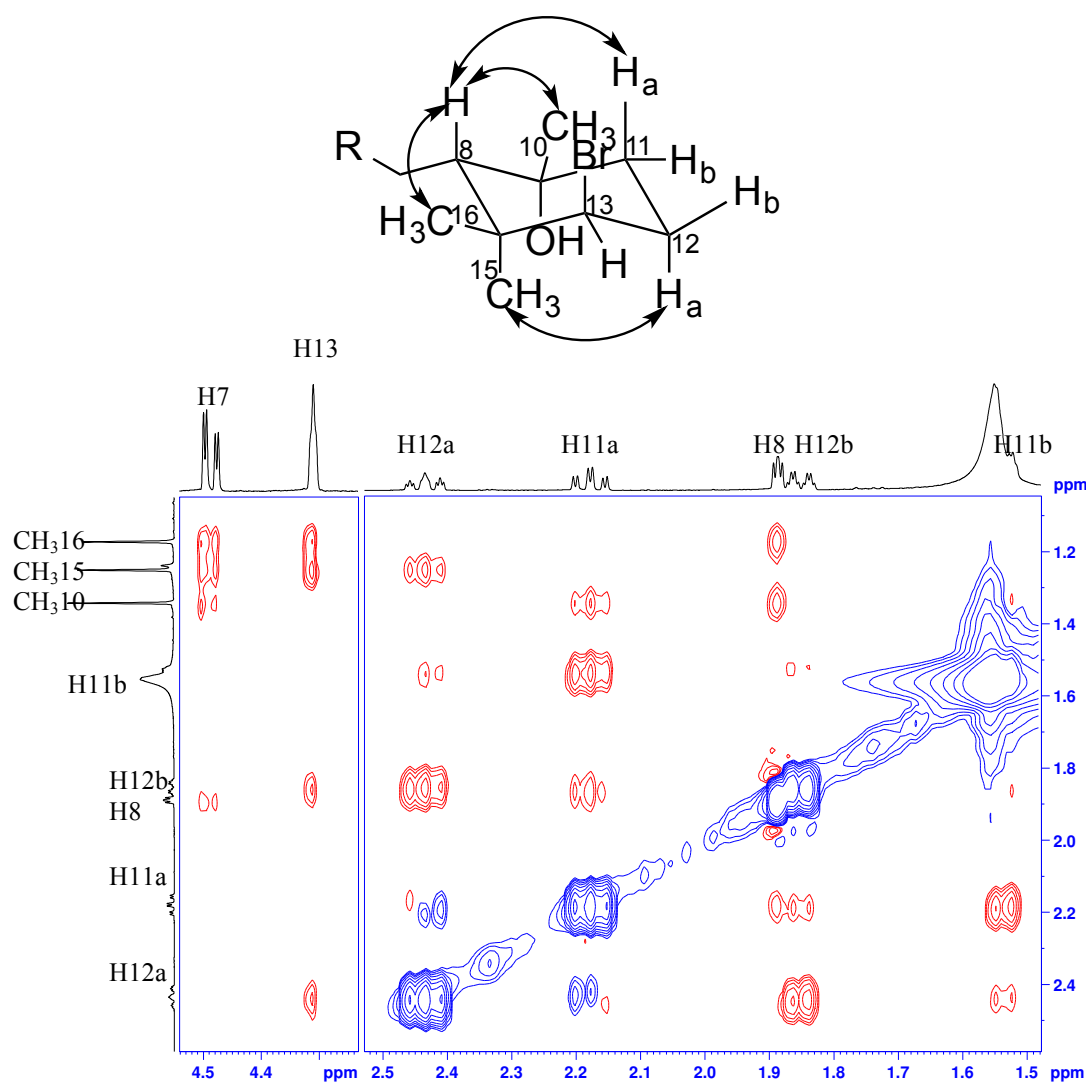


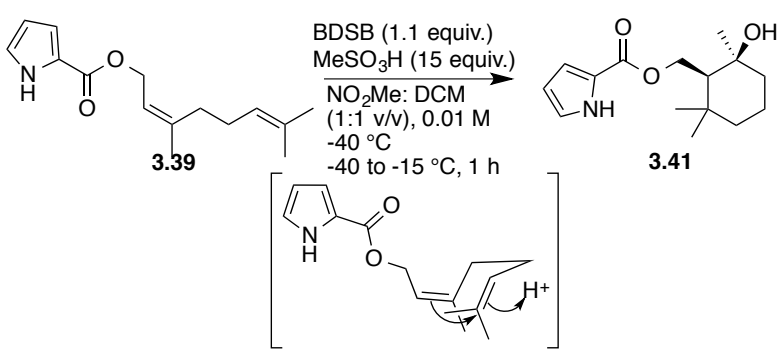
**Figure 3.4** Key NOESY correlations of **3.38d** are indicated by the arrows. Mixing time of 400 ms used.

#### 3.5.1.1. Effect of an Acid Additive

Methanesulfonic acid has been reported to promote complete intramolecular cyclisation with BDSB by being added at the end of the reaction.<sup>53</sup> The addition of 15 equivalents of methanesulfonic acid after 30 min resulted in a new product **3.41** that is the result of carbocation-induced cyclisation (**Entry 1**; **Table 3.5**). Adding methanesulfonic acid earlier during the course of the reaction led to a higher yield of this product (**Entry 2**). The highest yield was obtained when methanesulfonic acid was added initially to the reaction solution and prior to the addition of BDSB (**Entry**

3). In the absence of BDSB (**Entry 4**), **3.41** was obtained in comparable yield. When the reaction was stirred at  $-15^{\circ}\text{C}$  for an additional 30 min prior to the addition of  $\text{MeSO}_3\text{H}$ , **3.41** was not isolated (**Entry 5**). In the presence of a proton source, a carbocation-induced cyclisation reaction out-competes the bromonium-induced cyclisation pathway, particularly at lower temperatures. Again, intramolecular cyclisation was not observed.

**Table 3.6** Effect of  $\text{MeSO}_3\text{H}$  on the bromonium-induced cyclisation with BDSB.



Entry	Time added after start of reaction	Yield (%)
1	30 min	15
2	5 min	48
3	0 min	78
4 <sup>a</sup>	0 min	79
5 <sup>d</sup>	90 min	Not observed

a. BDSB not added; d. Stirred at  $-15^{\circ}\text{C}$  for an additional 30 min

The stereochemistry of **3.41**, where H8 and  $\text{CH}_3$ -10 are on the same side of the molecule, was assigned using NOESY. Proton H12a ( $J = 15.5, 13.9, 3.4, 3.4$  Hz), H11b (complex signal with only one large  $J$  observed) and H13a ( $J = 15.5, 13.9, 3.4, 3.4$  Hz) were assigned axial or equatorial based on their coupling constants and H12b, H11a and H13b were assigned by default. Proton 7 shows equal NOESY correlation with methyl groups 15 and 16, indicating that it must lie in the equatorial plane (**Figure 3.5**). Methyl group 10 has correlations to H11b, H11a and H8 and the

absence of diaxial NOESY correlation with H12a indicates that it lies on the equatorial plane.

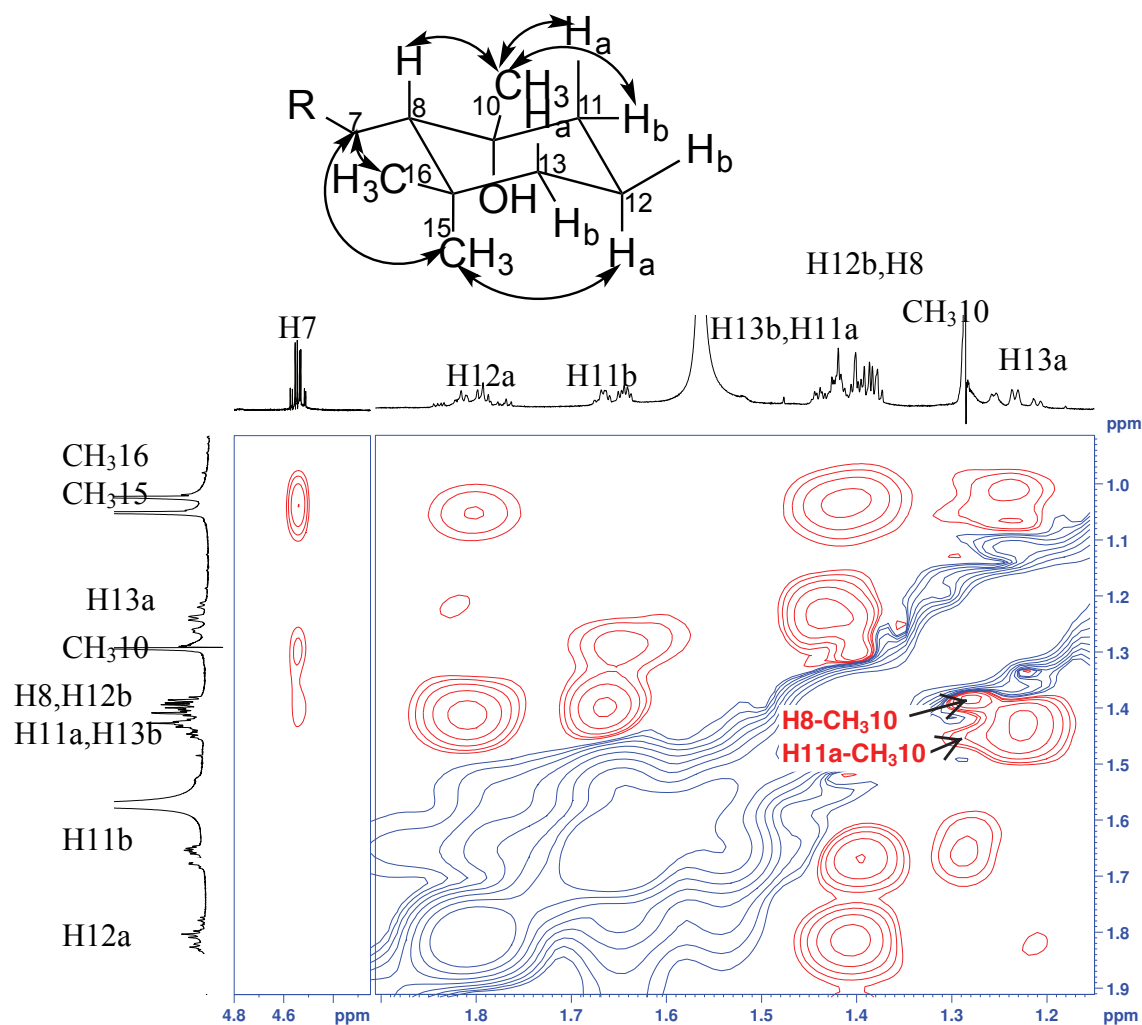


**Figure 3.5** Key NOESY correlations of **3.41** are indicated by the arrows. Mixing time of 300 ms used.

### 3.5.1.2. Addition of bases

The addition of a base was investigated as a way of increasing the nucleophilicity of the amide or pyrrole nitrogens (**Scheme 2.22**). Unfortunately, the use of both organic (pyridine, DMAP) and inorganic bases ( $K_2CO_3$ ) was not tolerated since the reactions of **3.39** were observed to remain incomplete with the formation of **3.39a-d** in low yields.



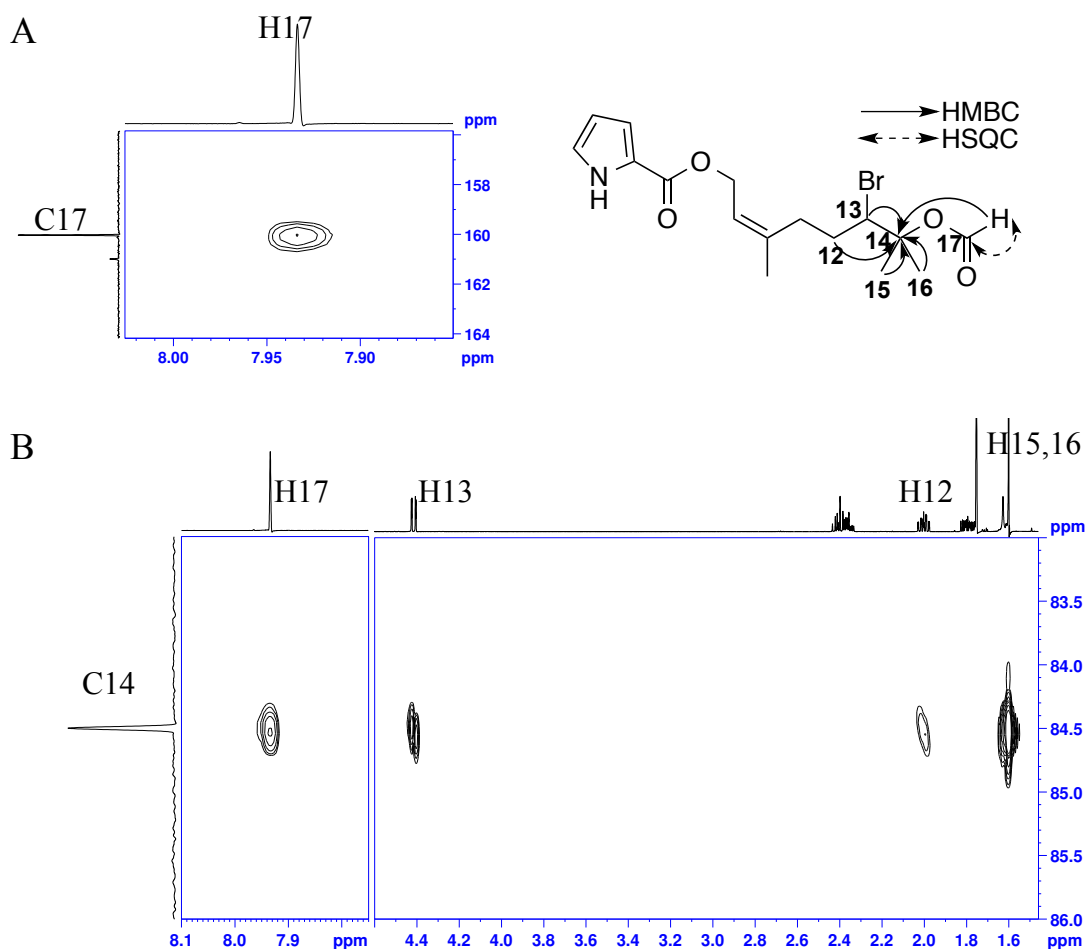
### 3.5.1.3 The Use of DMF as Solvent

Nitromethane is the solvent of choice for BDSB as it is known to have cation-solvating effects that help facilitate polyene cyclisations.<sup>54,55</sup> Cation solvation can lead to longer-lived cations that have a greater chance of undergoing cyclisation and are less likely to form undesired side products due to rearrangements or elimination.

However, the majority of our substrates are insoluble in MeNO<sub>2</sub>. Therefore the use of a cosolvent is required. Dihydrooroidin is soluble in the most polar solvents such as DMSO, DMF, MeOH, EtOH but not in MeNO<sub>2</sub> nor ACN. However BDSB has been shown to decompose<sup>35</sup> in polar solvents such as the alcohols, acetone and THF while DMSO can also act as an oxidant or reductant, thereby restricting the solvent choice to DMF. Therefore the use of DMF as part of the solvent system for the bromonium-induced cyclisation using BDSB was investigated using the pyrrole-nerol hybrid **3.39** as substrate. DMF is also known to stabilise carbocation (polar aprotic solvent).<sup>56</sup>

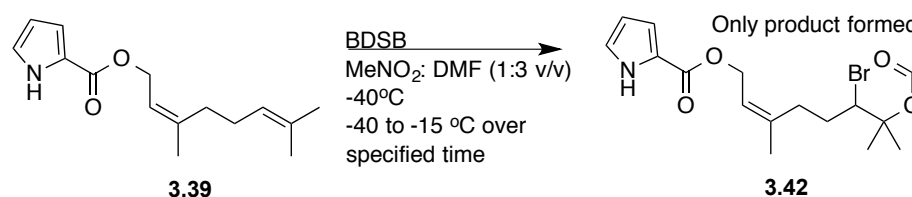
#### 3.5.1.3.1. Formylation of a Halohydrin or Bromoformyloxylolation

When DMF was used in combination with MeNO<sub>2</sub> as the solvent system with 1.1 equivalents of BDSB, the reaction proceeded cleanly to one product **3.42** but not to completion. We were surprised to find a proton singlet at around 8 ppm with HSQC correlation to a carbon at 160 ppm, which suggested a formyl group (**Figure 3.6A**). The proton showed only a single HMBC correlation to a quaternary carbon (C14,  $\delta$  161.0 ppm) (**Figure 3.6B**). EI-MS showed the parent ion M as two peaks 371/373 in the ratio of 1:1 corresponding to the presence of a single bromine atom and HRMS confirmed the molecular formula as C<sub>16</sub>H<sub>22</sub>BrNO<sub>4</sub> ( $\Delta$  0.0002 ppm).



**Figure 3.6** A. Key  $^1\text{H}$ - $^{13}\text{C}$  HSQC correlation for **3.42** and B. Key  $^1\text{H}$ - $^{13}\text{C}$  HMBC correlations for **3.42**.

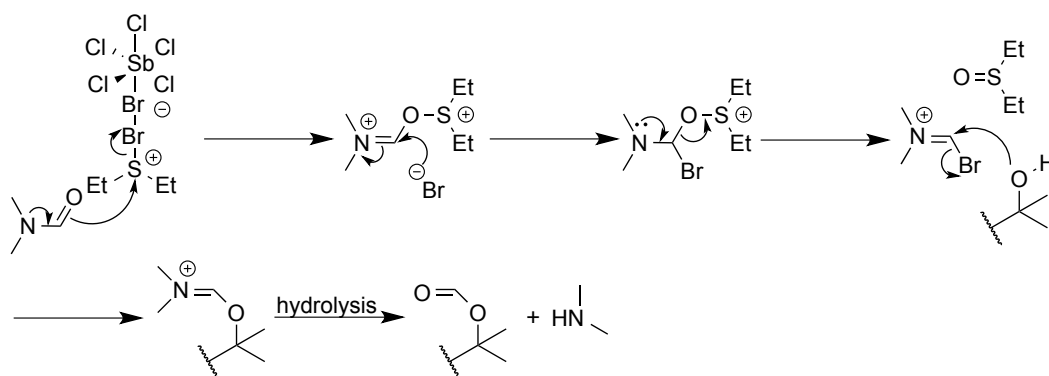
The use of an equimolar amount of BDSB, did not lead to the completion of the reaction (**Table 3.7**; **Entry 1**) while the use of 1.5 equivalents of the reagent was found to be optimum for the reaction (**Entry 2 and 3**) achieving 90% yield or better. The reaction time could be lowered by allowing the reaction to warm up from  $-40\text{ }^{\circ}\text{C}$  to  $-15\text{ }^{\circ}\text{C}$  over 30 min, after the addition of the reagent (**Entry 4**). The use of different percentages of DMF (75, 50 and 25% (v/v)) as part of the solvent system with  $\text{MeNO}_2$  led to the same outcome where only bromoformylation was observed. Lower percentages of DMF were not investigated since oroidin and dihydrooroidin are only soluble at and above 50% (v/v) of DMF in  $\text{MeNO}_2$ .

**Table 3.7** Effect of the number of equivalents of BDSB on the yield of the bromoformyloxylation product.

Entry	Equiv.	Time	Yield (%) <sup>a</sup>
1	1	1h	67
2	1.5	1h	91
3	2	1h	90
4	1.5	30 min	90

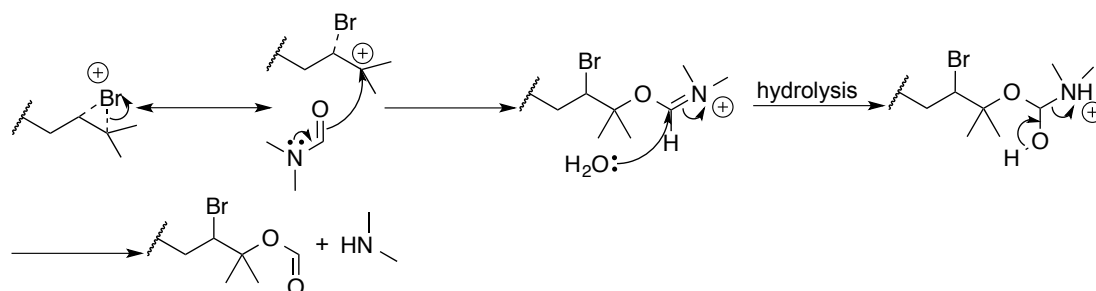
a. isolated yield.

The formation of the product can be explained by ring opening of the bromonium ion by water followed by the reaction of the alcohol with DMF with elimination of dimethylamine. The BDSB could be activating the DMF in a similar way as the Vilsmeier reagent (DMF-POCl<sub>3</sub>) (**Scheme 3.27**). Vilsmeier reagent has been used for the formylation of electron rich aromatic systems but is ineffective as a formylating agent for alcohols.<sup>57,58</sup>

**Scheme 3.27** Possible reaction mechanism for the formylation of a halohydrin using BDSB in the presence of DMF.

To test this hypothesis, bromohydrin **3.38c** was subjected to the same reaction condition as used in **entry 4** (**Table 3.7**). However, only starting material was

recovered. An alternative mechanism involves the ring opening of the bromonium ion with DMF and subsequent hydrolysis during an aqueous work-up (**Scheme 3.28**). As this bromoformyloxylation is highly regioselective, it can be inferred that the mechanism is highly SN1-like.



**Scheme 3.28** Possible reaction mechanism for the bromoformyloxylation using BDSB in the presence of DMF.

The traditional method for producing bromoformyloxylation product involves the acetylation of corresponding vicinal halohydrins, which require the synthesis of precursor halohydrins from the corresponding olefins. Bromoformyloxylation is a type of ‘cohalogenation’ reaction which uses a combination of halonium source and an appropriate nucleophile.<sup>59</sup> Reports of bromoformyloxylation in the literature, involve the use as bromine sources of NBS, *N*-Bromosaccharin or *N,N*-dibromobenzene sulfonamide, and as nucleophile source, DMF or formic acid as nucleophiles.<sup>60-62</sup> The most recently reported bromoformyloxylation procedure involves the use of *N,N*-dibromo-*p*-toluenesulfonamide in DMF at room temperature.<sup>63</sup> The use of BDSB in the presence of DMF provide a mild, quick and simple alternative to existing bromoformyloxylation procedures. Notwithstanding the discovery of a new reaction of BDSB, it was concluded that DMF is not a suitable solvent for BDSB in biomimetic bromonium ion cyclisations.

Despite the limited success of BDSB on our pyrrole-terpene hybrid substrates, we nevertheless investigated the application of this reagent to DHO and oroidin.

### 3.5.2. Investigation with DHO

Despite the possibility of bromoformyloxylation, we decided to try the reaction with DHO dissolved in a solvent mixture of MeNO<sub>2</sub> and DMF. Trials of different percentages of solvent mixture of MeNO<sub>2</sub> and DMF led to a 1:1 (v/v) ratio as the most suitable to avoid the precipitation of the substrate particularly when the reaction is conducted at very low temperatures.

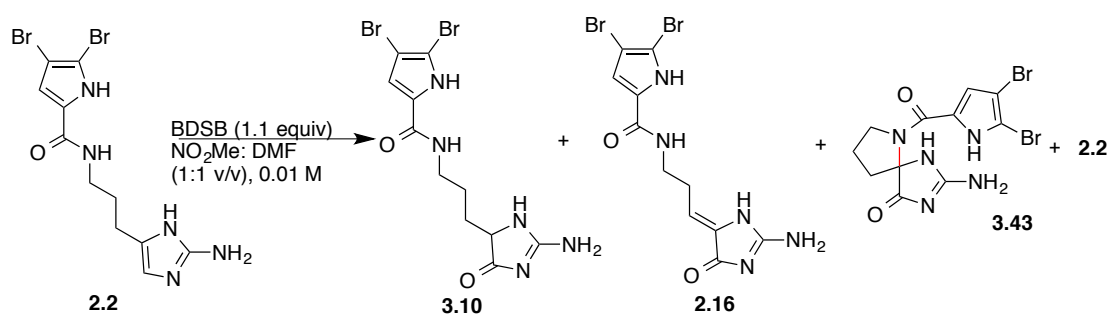
The initial reaction involved the addition of BDSB (1.2 equivalents in MeNO<sub>2</sub>) at –20 °C to a solution of DHO in a mixture of DMF/MeNO<sub>2</sub> (final solvent composition 1:1(v/v)). An instant formation of an intense red colour was observed. The reaction was allowed to stir at –20 °C for 1 hour during which time the red colour slowly dissipated to orangey before becoming a pale golden yellow.

Due to the highly polar nature of the substrate and its likely products, the reaction was quenched with a solutions 5% aqueous NaHCO<sub>3</sub> and 5% aqueous Na<sub>2</sub>SO<sub>3</sub> (1:1 v/v) and the reaction mixture was simply freeze-dried. The crude material was dissolved in methanol and any salt removed by filtration. TLC showed the formation of three main products. The crude material was subjected to LC-MS analysis whereby all the peaks with UV spectra with absorption maxima at around 270 nm (characteristic of 2-pyrrole carboxamide)<sup>64</sup>, showed only monomeric products. Silica column chromatography with ammonia as part of the solvent system allowed the isolation of three compounds. The major product corresponded to dihydrodispacamide A (**3.10**) (34%), along with dispacamide A (**2.16**) (21%) and a

new compound found to be a spirocyclic monomer (**3.43**) (14%). No formyloxylation was observed.

#### 3.5.2.1. Temperature Screening

With the aim of reducing the formation of the 2-aminoimidazolone products and promoting intramolecular cyclisation, the reaction was conducted at lower temperatures (**Table 3.8**). At  $-70\text{ }^{\circ}\text{C}$  for 30 min, mainly unreacted starting material was recovered from the reaction mixture together with dihydrodispacamide A (**3.10**) and dispacamide A (**2.16**) (**Entry 3**). When the reaction was allowed to proceed at a higher temperature of  $-40\text{ }^{\circ}\text{C}$  for 30 min, dispacamide A (**2.16**), dihydrodispacamide A (**3.10**) and the spirocyclic product (**3.43**) were isolated (**Entry 2**). These results suggest the high propensity of the bromonium ion to form the 2-aminoimidazolone products. The yield of the spirocyclic product **3.43** was improved to 18% by adding BDSB at  $-70\text{ }^{\circ}\text{C}$  and stirring to  $-40\text{ }^{\circ}\text{C}$  over 30 min before allowing the reaction to warm to  $-20\text{ }^{\circ}\text{C}$  over 1 h (**Entry 4**).

**Table 3.8** Outcome of the reaction with BDSB, conducted at different temperatures and times.

Entry	Temp.	additive	Time	<b>3.10</b> (%)	<b>2.16</b> (%)	<b>3.43</b> (%)	<b>2.2</b> (%)
1	−20 °C	-	1 h	34	21	14	0
2	−40 °C	-	30 min	23	14	11	40
3	−70 °C	-	30 min	17	11	0	64
4 <sup>a</sup>	−70 to −40 °C	-	30 min	29	22	18	0
	−40 to −20 °C	-	1 h				
5	−40 °C	K <sub>2</sub> CO <sub>3</sub> (1.1 equiv.)	30 min	trace	trace	0	95
6 <sup>a</sup>	−70 to −40 °C	K <sub>2</sub> CO <sub>3</sub> <sup>b</sup>	30 min	20	13	trace	35
	−40 to −20 °C	(1.1 equiv.)	1 h				
7	−40 to −20 °C	K <sub>2</sub> CO <sub>3</sub> <sup>b</sup> (1.1 equiv.)	1h	26	19	trace	0
8 <sup>a</sup>	−70 to −40 °C	butylamine <sup>b</sup>	30 min	25	20	trace	0
	−40 to −20 °C	(1.1 equiv.)	1 h				
9	−70 to −40 °C	MeSO <sub>3</sub> H	30 min	26	21	15	0
	−40 to −20 °C	(15 equiv.)	1h				

**a.** −70 to −40 °C over 30 min and −40 to −20 °C over 1 h; **b.** added 30 min after addition of BDSB; % = isolated yields

### 3.5.2.2. Acid/Base Screening

Similarly to the pyrrole-terpene hybrids, the inorganic base, K<sub>2</sub>CO<sub>3</sub> was added to the solution of DHO prior to the addition of BDSB in an attempt to promote intramolecular cyclisation by internal nucleophiles. From earlier investigation, we know that the use of a base is not compatible with BDSB. Therefore the addition of K<sub>2</sub>CO<sub>3</sub> was done before addition of BDSB (**Table 3.8; Entry 5**) or after 30 min

(**Entry 6 and 7**) to allow the formation of the bromonium ion to take place before the introduction of the base. If added early during the reaction, starting material was mainly recovered. When the base was introduced later, the reaction produced mainly dihydrodispacamide A (**3.10**) and dispacamide A (**2.16**). This indicates that the bromonium ion is short-lived and reacts immediately once formed. This implies that the addition of base will only hinder the formation of the key bromonium ion required for intramolecular cyclisation. The use of butylamine (**Entry 8**) to quench the bromonium ion had the same effect as the other organic bases trialed previously, inhibiting any reaction. No butylamine adduct of DHO was observed. On a different note, the presence of an excess of methanesulfonic acid in the reaction did not have any effect on the outcome of the reaction mixture (**Entry 9**).

### 3.5.2.3. Spirocyclic Monomer

ESI-MS of the new compound with max UV absorption of 284 nm showed  $[M+H]^+$  at  $m/z$  404/406/408 with two mass unit differences in the ratio of 1:2:1 corresponding to two bromines and HRMS confirmed the molecular formula as  $C_{11}H_{11}Br_2N_5O_2$  ( $\Delta$  0.0005 ppm). The structure of the spirocyclic ring was confirmed by HMBC correlation between H8 and H9 (strong) and H10 (weak) with quaternary carbon C11 (**Figure 3.7**). The absence of an imidazole proton and the presence of a carbonyl carbon (173.3 ppm) to which H10 has a correlation, indicated the oxidation of the imidazole ring to an imidazolone (**Figure 3.7**).



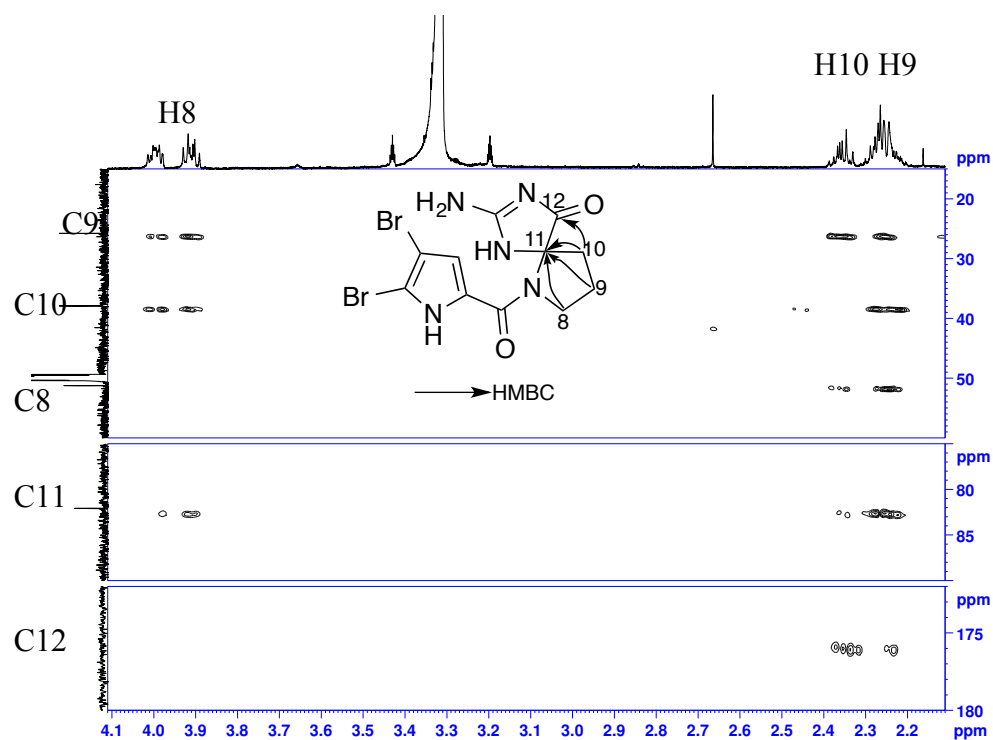
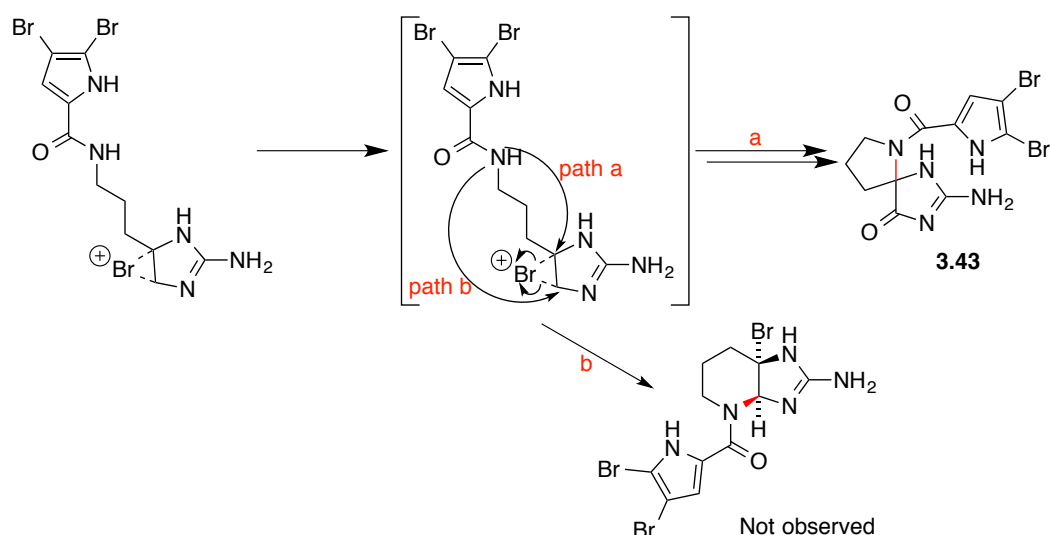


**Figure 3.7** Key  $^1\text{H}$ - $^{13}\text{C}$  HMBC correlations for **3.43**.

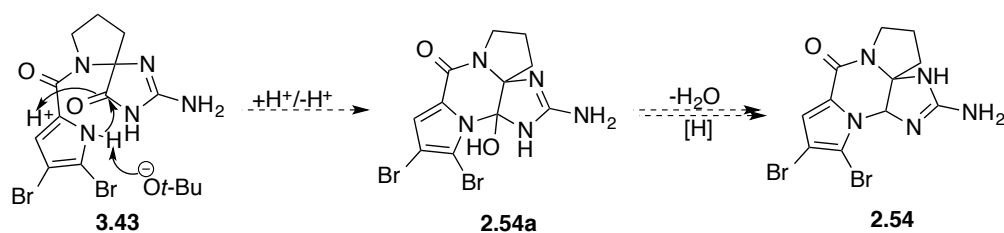
Two intramolecular cyclisation paths (**path a** and **b**) are possible (**Scheme 3.29**). **Path a** which involves the bromonium ion induced intramolecular cyclisation of the amide nitrogen at the C4 carbon of the imidazole ring, explains the formation of spirocycle **3.43**. It is possible for the ring opening of the bromonium ion to occur at the C5 carbon of the imidazole ring (**path b**) but no such product was observed.



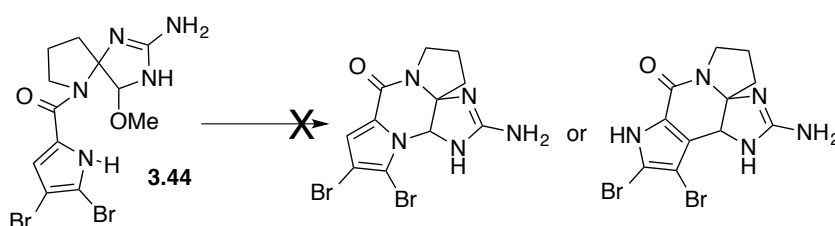
**Scheme 3.29** Two possible intramolecular cyclisation paths.

The spirocyclic monomer formed is likely an intermediate in the formation of **2.54a**, the hydroxyl derivative of the tetracyclic monomer dibromophakellin (**2.54**) through the nucleophilic attack of the pyrrole nitrogen onto the C5 imidazolone carbon (**Scheme 3.30**). Dibromohydroxyphakellin (**2.54a**) has been recently isolated from Indonesian marine sponges *Agelas linnaei* and *A. nakamurai*, just over 4 decades after dibromophakellin (**2.54**).<sup>65</sup> Further cyclisation of the spirocyclic monomer **3.43** was attempted using neat methansulfonic acid at room temperature. This resulted in a complex crude mixture. Büchi and co-workers have successfully used potassium *t*-butoxide to further cyclise their postulated spirocyclic intermediate (**Scheme 3.1**) in the formation of the tetracyclic ring of racemic dibromophakellin (**2.54**).<sup>1</sup> Under basic condition, the pyrrole nitrogen is deprotonated and the resulting highly nucleophilic anion can cyclise onto the amide carbon to first provide dibromohydroxyphakellin (**2.54a**) (**Scheme 3.30**). However, when 2.1 equivalents of potassium *t*-butoxide in *t*-butanol was added to **3.43** and stirred at room temperature for 1 hour, only starting material was recovered while the use of higher temperatures led to complex reaction mixtures. Horne was also unsuccessful in converting

spirocycle **3.44** into its tetracycle although there is no mention of the reaction conditions tried.

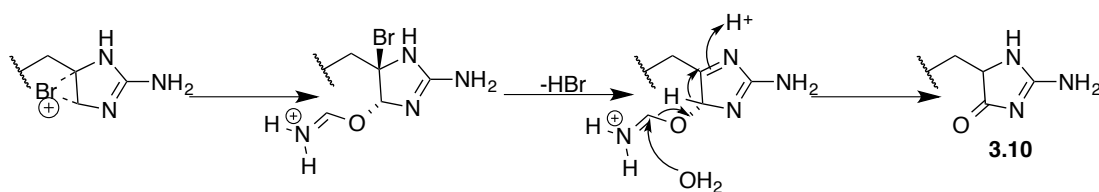


**Scheme 3.30** Possible formation of the tetracyclic oroidin alkaloid monomer, dibromophakellin (**2.54**) from **3.43**.



**Scheme 3.44** Horne reported the spirocycle **3.44** that failed to undergo further cyclisation.

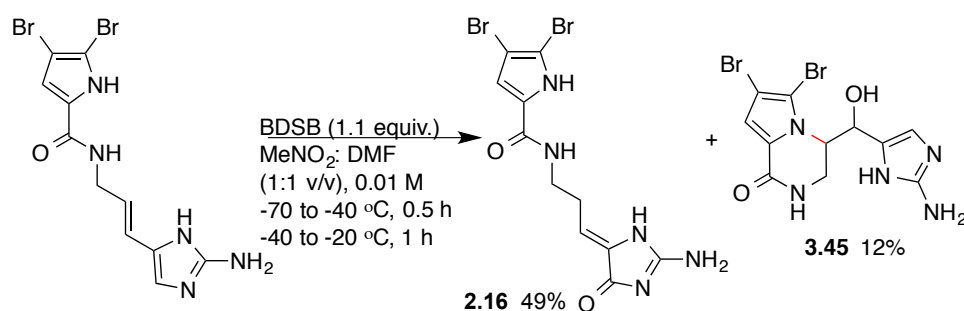
The isolation of dispacamide A (**2.16**) suggests further oxidation of dihydrodispacamide A (**3.11**) to the latter. The presence of trace amounts of water could be sufficient to convert the bromonium ion formed to an epoxide intermediate (**Scheme 2.18**) to eventually yield the different products that have been isolated and identified. Epoxide formation can be followed by a 1,2-hydride shift (**Scheme 3.11**) to provide the stable 2-aminoimidazolone. It is worth noting that unlike in the case of the pyrrole-terpene hybrids, the use of DMF did not lead to any observable formylated products. However, their intermediacy could explain the oxidation products (**Scheme 3.45**).



**Scheme 3.45** Intermediacy of formylated product formed in the presence of DMF, in the formation of the oxidation products observed.

### 3.5.3. Application to oroidin

Under the optimised reaction condition, BDSB was applied to oroidin (**Scheme 3.46**). An intense green colour was observed. The reaction was allowed to stir to  $-20\text{ }^{\circ}\text{C}$  over 1 hour during which time the green colour slowly changed to a faint yellow. TLC suggested the formation of two main products, along with decomposition (baseline). Silica column chromatography with ammonia as part of the solvent system allowed the isolation of the two compounds. The major product corresponded to dispacamide A **2.16** (49%) while the second one was characterised as the unnatural hydroxycyclooroidin **3.45** (12%). ESI-MS of **3.45** with max UV absorption of 277 nm showed the  $[\text{M}+\text{H}^+]$  at  $m/z$  404/406/408 with two mass unit differences in the ratio of 1:2:1 corresponding to two bromines and HRMS confirmed the molecular formula as  $\text{C}_{11}\text{H}_{11}\text{Br}_2\text{N}_5\text{O}_2$  ( $\Delta$  0.0005 ppm). The absence of the pyrrole proton (12-13 ppm in  $\text{DMSO}-d_6$ ) indicated the occurrence of intramolecular cyclisation via the pyrrole nitrogen. The presence of the imidazole proton (6.46 ppm) indicated the 2-aminoimidazole ring to be unoxidised. These results indicate that, under these conditions, BDSB preferentially oxidises the alkene over the imidazole double bond.



**Scheme 3.46** Application of BDSB on oroidin as substrate.

### 3.5.4. Dimerisation of DHO

There have only been two previous reports of biomimetic dimerisation (**Scheme 3.5** and **3.6**). In order to favour dimerisation we added 0.6 equivalent of BDSB at  $-40^{\circ}\text{C}$  before allowing the reaction to stir to  $-20^{\circ}\text{C}$  over an hour. We were delighted when a LCMS analysis of the crude reaction mixture indicated a small peak with max UV absorption of 276 nm and ESI-MS of  $[\text{M}+\text{H}]^{+}$  ion peaks at  $m/z$  793/795/797/799/801 (intensity of 1:4:6:4:1) corresponding to a dimer and HRMS indicated the molecular formula as  $\text{C}_{22}\text{H}_{24}\text{Br}_4\text{N}_{10}\text{O}_3$  ( $\Delta$  0.0005 ppm).

The reaction condition was optimised by increasing the concentration of the reaction solution from 0.01 M to 0.1 M and by adding 0.6 equivalent of BDSB over a period of 30 min at  $-70^{\circ}\text{C}$  before allowing the reaction to gradually warm up to  $-20^{\circ}\text{C}$  within an hour. This increased the yield of the dimer from <1% to 6%.

The dimer was isolated by repeated HPLC purification and analysed by 2D NMR spectroscopy. The absence of H12 and H12' were noted with the presence of two characteristic quaternary carbon signals at 67.6 ppm (C11') and 121.4 ppm (C12). Moreover, a carbonyl (C12') at 187.9 ppm in **3.46** suggests that a C12 to C11' link. The connectivity of the two dihydrooroidin units was established by HMBC correlations between H11 and H10' to C12 (**Figure 3.8**). This unnatural tetrahydromauritiamine (**3.46**) differs from mauritiamine (**2.76**) by the absence of the

alkenes.<sup>66</sup>

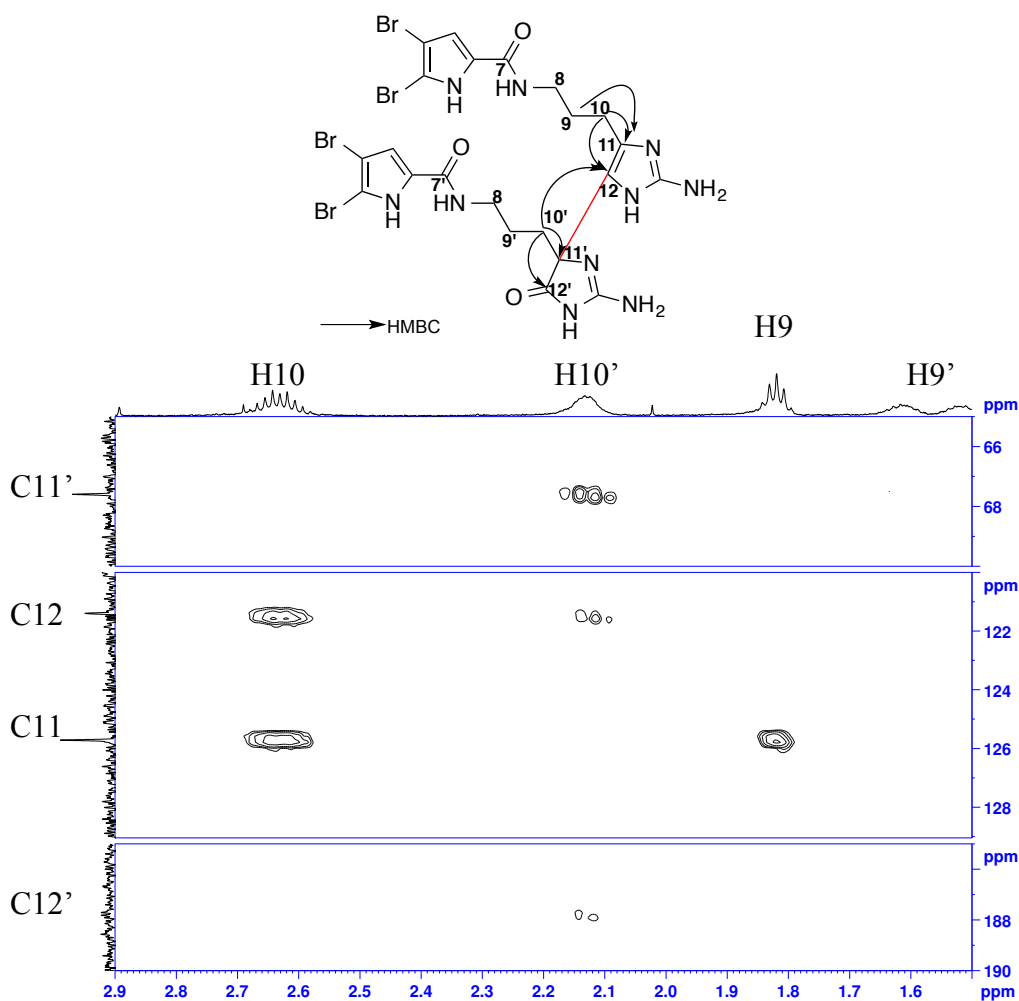
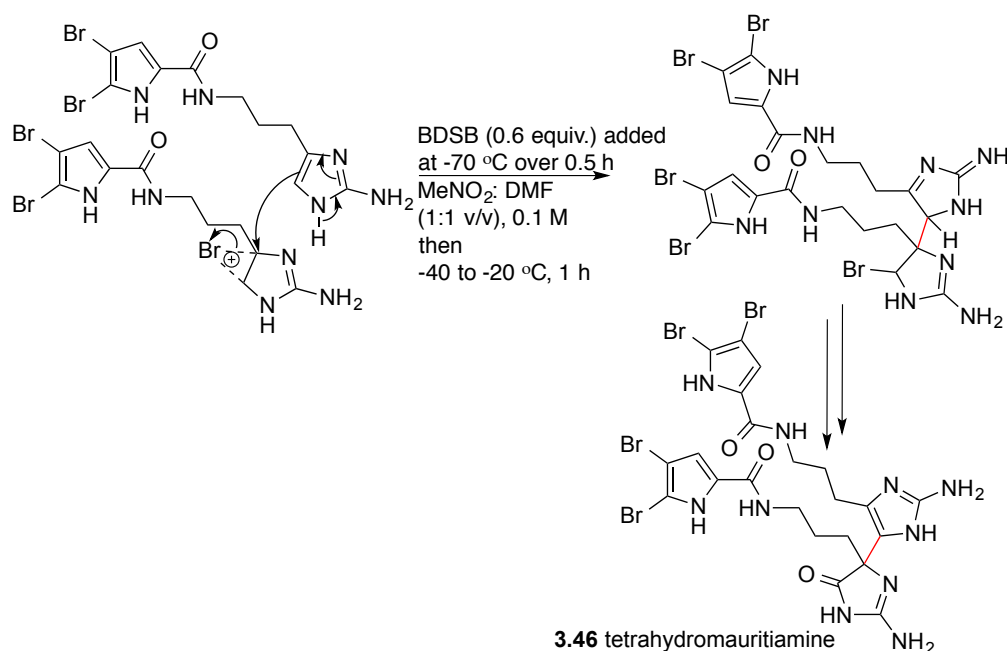


**Figure 3.8** Key <sup>1</sup>H-<sup>13</sup>C HMBC correlations (shown by arrows) for the dimer formed.

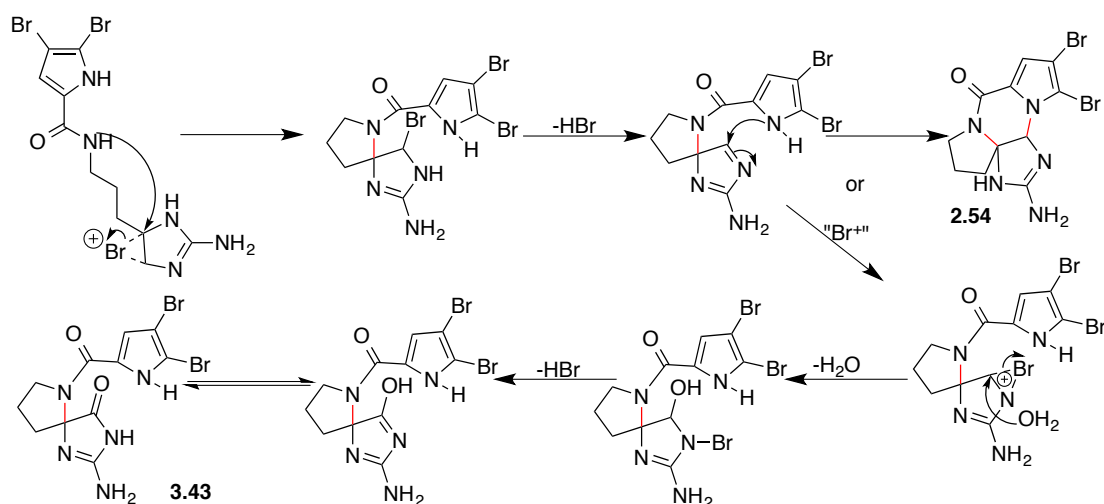
Tetrahydromauritiamine is likely to arise from the ring opening of a bromonium ion or an epoxide by the imidazole ring of another DHO (**Scheme 3.47**). In the case of a bromonium ion, subsequent substitution of the bromine with water eventually leads to the imidazolone ring. In the epoxide case, subsequent rearrangement leads to the imidazolone ring. It is worth noting that although other possible dimers are possible, only tetrahydromauritiamine was isolated.



**Scheme 3.47** Formation of tetrahydromauritiamine (**3.46**) via a bromonium ion.

Despite the optimised reaction condition used (**Scheme 3.47**), a relatively complex crude product was obtained from the reaction mixture, reminiscent of a marine sponge extract. This is not unexpected since various reaction pathways are possible. In order to gain better insight into the reactivity profile of the BDSB reagent on the DHO substrate, we purified all the products that were formed in isolable amount. Unsurprisingly, the ubiquitous formation of dihydrodispacamide (**3.10**) (21%) and dispacamide A (**2.16**) (18%) were observed. The third largest component of the reaction was the spirocyclic monomer **3.43** (12%) previously isolated.

Under the dimerisation reaction condition, the tetracycle dibromophakellin **2.54** was isolated in 2.5% yield and the NMR characteristics of the synthesised product as a racemic mixture are in agreement with previously reported data.<sup>67</sup> The isolation of dibromophakellin (**2.54**) and the failed attempts to convert spirocycle **3.43** to **2.54**, suggests the likelihood that the formation of the imidazolone competes with the formation of the tetracycle **2.54** (**Scheme 3.48**).

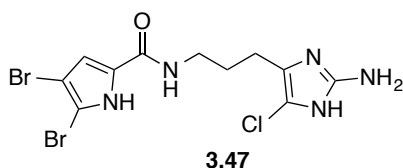


**Scheme 3.48** Formation of spirocyclic monomer **3.43** via bromonium ion.

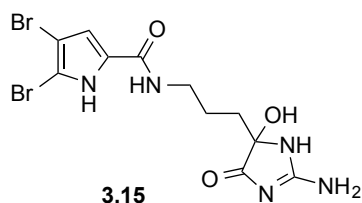
Amongst the other detectable products isolated and characterised from the reaction mixture, was oroidin (**2.1**) (2%). The isolation of oroidin from the reaction mixture is possible based on previously reported conversion of DHO to oroidin.<sup>11</sup> The use of a bromination reagent would suggest the formation of bromodihydrooroidin that could then undergo dehydrobromination to provide oroidin. However, bromodihydrooroidin was not isolated from the crude mixture nor was its corresponding mass observed on LCMS. The isolation of a product that has <sup>1</sup>H and <sup>13</sup>C NMR almost similar to dihydrooroidin with only the imidazole proton missing came as a mystery. The absence of both the imidazole proton and a carbonyl carbon suggested that the imidazole has not become oxidised to the imidazolone but rather, the imidazole proton has become substituted by another atom. ESI-MS showed the [M+H]<sup>+</sup> at *m/z* 424/426/428 with two mass unit differences in the ratio of 1:2:1 corresponding to two bromines and HRMS confirmed the molecular formula of C<sub>11</sub>H<sub>13</sub>Br<sub>2</sub>Cl<sub>2</sub>N<sub>5</sub>O (Δ 0.0002 ppm) with 2 bromines atoms and a chlorine atom. As previously observed in the case of the pyrrole-terpene hybrids, the presence of nucleophilic chloride ions from the antimony pentachloride could explain the



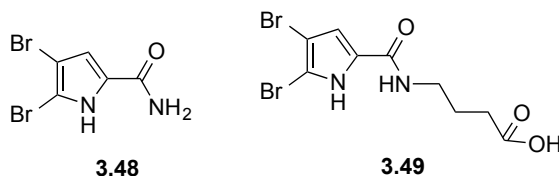
formation of chlorodihydrooroidin **3.47** (8%) which can be converted to oroidin (**2.1**) as reported by Lindel.<sup>11</sup>



Amongst other minor identifiable products that were isolated was a compound (2%) with ESI-MS showing  $[M+H]^+$  at  $m/z$  424/426/428 and for which the molecular formula was determined as  $C_{11}H_{13}Br_2N_5O_3$  from HRMS ( $\Delta$  0.0004 ppm). The NMR characteristics of the compound are in agreement with previously reported data for the  $\alpha$ -hydroxy-2-aminoimidazolone **3.15** which has been previously synthesised as an intermediate in the synthesis of dispacamide A (**2.16**) (Scheme 3.13) by Al-Mourabit.<sup>29</sup>

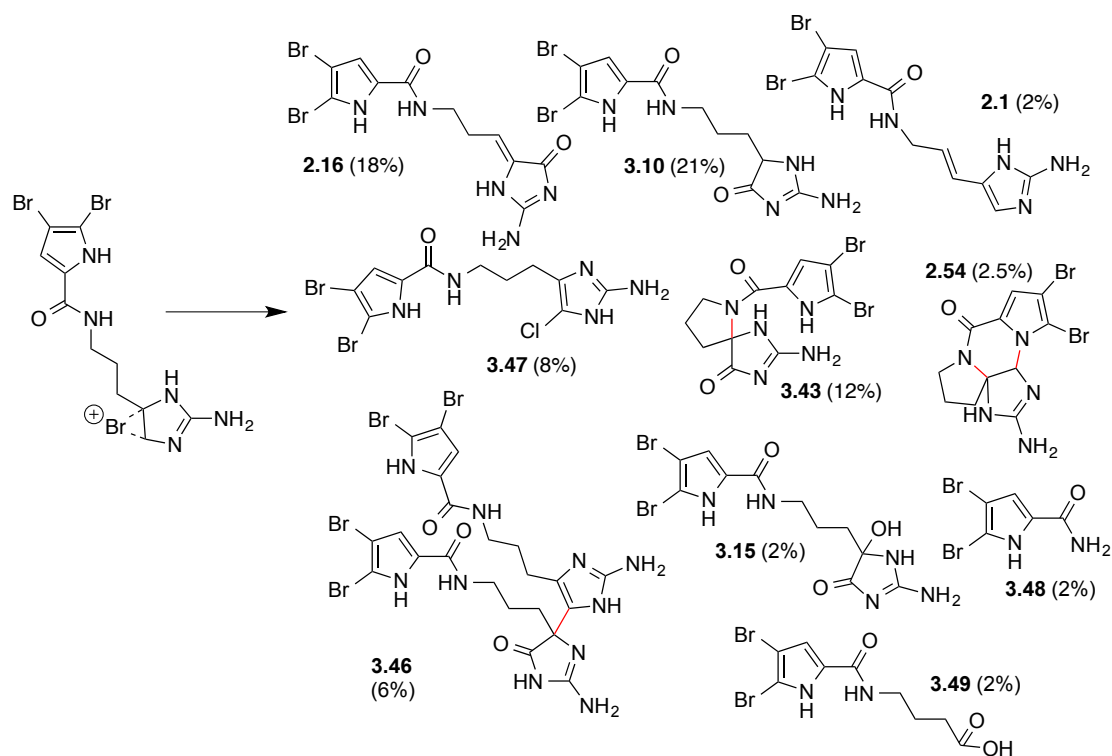


4,5-Dibromopyrrole-2-carboxamide **3.48** (2%) and its butanoic acid derivative **3.49** (2%) were other minor products. Compounds **3.48** and **3.49** have been previously isolated from marine sponges and have been described as key building blocks in the biosynthesis of bromopyrrole alkaloids.<sup>65</sup>



The characterisations of the isolable compounds (Scheme 3.49) provide some insights into the reaction profile of BDSB on DHO as a substrate. The formation of

dihydrodispacamide A (**3.10**) and displacamide A (**2.16**) appears to be ubiquitous. These together with decomposition reactions account for the low yield of dimerisation. Despite this, the formation of tetrahydromauritiamine directly from its monomer dihydrooroidin, brings further evidence to the generation of more complex oroidin alkaloids from a particular set of precursors. This also brings support to our biogenesis hypothesis whereby the haloperoxidases play an important role in the formation of key reactive intermediate(s) of the precursor(s) to generate the complexity observed in the oroidin alkaloids. Moreover, this is the second example of homodimerisation, albeit in low yield.



**Scheme 3.49** Isolated compounds from bromonium ion intermediate of DHO **2.2** under the optimised dimerisation condition.

### 3.5.5. Dimerisation of oroidin

The use of the optimised dimerisation reaction condition (**Scheme 3.47**) with oroidin on the same scale as with DHO, unfortunately did not lead to any isolable

amount of dimers. The outcome was the same as before where dispacamide A (40%) and hydroxycyclooroidin (**3.45**; 10%) were the only products that were isolated along with starting material and unidentified decomposition products. The presence of the alkene carbon double bond in addition to the imidazole carbon double bond provide more possible reaction pathways and could account for the formation of many different products in detectable but not isolable amounts.

### 3.6. Summary- Bromonium Ion Route

As has been already demonstrated, BDSB is a powerful reagent for electrophilic bromination.<sup>35,47,48,68</sup> However, the investigation of the reactivity of BDSB on the pyrrole-terpene hybrid substrates provided only modest findings. Products formed from these reactions consisted mainly of linear addition products and a monocyclised product was formed only as a minor component. The use of bases, both organic and inorganic, is not compatible with the reagent, leading to the inhibition of its reactivity. However when DMF was used as part of the solvent system with BDSB, bromoformyloxylation was observed as a clean reaction. This shows the utility of BDSB as a clean and efficient bromoformyloxylation reagent in the presence of DMF under mild conditions but that DMF is probably not an ideal solvent for bromonium ion formation.

The application of BDSB to oroidin (**2.1**), led to the isolation of two main products: dispacamide A (**2.16**) and a hydroxycyclooroidin (**3.45**). On the other hand, the application of BDSB to DHO (**2.2**), led to the formation of the ubiquitous oxidation products: dispacamide A (**2.16**) and dihydrodispacamide A (**3.10**), along with a spirocyclic monomer **3.43**, dibromophakellin (**2.54**) and eventually to a dimer

**3.46.** Attempts to convert spirocycle **3.43** into dibromohydroxyphakellin (**2.54a**) were unsuccessful. The formation of dimer, tetrahydromauritiamine (**3.46**) is the second example of dimerisation and the first example of dimerisation of the monomeric precursor DHO (**2.2**), without enzymatic catalysis. With this moderate success, we have demonstrated a biomimetic approach towards the generation of oroidin alkaloids, based on the recognition of the action of marine haloperoxidases in the biosynthesis of the wide diversity of marine natural products. The family of the oroidin alkaloids is continuously growing and it would not be surprising if some of the compounds we have synthesised here, are eventually isolated from a sponge.

### 3.7. References

- (1) Foley, L. H.; Buchi, G. *J. Am. Chem. Soc.* **1982**, *104*, 1776-1777.
- (2) Wiese, K. J.; Yakushijin, K.; Horne, D. A. *Tetrahedron Lett.* **2002**, *43*, 5135-5136.
- (3) Olofson, A.; Yakushijin, K.; Horne, D. A. *J. Org. Chem.* **1998**, *63*, 1248-1253.
- (4) Barrios Sosa, A. C.; Yakushijin, K.; Horne, D. A. *Org. Lett.* **2000**, *2*, 3443-3444.
- (5) Poverlein, C.; Breckle, G.; Lindel, T. *Org. Lett.* **2006**, *8*, 819-821.
- (6) Lejeune, C.; Tian, H.; Appenzeller, J.; Ermolenko, L.; Martin, M.-T.; Al-Mourabit, A. *J. Nat. Prod.* **2013**, *76*, 903-908.
- (7) Baran, P. S.; O'Malley, D. P.; Zografos, A. L. *Angew. Chem. Int. Ed. Engl.* **2004**, *43*, 2674-2677.
- (8) Grube, A.; Immel, S.; Baran, P. S.; Köck, M. *Angew. Chem. Int. Ed. Engl.* **2007**, *46*, 6721-6724.
- (9) O'Malley, D. P.; Yamaguchi, J.; Young, I. S.; Seiple, I. B.; Baran, P. S. *Angew. Chem. Int. Ed. Engl.* **2008**, *47*, 3581-3583.
- (10) Seiple, I. B.; Su, S.; Young, I. S.; Nakamura, A.; Yamaguchi, J.; Jørgensen, L.; Rodriguez, R. A.; O'Malley, D. P.; Gaich, T.; Köck, M.; Baran, P. S. *J. Am. Chem. Soc.* **2011**, *133*, 14710-14726.

- (11) Moldovan, R. P.; Lindel, T. Z. *Naturforsch., B: Chem. Sci.* **2009**, *64*, 1612-1616.
- (12) Murray, R. W.; Jeyaraman, R. *J. Org. Chem.* **1985**, *50*, 2847-2853.
- (13) Murray, R. W. *Chem. Rev.* **1989**, *89*, 1187-1201.
- (14) Bach, R. D. In *The Chemistry of Peroxides*; Patai, S., Ed.; Wiley: New York, 2006; Vol. 1, chapter 1.
- (15) Ferraz, H. M. C.; Muzzi, R. M.; de O. Vieira, T.; Viertler, H. *Tetrahedron Lett.* **2000**, *41*, 5021-5023.
- (16) Murray, R. W.; Singh, M. *Org. Synth.* **1997**, *74*, 91-96.
- (17) Kaur, N.; Kishore, D. *Synth. Commun.* **2013**, *44*, 721-747.
- (18) Zhdankin, V. V. *ARKIVOC* **2009**, *1*, 1-62.
- (19) Kirschning, A. *J. Prakt. Chem.* **1998**, *340*, 184-186.
- (20) Davis, F. A.; Lamendola, J.; Nadir, U.; Kluger, E. W.; Sedergran, T. C.; Panunto, T. W.; Billmers, R.; Jenkins, R.; Turchi, I. J. *J. Am. Chem. Soc.* **1980**, *102*, 2000-2005.
- (21) García Ruano, J. L.; Alemán, J.; Fajardo, C.; Parra, A. *Org. Lett.* **2005**, *7*, 5493-5496.
- (22) Davis, F. A.; Chen, B. C. *Chem. Rev.* **1992**, *92*, 919-934.
- (23) Grubbs, A. W.; Artman, G. D.; Tsukamoto, S.; Williams, R. M. *Angew. Chem. Int. Ed. Engl.* **2007**, *46*, 2257-2261.
- (24) Sivappa, R.; Koswatta, P.; Lovely, C. J. *Tetrahedron Lett.* **2007**, *48*, 5771-5775.
- (25) Cafieri, F.; Fattorusso, E.; Mangoni, A.; Taglialatela-Scafati, O. *Tetrahedron Lett.* **1996**, *37*, 3587-3590.
- (26) Lindel, T.; Hoffmann, H. *Tetrahedron Lett.* **1997**, *38*, 8935-8938.
- (27) Fresneda, P. M.; Molina, P.; Sanz, M. A. *Tetrahedron Lett.* **2001**, *42*, 851-854.
- (28) Ando, N.; Terashima, S. *Synlett* **2006**, 2836-2840.
- (29) Travert, N.; Al-Mourabit, A. *J. Am. Chem. Soc.* **2005**, *127*, 10454-10454.
- (30) Vergne, C.; Boury-Esnault, N.; Perez, T.; Martin, M. T.; Adeline, M. T.; Dau, E. T. H.; Al-Mourabit, A. *Org. Lett.* **2006**, *8*, 2421-2424.
- (31) Gonzalez, A. G.; Martin, J. D.; Perez, C.; Ramirez, M. A. *Tetrahedron Lett.* **1976**, *17*, 137-138.

- (32) Kato, T.; Ishii, K.; Ichinose, I.; Nakai, Y.; Kumagai, T. *J. Chem. Soc., Chem. Commun.* **1980**, 23, 1106-1108.
- (33) Kato, T.; Mochizuki, M.; Hirano, T.; Fujiwara, S.; Uyehara, T. *J. Chem. Soc., Chem. Commun.* **1984**, 1077-1078.
- (34) Shieh, H.-M.; Prestwich, G. D. *Tetrahedron Lett.* **1982**, 23, 4643-4646.
- (35) Snyder, S. A.; Treitler, D. S. *Angew. Chem. Int. Ed. Engl.* **2009**, 48, 7899-7903.
- (36) Van Tamelen, E. E.; Hessler, E. J. *Chem. Commun.* **1966**, 13, 411-413.
- (37) Wolinsky, L. E.; Faulkner, D. J. *J. Org. Chem.* **1976**, 41, 597-600.
- (38) Yamaguchi, Y.; Uyehara, T.; Kato, T. *Tetrahedron Lett.* **1985**, 26, 343-346.
- (39) Maimone, T. J.; Baran, P. S. *Nat. Chem. Biol.* **2007**, 3, 396-407.
- (40) Allemann, R. K. *Pure Appl. Chem.* **2008**, 80, 1791-1798.
- (41) Tantillo, D. J. *Nat. Prod. Rep.* **2011**, 28, 1035-1053.
- (42) Christianson, D. W. *Chem. Rev.* **2006**, 106, 3142-3442.
- (43) L., R.; Eschenmoser, A.; Heusser, H. *Experientia* **1953**, 9, 357-367.
- (44) Snyder, S. A.; Treitler, D. S. *Angew. Chem. Int. Ed. Engl.* **2009**, 48, 7899-7903.
- (45) Carter-Franklin, J. N.; Parrish, J. D.; Tschirret-Guth, R. A.; Little, R. D.; Butler, A. *J. Am. Chem. Soc.* **2003**, 125, 3688-3689.
- (46) Vaillancourt, F. H.; Yeh, E.; Vosburg, D. A.; Garneau-Tsodikova, S.; Walsh, C. T. *Chem. Rev.* **2006**, 106, 3364-3378.
- (47) Snyder, S. A.; Treitler, D. S.; Brucks, A. P.; Gollner, A.; Chiriac, M. I.; Wright, N. E.; Pflueger, J. J.; Breazzano, S. P. Patent WO2012037069 A2, 2012.
- (48) Snyder, S. A.; Treitler, D. S.; Brucks, A. P.; Sattler, W. *J. Am. Chem. Soc.* **2011**, 133, 15898-15901.
- (49) Bonney, K. J.; Braddock, D. C. *J. Org. Chem.* **2012**, 77, 9574-9584.
- (50) Lin, H.; Pochapsky, S. S.; Krauss, I. J. *Org. Lett.* **2011**, 13, 1222-1225.
- (51) Vignes, R. P. *J. Org. Chem.* **1974**, 39, 849-851.
- (52) Uemura, S.; Okazaki, H.; Onoe, A.; Okano, M. *J. Chem. Soc., Perkin Trans. 1* **1979**, 548-552.

- (53) Goodman, J. M.; Kirby, P. D.; Haustedt, L. O. *Tetrahedron Lett.* **2000**, *41*, 9879-9882.
- (54) Brunoldi, E.; Luparia, M.; Porta, A.; Zanoni, G.; Vidari, G. *Curr. Org. Chem.* **2006**, *10*, 2259-2282.
- (55) Johnson, W. S. *Bioorg. Chem.* **1976**, *5*, 51-98.
- (56) Reichardt, C.; Welton, T. *Solvents and Solvent Effects in Organic Chemistry*; 4th ed.; Wiley-VCH: Weinheim, Germany, 2010.
- (57) Vilsmeier, A.; Haack, A. *Ber. Bunsen-Ges. Phys. Chem.* **1927**, *60*, 119-122.
- (58) Barluenga, J.; Campos, P. J.; Gonzalez-Nunez, E.; G., A. *Synthesis* **1985**, 426-428.
- (59) Weber, F. C.; Hennion, G. F.; Vogt, R. R. *J. Am. Chem. Soc.* **1939**, *61*, 1457-1458.
- (60) de Souza, A. V. A.; Mendonca, G. F.; Bernini, R. B.; de Mattos, M. C. S. *J. Braz. Chem. Soc.* **2007**, *18*, 1575-1579.
- (61) Dalton, D. R.; Smith Jr, R. C.; Jones, D. G. *Tetrahedron* **1970**, *26*, 575-581.
- (62) Niizato, H.; Ueno, Y.; Takemura, S. *Chem. Pharm. Bull.* **1972**, *20*, 2707-2709.
- (63) Saikia, I.; Rajbongshi, K. K.; Phukan, P. *Tetrahedron Lett.* **2012**, *53*, 758-761.
- (64) *Theory and Application of Ultra Violet Spectroscopy*; Jaffe, H. H.; Orchin, M., Eds.; Wiley: New York, 1962.
- (65) Hertiani, T.; Edrada-Ebel, R.; Ortlepp, S.; van Soest, R. W. M.; de Voogd, N. J.; Wray, V.; Hentschel, U.; Kozytska, S.; Mueller, W. E. G.; Proksch, P. *Bioorg. Med. Chem.* **2010**, *18*, 1297-1311.
- (66) Tsukamoto, S.; Kato, H.; Hirota, H.; Fusetani, N. *J. Nat. Prod.* **1996**, *59*, 501-503.
- (67) Hewlett, N. M.; Tepe, J. J. *Org. Lett.* **2011**, *13*, 4550-4553.
- (68) Snyder, S. A.; Treitler, D. S. *Org. Synth.* **2011**, *88*, 54.





---

**CHAPTER 4**  
**SYNTHESIS OF EPICOCCONONE-HEMICYANINE HYBRIDS FOR**  
**NEAR INFRA-RED FLUORESCENCE**

---

## 4.1. Introduction

The earliest reports of the phenomenon of fluorescence, date back to the 16<sup>th</sup> century when a bluish glow was observed from an infusion known as *lignum nephriticum* (kidneywood) from the tree *Eysenhardtia polystachya* or *Pterocarpus indicus*, in daylight (**Figure 4.1**).<sup>1</sup> Neither the phenomenon nor its source was understood at the time but the intense blue fluorescence has been recently identified to come from the natural product matlaline found in the kidneywood.<sup>2</sup>

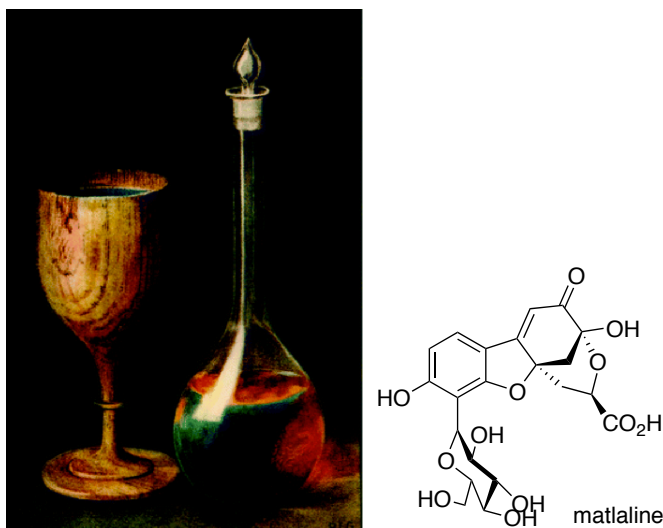


**Figure 4.1** Absorption and fluorescence colours of infusions of *lignum nephriticum* (Palo Azul) in daylight (left), taken from ref. 3 (public domain). Matlaline is the natural product responsible for the observed fluorescence (right).

It was not until the middle of the 19<sup>th</sup> century that the term “fluorescence” was introduced by G. G. Stokes to describe the phenomenon whereby substances with particular photophysical properties absorb light and emit it at a longer wavelength.<sup>4</sup> In his case, he observed a solution of quinine irradiated with UV light emitted blue light.<sup>4</sup>

### 4.1.2. Fluorescence

Fluorescence results from a three-stage process that occurs in certain molecules, that are generally polyaromatic hydrocarbons or heterocycles, called fluorophores or fluorescent dyes. The process responsible for the fluorescence is illustrated by the simple electronic-state diagram, the Jablonski diagram (**Figure 4.2**).

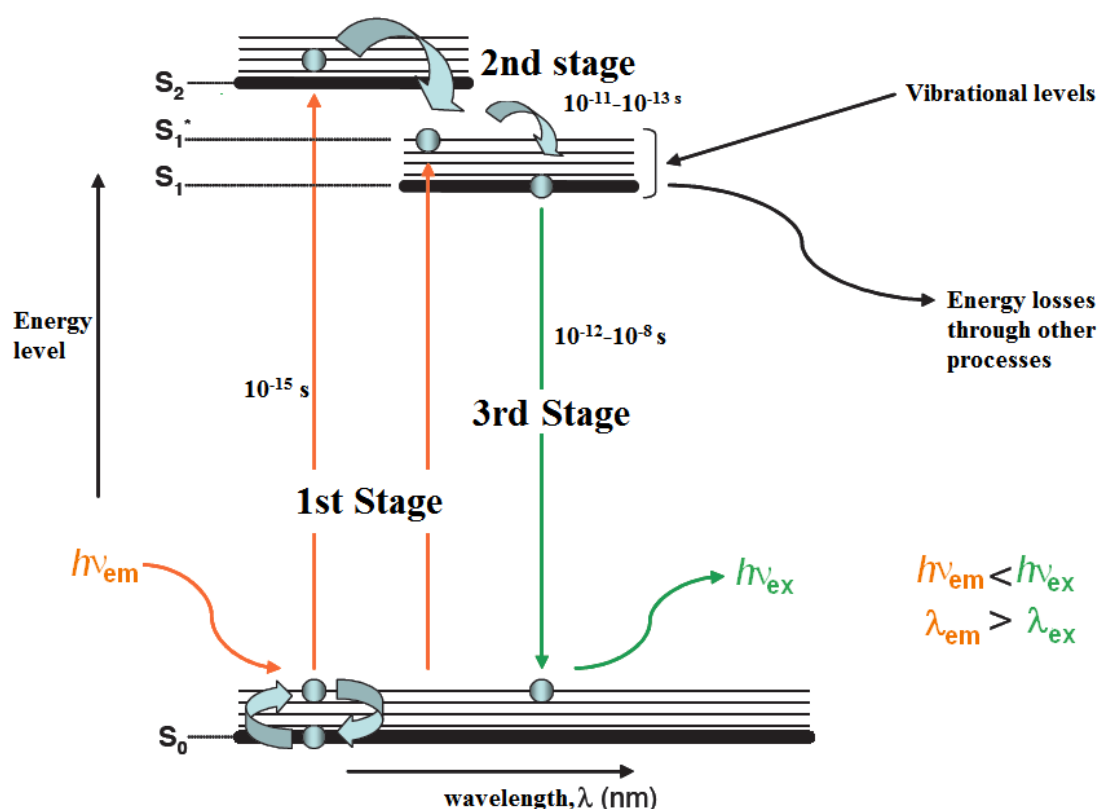


**Figure 4.2** Simplified Jablonski diagram, showing all three stages involved in fluorescence.<sup>5</sup>

In the first stage, a photon of energy  $h\nu_{ex}$  is supplied by an external source such as an incandescent lamp or a laser and absorbed by the fluorophore. The molecule of the fluorophore moves from ground state to an excited electronic singlet state ( $S_1'$ ). Such a transition corresponds to the promotion of an electron to an unoccupied orbital of higher energy. According to Born and Oppenheimer, such

electronic transitions are faster than electron movements due to molecular vibrations.<sup>6</sup> The time taken for an electron to move to an antibonding-orbital is in the order of  $10^{-15}$  s which is shorter than molecular vibrations which take  $10^{-10}$  to  $10^{-12}$  s to occur.<sup>6</sup> This observation follows the Franck-Condon principle which states that an electronic transition is most likely to occur without changes in the positions of the nuclei in the molecular entity and its environment.<sup>7,8</sup> The resulting state is called a Franck-Condon state (excited state), and the transition involved is a vertical transition.

In the second stage, the excited state exists for a finite time ( $10^{-10} - 10^{-13}$  s). During this time, the fluorophore undergoes conformational changes and is also subject to a multitude of possible interactions with its environment.<sup>5</sup> These processes have two important consequences. Firstly, the energy of  $S_1'$  is partially dissipated, yielding a relaxed singlet excited state ( $S_1$ ) from which fluorescence emission originates. Secondly, not all the molecules initially excited by absorption (Stage 1) return to the ground state ( $S_0$ ) by fluorescence emission. Other processes such as collisional quenching, fluorescence resonance energy transfer (FRET) and intersystem crossing may also depopulate  $S_1$ .<sup>5</sup> FRET is a strongly distance-dependent excited-state interaction in which emission of one fluorophore is coupled to the excitation of another.<sup>9</sup> Intersystem crossing is a non-radiative transition between two vibrational levels of two electronic states of different multiplicity ( $S_1$  to  $T_1$ ).<sup>10</sup> The fluorescence quantum yield, which is the ratio of the number of fluorescence photons emitted (Stage 3) to the number of photons absorbed (Stage 1), is a measure of the relative extent to which these processes occur.<sup>5</sup>

In the last stage, a photon of energy  $h\nu_{em}$  is emitted, returning the fluorophore to its ground state ( $S_0$ ). Due to energy dissipation during the excited-state lifetime,

the energy of this photon is lower, and therefore of longer wavelength, than the excitation photon  $h\nu_{\text{ex}}$ .<sup>5</sup> The difference in energy or wavelength represented by  $(h\nu_{\text{ex}} - h\nu_{\text{em}})$  is called the Stokes' shift.<sup>5</sup> The Stokes' shift is fundamental to the utility of fluorescence techniques as a long Stokes' shift minimises self-quenching and Rayleigh scattering.<sup>5</sup>

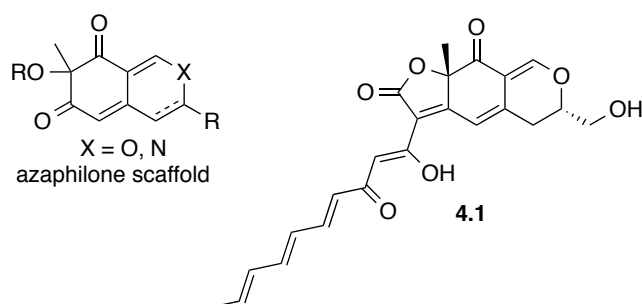
Accordingly, a large Stokes' shift is a desirable photophysical property of fluorophores. Others include a large extinction coefficient (ability to absorb light), a high quantum yield (ratio of photons absorbed to that emitted), good photostability (resistant to photobleaching) and good solubility in the medium it is to be used in. A large extinction coefficient and quantum yield result in fluorescence of high intensity. Fluorescence at longer wavelengths is highly desirable for use in biological systems to minimise photodamage and avoid interference from intrinsic fluorescence of biomolecules. The window where water and biological materials do not absorb (are transparent) is in the range of 750 – 900 nm.<sup>11</sup>

Fluorophores form an important class of molecules widely used in many areas of modern technology. They are used extensively as labelling agents and sensors in both chemical and biological systems, for cellular and molecular imaging as well as for detection and/or quantification of analytes.<sup>12,13</sup> Their wide applicability is due to the higher sensitivity of fluorescence over absorbance. Absorbance spectroscopy relies on the detection of a slight difference in the number of photons passing through the sample while fluorescence spectroscopy measures only the emitted photons from an ideal dark/zero background.<sup>5</sup> It is therefore possible to detect concentrations at sub-nM levels. Furthermore since few molecules have intrinsic fluorescence, the source of fluorescence is known and fluorescence measurements tend to be less

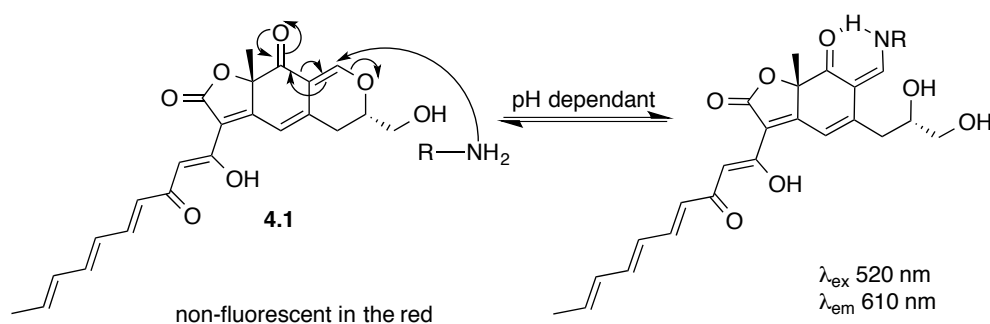
affected by interferences. Furthermore, fluorescence is generally more sensitive to the environment of the chromophore than is light absorption. This is due to the relatively longer time of  $10^{-9} - 10^{-8}$  s that a molecule stays in an excited singlet state before relaxation while absorption is a process that is over in  $10^{-15}$  s.<sup>5</sup> The relatively longer time is sufficient to allow the molecule to respond to its environment and exhibits changes to its fluorescence properties.<sup>5</sup> It is these responses that make fluorescence a widely used method in detecting changes in the environment of the fluorophore. Therefore, the development of fluorophores with desirable photophysical properties mentioned earlier, makes these molecules important targets for synthesis. Indeed, the wide applicability of fluorophores has led to the development and availability of a wide choice of fluorophores, each with their characteristic excitation and emission spectra.

#### 4.1.3. Epicocconone

In 2003, the fortuitous infection of a yeast culture by the fungus *Epicoccum nigrum* led to the growth of orangey-stained yeast which, when viewed under UV light, fluoresced red.<sup>14</sup> The isolation of the compound responsible for the observed fluorescence took place in our laboratory and led to a new member of the azaphilone family, which was named epicocconone (**4.1**).<sup>14</sup>



The azaphilone family, as its name suggests, have an affinity for molecules containing an amino group. Epicoconone will readily form an enamine with an amino group via the ring opening of its dihydropyran (**Scheme 4.1**). The enamine formed is stabilised by an intramolecular hydrogen bond, thus preventing the release of the protein and the reversal of the coupling reaction. However, the reaction is readily reversible through pH. At pH 2.4, the adduct is stable but reverts to the starting materials at higher or low pH's.<sup>15</sup> The natural product **4.1** is a pro-fluorophore as it is intrinsically non-fluorescent, or only weakly fluorescent at low wavelength (520 nm), but exhibits red fluorescence through its ability to covalently bond to amino groups, particularly to the amino side chain of lysine in proteins.<sup>15</sup> This results in the formation of an internal charge transfer (ICT) complex with a large Stokes' shift (90 nm).<sup>16</sup> The complex has fluorescence in the orange-red (610 nm) when subjected to UV or visible light (395 or 520 nm).<sup>14</sup>



**Scheme 4.1** Mechanism of protein fixation to epicoconone.

This pro-fluorophore has generated interest and led to its development as a sensitive stain for protein detection.<sup>17</sup> Its sensitivity is greatly improved by its long Stokes' shift since there is no overlap of excitation and emission wavelengths. In addition, this molecule has other advantageous characteristics, such as a small size (410 amu) and good solubility both in water and lipid. It has successfully entered the

market as Deep Purple (GE Healthcare) and FluoroProfile (Sigma-Aldrich) as a total protein stain in electrophoresis and for protein quantification respectively.<sup>17,18</sup>

However, epicocconone suffers from one main limitation; photobleaching with a lifetime of 11 minutes on a transilluminator.<sup>19</sup> Despite this, epicocconone has proven a very useful natural product and offers a scaffold for the synthesis of analogues to address its shortcomings and most importantly to improve on its photophysical properties. An understanding of the relationship between photophysical properties and molecular structures is also to be gained from the synthesis of analogues.

#### **4.1.3.1. Epicocconone Analogues**

In their efforts towards the total synthesis of the natural product epicocconone, Franck and co-workers have developed a synthetic route to access several epicocconone analogues and two different modifications were investigated.<sup>20-23</sup> The first was at the dihydropyran carbon bearing the methyl alcohol and the second involved the side chain of the molecule (**Figure 4.3**). This led to a first generation of analogues bearing a ketone on the side chain of the molecule and a second generation with a  $\beta$ -diketone. The results obtained have allowed some useful insights into the structure-photophysical relationships of epicocconone.



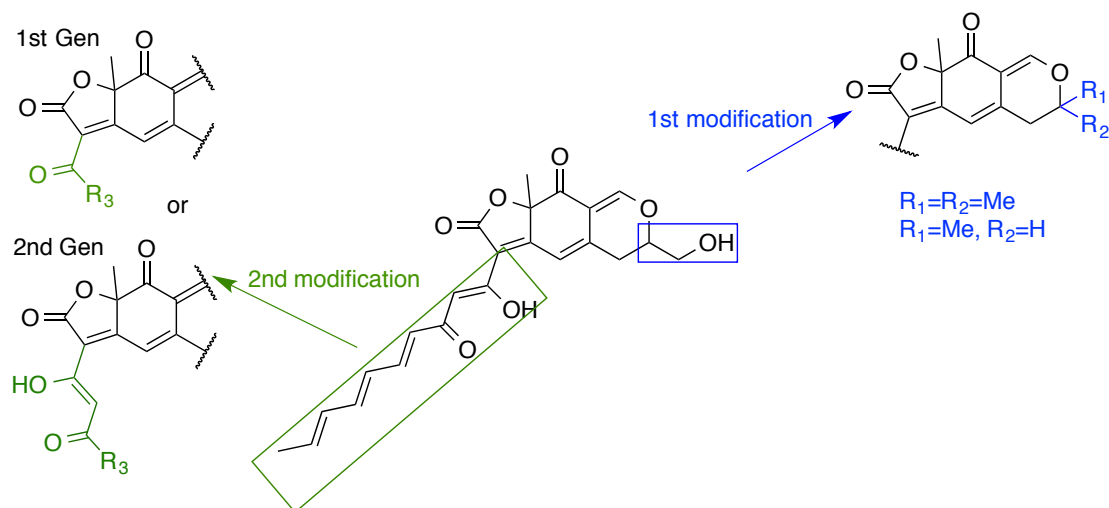
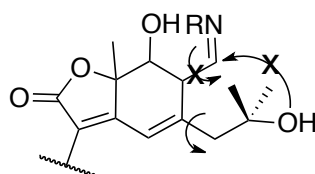


**Figure 4.3** Modifications that have already been investigated in the synthesis of epicocconone analogues. First and second generation (Gen) epicocconone analogues that have been synthesized.

The first generation analogues with the ketone on the side chain proved to be less fluorescent than the natural product itself while the second generation analogues with a  $\beta$ -diketone were of comparable fluorescence. This indicated the crucial role of the  $\beta$ -diketone in the formation of the internal charge transfer responsible for the fluorescence observed in epicocconone.<sup>24,25</sup> Compared to the latter, these second generation analogues are fluorescent in their native form as well as, as their enamines. The use of a 2-naphthyl group as the  $R_3$  group on the second generation analogue scaffold, has led to a brighter analogue **4.2** ( $\epsilon = 17\,500\text{ M}^{-1}\text{cm}^{-1}$ ,  $\Phi = 0.225$ ) than epicocconone ( $\epsilon = 13\,000\text{ M}^{-1}\text{cm}^{-1}$ ,  $\Phi = 0.147$ ) in the formation of the enamine adduct with butylamine (**Table 4.1**).

The presence of a dimethyl dihydropyran ring ( $R_1 = R_2 = \text{Me}$ ) was found to induce an increase (1.32 fold) in fluorescence emission intensity in the second generation analogues compared to the monomethyl counterpart ( $R_1 = \text{Me}$  and  $R_2 = \text{H}$ ) (**Figure 4.3**).<sup>20</sup> Steric hindrance is likely to cause restricted rotation of the enamine which could be a source of non-radiative energy loss of the excited state. It could also

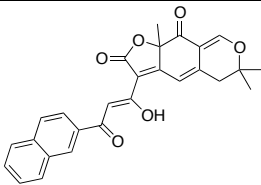
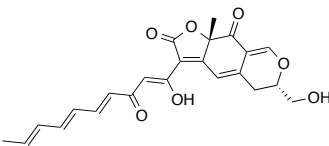
be inhibiting the recyclisation of the enamine that leads to the release of the native fluorescent molecule, the tertiary alcohol being far less nucleophilic (**Figure 4.4**).<sup>20</sup>



**Figure 4.4** The presence of the dimethyl groups restricts rotation of the enamine and potentially inhibits and slows down recyclisation.

The 2-naphthylepicocconone analogue has a signal-to-noise ratio, three times higher than that of epicocconone as a protein marker on gel electrophoresis, a better detection limit for five different proteins and a higher resistance to photobleaching with a half life of 33 min.<sup>20,26</sup> Therefore, an epicocconone analogue with better photophysical properties than the natural product was achieved (**Table 4.1**). These results encouraged us to investigate further analogues.

**Table 4.1** Comparison between the second generation analogue and the natural product, epicocconone.

Entry	Fluorophore	UV absorption $\lambda_{\text{max}}$ / nm	$\epsilon$ / $\text{M}^{-1}\text{cm}^{-1}$ at 2 <sup>nd</sup> max	Max $\lambda_{\text{em}}$ / nm	$\Phi$
<b>1</b>		<sup>a</sup> 310, 415	14 600	530	0.390
		<sup>b</sup> 370, 515	17 500	610	0.225
<b>2</b>		<sup>a</sup> 435	13 400	535	0.026
		<sup>b</sup> 396, 520	13 000	615	0.147

**a.** Measurements of the native molecule in ACN; **b.** Measurements of the enamine formed in the presence of butylamine (in excess) in ACN; Measurement of  $\epsilon$  at respective max  $\lambda_{\text{ex}}$ .<sup>25</sup>

#### 4.1.4. Near Infra-Red (NIR) Fluorescence

Even though visible-light fluorophores still dominate the field of fluorescence, dyes that fluoresce in the near infra-red region (NIR) have attracted much attention over the past decade.<sup>27,28</sup> In general, NIR fluorophores are defined as substances that emit fluorescence in the NIR region (700 – 900 nm) (**Figure 4.5**).<sup>29</sup> Compared to most other conventional fluorescent probes, those that rely on NIR fluorescence possess unique advantages for tracing molecular processes *in vivo*.<sup>11,30</sup>

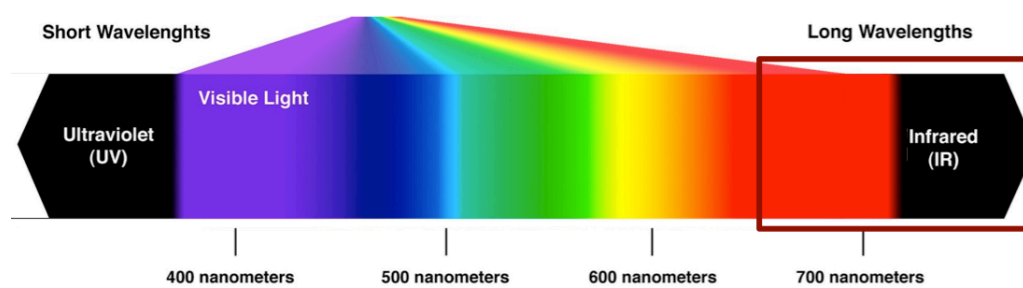


**Figure 4.5** The NIR region of the electromagnetic spectrum is indicated by the square.

The main advantage of using NIR fluorescence technology is an almost complete elimination of background fluorescence caused by autofluorescence from biomolecules in living systems.<sup>11,30,31</sup> Another benefit in the NIR region is that the scattered light from the excitation source will be greatly reduced since the scattering intensity is proportional to the inverse fourth power of the wavelength. Low background fluorescence and low scattering result in a high signal to noise ratios, which is essential for high sensitive detection in live animals. The low absorptivity and scattering of NIR photons in tissue enable *in vivo* imaging and subcellular detection applications which require the transmission of light through biological components.<sup>31,32</sup> NIR photons also mean less damage to biological samples.

A further advantage of NIR fluorescence is the availability and low cost of long-wavelength diode lasers for excitation and high efficiency silicon avalanche photodiodes for detection. However, commercial diode lasers are only available at a limited number of discrete wavelengths. To achieve optimum excitation, a fluorophore's maximum absorption wavelength should match these laser wavelength.

#### **4.1.4.1. Near Infra-red Fluorophores**

A variety of NIR-active organic dyes have been synthesised, with fluorescence maxima ranging from 700 nm to about 900 nm.<sup>29</sup> The principal limitations of most of these dyes in biological systems are the low quantum yields, poor chemical stability and/or photostability, and limited solubility in aqueous solutions.<sup>27</sup> Moreover, there are only a relatively few classes of NIR dyes that are readily available. These include the cyanine dyes, phthalocyanines and squaraine dyes.<sup>27</sup> There is thus a great interest in developing new NIR fluorescent dyes with improved properties for bioimaging applications.

##### **4.1.4.1.1. Cyanines**

The most widely employed NIR fluorophores are cyanine dyes. The cyanines are a unique class of charged chromophores with an odd number of carbons in a conjugated polymethine framework.<sup>33</sup> Cyanine dyes make excellent NIR dyes that have high molar absorptivity, strong fluorescence, and good photostability. However their intrinsically small Stokes' shifts may produce interference from Rayleigh and Raman Scattering.

The indocyanines are the most important type of cyanine dye, featuring two indole or benzindole rings linked by a polymethine chain (**Figure 4.6**). While Cy5 (**4.3**) fluoresces in the red, Cy7 (**4.4**), a more conjugated cyanine, fluoresces in the NIR region. The wavelength can be adjusted by varying the length of the polymethine chain and/or changing the heterocycle at the end of the chain. An example of the latter is the carbocyanine (**4.5**) where quinoline forms the heterocycle (**Figure 4.6**).<sup>34</sup> Derivatives of the cyanine dyes are the most commonly used NIR fluorescent dyes and popular in bioconjugation application. Indocyanine green (ICG, **4.6**) is a Cy7 cyanine dye, that has FDA approval for use in medical diagnosis and has allowed noninvasive deep tissue imaging.<sup>35-37</sup> In long chain ( $n > 3$ , where  $n$  is the number of double bonds as indicated in **Figure 4.6**), the decrease in rigidity of the double bond conjugation system leads to a reduction in brightness of the dye as the longer the polymethine chain the more likely occurrence of non-radiative isomerisations or oxidations. To circumvent this, a bridged polymethine chain is introduced to make the link less flexible.<sup>38</sup> Tung and co-workers reported a Cy7 derivative, NIR820 dye (**4.7**) with maximum emission at 820 nm which has a cyclohexene bridge heptamethine chain and has been functionalised with a *N*-hydroxysuccinimide ester on one of the indole ring for conjugation purposes (**Figure 4.6**).<sup>39</sup> In order to increase the solubility of cyanine dyes, sulfonate groups have been introduced on the aromatic rings or the *N*-alkyl chains. This has also led to the decrease of self-aggregation of cyanine dyes in aqueous solution. Self-aggregation along with a small Stokes' shift are the major problems of cyanine dyes.

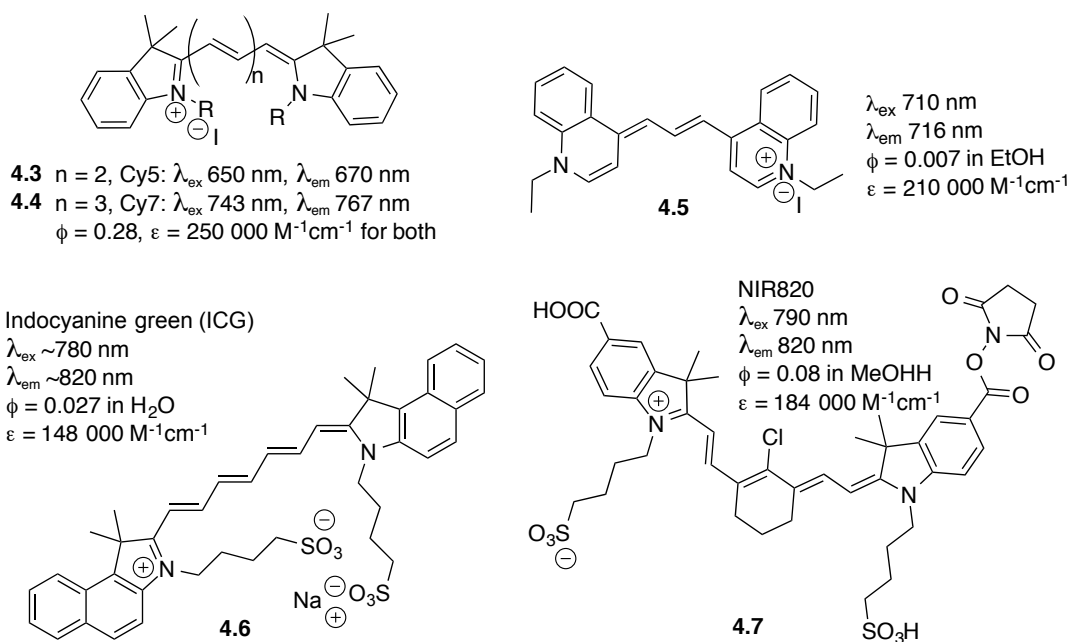


**Figure 4.6** Example of NIR cyanine dyes.

#### 4.1.4.1.2. Porphyrins and Phthalocyanines

Porphyrins and phthalocyanines and their metal complexes are amongst the most intensively studied NIR-active dyes. Phthalocyanines are an important class of NIR dyes used in many different fields, including as colourants, cancer therapy agents, detergents, and non-linear optical materials.<sup>40</sup> In general they demonstrate excellent chemical and photostability. However, most phthalocyanine dyes are hydrophobic, tend to aggregate in aqueous solution and also tend to have high phototoxicity in cells. They are also not easily functionalised for bioconjugation purposes. La Jolla Blue (**4.8**) is a NIR phthalocyanine that has two water-soluble axial polyethylene glycol moieties and bears two reactive carboxylic acid groups on the macrocycle useful for bioconjugation (**Figure 4.7**).<sup>41</sup> Generally, porphyrins absorb only weakly in the red region of the spectrum (600 – 700 nm) and not at all in the NIR region, whereas chlorins (dihydroporphyrins) absorb strongly in the red region, and bacteriochlorins (tetrahydroporphyrins) absorb even more strongly in the

NIR region.<sup>42</sup> NIR porphyrins were achieved through large fluorine-containing porphyrins **4.9-4.11** with emission bands at 746 – 953 nm, reported by Osuka and co-workers (**Figure 4.7**).<sup>43</sup> Synthetic chlorin and bacteriochlorin macrocycle dyads were created (example **4.12**) and displayed large Stoke' shifts (85 – 110 nm) and have narrow spectral widths ( $\leq 20$  nm).<sup>44</sup> However these lack the structural motifs required for bioconjugation and are not soluble in aqueous media as porphyrins tend to aggregate in water to form excimers that have different spectral properties.<sup>45</sup>

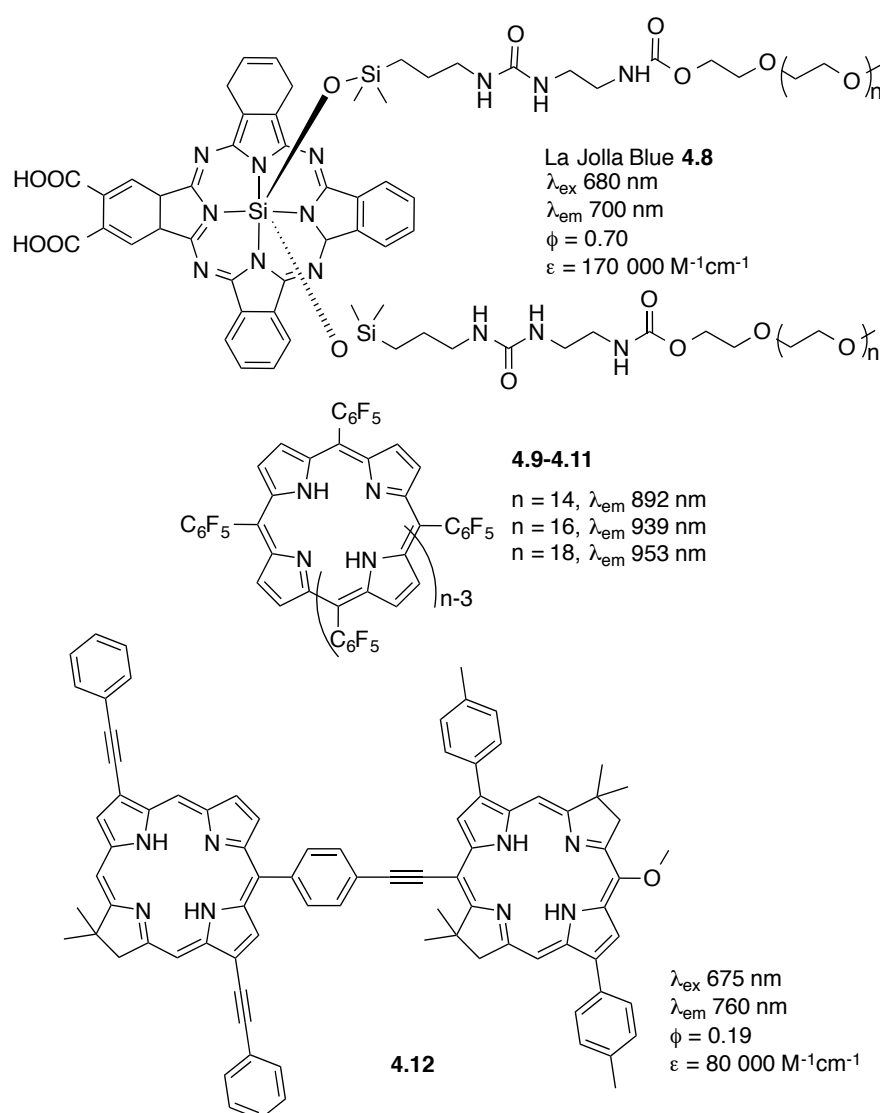


**Figure 4.7** Example of NIR macrocycle dyes: a phthalocyanine, large porphyrin macrocycles and a chlorin/ bacteriochlorin dyad.

#### 4.1.4.1.3. Squaraines

The squaraines are a class of organic dyes showing intense fluorescence, typically in the red and NIR.<sup>46</sup> Absorption maxima are found between 630 – 670 nm and their emission maxima are between 650 – 700 nm. They possess a unique aromatic four-membered ring system derived from squaric acid and a resonance stabilised zwitterionic structure. Most squaraines suffer from the nucleophilic attack of the highly electron deficient central four membered ring. This has been decreased by the formation of a rotaxane around the dye to protect it from nucleophiles. They are currently used as sensors for ions and have recently, with the advent of protected squaraine derivatives, been exploited in biomedical imaging.<sup>47</sup> Suzuki and co-worker reported a water soluble squaraine (**4.13**) (**Figure 4.8**), functionalised with sulfonate moieties which they have shown to be applicable to protein detection as covalent labeling probes, and as contrast agents for *in vivo* imaging.<sup>48</sup>

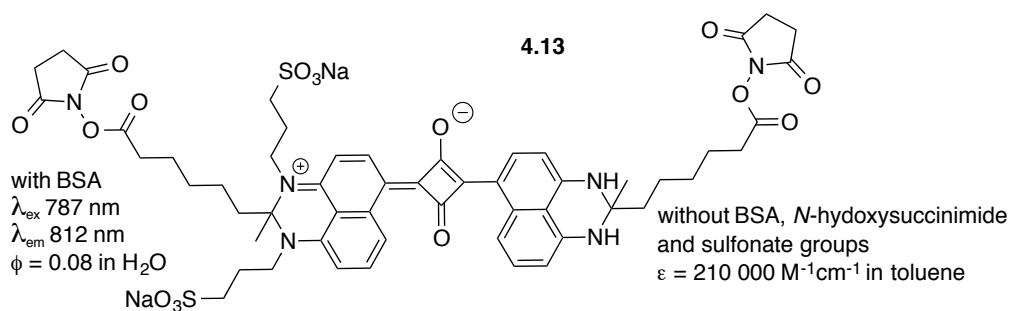


**Figure 4.8** Water-soluble NIR fluorescent probe based on a squaraine structure, exhibiting NIR fluorescence after protein labeling.

#### 4.1.4.1.4. BODIPY Dyes

The BODIPY dyes are composed of dipyrromethene complexed with a disubstituted boron atom, typically a BF<sub>2</sub> unit (**Figure 4.9**).<sup>49</sup> BODIPY dyes have



good and environment-independent brightness, and excellent photo-stability characteristics as compared to the cyanines and other NIR dyes.<sup>50</sup> However, they suffer from the fact that their absorption maxima lie in the visible region and, thus, they are not optimal for noninvasive *in vivo* imaging. They are also notable for their high extinction coefficients and small Stokes' shifts. O'Shea and co-workers has synthesised tetraarylazadipyrromethenes (example **4.14**) which contain aryl groups bonded to the chromophore and has resulted in emission into the NIR region (**Figure 4.9**).<sup>51-53</sup> Suzuki and co-workers have extended the emission of BODIPY analogues into the NIR region by fusing aromatic rings to the BODIPY core and by further increasing the conjugation by introducing aryl moieties (example **4.15**) (**Figure 4.9**).<sup>54,55</sup>

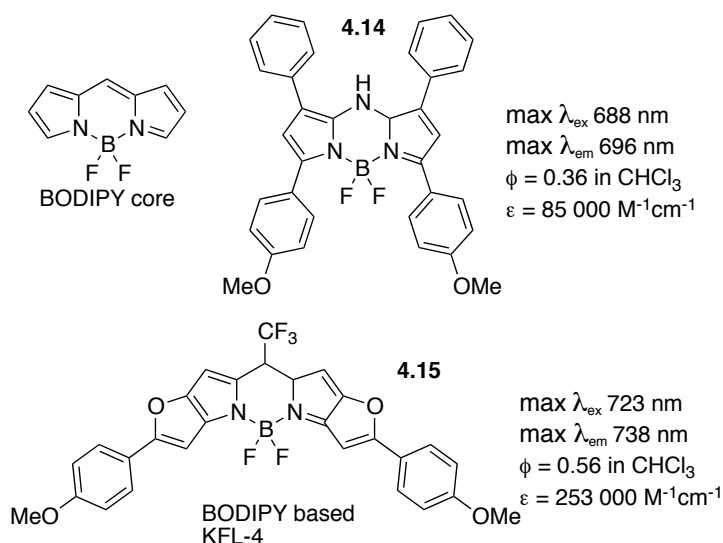


**Figure 4.9** The BODIPY core and examples of NIR BODIPY dyes.

#### 4.1.4.1.5. Xanthene/coumarin Derivatives

Xanthene-based dyes have good photochemical properties, such as high molar extinction coefficients, large fluorescence quantum yields and are relatively resistant to photobleaching.<sup>56</sup> They are widely used fluorescent probes and molecular markers

because of their excellent photophysical properties.<sup>57</sup> However, the absorption and emission wavelengths of most xanthene-based fluorophores as well as coumarin lie in the visible region. Nevertheless, fluorescein, rhodamine and coumarin (**Figure 4.10**) offer a platform onto which to develop stable analogues with absorption and emission in the red or NIR region. This has been achieved through chemical modifications of their xanthene core. Seminaphthofluorone xanthene dye **4.16** that exhibits NIR fluorescence, both in the neutral and anionic forms, with impressive Stokes' shifts, were synthesised by Strongin and co-workers (**Figure 4.10**).<sup>58</sup> NIR fluorescence was achieved by both the group of Lin and Song when they introduced a cyanine onto their respective developed xanthene-based scaffold **4.17** (**Figure 4.10**).<sup>59,60</sup> The fluorescence is very solvent-dependent and has relatively small Stokes' shift. Rhodamine 800 (Rhod 800, **4.18**), also known as MitoFluor Far Red 680, is a cationic lipophilic dye, which emits in the NIR region and is used for staining of the mitochondria.<sup>61</sup>

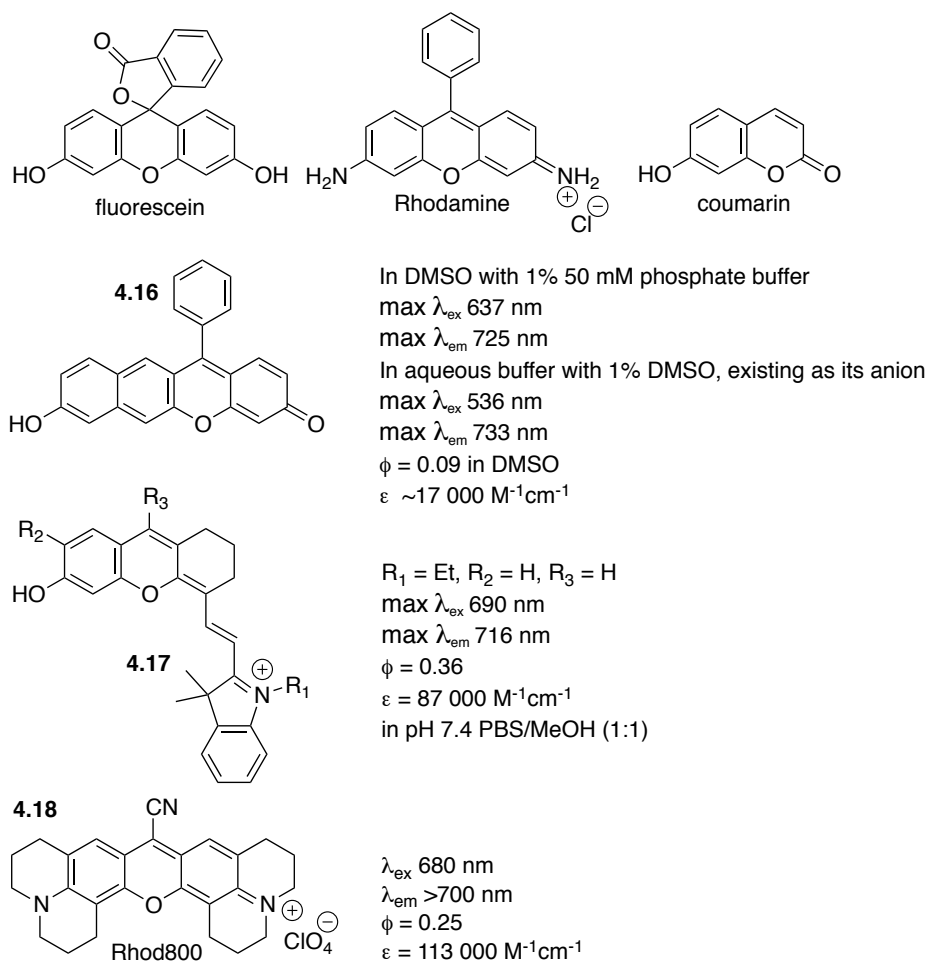


**Figure 4.10** Examples of NIR xanthene-based and coumarin-based dyes.

#### 4.1.4.1.6. Benzo[*c*]heterocycles

Push-pull type NIR dyes that contain isobenzofuran or isothianaphthene moieties have been reported by Swager and co-workers (**Figure 4.11**).<sup>62</sup>

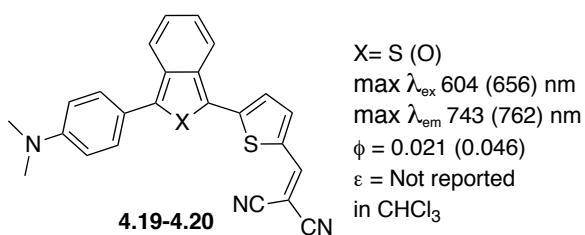
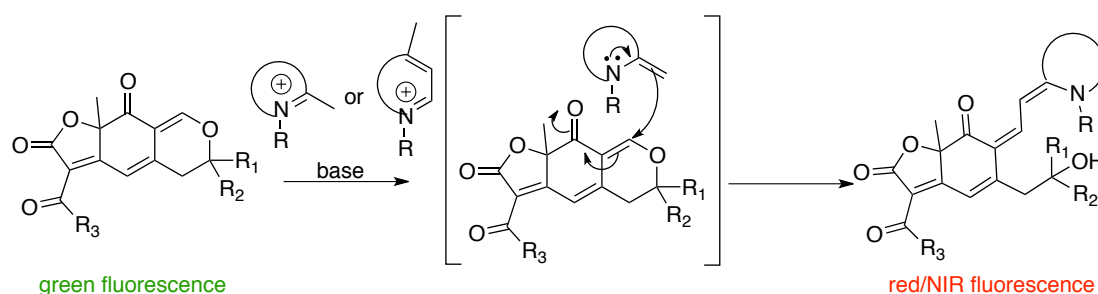


**Figure 4.11** Examples of NIR Benzo[*c*]heterocycle dyes.

#### 4.1.4.2. NIR Epicoconone Analogues

So far, in the synthesis of epicoconone analogues, structural modifications have only been made to the epicoconone sidechain (**Figure 4.3**). It was found that changing the triene to phenyl to naphthyl did not increase the emission wavelength. We reasoned that this may be possible by extending the conjugation of the other end of the molecule. This could be achieved in two ways: firstly by adding more conjugation to the reacting amine. Thus reacting aniline with epicoconone results in an adduct with  $\lambda_{\text{em}} = 630$  nm which is an increase in emission wavelength of 20 nm compared to the butylamine adduct (Coghlan and Karuso, *unpublished*) but the resulting adduct is unstable and only a modest increase in  $\lambda_{\text{em}}$  was achieved. Secondly the conjugation could be added in between the dihydropyran and the amine. This can be achieved by taking advantage of the fact that the dihydropyran is a masked aldehyde. Therefore in order to synthesise NIR epicoconone analogues, the high affinity of the dihydropyran ring in the epicoconone scaffold for nucleophiles has been exploited. This strategy has involved the introduction of nitrogen heterocycle-based ylides onto the epicoconone scaffold via the ring opening of the dihydropyran ring (**Scheme 4.2**). This would lead to the formation of epicoconone-hemicyanine hybrid dyes which we expected would extend the emission wavelength into the red to NIR region.



**Scheme 4.2** Synthesis of epicoconone-hemicyanine hybrid dyes.

## 4.2. Results and Discussion

With the aim of discovering new NIR dyes with improved photophysical properties over existing ones, we investigated the design and synthesis of epicocconone-hemicyanine hybrids (**Scheme 4.2**).

### 4.2.1. Hemicyanines

Hemicyanine is a class of cyanine. While cyanine is broadly used to refer to two nitrogens joined by an odd numbered polymethine chain, hemicyanine contain only one nitrogen as part of a heteroaromatic moiety, such as indole, quinoline, thiazole to name a few, and connects to a polymethine chain (examples **4.21** and **4.22**; **Figure 4.12**). Hemicyanine have been widely applied in different areas of technology due to their diverse properties.<sup>63</sup> Because of their spectroscopic properties they are commonly used as laser dyes and fluorescence probes.<sup>64</sup> They generally possess absorption and emission wavelengths below 600 nm but it has been possible to extend the latter to the red/NIR region by conjugation to existing fluorescent scaffolds (**4.17** in **Figure 4.11**). Their photophysical dependence on viscosity offers several applications in polymer science and analytical chemistry.<sup>65-67</sup> This is due to cis/trans isomerisation of the linking double bond, which is inhibited in viscous solvents.

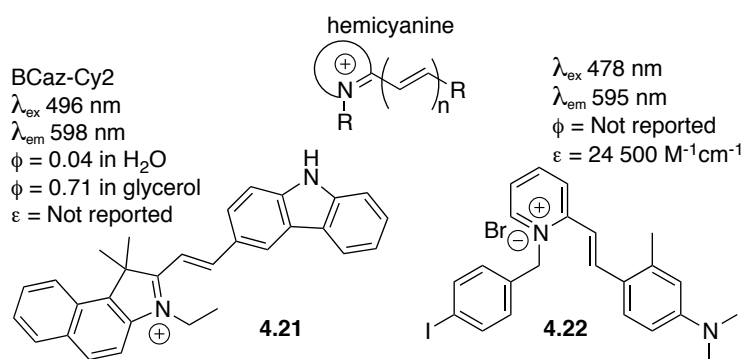
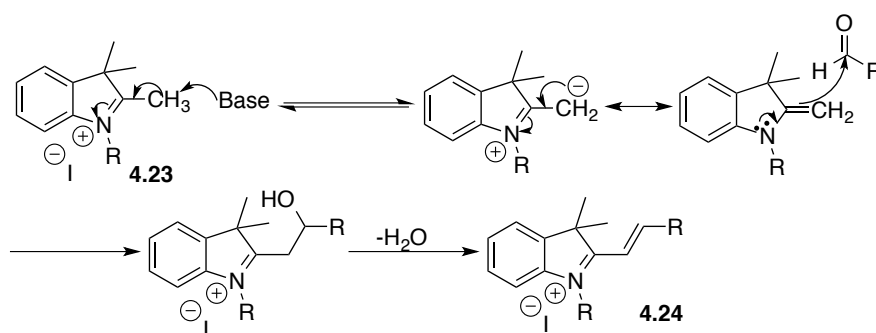


**Figure 4.12** General representation of a hemicyanine and two examples of hemicyanines.

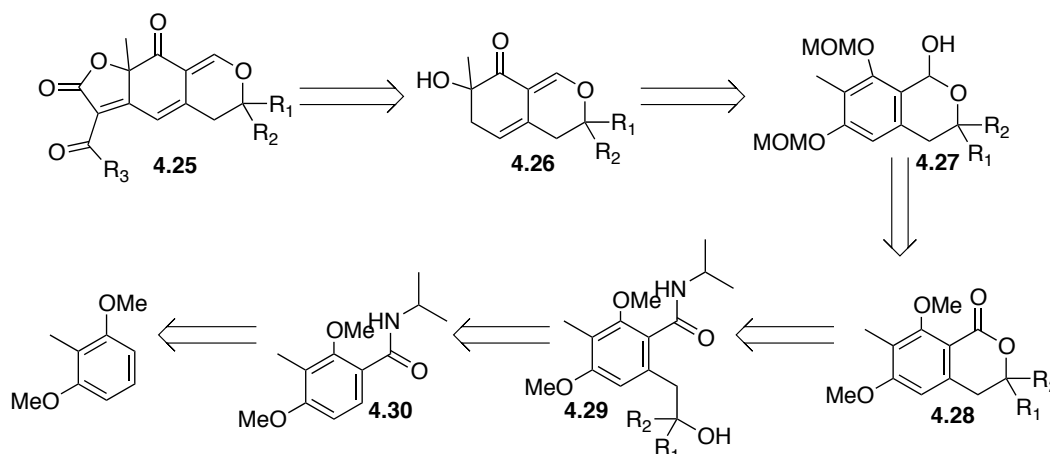
The general method used for the synthesis of hemicyanine dyes involves the condensation of nitrogen heterocycle-based ylides with a substituted benzaldehyde in the presence of a suitable base.<sup>68</sup> **Scheme 4.3** shows the condensation of an *N*-alkyl substituted 2-methyl-3,3-dimethylindolium iodide salt (**4.23**) with an aldehyde in the presence of a base. The reaction mechanism proceeds through an aldol-type reaction to eventually yield the *N*-alkyl-2-styryl-3,3-dimethylindolium iodide salt (**4.24**) as the hemicyanine dye.



**Scheme 4.3** Condensation of *N*-alkyl substituted 2-methyl-3,3-dimethylindolium iodide with an aldehyde to form a hemicyanine dye.

#### 4.2.2. Synthesis of the Second Generation Naphthyl Epicocconone Analogue

The dihydropyranic azaphilone (**4.25**) core framework of epicocconone skeleton has been accessed via an established route based on the introduction of acyl furanones to the  $\alpha$ -hydroxyketones (**Scheme 4.4**).<sup>20-23</sup> Retrosynthetically, the key  $\alpha$ -hydroxyketone **4.26** was the product of MOM deprotection of lactol **4.27**, followed by an oxidative dearomatisation. The lactol **4.27** was formed in four steps from the amidoalcohol **4.29** via a cyclisation to lactone **4.28**. The amido alcohol **4.29** was obtained from an orthometallation reaction with the subsequent trapping of the organometallic species with an epoxide. The amide **4.30** was synthesised from commercially available 2,6-dimethoxytoluene.

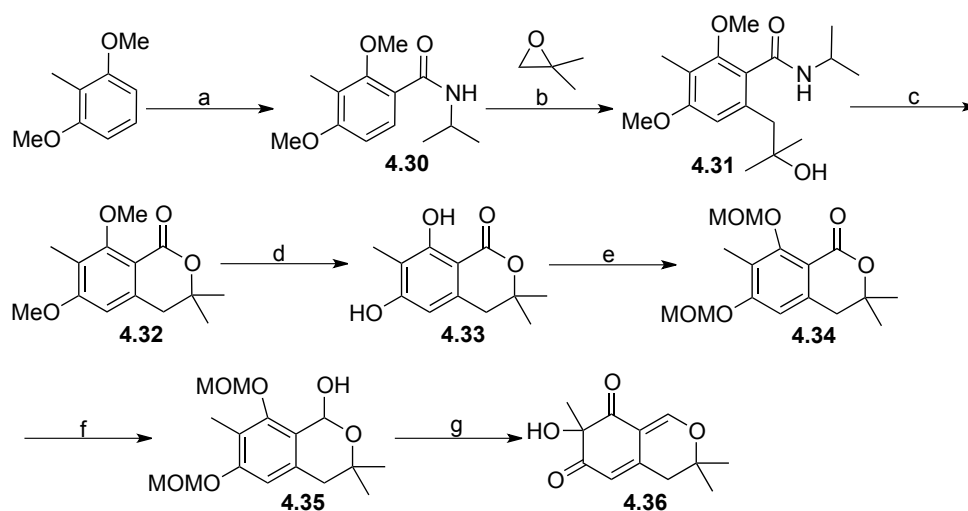


**Scheme 4.4** Retrosynthetic study of the epicocconone scaffold.

The most promising epicocconone analogue synthesised so far is **4.2** as it is brighter ( $\epsilon = 14\,600\text{ M}^{-1}\text{cm}^{-1}$ ,  $\Phi = 0.39$ ) than epicocconone ( $\epsilon = 13\,400\text{ M}^{-1}\text{cm}^{-1}$ ,  $\Phi = 0.026$ ). It also showed the best staining characteristics in gel electrophoresis as well as being more resistant to photobleaching.<sup>26</sup>

This analogue was prepared following the reported procedure with a few minor modifications, in 11 steps. Briefly, starting with the commercially available 2,6-dimethoxytoluene, the secondary amide **4.30** was obtained in excellent yield via an amidation reaction with isopropyl isocyanate in the presence of aluminium trichloride (**Scheme 4.5**). The epoxide, 2,2-dimethyloxirane was introduced by an ortho-lithiation reaction, directed by the amide at low temperature. The resulting alcohol **4.31** was subjected to lactonisation in the presence of camphorsulfonic acid to form lactone **4.32** in 95% yield. The latter was deprotected with aluminium trichloride to provide the diphenol **4.33**. The diphenol was protected with freshly prepared MOM-chloride to give the diMOM ether **4.34** which was then reduced by DIBAL-H to lactol **4.35**. Oxidative dearomatisation of the lactol was then carried out with IBX in the presence of TFA/water to afford the key diketone alcohol **4.36** in 58%

yield over the last two steps. This is a critical step as the presence of both TFA and water in the ratio 7:20 not only cleaves the MOM groups but accelerates the oxidation of the intermediate oxonium ion to yield the dearomatised product **4.36**. Since the completion of this work, a shorter synthetic route of only 5 steps has been devised to access the key  $\alpha$ -hydroxyketone **4.36** starting from commercially available methyl atarate.<sup>26</sup>

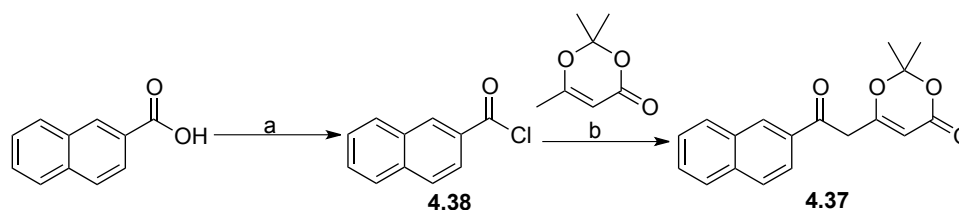


**Scheme 4.5** Synthesis of the key  $\alpha$ -hydroxyketone. Reaction conditions: **a.** *i*-PrNCO, AlCl<sub>3</sub>, DCM, r.t, 3 h, 95%; **b.** *t*-BuLi/TMEDA, THF, -78 °C then 2,2-dimethyloxirane, THF, -78 °C-r.t, 68%; **c.** camphorsulfonic acid, toluene, reflux, 95%; **d.** AlCl<sub>3</sub>, DCM, ref, 24 h, 98%; **e.** NaH, (MOM)Cl, THF, r.t, 100%; **f.** DIBAL-H, toluene, -78 °C, 100%; **g.** CH<sub>2</sub>Cl<sub>2</sub>, TFA/H<sub>2</sub>O (7:20, v/v), then IBX, 56%.

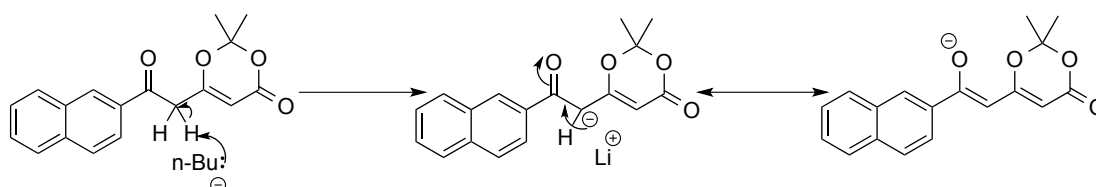
The formation of the acylfuranone ring and the addition of the  $\beta$ -diketo side chain take place using the dioxinone **4.37**. The 2-naphthoyl chloride (**4.38**) was obtained by the DMF catalysed nucleophilic acyl substitution of the corresponding carboxylic acid in dichloromethane in the presence of oxalyl chloride. The desired 2-naphthyldioxinone **4.37** was then obtained by the acylation of commercially available 2,2,6-trimethyl-4*H*-1,3-dioxin-4-one through the addition of its lithium enolate to the 2-naphthoyl acid chloride at -78 °C (**Scheme 4.6**). The low yield can be explained by the presence of the acidic protons on the 2-naphthyldioxinone that can themselves be



deprotonated to form the corresponding lithium enolate (**Scheme 4.7**). The purification of the commercial methylldioxinone on a short pad of silica prior to use, increased the yield of the 2-naphthyldioxinone.



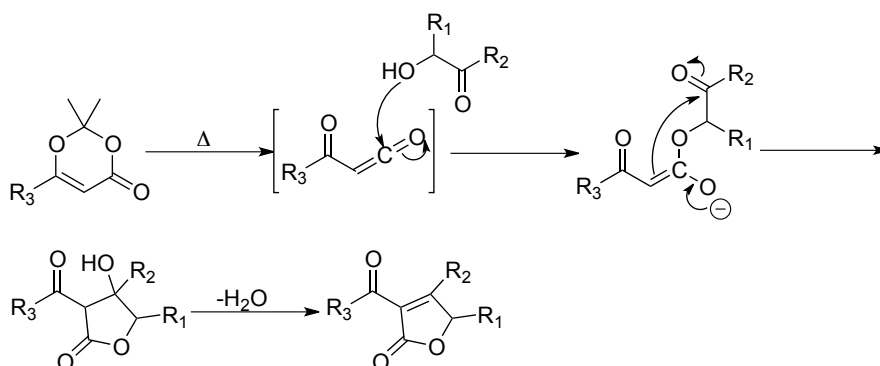
**Scheme 4.6** Synthesis of the 2-naphthyldioxinone. Reaction conditions: **a.** oxalyl chloride, DMF (catalytic amount), DCM, r.t., 2.5 h, qqt; **b.** *n*-BuLi/DIPA, THF,  $-78^{\circ}\text{C}$  then 2,2,6-trimethyl-4*H*-1,3-dioxin-4-one, THF,  $-78$  to  $-40^{\circ}\text{C}$ , 2.5 h, 75%.



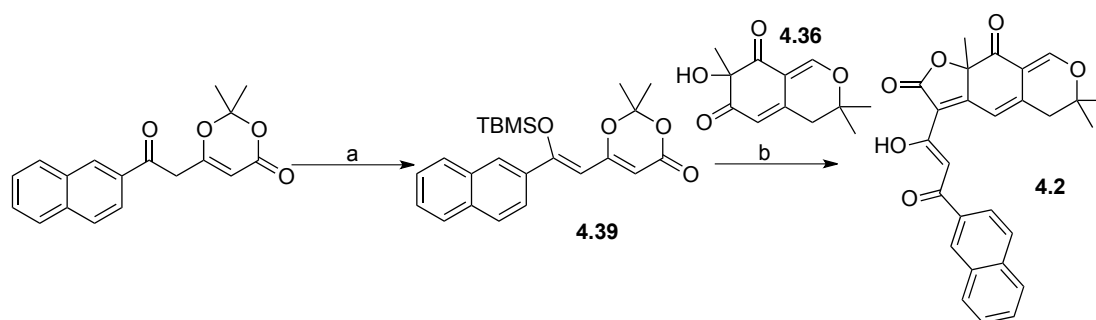
**Scheme 4.7** Unstability of the 2-naphthyldioxinone due to the presence of acidic protons.

The formation of the acylfuranone ring occurs via the *in situ* formation of an acyl ketene that is trapped by the hydroxy group of the  $\alpha$ -hydroxydiketone before cyclisation takes place (**Scheme 4.8**). The key acyl ketene is formed from the 2-naphthyldioxinone **4.37** at high temperature. However, **4.37** undergoes decomposition under basic conditions. The protection of the ketone in the form of the enol was necessary before the acylfuranone ring formation could proceed. The enol was therefore protected using *t*-butyldimethylsilyltriflate (TBDMS) to form **4.39**, as previously reported (**Scheme 4.9**). However the acylfuranone ring formation is low yielding (24%) and it is likely due to loss of the protecting group under the reaction

conditions. The loss of TBDMS during the reaction is apparent, as the epicocconone analogue **4.2** formed is non-silylated (**Scheme 4.9**).



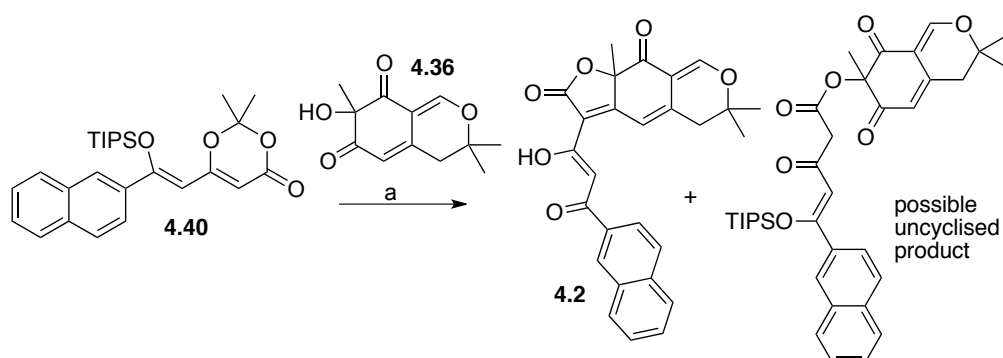
**Scheme 4.8** Formation of the acylfuranones from the cyclisation of in-situ formed acyl ketenes from dioxin-4-ones, with the key α-hydroxyketones.



**Scheme 4.9** Synthesis of the second generation, 2-naphthyl epicocconone analogue. Reaction conditions: **a.** TBDMSTF, DIEA, DCM, r.t, 2 h, 45%; **b.** TEA, 4Å MS, toluene, 100°C, 24%.

Consequently, the use of triisopropylsilyl (TIPS) as a protecting group, was investigated as a possible alternative to TBDMS. Thus TIPS protected dioxinone was synthesised and obtained in a comparable yield to TBDMS protected dioxinone after purification through a short pad of silica. The protected dioxinone must be used straight away as it is unstable and decomposes over a few hours at room temperature. TIPS-protected-2-naphthyldioxinone **4.40** was reacted for 7 h with **4.36** in refluxing toluene, in the presence of TEA and 4Å molecular sieves. After an aqueous work-up, crude <sup>1</sup>H NMR indicated a mixture of the desired product and an uncyclised

intermediate that possess the same  $R_f$  on TLC as the desired product (**Scheme 4.10**). Purification led to the isolation of **4.2** in 21% yield. While TIPS as a protecting group for the dioxinone is more robust to the reaction conditions used in the acylfuranone ring formation, this however appears to inhibit the desired cyclisation. Its removal with excess aqueous HF in THF did not lead to the desired cyclisation as the latter requires basic reaction conditions to proceed.



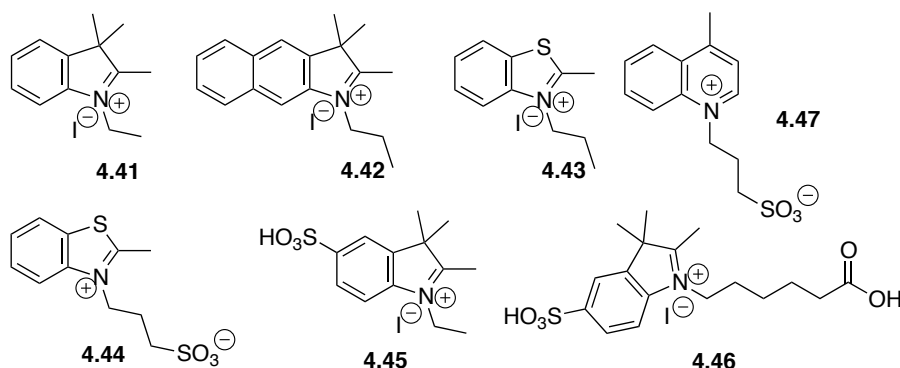
**Scheme 4.10** Synthesis of the second generation, 2-naphthyl epicocconone analogue using TIPS-protected-2-naphthyl dioxinone, led to a mixture of desired product and uncyclised intermediate. Reaction conditions: **a**. TEA, 4Å MS, toluene, 100°C, 7 h, 21% yield.

With the aim of improving on the yield of the acylfuranone reaction, the addition of the TBDMS protected dioxinone was effected in two different ways: (1) where the dioxinone was added all at once and (2) where the addition was conducted in 3 portions at 1 h intervals. The crude  $^1\text{H}$  NMR spectra of the two reactions were almost identical and the desired epicocconone analogue was isolated in 24% yield in the first instance and in 26% yield in the second.

### 4.2.3. Synthesis of the hemicyanine moieties

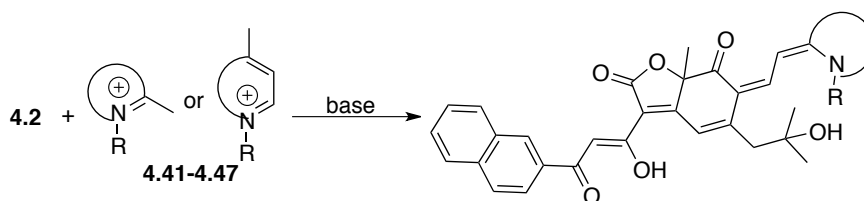
With the 2-naphthylepicocconone analogue **4.2** in hand, we turned our attention to the synthesis of the hemicyanine moieties. A range of quaternary salts **4.41-4.47** were purchased or synthesised from the base with alkyl iodides or sultones

(See **Experimental**). The presence of sulfonic acid groups has been reported to help decrease self-aggregation of cyanine dyes in aqueous solution.<sup>33</sup>



#### 4.2.4. Synthesis of the Epicocconone-Hemicyanine Hybrid Dyes

The coupling of **4.2** analogue with seven different *N*-alkyl-2-methyl or 4-methyl iodides (**4.41-4.47**) was effected for the preparation of the epicocconone-hemicyanine hybrid dyes (**Scheme 4.11**).

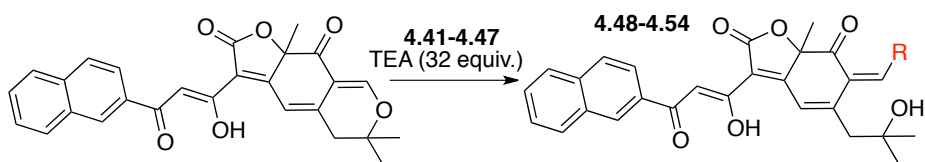


**Scheme 4.11** Synthesis of epicocconone-hemicyanine hybrid dyes.

The initial reaction trials were conducted with one equivalent of trimethylindolium iodide salt (**4.41**) in the presence of four equivalents of TEA in chloroform at room temperature. The desired epicocconone-hemicyanine hybrid was formed immediately as evident from a change in colour to deep purple. The product was isolated as a dark blue solid after silica chromatography in 30% yield. The use of

an inorganic base (for example potassium carbonate) provided only trace amount of the hybrid dye even after prolonged reaction time. The use of higher temperatures led to decomposition. When the reaction was conducted in methanol in the presence of TEA at room temperature, a dark blue colouration was initially observed but this turned brown over time. Crude  $^1\text{H}$  NMR indicated no evidence of the desired product. The use of a higher equivalent of TEA was observed to speed up the reaction considerably from 3 days to 1 day and allowed an improvement in the yield from 30% to 52%.

While chloroform was used as a solvent with the quaternary salts **4.41-4.43**, it proved inappropriate with quaternary salts **4.44-4.47** due to solubility issues. DMSO was found to be the only suitable solvent even so leading to poor to moderate yields of the hybrids because of difficulties in the purification of the sulfonic acid containing hybrids (**Table 4.2**).

**Table 4.2** Synthesis of the epicocconone-hemicyanine hybrid dyes.

Entry	<b>R</b>	Solvent	Time (days)	hybrid	Yield <sup>a</sup> (%)
<b>1</b>	<b>4.41</b>	CHCl <sub>3</sub>	1	<b>4.48</b>	52
<b>2</b>	<b>4.42</b>	CHCl <sub>3</sub>	1	<b>4.49</b>	62
<b>3</b>	<b>4.43</b>	CHCl <sub>3</sub>	1	<b>4.50</b>	60
<b>4</b>	<b>4.44</b>	DMSO	2	<b>4.51</b>	32
<b>5</b>	<b>4.45</b>	DMSO	2	<b>4.52</b>	29
<b>6</b>	<b>4.46</b>	DMSO	2	<b>4.53</b>	12
<b>7</b>	<b>4.47</b>	DMSO	2	<b>4.54</b>	15

**a.** Isolated yields.

Hybrids **4.48-4.50** were purified on silica either in a glass column or by preparative TLC using EtOAc/cyclohexane as eluent. A certain amount of the dye was irreversibly adsorbed onto the silica as evident by the persistent blue colouration of the silica even after stripping with methanol. The hybrids containing acidic group(s) would not travel on silica at all, so were subjected to HPLC purification using a kromasil-C18 column with a solvent system of ACN/H<sub>2</sub>O with 0.01% TFA. However, this led to extensive decomposition. LC-MS analysis of **4.52** (ACN/H<sub>2</sub>O with 0.05% formic acid), showed 2 main peaks with masses that corresponded to the hemicyanine moiety **4.45** and epicocconone analogue **4.2** (Figure 4.13).

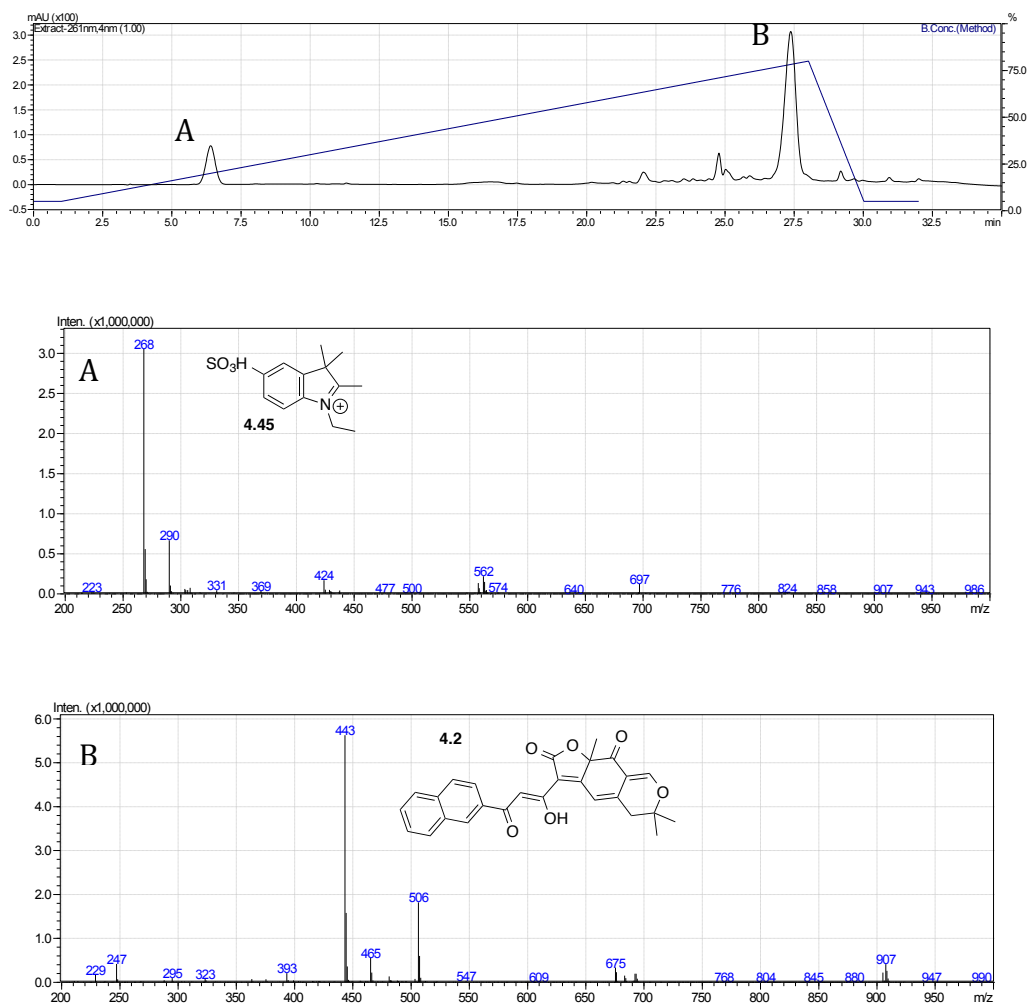


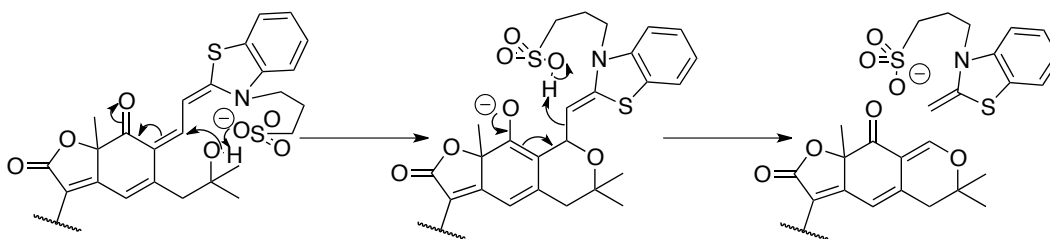
**Figure 4.13** LC-ESIMS analysis of **4.52** (ACN/H<sub>2</sub>O with 0.05% formic acid) showing 2 main peaks corresponding to **A**,  $M^+$  as **4.45** and **B**,  $[M+H]^+$  as **[4.2+H]^+**.

The acidic conditions appeared to be the cause of the decomposition observed.

HPLC in ACN/H<sub>2</sub>O on a Gemini C18 column resulted in no elution of the dye without the presence of an acid additive. Changing to an Alltech Econosphere C18 column eluted the dye but with decomposition. Switching to freshly distilled water instead of milliQ water allowed decomposition to be kept at a minimum and allowed more reproducible peaks to be obtained. The sulfonic acid dyes seem to be extremely acid sensitive.

While the hybrid dyes without any acid group were stable, the presence of an acidic group, sulfonic acid or carboxylic acid on the terminal *N*-alkyl chain led to the recyclisation of the hybrid back into its two components. Hybrid (**4.52**) with a sulfonic acid group on the indole does not appear to suffer from this instability, suggesting that the sulfonic acid sidechain catalyses the observed recyclisation. The hybrids **4.51**, **4.53** and **4.54** were stable as long as they are in the solid form and only start recyclising slowly when in solution.

A possible mechanism for the observed rapid decomposition of the hybrids with carboxylate or sulfonate side chains could involve intramolecular deprotonation-reprotonation (**Scheme 4.12**).



**Scheme 4.12** Possible reaction mechanism to explain the reversibility of the coupling reaction to provide the 2-naphthylepicocconone and hemicyanine back.

The structure of the prepared compounds was confirmed by NMR spectroscopy with the exception of the sulfonated quinolium hybrid **4.54** which gave only broad signals. Key <sup>1</sup>H-<sup>13</sup>C HMBC correlations in the spectrum of **4.48** indicated the success of the coupling (**Figure 4.14**). The <sup>1</sup>H NMR spectra display two characteristic doublets (<sup>3</sup>*J*<sub>HH</sub> 13–14 Hz) at 7.5 and 8.0 ppm, which are attributed to both vinyl protons. The coupling constant indicates an all *trans* configuration.



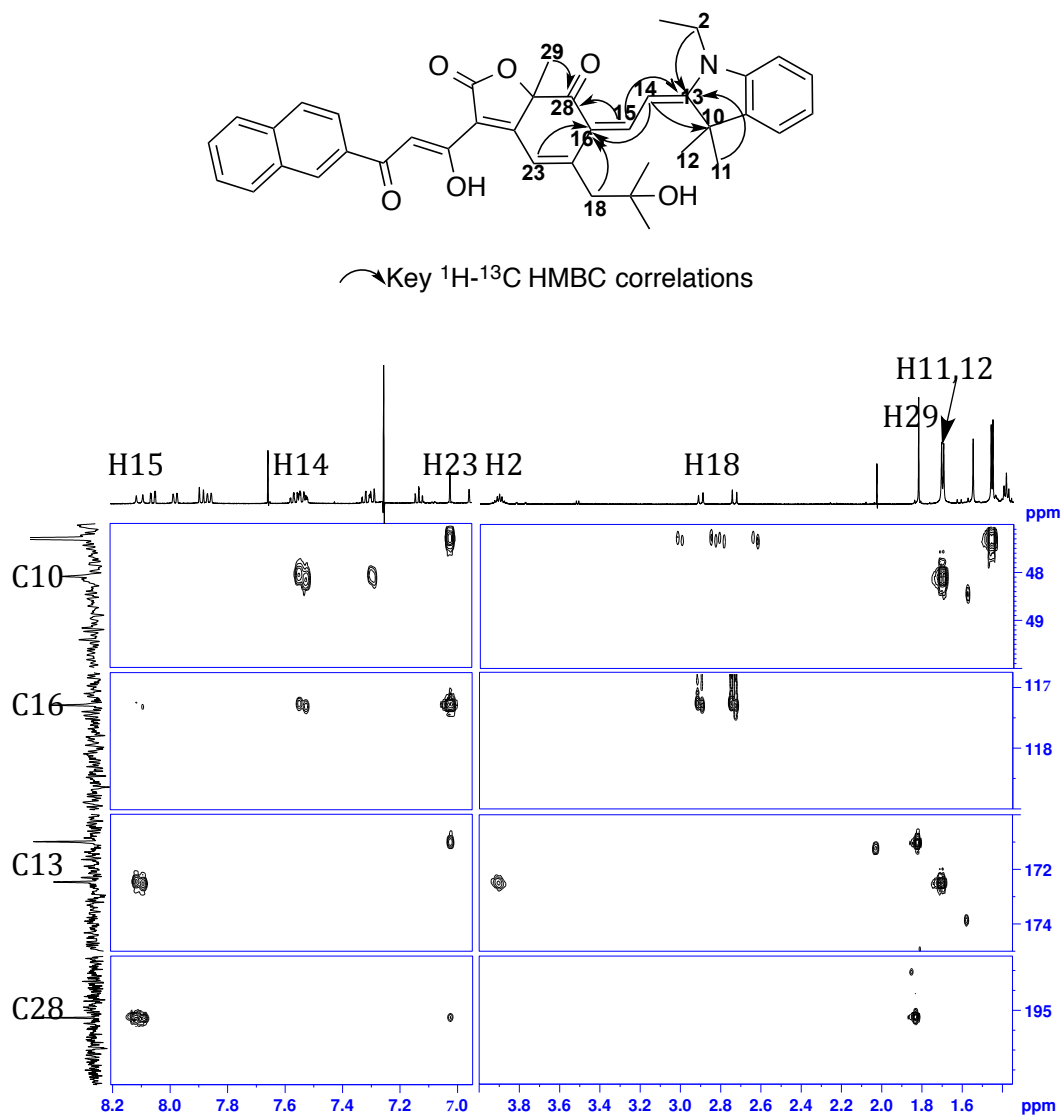
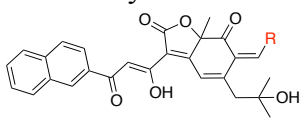


Figure 4.14 Key  $^1\text{H}$ - $^{13}\text{C}$  HMBC correlations of 4.48.

#### 4.2.5. Photophysical Properties of the Epicocconone-Hemicyanine Hybrid Dyes

The steady-state photophysical properties of the synthesised hybrid dyes were determined (details are in the **Experimental**) and the results are summarised in **Table 4.3** and the raw data in **Appendix 6.2**.

**Table 4.3** Summary of photophysical properties of the synthesized hemicyanine-epicocconone hybrid dyes.

Entry	Hybrid	UV absorption $\lambda_{\text{max}}$ (nm)	$\epsilon$ ( $\text{M}^{-1}\text{cm}^{-1}$ ) at longer $\lambda_{\text{max}}$	Max $\lambda_{\text{em}}$ (nm)	Stokes' shift (nm)	$\Phi$
<b>1</b>						
	<b>4.48</b>	470, 630	12 000	715	85	0.056 <sup>a</sup>
<b>2</b>						
	<b>4.49</b>	480, 650	72 000	730	80	0.033 <sup>a</sup>
<b>3</b>						
	<b>4.50</b>	480, 650	37 000	725	75	0.033 <sup>a</sup>
<b>4</b>						
	<b>4.51</b>	470, 630	71 000	725	95	0.028 <sup>a</sup>
<b>5</b>						
	<b>4.52</b>	470, 630	41 000	720	90	0.066 <sup>a</sup>
<b>6</b>						
	<b>4.53</b>	470, 630	19 000	720	90	0.058 <sup>a</sup>
<b>7</b>						
	<b>4.54</b>	530, 720	37 000	795	75	0.0027 <sup>a</sup>

1,1'-diethyl-4,4'-carbocyanine iodide ( $\Phi = 0.007$  in EtOH) used as a standard; **a.** Measurements done in acetonitrile; **b.** Measurement done in DMSO.

The fluorescence spectrum of **4.49** (Figure 4.15), representative of the epicocconone-hemicyanine hybrids synthesised (Appendix 6.2), is similar to epicocconone and its analogue with relatively broad absorption and emission and a large Stokes' shift.

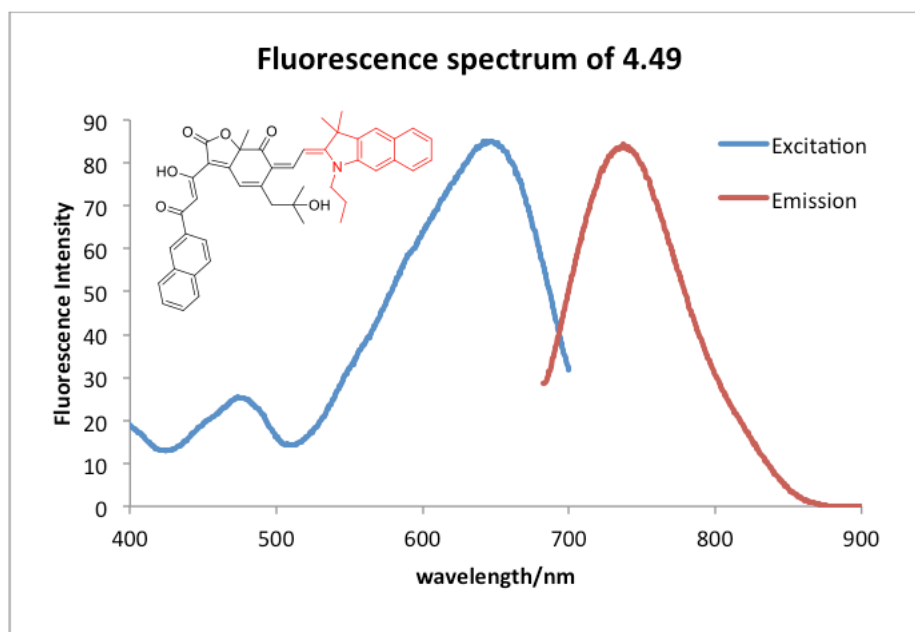


**Figure 4.15** Fluorescence spectrum of **4.49** in acetonitrile.

The UV absorption is red shifted by  $\sim 110$  nm indicating an increase of about 4 double bonds (1 double bond  $\sim +30$  nm) in conjugation of the chromophore. This sort of increase was not seen with the change from phenyl to naphthyl at the other end of the molecule. As expected, the fluorescence emission of **4.48–4.54** became red-shifted compared to **4.2** or **4.1** after coupling with the hemicyanine moieties **4.41–4.46**. The difference in wavelengths is about 165 nm as compared to the native 2–naphthylepicocconone and about 110 nm when compared to the butylamine adduct of the latter again indicating a 4 double bond equivalents increase in wavelength. Excitation at their respective absorption maxima, leads to maximum emission wavelengths between 715 – 730 nm. Laser diodes manufactured from gallium indium phosphide or aluminium gallium indium phosphide or the krypton laser emitting near 650 nm<sup>69</sup>, should be excellent excitation sources for these hybrid dyes.

Like the Cy5 dyes, the epicocconone-hemicyanine hybrids have  $\lambda_{\text{ex}}$  around 650 nm but unlike Cy5, which has a  $\lambda_{\text{em}}$  of 670 nm, these new dyes emit around 730 nm. Thus while Cy5 dyes suffer from a small Stokes' shift of 20 nm, the hybrids synthesised benefit from a relatively large Stokes' shifts ranging from 75 – 95 nm. However, the hybrid dyes possess relatively small extinction coefficients, the highest being  $72\,000\text{ M}^{-1}\text{cm}^{-1}$  for the benzoindole derivative **4.49**, in comparison to the cyanines that are often over  $200\,000\text{ M}^{-1}\text{cm}^{-1}$ .<sup>63</sup> Nevertheless, the extinction coefficients are all above that of the butylamine adduct of epicocconone ( $13\,000\text{ M}^{-1}\text{cm}^{-1}$  in ACN).<sup>25</sup> However, the hybrid dyes were found to possess a quantum yield 100 times lower than Cy5 ( $\Phi$  0.28.)

The sulfonated quinolinium derivative **4.54** achieved the longest emission wavelength of 795 nm, which is suitable for whole body imaging.<sup>70,71</sup> This work demonstrates that fluorescence of the epicocconone-hemicyanine hybrid dyes can be further red-shifted by attaching the appropriate heterocycle to the dihydropyran end of the epicocconone scaffold but stability issues need to be overcome.

#### 4.2.6. Investigation of the Hybrid Dyes as Fluorescent Probes

A fluorescent probe is a fluorophore with 'function', that is, it interacts specifically with its environment to induce a concomitant change of its photophysical properties. The utility of the epicocconone-hemicyanine hybrid dyes as fluorescent probes was investigated by measuring their change in fluorescence with pH, surfactant, protein and oligonucleotide concentrations. The full data is provided in **Appendix 6.3, 6.4, 6.5 and 6.6**, and the most interesting results are discussed in the following sections.

#### 4.2.6.1. Effect of pH on the Fluorescence of the Hybrid Dyes

The UV absorbance and fluorescence of the epicocconone-hemicyanine hybrid dyes was measured at different pHs in universal buffer and graphs of absorbance against pH and fluorescence against pH were constructed (**Appendix 6.3; e.g Figure 4.16A and B for 4.49**). The presence of isobestic points in the absorbance spectrum (**Figure 4.16A**) indicates that this change corresponds to a reversible change such as protonation/deprotonation. In **4.49**, this corresponds to the deprotonation/protonation (**Figure 4.17**) of the  $\beta$ -diketone of the hybrid with an apparent  $pK_{a2}$  at ground state of 10.26, which was determined by fitting a sigmoidal curve (GraphPad Prism (v 4.0)) to absorbance at the maximum absorbance wavelength (625 nm for **4.49**) at different pHs (**Figure 4.16C**). Similarly, a sigmoidal curve was fitted to fluorescence intensity at the maximum emission wavelength (635 nm for **4.49**) at different pHs (**Figure 4.16D**). The apparent  $pK_{a2}$  at the excited state for **4.49** was determined to be 10.02.

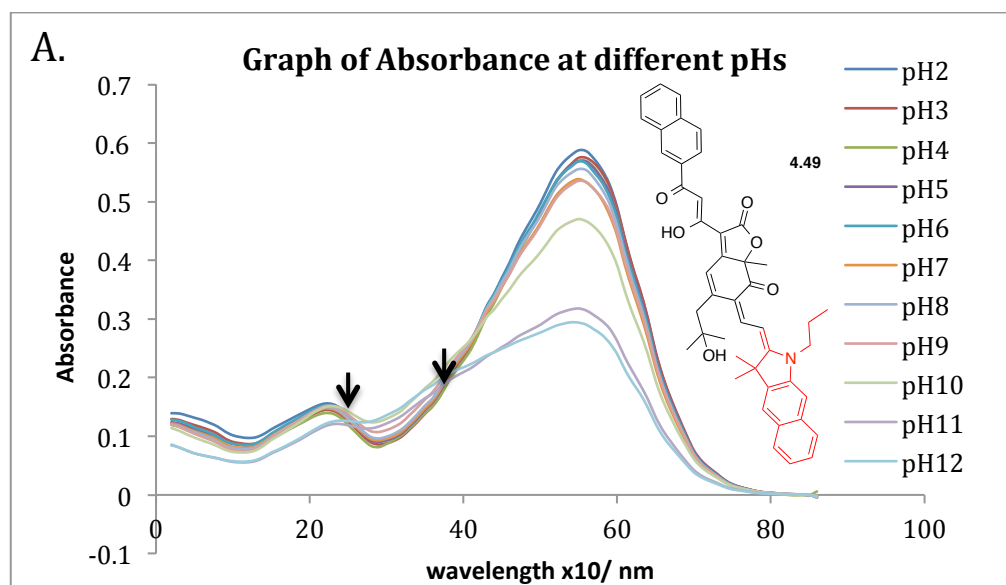


**Figure 4.16 A.** Presence of isobestic points (shown by arrows) in the absorbance spectrum of **4.49**.

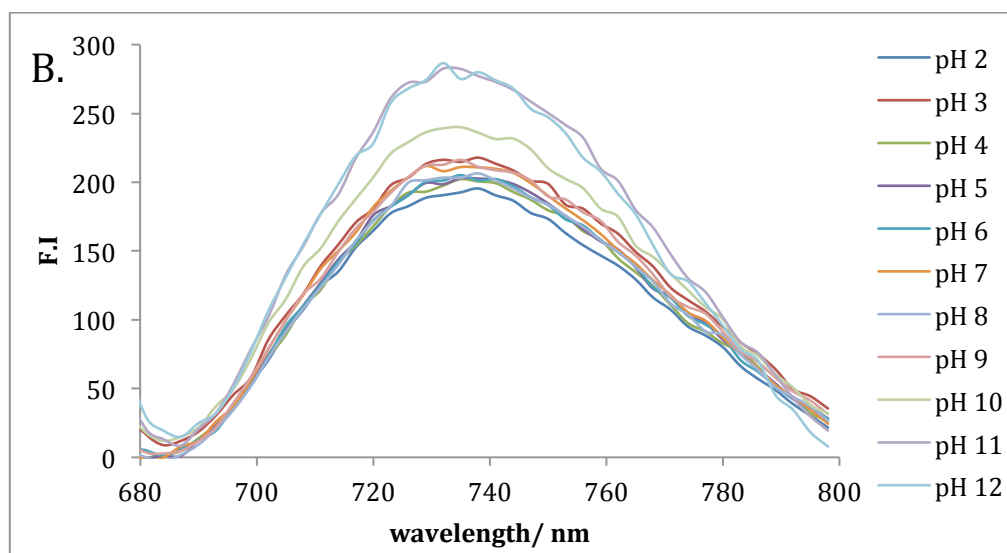


**Figure 4.16 B.** Fluorescence intensity spectrum of **4.49** at different pHs initially.

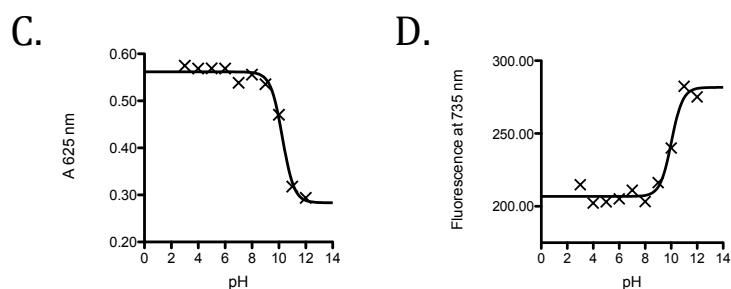


**Figure 4.16 C.** Absorbance vs pH plot and **D.** Corrected fluorescence vs pH plot for **4.49** fitted to a sigmoidal  $pK_a$  plot;  $Y = (\text{Bottom} \cdot 10^{(X-pK_a)} + \text{Top}) / (1 + 10^{(X-pK_a)})$  (GraphPad Prism (v 4.0)); point of inflection give the  $pK_a$ .

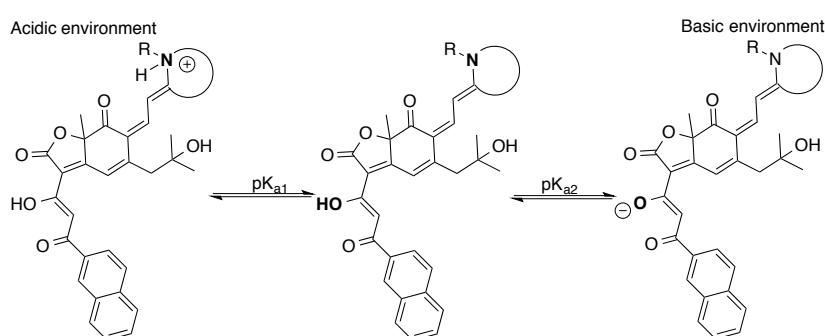


**Figure 4.17** Species of the epicocconone-hemicyanine hybrid dye **4.49** at different pHs.

The  $pK_a$  values for all the hybrid dyes were calculated (**Table 4.4**). In general, the  $pK_a$  value for the  $\beta$ -diketone in the excited state is lower *ca* 0.2  $pK_a$  units than in

the ground state, unlike with epicocconone **4.1** where an increase in  $pK_a$  is observed in the excited state.<sup>21</sup> This indicates that in the hybrid dyes in the excited state, the enol proton is less tightly held, leading to the decrease in  $pK_a$ . The hybrid dyes **4.48** and **4.53** display much lower  $pK_a$  values (in the range of 3.5 – 4.5) (**Appendix 6.3.1**) which likely correspond to the  $pK_a$  of the hemicyanine nitrogen ( $pK_{a1}$ ; **Figure 4.17**) in the excited state.

**Table 4.4** Calculated ground state and excited state  $pK_a$  values for hybrid dyes. GS= ground state; ES = excited state; **a.** sigmoidal curve could not be fitted; **b.** not calculated but in the range of 3.5 – 4.5.

	<b>4.48</b>	<b>4.49</b>	<b>4.50</b>	<b>4.51</b>	<b>4.52</b>	<b>4.53</b>	<b>4.54</b>
$pK_a$ (GS)	- <sup>a</sup>	10.26	10.14	10.24	10.02	10.18	8.56
$R^2$	-	0.9885	0.9811	0.9839	0.9943	0.9435	0.9881
$pK_a$ (ES)	- <sup>b</sup>	10.02	10.04	10.09	9.81	- <sup>b</sup>	8.20
$R^2$	-	0.9696	0.9337	0.9799	0.8141	-	0.9754

The mechanism of fluorescence for epicocconone and its analogues has been explained by the occurrence of an internal charge transfer (ICT) within the fluorophore.<sup>16,24,72</sup> An ICT occurs in a push-pull system with an electron donating and an electron withdrawing group at opposite ends, linked through conjugation that will allow delocalisation of electrons but not aromaticity. In the hybrid dyes, a push-pull system exists between the heterocyclic nitrogen (electron source) of the hemicyanine moiety and the ketoenol (electron sink) at the epicocconone end of the hybrid (**Figure 4.18**). At  $pHs < pK_1$ , the lone pair of electrons of the heterocyclic nitrogen is not available for delocalisation into the epicocconone moiety thus explaining the low fluorescence emission. At  $pHs > pK_2$ , the presence of a negative charge and the available lone pair of electrons of the heterocyclic nitrogen lead to a strong ICT, thus explaining the strong fluorescence emission. If an ICT is present, the fluorescence within a hydrophobic medium should be greater than in polar medium where the dipole can be dispersed through H-bonding.<sup>5</sup>

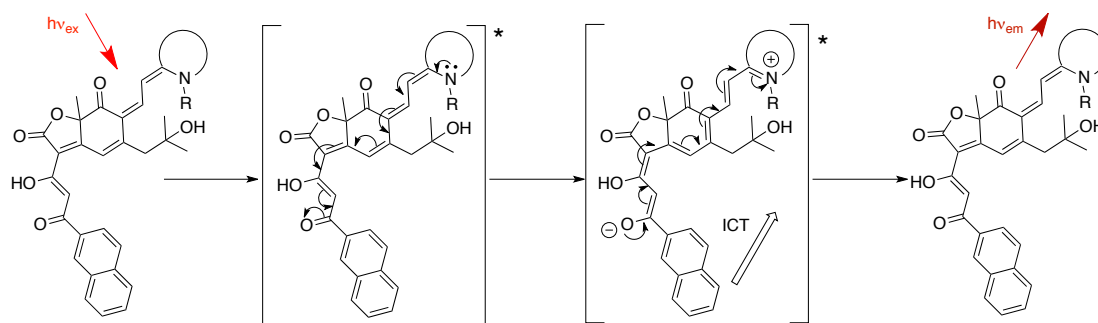


**Figure 4.18** Possible mechanism of fluorescence of the epicocconone-hemicyanine hybrid dye based on ICT.

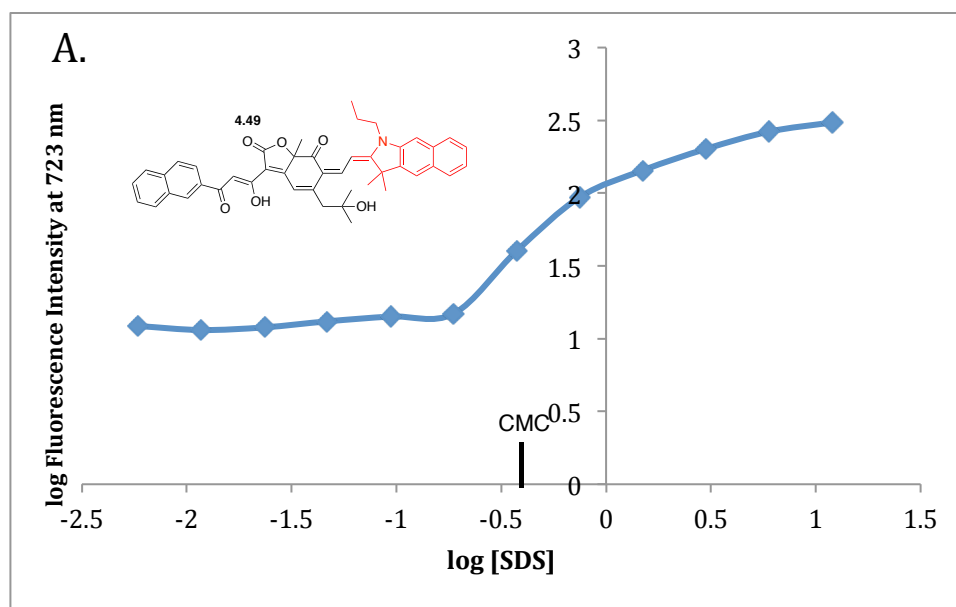
After 3 hours in buffer, the fluorescence generally decreased and the absorption spectra change such that there was no longer an isobestic point indicative of decomposition. This was a general phenomenon for all the hybrid dyes (**Appendix 6.3**).

#### 4.2.6.2. Influence of SDS on the fluorescence of the hybrid dyes

Membranes typically do not display intrinsic fluorescence. For this reason it is common to label membranes with probes which partition into the non-polar hydrocarbon chain region of the membranes. In order to investigate the potential of the hybrid fluorophores as membrane probes, sodium dodecyl sulfate (SDS), an anionic surfactant was used as a model. A general characteristic of surfactants is the formation of micelles in aqueous solution above a certain concentration, known as the critical micellar concentration (CMC) which correspond to a concentration of ~0.25% (w/v) of SDS.<sup>73</sup> As such, micelles can be used as a model for the lipid membrane environment.



At concentration of SDS greater than 0.2% (w/v), an increase in fluorescence intensity was observed for the hybrid dyes (**Appendix 6.4**). Such behaviour is common for internal charge transfer (ICT) fluorophores where H-bonding to water decreases the polarity of the excited state and quenches it.<sup>5</sup> However, the fluorescence did not show a point of inflection at the CMC but continued to increase (**Figure 4.19A and Appendix 6.4**). A point of inflection was observed at CMC when fluorescence was plotted against viscosity of SDS micelles which was measured in water using electron spin resonance spectroscopy of the nitroxide labelled fatty acid probes (5,16-doxylstearic acid) and reported by Bahri and co-workers<sup>74</sup> (**Figure 4.19B**). Therefore, these hybrid dyes appeared to be responding not only to the formation of micelles but also to increasing microviscosity of the micelles that result from the increasing concentration of SDS.



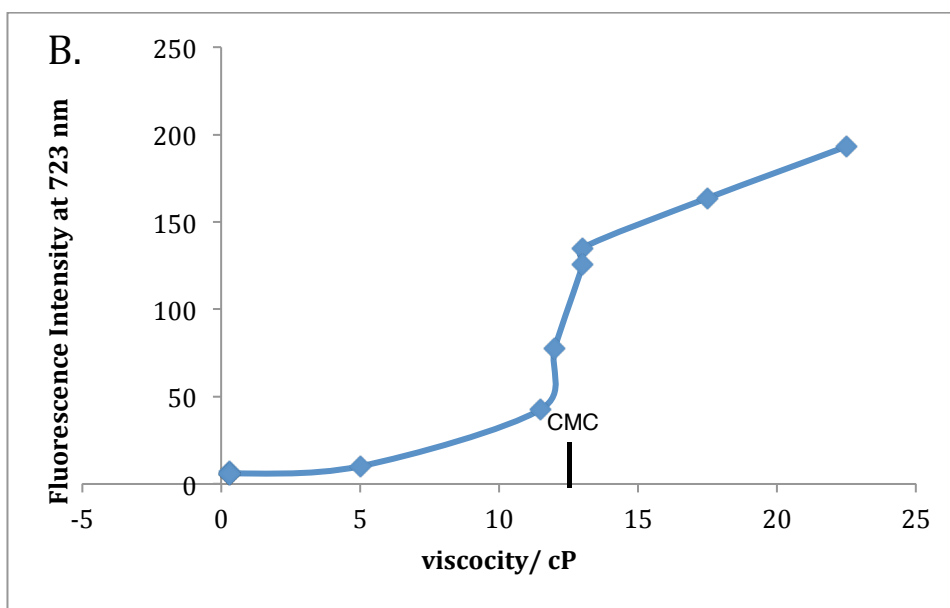


**Figure 4.19 A.** Fluorescence response at  $\lambda_{em} = 723$  nm for **4.49** with SDS concentration log (% w/v). An increase in fluorescence was observed above CMC; **B.** Fluorescence response at  $\lambda_{em} = 723$  nm for **4.49** with microviscosity of SDS in water.

Increasing viscosity inhibits free bond rotation suggesting this is a major non-radiative decay mechanism for these compounds.<sup>65</sup> Hemicyanine dyes have been applied as molecular rotors to determine viscosity in solutions or biological fluids.<sup>65</sup>

#### 4.2.6.3. Fluorescence of the Hybrid Dyes in the Presence of Biomolecules

Fluorophores are both useful in covalent and non-covalent labelling of biomolecules. These would ideally be weakly or non-fluorescent in water, but fluoresce strongly when bound to the analyte of interest. A marked shift in  $\lambda_{em}$  is also useful. Epicocconone is unique in that it has the ability to covalently bond to amino groups in a reversible fashion and in so doing, exhibits a red fluorescence. Non-covalent bonding on the other hand requires some sort of intermolecular interaction between the fluorophore and the analyte that will lead to a measurable change in fluorescence. For example, sensitive visualisation and quantification of

DNA, requires staining with dyes such as acridines, ethidium bromide, and other planar cationic species, that can intercalate with DNA and thereby become highly fluorescent. Similarly, minor groove binding dyes, such as Hoechst 33342, are specific to double stranded DNA. Cyanine dyes have been used as oligonucleotide probes due to their capacity to bind to DNA through non-covalent interactions either by intercalation between base pairs (monomethine ( $n = 0$ ) cyanine dyes) or minor groove binding of double-stranded DNA (trimethine ( $n = 1$ ) and penta-methine ( $n = 2$ ) cyanine dyes).<sup>75-78</sup> There was no detectable response of fluorescence of the hybrid dyes to double strand of DNA (**Appendix 6.5**).

However, fluorescence response to changes in the concentration of protein (bovine serum albumin; BSA) was observed for some of the hybrid dyes. A blue-shift ( $\Delta\lambda$  5-10 nm) in emission wavelength was noted indicative of a lower polarity in the local environment around the protein.<sup>5</sup> In addition, an increase in fluorescence intensity was observed with increasing concentration of BSA. Hybrids **4.50**, **4.51** and **4.53** (**Appendix 6.6**) were found to respond to BSA with the best response obtained with **4.51** (**Figure 4.20**). The other hybrids either have negligible response to BSA or no response at all. The detection limit for **4.51** determined to be 1.0  $\mu\text{g/mL}$ , suggesting this particular probe could be useful in protein visualisation/quantification.

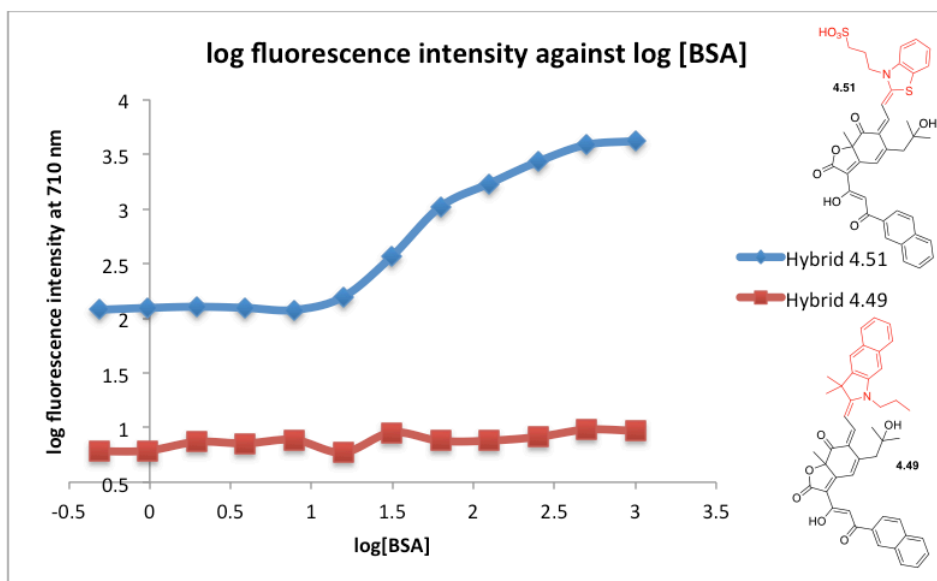


**Figure 4.20** Fluorescence response at  $\lambda = 710$  nm for hybrid **4.51** and **4.49** at different concentrations of BSA ( $\mu\text{g/mL}$ ).

#### 4.2.7. Total Protein Stain in Gel Electrophoresis

Gel electrophoresis is a routinely used method for the separation and analysis of macromolecules and their fragments, based on their size and charge. The gel electrophoresis apparatus consists of a gel in a buffer-filled box and an electrical field that is applied via the power supply to create positive and negative terminals across the gel along which the analyte will move due to its inherent or induced charge.

A commonly used technique to analyse proteins is sodium dodecyl sulfate polyacrylamide gel electrophoresis (SDS-PAGE).<sup>79</sup> As is suggested by its name, the gel used is made of polyacrylamide. The proteins are first denatured in the presence of SDS before being loaded on the gel at the cathode. SDS coats the proteins with a negative charge. The amount of SDS bound is relative to the size of the protein so that the resulting denatured proteins have an overall negative charge, and all the proteins have a similar charge to mass ratio. Since denatured proteins act like long

rods instead of having a complex tertiary shape, the rate at which the resulting SDS coated proteins migrate in the gel to the anode is relative only to its size and not its charge or shape.<sup>80</sup>

In order to visualise proteins on a gel, gel stains are used (**Figure 4.21**).<sup>81</sup> Traditional colourimetric stains which include Coomassie Blue and silver, suffer from sensitivity and/or low and limited dynamic range and/or reproducibility of results. These limitations have prompted the development of a number of fluorescent stains that are more accurate, sensitive and have larger dynamic ranges. The most commonly used fluorescent dye is SYPRO Ruby which is a formulation of a bathophenanthroline complex of ruthenium (II) (**4.56**) that associates with cationic residues on the protein, similar to Coomassie blue.<sup>82</sup> More recently introduced dyes such as Krypton (**4.58**), Flamingo (**4.59**) and SYPRO Orange (**4.57**) similarly contain sulphonic acids that bind to proteins in the same way as SDS.<sup>83</sup> Deep Purple is unique in that it contains no sulfonic acid, reacts covalently with amino groups in proteins and then becomes amphiphilic, one end being very hydrophobic (triene) and the other polar (ammonium ion, diol).<sup>15,81</sup>

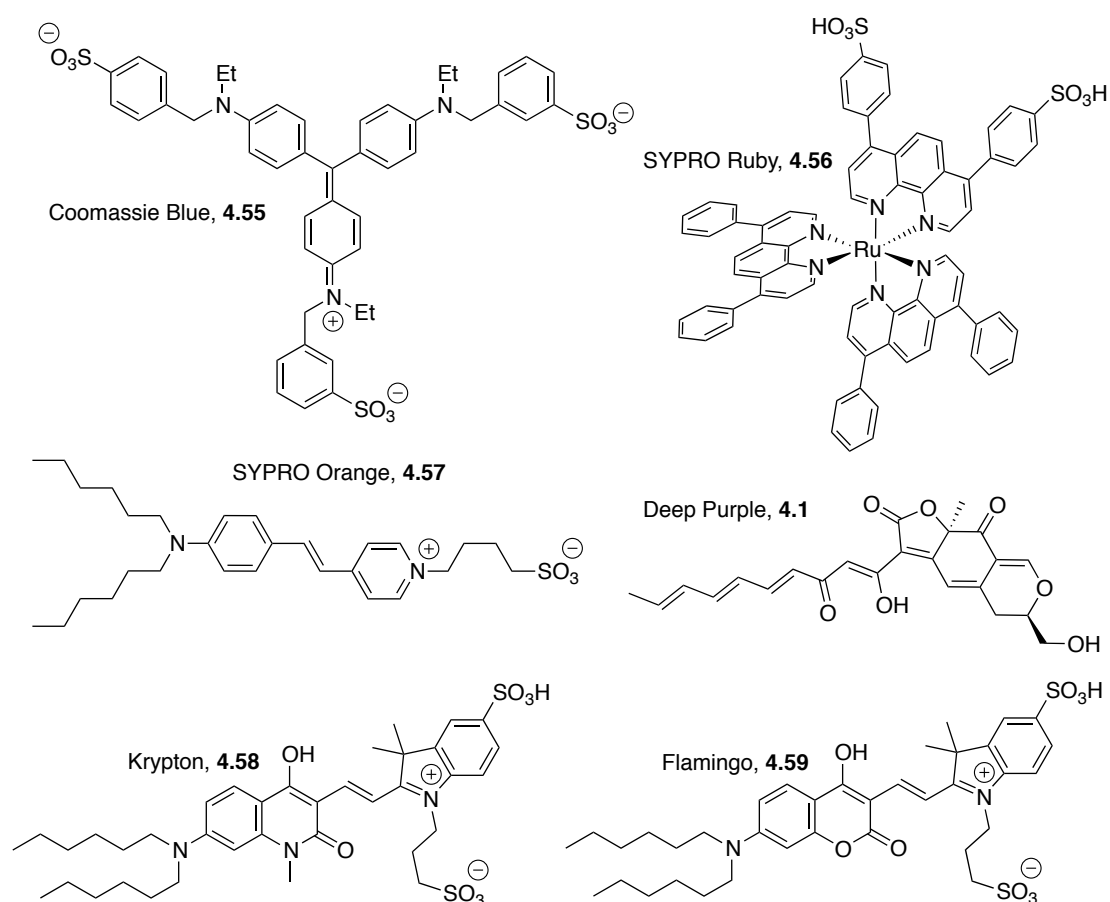


**Figure 4.21** Structural motifs of common fluorescent protein gel stains used in electrophoresis.

The epicocconone hybrid dyes that contain sulfonic acids similarly bound to protein in gels. Hybrid dye **4.53** (**Figure 4.22**) was the most sensitive of the dyes tested with a limit of detection (**Appendix 6.7.2**) for BSA determined to be 0.22 ng/band (**Table 4.4, Entry 6**) which is more sensitive than silver and comparable to the limit of detection of epicocconone (**4.1**) (0.92 ng) or the 2-naphthylepicocconone analogue **4.2** (0.56 ng).<sup>20</sup> **Figure 4.22** (and **Appendix 6.7.1**) are the result of one experiment using the protocol developed for **4.1**,<sup>84</sup> which would not be optimum for the hybrid dyes. Nonetheless, the epicocconone-hemicyanine hybrid dyes have potential as a new class of protein stain on gel because they are at least sensitive as Deep Purple (**Table 4.4**) and with optimisation could be much more sensitive. They

would make excellent sensitive counter stains for DIGE, for example, which uses Cy3, Cy5 and Cy7 staining that do not overlap with that of **4.53**.

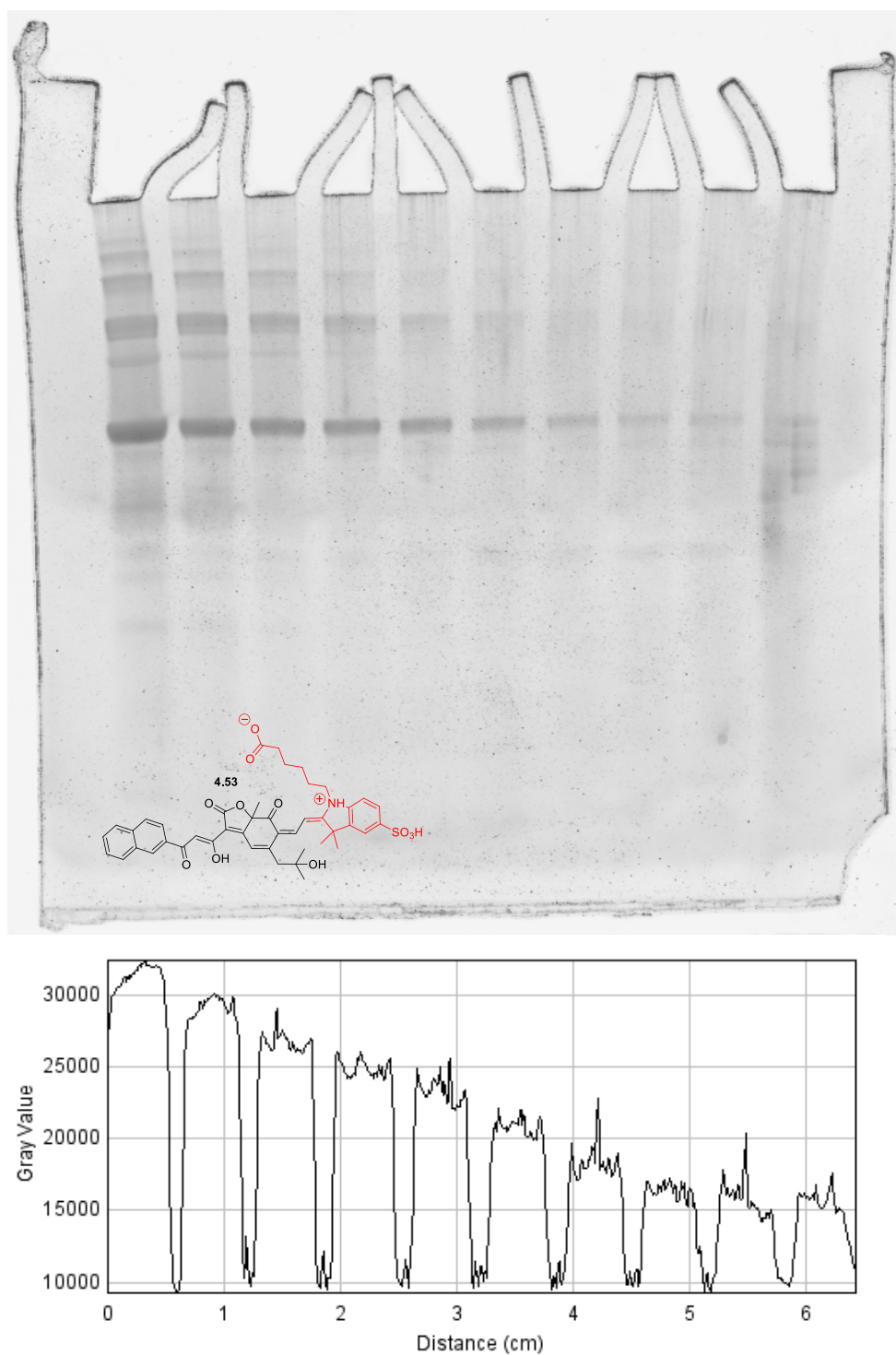


**Figure 4.22** Typhoon scan of the gels for **4.53** and its respective Profile Plot using ImageJ.

**Table 4.4** Limit of detection of BSA (see **Appendix 6.7.2**) detected on gel in ng of the synthesised hemicyanine-epicocconone hybrid dyes.

Entry	Hybrid dye	Limit of detection of BSA on gel ng/band
1	4.48	10.5
2	4.49	136
3	4.50	7.1
4	4.51	24.2
5	4.52	1.9
6	4.53	0.22

#### 4.2.8. The Hybrid Dyes in Fluorescence Microscopy

Fluorescence microscopy has gained importance in a lot of different fields in biomedical research.<sup>85</sup> Fluorescence is widely used nowadays in the identification, classification and quantitative measurements of biological structures and processes. As mentioned in the **section 4.1.4**, compared with fluorescent imaging in the visible region, biological imaging in the NIR region is favourable because it reduces photodamage, allows deep tissue penetration, minimises background autofluorescence, has lower light scattering and can use low-cost light sources.

##### 4.2.8.1. Live Cell Imaging using the NIR Hybrid Dyes

As proof of concept for cell imaging, we explored live cell imaging using the NIR emission of two hybrid dyes, the benzoindole **4.49** and the sulfonated thiazolium **4.51** hybrids. Live colon cancer cells (SW430) exposed to **4.49** (200 nM) rapidly absorbed the dye within 15 min. Adequate NIR fluorescence intensity was observed after 25 min and was detected in the cytoplasmic rather than nuclear regions. This



was confirmed by co-staining the nucleus with Hoechst 33342 where no co-localisation was observed. **4.49** appeared to become localised in organelles (**Figure 4.23**) distributed evenly throughout each stained cells, not on or near the surface of the cell membrane. Staining was partially retained after fixing the cells with 2% formaldehyde. However, when the dye was used on already fixed colon cancer cells, little to no staining was observed even after an extended period of incubation time. This suggests the dye is taken up by an active transport mechanism such as endocytosis.<sup>86</sup>

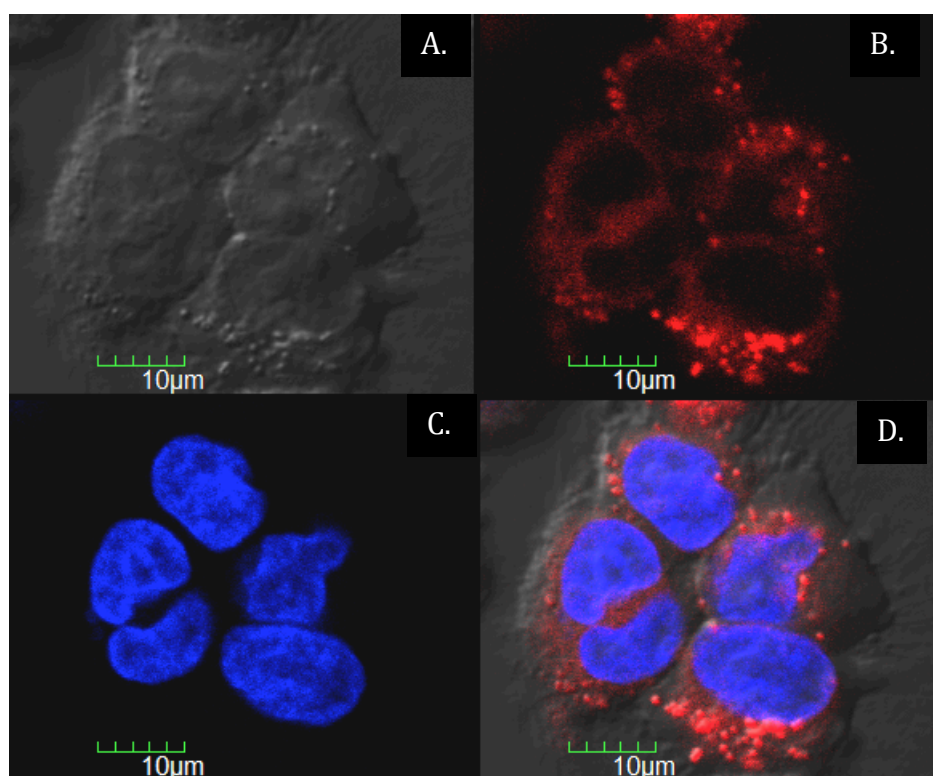


**Figure 4.23** Uptake of **4.49** (200 nM) by live colon cancer cells (SW430) within 25 min. Images: **A.** bright-field image; **B.** dye become localized in circular vesicles (red); **C.** nucleus stained with Hoechst (blue); **D.** overlays on a bright-field image.

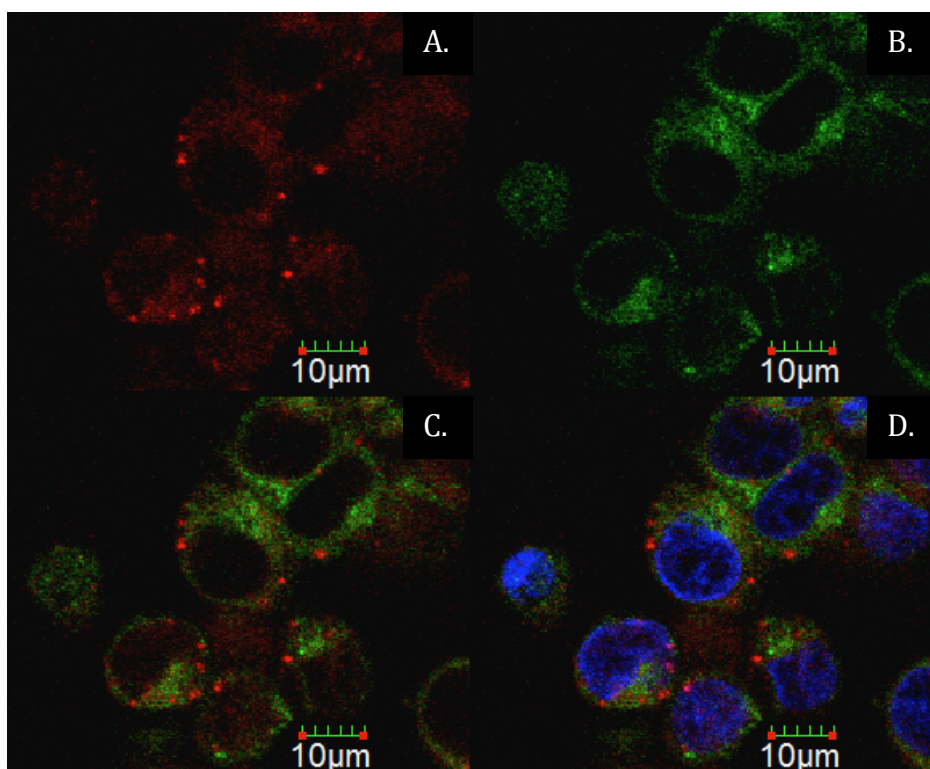


**Figure 4.24** Co-staining with ER-Tracker Green: **A.** 4.49 in the cytoplasm and concentrated in circular vesicles (red); **B.** ER-Tracker Green staining the ER (green); **C.** overlay of **A.** and **B.**; **D.** overlay of **C.** with nucleus stained with Hoechst (blue).

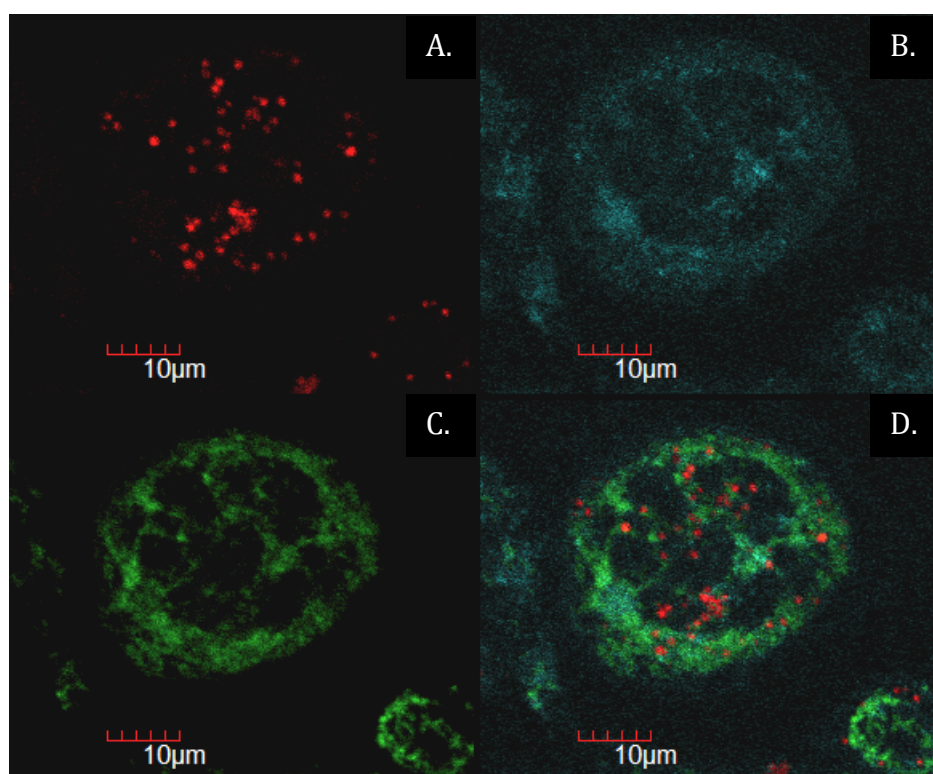


**Figure 4.25** Co-staining with LysoTracker Red and MitoTracker Green: **A.** hybrid dye localised in circular vesicles (red); **B.** LysoTracker Red staining the ER (cyan); **C.** Mitotracker Green staining the mitochondria; **D.** overlay of **B.**, **C** and **D.**

Co-staining **4.49** with ER tracker Green (**Figure 4.24**), Mitotracker Green and LysoTracker Red (**Figure 4.25**) showed that **4.49** did not stain endoplasmic reticulum, mitochondria or lysosomes.

From our investigation of the effect of SDS (**Figure 4.19**) on the fluorescence of the hybrid dyes, we know that fluorescence is weak in water but that it increases with viscosity. Therefore it is very likely that for adequate NIR fluorescence to be observed, the dye must be in a hydrophobic or viscous environment similar to that provided by SDS after micelles formation. The dye is likely to be entering the cell by endocytosis (*vide supra*) and therefore the circular organelles being stained could well be cytoplasmic vesicles (endosomes) in which the dye has become trapped.

In order to investigate this, co-staining was conducted with CM-DiI, a cell tracker that enters cells by endocytosis. **4.49**, Hoechst 33342 and CM-DiI were co-incubated for 25 min, to promote endocytosis and confocal images obtained for each dye. Similarities in the pattern of staining between CM-DiI and the hybrid dye were observed (**Figure 4.26**) but the co-localisation was not general for the whole population of cells stained. Moreover cells stained with both CM-DiI and the hybrid dye, were low in number. Mostly, observed were cells either stained with CM-DiI or with the **4.49** but not both. Different rates of uptake of the dyes by the cells and/or by cells at different stages of life, could explain their poor co-localisation despite the same pattern of staining for some cells. These observations together with a closer look at the morphology of the stained organelles (**Figure 4.27**, also **Figure 4.23A and B**), have allowed the latter to be identified as most likely to be caveolae.

Caveolae are spherical or flask-shaped invaginations of the plasma membrane and associated vesicles of uniform size (70 nm average outer diameter), that occur

either singly or in clusters, attached to either front of the cell or apparently free in the cytoplasm.<sup>87</sup> These subcellular structures are rich in proteins as well as lipids such as cholesterol and sphingolipids.<sup>88</sup> Caveolae have been involved in functions such as transcytosis of molecules across the cell, endocytosis, control of cholesterol trafficking, the uptake of pathogenic bacteria and certain viruses, and signal transduction influencing cell growth, apoptosis and angiogenesis.<sup>87,89-91</sup> The caveosome is an endosomal compartment with neutral pH which contains molecules internalised by caveolar endocytosis.<sup>92</sup> It is by this process that the hybrid dye **4.49** is being taken into the cell and this explains the partial co-localisation observed with CM-DiI. The presence of the hybrid dye in a lipid-rich and a neutral pH environment accounts respectively for the adequate NIR fluorescence observed and the stability of the dye over a period of 24 h.

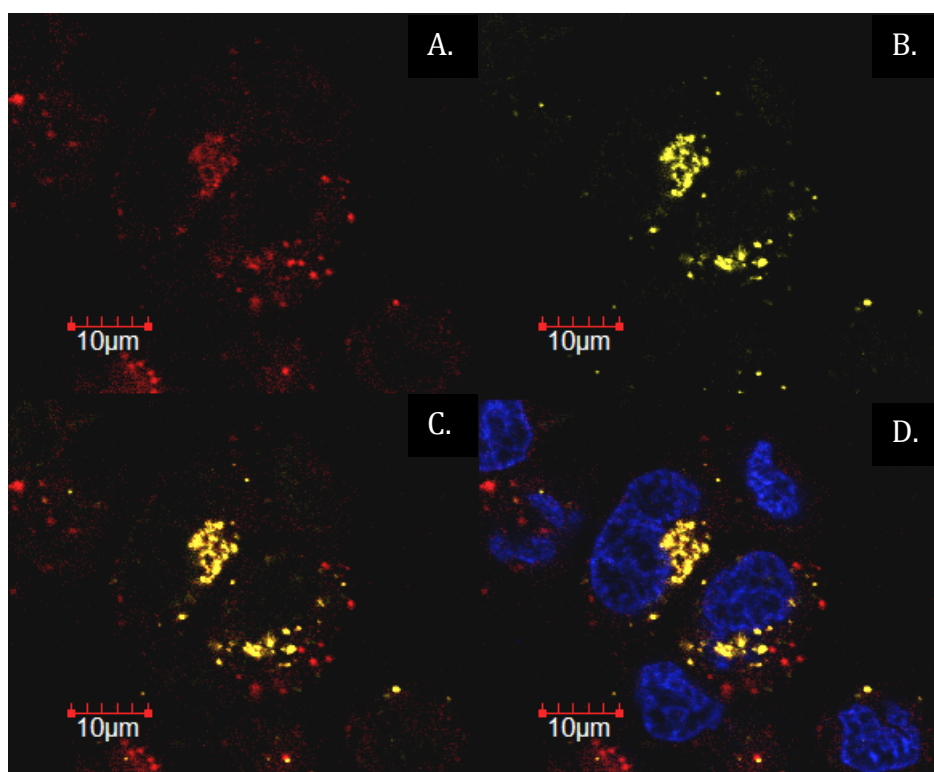


**Figure 4.26** Co-staining with CM-DiI, a lipophilic tracer: **A.** hybrid dye localised in circular vesicles (red); **B.** CM-DiI localized in cytoplasmic vesicles (yellow); **C.** overlay of **A** and **B**; **D.** overlay **C** with nucleus stained with Hoescht (blue).

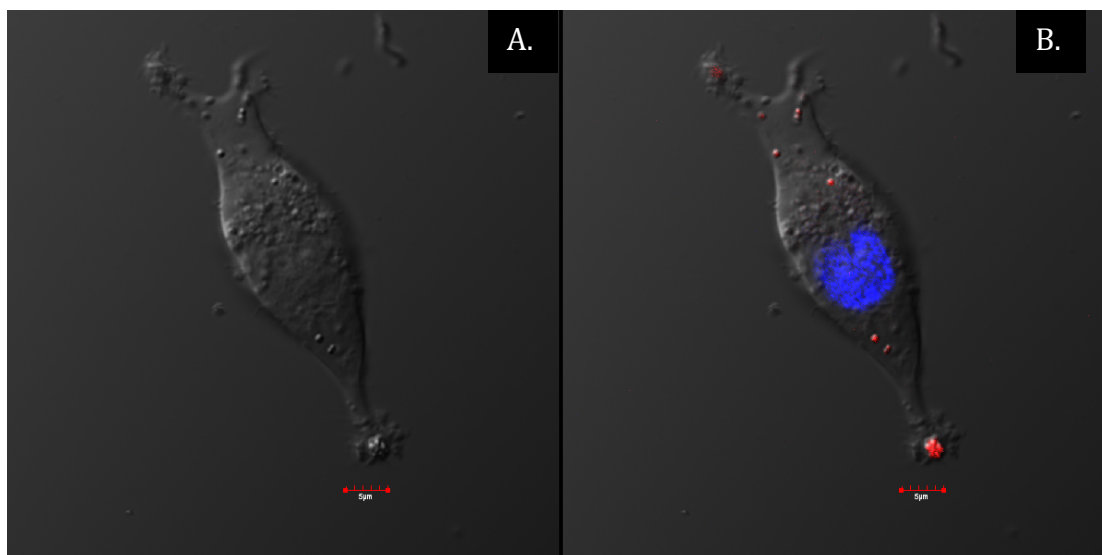


**Figure 4.27** Single cell imaging: **A.** Bright-field image and **B.** cell stained with Hoescht (blue) and **4.49** (red) staining caveola which are spherical structures either single or in clusters as observed in the image. Scale bar is 5  $\mu\text{m}$ .

The dye was also found to have low cytotoxicity. Incubation of cells overnight in the presence of 200 nM **4.49** had no effect on growth or morphology. It was observed that even after 24 h the same small vesicles were stained. Epicocconone itself has been found to be a neutral, non-toxic, small molecule that appears to diffuse readily into live or fixed cells without the need for permeabilisation.<sup>93</sup>

When the cells were incubated with the sulfonated thiazole hybrid dye **4.51** (200 nM) for up to 24 hours, no evidence of NIR fluorescence was observed even though the nucleus was stained perfectly well with Hoechst. This suggests that the hydrophilic sulfonate group inhibits its membrane permeability/uptake.

These results suggest that the epicocconone-hemicyanine hybrid dyes lacking any acidic group(s), can readily enter live cells (uptake time within 25 min at 200 nM) without the need for permeabilisation, is retained after fixing and is non-cytotoxic. Cells stained with hybrid dyes are excitable by the common HeNe laser (633 nm) or

LED lasers. These features enable the real-time imaging of live cells and the study of organelle movements using NIR fluorescence. One drawback is photobleaching of the dye, that was most evident when z-stacking was conducted with a large number of slices at small depth increments. This can be minimised by reducing the number of slices or perhaps adding an antifade reagent but this is yet to be investigated.

### 4.3. Conclusions

The epicocconone-hemicyanine hybrid dyes show two UV absorbance bands with a small maxima between 470 – 480 nm and a large maxima between 630 – 650 nm and have a maximum emission between 715 – 730 nm. The spectral window covered by the epicocconone-hemicyanine hybrid dyes is unlike any other reported fluorescent dyes. Therefore they come to complement existing commercially available fluorescent dyes. Moreover they benefit from unusually large Stokes' shifts for NIR dyes, ranging from 75 – 95 nm. However, the hybrid dyes possess relatively low extinction coefficients ( $12\,000 - 72\,000\text{ M}^{-1}\text{cm}^{-1}$ ). Even though their measured quantum yields are also relatively low (0.0027 – 0.066), the fluorescence of the hybrid dye has shown enhancement in the presence of SDS, which pointed to an environment-dependence in the brightness of the dyes. The fluorescence of the hybrid dyes can be further red-shifted by attaching hemicyanines which can provide extended conjugation to the epicocconone scaffold as shown by the sulfonated quinolinium hybrid **4.54** which achieved the longest emission wavelength of 795 nm.

Some of the epicocconone-hemicyanine hybrid dyes have been found to respond to the presence of protein, both in solution and in PAGE. Since the hybrid dyes lack the dihydropyran ring, the response is from a non-covalent interaction with proteins in a similar fashion to Coomassie Blue, SYPRO Ruby and other total protein

stains. The carboxylic group-containing hybrid dye **4.53** has shown sensitivity better than Deep Purple.

We have shown proof of concept of the application of the non-cytotoxic, cell-permeable benzoindole hybrid dye **4.49** in *in vivo* imaging of selectively-stained caveolae of live colon cancer cells. This would need to be confirmed through colocalisation with caveolin-1 antibody. We wish also to explore the application of the novel NIR dyes for non-invasive live-animal imaging.

A major limitation of the hybrid dyes is their poor stability, particularly at low pHs. The hybrid dyes undergo a recyclisation reaction to provide the initial two components of the coupling reaction. A possible solution involves the protection of the alcohol to prevent recyclisation. The presence of acid group at the end of the N-alkyl chain leads to the self-catalysis of the recyclisation and thus having the acid group as a solubilising group at another position on the molecule instead on the end of the N-alkyl chain, would solve this problem. Photobleaching has been a recurring issue with the epicocconone scaffold as a fluorophore and is still being addressed.<sup>23</sup> The results are very encouraging for further development of the epicocconone-hemicyanine hybrid as useful NIR dyes.

#### 4.4. References

- (1) Acuna, A. U.; Amat-Guerri, F. In *Fluorescence of Supramolecules, Polymers, and Nanosystems*; BerberanSantos, M. N., Ed. 2008; Vol. 04, p 3-20.
- (2) Acuna, A. U.; Amat-Guerri, F.; Morcillo, P.; Liras, M.; Rodriguez, B. *Org. Lett.* **2009**, *11*, 3020-3023.
- (3) Safford, W. E. *Ann. Rep. Smithsonian Inst.* **1915**, 271-298.
- (4) Stokes, G. G. *Phil. Trans. R. Soc. Lond. B, Biol. Sci.* **1852**, *143*, 385.

- (5) Lakowicz, J. R. *Principles of Fluorescence Spectroscopy*; 3rd ed.; Springer, 2006.
- (6) Born, M.; Oppenheimer, R. *Ann. Phys.* **1927**, *389*, 457-484.
- (7) Franck, J.; Dymond, E. G. *Trans. Faraday Soc.* **1926**, *21*, 536-542.
- (8) Condon, E. *Phys. Rev.* **1926**, *28*, 1182-1201.
- (9) Förster, T. *Ann. Phys.* **1948**, *437*, 55-75.
- (10) Atkins, P.; De Paula, J. *Atkins Physical Chemistry*; Oxford, 2006.
- (11) Frangioni, J. V. *Curr. Opin. Chem. Biol.* **2003**, *7*, 626-634.
- (12) de Silva, A. P.; Gunaratne, H. Q. N.; Gunnlaugsson, T.; Huxley, A. J. M.; McCoy, C. P.; Rademacher, J. T.; Rice, T. E. *Chem. Rev.* **1997**, *97*, 1515-1566.
- (13) Sameiro, M.; Goncalves, T. *Chem. Rev.* **2009**, *109*, 190-212.
- (14) Bell, P. J. L.; Karuso, P. *J. Am. Chem. Soc.* **2003**, *125*, 9304-9305.
- (15) Coghlan, D. R.; Mackintosh, J. A.; Karuso, P. *Org. Lett.* **2005**, *7*, 2401-2404.
- (16) Karuso, P.; Crawford, A. S.; Veal, D. A.; Scott, G. B. I.; Choi, H.-Y. *J. Proteome Res.* **2007**, *7*, 361-366.
- (17) Mackintosh, J. A.; Choi, H. Y.; Bae, S. H.; Veal, D. A.; Bell, P. J.; Ferrari, B. C.; Van Dyk, D. D.; Verrills, N. M.; Paik, Y. K.; Karuso, P. *Proteomics* **2003**, *3*, 2273-2288.
- (18) Mackintosh, J. A.; Veal, D. A.; Karuso, P. *Proteomics* **2005**, *5*, 4673-4677.
- (19) Smejkal, G. B.; Robinson, M. H.; Lazarev, A. *Electrophoresis* **2004**, *25*, 2511-2519.
- (20) Boulangé, A. *PhD Thesis* **2011**, IRCOF, University of Rouen.
- (21) Boulangé, A.; Peixoto, P. A.; Franck, X. *Chem. Eur. J.* **2011**, *17*, 10241-10245.
- (22) Peixoto, P. A. *PhD Thesis* **2009**, IRCOF, University of Rouen.
- (23) Franck, X.; Peixoto, P.; Karuso, P. H. Patent WO2011051225 A1, 2011.
- (24) Chatterjee, S.; Burai, T. N.; Karuso, P.; Datta, A. *J. Phys. Chem. A* **2011**, *115*, 10154-10158.
- (25) Chatterjee, S.; Karuso, P.; Boulangé, A.; Peixoto, P. A.; Franck, X.; Datta, A. *J. Phys. Chem. B* **2013**, *117*, 14951-14959.



- (26) Peixoto, P.; Boulangé, A.; Ball, M. S.; Naudin, B.; Alle, T.; Cosette, P.; Karuso, P.; Franck, X. *J. Am. Chem. Soc.* **2014**, *Submitted*.
- (27) Escobedo, J. O.; Rusin, O.; Lim, S.; Strongin, R. M. *Curr. Opin. Chem. Biol.* **2010**, *14*, 64-70.
- (28) Guo, Z.; Park, S.; Yoon, J.; Shin, I. *Chem. Soc. Rev.* **2014**, *43*, 16-29.
- (29) Kovar, J. L.; Simpson, M. A.; Schutz-Geschwender, A.; Olive, D. M. *Anal. Biochem.* **2007**, *367*, 1-12.
- (30) Weissleder, R. *Nat. Biotechnol.* **2001**, *19*, 316-317.
- (31) Monici, M. In *Biotechnology Annual Review*; El-Gewely, M. R., Ed.; Elsevier: 2005; Vol. Volume 11, p 227-256.
- (32) Pansare, V. J.; Hejazi, S.; Faenza, W. J.; Prud'homme, R. K. *Chem. Mater.* **2012**, *24*, 812-827.
- (33) Mishra, A.; Behera, R. K.; Behera, P. K.; Mishra, B. K.; Behera, G. B. *Chem. Rev.* **2000**, *100*, 1973-2012.
- (34) Dempster, D. N.; Morrow, T.; Rankin, R.; Thompson, G. F. *Chem. Phys. Lett.* **1973**, *18*, 488-492.
- (35) Fox, I. J.; Wood, E. H. *Mayo Clin. Proc.* **1960**, *35*, 732-744.
- (36) Dzurinko, V. L.; Gurwood, A. S.; Price, J. R. *Optometry*, **75**, 743-755.
- (37) Schaafsma, B. E.; Mieog, J. S. D.; Hutteman, M.; van der Vorst, J. R.; Kuppen, P. J. K.; Löwik, C. W. G. M.; Frangioni, J. V.; van de Velde, C. J. H.; Vahrmeijer, A. L. *J. Surg. Oncol.* **2011**, *104*, 323-332.
- (38) Lee, H.; Mason, J. C.; Achilefu, S. *J. Org. Chem.* **2006**, *71*, 7862-7865.
- (39) Pham, W.; Lai, W.-F.; Weissleder, R.; Tung, C.-H. *Bioconjugate Chem.* **2003**, *14*, 1048-1051.
- (40) Löbber, G. In *Ullmann's Encyclopedia of Industrial Chemistry*; Wiley-VCH Verlag GmbH & Co. KGaA: 2000.
- (41) Devlin, R.; Dandliker, W. B.; Arrhenius, P. O. G. Patent US6060598, 2000.
- (42) Kobayashi, M.; Akiyama, M.; Kano, H.; Kise, H. *Chlorophylls and Bacteriochlorophylls: Biochemistry, Biophysics, Functions and Applications*; Springer: Dordrecht, The Netherlands, 2006.
- (43) Tanaka, Y.; Shin, J.-Y.; Osuka, A. *Eur. J. Org. Chem.* **2008**, *2008*, 1341-1349.
- (44) Kee, H. L.; Nothdurft, R.; Muthiah, C.; Diers, J. R.; Fan, D.; Ptaszek, M.; Bocian, D. F.; Lindsey, J. S.; Culver, J. P.; Holten, D. *Photochem. Photobiol.* **2008**, *84*, 1061-1072.

- (45) Callis, J. B.; Knowles, J. M.; Gouterman, M. *The Journal of Physical Chemistry* **1973**, *77*, 154-157.
- (46) Terpetschnig, E.; Szmecinski, H.; Lakowicz, J. *J. Fluoresc.* **1993**, *3*, 153-155.
- (47) Luo, S.; Zhang, E.; Su, Y.; Cheng, T.; Shi, C. *Biomaterials* **2011**, *32*, 7127-7138.
- (48) Umezawa, K.; Cittierio, D.; Suzuki, K. *Anal. Sci.* **2008**, *24*, 213-217.
- (49) Treibs, A.; Kreuzer, F.-H. *Justus Liebigs Ann. Chem.* **1968**, *718*, 208-223.
- (50) Loudet, A.; Burgess, K. *Chem. Rev.* **2007**, *107*, 4891-4932.
- (51) Killoran, J.; Allen, L.; Gallagher, J. F.; Gallagher, W. M.; O'Shea, D. F. *Chem. Commun.* **2002**, 1862-1863.
- (52) Tasior, M.; O'Shea, D. F. *Bioconjugate Chem.* **2010**, *21*, 1130-1133.
- (53) Gorman, A.; Killoran, J.; O'Shea, C.; Kenna, T.; Gallagher, W. M.; O'Shea, D. F. *J. Am. Chem. Soc.* **2004**, *126*, 10619-10631.
- (54) Umezawa, K.; Nakamura, Y.; Makino, H.; Citterio, D.; Suzuki, K. *J. Am. Chem. Soc.* **2008**, *130*, 1550-1551.
- (55) Umezawa, K.; Matsui, A.; Nakamura, Y.; Citterio, D.; Suzuki, K. *Chem. Eur. J.* **2009**, *15*, 1096-1106.
- (56) Sparano, B. A.; Koide, K. *J. Am. Chem. Soc.* **2007**, *129*, 4785-4794.
- (57) Beija, M.; Afonso, C. A. M.; Martinho, J. M. G. *Chem. Soc. Rev.* **2009**, *38*, 2410-2433.
- (58) Yang, Y. J.; Lowry, M.; Xu, X. Y.; Escobedo, J. O.; Sibrian-Vazcluez, M.; Wong, L.; Schowalter, C. M.; Jensen, T. J.; Fronczek, F. R.; Warner, I. M.; Strongin, R. M. *Proc. Natl. Acad. Sci. U. S. A.* **2008**, *105*, 8829-8834.
- (59) Yuan, L.; Lin, W.; Zhao, S.; Gao, W.; Chen, B.; He, L.; Zhu, S. *J. Am. Chem. Soc.* **2012**, *134*, 13510-13523.
- (60) Xiong, X.; Song, F.; Chen, G.; Sun, W.; Wang, J.; Gao, P.; Zhang, Y.; Qiao, B.; Li, W.; Sun, S.; Fan, J.; Peng, X. *Chem. Eur. J.* **2013**, *19*, 6538-6545.
- (61) Alessi, A.; Salvalaggio, M.; Ruzzon, G. *J. Lumin.* **2013**, *134*, 385-389.
- (62) Meek, S. T.; Nesterov, E. E.; Swager, T. M. *Org. Lett.* **2008**, *10*, 2991-2993.
- (63) Jedrzejewska, B.; Kabatc, J.; Pietrzak, M.; Paczkowski, J. *Dyes Pigm.* **2003**, *58*, 47-58.
- (64) Strehmel, B.; Seifert, H.; Rettig, W. *J. Phys. Chem. B* **1997**, *101*, 2232-2243.

- (65) Cao, J. F.; Hu, C.; Liu, F.; Sun, W.; Fan, J. L.; Song, F. L.; Sun, S. G.; Peng, X. *J. ChemPhysChem* **2013**, *14*, 1601-1608.
- (66) Zhao, C. F.; Gvishi, R.; Narang, U.; Ruland, G.; Prasad, P. N. *J. Phys. Chem.* **1996**, *100*, 4526-4532.
- (67) Szczepan, M.; Rettig, W.; Bricks, Y. L.; Slominski, Y. L.; Tolmachev, A. I. *J. Photochem. Photobiol., A* **1999**, *124*, 75-84.
- (68) Gawinecki, R.; Trzebiatowska, K. *Dyes Pigm.* **2000**, *45*, 103-107.
- (69) Weber, M. J. *Handbook of laser wavelengths*; CRC Press, 1999.
- (70) Mourant, J. R.; Fuselier, T.; Boyer, J.; Johnson, T. M.; Bigio, I. J. *Appl. Opt.* **1997**, *36*, 949-957.
- (71) Ntziachristos, V.; Bremer, C.; Weissleder, R. *European Radiology* **2003**, *13*, 195-208.
- (72) Syzgantseva, O. A.; Tognetti, V.; Boulangé, A.; Peixoto, P. A.; Leleu, S.; Franck, X.; Joubert, L. *J. Phys. Chem. A* **2014**, *118*, 757-764.
- (73) Chaudhuri, R.; Guharay, J.; Sengupta, P. K. *J. Photochem. Photobiol., A* **1996**, *101*, 241-244.
- (74) Bahri, M. A.; Hoebeke, M.; Grammenos, A.; Delanaye, L.; Vandewalle, N.; Seret, A. *Colloids and Surfaces A: Physicochemical and Engineering Aspects* **2006**, *290*, 206-212.
- (75) Armitage, B. A. In *DNA Binders and Related Subjects*; Waring, M. J., Chaires, J. B., Eds. 2005; Vol. 253, p 55-76.
- (76) Ferguson, L. R.; Denny, W. A. *Mutation Research-Fundamental and Molecular Mechanisms of Mutagenesis* **2007**, *623*, 14-23.
- (77) Karlsson, H. J.; Bergqvist, M. H.; Lincoln, P.; Westman, G. *Bioorg. Med. Chem.* **2004**, *12*, 2369-2384.
- (78) Nygren, J.; Svanvik, N.; Kubista, M. *Biopolymers* **1998**, *46*, 39-51.
- (79) Weber, K.; Osborn, M. *J. Biol. Chem.* **1969**, *244*, 4406-4412.
- (80) Berg, J. M.; Tymoczko, J. L.; Stryer, L. *Biochemistry*; 7th ed.; W. H. Freeman: New York, 2012.
- (81) Ball, M. S.; Karuso, P. *J. Proteome Res.* **2007**, *6*, 4313-4320.
- (82) Lopez, M. F.; Berggren, K.; Chernokalskaya, E.; Lazarev, A.; Robinson, M.; Patton, W. F. *Electrophoresis* **2000**, *21*, 3673-3683.
- (83) Czerney, P.; Lehmann, F.; Schweder, B.; Wenzel, M. Patent WO2006079334 A3, 2006.

- (84) [http://www.fluorotechnics.com.au/pdf/LavaPurple\\_protocol.pdf](http://www.fluorotechnics.com.au/pdf/LavaPurple_protocol.pdf); Accessed: 18/11/2013.
- (85) Drummen, G. *Molecules* **2012**, *17*, 14067-14090.
- (86) Doherty, G. J.; McMahon, H. T. *Annu. Rev. Biochem.* **2009**, *78*, 857-902.
- (87) Stan, R.-V. *Microsc. Res. Tech.* **2002**, *57*, 350-364.
- (88) Anderson, R. G. *Annu. Rev. Biochem.* **1998**, *67*, 199-225.
- (89) Carver, L. A.; Schnitzer, J. E. *Nat. Rev. Cancer* **2003**, *3*, 571-581.
- (90) Frank, P.; Lisanti, M. *Curr. Opin. Lipidol.* **2004**, *15*, 523-529.
- (91) Pelkmans, L. *Biochim. Biophys. Acta* **2005**, *1746*, 295-304.
- (92) Lajoie, P.; Nabi, I. R. *Int. Rev. Cell. Mol. Biol.* **2010**, *282*, 135-163.
- (93) Choi, H. Y.; Veal, D. A.; Karuso, P. *J. Fluoresc.* **2006**, *16*, 475-482.

---

## **CHAPTER 5**

### **EXPERIMENTAL**

---

## 5.1. General

Reagents were purchased from Sigma Aldrich and Alfa Aesar and used without purification unless specified. Calcein, bovine serum albumin (BSA), sodium dodecyl sulfate (SDS), 1,1'-diethyl-4,4'-carbocyanine iodide and spectroscopic grade solvents: acetonitrile, DMSO and ethanol were purchased from Sigma Aldrich. Hoechst 33342, ER-Tracker<sup>TM</sup> Green, MitoTracker® Green, LysoTracker® Red DND-99 and CellTracker<sup>TM</sup> CM-DiI were purchased from Invitrogen. Molecular sieves were freshly activated either in an oven at > 400 °C or in the microwave. Ratios provided in “general procedures” and percentage yields are with respect to the limiting reagent. Temperatures specified are those of the heating or cooling bath. Methanol was distilled from magnesium/iodide, and stored under nitrogen over oven-activated 4Å MS. Nitromethane was fractionally distilled before being freshly redistilled over CaH before use. TLC was performed on aluminium backed silica gel 60 F254 plates (Merck) and visualised using either a UV lamp (254 or 365 nm) or heating with phosphomolybdic acid or ninhydrin stain. All microwave irradiation experiments were carried out in a dedicated CEM-Discover LabMate microwave apparatus, operating at a frequency of 2.45 GHz with continuous irradiation power from 0 to 300 W. The reactions were carried out in 10 mL glass vials sealed with a Teflon crimp cap, which can be exposed to a maximum of 250 °C and 20 bar internal pressure. Purifications were conducted as specified with flash column chromatography using silica gel 60 (Merck, 230-400 mesh) or with preparative TLC plates (Analtech, 1 000 µm thickness) or basic aluminium oxide (S grade, 100-290 mesh, gravity) or activated charcoal Darco G-60, 100 mesh or a 50% (w/w) mixture of charcoal Darco G-60, 100 mesh and celite 545 (50% (w/w)). The charcoal and celite were pre-washed with MeOH and water before used. HPLC purification was conducted as specified using an Alltech Econosphere C18 column 100 × 10 mm, 10 µm or Gemini NX C18 column 150 × 21.22 mm, 5 µm. As specified <sup>1</sup>H NMR spectra were recorded on either a Bruker AVIII-300 MHz spectrometer or a Bruker DPX400 (400 MHz) spectrometer or a Bruker AVII600K (600 MHz) spectrometer and reported in ppm using the specified solvent as internal standard (CDCl<sub>3</sub> at 7.24 ppm, DMSO-*d*<sub>6</sub> at 2.49 ppm, D<sub>2</sub>O at 4.66 ppm and MeOD-*d*<sub>4</sub> at 3.34 ppm). As specified, <sup>13</sup>C NMR spectra were recorded on a Bruker DPX400 (101 MHz) spectrometer or a Bruker AVII600K (150 MHz) spectrometer and reported in ppm

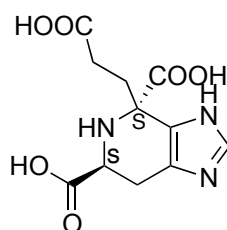
using the specified solvent as internal standard ( $\text{CDCl}_3$  at 77.06 ppm,  $\text{DMSO}-d_6$  at 39.50 ppm and  $\text{MeOD}-d_4$  at 49.86 ppm). HRMS were performed at Illinois University Mass Spectrometry Unit, USA, using a Waters Q-ToF Ultima Tandem Quadrupole/Time-of-Flight Instrument or at the Australian Proteome analysis Facility (APAF), Macquarie University, Australia using a Thermo Orbitrap Elite with ETD. LRMS (ESI) data were obtained by direct injection using a Shimadzu GCMS-QP5000. Specific optical rotation was measured on a Jasco P-1010 Polarimeter (Jasco, Japan). UV-vis absorption and fluorescence measurements were conducted on a Spectramax M5 fluorescence spectrophotometer with the use of the plate reader, a CARY 1Bio UV-Visible spectrophotometer and a LS50B fluorometer (Perkin Elmer). A FV1000 confocal laser-scanning microscope was used for imaging purposes.

## 5.2. Experimental for Chapter 1

### 5.2.1. General Procedure for Conducting the Pictet-Spengler Reaction

Base or Lewis acid (no. of equiv as specified) was added to a solution of L-histidine (1 equiv) and ketone (1 equiv) in the solvent as specified ( $0.06 \text{ mL mg}^{-1}$ ). The mixture was then subjected to the reaction conditions (temperature and time) as specified. The solvent was evaporated under reduced pressure and the crude  $^1\text{H}$  NMR was taken. The diastereomers were separated as specified and yields are as reported in Chapter 1 (Table 1.1, 1.2, 1.3, 1.4, 1.5 and 1.6).

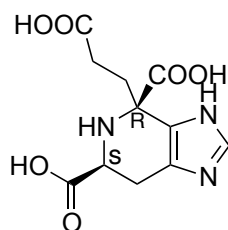
**(4*S*,6*S*)-4-(2-carboxyethyl)-4,5,6,7-tetrahydro-3*H*-imidazo[4,5-*c*]pyridine-4,6-dicarboxylic acid, cucumopine (1.5) (from Table 1.3; Entry 2)**



TEA (7.2 mL, 51.6 mmol) was added to a solution of L-histidine (500 mg, 3.2 mmol) and  $\alpha$ -ketoglutaric acid (471 mg, 3.2 mmol) in MeOH (30 mL). The mixture was refluxed for 17 h after which the solvent was evaporated under reduced pressure. The crude reaction mixture was adsorbed onto a column of activated charcoal ( $15 \times 1.5 \text{ cm}$ ) and eluted with  $\text{H}_2\text{O}$ . Cucumopine eluted after 60 mL. The fractions containing the latter were freeze-dried and cucumopine was isolated (788 mg, 86%)

as a white powder.  $^1\text{H}$  NMR (400 MHz,  $\text{D}_2\text{O}$ )  $\delta$  7.82 (s, 1H), 4.00 (dd,  $J$  = 6.0 Hz, 1H), 3.21 (dd,  $J$  = 6.0 Hz, 1H), 2.88 (dd,  $J$  = 12.0 Hz, 1H), 2.2-2.6 (m, 2H);  $^{13}\text{C}$  NMR (100 MHz,  $\text{D}_2\text{O}$ )  $\delta$  182.6, 175.3, 175.2, 137.8, 127.8, 127.8, 67.1, 57.1, 33.5, 33.2, 24.7; **mass** (ESI)  $m/z$  282  $[\text{M}-\text{H}^+]$ ;  $[\alpha]_{\text{D}}^{22.3}$ :  $-43$  ( $\text{H}_2\text{O}$ ; c 1.0),  $\text{lit}^2$   $[\alpha]_{\text{D}}$ :  $-41$  ( $\text{H}_2\text{O}$ ; c 2.92).

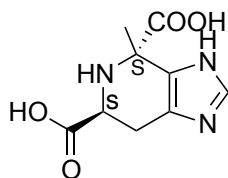
**(4*R*,6*S*)-4-(2-carboxyethyl)-4,5,6,7-tetrahydro-3*H*-imidazo[4,5-*c*]pyridine-4,6-dicarboxylic acid, mikimopine (1.6)**



After a further 40 mL mikimopine eluted, was freeze dried and isolated (77.9 mg, 8.6%) as a white powder.  $^1\text{H}$  NMR (400 MHz,  $\text{D}_2\text{O}$ )  $\delta$  5.15 (dt,  $J$  = 7.0, 6.8, 1H), 5.04 (tt,  $J$  = 6.8, 6.6, 1.3 Hz, 1H), 4.41 (br s, 1H), 3.68 (br t,  $J$  = 5.9 Hz, 2H), 2.03 (m, 2H), 1.96 (m, 2H), 1.65 (s, 3H), 1.62 (s, 3H), 1.56 (s, 3H), 1.41 (s 9H);  $^{13}\text{C}$  NMR (100 MHz,  $\text{D}_2\text{O}$ )  $\delta$  155.8, 139.1, 131.7, 123.9, 120.6, 79.1, 39.4, 38.4, 28.4, 26.4, 25.6, 17.5, 16.2; **mass** (ESI)  $m/z$  282  $[\text{M}-\text{H}^+]$ ;  $[\alpha]_{\text{D}}^{22.5}$ :  $-88$  ( $\text{H}_2\text{O}$ ; c 1.0),  $\text{lit}^2$   $[\alpha]_{\text{D}}$ :  $-89$  ( $\text{H}_2\text{O}$ ; c 1.0).

All physicochemical and spectral data of **1.5** and **1.6** are as previously reported.<sup>1,2</sup>

**(4*S*,6*S*)-4-methyl-4,5,6,7-tetrahydro-3*H*-imidazo[4,5-*c*]pyridine-4,6-dicarboxylic acid (1.8)**

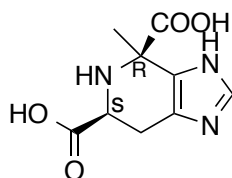


TEA (0.7 mL, 5.2 mmol) was added to a solution of L-histidine (50.0 mg, 0.32 mmol) and ketone (28.4 mg, 0.32 mmol) in MeOH (3 mL). The mixture was refluxed for 17 h after which the solvent was evaporated under reduced pressure. The crude reaction mixture was adsorbed onto a column of activated charcoal and eluted using a



gradient of 0-30% MeOH in H<sub>2</sub>O as eluant. The *trans*-(S,S) diastereomer **1.8** was eluted first. After removal of methanol, the residue was freeze-dried to yield **1.8** (52.8 mg, 72.8%) as a white powder. <sup>1</sup>H NMR (600 MHz, D<sub>2</sub>O) δ 8.63 (s, 1H), 4.42 (dd, *J* = 11.9, 5.3 Hz, 1H), 3.33 (dd, *J* = 17.0, 5.3 Hz, 1H), 3.00 (dd, *J* = 17.0, 11.9 Hz, 1H), 1.83 (s, 1H); <sup>13</sup>C NMR (150 MHz, D<sub>2</sub>O) δ 169.95, 169.85, 135.3, 124.5, 123.6, 61.3, 53.9, 21.32, 21.29; IR (neat) cm<sup>-1</sup> 3048, 1668, 1631, 1199, 1139; [α]<sub>D</sub><sup>23.4</sup>: -61 (H<sub>2</sub>O; c 0.11); mass (ESI) *m/z* 224 [M-H<sup>+</sup>]; HRMS (ESI) *m/z* [M+H<sup>+</sup>] calcd for C<sub>9</sub>H<sub>12</sub>N<sub>3</sub>O<sub>4</sub> 226.0828, found 226.0822.

**(4*S*,6*S*)-4-methyl-4,5,6,7-tetrahydro-3*H*-imidazo[4,5-*c*]pyridine-4,6-dicarboxylic acid (**1.9**)**



The *cis*-(S,R) diastereomer **1.9** was eluted with 30% methanol and isolated (5.2 mg, 7.2%) as a white powder. <sup>1</sup>H NMR (600 MHz, D<sub>2</sub>O) δ 8.59 (s, 1H), 4.42 (dd, *J* = 11.7, 5.5 Hz, 1H), 3.35 (dd, *J* = 17.0, 5.5 Hz, 1H), 3.02 (dd, *J* = 17.0, 11.7 Hz, 1H), 1.74 (s, 1H); <sup>13</sup>C NMR (150 MHz, D<sub>2</sub>O) δ 170.3, 169.9, 134.9, 124.5, 123.4, 60.6, 51.5, 22.4, 21.5; IR (neat) cm<sup>-1</sup> 3041, 1673, 1623, 1201, 1138; [α]<sub>D</sub><sup>23.7</sup>: -30 (H<sub>2</sub>O; c 0.11); mass (ESI) *m/z* 224 [M-H<sup>+</sup>]; HRMS (ESI) *m/z* [M+H<sup>+</sup>] calcd for C<sub>9</sub>H<sub>12</sub>N<sub>3</sub>O<sub>4</sub> 226.0828, found 226.0824.

## 5.2.2. Fluorescence-based Assay to Assess the Fe(III) Chelating Ability of Mikimopine

### Apparatus and reagents

Fluorescent measurements were conducted on a Spectramax M5 fluorescence spectrophotometer with the use of the plate reader. Calcein and ammonium iron (III) citrate were purchased from Sigma Aldrich and used as received.

## Preparation of solutions

A 200  $\mu\text{M}$  stock solution of calcein was prepared in a buffer of 40 mM HEPES at pH 7.65 and 150 mM NaCl. A 50 mM stock solution of Fe(III) and a 50 mM stock solution of EDTA were prepared. Ten times serial dilutions of each stock solution were conducted to make solutions of concentrations 5000-0.5  $\mu\text{M}$  of Fe(III), EDTA and mikimopine in a buffer of 40 mM HEPES (pH 7.65), 150 mM NaCl.

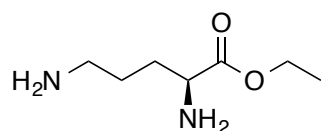
## Determination of Fe(III) Chelating Ability

Serial dilutions of Fe(III) citrate (5000-0.5  $\mu\text{M}$ ) were added to the rows of a black 96 well plate (20  $\mu\text{L}$ ) plus a blank. To the columns was added serially diluted EDTA (5000-0.5  $\mu\text{M}$ ) plus a blank (20  $\mu\text{L}$ ). To each well was added calcein stock (5  $\mu\text{L}$ ) and buffer (155  $\mu\text{L}$ ) and the plate allowed to equilibrate at room temperature in the dark for 5 h. Each experiment was conducted in triplicate. Fluorescence ( $\lambda_{\text{ex}}$  490 nm;  $\lambda_{\text{em}}$  520 nm) was recorded and plotted against  $\log[\text{Fe(III)}]$  and fitted to a Gaddum-Schild  $\text{EC}_{50}$  shift equation<sup>3</sup> using GraphPad Prism (v 4.0) (**Chapter 1; Figure 1.10A and B**).

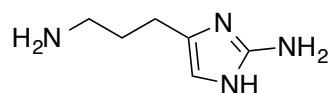
## 5.3. Experimental for Chapter 3

### 5.3.1. Synthesis of DHO (2.2) and Oroidin (2.1)

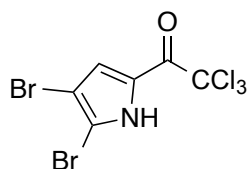
#### ethyl (*S*)-2,5-diaminopentanoate (3.9)



Ornithine hydrochloride (5 g, 0.029 mol) was dissolved in a dry ethanol (50 mL) and the reaction mixture cooled to 0 °C. After 10 min. Thionyl chloride (2.83 mL, 0.037 mol) was slowly added to the reaction mixture. After completion of the addition, the reaction mixture was warmed to r.t. and then refluxed for 8 h, after which, solvent was removed under reduced pressure yielding ornithine ethyl ester dihydrochloride (**3.9**) as a white solid (5.82 g, 89%). <sup>1</sup>H NMR (400 MHz, DMSO-*d*<sub>6</sub>)  $\delta$  8.76 (br s, 3H), 8.27 (br s, 3H), 4.16 (m, 2H), 3.94 (t,  $J$  = 6.6 Hz, 1H), 2.79-2.68 (m, 2H), 1.90-1.80 (m, 2H), 1.79-1.58 (m, 2H), 1.21 (t,  $J$  = 7.4 Hz, 3H).

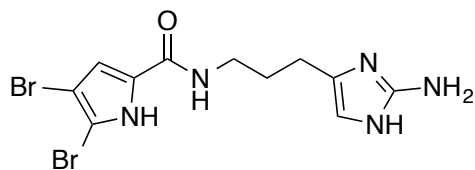
**4-(3-aminopropyl)-1*H*-imidazol-2-amine (1.4)**

Compound **1.4** was synthesised using a method of Horne *et al.*<sup>4</sup> Briefly, **3.9** was dissolved in water (50 mL) and the solution cooled to 0 °C. Sodium amalgam<sup>5</sup> (109.2 g, 0.22 mol) was slowly added to the solution over a period of 30 min. During the addition the pH of the reaction mixture was maintained at 1-3 using dropwise addition of 15% hydrochloric acid. When the pH remained constant and the evolution of the gas had ceased, the solution was decanted from the residual mercury. The pH of the solution was changed to and maintained at 4.5 by addition of 1*N* sodium hydroxide. The crude aldehyde so formed is further heated to 95 °C with an aqueous solution of cyanamide (9.6 mL, 0.114 mol) for 2 h. The solvent was removed leaving behind a thick yellow residue. Methanol was then added and the precipitated salt removed by filtration. The filtrate was concentrate and recrystallised from ethanol to give **1.4** (1.92 g, 42%) as a yellow solid. <sup>1</sup>H NMR (400 MHz, DMSO-*d*<sub>6</sub>) δ 12.33 (s, 1H), 11.79 (s, 1H), 8.31 (br s, 2H), 7.37 (br s, 3H), 6.61 (s, 1H), 2.77-2.65 (m, 2H), 2.50 (t, *J* = 6.7 Hz, 2H), 1.88-1.77 (m, 2H).

**2,2,2-trichloro-1-(4,5-dibromo-1*H*-pyrrol-2-yl)ethanone (3.6)**

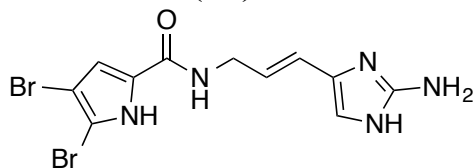
Bromine (1.50 g, 9.42 mol) was added dropwise to a solution of 2-trichloroacetylpyrrole (1.00 g, 4.71 mol) in chloroform (50 mL) at 0 °C. The reaction mixture was then allowed to warm to r.t. and stirred overnight. The solvent was removed on the rotary evaporator and the crude was purified by flash chromatography (SiO<sub>2</sub>, 5% EtOAc in Pet ether) affording **3.6** (1.95 g; 95%) as a white solid. <sup>1</sup>H NMR (400 MHz, CDCl<sub>3</sub>) δ 9.10 (br s, 1H), 8.11 (d, *J* = 1.2 Hz, 1H).

***N*-(3-(2-amino-1*H*-imidazol-4-yl)propyl)-4,5-dibromo-1*H*-pyrrole-2-carboxamide (2.2)**



To a solution of **1.4** (1.4 g, 0.01 mol) in DMF (30 mL) was added **3.6** (4.17, 0.011 mol) followed by K<sub>2</sub>CO<sub>3</sub> (3.18, 0.03 mol). The reaction mixture was stirred at r.t. for 24 h. The solvent was removed under high vacuum and the crude product was purified by flash chromatography (alumina, 10-40% MeOH in CHCl<sub>3</sub> saturated with NH<sub>3</sub>) to give DHO (**2.2**) as an orange solid (1.0 g, 53%). <sup>1</sup>H NMR (400 MHz, MeOD-*d*<sub>4</sub>) δ 6.83 (s, 1H), 6.32 (s, 1H), 3.36 (t, *J* = 7.5 Hz, 2H), 2.50 (t, *J* = 7.5 Hz, 2H), 1.85 (q, *J* = 7.2 Hz, 2H).

**(*E*)-*N*-(3-(2-amino-1*H*-imidazol-4-yl)allyl)-4,5-dibromo-1*H*-pyrrole-2-carboxamide (2.1)**



DHO (**2.2**) was converted to oroidin following a method reported by Lindel and coworkers.<sup>6</sup> Refluxing in MeOH for 15 min in the presence of a few drops of conc. HCl gave dihydrooroidin-HCl. A solution of *N*-chlorosuccinimide (30.5 mg, 0.22 mmol) and DHO-HCl (100 mg, 0.22 mmol) in dry DMF (10 mL) was stirred at r.t. for 1 h and then at 100 °C for 1 h. The solvent was evaporated under reduced pressure, and the residue was purified by flash chromatography (alumina, 2-16% MeOH in CHCl<sub>3</sub> saturated with NH<sub>3</sub>) to give **2.1** as yellow solid (41.0 mg, 55%). <sup>1</sup>H NMR (400 MHz, DMSO-*d*<sub>6</sub>) δ 8.45 (t, *J* = 5.8 Hz, 1H), 8.23 (s, 3H), 7.77 (br s, 2H), 6.97 (s, 1H), 6.80 (s, 1H), 6.19 (d, *J* = 16.0 Hz, 1H), 6.08 (dt, *J* = 16.0, 5.2 Hz, 1H), 3.95 (d, *J* = 5.1 Hz, 2H).

NMR spectral data of **3.9**, **1.4**, **3.6**, **2.2** and **2.1** were as previously reported.<sup>4,6</sup>

### 5.3.2. Epoxidation Reactions

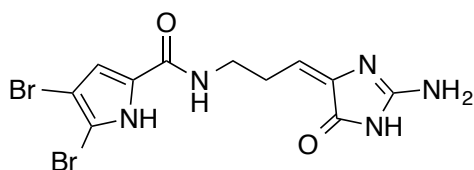
#### Reaction using *in situ* generation of dimethyldioxirane, DMDO

To a stirred solution of DHO (**2.2**) or oroidin (**2.1**) (1 equiv) in acetone/H<sub>2</sub>O (1:3 v/v) (0.1 mL/mg) at 0 °C was added Oxone (1.2 equiv) and NaHCO<sub>3</sub> (2.4 equiv) in portions. The reaction was allowed to warm up to r.t. after which acetone was removed under vacuum and the water was removed by freeze-drying. The crude was then subjected to purification by flash chromatography (SiO<sub>2</sub>, 2-20% MeOH in CHCl<sub>3</sub> saturated with NH<sub>3</sub>) to yield the product in amounts as reported (**Table 3.1**; Entry **1** and **2**).

#### Preparation of DMDO

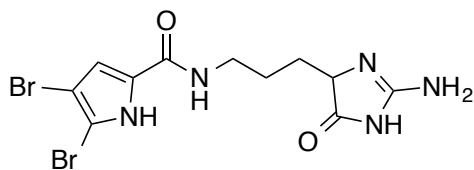
DMDO was prepared using the procedure reported by Murray and Singh.<sup>7</sup> The concentration of DMDO was determined by iodometric titration before use and found to be in the range of 0.05-0.09 M.

#### (*E*)-*N*-(3-(2-amino-5-oxo-4,5-dihydro-1*H*-imidazol-4-yl)allyl)-4,5-dibromo-1*H*-pyrrole-2-carboxamide, dispacamide A (**2.16**) (from **Table 3.1**; Entry **5**)



A solution of DMDO in acetone (660  $\mu$ L, 0.07 M, 0.046 mmol) was added to oroidin (15 mg, 0.039 mmol) dissolved in DMF (1 mL) at 0 °C. The reaction mixture was then allowed to warm up to r.t. over 1 h. The solvent was removed under reduced pressure and the crude purified by flash chromatography (SiO<sub>2</sub>, 2-16% MeOH in CHCl<sub>3</sub> saturated with NH<sub>3</sub>) to give **2.16** as a white solid (9.4 mg, 60 %). <sup>1</sup>H NMR (MeOD-*d*<sub>4</sub>)  $\delta$  6.81 (s, 1H), 6.20 (t, *J* = 8.2 Hz, 1H), 3.51 (t, *J* = 6.6 Hz, 2H), 2.63 (q, *J* = 7.1 Hz, 2H); HRMS (ESI) *m/z* [M+H<sup>+</sup>] calcd for C<sub>11</sub>H<sub>12</sub>Br<sup>79</sup>Br<sup>81</sup>N<sub>5</sub>O<sub>2</sub><sup>+</sup>, 405.9332, found 405.9333.

#### *N*-(3-(2-amino-5-oxo-4,5-dihydro-1*H*-imidazol-4-yl)propyl)-4,5-dibromo-1*H*-pyrrole-2-carboxamide, dihydrodispacamide A (**3.10**)



A solution of DMDO in acetone (660  $\mu$ L, 0.07 M, 0.046 mmol) was added to DHO (15 mg, 0.038 mmol) dissolved in DMF (1 mL) at 0  $^{\circ}$ C. The reaction mixture was then allowed to warm up to r.t. over 1 h. The solvent was removed under reduced pressure and the crude purified by flash chromatography (SiO<sub>2</sub>, 2-16% MeOH in CHCl<sub>3</sub> saturated with NH<sub>3</sub>) to give **3.10** as a white solid (8.7 mg, 56 %). <sup>1</sup>H NMR (DMSO-*d*<sub>6</sub>)  $\delta$  12.67 (br s, 1H), 9.77 (br s, 1H), 8.98 (br s, 2H), 8.17 (t, *J* = 5.8 Hz, 1H), 6.90 (s, 1H), 4.28 (t, *J* = 6.0 Hz, 1H), 3.20 (q, *J* = 6.0 Hz, 2H), 1.77 (m, 1H), 1.66 (m, 1H), 1.55 (m, 1H), 1.48 (m, 1H); HRMS (ESI) *m/z* [M+H<sup>+</sup>] calcd for C<sub>11</sub>H<sub>14</sub>Br<sup>79</sup>Br<sup>81</sup>N<sub>5</sub>O<sub>2</sub> 407.9488, found 407.9479.

NMR spectral data of **2.16** and **3.10** were as previously reported.<sup>4,6</sup>

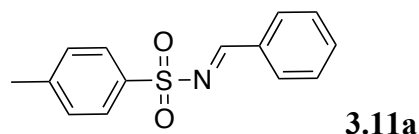
### Reaction with DIB

A solution of DIB (8.2 mg, 0.026 mmol) and TFA (2.5  $\mu$ L, 0.033 mmol) in ACN (0.3 mL) was added to DHO (10 mg, 0.026 mmol) dissolved in DMF (0.5 mL) at 0  $^{\circ}$ C. The reaction mixture was then allowed to warm up to r.t. over 1 h. The solvent was removed under reduced pressure and the crude purified by flash chromatography (SiO<sub>2</sub>, 2-16% MeOH in CHCl<sub>3</sub> saturated with NH<sub>3</sub>) to give **3.10** as a white solid (1.1 mg, 11 %). <sup>1</sup>H NMR characteristics as reported before for **3.10**.

### Reaction with m-CPBA

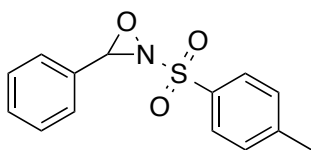
m-CPBA (6.6 mg, 0.038 mmol) was added to DHO (15 mg, 0.038 mmol) dissolved in MeOH (1 mL) at 0  $^{\circ}$ C. The reaction mixture was then allowed to warm up to r.t. over 1 h then stirred overnight. The solvent was removed under reduced pressure and the crude purified by flash chromatography (SiO<sub>2</sub>, 2-16% MeOH in CHCl<sub>3</sub> saturated with NH<sub>3</sub>) to give **3.10** as a white solid (0.5 mg, 3 %). <sup>1</sup>H NMR characteristics as reported before for **3.10**.

### Synthesis of 3-phenyl-2-tosyl-1,2-oxaziridine (**3.11**)



Aziridine **3.11** was synthesised following the procedure reported by Chang *et*

*al.*<sup>8</sup> To a solution of benzaldehyde (1.01 mL, 10 mmol) and *p*-toluenesulfonamide (1.71 g, 10 mmol) in 50 mL of CH<sub>2</sub>Cl<sub>2</sub> was added trifluoroacetic anhydride (1.53 mL, 11 mmol). The reaction was refluxed for 12 h after which the reaction mixture was poured into cold water, extracted with CH<sub>2</sub>Cl<sub>2</sub>, dried with MgSO<sub>4</sub>, evaporated to dryness and purified by flash chromatography (SiO<sub>2</sub>, 10% EtOAc in Pet ether) to give **3.11** as a white solid (2.28 g, 76%). <sup>1</sup>H NMR δ 9.03 (s, 1H) 7.94-7.88 (m, 4H), 7.62 (t, *J* = 6.2 Hz, 1H) 7.49 (d, *J* = 7.4 Hz, 2H), 7.36 (d, *J* = 8.1 Hz, 2H), 2.44 (s, 3H).



To a suspension of powdered KOH (392 mg, 7 mmol) and *m*-chloroperoxybenzoic acid (380.6 mg, 2.2 mmol) in 1 mL of CH<sub>2</sub>Cl<sub>2</sub> was added a solution of **3.11a** (518.6 mg, 2.2 mmol) in 3 mL of CH<sub>2</sub>Cl<sub>2</sub>. After 5 min, the suspension was filtered, evaporated to dryness and dried under vacuum to afford the product as a white solid (528 mg, 95%). <sup>1</sup>H NMR δ 7.93 (d, *J* = 8.0 Hz, 2H), 7.46-7.40 (m, 7H), 5.45 (s, 1H), 2.49 (s, 3H).

NMR spectral data of **3.11a** and **3.11** were as previously reported.<sup>8</sup>

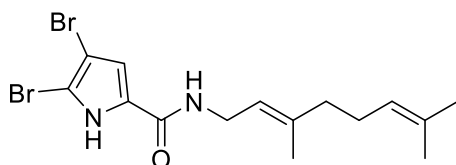
### Reaction with the oxaziridines (Table 3.2; Entry 4-6, and Table 3.3; Entry 4-5)

The oxaziridine (No. of equiv as specified) was added to a solution of DHO or oroidin (1 equiv) in MeOH at r.t. The reaction was allowed to stir for the specified amount of time. The solvent was removed under reduced pressure and the crude purified by flash chromatography (SiO<sub>2</sub>, 2-16% MeOH in CHCl<sub>3</sub> saturated with NH<sub>3</sub>) to give the product in the amount specified.

### 5.3.3. Reactions with Snyder's Reagent, BDSB (3.26)

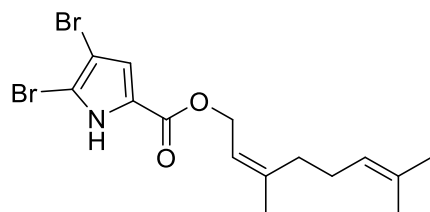
#### Synthesis of Pyrrole-terpene Substrates

#### (*E*)-4,5-dibromo-*N*-(3,7-dimethylocta-2,6-dien-1-yl)-1*H*-pyrrole-2-carboxamide (**3.37**)



To a solution of the gerylamine (188 mg, 1.22 mmol) in DMF (5 mL) was added dibromotrichloroacetylpyrrole (455 mg, 1.22 mmol) followed by  $K_2CO_3$  (510 mg, 3.69 mmol). The reaction mixture was stirred at r.t. for 24 h. Water (5 mL) was added to the reaction mixture which was extracted with EtOAc ( $3 \times 8$  mL). The combined organic layers was then washed with water, dried with  $MgSO_4$  and evaporated under vacuum to yield the desired crude product which purified as specified by flash chromatography ( $SiO_2$ , 30% EtOAc in Pet ether) to give **3.36** was obtained as a cream solid (508 mg, 98%).  $^1H$  NMR (400 MHz,  $CDCl_3$ )  $\delta$  11.45 (br s, 1H), 6.54 (s, 1H), 5.82 (t,  $J = 5.0$  Hz, 1H), 5.24 (t,  $J = 7.0$  Hz, 1H), 5.06 (t,  $J = 6.6$  Hz, 1H), 4.03 (t,  $J = 6.1$  Hz, 2H), 2.06 (m, 2H), 2.00 (m, 2H), 1.67 (s, 3H), 1.66 (s, 3H), 1.58 (s, 3H);  $^{13}C$  NMR (100 MHz,  $CDCl_3$ )  $\delta$  159.7, 140.8, 131.9, 126.8, 123.7, 119.4, 112.4, 106.0, 99.4, 39.5, 37.6, 26.4, 25.7, 17.8, 16.4; IR (neat)  $cm^{-1}$  3415, 3146, 1640, 1561, 1520, 1241, 806.6, 755; HRMS (EI)  $m/z$  [ $M^+$ ] calcd for  $C_{15}H_{20}Br_2^{79}N_2O$  401.9943, found 401.9947.

**(Z)-3,7-dimethylocta-2,6-dien-1-yl 4,5-dibromo-1H-pyrrole-2-carboxylate (3.38)**

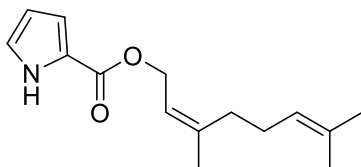


To a solution of the nerol (166 mg, 1.08 mmol) in DMF (5 mL) was added dibromotrichloroacetylpyrrole (400 mg, 1.08 mmol) followed by  $K_2CO_3$  (448 mg, 3.24 mmol). The reaction mixture was stirred at r.t. for 24 h. Water (5 mL) was added to the reaction mixture which was extracted with EtOAc ( $3 \times 8$  mL). The combined organic layers was then washed with water, dried with  $MgSO_4$  and evaporated under vacuum to yield the desired crude product which purified as specified by flash chromatography ( $SiO_2$ , 25% EtOAc in Pet ether) to give **3.37** as a cream solid (410 mg, 95%).  $^1H$  NMR (400 MHz,  $CDCl_3$ )  $\delta$  10.43 (br s, 1H), 6.87 (d,  $J = 2.9$  Hz, 1H), 5.43 (t,  $J = 7.1$  Hz, 1H), 5.07 (tt,  $J = 6.9, 6.8, 1.4$  Hz, 1H), 4.78 (d,  $J = 7.3$  Hz, 2H), 2.14 (m, 2H), 2.09 (m, 2H), 1.76 (s, 3H), 1.65 (s, 3H), 1.58 (s, 3H);  $^{13}C$  NMR (100 MHz,  $CDCl_3$ )  $\delta$  160.2, 143.6, 132.3, 123.9, 123.9, 118.8, 118.0, 107.3,



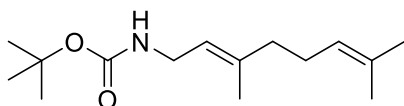
100.5, 61.8, 32.3, 26.7, 25.7, 23.6, 17.7; **IR** (neat)  $\text{cm}^{-1}$  3233, 2917, 1603, 1407, 1231, 1196, 973, 830, 761; **HRMS**  $m/z$  [ $\text{M}^+$ ] calcd for  $\text{C}_{15}\text{H}_{19}\text{Br}_2^{79}\text{N}_2\text{O}$  402.9783, found 402.9783.

**(Z)-3,7-dimethylocta-2,6-dien-1-yl 1H-pyrrole-2-carboxylate (3.39)**



To a solution of the nerol (215 mg, 1.40 mmol) in DMF (5 mL) was added trichloroacetylpyrrole (297 mg, 1.40 mmol) followed by  $\text{K}_2\text{CO}_3$  (579 mg, 4.19 mmol). The reaction mixture was stirred at r.t. for 24 h. Water (5 mL) was added to the reaction mixture which was extracted with EtOAc ( $3 \times 8$  mL). The combined organic layers was then washed with water, dried with  $\text{MgSO}_4$  and evaporated under vacuum to yield the desired crude product which purified as specified by flash chromatography ( $\text{SiO}_2$ , 30% EtOAc in Pet ether) to give **3.38** as a yellow oil (310 mg, 90%).  **$^1\text{H}$  NMR** (400 MHz,  $\text{CDCl}_3$ )  $\delta$  9.62 (br s, 1H), 6.92 (m, 2H), 5.82 (dd,  $J = 6.2$ , 2.6 Hz, 1H), 5.44 (t,  $J = 7.2$  Hz, 1H), 5.11 (tt,  $J = 7.0$ , 6.9, 1.4 Hz, 1H), 4.75 (dd,  $J = 7.1$ , 0.73 Hz, 2H), 2.17 (m, 2H), 2.10 (m, 2H), 1.77 (s, 3H), 1.66 (s, 3H), 1.59 (s, 3H);  **$^{13}\text{C}$  NMR** (100 MHz,  $\text{CDCl}_3$ )  $\delta$  161.5, 142.5, 132.2, 123.6, 122.9, 119.4, 115.3, 110.3, 60.9, 32.1, 26.7, 25.7, 23.5, 17.6; **IR** (neat)  $\text{cm}^{-1}$  3309, 2916, 1679, 1412, 1304, 1185, 1125, 956, 742; **HRMS**  $m/z$  [ $\text{M}^+$ ] calcd for  $\text{C}_{15}\text{H}_{21}\text{NO}_2$  247.1572, found 247.1574.

**(E)-tert-butyl (3,7-dimethylocta-2,6-dien-1-yl)carbamate (3.40)**



To the solution of gerylamine (0.50 g, 0.0030 mol) in  $\text{EtO}_2$ /pentane (3 mL) was added TEA (0.4 mL, 0.0030 mol) followed by boc-anhydride (0.66 g, 0.0030 mol). The solution was stirred for 24 h at r.t. after which solvent was removed under reduced pressure and the crude was purified by flash chromatography ( $\text{SiO}_2$ , 2-10% EtOAc in

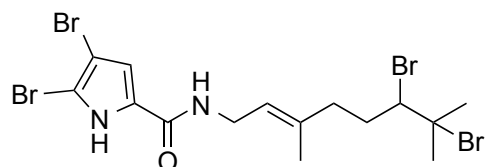
petroleum ether) affording **3.39** (380 mg; 50%) as a colourless oil.  $^1\text{H NMR}$  (400 MHz,  $\text{CDCl}_3$ )  $\delta$  5.15 (dt,  $J = 7.0, 6.8$  Hz, 1H), 5.04 (tt,  $J = 6.8, 6.6, 1.3$  Hz, 1H), 4.41 (br s, 1H), 3.68 (br t,  $J = 5.9$  Hz, 2H), 2.03 (m, 2H), 1.96 (m, 2H), 1.65 (s, 3H), 1.62 (s, 3H), 1.56 (s, 3H), 1.41 (s, 9H);  $^{13}\text{C NMR}$  (100 MHz,  $\text{CDCl}_3$ )  $\delta$  155.9, 139.2, 131.7, 123.9, 120.7, 79.1, 39.5, 38.5, 28.4, 26.4, 25.7, 17.7, 16.2; **IR** (neat)  $\text{cm}^{-1}$  3359, 2976, 2921, 1699, 1366, 1150; **HRMS** (ESI)  $m/z$   $[\text{M}+\text{H}^+]$  calcd for  $\text{C}_{15}\text{H}_{28}\text{NO}_2$  254.2120, found 254.2131.

**Bromodiethylsulfoniumbromopentachloroantimonate, BDSB (3.26)** was prepared according to the procedure reported by Snyder.<sup>9</sup>

### Reaction with pyrrole-terpene substrate **3.37**

A solution of BDSB (22.4 mg, 0.041 mmol) in  $\text{MeNO}_2$  (1.0 mL) was added quickly via syringe to a solution of **3.37** (15 mg, 0.037 mmol) in a mixture of  $\text{MeNO}_2$  (0.75 mL) and  $\text{CH}_2\text{Cl}_2$  (1.75 mL) at  $-40^\circ\text{C}$ . The reaction was allowed to warm up to  $-15^\circ\text{C}$  over a period of 1 h and further stirred at  $-15^\circ\text{C}$  for 30 min before the reaction mixture was quenched by the addition of 5% aqueous  $\text{NaHCO}_3$ : 5% aqueous  $\text{Na}_2\text{SO}_3$  (1:1 v/v, 5 mL), stirred for 15 min, poured into water (3 mL), and extracted with  $\text{CH}_2\text{Cl}_2$  ( $3 \times 10$  mL). The combined organic layers were then dried with  $\text{MgSO}_4$ , concentrated, and purified by flash column chromatography ( $\text{SiO}_2$ , 2.5–22.5% EtOAc in Pet ether) give the products in the amounts and yields as indicated.

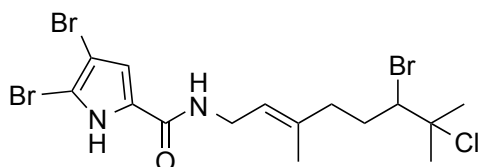
### (E)-4,5-dibromo-N-(6,7-dibromo-3,7-dimethyloct-2-en-1-yl)-1H-pyrrole-2-carboxamide (**3.37a**)



Compound **3.37a** was obtained as a white solid (8.8 mg, 42%).  $^1\text{H NMR}$  ( $\text{CDCl}_3$ , 600 MHz)  $\delta$  10.48 (br s, 1H), 6.53 (d,  $J = 2.9$  Hz, 1H), 5.73 (t,  $J = 5.0$  Hz, 1H), 5.34 (t,  $J = 6.9$  Hz, 1H), 4.11 (dd,  $J = 11.0, 1.1$  Hz, 1H), 4.04 (t,  $J = 6.2$  Hz, 2H), 2.56 (m, 1H), 2.38 (m, 1H), 2.18 (m, 1H), 1.96 (s, 3H), 1.88 (m, 1H), 1.79 (s, 3H),

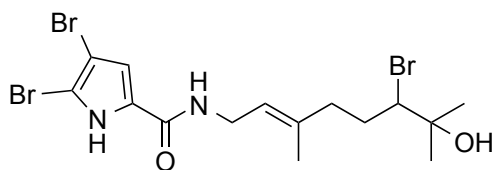
1.73 (s, 3H);  $^{13}\text{C}$  NMR ( $\text{CDCl}_3$ , 150 MHz)  $\delta$  159.3, 138.8, 126.9, 121.1, 111.8, 105.5, 99.7, 68.9, 65.6, 37.7, 37.5, 35.5, 33.6, 28.0, 16.4; IR (neat)  $\text{cm}^{-1}$  3242, 2928, 1682, 1509, 1404, 1196, 1097, 973, 765; HRMS (ESI)  $m/z$   $[(\text{M}+\text{H})^+]$  calcd for  $\text{C}_{15}\text{H}_{21}^{79}\text{Br}_4\text{N}_2\text{O}$  560.8387, found 560.8380.

**(E)-4,5-dibromo-N-(6-bromo-7-chloro-3,7-dimethyloct-2-en-1-yl)-1H-pyrrole-2-carboxamide (3.37b)**



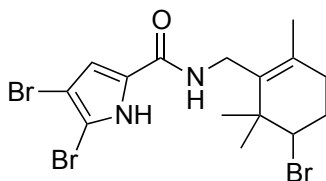
Compound **3.37b** was obtained as a white solid (3.8 mg, 20%).  $^1\text{H}$  NMR ( $\text{CDCl}_3$ , 600 MHz)  $\delta$  10.12 (br s, 1H), 6.52 (d,  $J = 1.62$  Hz, 1H), 5.70 (br s, 1H), 5.32 (t,  $J = 6.9$  Hz, 1H), 4.02 (t,  $J = 6.1$  Hz, 2H), 3.96 (d,  $J = 11.0$  Hz, 1H), 2.43 (m, 1H), 2.38 (m, 1H), 2.15 (m, 1H), 1.83 (m, 1H), 1.77 (s, 3H), 1.71 (s, 3H), 1.65 (s, 3H);  $^{13}\text{C}$  NMR ( $\text{CDCl}_3$ , 150 MHz)  $\delta$  159.1, 139.0, 127.0, 121.0, 111.7, 105.3, 100.1, 72.2, 64.8, 37.7, 37.5, 33.4, 32.3, 26.9, 16.4; IR (neat)  $\text{cm}^{-1}$  3243, 2975, 1637, 1559, 1405, 1230, 1097, 973, 824, 765; HRMS (ESI)  $m/z$   $[\text{M}+\text{H}^+]$  calcd  $\text{C}_{15}\text{H}_{21}^{79}\text{Br}_3\text{ClN}_2\text{O}$  516.8892, found 516.8888.

**(E)-4,5-dibromo-N-(6-bromo-7-hydroxy-3,7-dimethyloct-2-en-1-yl)-1H-pyrrole-2-carboxamide (3.37c)**



Compound **3.37c** was obtained as a white solid (3.2 mg, 17%).  $^1\text{H}$  NMR ( $\text{CDCl}_3$ , 600 MHz)  $\delta$  10.30 (br s, 1H), 6.53 (d,  $J = 2.9$  Hz, 1H), 5.74 (t,  $J = 5.0$  Hz, 1H), 5.30 (t,  $J = 6.9$  Hz, 1H), 4.02 (dd,  $J = 11.0, 1.1$  Hz, 2H), 3.92 (d,  $J = 6.2$  Hz, 1H), 2.38 (m, 1H), 2.13 (m, 1H), 2.00 (m, 1H), 1.80 (m, 1H), 1.70 (s, 3H), 1.34 (s, 3H), 1.32 (s, 3H);  $^{13}\text{C}$  NMR ( $\text{CDCl}_3$ , 150 MHz)  $\delta$  159.2, 138.9, 126.9, 120.9, 111.6, 105.3, 99.8, 72.6, 70.2, 38.1, 37.5, 36.1, 31.8, 26.6, 26.1, 16.4; IR (neat)  $\text{cm}^{-1}$  3210, 2923, 1648, 1509, 1409, 1221, 1092, 978, 735; HRMS (ESI)  $m/z$   $[\text{M}+\text{H}^+]$  calcd for  $\text{C}_{15}\text{H}_{22}^{79}\text{Br}_3\text{N}_2\text{O}_2$  498.9231, found 498.9225.

**4,5-dibromo-*N*-((5-bromo-2,6,6-trimethylcyclohex-1-en-1-yl)methyl)-1*H*-pyrrole-2-carboxamide (3.37d)**

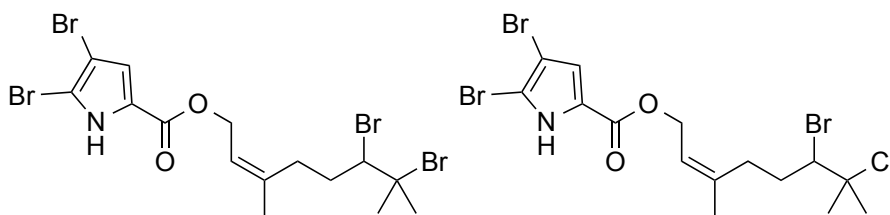


Compound **3.37c** was further purified on the HPLC (Gemini, 50-90% MeOH in H<sub>2</sub>O with 0.05% TFA) and obtained as a white solid (0.4 mg, 2%). **<sup>1</sup>H NMR** (600 MHz, CDCl<sub>3</sub>)  $\delta$  9.72 (br s, 1H), 6.50 (d,  $J$  = 2.82 Hz, 1H), 5.37 (br t,  $J$  = 4.11 Hz, 1H), 4.21 (m, 2H), 4.00 (d,  $J$  = 4.98 Hz, 1H), 2.23 (m, 1H), 2.16 (m, 3H), 1.69 (s, 3H), 1.17 (s, 3H), 1.165 (s, 3H); **<sup>13</sup>C NMR** (150 MHz, CDCl<sub>3</sub>)  $\delta$  158.8, 133.4, 131.8, 126.0, 111.6, 105.3, 99.9, 65.0, 40.0, 38.0, 31.9, 29.6, 27.4, 25.0, 19.6; **IR** (neat) cm<sup>-1</sup> 3129, 2930, 1647, 1510, 1409, 1221, 1101, 732; **HRMS** (ESI)  $m/z$  [M+H<sup>+</sup>] calcd for C<sub>15</sub>H<sub>20</sub><sup>79</sup>Br<sub>3</sub>N<sub>2</sub>O 480.9126, found 480.9128.

**Reaction with pyrrole-terpene substrate 3.38**

A solution of BDSB (22.4 mg, 0.041 mmol) in MeNO<sub>2</sub> (0.75 mL) was added quickly via syringe to a solution of **3.38** (15 mg, 0.037 mmol) in a mixture of MeNO<sub>2</sub> (0.75 mL) and CH<sub>2</sub>Cl<sub>2</sub> (1.75 mL) at -40 °C. The reaction was allowed to warm up to -15 °C over a period of 1 h and further stirred at -15 °C for 30 min before the reaction mixture was quenched by the addition of 5% aqueous NaHCO<sub>3</sub>: 5% aqueous Na<sub>2</sub>SO<sub>3</sub> (1:1 v/v, 5 mL), stirred for 10 min, poured into water (3 mL), and extracted with CH<sub>2</sub>Cl<sub>2</sub> (3 × 10 mL). The combined organic layers were then dried with MgSO<sub>4</sub>, concentrated, and purified by flash column chromatography (SiO<sub>2</sub>, 2.5-30% EtOAc in Pet ether) give the products in the amounts and yields as indicated.

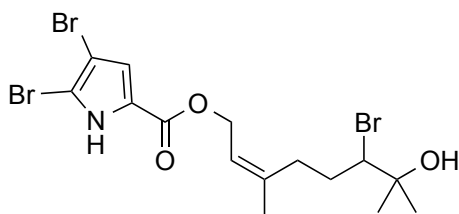
(*Z*)-6,7-dibromo-3,7-dimethyloct-2-en-1-yl 4,5-dibromo-1H-pyrrole-2-carboxylate (**3.38a**) and (*Z*)-6-bromo-7-chloro-3,7-dimethyloct-2-en-1-yl 4,5-dibromo-1H-pyrrole-2-carboxylate (**3.38b**)



Compound **3.38a** (9.0 mg, 43%) and **3.38b** (3.3 mg, 17%), isolated as a mixture, were obtained as white solids.  $^1\text{H NMR}$  (600 MHz,  $\text{CDCl}_3$ )  $\delta$  9.33 (br s, 1H), 6.88 (s, 1H), 5.52 (t,  $J = 6.9$  Hz, 1H), 4.81 (ddd,  $J = 7.6, 12.4, 40.0$  Hz, 2H), 4.11(3.96) (d,  $J = 11.0$  Hz, 1H), 2.59 (1H, m), 2.46 (m, 1H), 2.35 (m, 1H), 1.96(1.76) (s, 3H), 1.90 (1H, m), 1.80 (s, 3H), 1.78(1.64) (s, 3H);  $^{13}\text{C NMR}$  (150 MHz,  $\text{CDCl}_3$ )  $\delta$  159.4, 141.7, 124.1, 120.8, 118.0, 106.5, 100.8, 68.6(72.0), 65.6(64.7), 61.4, 35.4(32.5), 34.0(33.3), 30.3, 28.0(26.9), 23.4; **IR** (neat)  $\text{cm}^{-1}$  2975, 2927, 1681, 1404, 1304, 1229, 1195, 1097, 972, 823, 764; **HRMS** (EI)  $m/z$  [ $\text{M}^+$ ] calcd for  $\text{C}_{15}\text{H}_{19}\text{Br}_4\text{NO}_2$  560.8149, found 560.8144 and calcd for  $\text{C}_{15}\text{H}_{19}\text{Br}_3\text{ClNO}_2$  516.8654, found 516.8658.

Signals in bracket correspond to the minor chloro compound which was inseparable from the bromo compound. Yields and amounts based on ratios from  $^1\text{H NMR}$  of the combined mixed fractions.

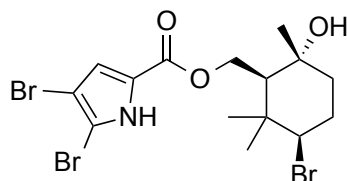
(*Z*)-6-bromo-7-hydroxy-3,7-dimethyloct-2-en-1-yl 4,5-dibromo-1H-pyrrole-2-carboxylate (**3.38c**)



Compound **3.38c** was obtained as a white solid (1.7 mg, 9%).  $^1\text{H NMR}$  (600 MHz,  $\text{CDCl}_3$ )  $\delta$  9.45 (br s, 1H), 6.88 (d,  $J = 2.9$  Hz, 1H), 5.49 (t,  $J = 7.5$  Hz, 1H), 4.79 (m, 2H), 3.96 (dd,  $J = 11.3, 1.8$  Hz, 1H), 2.38 (m, 2H), 2.03 (m, 1H), 1.83 (m, 1H), 1.76 (s, 3H), 1.33 (s, 6H);  $^{13}\text{C NMR}$  (150 MHz,  $\text{CDCl}_3$ )  $\delta$  159.3, 142.1, 124.0, 120.5, 118.0, 106.5, 100.7, 72.7, 69.9, 61.2, 32.2, 30.8, 26.3, 23.4; **IR** (neat)  $\text{cm}^{-1}$  3230, 2924,

1687, 1310, 1406, 1190, 975, 764; **HRMS** (ESI)  $m/z$   $[M+H]^+$  calcd for  $C_{15}H_{21}^{79}Br_3NO_3$  499.9072, found 499.9069.

**((1*S*,3*R*,6*R*)-3-bromo-6-hydroxy-2,2,6-trimethylcyclohexyl)methyl 4,5-dibromo-1*H*-pyrrole-2-carboxylate (3.37d)**

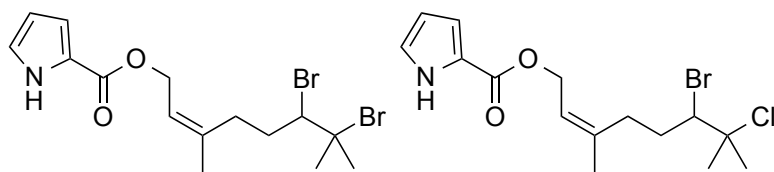


Compound **3.38d** was obtained as a white solid (2.2 mg, 12%). **<sup>1</sup>H NMR** (600 MHz,  $CDCl_3$ )  $\delta$  9.32 (br s, 1H), 6.81 (d,  $J = 2.9$  Hz, 1H), 4.61 (dd,  $J = 5.0, 20.7, 4.0$  Hz, 2H), 4.49 (dd,  $J = 12.2, 3.2$  Hz, 1H), 4.31 (t,  $J = 3.0$  Hz, 1H), 2.46 (dddd,  $J = 14.7, 14.1, 3.7, 3.4$  Hz, 1H), 2.17 (ddd,  $J = 13.9, 13.9, 4.1$  Hz, 1H), 1.89 (dd,  $J = 4.4, 3.8$  Hz, 1H), 1.85 (dddd,  $J = 14.9, 6.5, 3.5, 3.5$  Hz, 1H), 1.53 (1H, m), 1.34 (3H, s), 1.25 (3H, s), 1.17 (3H, s); **<sup>13</sup>C NMR** (150 MHz,  $CDCl_3$ )  $\delta$  159.5, 124.0, 117.9, 107.2, 100.9, 71.9, 69.7, 62.9, 47.2, 38.8, 36.2, 32.4, 31.2, 27.7, 23.1; **IR** (neat)  $cm^{-1}$  3228, 2964, 2924, 1686, 1410, 1194, 978, 764; **HRMS** (ESI)  $m/z$   $[M+Na]^+$  calcd for  $C_{15}H_{20}^{79}Br_3NO_3Na$  521.8891, found 521.8898.

**Reaction with pyrrole-terpene substrate 3.39**

A solution of BDSB (37.1 mg, 0.068 mmol) in  $MeNO_2$  (1.5 mL) was added quickly via syringe to a solution of **3.39** (15.2 mg, 0.061 mmol) in a mixture of  $MeNO_2$  (1.5 mL) and  $CH_2Cl_2$  (3.0 mL) at  $-40^\circ C$ . The reaction was allowed to warm up to  $-15^\circ C$  over a period of 1 h and further stirred at  $-15^\circ C$  for 30 min before the reaction mixture was quenched by the addition of 5% aqueous  $NaHCO_3$ : 5% aqueous  $Na_2SO_3$  (1:1 v/v, 5 mL), stirred for 10 min, poured into water (5 mL), and extracted with  $CH_2Cl_2$  ( $3 \times 8$  mL). The combined organic layers were then dried with  $MgSO_4$ , concentrated, and purified by flash column chromatography ( $SiO_2$ , 2.5-30% EtOAc in Pet ether) give the products in the amounts and yields as indicated.

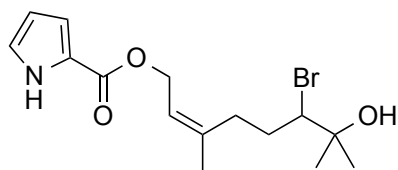
**(Z)-6,7-dibromo-3,7-dimethyloct-2-en-1-yl 1H-pyrrole-2-carboxylate (3.39a) and (Z)-6-bromo-7-chloro-3,7-dimethyloct-2-en-1-yl 1H-pyrrole-2-carboxylate (3.39b)**



Compound **3.39a** (10.6 mg, 42%) and **3.39b** (3.1 mg, 14%), isolated as a mixture, were obtained as white solids.  $^1\text{H NMR}$  (600 MHz,  $\text{CDCl}_3$ )  $\delta$  9.11 (br s, 1H), 6.92 (m, 2H), 6.24 (m, 1H), 5.54 (t,  $J = 6.8$  Hz, 1H), 4.80 (ddd,  $J = 38.1, 12.4, 7.3$  Hz, 2H), 4.12(3.98) (dd,  $J = 11.2, 1.3$  Hz, 1H), 2.58 (1H, m), 2.48 (m, 1H), 2.37 (m, 1H), 1.95(1.76) (s, 3H), 1.90 (m, 1H), 1.80 (s, 3H), 1.78(1.64) (s, 3H);  $^{13}\text{C NMR}$  (150 MHz,  $\text{CDCl}_3$ )  $\delta$  161.0, 140.7(140.8), 122.9, 122.6, 121.3(121.28), 115.3, 110.4, 68.7(71.9), 65.6(64.7), 60.8(60.7), 35.4(33.2), 34.0, 30.2, 28.0(26.9), 23.3(23.26); **IR** (neat)  $\text{cm}^{-1}$  3311, 2933, 1683, 1413, 1307, 1168, 1126, 749; **HRMS** (ESI)  $m/z$   $[\text{M}+\text{H}^+]$  calcd for  $\text{C}_{15}\text{H}_{22}^{79}\text{Br}_2\text{NO}_2$  406.0017, found 406.0023, calcd for  $\text{C}_{15}\text{H}_{21}^{79}\text{BrClNO}_2$  362.0522, found 362.0521.

Signals in bracket correspond to the minor chloro compound which was inseparable from the bromo compound. Yields and amounts based on ratios from  $^1\text{H NMR}$  of the combined mixed fractions.

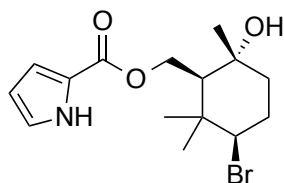
**(Z)-6-bromo-7-hydroxy-3,7-dimethyloct-2-en-1-yl 1H-pyrrole-2-carboxylate (3.39c)**



Compound **3.38c** was obtained as a colourless oil (2.1 mg, 10%).  $^1\text{H NMR}$  (600 MHz,  $\text{CDCl}_3$ )  $\delta$  9.12 (br s, 1H), 6.91 (m, 2H), 6.24 (q,  $J = 2.96$  Hz, 1H), 5.52 (t,  $J = 7.50$  Hz, 1H), 4.79 (ddd,  $J = 38.1, 12.4, 7.3$  Hz, 2H), 3.96 (dd,  $J = 11.2, 1.86$  Hz, 1H), 2.39 (m, 2H), 2.02 (m, 1H), 1.84 (m, 1H), 1.76 (s, 3H), 1.33 (s, 3H), 1.32 (s, 3H);  $^{13}\text{C NMR}$  (150 MHz,  $\text{CDCl}_3$ )  $\delta$  159.0, 136.6, 122.7, 122.67, 121.2, 115.4, 110.5, 72.6, 70.2, 60.6, 32.3, 30.9, 26.5, 26.0, 23.4; **IR** (neat)  $\text{cm}^{-1}$  3310, 2966, 2928, 1689,

1685, 1413, 1306, 1163, 1125, 959, 748; **HRMS** (ESI)  $m/z$   $[M+Na^+]$  calcd for  $C_{15}H_{22}^{79}BrNO_3Na$  366.0681, found 343.0677.

**((1*S*,3*R*,6*R*)-3-bromo-6-hydroxy-2,2,6-trimethylcyclohexyl)methyl 1*H*-pyrrole-2-carboxylate (3.39d)**



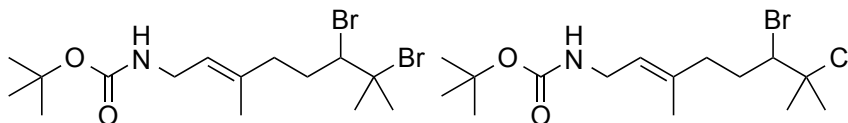
Compound **3.39d** was obtained as a colourless oil (1.1 mg, 5%). **<sup>1</sup>H NMR** (600 MHz,  $CDCl_3$ )  $\delta$  9.08 (br s, 1H), 6.97 (m, 1H), 6.85 (m, 1H), 6.26 (m, 1H), 4.61 (dd,  $J$  = 12.1, 4.4 Hz, 1H), 4.53 (dd,  $J$  = 12.2, 3.33 Hz, 1H), 4.32 (t,  $J$  = 2.7 Hz, 1H), 2.46 (dddd,  $J$  = 14.4, 13.9, 3.6, 2.8 Hz, 1H), 2.17 (ddd,  $J$  = 14.8, 13.4, 4.1 Hz, 1H), 1.89 (dd,  $J$  = 4.4, 3.6 Hz, 1H), 1.85 (dddd,  $J$  = 14.9, 7.9, 4.0, 3.1 Hz, 1H), 1.53 (m, 1H), 1.36 (s, 3H), 1.29 (s, 3H), 1.18 (s, 3H); **<sup>13</sup>C NMR** (150 MHz,  $CDCl_3$ )  $\delta$  158.0, 123.4, 122.6, 115.2, 110.6, 72.1, 70.1, 62.3, 47.1, 38.8, 36.1, 32.4, 31.1, 27.8, 23.3; **IR** (neat)  $cm^{-1}$  3230, 2965, 2923, 1684, 1410, 1194, 763; **HRMS** (ESI)  $m/z$   $[M+Na^+]$  calcd for  $C_{15}H_{22}^{79}BrNO_3Na$  366.0681, found 366.0677.

**Reaction with pyrrole-terpene substrate 3.40**

A solution of BDSB (37.2 mg, 0.068 mmol) in  $MeNO_2$  (1.5 mL) was added quickly via syringe to a solution of **3.39** (15.6 mg, 0.062 mmol) in a mixture of  $MeNO_2$  (1.5 mL) and  $CH_2Cl_2$  (3.0 mL) at  $-40^\circ C$ . The reaction was allowed to warm up to  $-15^\circ C$  over a period of 1 h and further stirred at  $-15^\circ C$  for 30 min before the reaction mixture was quenched by the addition of 5% aqueous  $NaHCO_3$ : 5% aqueous  $Na_2SO_3$  (1:1 v/v, 5 mL), stirred for 10 min, poured into water (5 mL), and extracted with  $CH_2Cl_2$  ( $3 \times 8$  mL). The combined organic layers were then dried with  $MgSO_4$ , concentrated, and purified by flash column chromatography ( $SiO_2$ , 2.5-22.5% EtOAc in Pet ether) give the products in the amounts and yields as indicated.



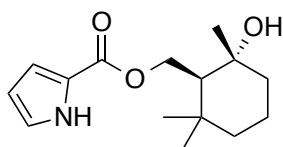
***tert*-butyl (*E*)-(6,7-dibromo-3,7-dimethyloct-2-en-1-yl)carbamate (3.40a) and *tert*-butyl (*E*)-(6-bromo-7-chloro-3,7-dimethyloct-2-en-1-yl)carbamate (3.40b)**



Compound **3.40a** (14.1 mg, 55%) and **3.40b** (trace), isolated as a mixture, were obtained as a colourless oil.  $^1\text{H NMR}$  (600 MHz,  $\text{CDCl}_3$ )  $\delta$  5.27 (t,  $J = 6.7$  Hz, 1H), 4.45 (br s, 1H), 4.11(3.96) (d,  $J = 11.1$  Hz, 1H), 3.73 (br t, 2H), 2.53 (1H, m), 2.35 (m, 1H), 2.15 (m, 1H), 1.96(1.76) (s, 3H), 1.85 (m, 1H), 1.79 (s, 3H), 1.67(1.65) (s, 3H), 1.43 (s, 9H);  $^{13}\text{C NMR}$  (150 MHz,  $\text{CDCl}_3$ )  $\delta$  160.0, 140.9, 122.5, 79.5, 68.8, 65.7 (65.5), 38.5, 37.7(33.3), 35.5, 33.7(32.1), 29.8, 28.5, 28.2; **IR** (neat)  $\text{cm}^{-1}$  3359, 2976, 2921, 1701, 1365, 1151, 860, 765; **HRMS** (ESI)  $m/z$   $[\text{M}+\text{H}^+]$  calcd for  $\text{C}_{15}\text{H}_{28}^{79}\text{Br}_2\text{NO}_2$  412.0487, found 412.0484, calcd for  $\text{C}_{15}\text{H}_{28}^{79}\text{BrClNO}_2$  368.0992, found 368.1000.

### Reaction with methanesulfonic acid additive

**((1*S*,2*S*)-2-hydroxy-2,6,6-trimethylcyclohexyl)methyl 1*H*-pyrrole-2-carboxylate (3.41)**

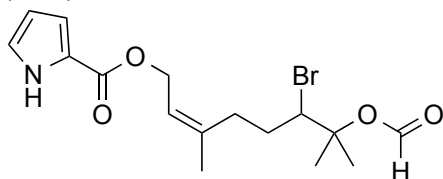


Methanesulfonic acid (60.1  $\mu\text{L}$ , 0.93 mmol) was added to a solution of **3.38** (15.2 mg, 0.062 mmol) in a mixture of  $\text{MeNO}_2$  (6.0 mL) and  $\text{CH}_2\text{Cl}_2$  (6.0 mL) at  $-40^\circ\text{C}$ . The reaction was allowed to warm up to  $-15^\circ\text{C}$  over a period of 1 h before the reaction mixture was quenched by the addition of saturated  $\text{NaHCO}_3$  (10 mL), stirred for 5 min, poured into water (6 mL), and extracted with  $\text{CH}_2\text{Cl}_2$  ( $3 \times 15$  mL). The combined organic layers were then dried with  $\text{MgSO}_4$ , concentrated, and purified by flash column chromatography ( $\text{SiO}_2$ , 2.5-30%  $\text{EtOAc}$  in  $\text{Pet ether}$ ) give **3.41** as a colourless oil (12.5 mg, 76%).  $^1\text{H NMR}$  (600 MHz,  $\text{CDCl}_3$ )  $\delta$  9.14 (br s, 1H), 6.95 (m, 1H), 6.84 (m, 1H), 6.24 (m, 1H), 4.54 (dd,  $J = 11.9, 8.17$  Hz, 2H), 1.81 (dddd,  $J = 15.5, 13.9, 3.4, 3.4$  Hz, 1H), 1.66 (m, 1H), 1.43 (m, 1H), 1.41 (m, 1H), 1.40 (m, 1H),

1.39 (m, 1H), 1.29 (s, 3H), 1.23 (ddd,  $J = 14.3, 14.3, 4.2$  Hz, 1H), 1.02 (s, 3H), 1.05 (s, 3H);  $^{13}\text{C}$  NMR (150 MHz,  $\text{CDCl}_3$ )  $\delta$  161.0, 123.0, 123.9, 115.1, 110.6, 72.2, 62.6, 52.6, 42.3, 41.6, 33.8, 32.4, 31.3, 22.3, 18.3; IR (neat)  $\text{cm}^{-1}$  3309, 2930, 1679, 1415, 1323, 1176, 1128, 746; HRMS (ESI)  $m/z$   $[\text{M}+\text{Na}^+]$  calcd for  $\text{C}_{15}\text{H}_{23}\text{NO}_3\text{Na}$  288.1576, found 288.1579.

### Reaction using DMF as co-solvent

#### (*Z*)-6-bromo-7-(formyloxy)-3,7-dimethyloct-2-en-1-yl 1*H*-pyrrole-2-carboxylate (3.42)



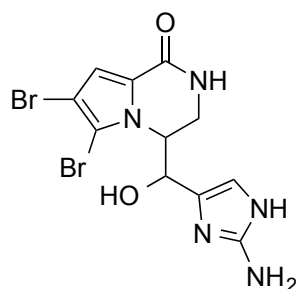
A solution of BDSB (50.8 mg, 0.093 mmol) in  $\text{MeNO}_2$  (1.5 mL) was added quickly via syringe to a solution of **3.38** (15.2 mg, 0.062 mmol) in a mixture of  $\text{MeNO}_2$  (1.5 mL) and DMF (9.0 mL) at  $-40$  °C. The reaction was allowed to warm up to  $-15$  °C over a period of 30 min before the reaction mixture was quenched by the addition of 5% aqueous  $\text{NaHCO}_3$ : 5% aqueous  $\text{Na}_2\text{SO}_3$  (1:1 v/v, 10 mL), stirred for 15 min, poured into water (6 mL), and extracted with  $\text{CH}_2\text{Cl}_2$  ( $3 \times 15$  mL). The combined organic layers were then dried with  $\text{MgSO}_4$ , concentrated, and purified by flash column chromatography ( $\text{SiO}_2$ , 2.5-17.5% EtOAc in Pet ether) to give **3.42** as a colourless oil (20.8 mg, 90%).  $^1\text{H}$  NMR (600 MHz,  $\text{CDCl}_3$ )  $\delta$  9.26 (br s, 1H), 7.93 (s, 1H), 6.92 (m, 1 H), 6.91 (m, 1H), 6.22 (m, 1H), 5.52 (t,  $J = 7.4$  Hz, 1H), 4.78 (ddd,  $J = 24.3, 12.4, 7.38$  Hz, 2H), 4.42 (dd,  $J = 11.5, 1.7$  Hz, 1H), 2.39 (m, 2H), 2.00 (m, 1H), 1.80 (m, 1H), 1.75 (s, 3H), 1.60 (s, 6H);  $^{13}\text{C}$  NMR (150 MHz,  $\text{CDCl}_3$ )  $\delta$  161.0, 160.0, 140.8, 122.9, 122.7, 121.3, 110.5, 84.5, 61.2, 60.6, 31.5, 30.4, 29.7, 24.6, 23.3, 23.1; IR (neat)  $\text{cm}^{-1}$  3309, 2926, 1720, 1682, 1412, 1304, 1162, 1123, 747; mass (EI)  $m/z$  371, 373  $[\text{M}^+]$ ; HRMS (EI)  $m/z$   $[\text{M}^+]$  calcd for  $\text{C}_{16}\text{H}_{22}^{79}\text{BrNO}_4$ , 371.0732, found 371.0730.

### 5.3.4. Application of BDSB to DHO (2.2) and oroidin (2.1)

#### Reaction with oroidin (2.1)

A solution of BDSB (23.3 mg, 0.042 mmol) in MeNO<sub>2</sub> (1.0 mL) was added quickly via syringe to a solution of **2.1** (15 mg, 0.039 mmol) in a mixture of MeNO<sub>2</sub> (0.5 mL) and DMF (1.5 mL) at −70 °C. The reaction was allowed to warm up to −40 °C over a period of 30 min and further warm up to −20 °C over 1 h before the reaction mixture was quenched by the addition of 5% aqueous NaHCO<sub>3</sub>: 5% aqueous Na<sub>2</sub>SO<sub>3</sub> (1:1 v/v, 3 mL), stirred for 15 min, and the reaction solution lyophilised. The crude was triturated with MeOH and the salt filtered off. The filtrate was evaporated to give a yellow solid which was purified by flash column chromatography (Alumina, 2.5–25% MeOH in CHCl<sub>3</sub>, saturated with NH<sub>3</sub>) to give dispacamide A (**2.16**) (8.3 mg, 49%) as a white solid and **3.45** (2.0 mg, 12%) as a yellow solid.

#### 4-((2-amino-1*H*-imidazol-4-yl)(hydroxy)methyl)-6,7-dibromo-3,4-dihydropyrrolo[1,2-*a*]pyrazin-1(2*H*)-one (**3.45**)



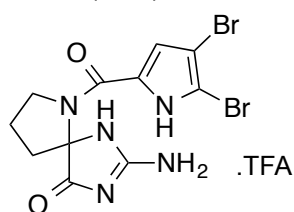
**<sup>1</sup>H NMR** (600 MHz, DMSO-*d*<sub>6</sub>) δ 8.03 (t, *J* = 5.8 Hz, 1H), 6.89 (s, 1H), 6.46 (s, 1H), 5.26 (br s, 2H), 4.04 (d, *J* = 4.6 Hz, 1H), 3.53 (dt, *J* = 8.6, 3.7 Hz, 1H), 3.46 (ddd, *J* = 13.8, 5.3, 4.2 Hz, 1H), 3.28 (dd, *J* = 14.0, 6.7 Hz, 1H); **<sup>13</sup>C NMR** (150 MHz, DMSO-*d*<sub>6</sub>) δ 159.3, 149.7, 128.7, 127.2, 113.7, 112.6, 104.9, 97.3, 81.3, 76.9, 39.2; **IR** (neat) cm<sup>−1</sup> 3311, 2929, 1682, 1635, 1561, 1541, 1416, 1113; **HRMS** (ESI) *m/z* [M+H<sup>+</sup>] calcd for C<sub>11</sub>H<sub>12</sub><sup>79</sup>Br<sub>2</sub>N<sub>5</sub>O<sub>2</sub> 403.9352, found 403.9357.

#### Reaction with DHO (2.2) with the isolation of a dimer

A solution of BDSB (42.1 mg, 0.077 mmol) in MeNO<sub>2</sub> (1.0 mL) was added via syringe to a solution of **2.1** (50.0 mg, 0.13 mmol) in a mixture of MeNO<sub>2</sub> (0.25 mL) and DMF (1.25 mL) at −70 °C over 30 min. The reaction was allowed to warm

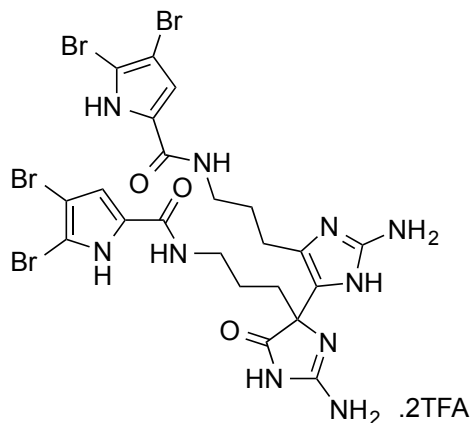
up to  $-20\text{ }^{\circ}\text{C}$  over a period of 1 h before the reaction mixture was quenched by the addition of 5% aqueous  $\text{NaHCO}_3$ : 5% aqueous  $\text{Na}_2\text{SO}_3$  (1:1 v/v, 3 mL), stirred for 15 min, and the reaction solution lyophilised. The crude was triturated with MeOH and the salt filtered off. The filtrate was evaporated to give a crude residue which was subjected to repeated HPLC purifications (Gemini, 10-40% ACN in  $\text{H}_2\text{O}$  with 0.05% TFA) to give dihydrodispacamide (**3.10**) (13.5 mg, 21%), dispacamide A (**2.16**) (11.6 mg, 18%) as white solids, oroidin (**2.1**) (1.0 mg, 3%) as a yellowish solid and other products in the amounts and yields as indicated below.

**2-amino-6-(4,5-dibromo-1H-pyrrole-2-carbonyl)-1,3,6-triazaspiro[4.4]non-2-en-4-one (3.43)**



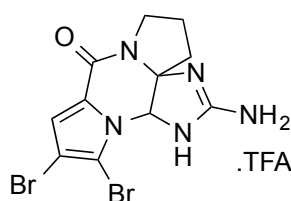
Compound **3.43** was obtained as a white solid (7.7 mg, 12%).  $^1\text{H NMR}$  (600 MHz,  $\text{DMSO}-d_6$ )  $\delta$  12.88 (s, 1H), 10.28 (br s, 1H), 6.82 (s, 1H), 9.30 (br s, 1H), 9.24 (br s, 1H), 6.96 (d,  $J = 2.52$  Hz, 1H), 3.88 (q,  $J = 6.5$  Hz, 1H), 3.80 (q,  $J = 7.7$  Hz, 1H), 2.18 (m, 2H), 2.12 (m, 2H);  $^{13}\text{C NMR}$  (150 MHz,  $\text{DMSO}-d_6$ )  $\delta$  173.3, 158.2, 157.5, 125.7, 116.3, 107.5, 98.9, 79.6, 48.7, 35.5, 23.5; **mass** (ESI)  $m/z$  404, 406, 408  $[\text{M}+\text{H}^+]$ ; **IR** (neat)  $\text{cm}^{-1}$  3377, 1710, 1679, 1436, 1417, 1203, 1139, 724.7; **HRMS** (ESI)  $m/z$   $[\text{M}+\text{H}^+]$  calcd for  $\text{C}_{11}\text{H}_{12}^{79}\text{Br}^{81}\text{BrN}_5\text{O}_2$  405.9332, found 405.9327.

**N,N'-((2,2'-diamino-5'-oxo-1',5'-dihydro-3H,4'H-[4,4'-biimidazole]-4',5'-diyl)bis(propane-3,1-diyl))bis(4,5-dibromo-1H-pyrrole-2-carboxamide) (3.46)**



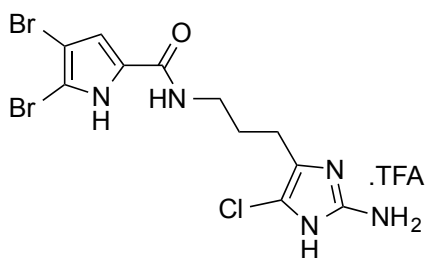
Compound **3.46** was obtained as a white powder (6.1 mg, 6%).  $^1\text{H}$  NMR (600 MHz, MeOD- $d_4$ )  $\delta$  6.85 (s, 1H), 6.82 (s, 1 H), 3.37 (m, 2H), 3.34 (m, 2H), 2.63 (m, 2H), 2.15 (br m, 2H), 1.82 (q,  $J$  = 7.08 Hz, 2H), 1.56 (br m, 2H);  $^{13}\text{C}$  NMR (150 MHz, MeOD- $d_4$ )  $\delta$  187.9, 162.9, 162.8, 148.9 (x2), 129.6, 129.4, 125.7, 121.4, 115.2, 115.1, 67.6, 40.5, 40.3, 35.4, 31.5, 25.7, 23.4; IR (neat)  $\text{cm}^{-1}$  3338, 1684, 1638, 1203, 1139, 725; mass (ESI)  $m/z$  793, 795, 797, 799, 801  $[\text{M}+\text{H}^+]$ ; HRMS (ESI)  $m/z$   $[\text{M}+\text{H}^+]$  calcd for  $\text{C}_{22}\text{H}_{25}^{79}\text{Br}_2^{81}\text{Br}_2\text{N}_{10}\text{O}_3$  796.8798, found 796.8803.

**2-amino-10,11-dibromo-1,5,6,12a-tetrahydro-4H,8H-imidazo[4,5-*b*]dipyrrolo[1,2-*a*:1',2'-*d*]pyrazin-8-one (2.54)**



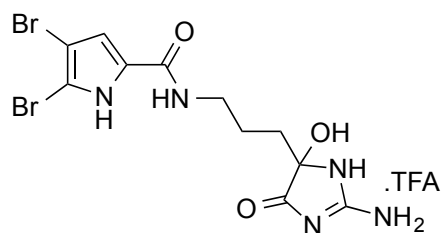
Compound **2.54** was obtained as a white solid (1.6 mg, 2.5%).  $^1\text{H}$  NMR (600 MHz, MeOD- $d_4$ )  $\delta$  6.94 (s, 1H), 5.92 (s, 1 H), 3.82 (m, 1H), 3.67 (m, 1H), 2.21 (m, 4H); mass (ESI)  $m/z$  388, 390, 392  $[\text{M}+\text{H}^+]$ ; HRMS (ESI)  $m/z$   $[\text{M}+\text{H}^+]$  calcd for  $\text{C}_{11}\text{H}_{12}^{79}\text{Br}^{81}\text{BrN}_5\text{O}$  389.9383, found 389.9387.

***N*-(3-(2-amino-5-chloro-1H-imidazol-4-yl)propyl)-4,5-dibromo-1H-pyrrole-2-carboxamide (3.49)**



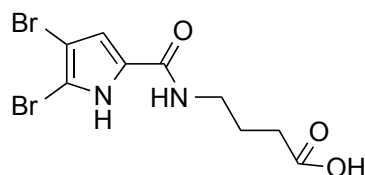
Compound **3.49** was obtained as a yellowish solid (5.3 mg, 8%).  $^1\text{H}$  NMR (600 MHz, MeOD- $d_4$ )  $\delta$  6.84 (s, 1H), 3.37 (t,  $J$  = 6.8 Hz, 2H), 2.58 (t,  $J$  = 7.4 Hz, 2H), 1.88 (quint,  $J$  = 7.1 Hz, 2H); mass (ESI)  $m/z$  424, 426, 428  $[\text{M}+\text{H}]^+$ ; HRMS (ESI)  $m/z$   $[\text{M}+\text{H}^+]$  calcd for  $\text{C}_{11}\text{H}_{13}^{79}\text{Br}^{81}\text{BrClN}_5\text{O}$  425.9149, found 423.9151.

***N*-(3-(2-amino-5-hydroxy-4-oxo-4,5-dihydro-1*H*-imidazol-5-yl)propyl)-4,5-dibromo-1*H*-pyrrole-2-carboxamide (3.15)**



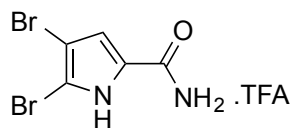
Compound **3.15** was obtained as a colourless solid (1.3 mg, 2%). **<sup>1</sup>H NMR** (600 MHz, MeOD-*d*<sub>4</sub>)  $\delta$  6.83 (s, 1H), 3.36 (m, 2H), 1.96 (t, *J* = 8.3 Hz, 2H), 1.71 (m, 1H), 1.58 (m, 1H); **mass** (ESI) *m/z* 424, 426, 428 [*M*+*H*<sup>+</sup>]; **HRMS** (ESI) *m/z* [*M*+*H*<sup>+</sup>] calcd for C<sub>11</sub>H<sub>14</sub><sup>79</sup>Br<sup>81</sup>BrN<sub>5</sub>O<sub>3</sub> 423.9437, found 423.9441.

**4-(4,5-dibromo-1*H*-pyrrole-2-carboxamido)butanoic acid (3.49)**



Compound **3.49** was obtained as a colourless solid (0.9 mg, 2%). **<sup>1</sup>H NMR** (600 MHz, MeOD-*d*<sub>4</sub>)  $\delta$  6.83 (s, 1H), 3.37 (t, *J* = 7.2 Hz, 2H), 2.38 (t, *J* = 7.4 Hz, 2H), 1.89 (quint, *J* = 7.1 Hz, 2H); **HRMS** (ESI) *m/z* [*M*+*H*<sup>+</sup>] calcd for C<sub>9</sub>H<sub>11</sub><sup>79</sup>Br<sup>81</sup>BrN<sub>2</sub>O<sub>3</sub> 354.9110, found 354.9114.

**4,5-dibromo-1*H*-pyrrole-2-carboxamide (3.48)**



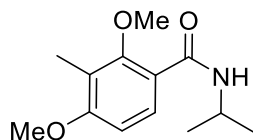
Compound **3.48** was obtained as a colourless oil (0.9 mg, 2%). **<sup>1</sup>H NMR** (600 MHz, MeOD-*d*<sub>4</sub>)  $\delta$  6.83 (s, 1H); **mass** (ESI) *m/z* 269 [*M*+*H*<sup>+</sup>].

NMR spectral data of **2.54**, **3.49**, **3.48** and **3.15** were as previously reported.<sup>6,10,11</sup>

## 5.4. Experimental for Chapter 4

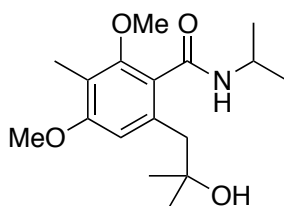
### 5.4.1. Synthesis of the Second Generation Epicocconone Analogue (4.2)

#### *N*-isopropyl-2,4-dimethoxy-3-methylbenzamide (4.30)



To a solution of dimethoxytoluene (22.8 g, 150 mmol) in  $\text{CH}_2\text{Cl}_2$  (200 mL) was slowly added aluminium trichloride (21.0 g, 158 mmol) at r.t. The mixture was allowed to stir for 10 min before the dropwise addition of isopropylisocyanate (17.7 mL, 188 mmol) at r.t. After 3h, the reaction was quenched at 0 °C with a 1 N solution of HCl (150 mL) and extracted with  $\text{CH}_2\text{Cl}_2$  ( $2 \times 150$  mL). The combined organic layer was washed with a 1 N solution of HCl followed by a saturated solution of  $\text{NaHCO}_3$ . The organic layer was dried over  $\text{MgSO}_4$  and concentrated under vacuum. The crude was purified by flash chromatography ( $\text{SiO}_2$ , 20 % EtOAc in cyclohexane) affording **4.30** (33.8 g; 95%) as a white solid.  $^1\text{H}$  NMR (400 MHz,  $\text{CDCl}_3$ )  $\delta$  7.94 (d,  $J = 8.8$  Hz, 1H), 7.68 (d,  $J = 5.6$  Hz, 1H), 6.72 (d,  $J = 8.7$  Hz, 1H), 4.26-4.37 (m, 1H), 3.86 (s, 3H), 3.73 (s, 3H), 2.15 (s, 3H), 1.25 (d,  $J = 6.5$  Hz, 6H), 1.25 (d,  $J = 6.5$  Hz, 6H).

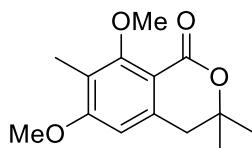
#### 6-(2-hydroxypropyl)-*N*-isopropyl-2,4-dimethoxy-3-methylbenzamide (4.31)



Tetramethylethylenediamine (15.0 mL, 100 mmol) was added to a solution of compound **4.30** (11.85 g, 50 mmol) in THF (200 mL) at r.t. The reaction mixture was cooled to -78 °C before the dropwise addition of *t*-BuLi (65 mL, 1.7 M in hexane). The solution was allowed to warm up to -15 °C and stirred for 30 min before being recooled to -78 °C after the formation of the characteristic red orthometallated intermediate. The 2,2-dimethyloxirane was then added dropwise at -78 °C and the reaction mixture was warmed to -10 °C and then allowed to warm slowly to rt over

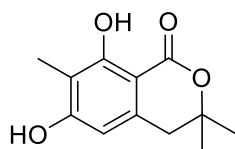
1.5 h. The reaction mixture was then quenched with H<sub>2</sub>O (250 mL) and extracted with EtOAc (3 × 200 mL). The combined organic layers were then washed with saturated NH<sub>4</sub>Cl followed by saturated NaHCO<sub>3</sub>. The organic layer was dried over MgSO<sub>4</sub> and concentrated under vacuum. The crude product was purified by flash chromatography (SiO<sub>2</sub>, 30% EtOAc in Cyclohexane) to give the desired compound **4.31** (10.0 g, 68%) as a cream solid. <sup>1</sup>H NMR (400 MHz, CDCl<sub>3</sub>) δ 6.48 (s, 1H), 6.26 (d, *J* = 7.4 Hz, 1H), 5.68 (s, 1H), 4.24-4.31 (m, 1H), 3.83 (s, 3H), 3.70 (s, 3H), 2.79 (s, 2H), 2.10 (s, 3H), 1.30 (s, 6H), 1.25 (d, *J* = 6.6 Hz, 6H).

#### 6,8-dimethoxy-3,3,7-trimethylisochroman-1-one (4.32)



Camphorsulfonic acid (11.7 g, 49.4 mmol) was added to a 400 mL toluene solution of **4.31** (12.1 g, 41.0 mmol) at r.t. The reaction mixture was refluxed for 2 h before being quenched at r.t. with saturated NaHCO<sub>3</sub> (200 mL) and extracted with EtOAc (3 × 150 mL). The organic layer was then washed with saturated NaHCO<sub>3</sub> and then with saturated NH<sub>4</sub>Cl. The organic layer was dried over MgSO<sub>4</sub> and concentrated under vacuum. The crude product was finally precipitated in cyclohexane to give the lactone **4.32** (9.75 g, 95%) as a cream powder. <sup>1</sup>H NMR (400 MHz, CDCl<sub>3</sub>) δ 6.40 (s, 1H) 3.82 (s, 3H), 3.76 (s, 3H), 2.86 (s, 2H), 2.07 (s, 3H), 1.34 (s, 6H).

#### 6,8-dihydroxy-3,3,7-trimethylisochroman-1-one (4.33)

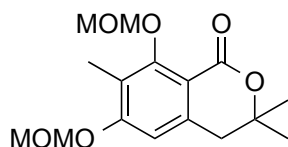


Aluminium trichloride (30.9 g, 220 mmol) was added at r.t. to a solution of **4.32** in CH<sub>2</sub>Cl<sub>2</sub>, which was then refluxed for 20 h. The reaction mixture was quenched at r.t. with 1 N HCl and extracted with EtOAc. The combined organic layer was then dried over MgSO<sub>4</sub> and concentrated under vacuum. The crude product was



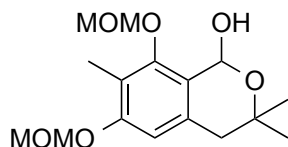
finally precipitated in 5 mL of  $\text{CH}_2\text{Cl}_2$  to give 4.80 g (98%) of compound **4.33**.  $^1\text{H}$  NMR (400 MHz,  $\text{CDCl}_3$ )  $\delta$  11.60 (s, 1H), 7.76 (s, 1H), 6.26 (s, 1H), 2.91 (s, 2H), 2.01 (s, 3H), 1.40 (s, 6H).

**6,8-bis(methoxymethoxy)-3,3,7-trimethylisochroman-1-one (4.34)**



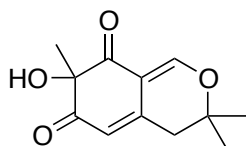
Under an inert atmosphere of argon, sodium hydride (2.78 g, 110 mmol; 95% grade) and MOM-Cl (65 mL, 137.3 mmol; 2.1 M in toluene) were added at r.t. to a 250 mL THF solution of compound **4.33** (6.11 g, 27.5 mmol). After 2 h, the reaction was quenched with saturated  $\text{NH}_4\text{Cl}$  (350 mL) and extracted with EtOAc ( $3 \times 250$  mL). The combined organic layers were then dried over  $\text{MgSO}_4$  and concentrated under vacuum. Compound **4.34** (8.53 g, 100 %) was obtained and used without further purification.

**6,8-bis(methoxymethoxy)-3,3,7-trimethylisochroman-1-ol (4.35)**



DIBAL-H (21.3 mL, 25.6 mmol, 1.2 M in toluene) was added to a solution of **4.34** (6.11 g, 19.7 mmol) in toluene (200 mL) at  $-78^\circ\text{C}$ . After 20 min, the reaction was quenched at  $0^\circ\text{C}$  with  $\text{H}_2\text{O}$  and extracted with EtOAc. The organic layer was then washed with HCl 1 N and then with a saturated solution of sodium chloride ( $\text{NaCl}$  sat.). The organic layer was dried over  $\text{MgSO}_4$  and concentrated under vacuum. Compound **4.35** (8.59 g, 100 %) was obtained and used without further purification.

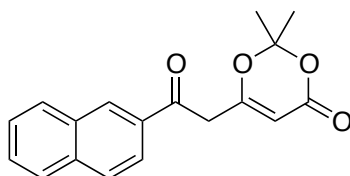
**7-hydroxy-3,3,7-trimethyl-3*H*-isochromene-6,8(4*H*,7*H*)-dione (4.36)**



To a solution of compound **4.35** (1.25 g, 4 mmol) in CH<sub>2</sub>Cl<sub>2</sub> (40 mL) at r.t., was added TFA (6.0 mL, 28 mmol), H<sub>2</sub>O (1.44 mL, 80 mmol) and IBX (2.24 g, 8 mmol). After 3 h at r.t, the reaction mixture was filtered to remove the IBX residue and the filtrate was evaporated under vacuum to give the crude which was purified by flash chromatography (SiO<sub>2</sub>, 20-60% EtOAc in pentane) affording **4.36** (498 mg; 56%) as a pale cream solid. <sup>1</sup>H NMR (400 MHz, CDCl<sub>3</sub>) δ 7.75 (s, 1H), 5.78 (s, 1H), 4.05 (br s, 1H), 2.66 (s, 2H), 1.49 (s, 3H), 1.36 (s, 6H).

NMR spectral data of **4.30-4.36** were as previously reported.<sup>12</sup>

**2,2-dimethyl-6-(2-(naphthalen-2-yl)-2-oxoethyl)-4*H*-1,3-dioxin-4-one (4.37)**

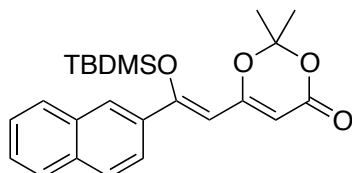


Prior to being used, the commercially available 2,2,6-trimethyl-4*H*-1,3-dioxin-4-one was purified by flash chromatography (SiO<sub>2</sub>, 5-50% EtOAc in cyclohexane) to give a golden yellow oil.

Oxalyl chloride (5.23 mL, 58.9 mmol) was added dropwise to a suspension of 2-naphthoic acid (5.07 g, 29.4 mmol) in CH<sub>2</sub>Cl<sub>2</sub> (100 mL), followed by the addition of 10 drops of DMF (catalytic amount). The reaction mixture was stirred at r.t. for 3 h until a further addition of a drop of DMF show no bubble of gas formed. The solution was evaporated under vacuum and the crude 2-naphthoyl chloride **4.38** was used in the next step without purification.

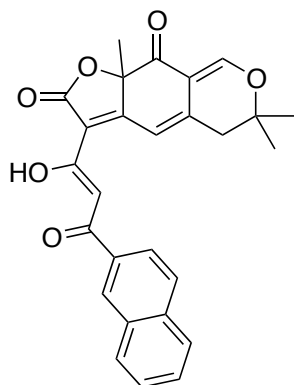
A solution of *n*-BuLi (24.7 mL, 61.7 mmol, 2.5 M in hexane) was added dropwise to a solution of DIPA (8.26 mL, 58.8 mmol) in THF (300 mL) at  $-78\text{ }^{\circ}\text{C}$ . The mixture was allowed to warm up to  $0\text{ }^{\circ}\text{C}$  and stirred at this temperature for 30 min before being cooled back to  $-78\text{ }^{\circ}\text{C}$  and 2,2,6-trimethyl-4*H*-1,3-dioxin-4-one (7.81 mL, 58.8 mmol) added. After another 30 min at  $-78\text{ }^{\circ}\text{C}$ , the crude 2-naphthoyl chloride (5.61 g, 29.4 mmol) dissolved in THF (40 mL) was finally added. The reaction mixture was allowed to warm up to  $-40\text{ }^{\circ}\text{C}$  and stirred at this temperature for 2 h. It was then quenched at  $0\text{ }^{\circ}\text{C}$  with 1 N HCl and extracted twice with EtOAc. The combined organic layers were dried over  $\text{MgSO}_4$  and concentrated under vacuum to give the crude product was a reddish gum. The desired product was finally precipitated using a 1:10 mixture of  $\text{Et}_2\text{O}$ /pentane (first  $\text{Et}_2\text{O}$  and then pentane) to give the desired dioxinone **4.37** (6.53 g, 75%) as an orange solid.  $^1\text{H NMR}$  (400 MHz,  $\text{CDCl}_3$ )  $\delta$  8.45 (s, 1H), 7.89-8.01 (m, 4H), 7.57-7.68 (m, 2H), 5.48 (s, 1H), 4.04 (s, 2H), 1.72 (s, 6H).

**(*Z*)-6-(2-((*tert*-butyldimethylsilyl)oxy)-2-(naphthalen-2-yl)vinyl)-2,2-dimethyl-4*H*-1,3-dioxin-4-one (4.39)**



To a solution of the dioxinone **4.37** (2.00 g, 6.7 mmol) in  $\text{CH}_2\text{Cl}_2$  (60 mL) at r.t., was added DIEA (3.5 mL, 20.1 mmol) followed by *t*-butyldimethylsilyl triflate (TBSOTf) (2.3 mL, 10.1 mmol). After 2 h, the reaction was quenched at r.t. with saturated  $\text{NaHCO}_3$  and extracted with of EtOAc ( $3 \times 50\text{ mL}$ ). The combined organic layers were washed with saturated  $\text{NH}_4\text{Cl}$ , dried over  $\text{MgSO}_4$  and then concentrated under vacuum. The crude product was purified through a short pad of silica (20-50% EtOAc in cyclohexane) to give the silylated dioxinone (1.03 g, 45%).  $^1\text{H NMR}$  (400 MHz,  $\text{CDCl}_3$ )  $\delta$  7.99 (s, 1H), 7.82-7.87 (m, 3H), 7.52-7.60 (m, 3H), 5.92 (s, 1H), 5.60 (s, 1H), 1.74 (s, 6H), 1.03 (s, 9H), 0.02 (s, 6H).

**(Z)-3-(1-hydroxy-3-(naphthalen-2-yl)-3-oxoprop-1-en-1-yl)-6,6,9a-trimethyl-5,6-dihydro-2H-furo[3,2-g]isochromene-2,9(9aH)-dione (4.2)**

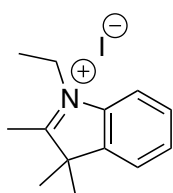


TEA (0.34 mL, 2.43 mmol), dioxinone **4.39** (980 mg, 2.19 mmol) and 4Å molecular sieves (250 mg per mmol) were added to a solution of the alcohol **4.36** (270 mg, 1.21 mmol) in toluene (40 mL) at r.t. The reaction mixture was heated at 100°C. After 3 h, the reaction was quenched at r.t. with 1N HCl and extracted with EtOAc (2 × 40 mL). The combined organic layers were then dried over MgSO<sub>4</sub> and concentrated under vacuum. The crude was purified by flash chromatography (SiO<sub>2</sub>, 30-80% EtOAc in cyclohexane) to give a yellow gum which was dissolved in a minimum amount of CH<sub>2</sub>Cl<sub>2</sub> then precipitated with cyclohexane to give the desired product as a yellow powder (128.5 mg, 24%). <sup>1</sup>H NMR (400 MHz, CDCl<sub>3</sub>) δ 8.00 (d, *J* = 7.4 Hz, 2H), 7.76 (s, 1H), 7.55 (t, *J* = 7.2 Hz, 1H), 7.50 (s, 1H), 7.46 (t, *J* = 7.2 Hz, 2H), 7.11 (s, 1H), 2.78 (d, *J* = 16.6 Hz, 1H), 2.71 (d, *J* = 16.6 Hz, 1H), 1.73 (s, 3H), 1.46 (s, 3H), 1.40 (s, 3H).

NMR spectral data of **4.37**, **4.39** and **4.2** were as previously reported.<sup>12</sup>

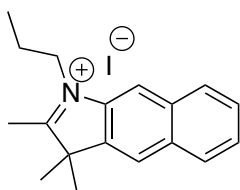
#### 5.4.2. Synthesis of the Hemicyanine Moieties

##### 1-ethyl-2,3,3-trimethyl-3H-indol-1-ium iodide (4.41)



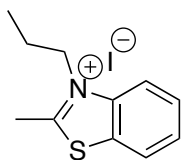
2,3,3-trimethyl-3H-indolenine (1 mL, 6.24 mmol) and iodoethane (1.2 g, 7.68 mmol) were refluxed in 2 mL dry toluene for 12 h. Upon cooling, a precipitate was formed and was filtered and the residue washed with diethyl ether and dried in vacuo to afford **4.41** as a pink solid (1.57 g, 80%).  $^1\text{H NMR}$  (300 MHz,  $\text{CDCl}_3$ )  $\delta$  1.60 (t,  $J$  = 7.5 Hz, 3H), 1.70 (s, 6H) 3.09 (s, 3H) 4.70, 4.74 (q,  $J$  = 7.5 Hz, 2H), 7.55-7.70 (m, 3H), 7.71 (d,  $J$  = 7.8 Hz, 1H).

#### 2,3,3-trimethyl-1-propyl-3H-benzo[*f*]indol-1-ium iodide (**4.42**)



2,3,3-trimethyl-3H-benzo[*f*]indole (300 mg, 1.44 mmol) was refluxed in iodoethane (10 mL) for 24 h. Upon cooling, a precipitate was formed. It was filtered off, washed with diethyl ether and dried in vacuo to afford **4.43** as a dark green solid (235.1 mg, 65%).  $^1\text{H NMR}$  (400 MHz,  $\text{CDCl}_3$ )  $\delta$  8.04 (d,  $J$  = 8.8 Hz, 1H), 8.03 (d,  $J$  = 8.4 Hz, 1H), 7.97 (d,  $J$  = 8.0 Hz, 1H), 7.79 (d,  $J$  = 8.8 Hz, 1H), 4.70 (t,  $J$  = 7.6 Hz, 1H), 3.14 (s, 3H), 2.02 (q,  $J$  = 7.6 Hz, 1H), 1.81 (s, 6H), 1.04 (t,  $J$  = 7.4 Hz, 1H).

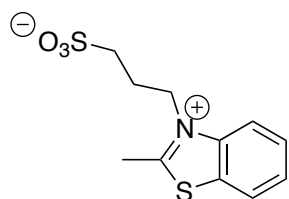
#### 2-methyl-3-propylbenzo[*d*]thiazol-3-ium iodide (**4.43**)



2-methylbenzothiazole (300 mg, 2.01 mmol) was refluxed with iodoethane (10 mL) for 24 h. Upon cooling, a precipitate was formed. It was filtered off, washed with diethyl ether and dried in vacuo to afford **4.43** as a pale grey solid (299.6 mg, 55%).  $^1\text{H NMR}$  (400 MHz,  $\text{CDCl}_3$ )  $\delta$  8.22 (d,  $J$  = 6.9 Hz, 1H), 7.99 (d,  $J$  = 8.4 Hz,

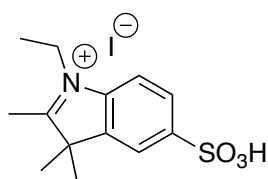
1H), 7.83 (t,  $J = 7.9$  Hz, 1H), 7.73 (t,  $J = 7.5$  Hz, 1H), 4.86 (t,  $J = 7.7$  Hz, 1H), 2.04 (q,  $J = 7.5$  Hz, 1H), 1.13 (t,  $J = 7.4$  Hz, 1H).

### 3-(2-methylbenzo[d]thiazol-3-ium-3-yl)propane-1-sulfonate (4.44)

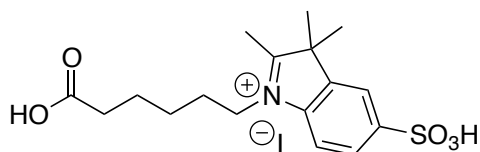


2-methylbenzothiazole (300 mg, 2.01 mmol) and propane sultone (491 mg, 4.02 mmol) were refluxed in 1,2-dichlorobenzene (15 mL) for 12 h. Upon cooling, a precipitate was formed and was filtered, and the residue washed with diethyl ether and dried in vacuo to afford **4.44** as a pale yellow solid (332 mg, 61%).  $^1\text{H NMR}$  (400 MHz,  $\text{CDCl}_3$ )  $\delta$  8.42 (d,  $J = 8.5$  Hz, 1H), 8.31 (d,  $J = 8.3$  Hz, 1H), 7.95 (dt,  $J = 7.9$ , 1.3 Hz, 1H), 7.84 (t,  $J = 7.6$  Hz, 1H), 5.04 (m, 2H), 3.28 (s, 3H), 3.07 (t,  $J = 6.4$  Hz, 2H), 2.14 (m, 2H).

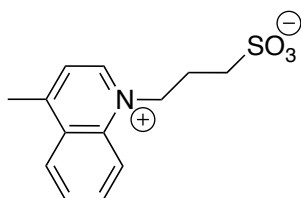
### 1-ethyl-2,3,3-trimethyl-5-sulfo-3*H*-indol-1-ium iodide (4.45)



Compound **4.45** was available in the laboratory from previous synthesis and used as obtained.

**1-(5-carboxypentyl)-2,3,3-trimethyl-5-sulfo-3*H*-indol-1-ium iodide (4.46)**

Compound **4.46** was available in the laboratory from previous synthesis and used as obtained.

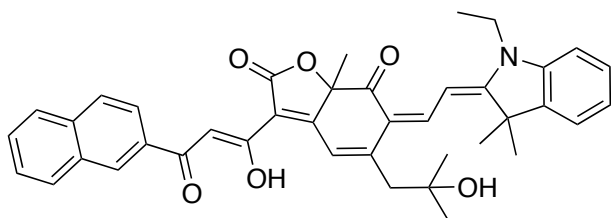
**3-(4-methylquinolin-1-ium-1-yl)propane-1-sulfonate (4.47)**

Lepidine (0.77 g, 5.35 mmol) was heated with propanesultone (0.625 g, 5.1 mmol) at 110 °C for 1.5 h. Upon cooling, the reaction mixture solidified. The solid was crushed and washed several times with diethyl ether, dried under vacuum to afford **4.47** as an off white solid (1.42 g, 90%). <sup>1</sup>H NMR (300 MHz, DMSO-*d*<sub>6</sub>) δ 9.39 (d, *J* = 6.0 Hz, 1H), 8.71 (d, *J* = 9.0 Hz, 1H), 8.55 (dd, *J* = 8.4, 1.2 Hz, 1H), 8.27 (ddd, *J* = 9.1, 7.0, 1.5 Hz, 1H), 8.06(m, 2H), 5.18 (t, *J* = 7.2 Hz, 2H), 3.01 (3H, s), 2.55 (t, *J* = 7.2 Hz, 2H), 2.28 (q, *J* = 7.2 Hz, 2H).

The NMR spectra of synthesised hemicyanines moities were as previously reported.<sup>13-</sup>

### 5.4.3. Synthesis of the Epicocconone-Hemicyanine Hybrids

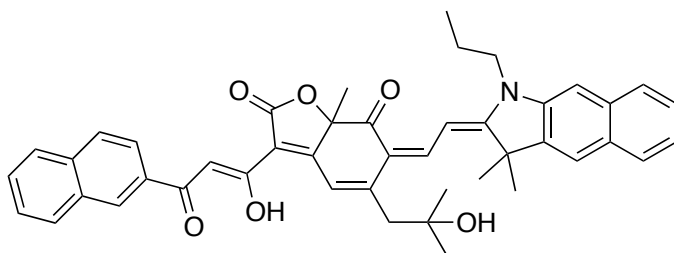
**(Z)-6-((E)-2-(1-ethyl-3,3-dimethylindolin-2-ylidene)ethylidene)-5-(2-hydroxy-2-methylpropyl)-3-((Z)-1-hydroxy-3-(naphthalen-2-yl)-3-oxoprop-1-en-1-yl)-7a-methylbenzofuran-2,7(6H,7aH)-dione (4.48)**



To **4.2** (6.8 mg, 0.015 mmol) in  $\text{CHCl}_3$  (0.8 mL), was added **4.41** (7.2 mg, 0.23 mmol) followed by TEA (68  $\mu\text{L}$ , 0.49 mmol). The reaction mixture was observed to turn reddish then purple or blue immediately upon or within minutes of the addition of TEA. The reaction mixture was allowed to stir at r.t. in the dark for 1 day. The solvent was removed on the rotary evaporator and the crude was purified by flash chromatography ( $\text{SiO}_2$ , 30-90% EtOAc in hexane) to give the hybrid (5 mg, 52%) as a dark blue solid.  $^1\text{H NMR}$  (600 MHz,  $\text{CDCl}_3$ )  $\delta$  8.56 (s, 1H), 8.11 (d,  $J$  = 13.5 Hz, 1H), 8.06 (dd,  $J$  = 8.6, 1.8 Hz, 1H), 7.98 (d,  $J$  = 7.8 Hz, 1H), 7.89 (d,  $J$  = 8.6 Hz, 1H), 7.86 (d,  $J$  = 7.9 Hz, 1H), 7.66 (s, 1H), 7.57 (m, 1H), 7.55 (m, 1H), 7.54 (d,  $J$  = 13.5 Hz, 1H), 7.32 (t,  $J$  = 7.6 Hz, 1H), 7.30 (d,  $J$  = 7.5 Hz, 1H), 7.13 (t,  $J$  = 7.4 Hz, 1H), 7.03 (s, 1H), 6.95 (d,  $J$  = 7.8 Hz, 1H), 3.95 (q,  $J$  = 7.3 Hz, 2H), 2.93 (d,  $J$  = 13.5 Hz, 1H), 2.76 (d,  $J$  = 13.5 Hz, 1H), 1.83 (s, 3H), 1.71 (s, 3H), 1.70 (s, 3H), 1.46 (s, 3H), 1.45 (s, 3H), 1.39 (t,  $J$  = 7.3 Hz, 3H);  $^{13}\text{C NMR}$  (150 MHz,  $\text{CDCl}_3$ )  $\delta$  195.4, 188.3, 176.9, 172.5, 171.1, 169.6, 154.1, 146.1, 142.3, 140.8, 135.5, 135.5, 133.4, 132.8, 129.6, 128.8, 128.4, 128.1, 127.8, 126.7, 123.7, 123.66, 122.1, 116.6, 114.9, 110.2, 109.1, 98.0, 96.7, 87.3, 72.1, 48.1, 47.3, 38.7, 31.2, 30.5, 29.6, 28.5, 28.3, 11.8; **IR** (neat)  $\text{cm}^{-1}$  2969, 2925, 1746, 1485, 1459, 1327, 1261, 1206, 1127; **mass** (ESI)  $m/z$  630  $[\text{M}+\text{H}^+]$ ; **HRMS** (ESI)  $m/z$   $[\text{M}+\text{H}^+]$  calcd for  $\text{C}_{40}\text{H}_{40}\text{NO}_6$  630.2856, found 630.2857.

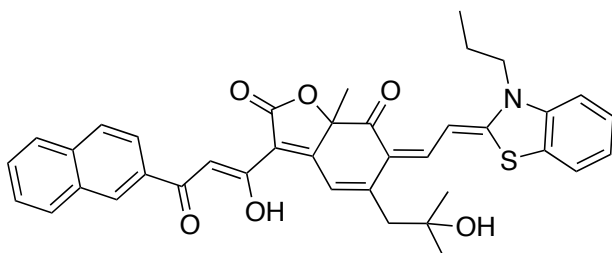


**(Z)-6-((E)-2-(3,3-dimethyl-1-propyl-1*H*-benzo[*f*]indol-2(3*H*)-ylidene)ethylidene)-5-(2-hydroxy-2-methylpropyl)-3-((Z)-1-hydroxy-3-(naphthalen-2-yl)-3-oxoprop-1-en-1-yl)-7a-methylbenzofuran-2,7(6*H*,7a*H*)-dione (4.49)**



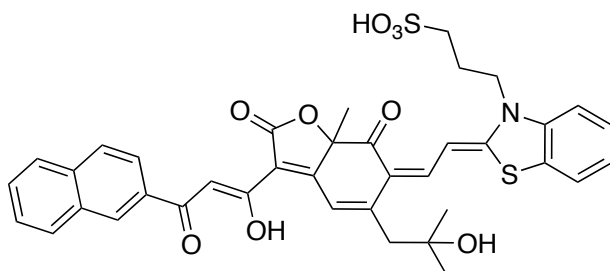
To **4.2** (15.4 mg, 0.035 mmol) in  $\text{CHCl}_3$  (1.7 mL), was added **4.42** (19.8 mg, 0.052 mmol) followed by TEA (156  $\mu\text{L}$ , 1.12 mmol). The reaction mixture was observed to turn reddish then purple or blue immediately upon or within minutes of the addition of TEA. The reaction mixture was allowed to stir at r.t. in the dark for 1 day. The solvent was removed on the rotary evaporator and the crude was purified by flash chromatography ( $\text{SiO}_2$ , 30-80% EtOAc in hexane) to give the hybrid (15 mg, 62%) as a dark blue solid.  $^1\text{H NMR}$  (600 MHz,  $\text{CDCl}_3$ )  $\delta$  8.54 (s, 1H), 8.10 (d,  $J = 8.44$  Hz, 1H), 8.05 (dd,  $J = 8.53, 1.74$  Hz, 1H), 8.25 (d,  $J = 13.9$  Hz, 1H), 7.96 (d,  $J = 7.74$  Hz, 1H), 7.88 (m, 1H), 7.87 (m, 1H), 7.84 (m, 1H), 7.66 (s, 1H), 7.62 (d,  $J = 13.7$  Hz, 1H), 7.56 (m, 1H), 7.55 (m, 1H), 7.52 (m, 1H), 7.85 (m, 1H), 7.40 (d,  $J = 7.38$  Hz, 1H), 7.24 (d,  $J = 8.49$  Hz, 1H), 7.03 (s, 1H), 3.98 (m, 2H), 2.98 (d,  $J = 13.5$  Hz, 1H), 2.80 (d,  $J = 13.4$  Hz, 1H), 2.03 (s, 3H), 2.01 (s, 3H), 1.90 (q,  $J = 7.3$  Hz, 2H), 1.84 (s, 3H), 1.50 (s, 3H), 1.49 (s, 3H), 1.07 (t,  $J = 7.4$  Hz, 3H);  $^{13}\text{C NMR}$  (150 MHz,  $\text{CDCl}_3$ )  $\delta$  195.7, 187.9, 177.2, 175.1, 171.3, 169.6, 154.6, 145.7, 140.0, 135.4, 133.4, 133.3, 132.69, 132.64, 131.3, 130.2, 130.0, 129.6, 128.7, 128.3, 128.0, 127.7, 127.5, 126.6, 124.3, 123.7, 121.9, 116.1, 114.6, 110.2, 109.6, 97.9, 96.5, 87.3, 72.1, 50.1, 47.4, 45.4, 31.2, 30.5, 29.8, 28.0, 27.9, 20.6, 11.5; **IR** (neat)  $\text{cm}^{-1}$  2968, 2927, 1739, 1450, 1255, 1193, 1126, 940; **mass** (ESI)  $m/z$  694  $[\text{M}+\text{H}^+]$ ; **HRMS** (ESI)  $m/z$   $[\text{M}+\text{H}^+]$  calcd for  $\text{C}_{45}\text{H}_{44}\text{NO}_6$  694.3169, found 694.3165.

**(Z)-5-(2-hydroxy-2-methylpropyl)-3-((Z)-1-hydroxy-3-(naphthalen-2-yl)-3-oxoprop-1-en-1-yl)-7a-methyl-6-((Z)-2-(3-propylbenzo[d]thiazol-2(3H)-ylidene)ethylidene)benzofuran-2,7(6H,7aH)-dione (4.50)**



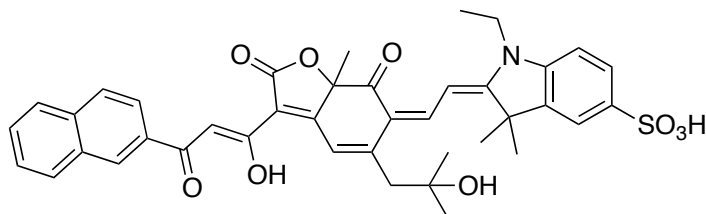
To **4.2** (18.6 mg, 0.042 mmol) in  $\text{CHCl}_3$  (2.1 mL), was added **4.43** (20.2 mg, 0.063 mmol) followed by TEA (188  $\mu\text{L}$ , 1.35 mmol). The reaction mixture was observed to turn reddish then purple or blue immediately upon or within minutes of the addition of TEA. The reaction mixture was allowed to stir at r.t. in the dark for 1 day. The solvent was removed on the rotary evaporator and the crude was purified by preparative TLC ( $\text{SiO}_2$ , 80% EtOAc in cyclohexane) to give the hybrid (16 mg, 60%) as a dark blue solid.  $^1\text{H NMR}$  (600 MHz,  $\text{CDCl}_3$ )  $\delta$  8.52 (s, 1H), 8.03 (d,  $J = 8.65$  Hz, 1H), 7.95 (d,  $J = 7.98$  Hz, 1H), 7.86 (d,  $J = 8.65$  Hz, 1H), 7.84 (d,  $J = 7.91$  Hz, 1H), 7.75 (d,  $J = 13.0$  Hz, 1H), 7.63 (d,  $J = 13.0$  Hz, 1H), 7.60 (s, 1H), 7.54 (m, 1H), 7.51 (m, 1H), 7.40 (m, 1H), 7.36 (m, 1H), 7.22 (d,  $J = 7.54$  Hz, 1H), 7.09 (d,  $J = 7.69$  Hz, 1H), 6.96 (s, 1H), 4.07 (br s, 2H), 2.95 (d,  $J = 13.5$  Hz, 1H), 2.77 (d,  $J = 13.4$  Hz, 1H), 1.77 (s, 3H), 1.43 (s, 3H), 1.42 (s, 3H), 1.07 (t,  $J = 15.6$  Hz, 3H);  $^{13}\text{C NMR}$  (150 MHz,  $\text{CDCl}_3$ )  $\delta$  195.2, 187.5, 177.5, 171.8, 169.7, 166.4, 155.0, 145.4, 141.6, 135.4, 133.3, 132.7, 129.6, 128.3, 128.0, 127.7, 127.6, 126.6, 125.2, 124.5, 123.7, 122.2, 114.5, 113.7, 111.8, 109.1, 96.9, 96.4, 71.9, 48.1, 47.5, 31.0, 30.6, 30.2, 20.8, 11.5; **IR** (neat)  $\text{cm}^{-1}$  2968, 2927, 1735, 1526, 1452, 1201, 1129, 825, 696; **mass** (ESI)  $m/z$  634  $[\text{M}+\text{H}^+]$ ; **HRMS** (ESI)  $m/z$   $[\text{M}+\text{H}^+]$  calcd for  $\text{C}_{38}\text{H}_{36}\text{NO}_6\text{S}$  634.2263, found 634.2268.

**3-((*Z*)-2-((*Z*)-2-(5-(2-hydroxy-2-methylpropyl)-3-((*Z*)-1-hydroxy-3-(naphthalen-2-yl)-3-oxoprop-1-en-1-yl)-7a-methyl-2,7-dioxo-7,7a-dihydrobenzofuran-6(2*H*)-ylidene)ethylidene)benzo[*d*]thiazol-3(2*H*)-yl)propane-1-sulfonic acid (4.51)**



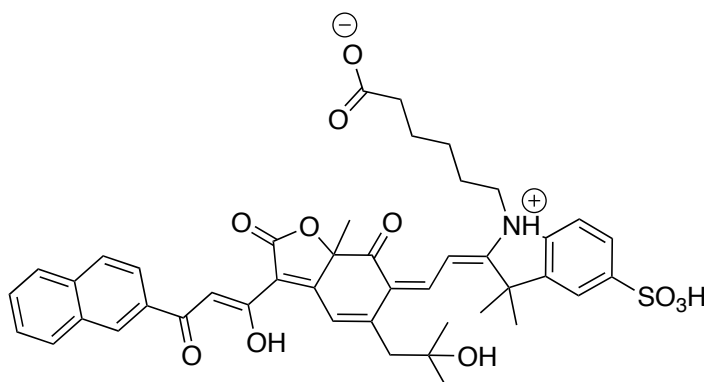
To **4.2** (15.5 mg, 0.035 mmol) in DMSO (1.8 mL), was added **4.44** (14.3 mg, 0.053 mmol) followed by TEA (156  $\mu$ L, 1.12 mmol). The reaction mixture was observed to turn reddish then purple or blue immediately upon or within minutes of the addition of TEA. The reaction mixture was allowed to stir at r.t. in the dark for 2 day. The solvent was removed by freeze-drying and the crude was purified by preparative HPLC (Econosphere, 10-40% ACN in distilled H<sub>2</sub>O) to give the hybrid (8 mg, 32%) as a dark blue solid. **<sup>1</sup>H NMR** (600 MHz, DMSO-*d*<sub>6</sub>)  $\delta$  8.53 (s, 1H), 8.15 (d, *J* = 7.86 Hz, 1H), 8.06 (d, *J* = 8.70 Hz, 1H), 8.01 (m, 1H), 8.00 (m, 1H), 7.94 (d, *J* = 13.0 Hz, 1H), 7.92 (m, 1H), 7.91 (d, *J* = 8.94 Hz, 1H), 7.65 (m, 1H), 7.60 (d, *J* = 13.0 Hz), 7.49 (s, 1H), 7.59 (d, *J* = 8.65 Hz, 1H), 7.55 (t, *J* = 7.62 Hz, 1H), 7.49 (s, 1H), 7.40 (t, *J* = 7.50 Hz, 1H), 6.81 (s, 1H), 6.53 (s, 1H), 4.76 (s, 1H), 4.46 (m, 2H), 2.94 (d, *J* = 12.8 Hz, 1H), 2.66 (d, *J* = 12.8 Hz, 1H), 2.59 (m, 2H), 2.08 (q, *J* = 7.2 Hz, 2H), 1.70 (s, 3H), 1.29 (s, 3H), 1.27 (s, 3H); **<sup>13</sup>C NMR** (150 MHz, DMSO-*d*<sub>6</sub>)  $\delta$  195.0, 184.0, 179.7, 172.9, 169.5, 168.0, 159.6, 146.3, 141.7, 134.8, 132.5, 132.4, 129.5, 128.4, 128.4, 128.0, 127.7, 127.6, 127.0, 125.16, 125.14, 123.0, 122.9, 113.9, 113.8, 111.8, 105.1, 97.9, 95.0, 86.7, 70.3, 47.9, 47.7, 45.7, 31.1, 30.8, 30.1, 23.8; **IR** (neat)  $\text{cm}^{-1}$  3389, 1524, 1440, 1197, 1161, 1133, 1023, 818, 696; **mass** (ESI) *m/z* 714 [M+H<sup>+</sup>]; **HRMS** (ESI) *m/z* [M+H<sup>+</sup>] calcd for C<sub>38</sub>H<sub>36</sub>NO<sub>9</sub>S<sub>2</sub> 714.1832, found 714.1829.

**(*E*)-1-ethyl-2-((*Z*)-2-(5-(2-hydroxy-2-methylpropyl)-3-((*Z*)-1-hydroxy-3-(naphthalen-2-yl)-3-oxoprop-1-en-1-yl)-7a-methyl-2,7-dioxo-7,7a-dihydrobenzofuran-6(2*H*)-ylidene)ethylidene)-3,3-dimethylindoline-5-sulfonic acid (4.52)**



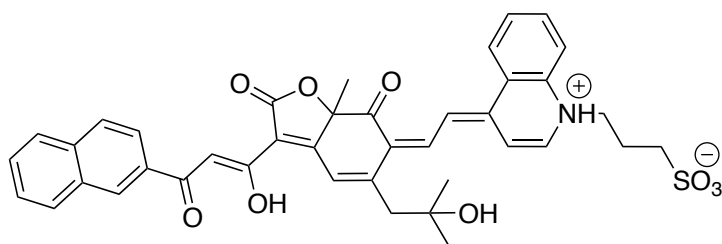
To **4.2** (19.3 mg, 0.044 mmol) in DMSO (2.2 mL), was added **4.45** (25.9 mg, 0.066 mmol) followed by TEA (195  $\mu$ L, 1.40 mmol). The reaction mixture was observed to turn reddish then purple or blue immediately upon or within minutes of the addition of TEA. The reaction mixture was allowed to stir at r.t. in the dark for 2 day. The solvent was removed by freeze-drying and the crude was purified by preparative HPLC (Econosphere, 10-40% ACN in distilled H<sub>2</sub>O) to give the hybrid (9 mg, 29%) as a dark blue solid. <sup>1</sup>H NMR (600 MHz, DMSO-*d*<sub>6</sub>)  $\delta$  8.55 (s, 1H), 8.20 (d, *J* = 14.0 Hz, 1H), 8.16 (d, *J* = 8.06 Hz, 1H), 8.07 (d, *J* = 9.04 Hz, 1H), 8.00 (d, *J* = 7.97 Hz, 1H), 7.93 (d, *J* = 8.55 Hz, 1H), 7.69 (s, 1H), 7.66 (m, 1H), 7.62 (t, *J* = 7.15 Hz, 1H), 7.61 (m, 1H), 7.26 (d, *J* = 8.22 Hz, 1H), 7.50 (s, 1H), 7.40 (d, *J* = 14.0 Hz, 1H), 6.90 (s, 1H), 4.01 (br m, 2H), 2.88 (d, *J* = 13.2 Hz, 1H), 2.66 (d, *J* = 13.2 Hz, 1H), 1.74 (s, 3H), 1.67 (s, 6H), 1.34 (s, 3H), 1.30 (s, 3H), 1.16 (t, *J* = 7.3 Hz, 3H); <sup>13</sup>C NMR (150 MHz, DMSO-*d*<sub>6</sub>)  $\delta$  195.2, 185.1, 178.7, 173.6, 172.1, 169.4, 158.5, 147.5, 144.5, 141.9, 140.2, 134.9, 132.5, 132.4, 129.5, 128.8, 128.5, 127.8, 127.1, 126.1, 123.1, 119.7, 116.8, 113.4, 113.1, 109.3, 98.2, 95.4, 87.0, 70.6, 48.2, 47.5, 38.6, 31.5, 29.9, 29.85, 27.8, 27.5, 11.6; IR (neat) cm<sup>-1</sup> 3385, 2971, 1740, 1473, 1196, 1114, 1024; mass (ESI) *m/z* 710 [M+H<sup>+</sup>]; HRMS (ESI) *m/z* [M+H<sup>+</sup>] calcd for C<sub>40</sub>H<sub>40</sub>NO<sub>9</sub>S 710.2424, found 710.2427.

**6-((*E*)-2-((*Z*)-2-(5-(2-hydroxy-2-methylpropyl)-3-((*Z*)-1-hydroxy-3-(naphthalen-2-yl)-3-oxoprop-1-en-1-yl)-7a-methyl-2,7-dioxo-7,7a-dihydrobenzofuran-6(2*H*)-ylidene)ethylidene)-3,3-dimethyl-5-sulfoindolin-1-ium-1-yl)hexanoate (4.53)**



To **4.2** (27.8 mg, 0.063 mmol) in DMSO (3.1 mL), was added **4.46** (45.4 mg, 0.094 mmol) followed by TEA (280  $\mu$ L, 2.01 mmol). The reaction mixture was observed to turn reddish then purple or blue immediately upon or within minutes of the addition of TEA. The reaction mixture was allowed to stir at r.t. in the dark for 2 day. The solvent was removed by freeze-drying and the crude was purified by preparative HPLC (Econosphere, 10-40% ACN in distilled H<sub>2</sub>O) to give the hybrid (**6** mg, 12%) as a dark blue solid. **<sup>1</sup>H NMR** (400 MHz, DMSO-*d*<sub>6</sub>)  $\delta$  8.55 (s, 1H), 8.20 (d, *J* = 14.0 Hz, 1H), 8.16 (d, *J* = 7.67 Hz, 1H), 8.07 (m, 1H), 8.00 (m, 1H), 7.94 (m, 1H), 7.67 (m, 1H), 7.66 (m, 1H), 7.62 (m, 1H), 7.60 (m, 1H), 7.49 (s, 1H), 7.40 (d, *J* = 14.0 Hz, 1H), 7.25 (d, *J* = 8.33 Hz, 1H), 6.90 (s, 1H), 6.53 (s, 1H), 4.82 (s, 1H), 3.94 (m, 2H), 2.87 (d, *J* = 13.2 Hz, 1H), 2.65 (d, *J* = 13.2 Hz, 1H), 2.20 (t, *J* = 7.13 Hz, 2H), 1.74 (s, 3H), 1.73 (m, 2H), 1.67 (s, 6H), 1.56 (m, 2H), 1.39 (m, 2H), 1.34 (s, 3H), 1.30 (s, 3H); **<sup>13</sup>C NMR** (100 MHz, DMSO-*d*<sub>6</sub>)  $\delta$  197.1, 195.1, 185.2, 178.9, 174.4, 174.0, 172.3, 159.0, 147.4, 144.6, 142.3, 140.1, 134.9, 132.5, 132.4, 129.5, 128.8, 128.5, 127.7, 127.1, 126.0, 122.9, 119.5, 116.8, 113.3, 109.5, 106.6, 99.6, 95.4, 87.1, 70.6, 48.1, 47.5, 43.5, 33.6, 31.5, 29.9, 29.8, 27.9, 27.6, 26.2, 25.9, 24.2; **IR** (neat)  $\text{cm}^{-1}$  3382, 2973, 1719, 1473, 1458, 1258, 1115, 1024; **HRMS** (ESI) *m/z* [M-H<sup>+</sup>] calcd for C<sub>44</sub>H<sub>44</sub>NO<sub>11</sub>S 794.332, found 794.332.

**3-((*E*)-4-((*Z*)-2-(5-(2-hydroxy-2-methylpropyl)-3-((*Z*)-1-hydroxy-3-(naphthalen-2-yl)-3-oxoprop-1-en-1-yl)-7a-methyl-2,7-dioxo-7,7a-dihydrobenzofuran-6(2*H*)-ylidene)ethylidene)-1,4-dihydroquinolin-1-ium-1-yl)propane-1-sulfonate (4.54)**



To **4.2** (33.3 mg, 0.075 mmol) in DMSO (3.8 mL), was added **4.47** (30.0 mg, 0.11 mmol) followed by TEA (336  $\mu$ L, 2.41 mmol). The reaction mixture was observed to turn reddish then purple or blue immediately upon or within minutes of the addition of TEA. The reaction mixture was allowed to stir at r.t. in the dark for 2 day. The solvent was removed by freeze-drying and the crude was purified by preparative HPLC (Econosphere, 10-40% ACN in distilled H<sub>2</sub>O) to give the hybrid (8 mg, 15%) as a dark blue solid. Interpretable NMR data could not be unobtained. **IR** (neat)  $\text{cm}^{-1}$  3426, 2974, 1648, 1529, 1471, 1395, 1196, 1046; **Mass** (ESI)  $m/z$  708 [ $\text{M}+\text{H}^+$ ]; **HRMS** (ESI)  $m/z$  [ $\text{M}+\text{H}^+$ ] calcd for C<sub>40</sub>H<sub>38</sub>NO<sub>9</sub>S<sup>+</sup> 708.2265, found 708.2267.

#### 5.4.4. Determination of the Extinction Coefficient and Fluorescence Quantum Yield

Measurement of absorbance was conducted from 200 to 900 nm at 25 °C in a solution of acetonitrile using a CARY 1Bio UV-Visible spectrophotometer. The Beer-Lambert equation ( $A = \epsilon cl$ ) was used to calculate the extinction coefficient,  $\epsilon$  at a concentration where the absorbance,  $A$  is less than 1,  $c$  is concentration of fluorophore (M) and  $l$  path length (cm) of light through the sample.

Each of the hybrid dyes was scanned for its maximum excitation wavelength,  $\text{max } \lambda_{\text{ex}}$  and maximum emission wavelength,  $\text{max } \lambda_{\text{em}}$  to obtain its fluorescence spectrum using a LS50B fluorometer (Perkin Elmer).

For the recording of quantum yields, the comparative method of Williams<sup>17</sup> was chosen over that of Demas<sup>18</sup> mainly because the former takes into consideration

the presence of concentration effects such as self-quenching by working within a carefully chosen concentration range and acquiring data at a number of different absorbances (*i.e.* concentrations), thus ensuring linearity across the concentration range.

The relative quantum yields were measured at 25 °C in acetonitrile, using 1,1'-diethyl-4,4'-carbocyanine iodide ( $\Phi_F = 0.007$  in ethanol) as standard according to equation 1.

$$\text{Equation 1: } F_x = F_{\text{std}}(\text{Grad}_x/\text{Grad}_{\text{std}})(h_x/h_{\text{std}})^2$$

Where subscripts x and std denote sample and standard respectively, Grad refer to the gradient from a plot of integrated fluorescence intensity vs absorbance of a range of concentrations of the fluorophores that shows linearity,  $\eta$  = refractive index of solvents used ( $\eta = 1.3441$  for acetonitrile,  $\eta = 1.3614$  for ethanol and  $\eta = 1.4783$  for DMSO). Spectroscopic grade solvents were used.

#### 5.4.5. Investigation of the Hybrid Dyes as Fluorescent Probes

For fluorescent probes evaluation, the following solutions were prepared:

- (i) a solution of BSA of concentration 1000, 500, 250, 125, 62.5, 31, 15.6, 8, 4, 2, 1, 0.5  $\mu\text{g/mL}$
- (ii) a solution of dsDNA ( $\text{Na}^+$  salt from salmon testes) of concentration 10, 5, 2.5, 1.25, 0.625, 0.3125, 0.156, 0.0781, 0.0391, 0.0195, 0.0098, 0.0049, 0.0012, 0.0003, 0.0001  $\text{mg/mL}$ ,
- (iii) a solution of SDS of concentration 8, 4, 2, 1, 0.5, 0.25, 0.125, 0.0625, 0.0313, 0.0156 % (w/v)
- (iv) universal pH buffer solutions of pH 2-12, prepared using a solution of 0.04 M  $\text{H}_3\text{BO}_3$ , 0.04 M  $\text{H}_3\text{PO}_4$  and 0.04 M  $\text{CH}_3\text{COOH}$  that has been titrated to the desired pH with 0.2 M NaOH.<sup>19</sup>

Fluorescence readings were taken in 96-well plates using the fluorescence plate reader (Spectramax M5). The total volume of each well was 200  $\mu$ L. The concentrations of each dye used, is indicated in **Table 5.1**.

**Table 5.1** Concentration of hybrid dyes used in each test.

Hybrid dye	Conc. of dye tested against dsDNA, BSA and SDS/ $\mu$ M	Conc. of dye tested in buffer/ $\mu$ M
<b>4.48</b>	7.8	23
<b>4.49</b>	4.9	15
<b>4.50</b>	8.0	24
<b>4.51</b>	7.7	23
<b>4.52</b>	7.3	22
<b>4.53</b>	3.6	11
<b>4.54</b>	5.4	16

#### 5.4.6. Staining of 1D PAGE Gels

The epicocconone-hemicyanine hybrids (**4.48-4.53**) were dissolved in DMSO (1 mg/mL). A stock solution of BSA was made by dissolving 5.3 mg of BSA in 10 mL distilled water. The stock solution was serially diluted (2 $\times$ ) from 0.53 mg/mL to 5.2  $\mu$ g/mL. Seven 4-12% Bis-Tris Novex NuPAGE (Invitrogen NP0321BOX), 1 mm thick gels were loaded with the dilution series of BSA (5  $\mu$ L of each dilution) to obtain the amounts of 2650, 1325, 662.5, 331.3, 165.6, 82.8, 41.4, 20.7, 10.4, 5.2 ng per lane. The gels were run in Xcell SureLock minigel systems (Invitrogen, EI0001) at 240 V for approximately 45 min (buffer front just off gel) using MES buffer (50 mM MES, 50 mM Tris, 1 mM EDTA, 0.1% SDS, pH 7.3).

The gels were removed and fixed in 15% ethanol (v/v), 1% citric acid (100 mL) on a rocker for 1 h before the addition of fresh fixative overnight. The next day, the gels were placed into fresh fixative (100 mL) for 1 h, drained, then stained in 100 mM sodium borate buffer (50 mL; pH 10.9) containing one of the hybrids each (50



$\mu\text{L}$  of a 1 mg/mL solution in DMSO). These concentrations resulted in approximately 1  $\mu\text{g/mL}$  active dye in each staining solution. After 1 h staining the gels were de-stained in 15% ethanol (100 mL) for 30 min and transferred to fixative (100 mL; 15% ethanol (v/v), 1% citric acid (w/v)) for 30 min. All gels were imaged using a Typhoon Trio (GE, 63-0055-87) using the 633 nm red laser, 600 PMT, 100  $\mu\text{m}$  resolution and normal sensitivity.

The Typhoon scans were analysed using ImageJ and a Plot Profile was obtained across the main protein band stain (**Appendix 6.7.1**).

#### 5.4.7. Live Cell Imaging Using the NIR Hybrids

The human colon cancer cell line SW480 (Australian Proteomic Analysis Facility, Sydney, Australia) was cultured in Dulbecco's Modified Eagle Medium (DMEM, Gibco, NY, USA) containing 10% FBS and 1% Geneticin. Cultures were maintained at 37 °C under a humidified atmosphere containing 5% CO<sub>2</sub>.

The hybrid dyes were diluted in phenol red-free Dulbecco's Modified Eagle Medium (DMEM, Gibco, NY, USA) containing 10% FBS and 1% Geneticin for cell staining. For washing cells, Dulbecco's phosphate buffered saline (pH 7.4 $\pm$ 0.2; Gibco, NY, USA) was used. For fixing cells, 2% formaldehyde (Sigma-Aldrich, Sydney, Australia) in Dulbecco's PBS was used.

Fluorescent images were acquired on a FV1000 confocal laser-scanning microscope (Carl Zeiss Co., Ltd.) with an objective lens (up to  $\times 40$ ). Prior to imaging, the medium was removed. Cell imaging was carried out after washing cells with PBS for three times before being view in fresh PBS.

For the epicocconone-hemicyanine dye, the excitation wavelength used was 633 nm (Alexa Fluor-633 laser) and emission wavelength scanned from 690-790 nm. In the co-staining studies, up to 3 channels were used at any one time, the excitation wavelengths used to view the co-stains were based on the recommended excitation and emission wavelengths as follows (Ex/Em nm): 350/461 Hoechst, 504/511 ER-Tracker Green, 470/516 MitoTracker Green, 577/590 LysoTracker Red, 553/570 CM-

DiI. The final concentrations of the co-stains used were as follows: Hoechst 2 µg/mL, ER-Tracker 200 nM, LysoTracker 70 nM, MitoTracker 70 nM and CM-DiI 2 µM.

## 5.5. References

- (1) Davioud, E.; Petit, A.; Tate, M. E.; Ryder, M. H.; Tempé, J. *Phytochemistry* **1988**, *27*, 2429-2433.
- (2) Isogai, A.; Fukuchi, N.; Hayashi, M.; Kamada, H.; Harada, H.; Suzuki, A. *Phytochemistry* **1990**, *29*, 3131-3134.
- (3) [http://www.graphpad.com/guides/prism/6/curve-fitting/index.htm?reg\\_gaddumschild.htm](http://www.graphpad.com/guides/prism/6/curve-fitting/index.htm?reg_gaddumschild.htm); Accessed: 01/08/2011.
- (4) Olofson, A.; Yakushijin, K.; Horne, D. A. *J. Org. Chem.* **1998**, *63*, 1248-1253.
- (5) Isbell, H. S.; Frush, H. L.; Holt, N. B. *J. Res. Natl. Bur. Stand., Sect. A* **1960**, *64A*, 135-136.
- (6) Moldovan, R. P.; Lindel, T. Z. *Naturforsch., B: Chem. Sci.* **2009**, *64*, 1612-1616.
- (7) Murray, R. W.; Sing, M. *Org. Synth.* **1997**, *74*, 91.
- (8) Chang, J. W. W.; Ton, T. M. U.; Tania, S.; Taylor, P. C.; Chan, P. W. H. *Chem. Commun.* **2010**, *46*, 922-924.
- (9) Snyder, S. A.; Treitler, D. S.; Brucks, A. P.; Gollner, A.; Chiriac, M. I.; Wright, N. E.; Pflueger, J. J.; Breazzano, S. P. Patent WO2012037069 A2, 2012.
- (10) Travert, N.; Al-Mourabit, A. *J. Am. Chem. Soc.* **2005**, *127*, 10454-10454.
- (11) Hewlett, N. M.; Tepe, J. J. *Org. Lett.* **2011**, *13*, 4550-4553.
- (12) Boulangé, A.; Peixoto, P. A.; Franck, X. *Chem. Eur. J.* **2011**, *17*, 10241-10245.
- (13) Constantin, T. P.; Silva, G. L.; Robertson, K. L.; Hamilton, T. P.; Fague, K.; Waggoner, A. S.; Armitage, B. A. *Org. Lett.* **2008**, *10*, 1561-1564.
- (14) Horiuchi, H.; Ishida, S.; Matsuzaki, K.; Tani, K.; Hashimoto, T.; Hotta, H.; Tsunoda, K.-i.; Kodaira, T.; Okutsu, T.; Hiratsuka, H. *J. Phys. Chem. C* **2011**, *115*, 6902-6909.
- (15) Park, J. W.; Kim, Y.; Lee, K.-J.; Kim, D. J. *Bioconjugate Chem.* **2012**, *23*, 350-362.
- (16) Tyler, A. R.; Okoh, A. O.; Lawrence, C. L.; Jones, V. C.; Moffatt, C.; Smith, R. B. *Eur. J. Med. Chem.* **2013**, *64*, 222-227.

- (17) Williams, A. T. R.; Winfield, S. A.; Miller, J. N. *Analyst* **1983**, 108, 1067-1071.
- (18) Demas, J. N. *J. Phys. Chem.* **1971**, 75, 991-1025.
- (19) Britton, H. T. S.; Robinson, R. A. *J. Chem. Soc., Chem. Commun.* **1931**, 1456-1462.



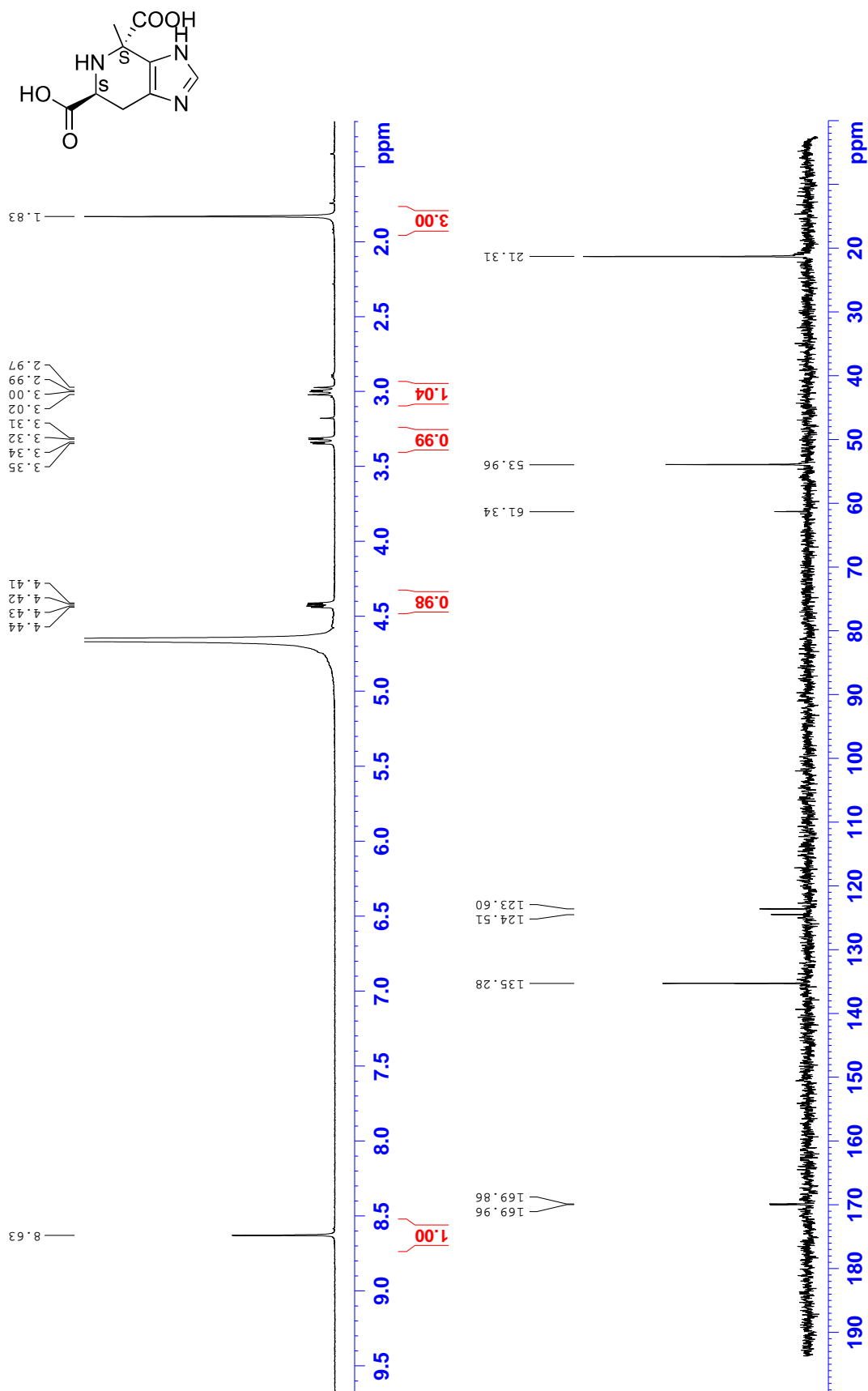
---

**CHAPTER 6**  
**APPENDICES**

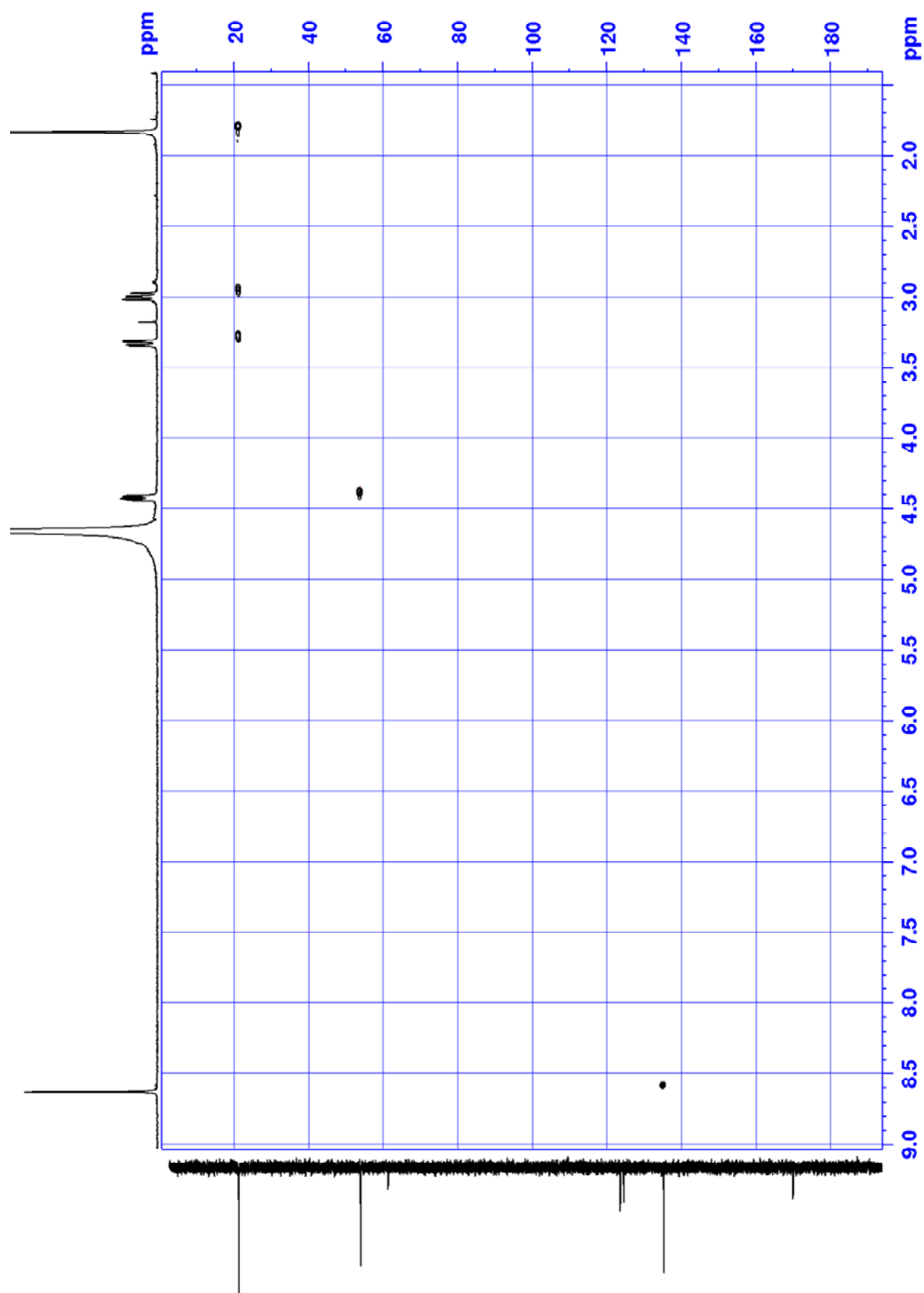
---

## 6.1. NMR Spectra of Newly Synthesised Compounds

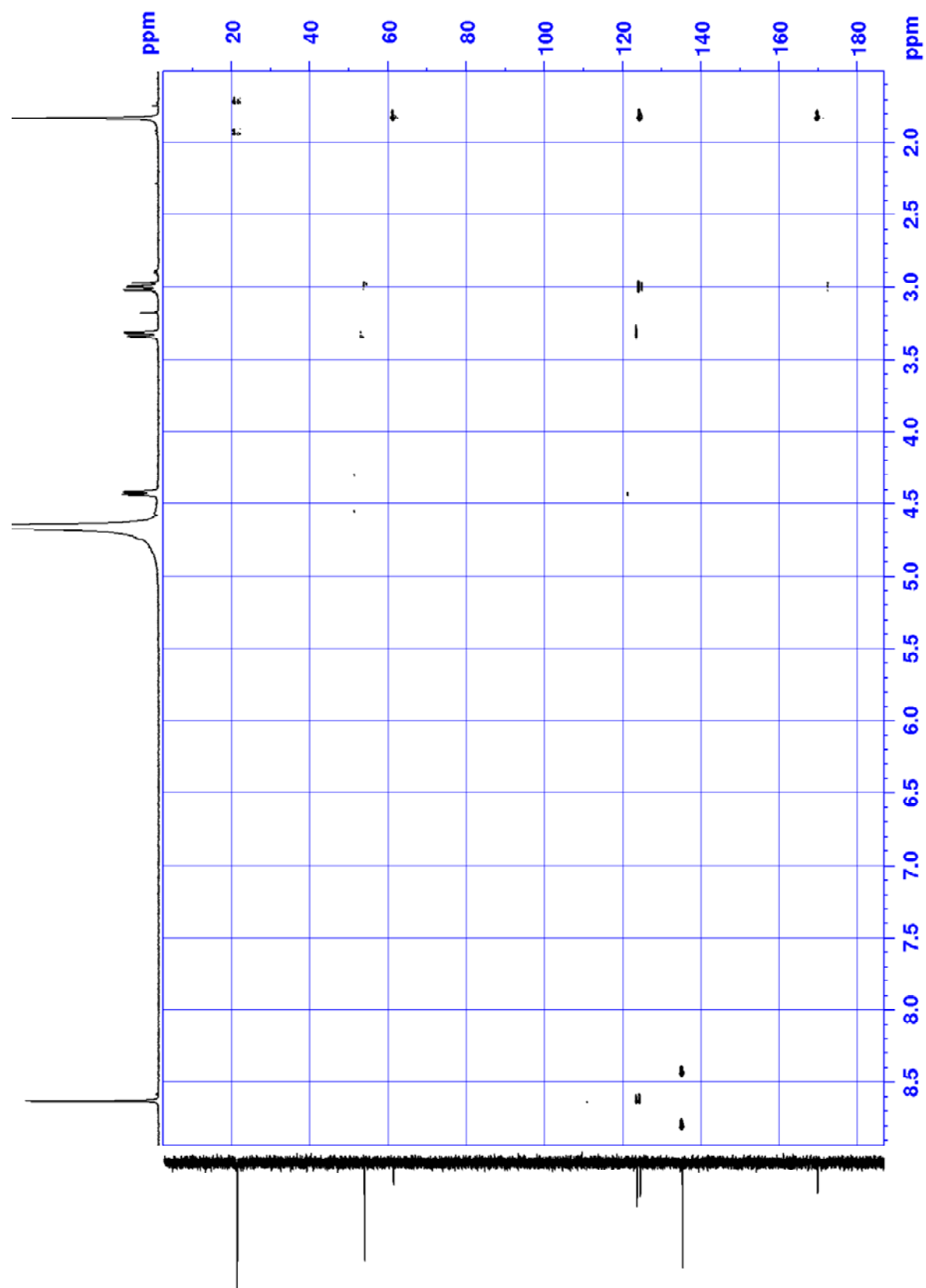
**((1S,3R,6R)-3-bromo-6-hydroxy-2,2,6-trimethylcyclohexyl)methyl 1H-pyrrole-2-carboxylate (1.8)**



HSQC (1.8)

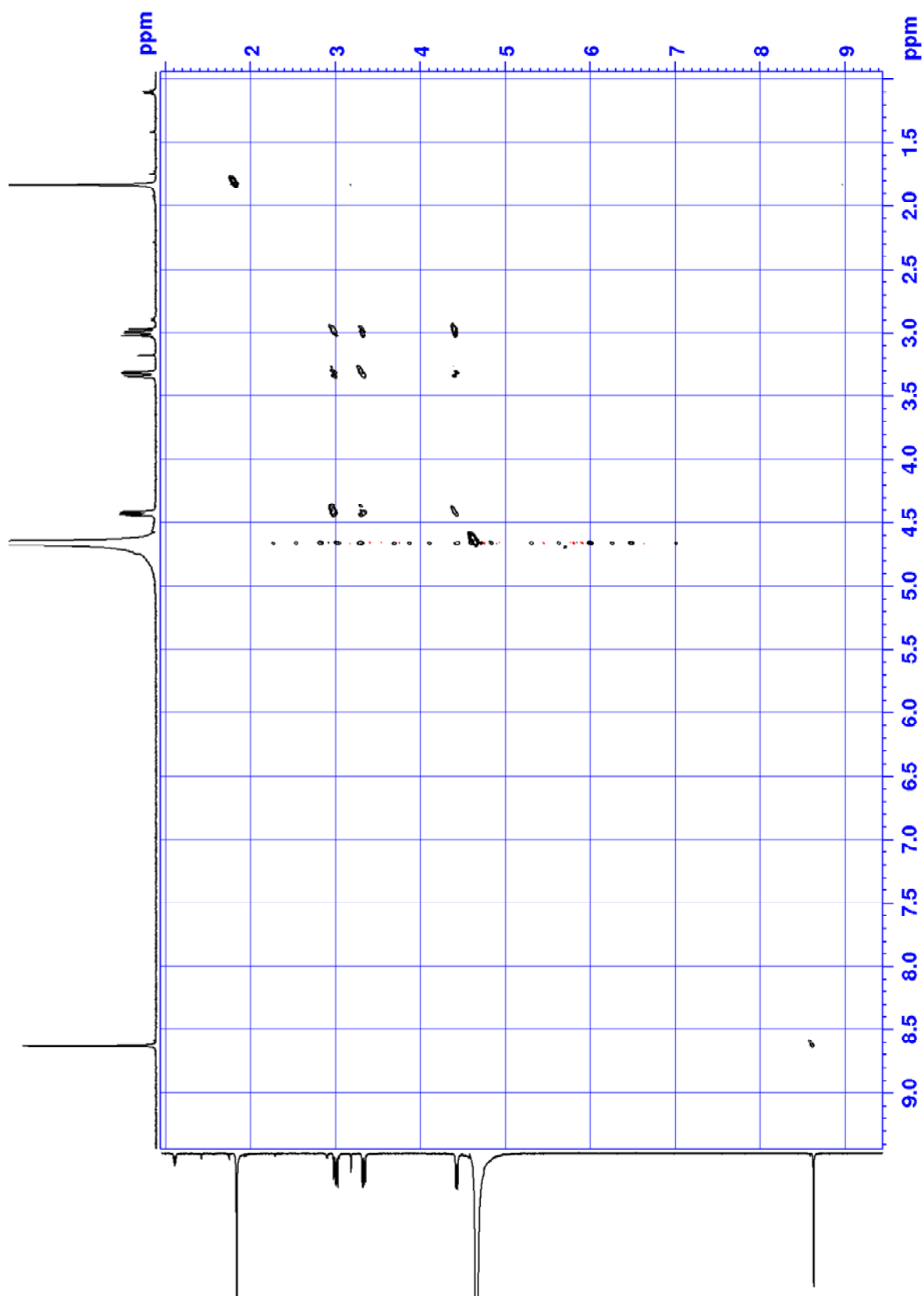


HMBC (1.8)

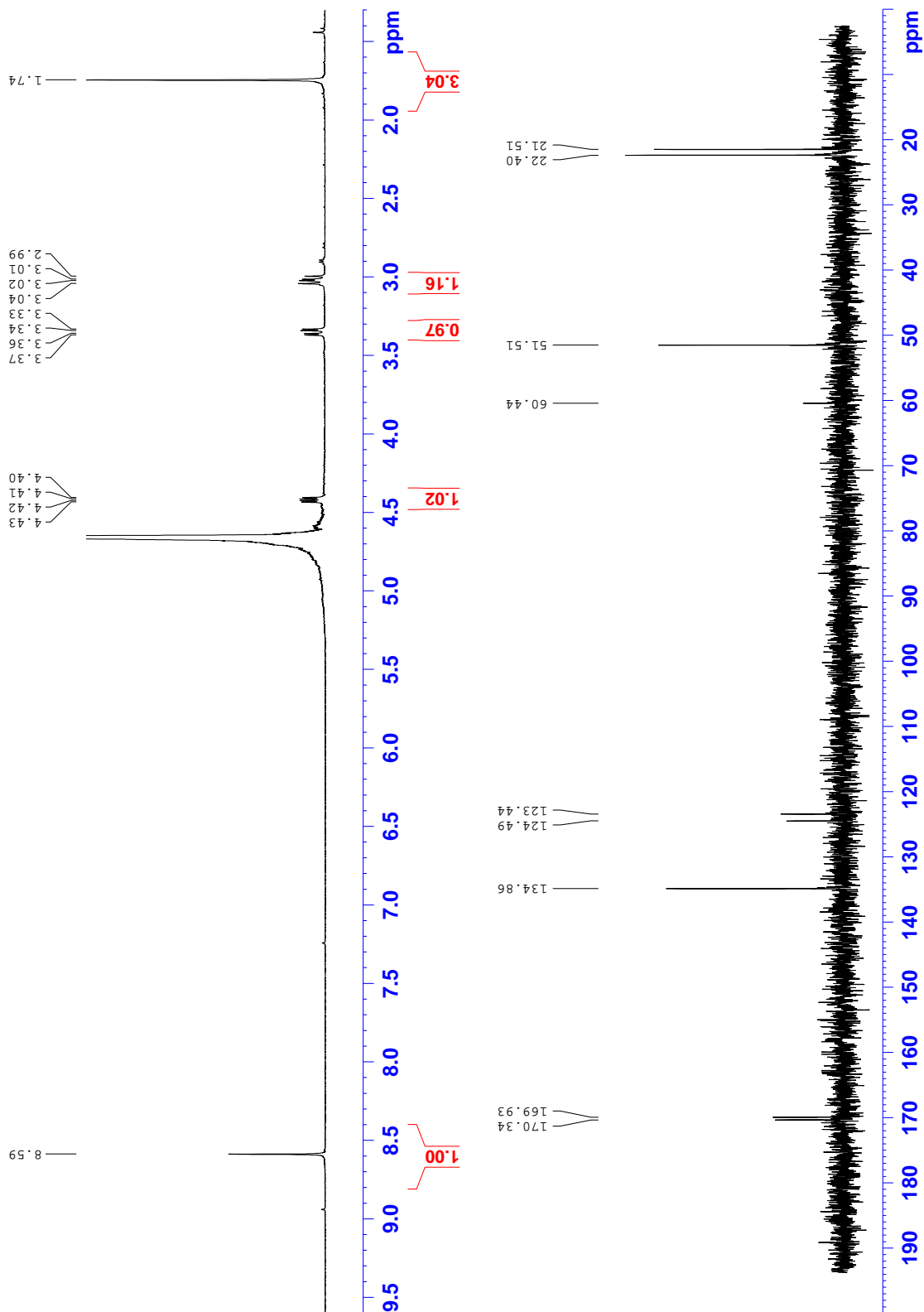
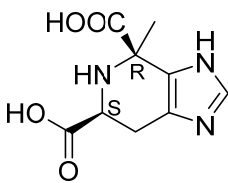


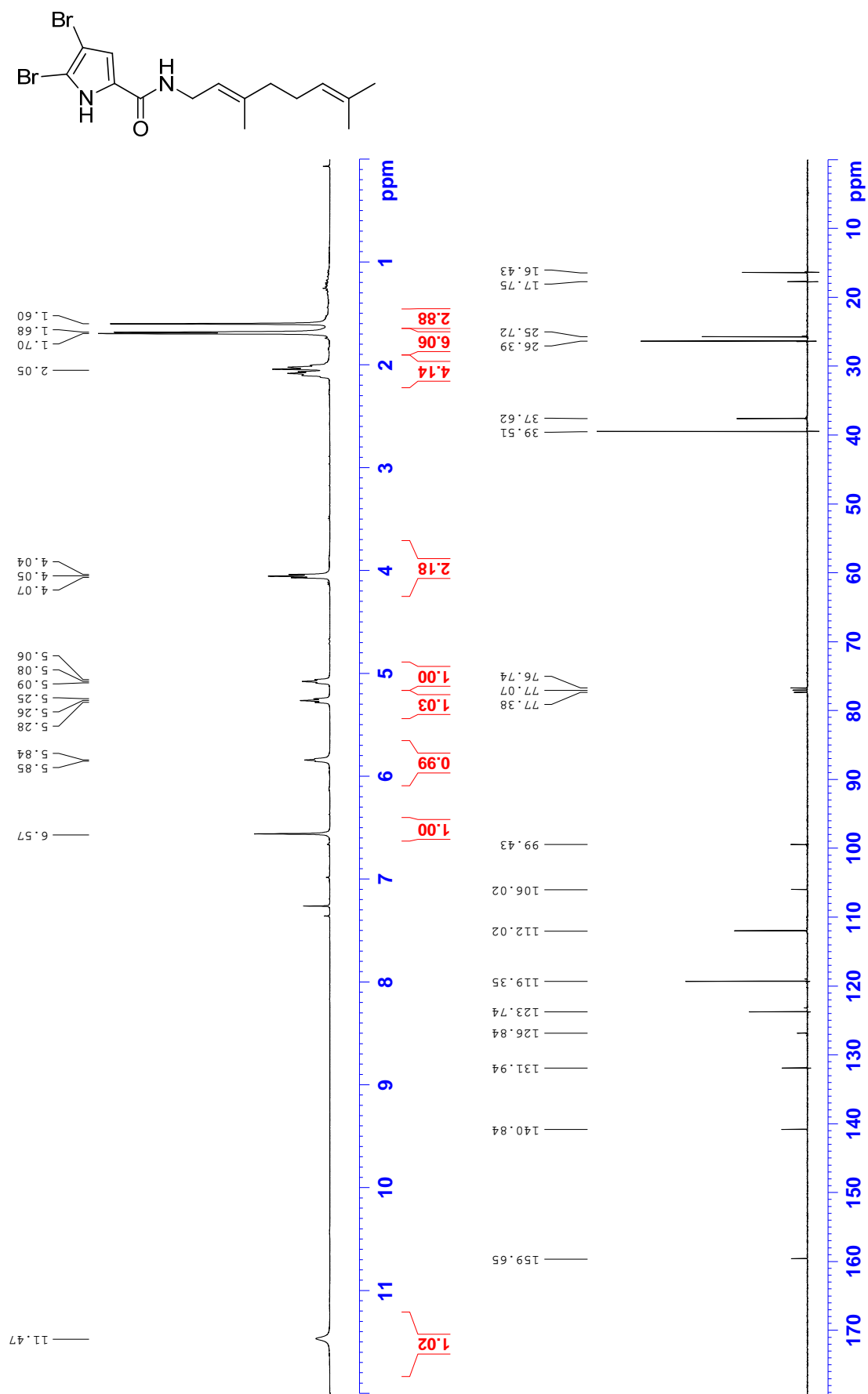


COSY (1.8)

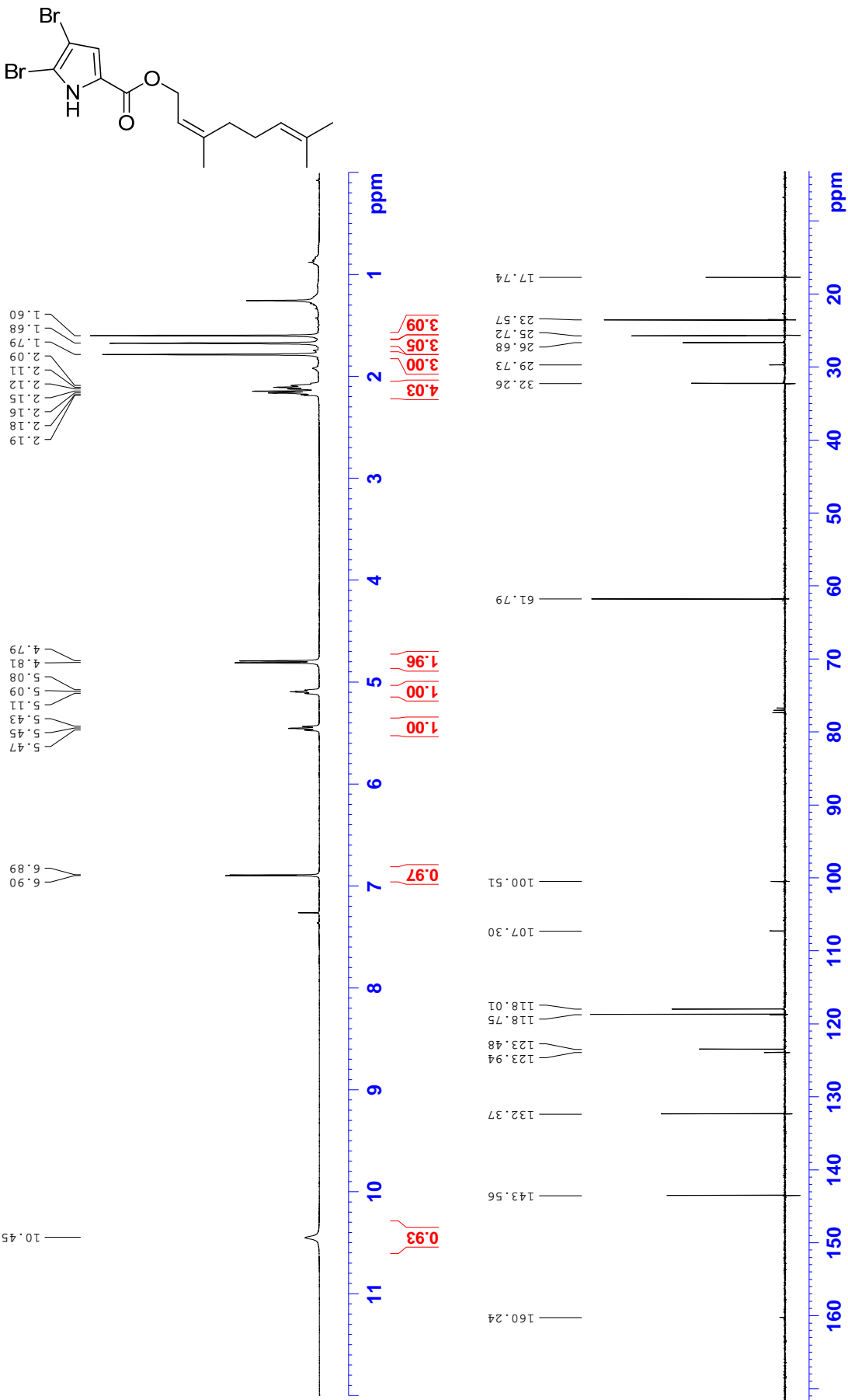


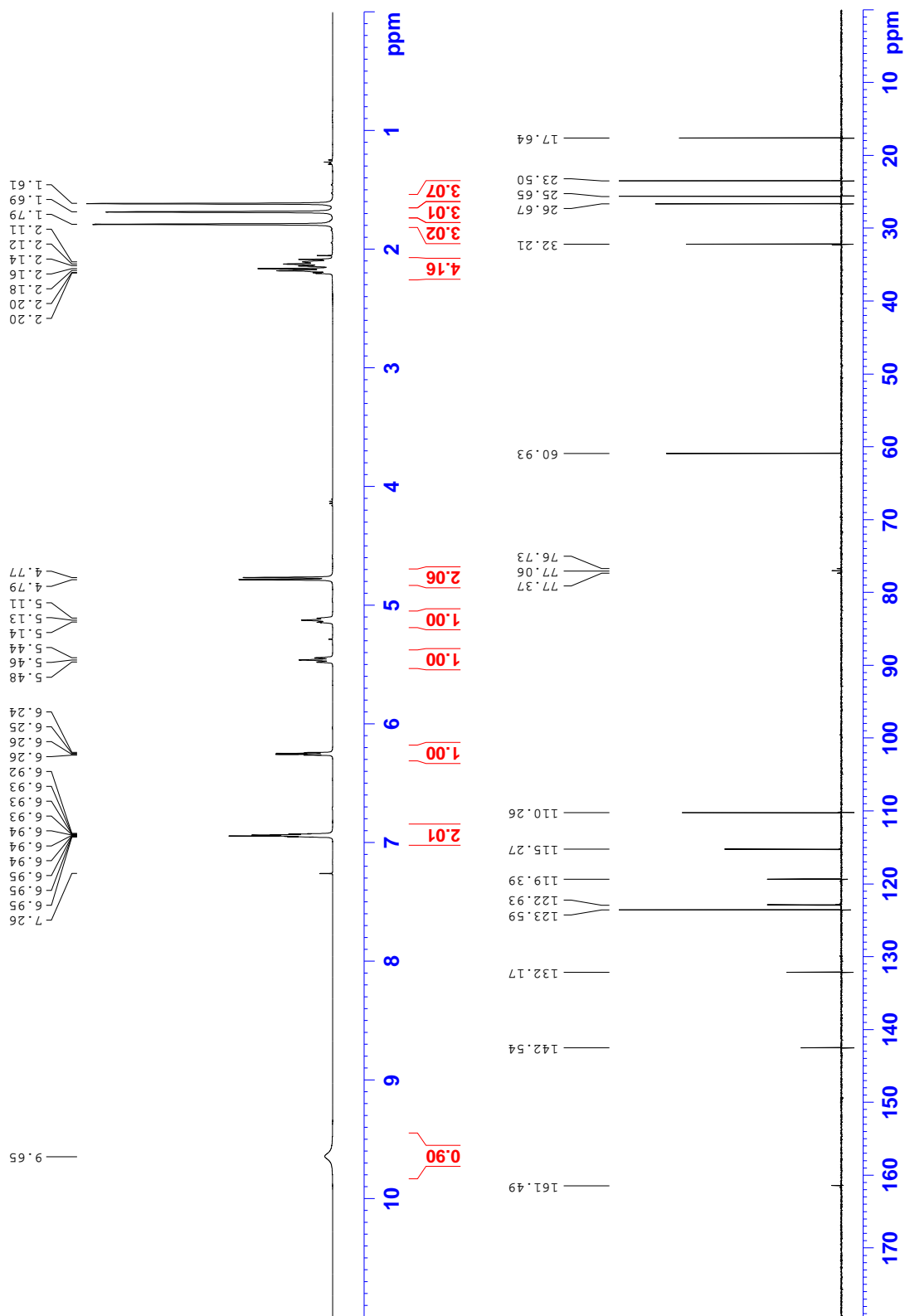
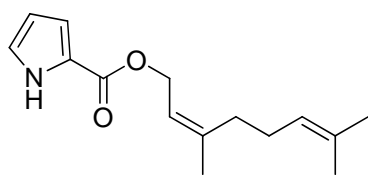
(4*R*,6*S*)-4-methyl-4,5,6,7-tetrahydro-3*H*-imidazo[4,5-*c*]pyridine-4,6-dicarboxylic acid (1.9)



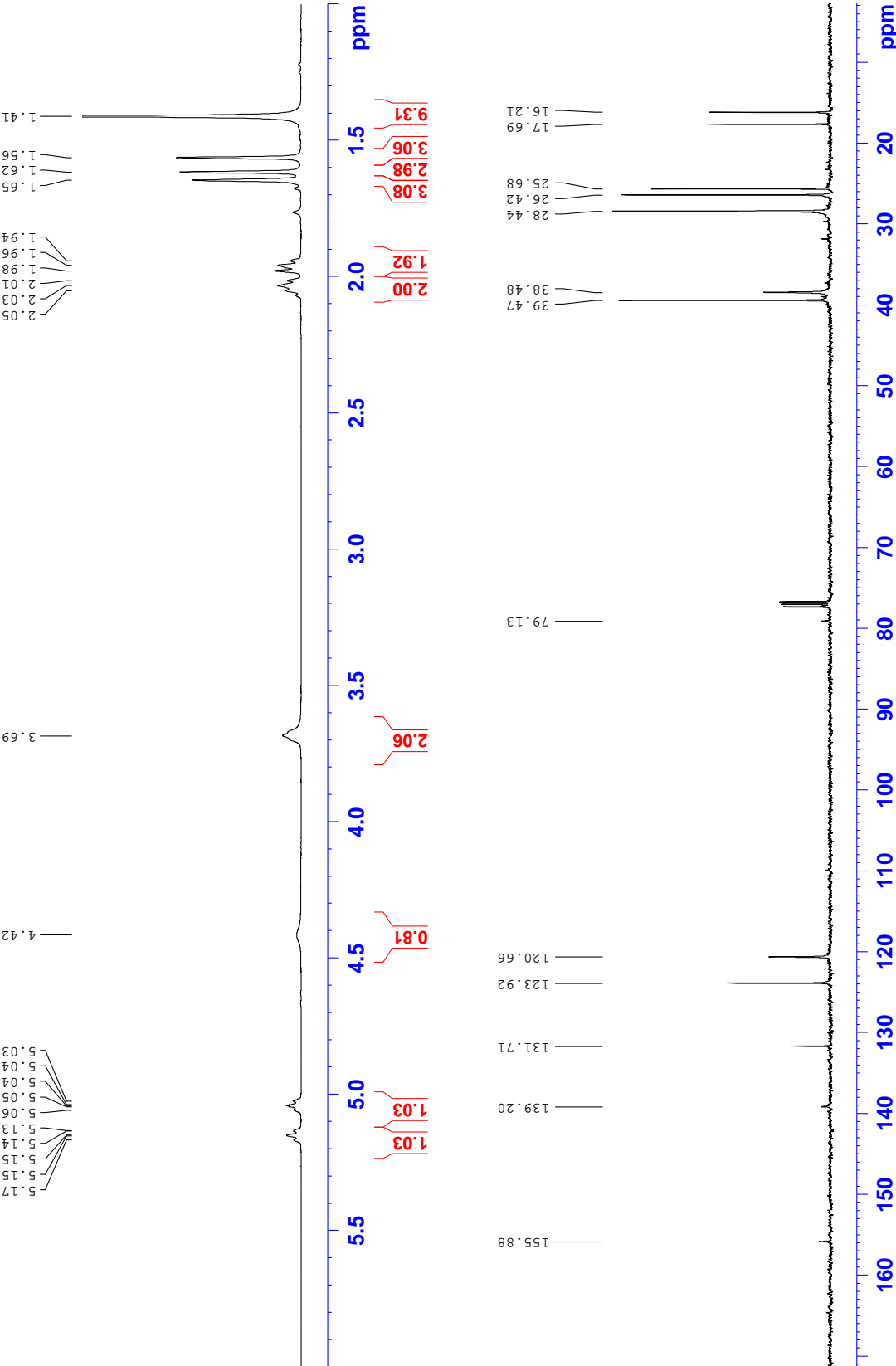
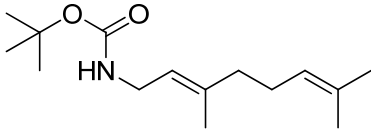
**(E)-4,5-dibromo-N-(3,7-dimethylocta-2,6-dien-1-yl)-1H-pyrrole-2-carboxamide (3.37)**

(Z)-3,7-dimethylocta-2,6-dien-1-yl 4,5-dibromo-1H-pyrrole-2-carboxylate (3.38)

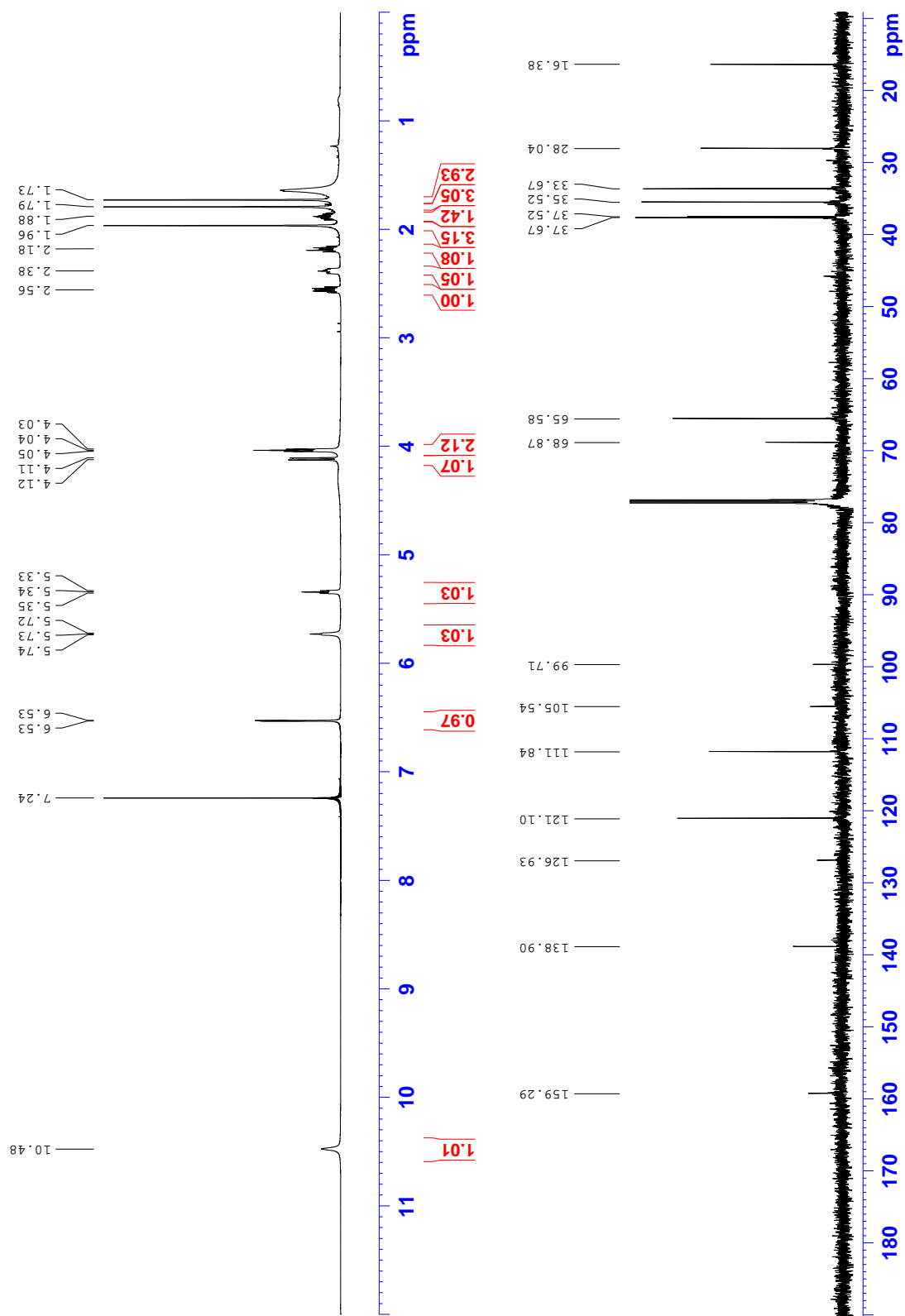
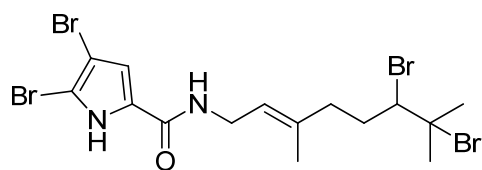


**(Z)-3,7-dimethylocta-2,6-dien-1-yl 1H-pyrrole-2-carboxylate (3.39)**

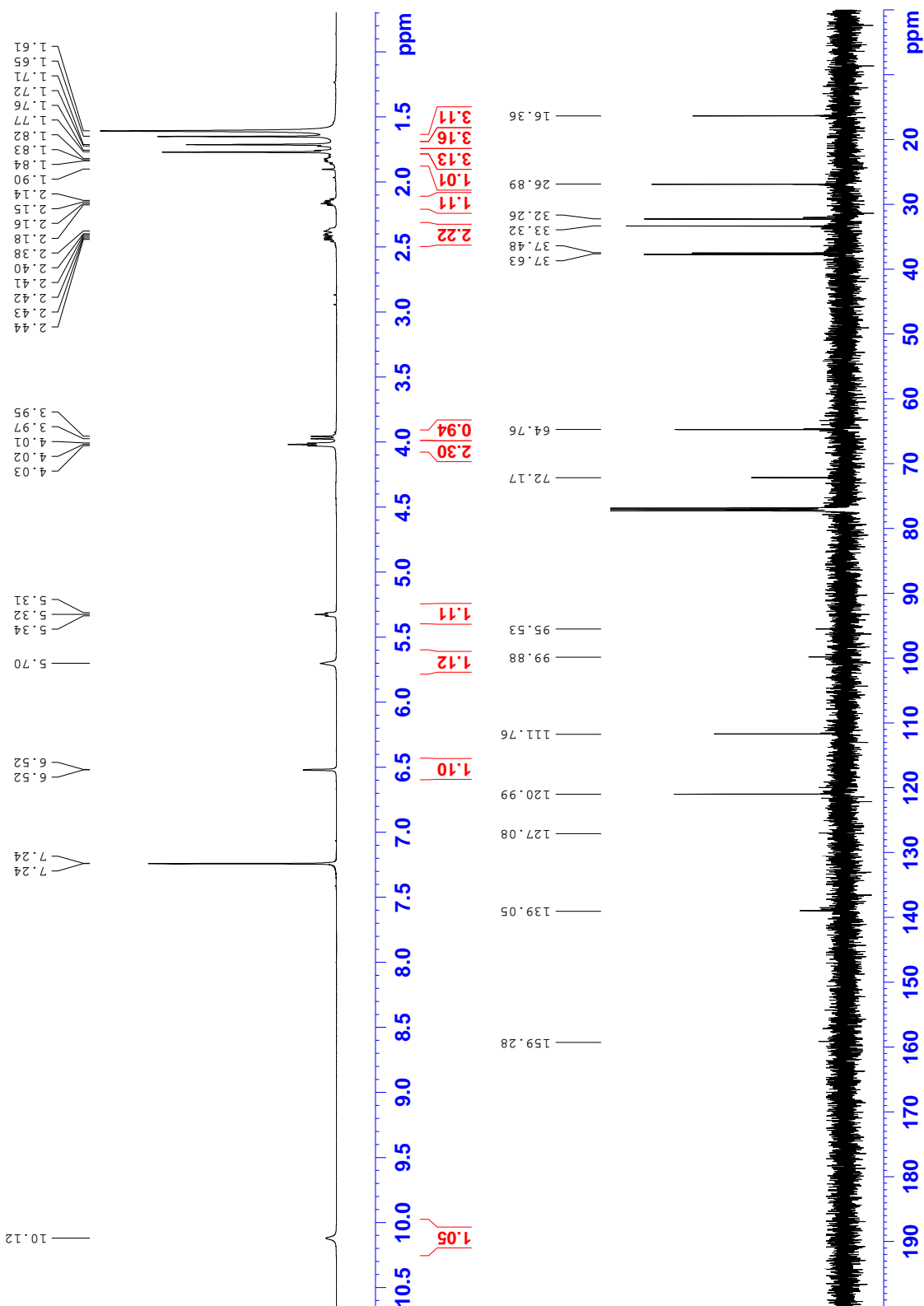
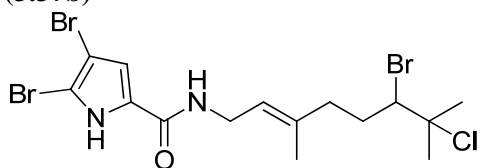
**(*E*)-tert-butyl (3,7-dimethylocta-2,6-dien-1-yl)carbamate (3.40)**



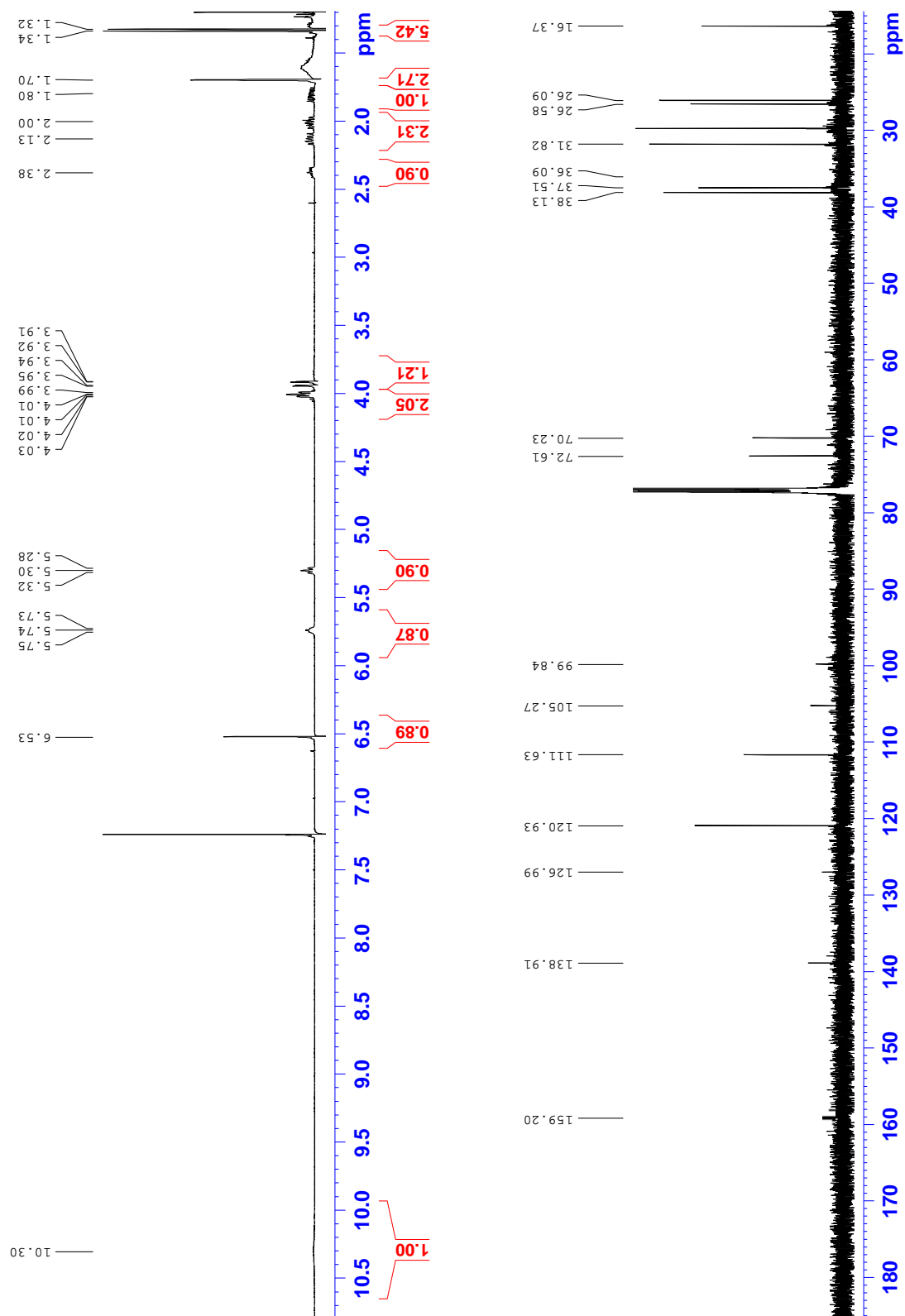
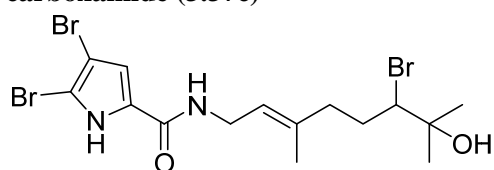
**(E)-4,5-dibromo-N-(6,7-dibromo-3,7-dimethyloct-2-en-1-yl)-1H-pyrrole-2-carboxamide**  
**(3.37a)**



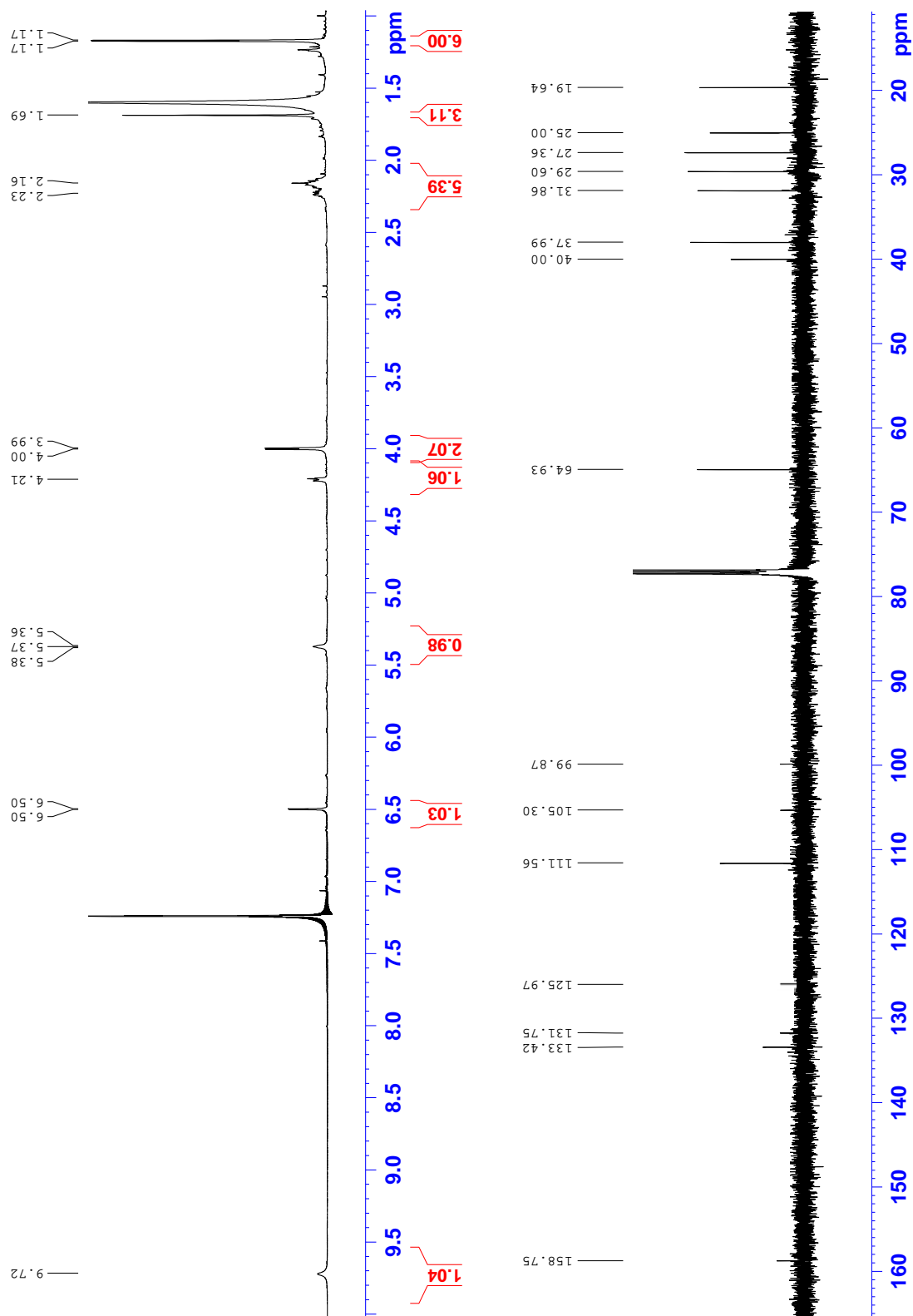
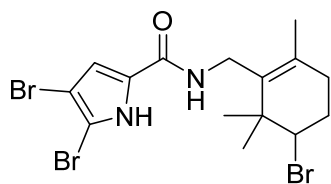
**(E)-4,5-dibromo-N-(6-bromo-7-chloro-3,7-dimethyloct-2-en-1-yl)-1H-pyrrole-2-carboxamide (3.37b)**



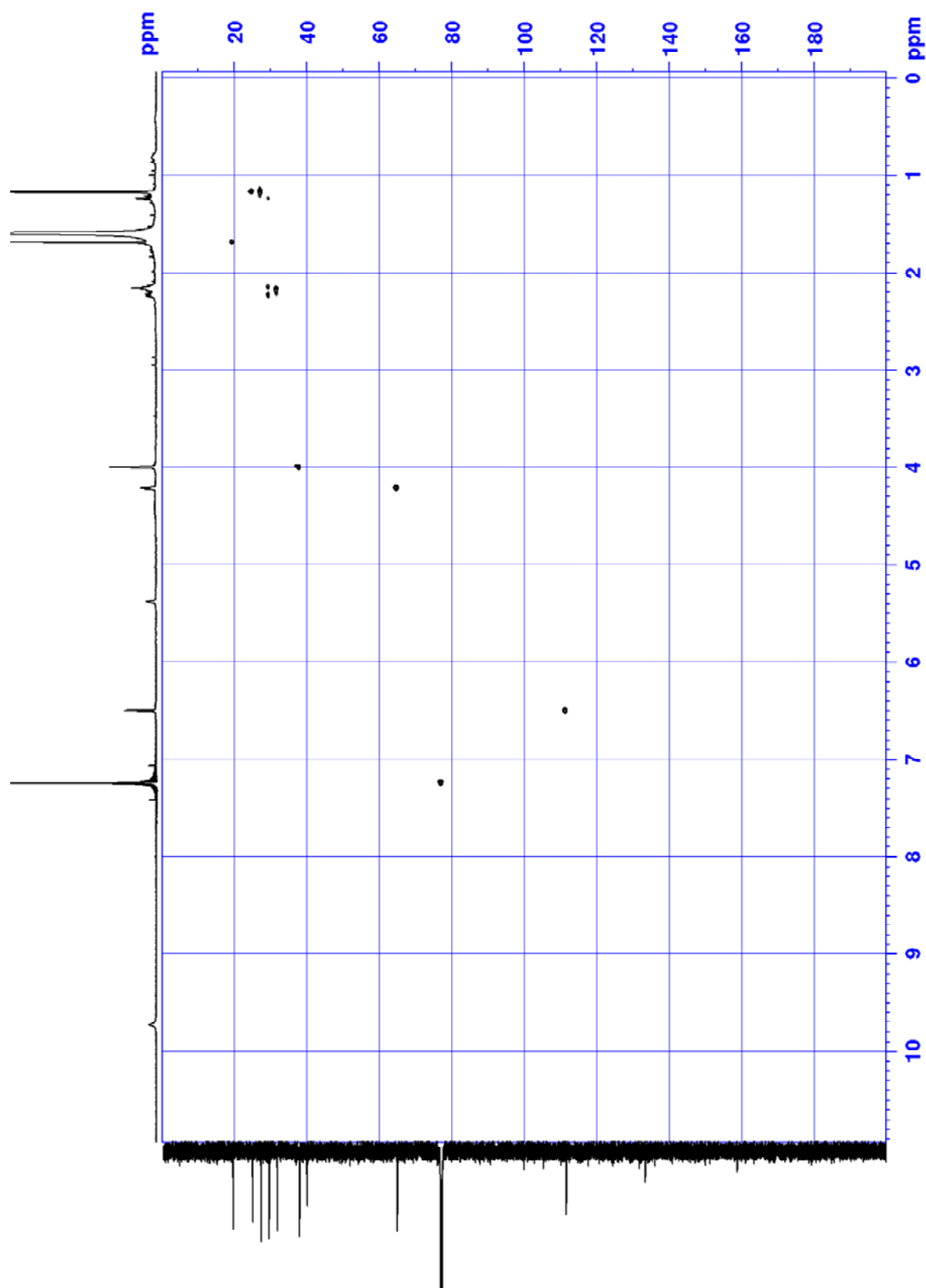


**(E)-4,5-dibromo-N-(6-bromo-7-hydroxy-3,7-dimethyloct-2-en-1-yl)-1H-pyrrole-2-carboxamide (3.37c)**

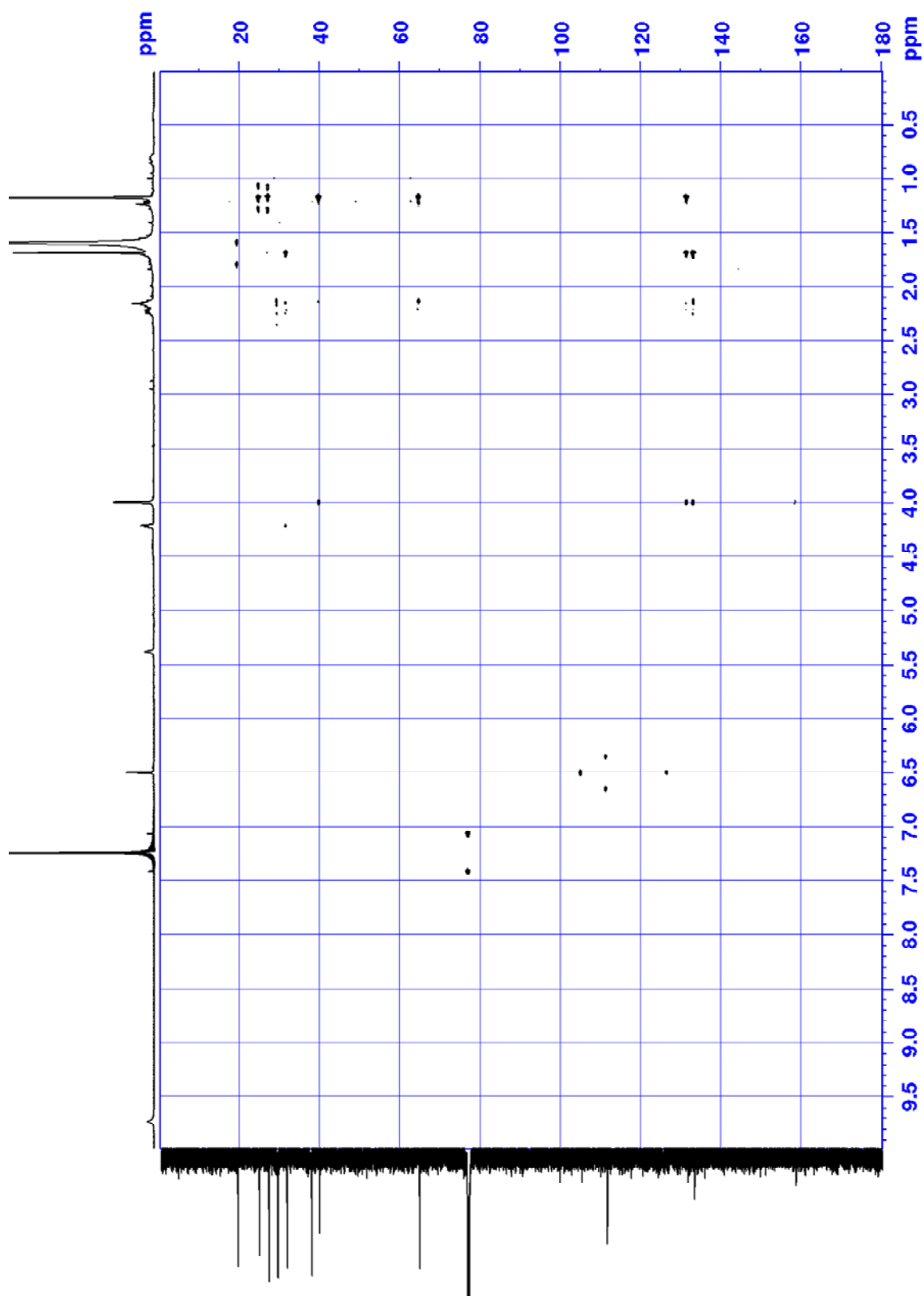
**4,5-dibromo-N-((5-bromo-2,6,6-trimethylcyclohex-1-en-1-yl)methyl)-1H-pyrrole-2-carboxamide (3.37d)**



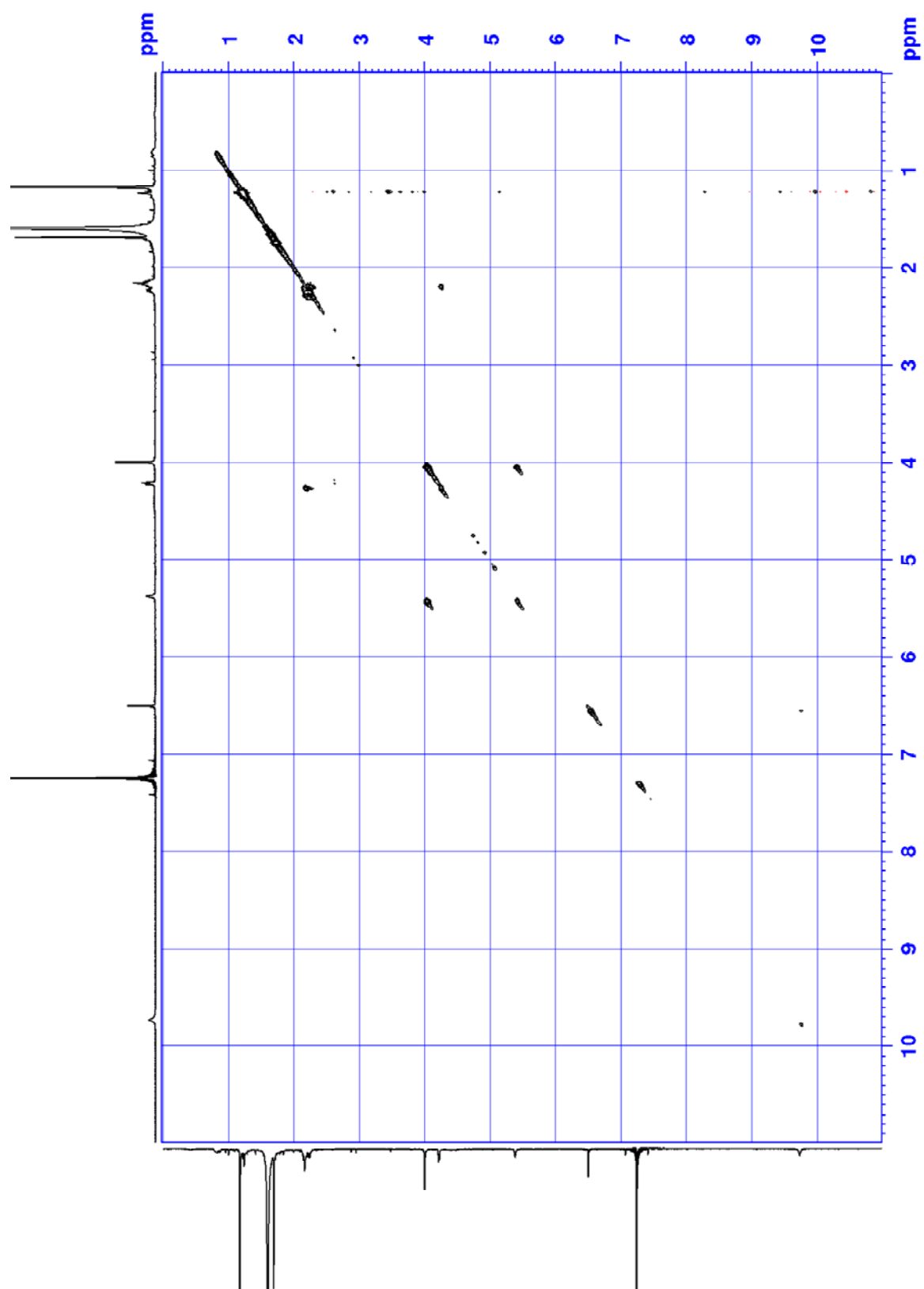
HSQC (3.37d)



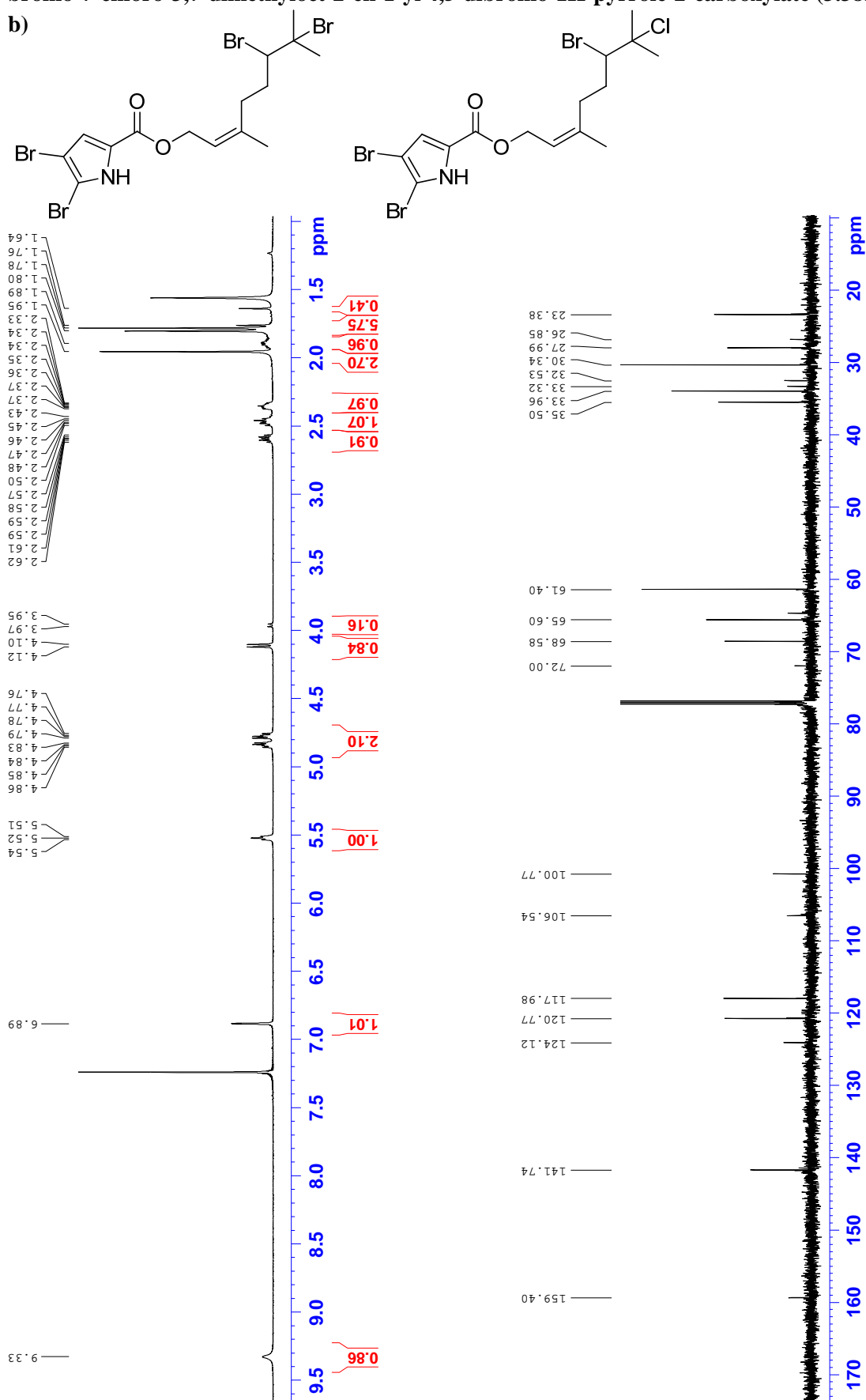
HMBC (3.37d)



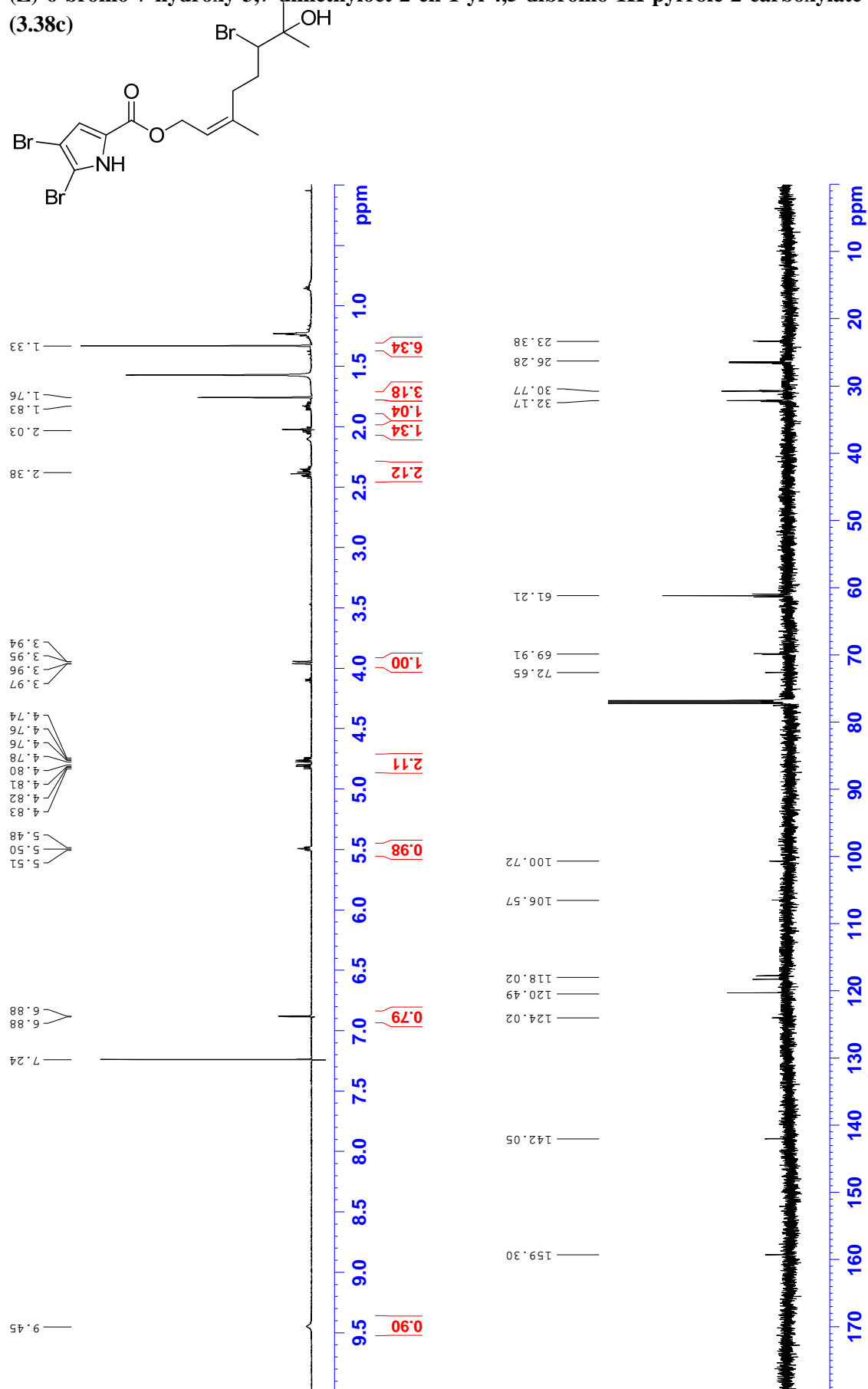
COSY (3.37d)



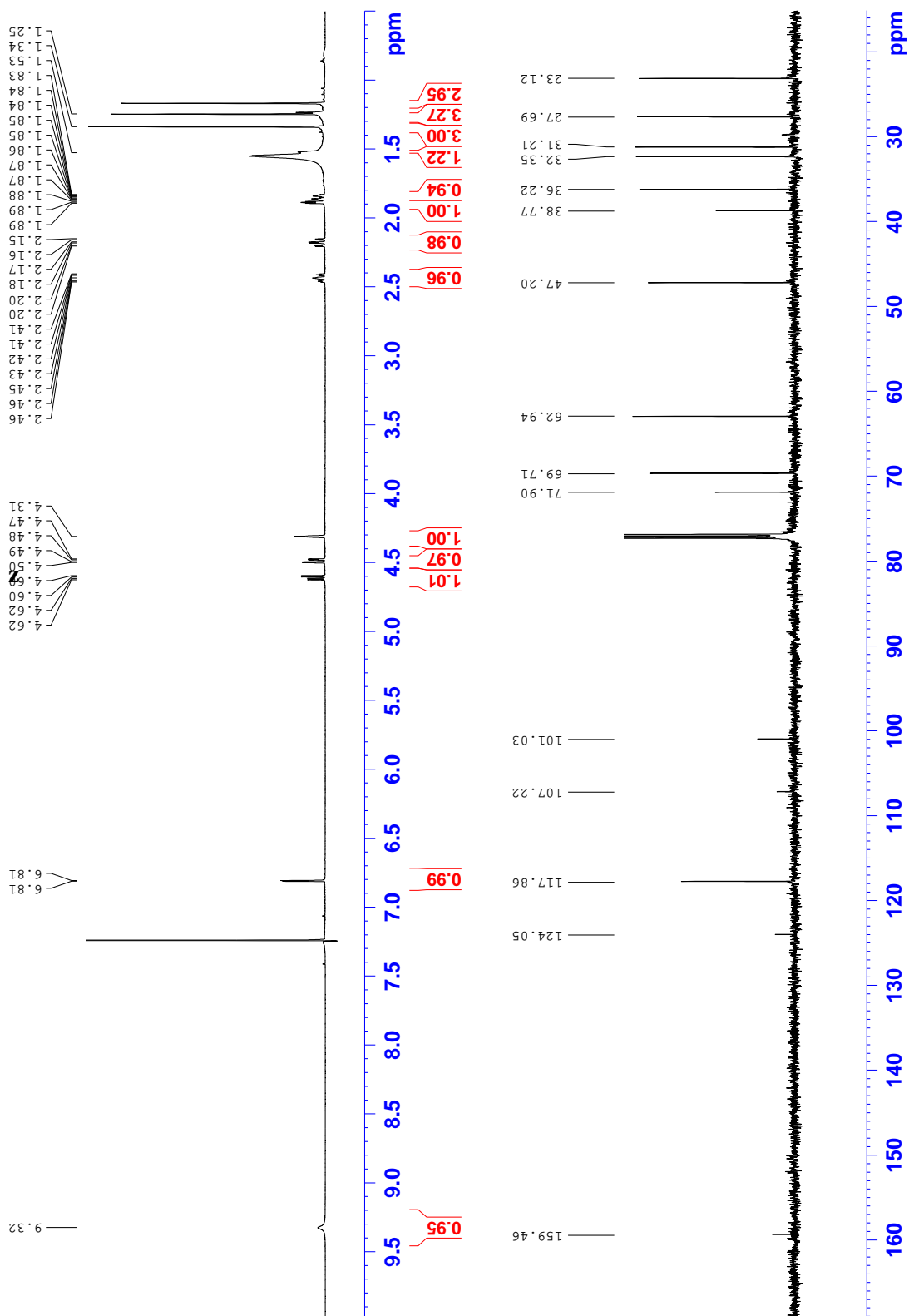
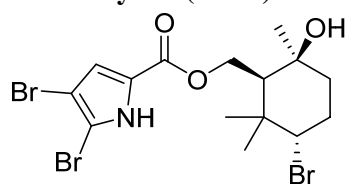
(Z)-6,7-dibromo-3,7-dimethyloct-2-en-1-yl 4,5-dibromo-1H-pyrrole-2-carboxylate and (Z)-6-bromo-7-chloro-3,7-dimethyloct-2-en-1-yl 4,5-dibromo-1H-pyrrole-2-carboxylate (3.38a and b)



**(Z)-6-bromo-7-hydroxy-3,7-dimethyloct-2-en-1-yl 4,5-dibromo-1H-pyrrole-2-carboxylate (3.38c)**

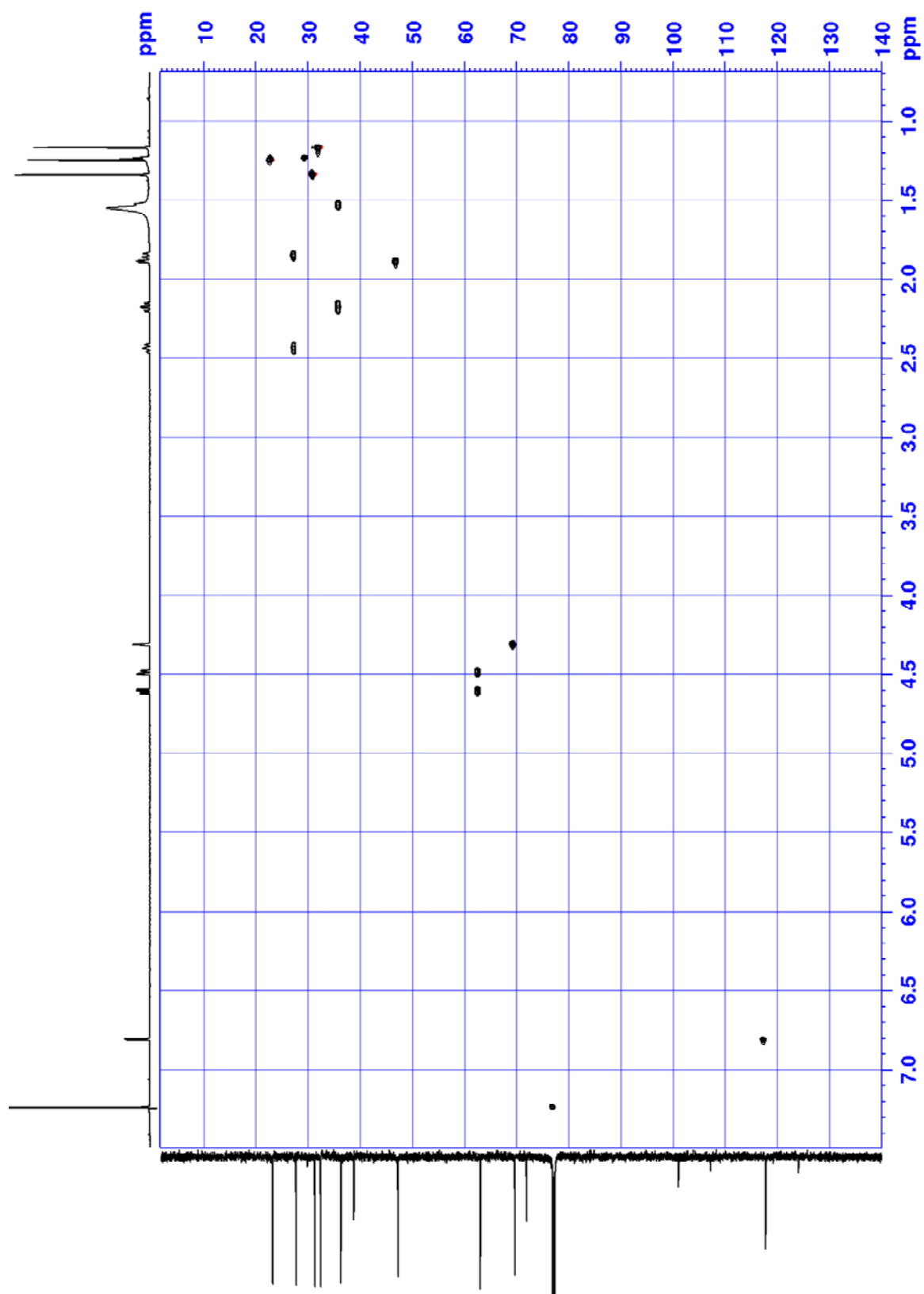


**((1R,3R,6R)-3-bromo-6-hydroxy-2,2,6-trimethylcyclohexyl)methyl 4,5-dibromo-1H-pyrrole-2-carboxylate (3.38d)**

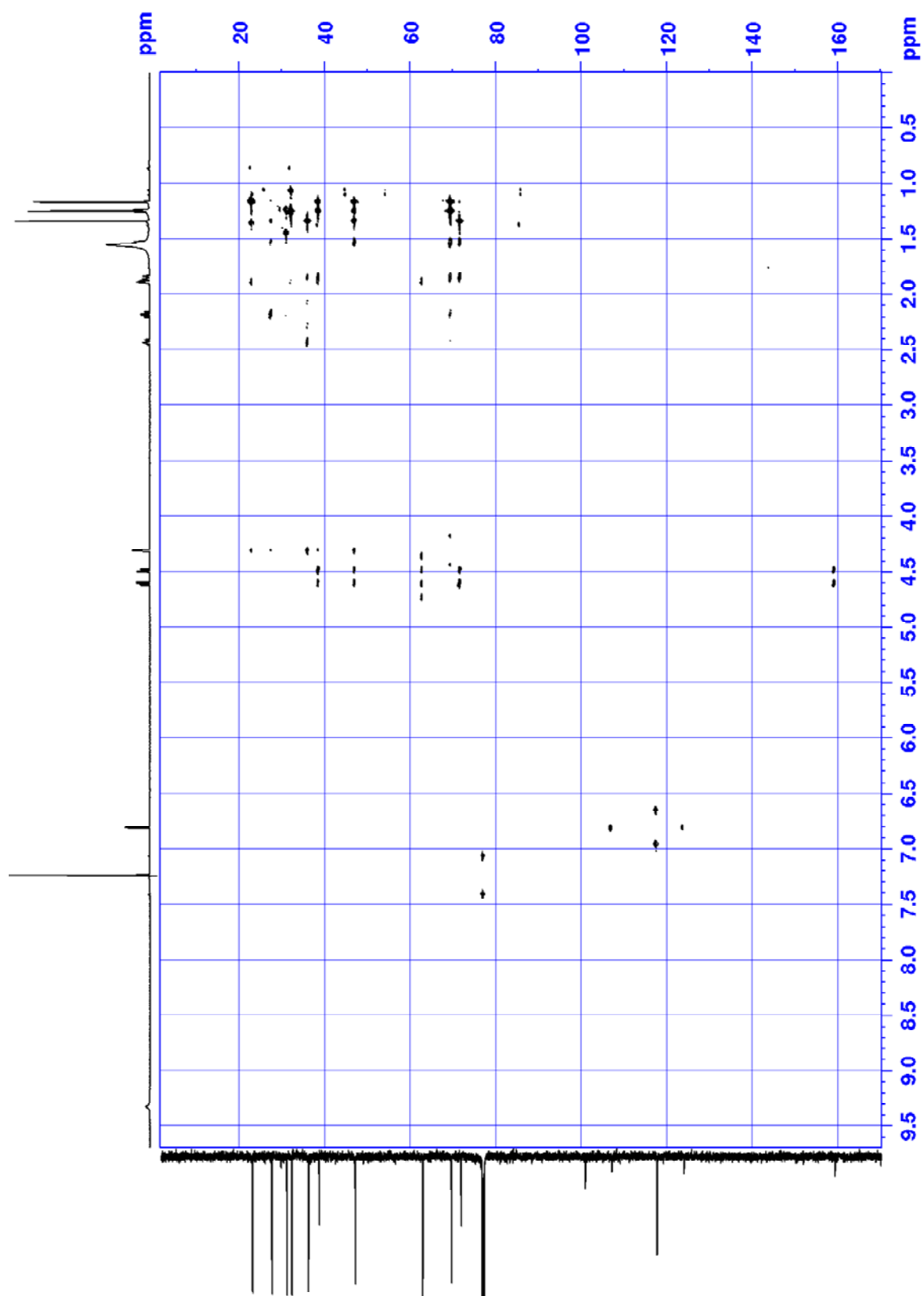




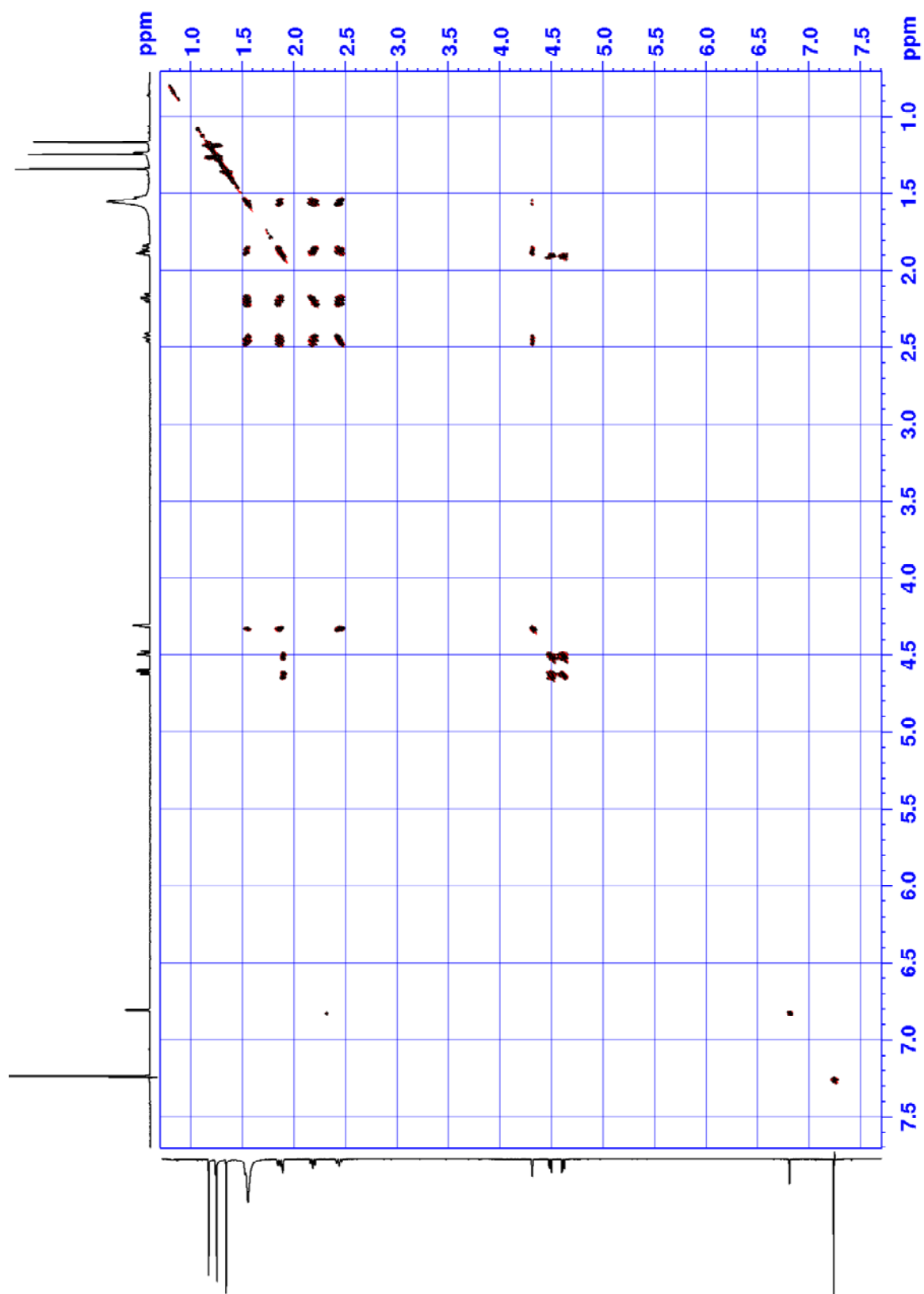
HSQC (3.38d)



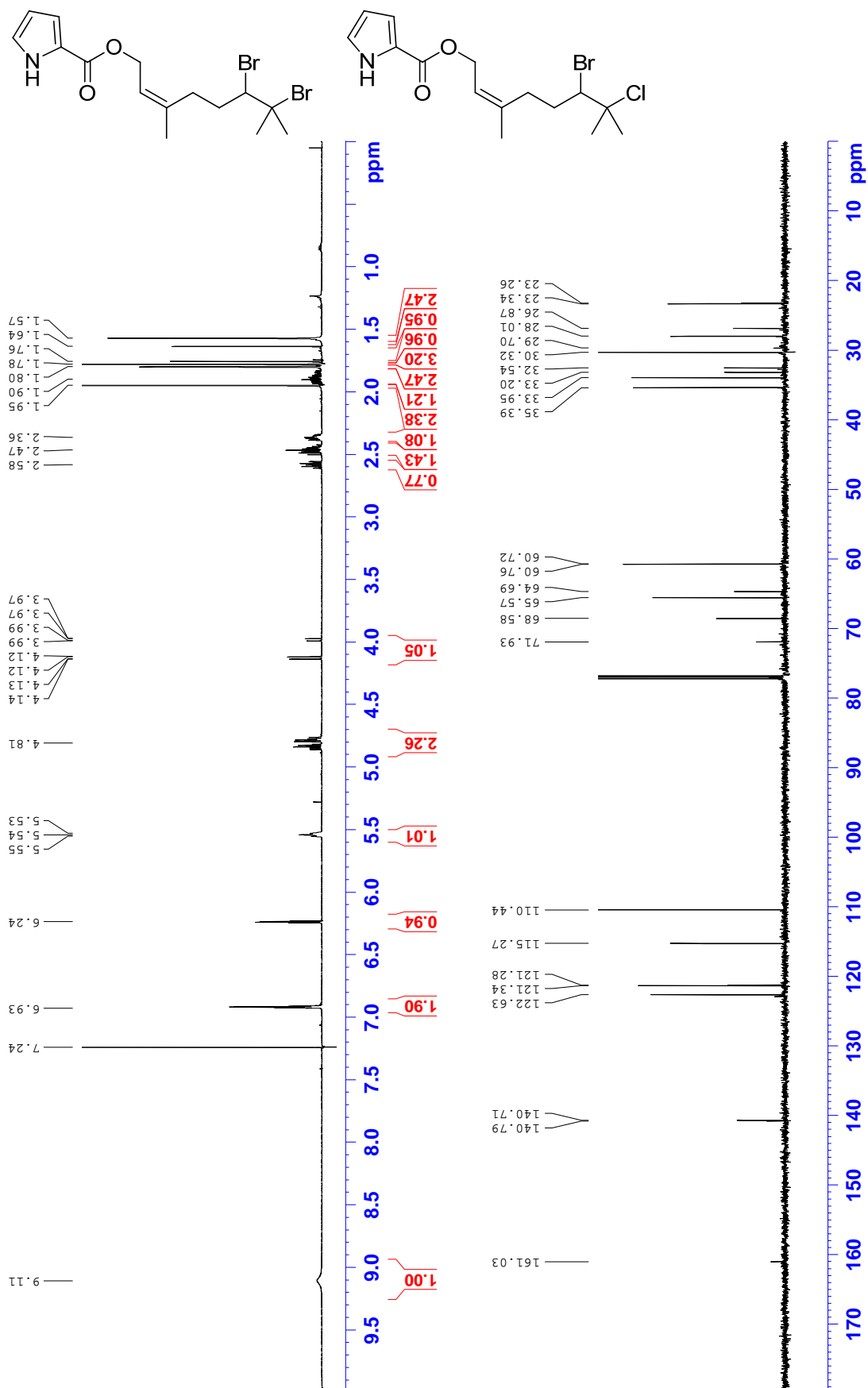
HMBC (3.38d)



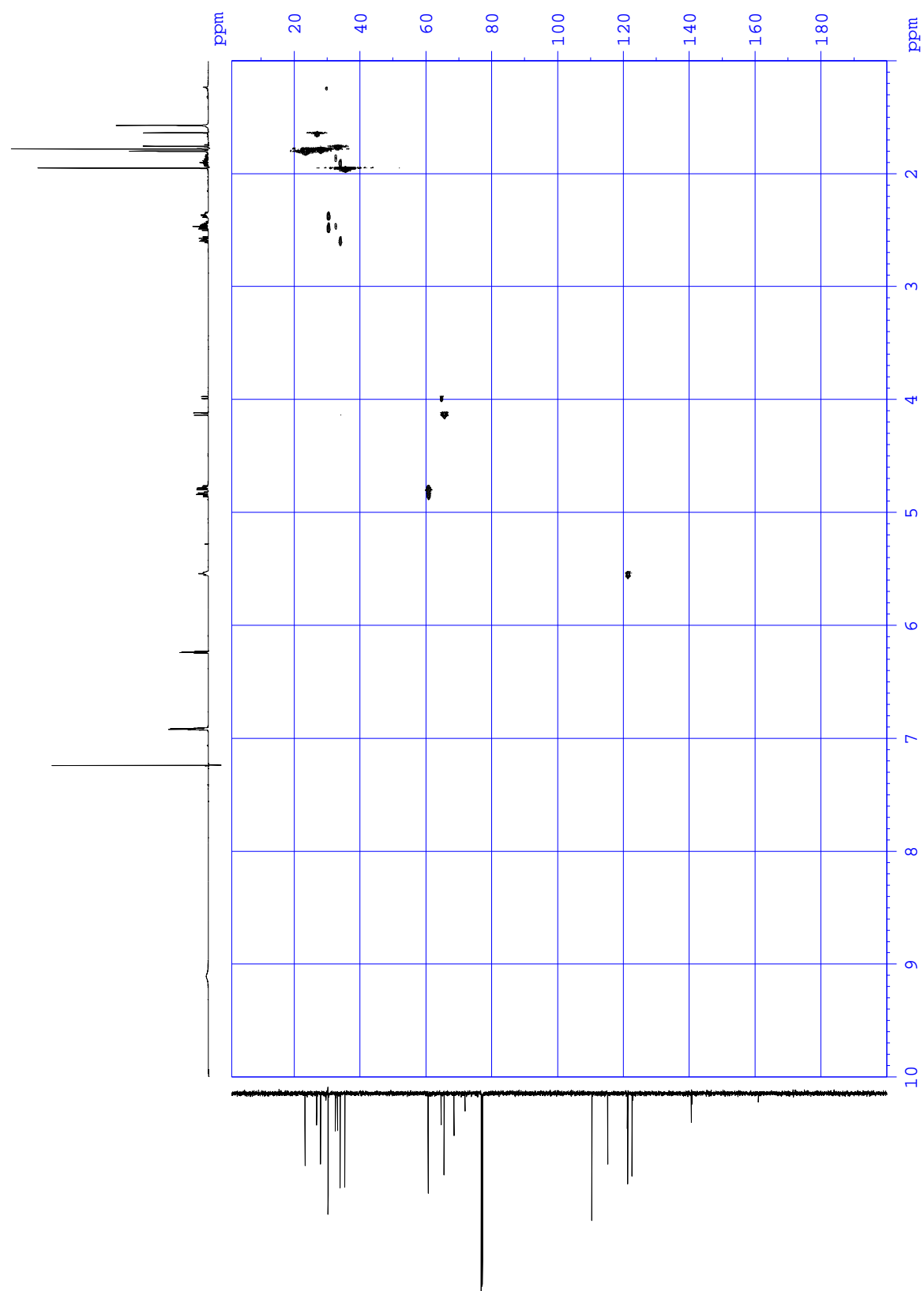
COSY (3.38d)



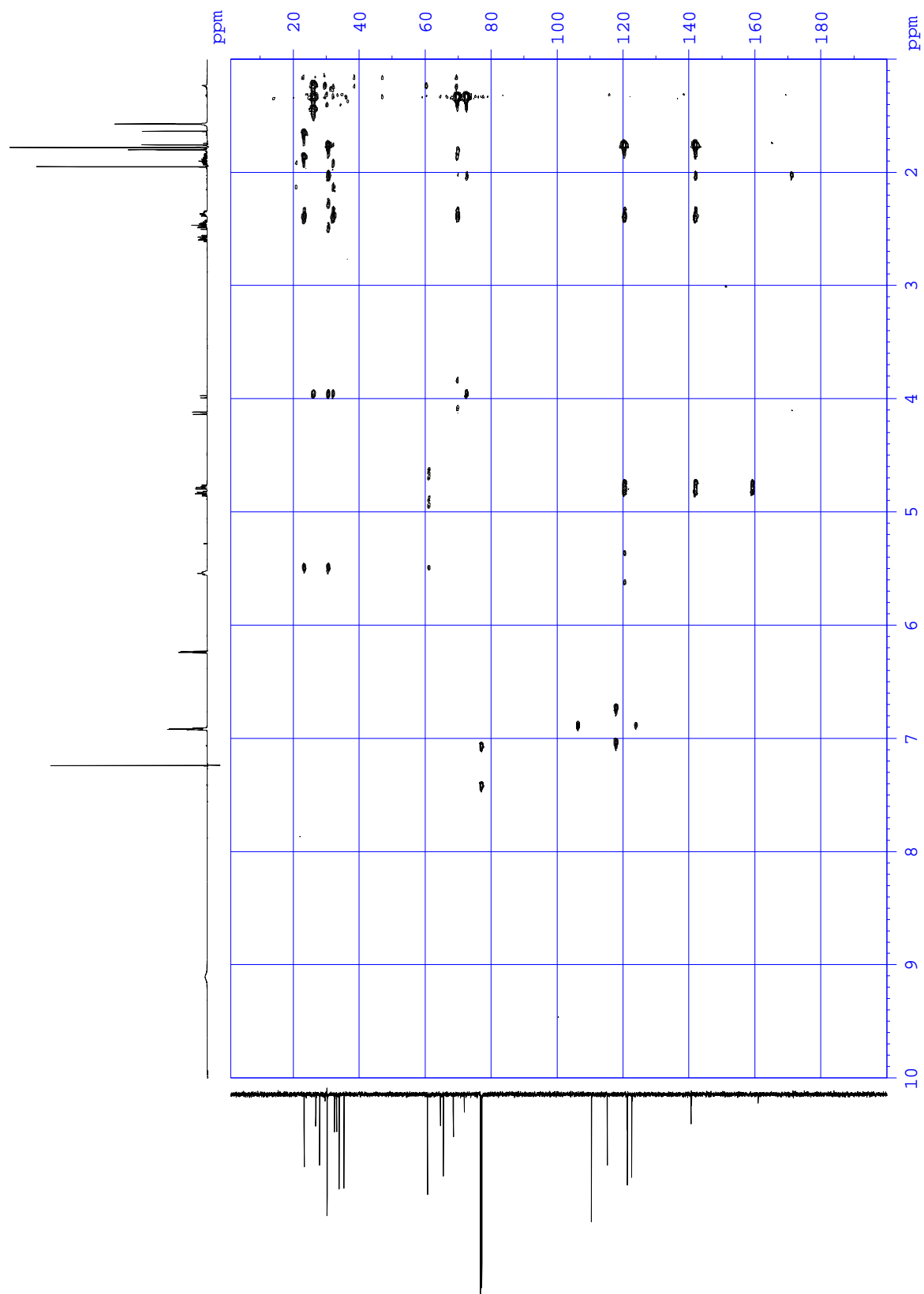
**(Z)-6,7-dibromo-3,7-dimethyloct-2-en-1-yl 1H-pyrrole-2-carboxylate and (Z)-6-bromo-7-chloro-3,7-dimethyloct-2-en-1-yl 1H-pyrrole-2-carboxylate (3.39a and b)**



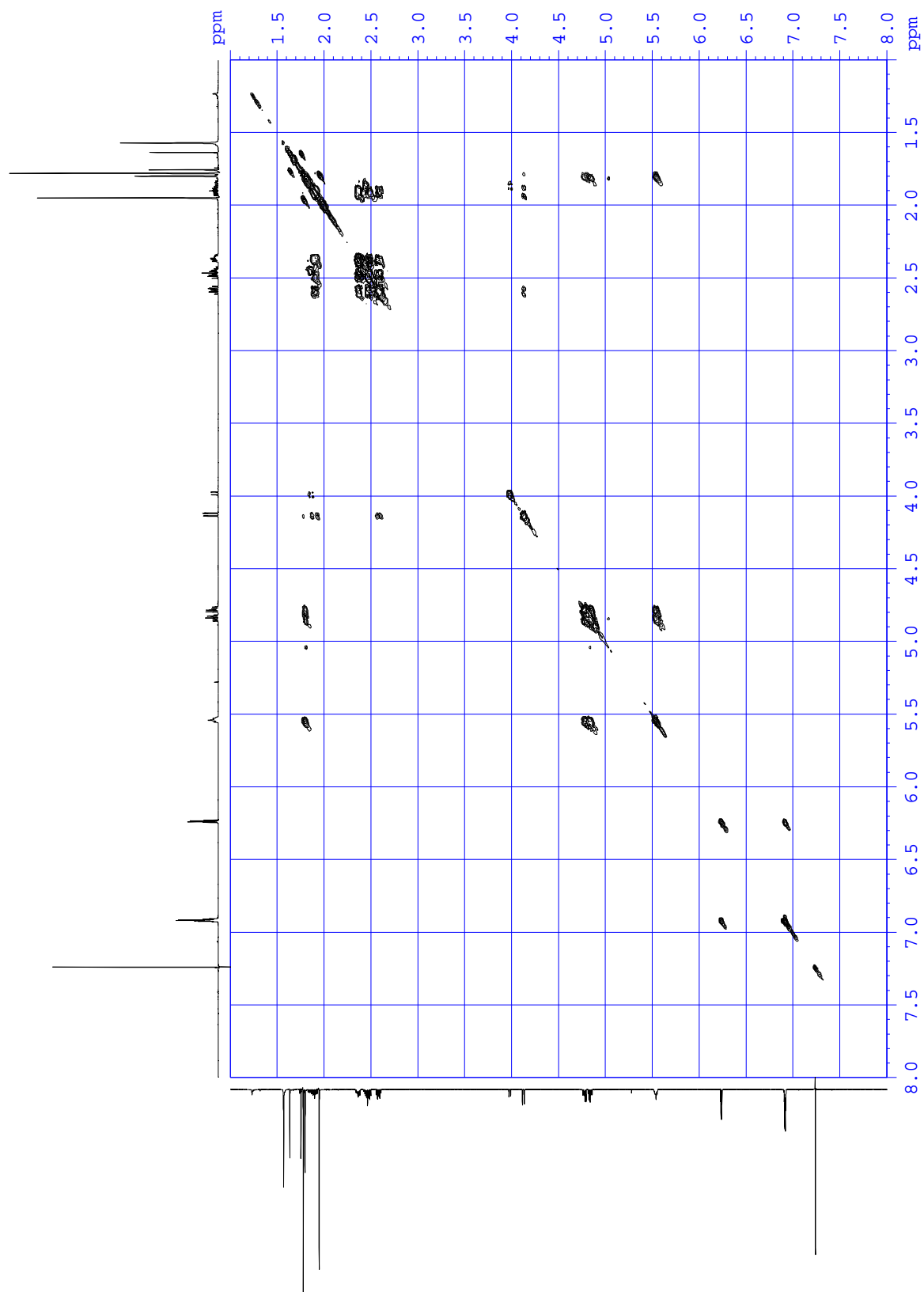
HSQC (3.39a and b)



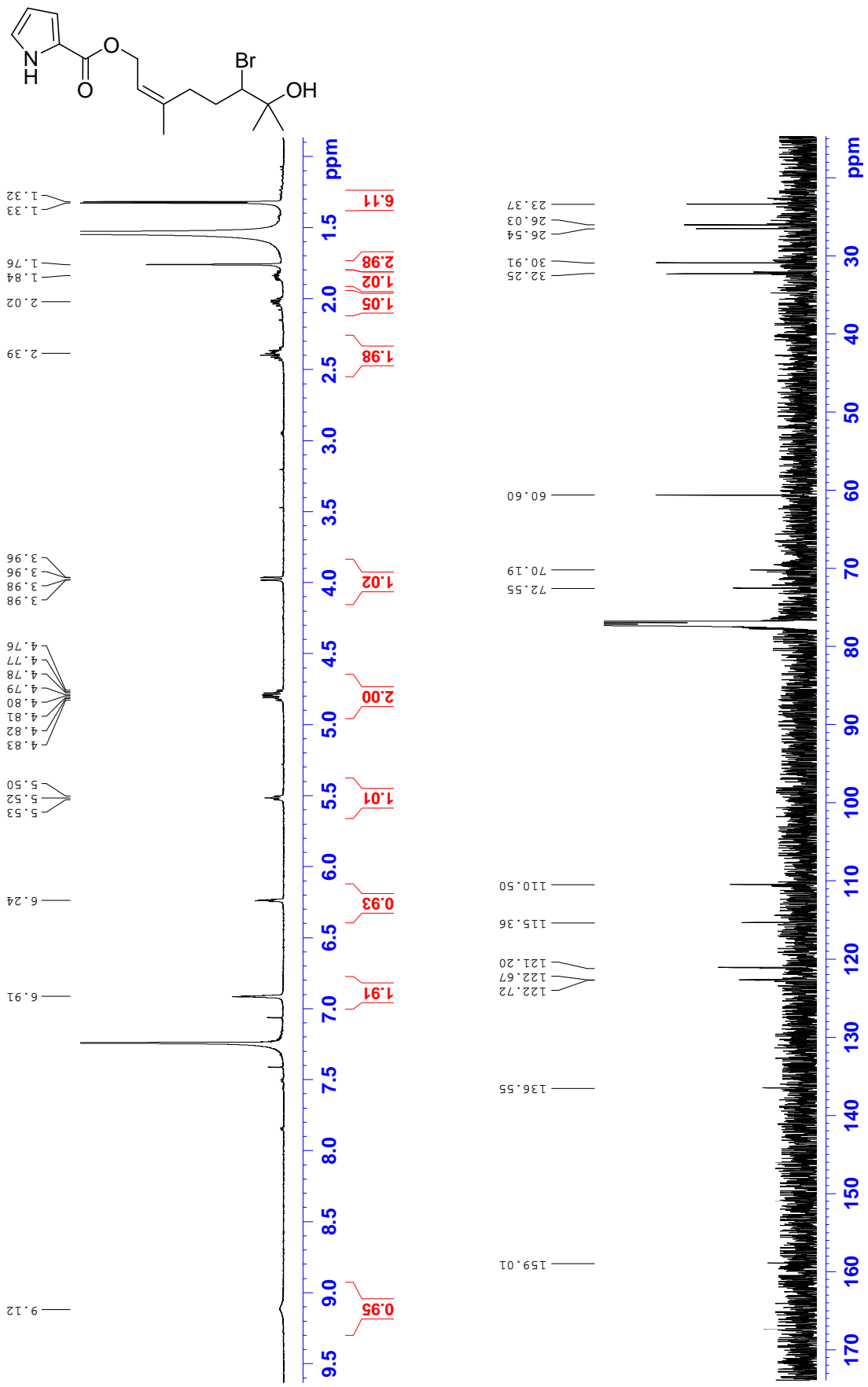
HMBC (3.39a and b)



COSY (3.39a and b)

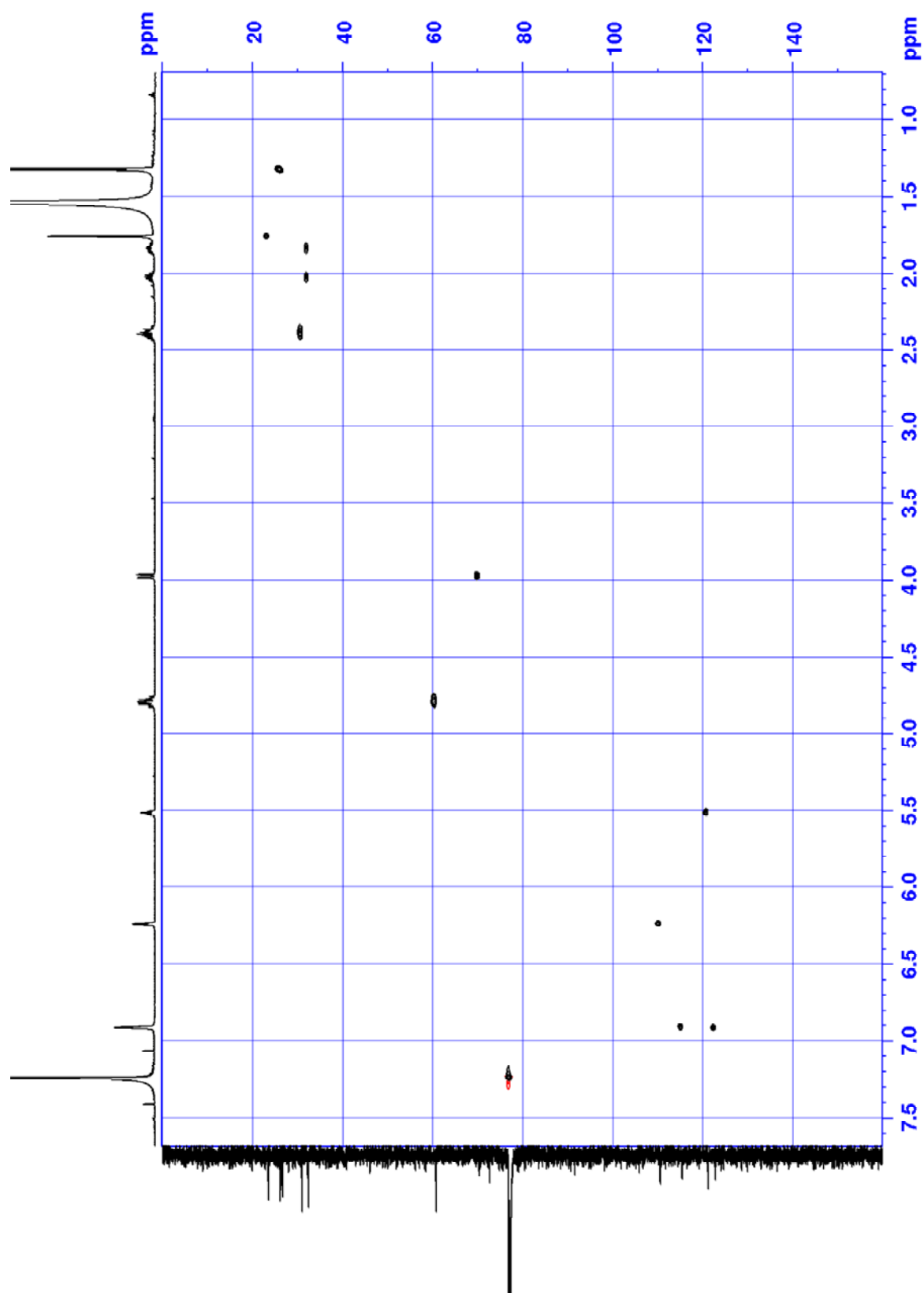


(Z)-6-bromo-7-hydroxy-3,7-dimethyloct-2-en-1-yl 1H-pyrrole-2-carboxylate (3.39c)

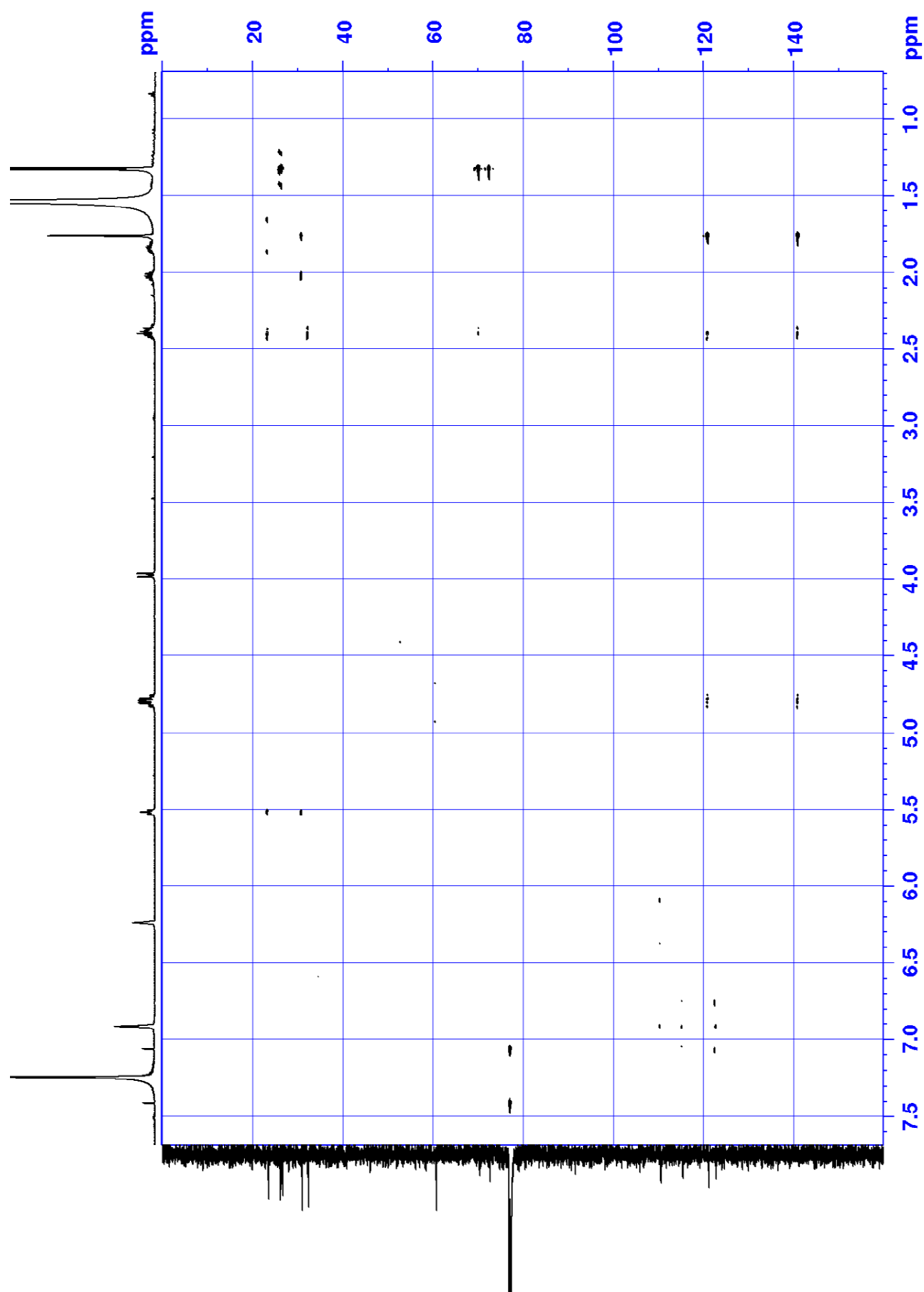




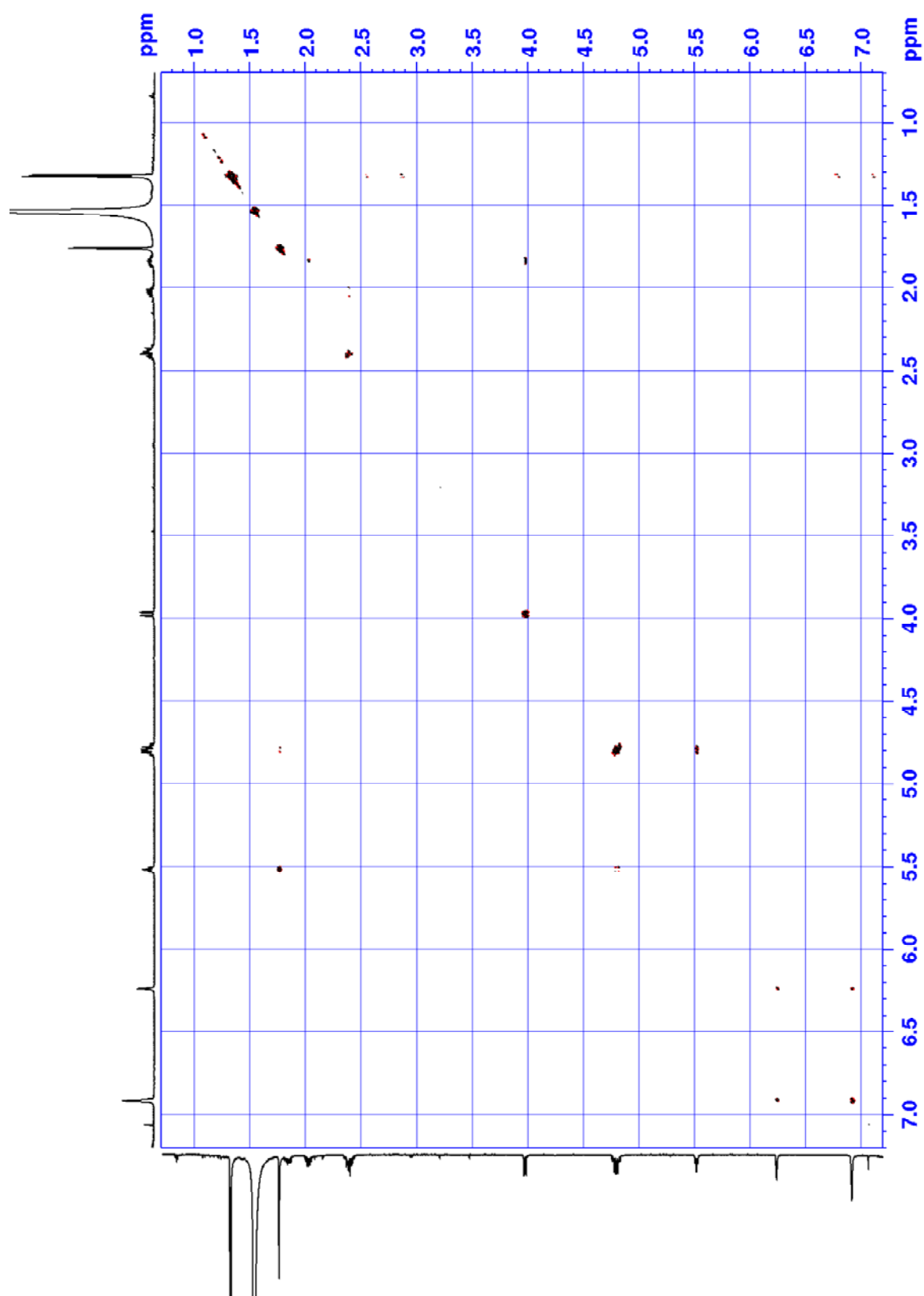
HSQC (3.39c)



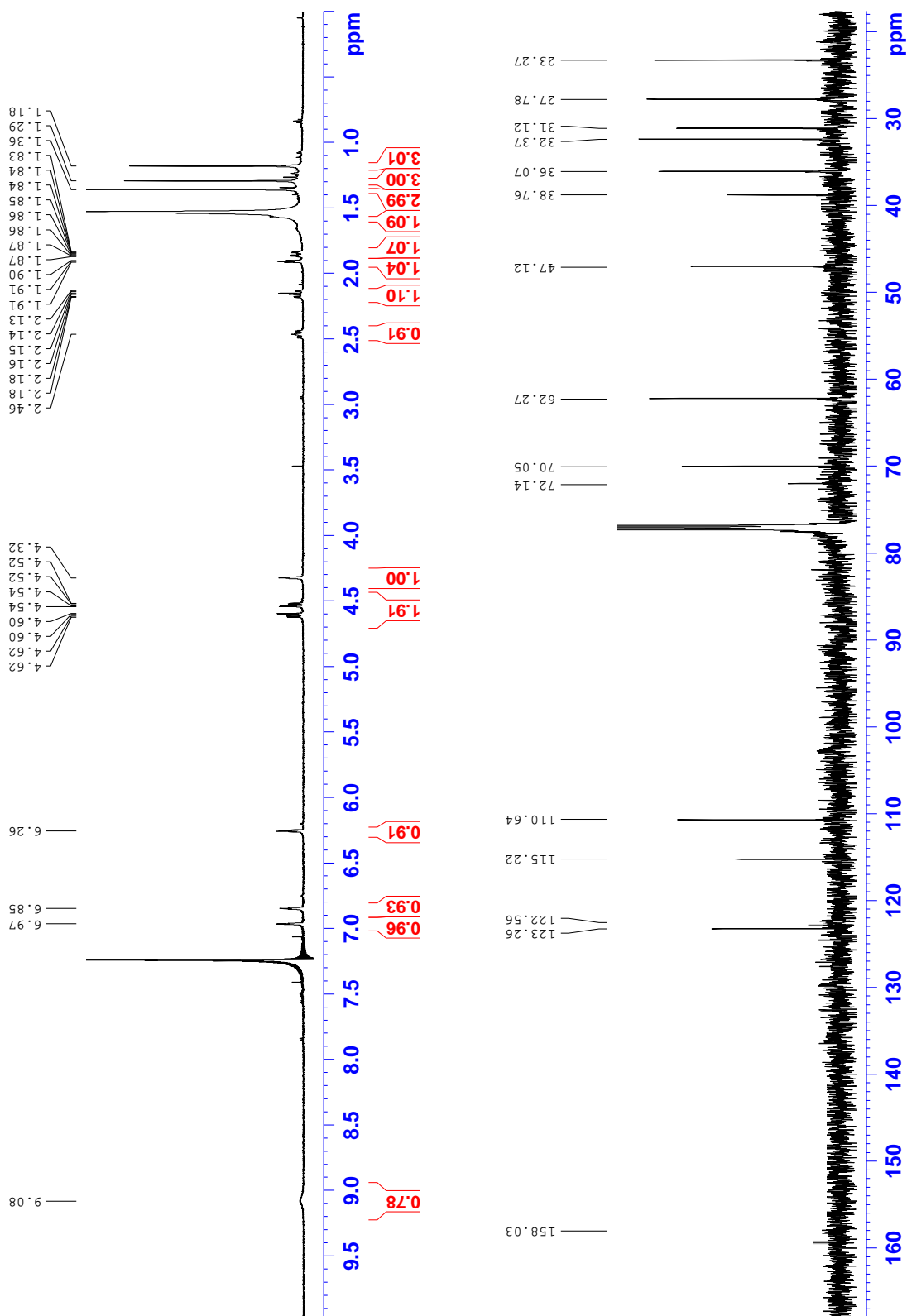
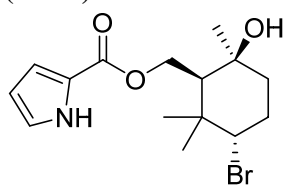
HMBC (3.39c)



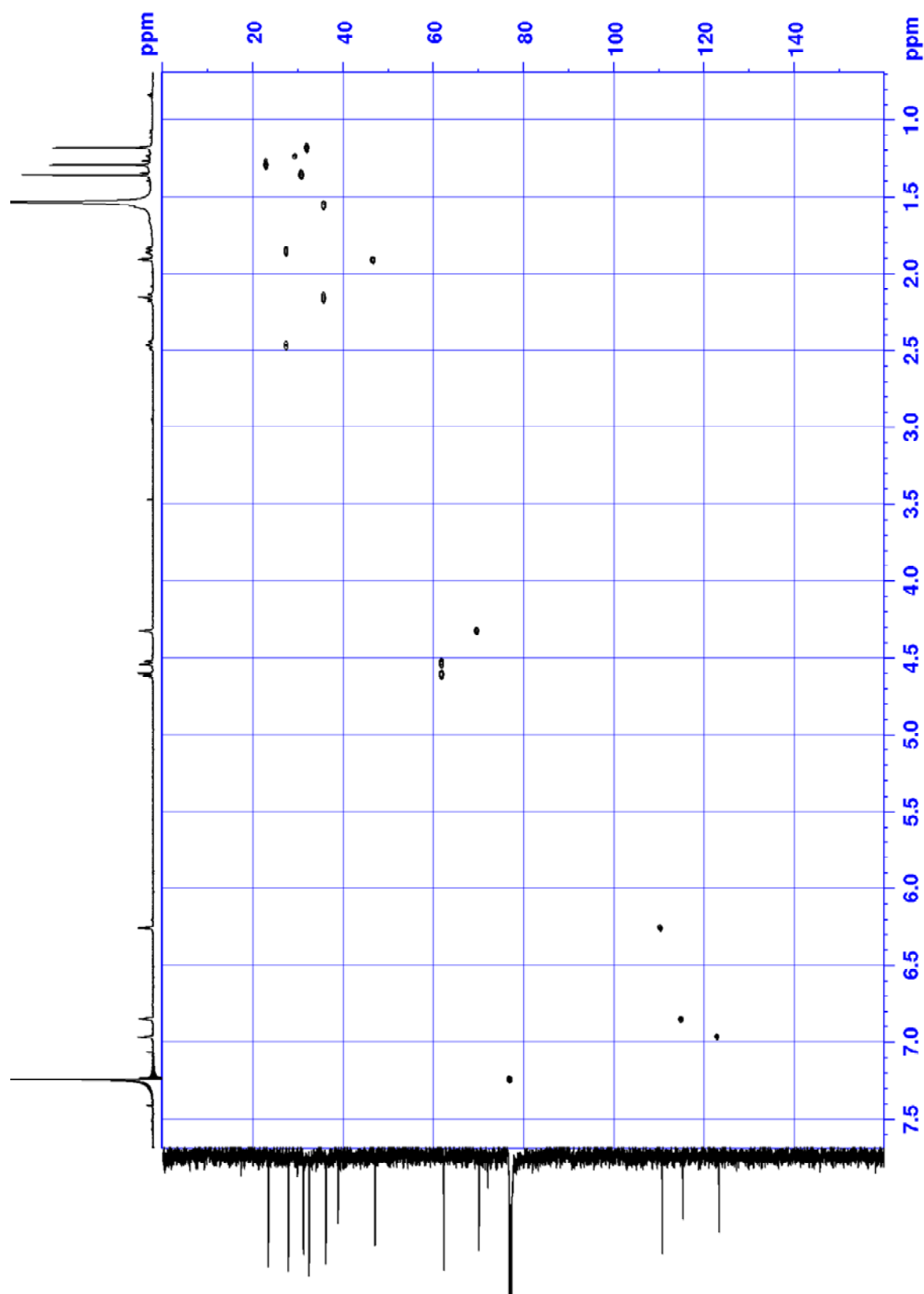
COSY (3.39c)



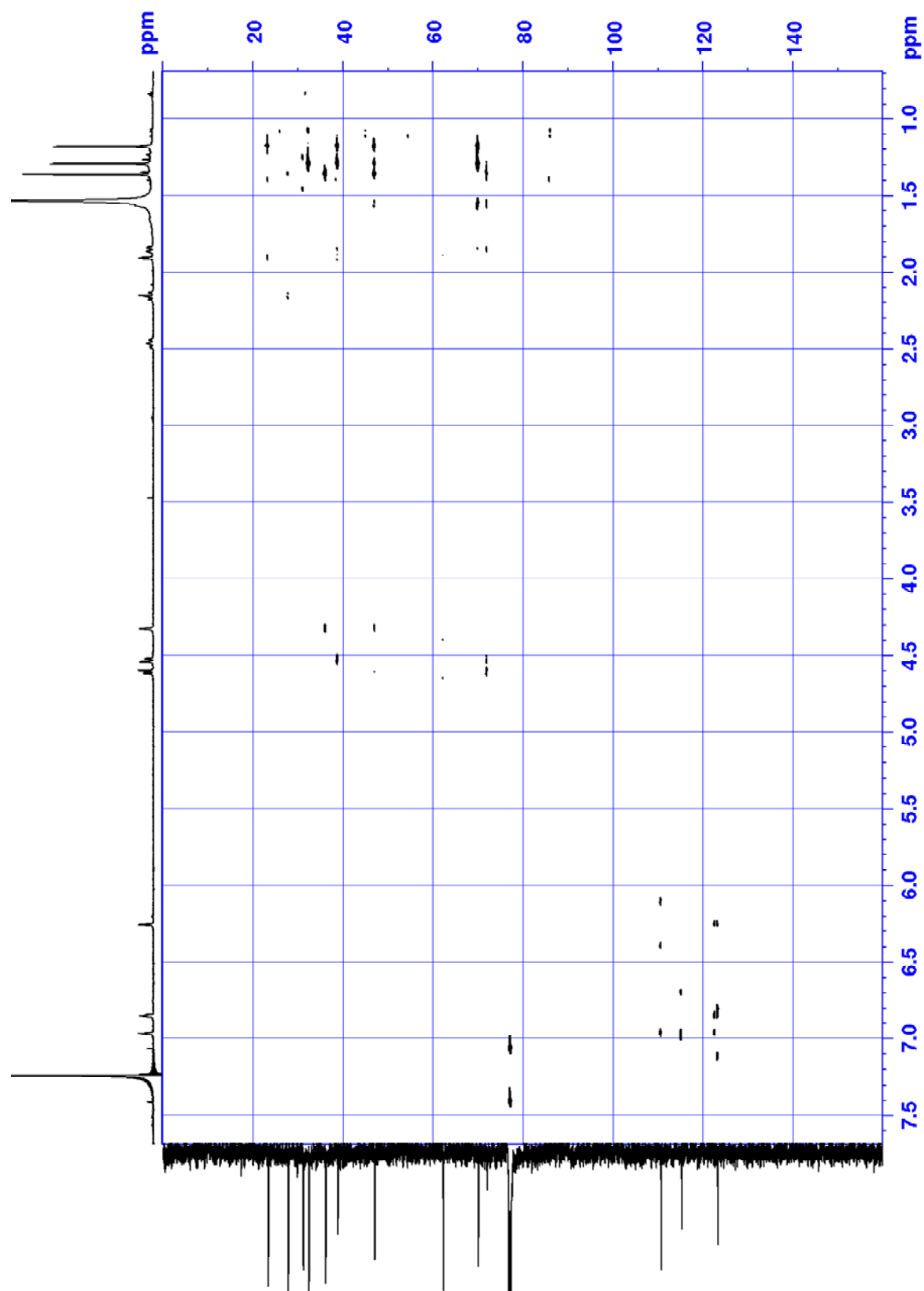
**((1R,3R,6R)-3-bromo-6-hydroxy-2,2,6-trimethylcyclohexyl)methyl 1H-pyrrole-2-carboxylate (3.39d)**



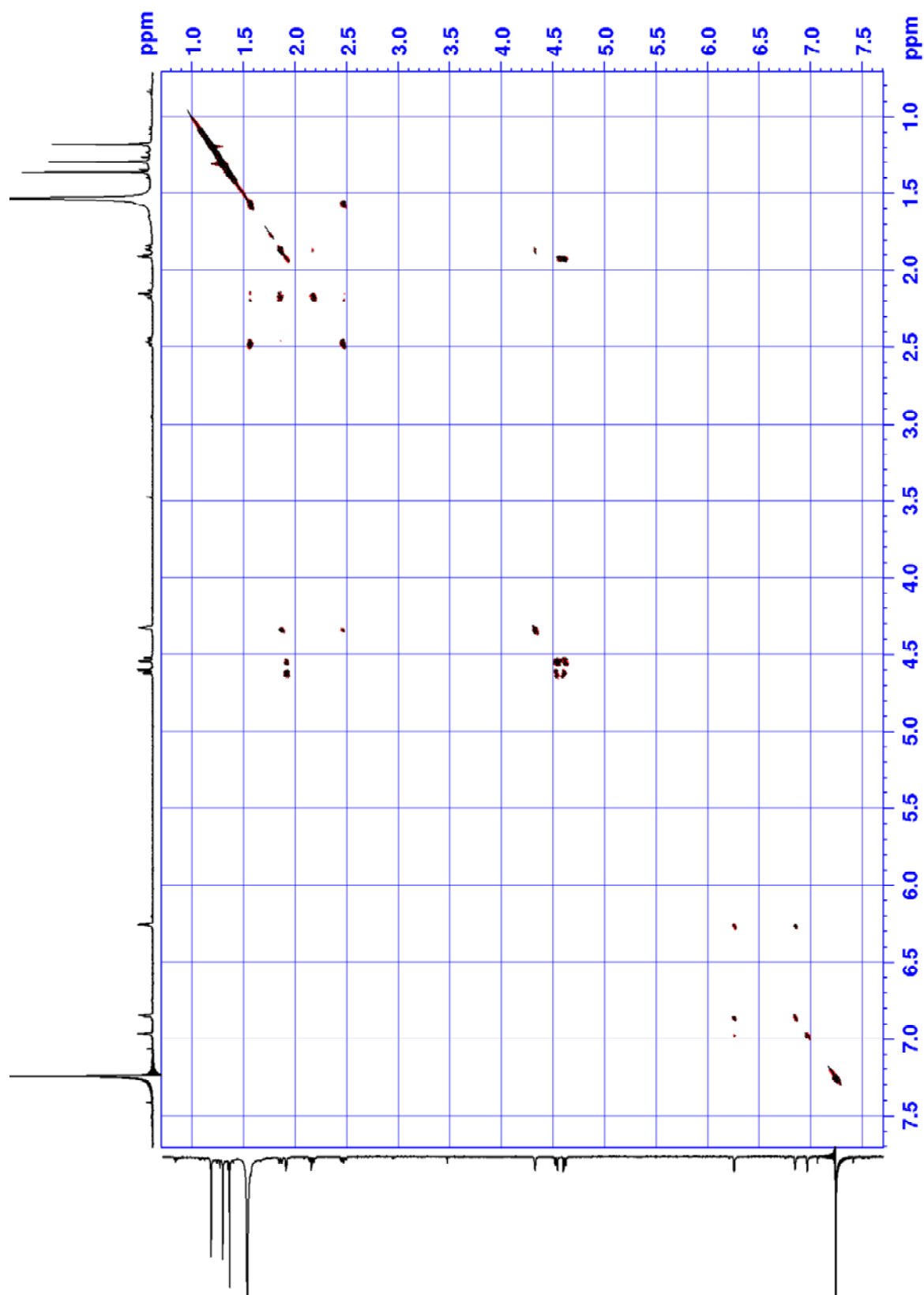
HSQC (3.39d)



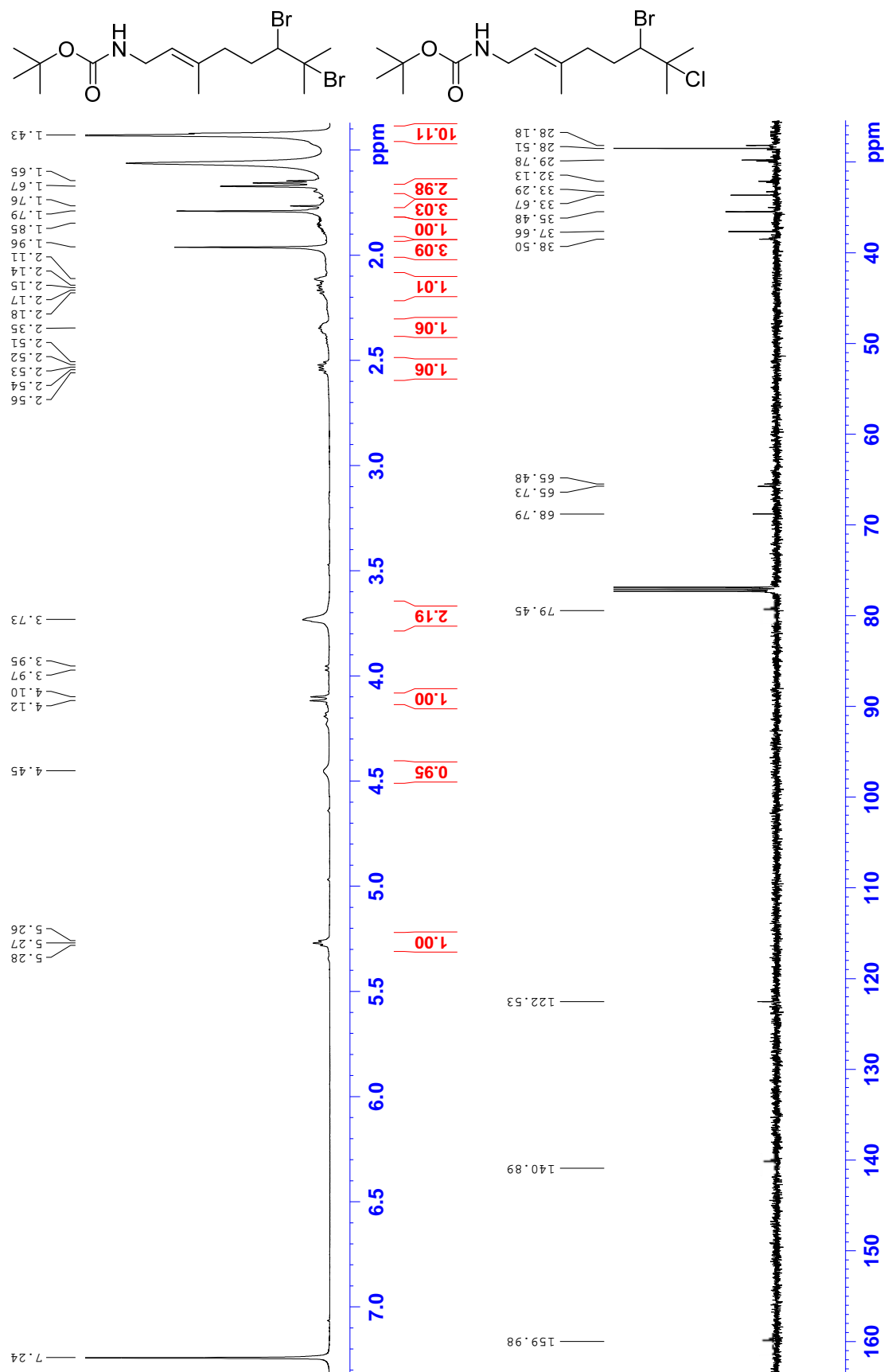
HMBC (3.39d)



COSY (3.39d)

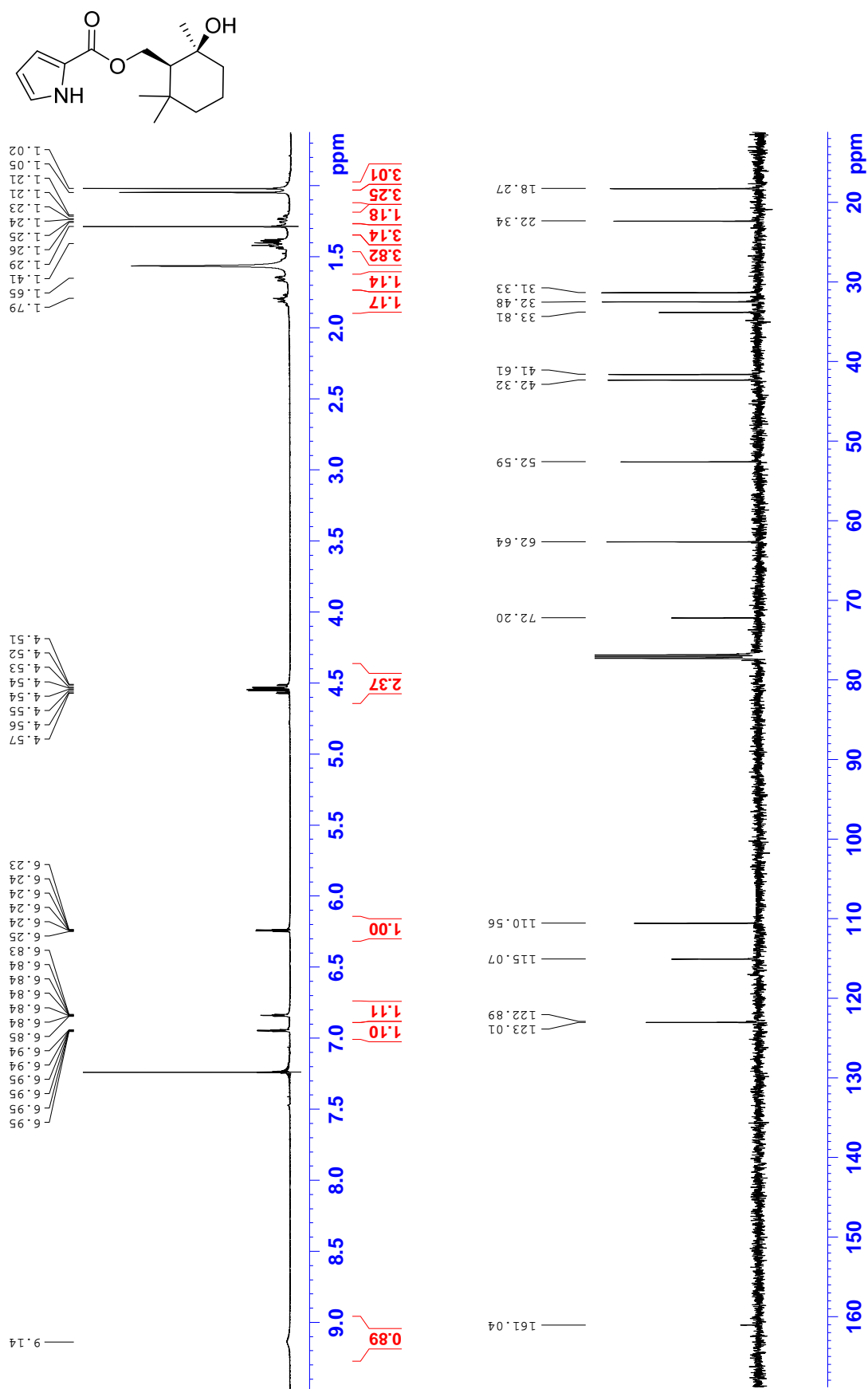


***tert*-butyl (E)-(6,7-dibromo-3,7-dimethyloct-2-en-1-yl)carbamate (3.40a) and *tert*-butyl (E)-(6-bromo-7-chloro-3,7-dimethyloct-2-en-1-yl)carbamate (3.40b) (trace amount)**

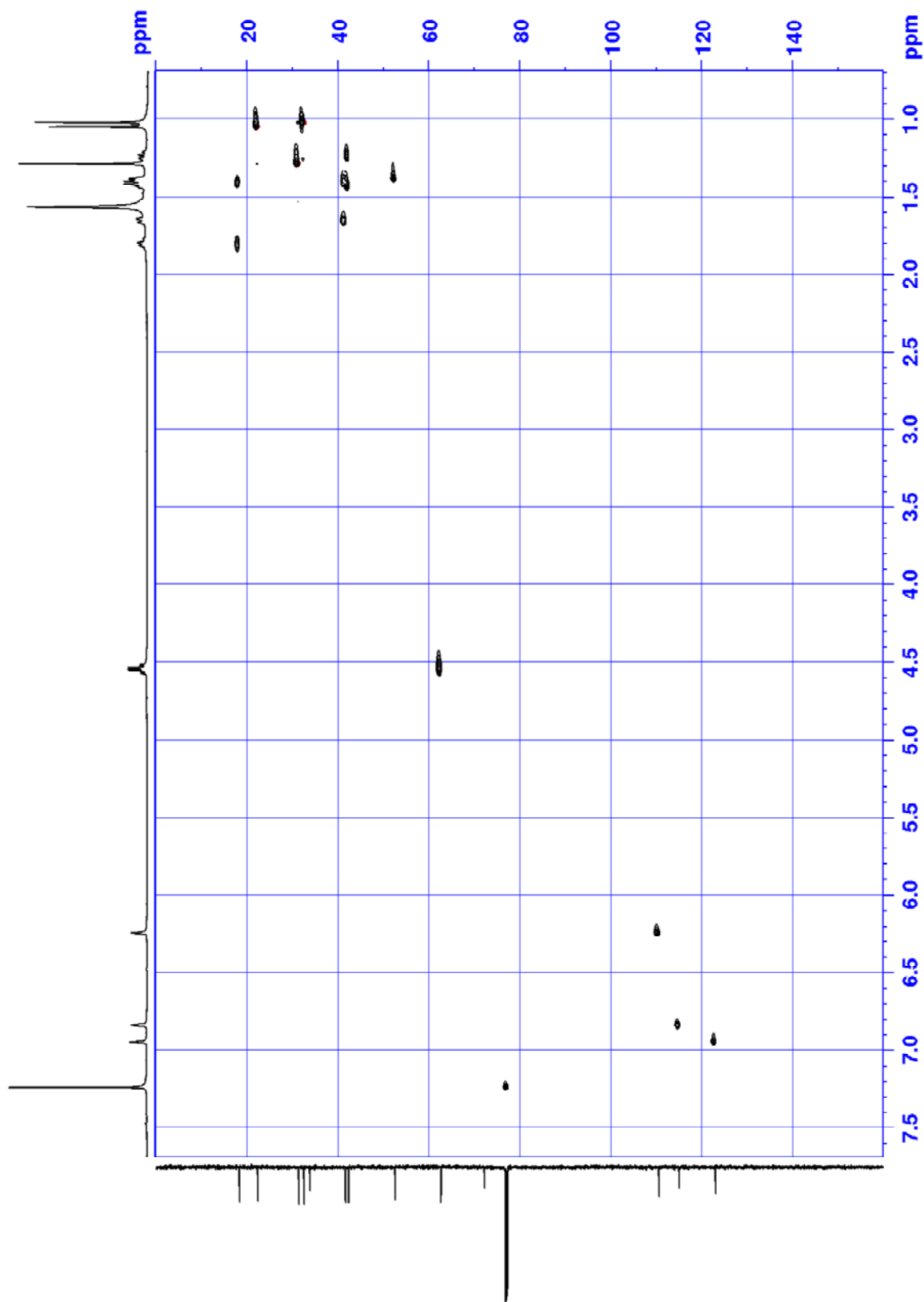




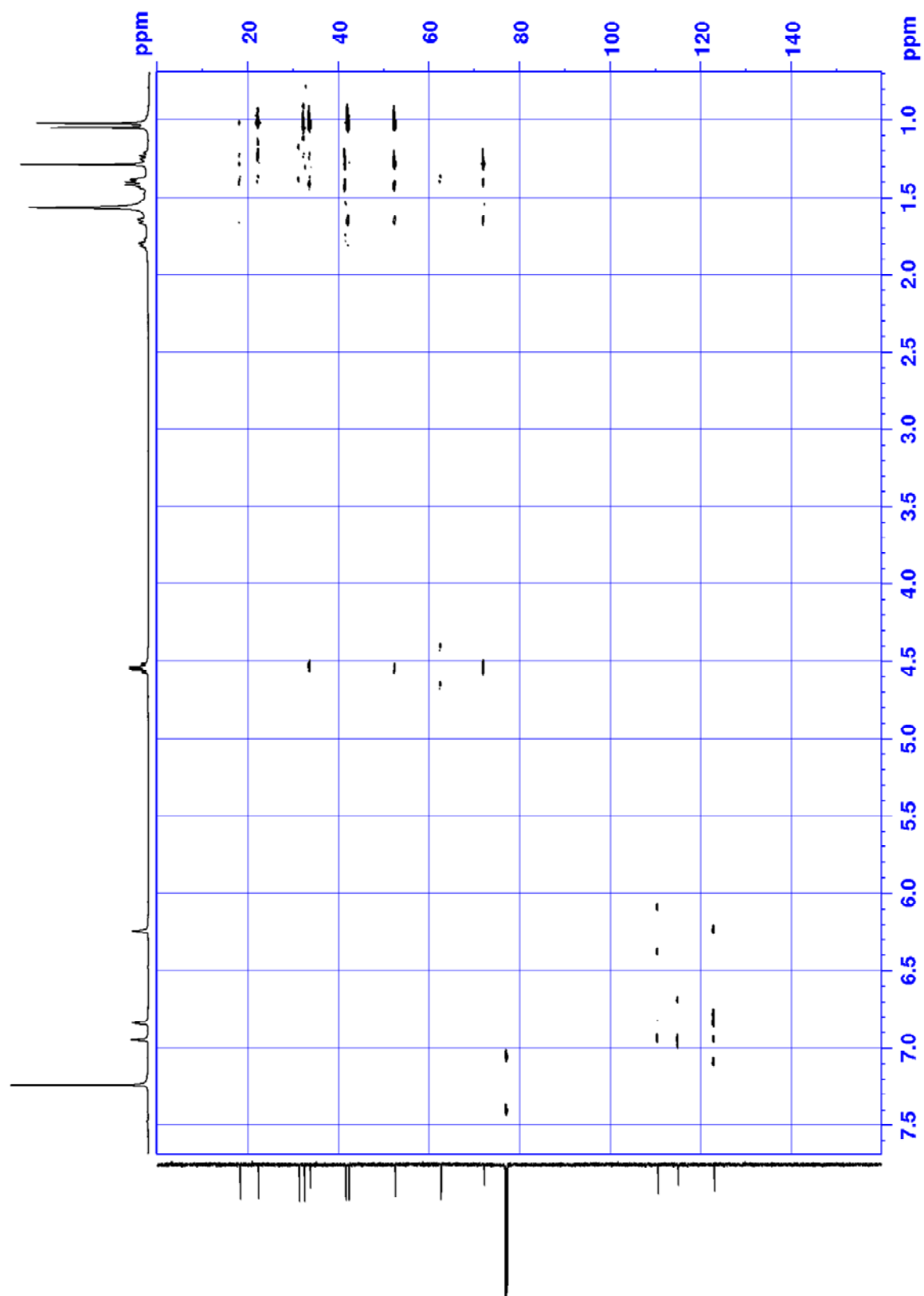
**((1R,3R,6R)-3-bromo-6-hydroxy-2,2,6-trimethylcyclohexyl)methyl 1H-pyrrole-2-carboxylate**  
**(3.41)**



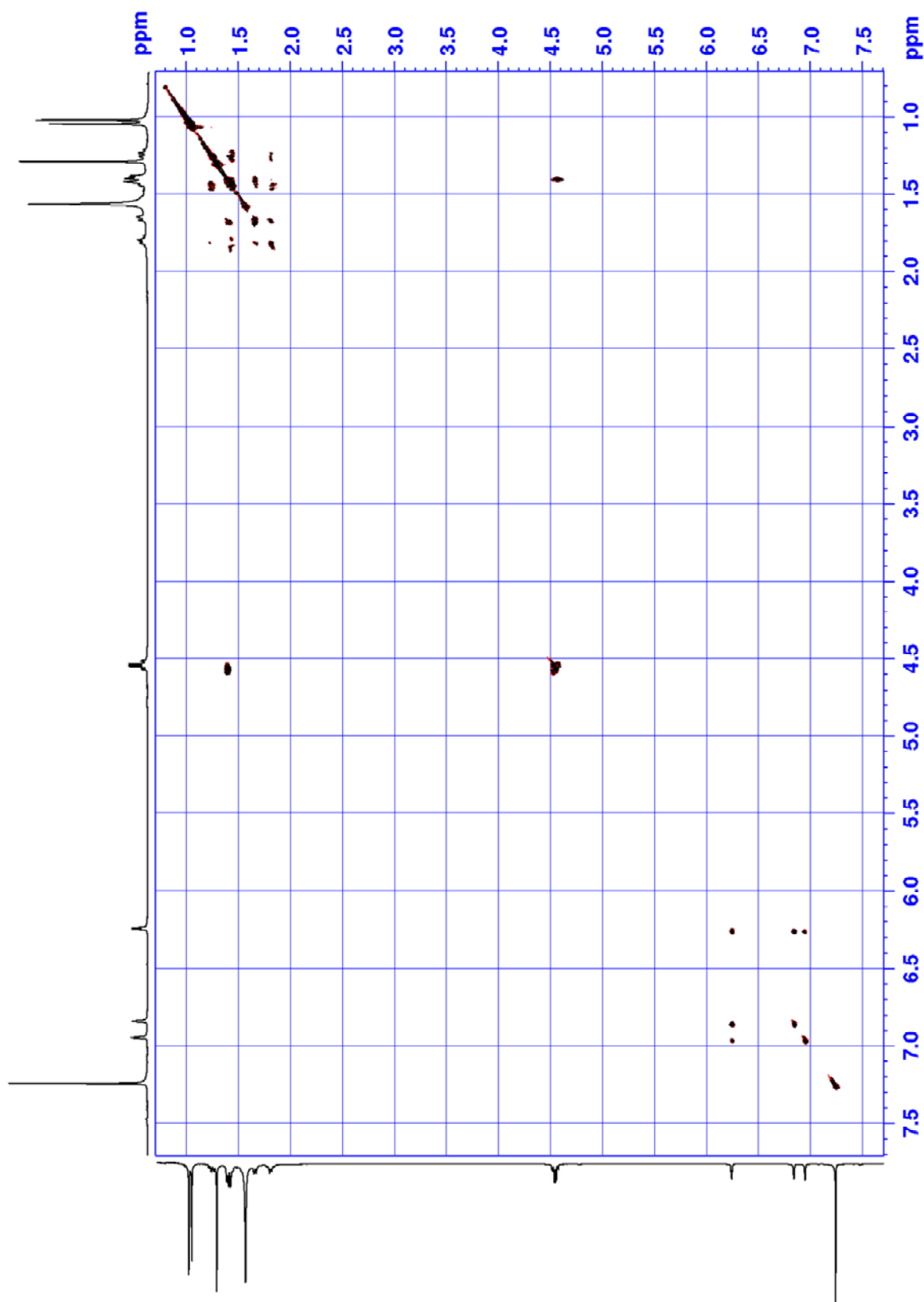
HSQC (3.41)

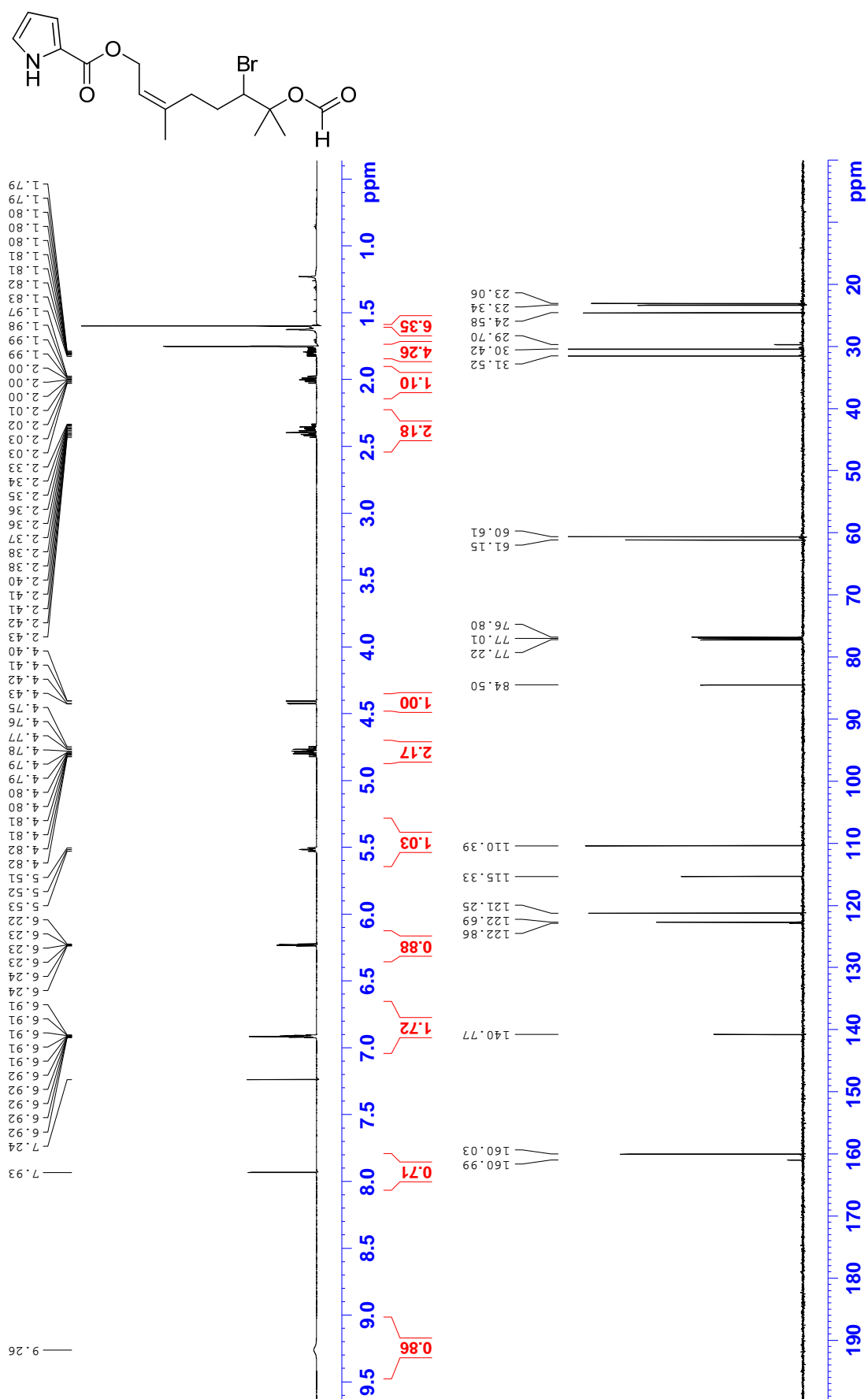


HMBC (3.41)

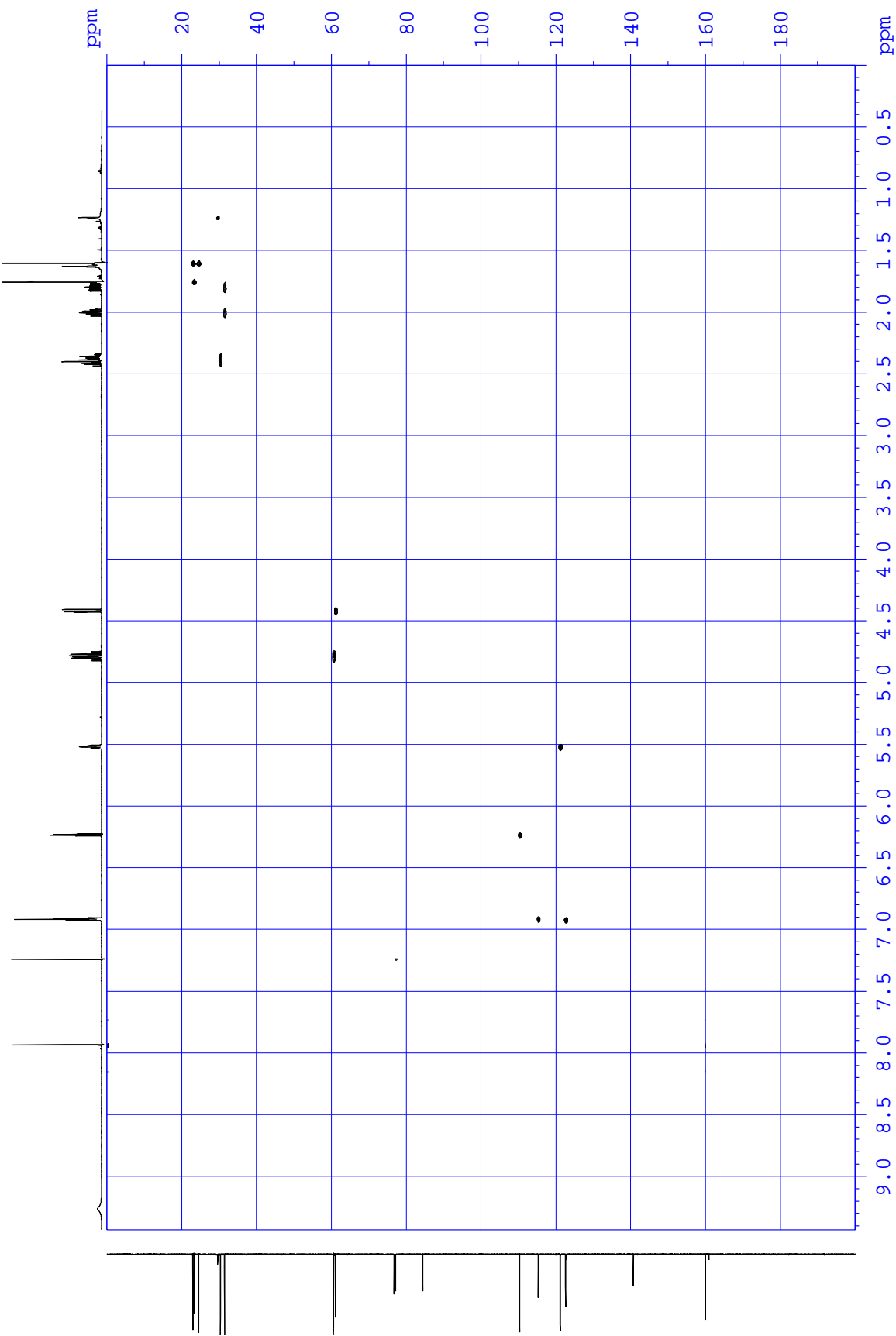


COSY (3.41)

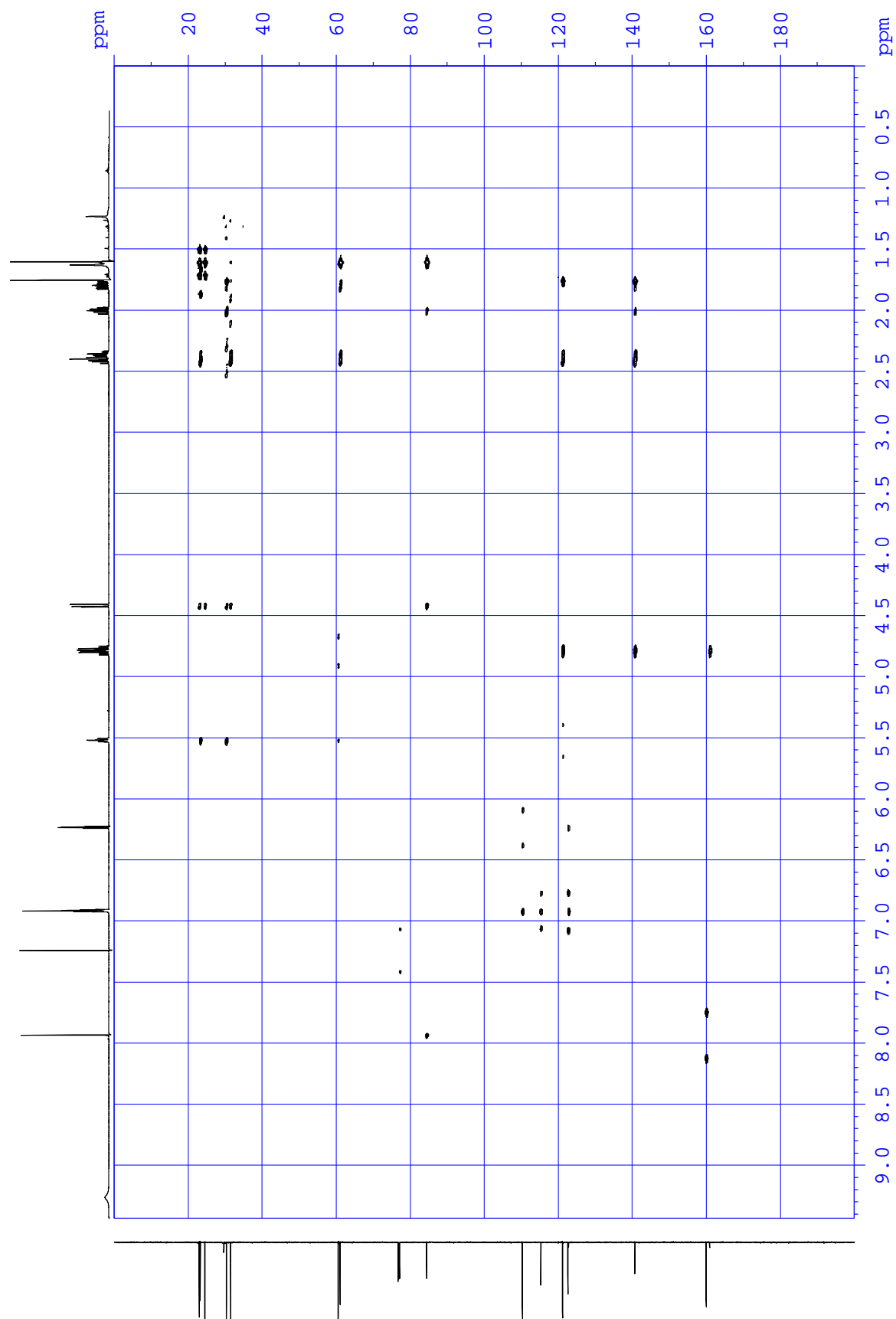


**(Z)-6-bromo-7-(formyloxy)-3,7-dimethyloct-2-en-1-yl 1H-pyrrole-2-carboxylate (3.42)**

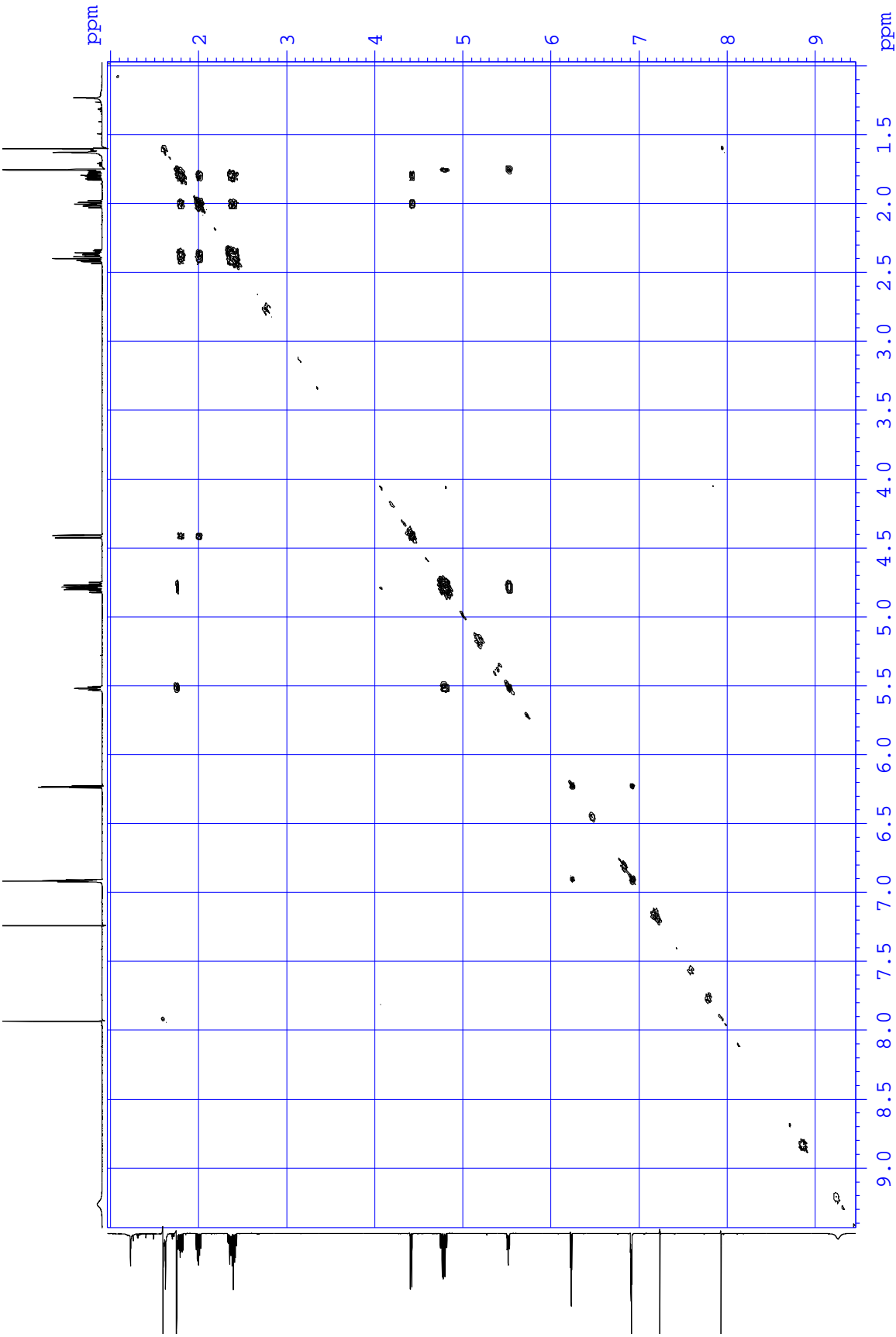
HSQC (3.42)



HMBC (3.42)

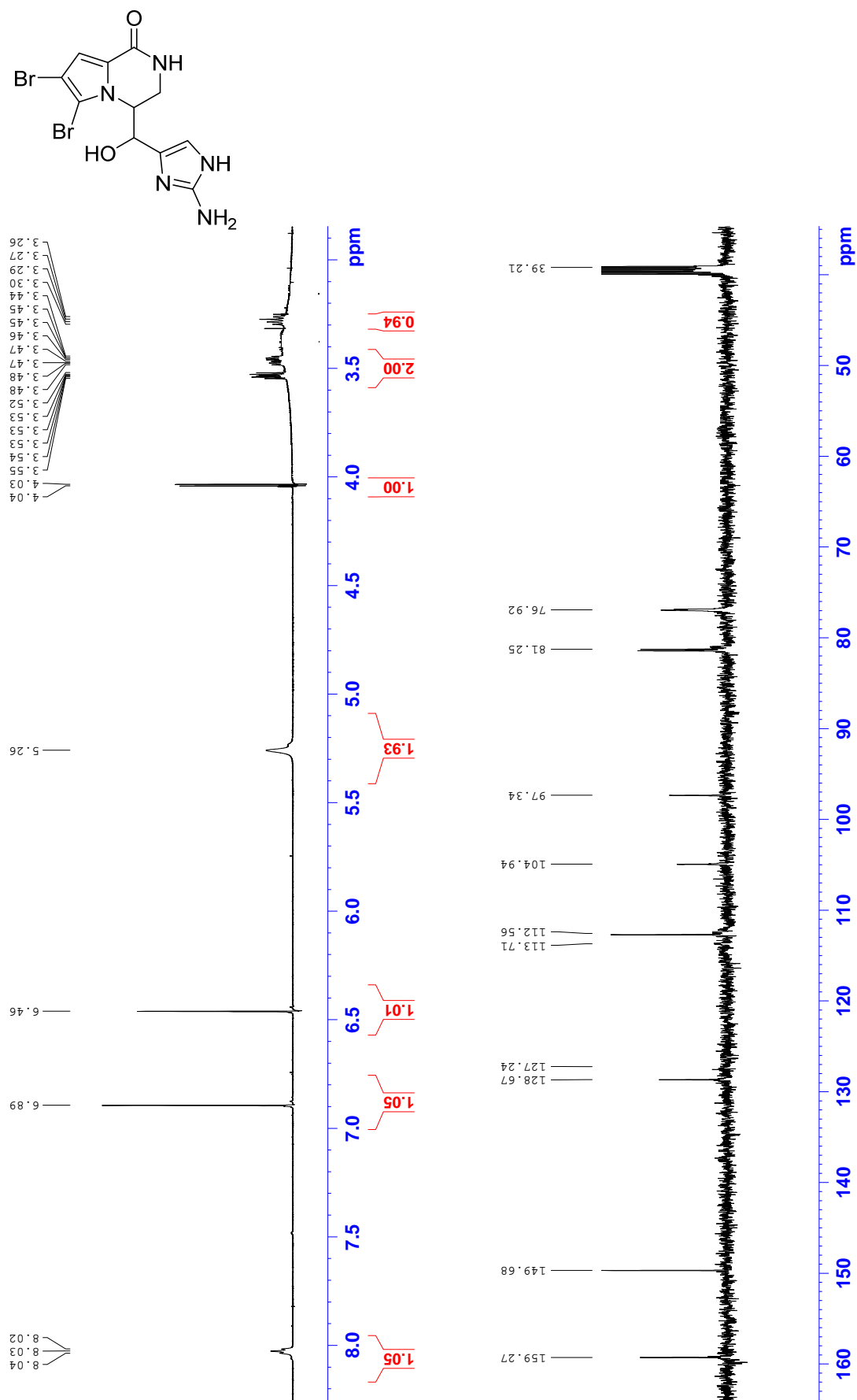


COSY (3.42)

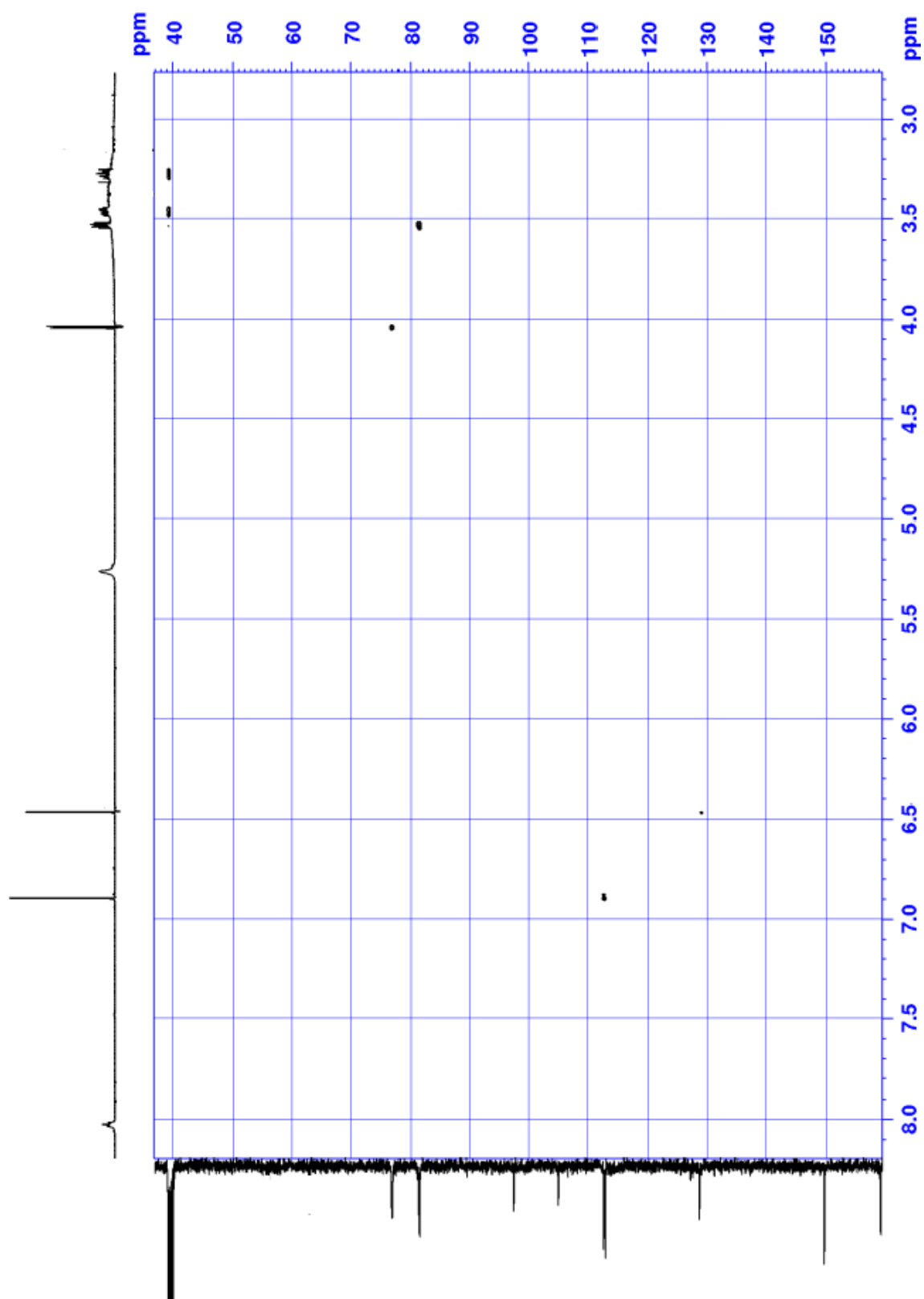




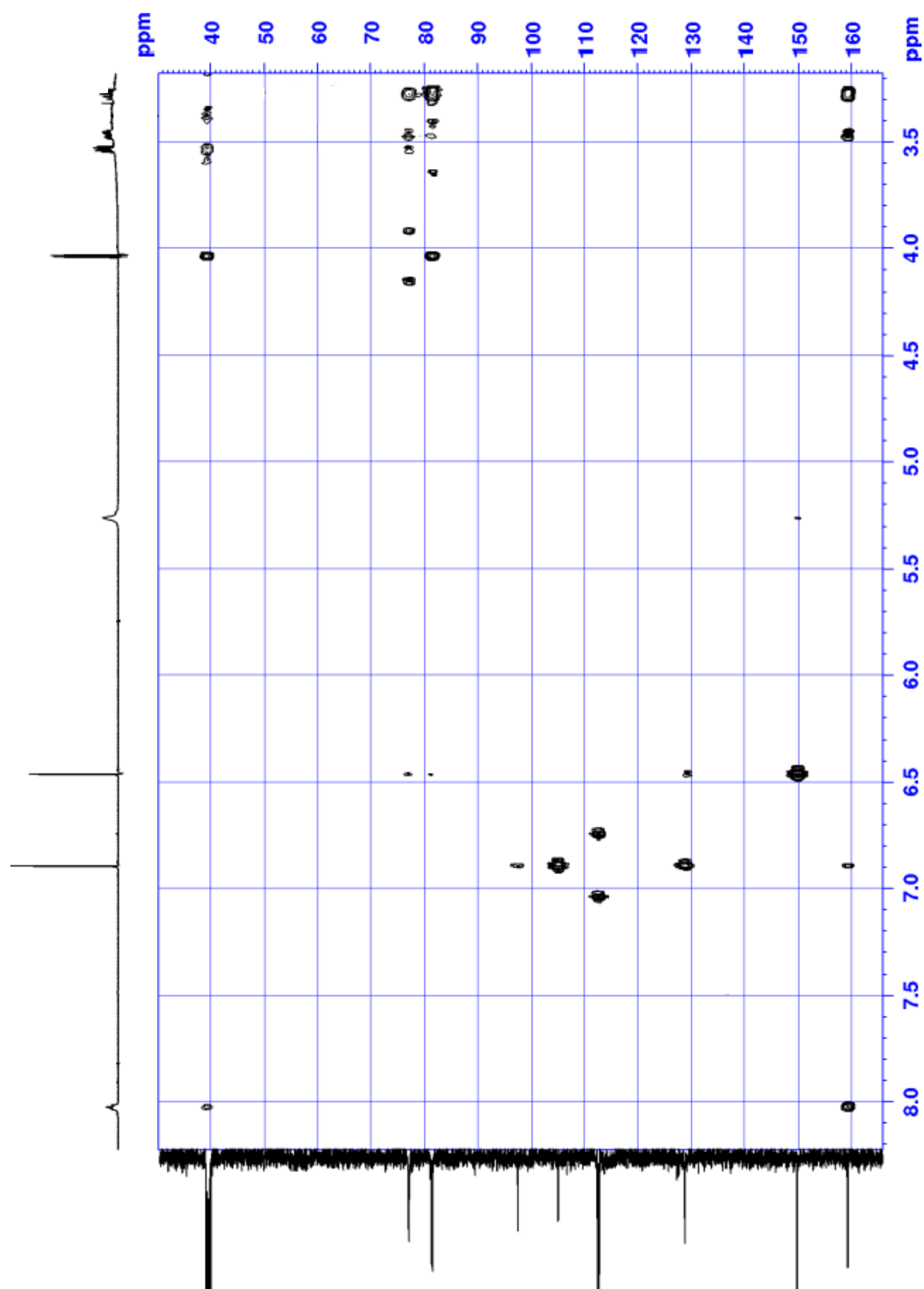
**4-((2-amino-1H-imidazol-4-yl)(hydroxy)methyl)-6,7-dibromo-3,4-dihydropyrrolo[1,2-a]pyrazin-1(2H)-one (3.45)**



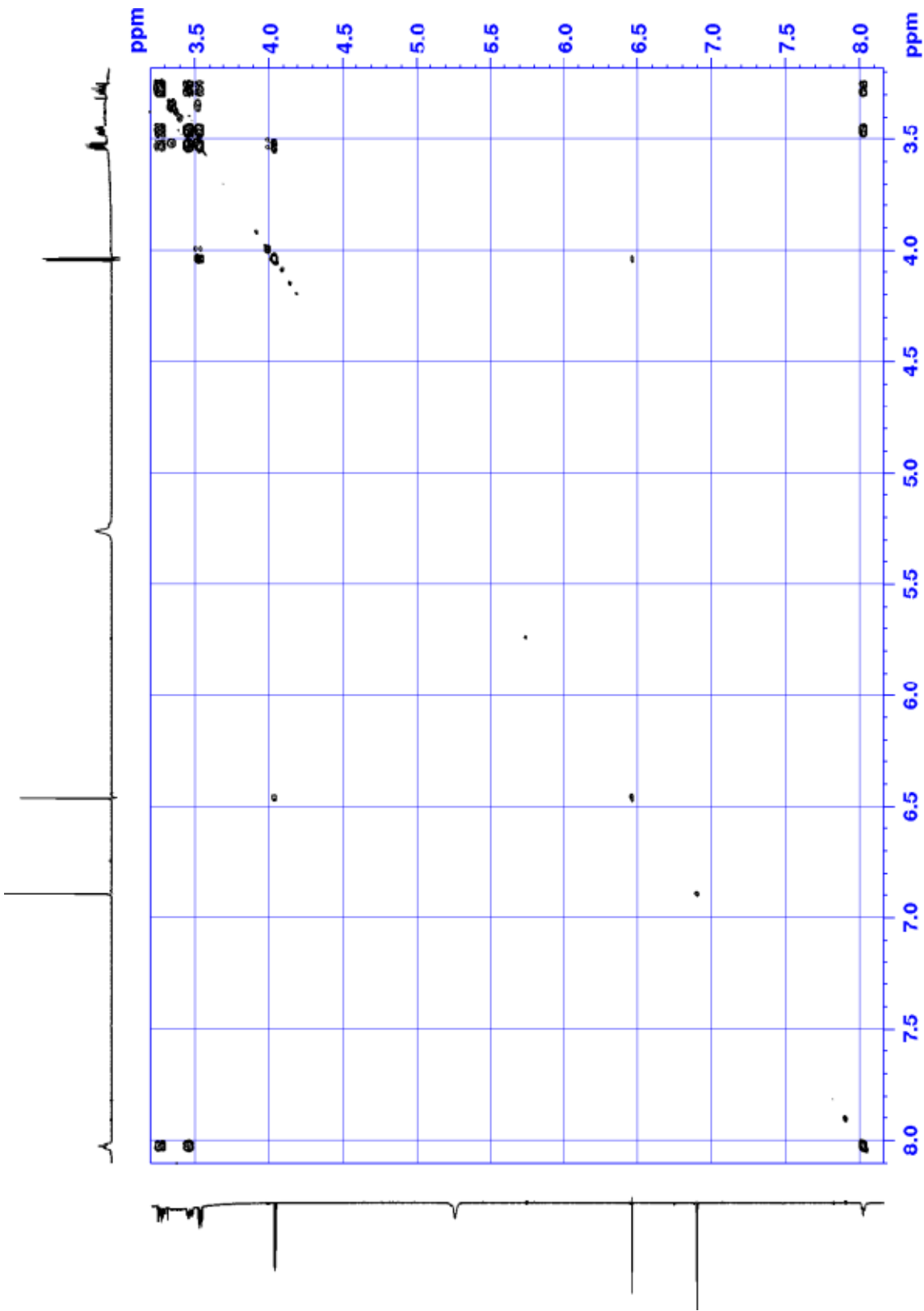
HSQC (3.45)



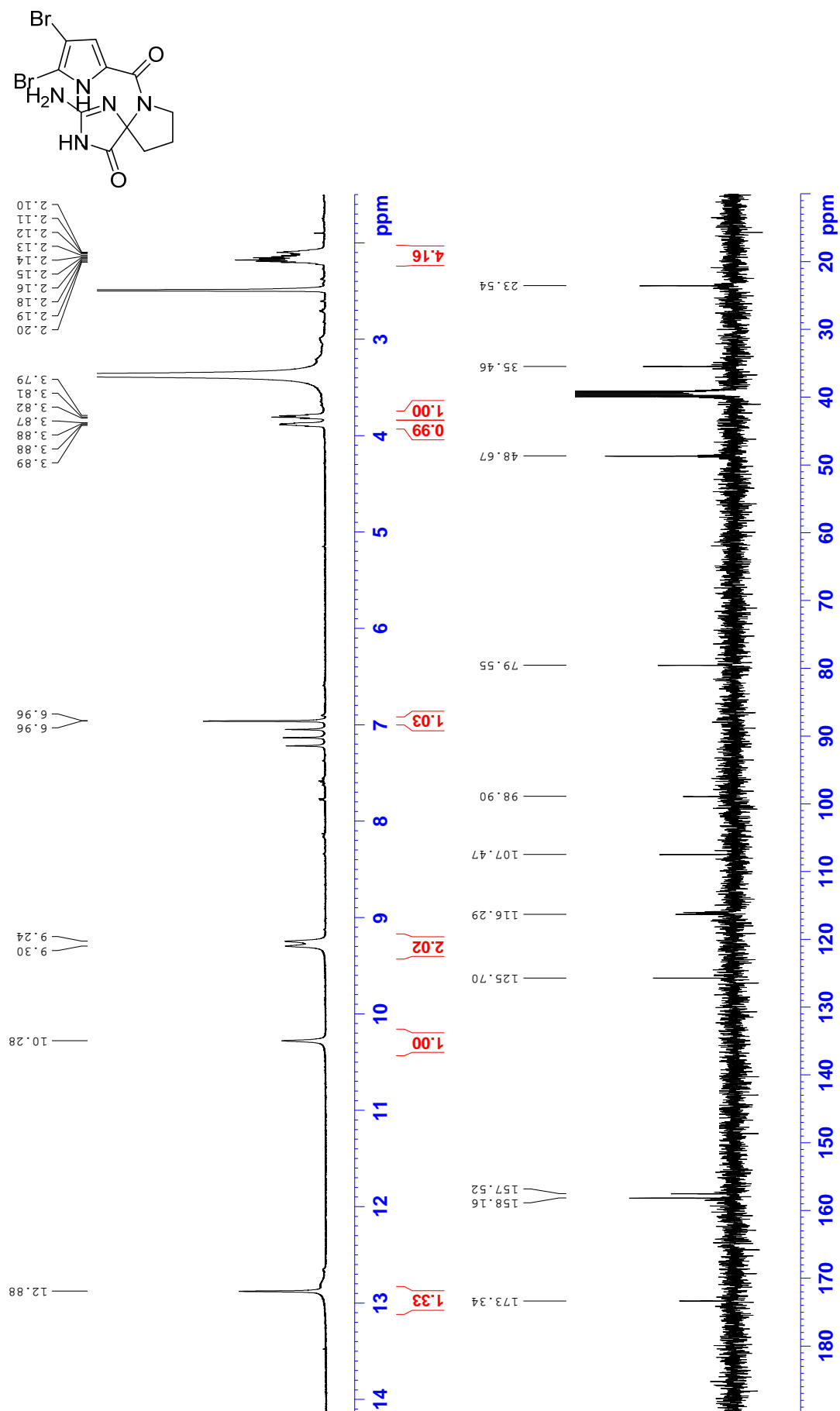
HMBC (3.45)



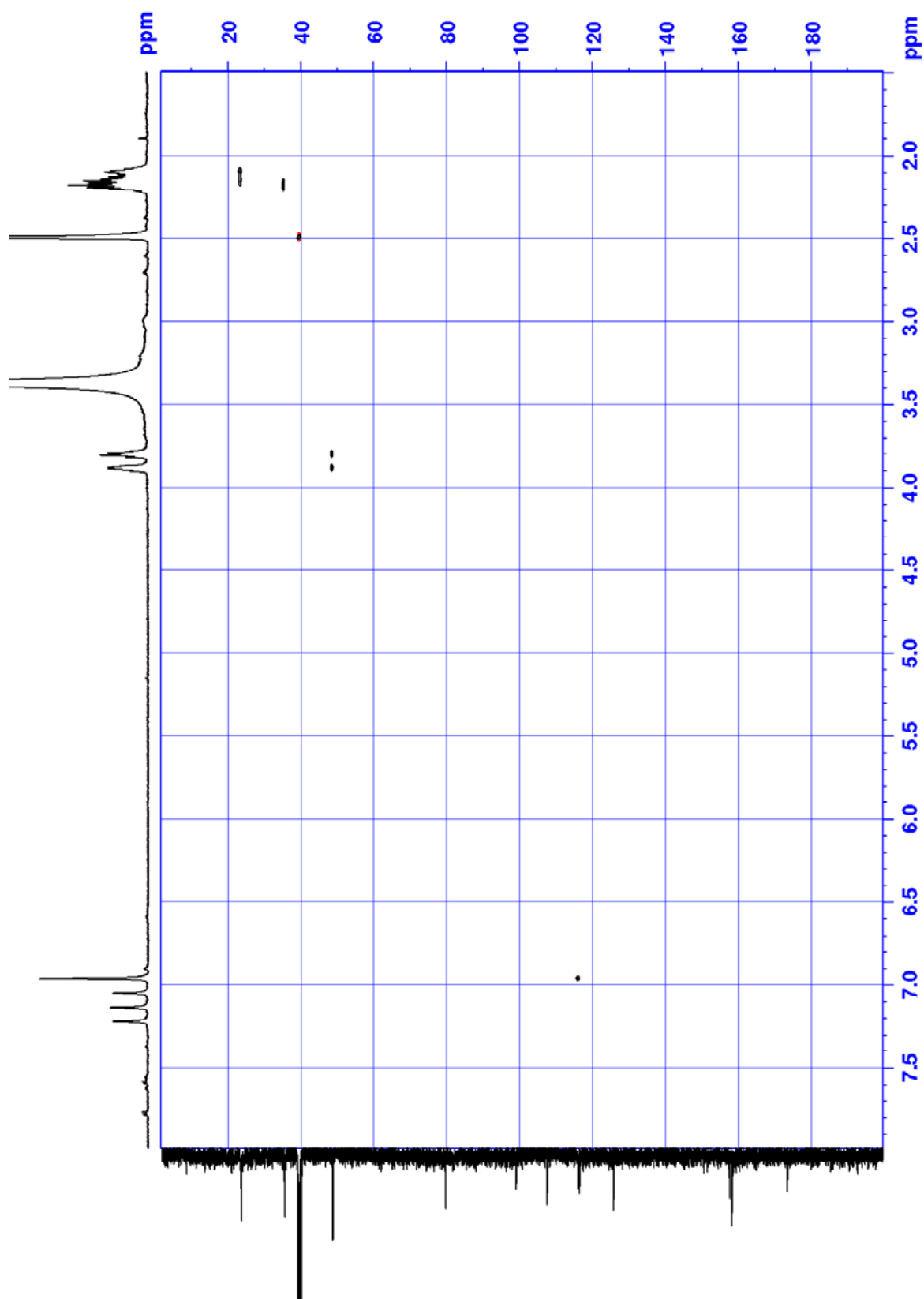
COSY (3.45)



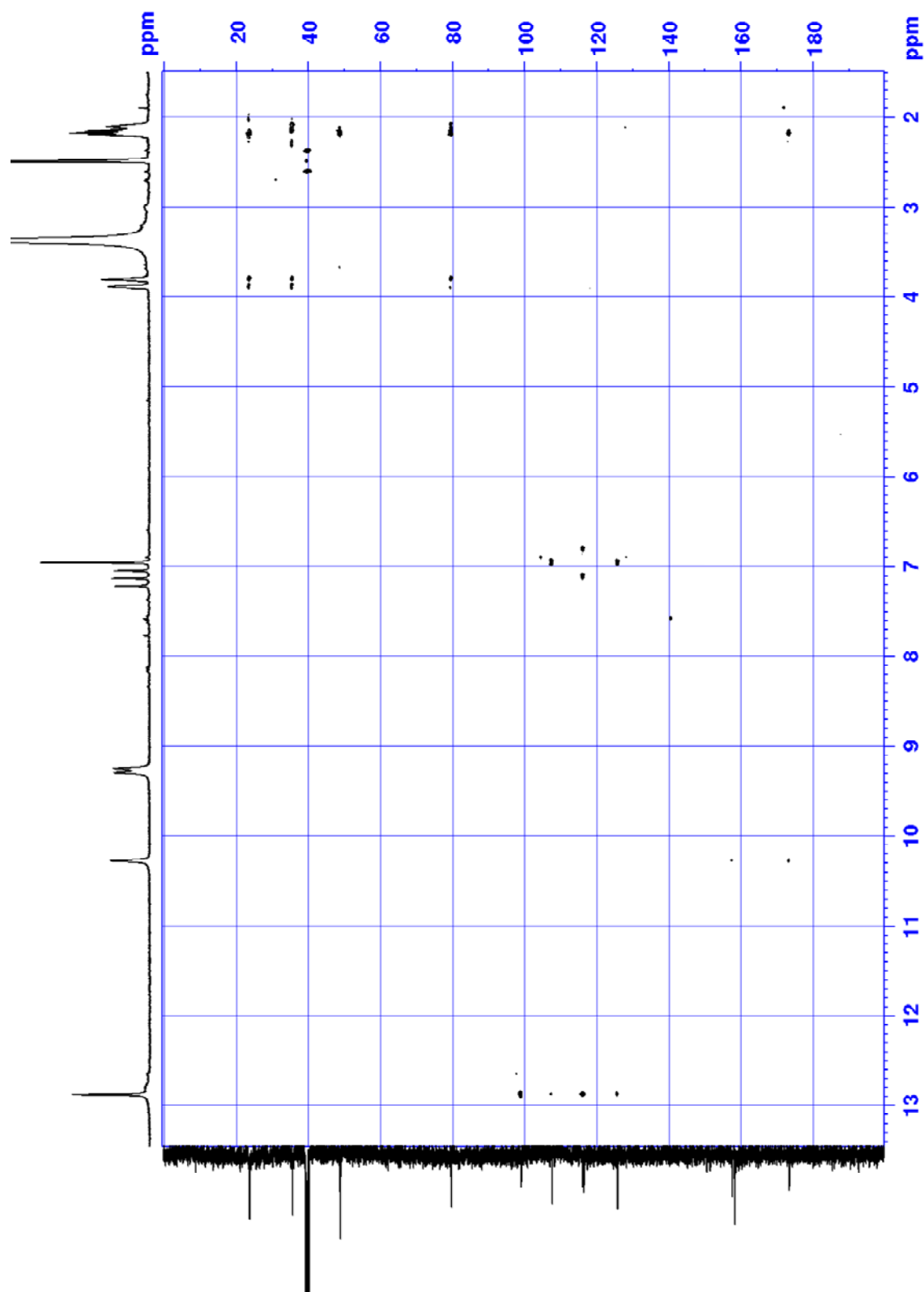
## 2-amino-6-(4,5-dibromo-1H-pyrrole-2-carbonyl)-1,3,6-triazaspiro[4.4]non-1-en-4-one (3.43)



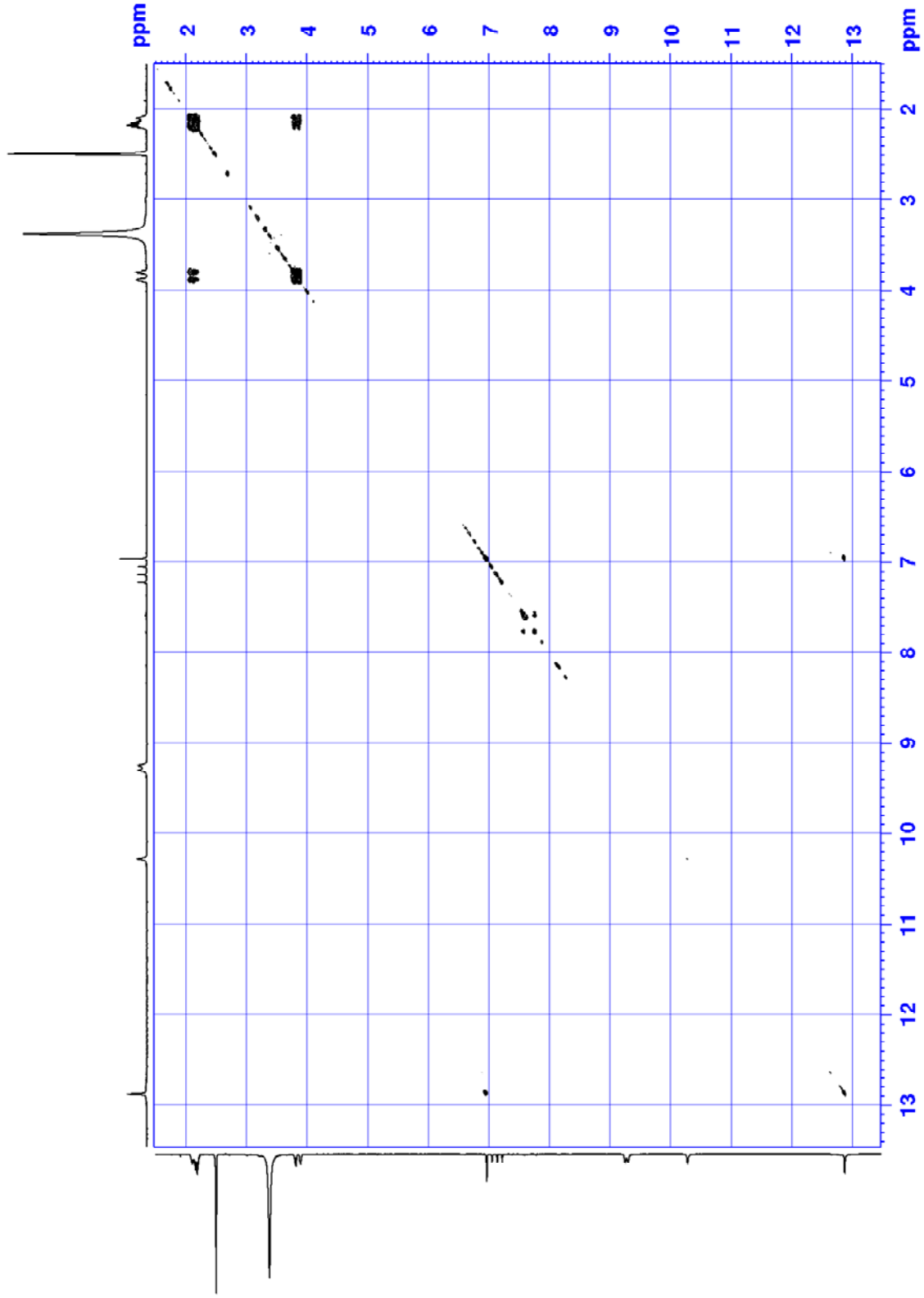
HSQC (3.43)



HMBC (3.43)

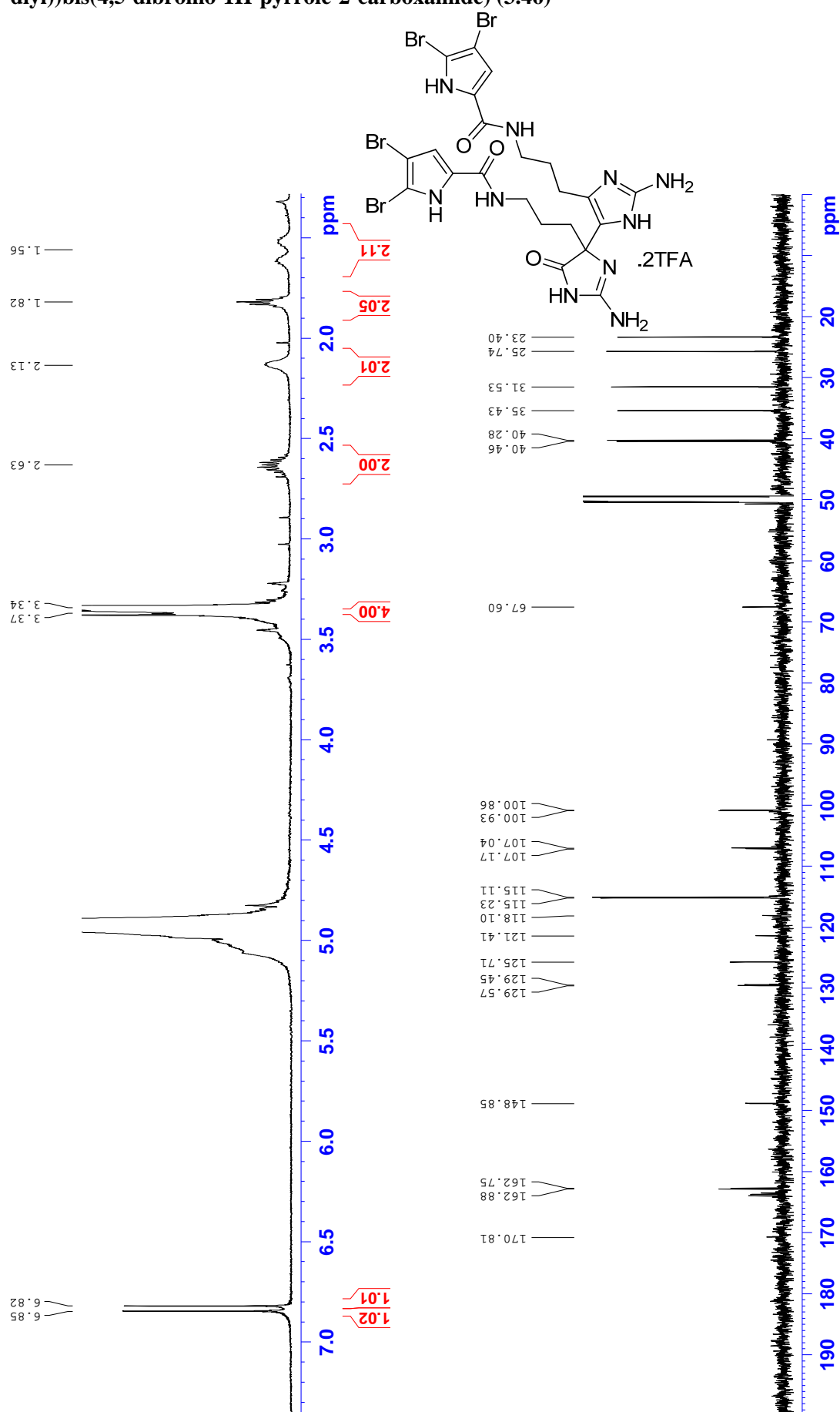


COSY (3.43)

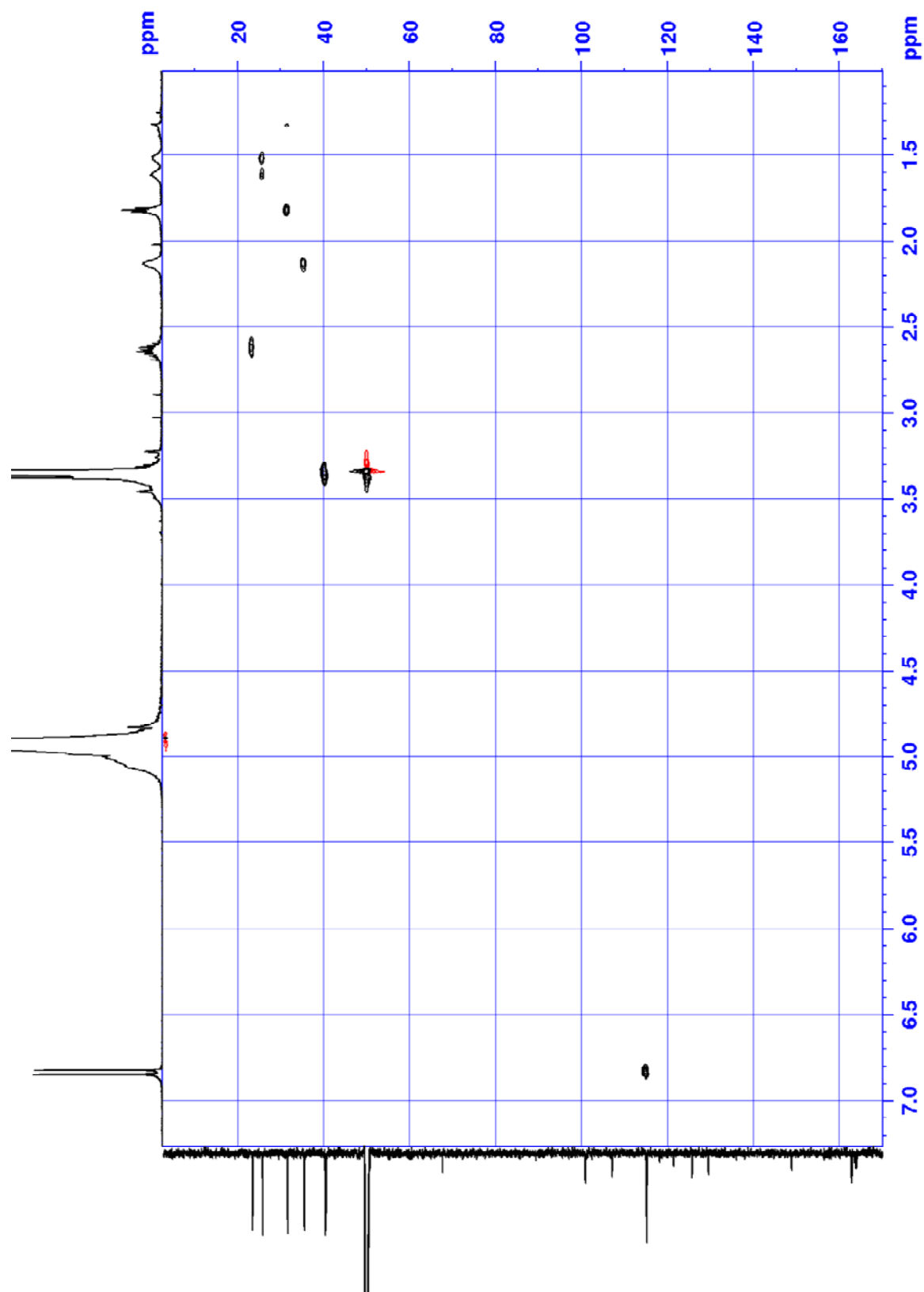




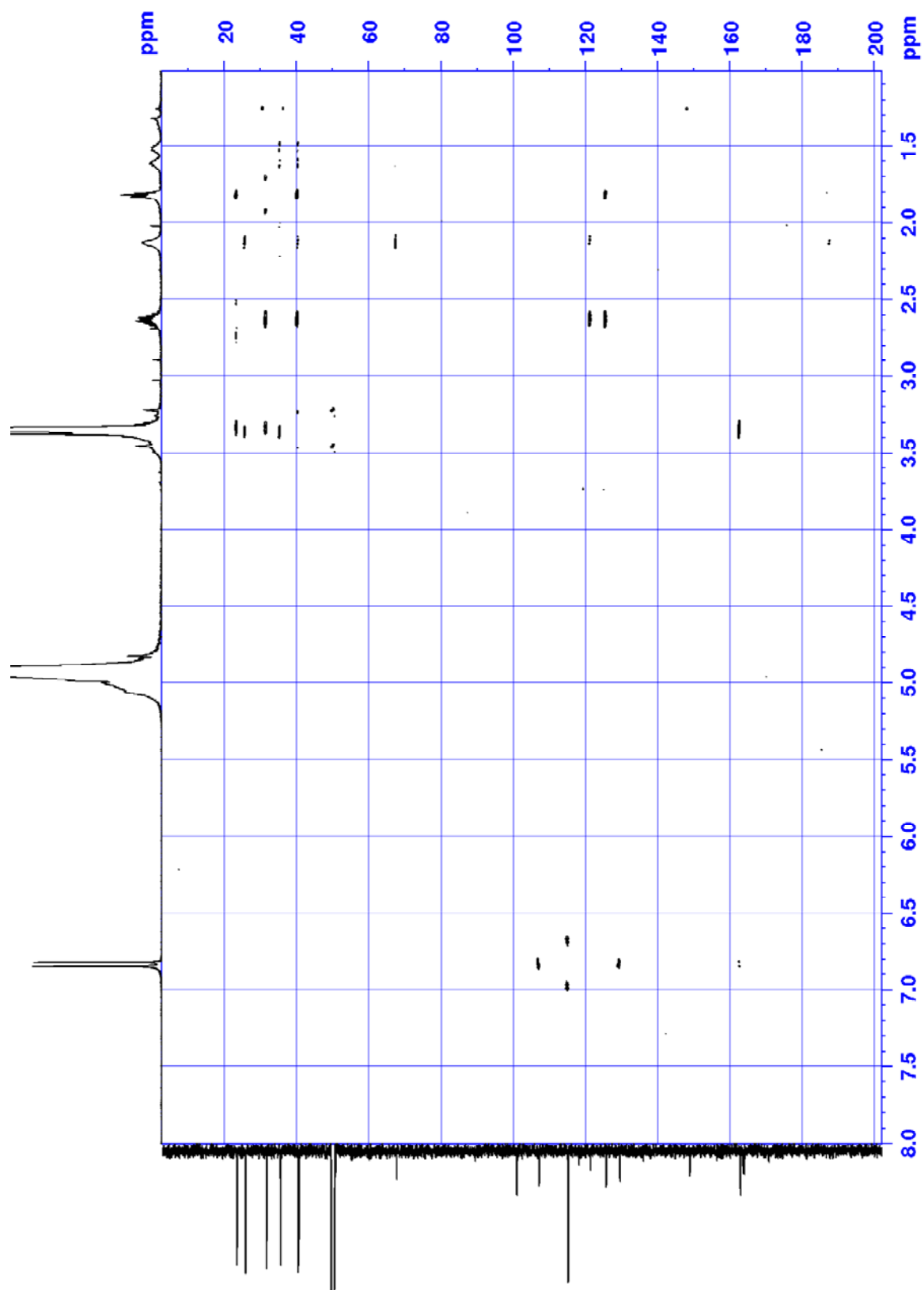
**N,N'-((2,2'-diamino-5'-oxo-1',5'-dihydro-3H,4'H-[4,4'-biimidazole]-4',5-diyl)bis(propane-3,1-diyl))bis(4,5-dibromo-1H-pyrrole-2-carboxamide) (3.46)**



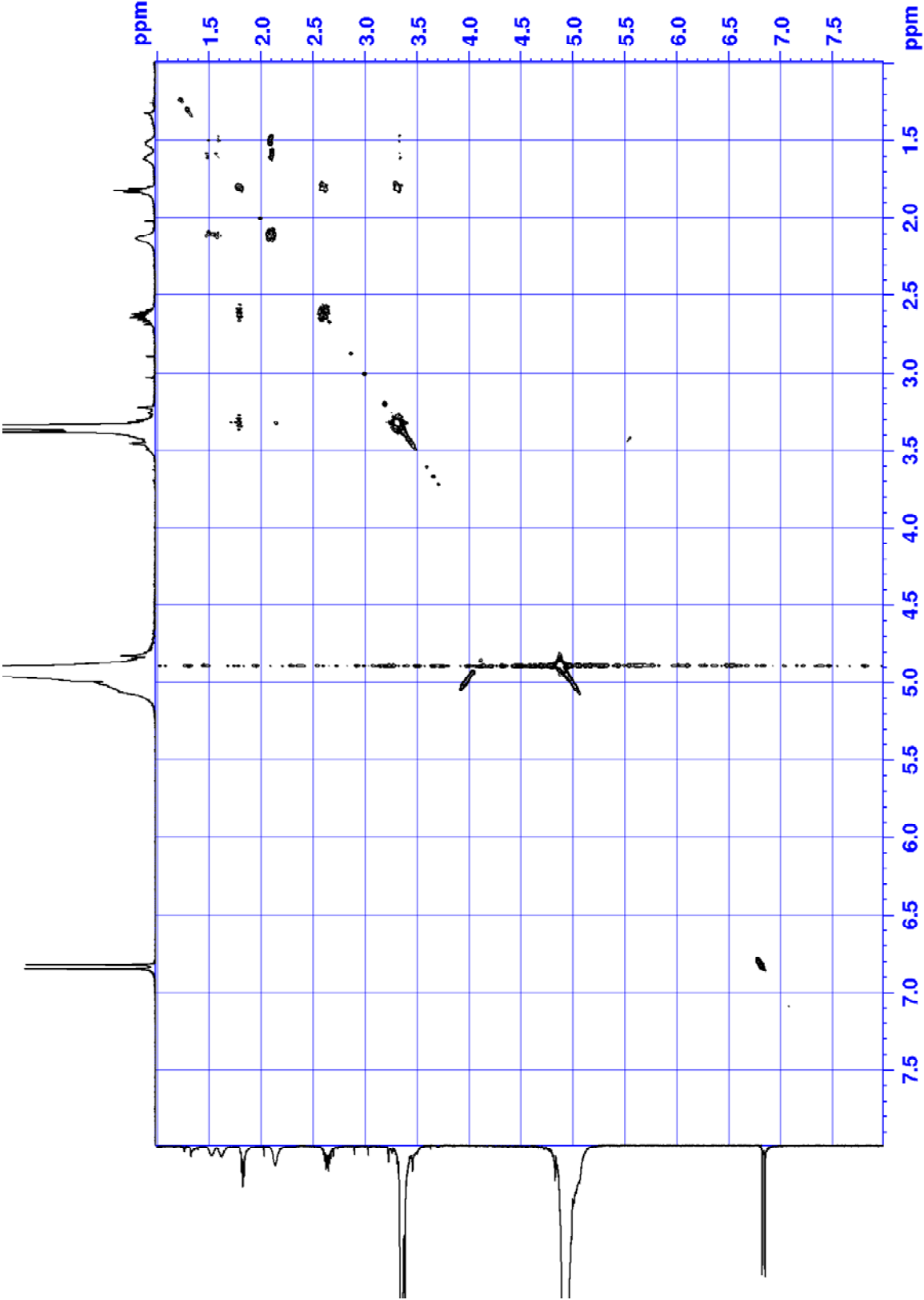
HSQC (3.46)



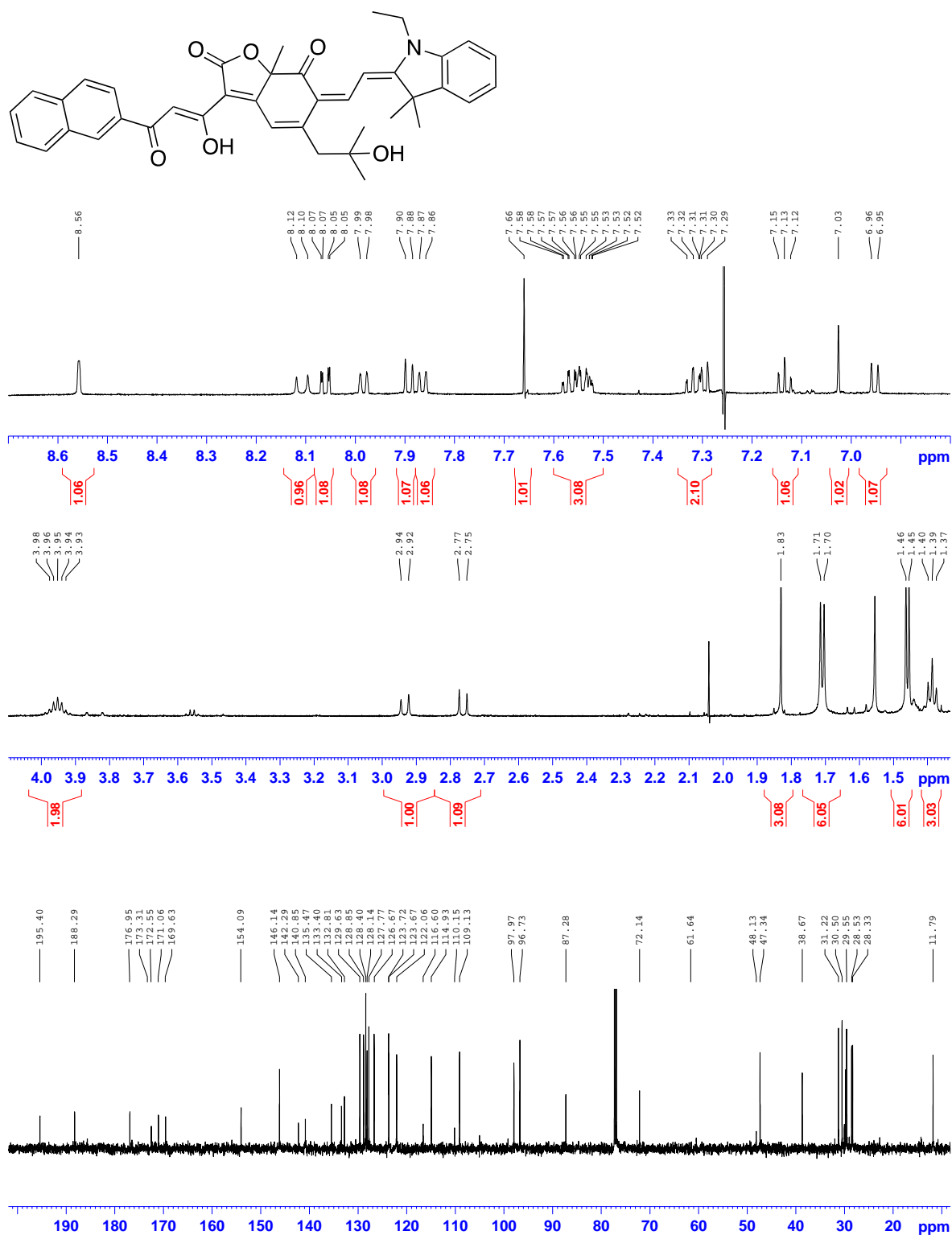
HMBC (3.46)



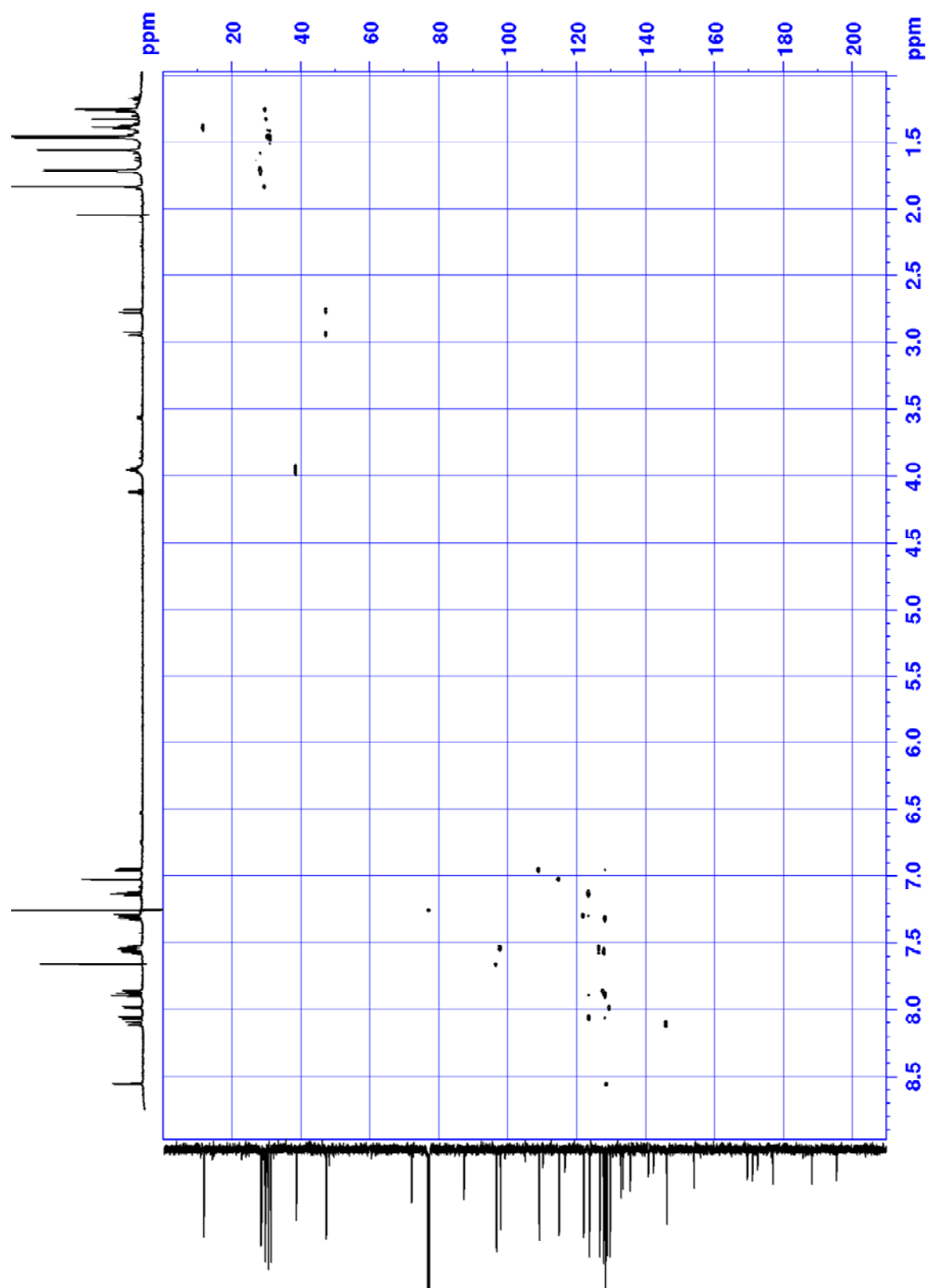
COSY (3.46)



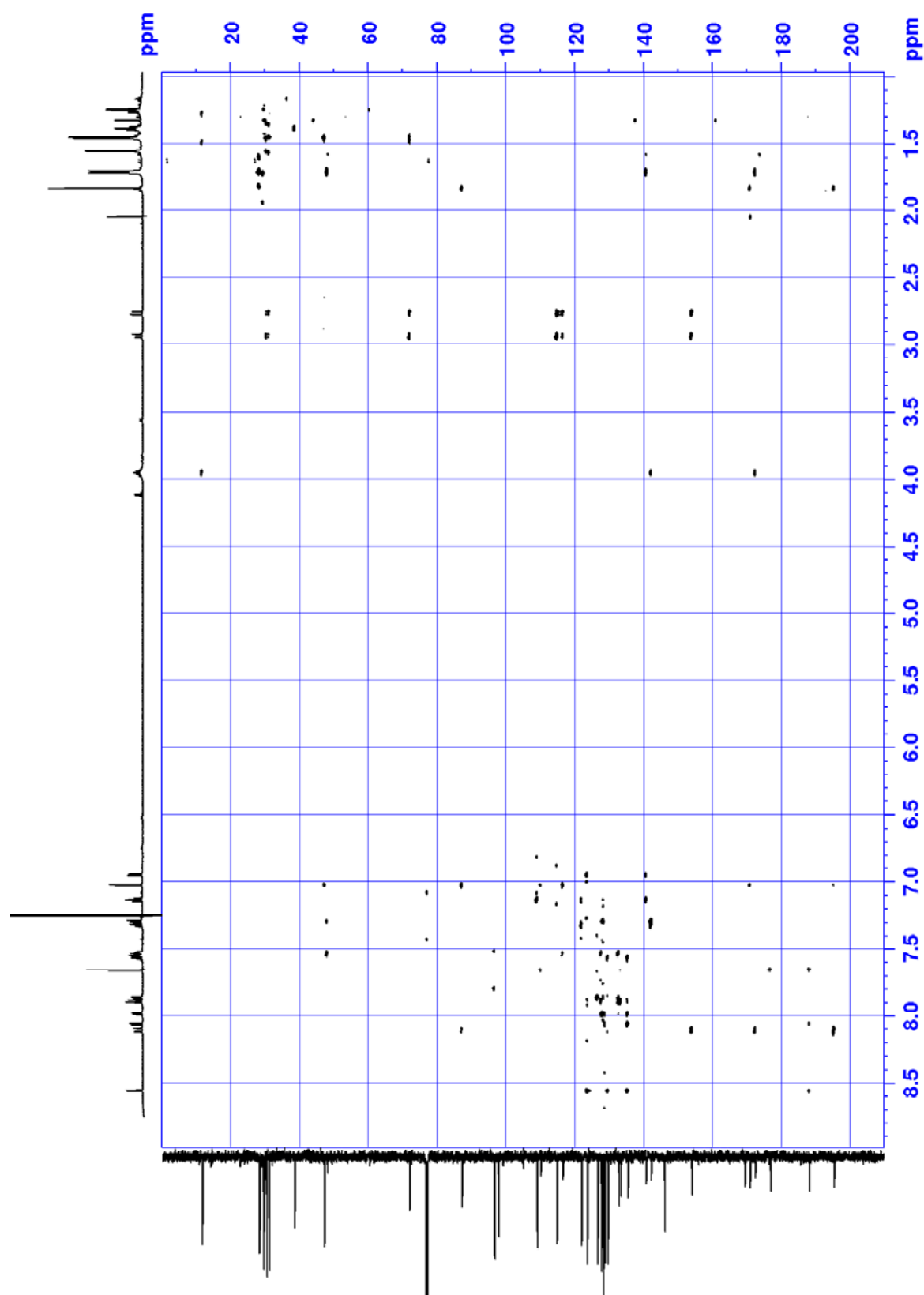
**(Z)-6-((E)-2-(1-ethyl-3,3-dimethylindolin-2-ylidene)ethylidene)-5-(2-hydroxy-2-methylpropyl)-3-((Z)-1-hydroxy-3-(naphthalen-2-yl)-3-oxoprop-1-en-1-yl)-7a-methylbenzofuran-2,7(6H,7aH)-dione (4.48)**



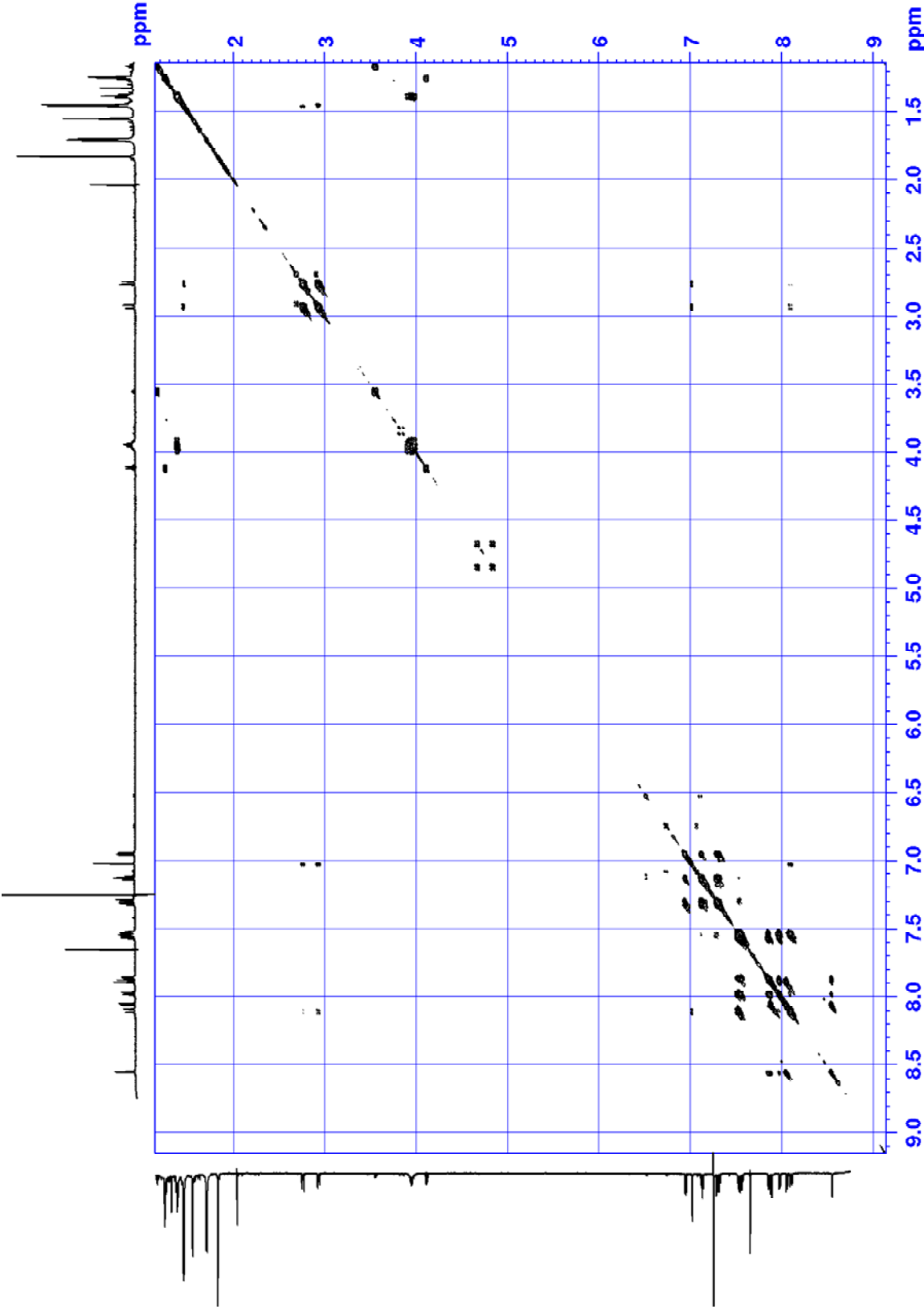
HSQC (4.48)



HMBC (4.48)

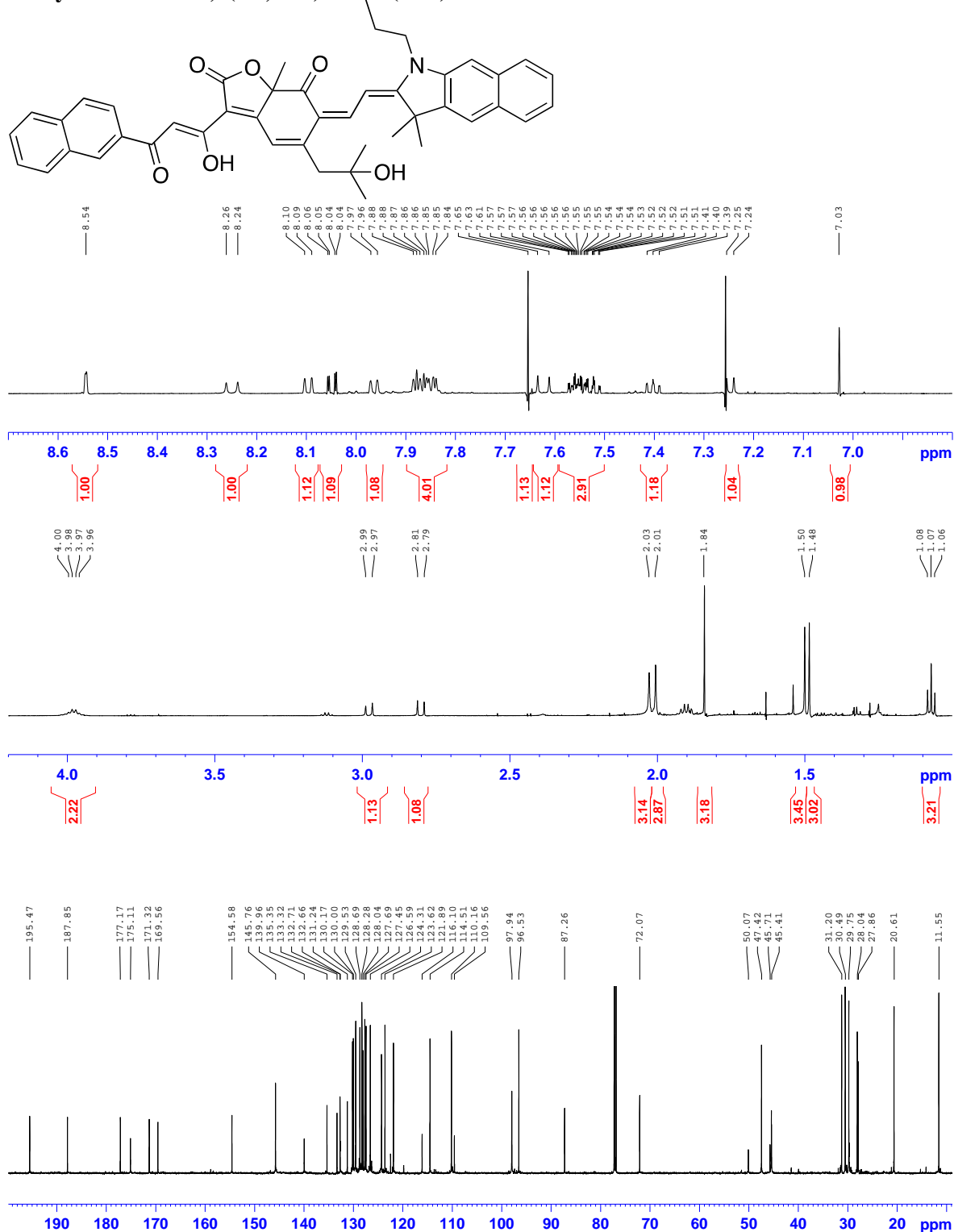


COSY (4.48)

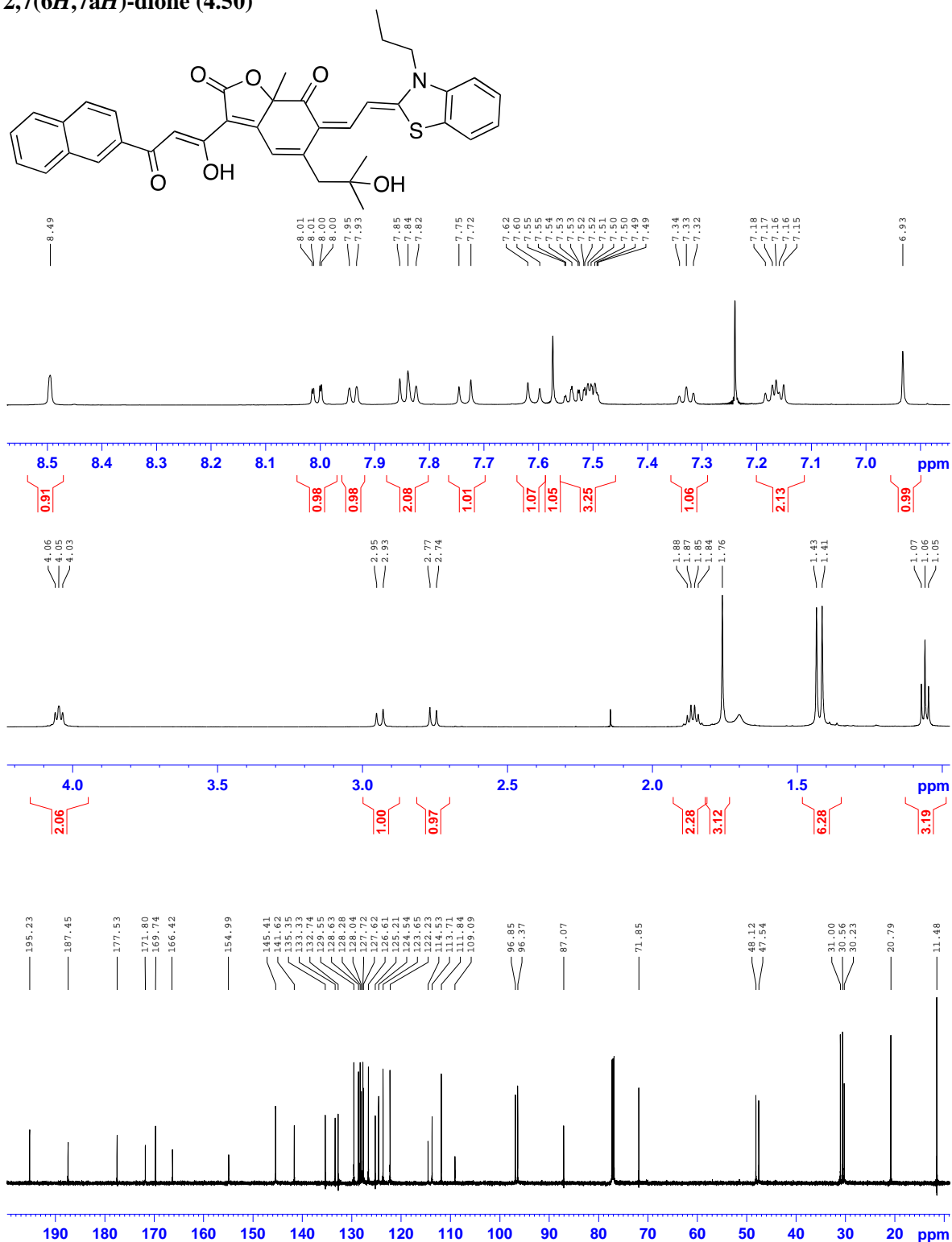




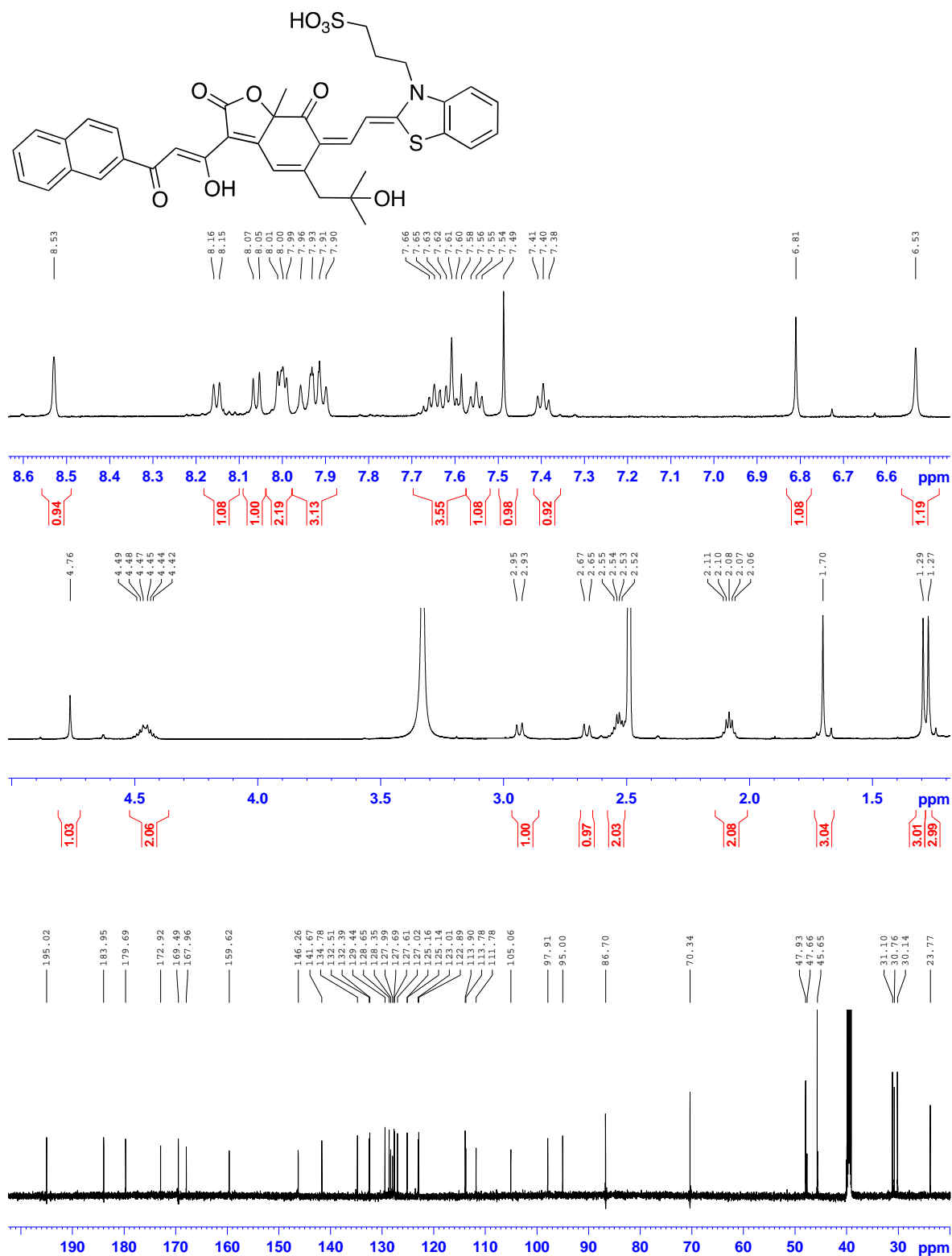
**(Z)-6-((E)-2-(3,3-dimethyl-1-propyl-1H-benzo[f]indol-2(3H)-ylidene)ethylidene)-5-(2-hydroxy-2-methylpropyl)-3-((Z)-1-hydroxy-3-(naphthalen-2-yl)-3-oxoprop-1-en-1-yl)-7a-methylbenzofuran-2,7(6H,7aH)-dione (4.49)**



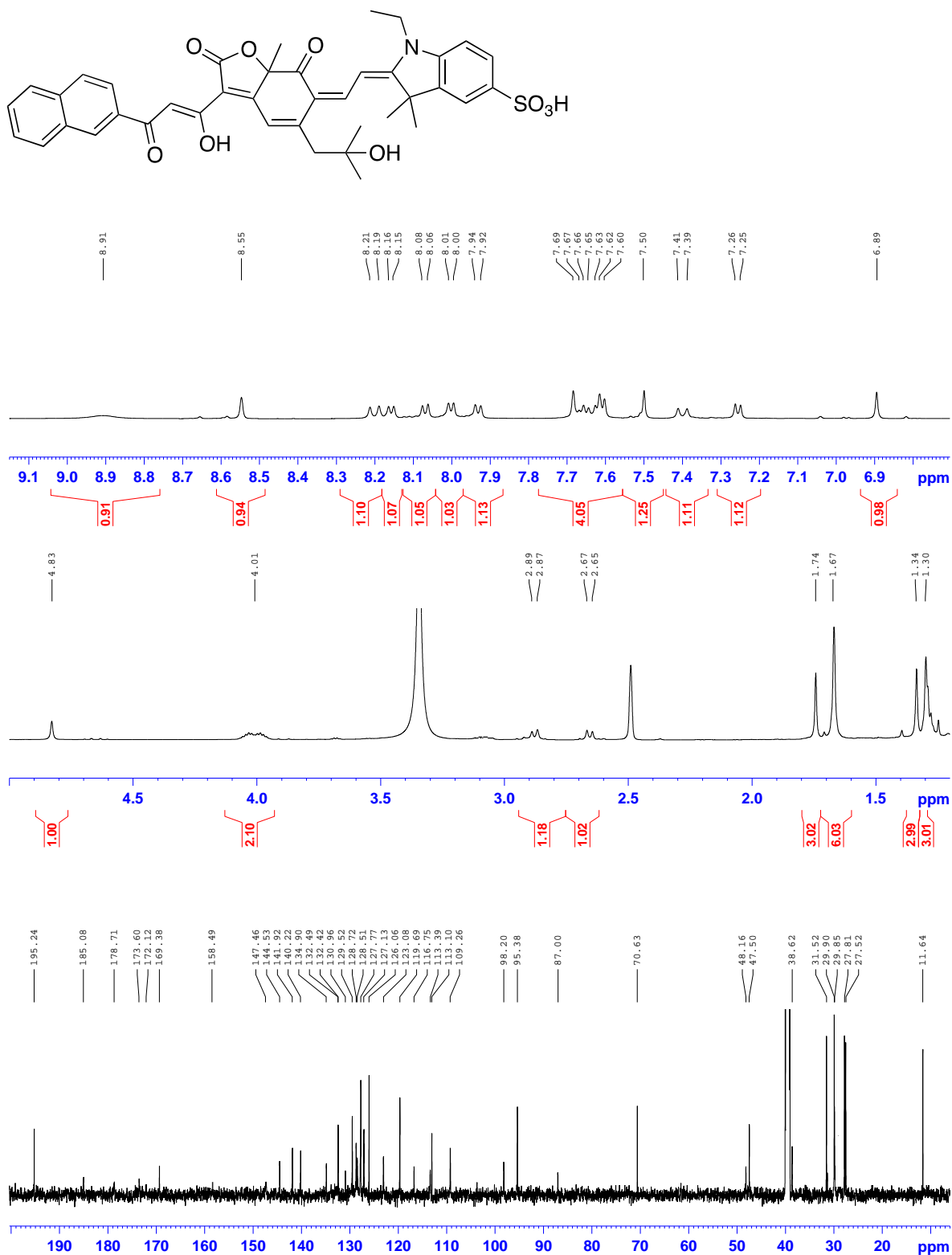
**(Z)-5-(2-hydroxy-2-methylpropyl)-3-((Z)-1-hydroxy-3-(naphthalen-2-yl)-3-oxoprop-1-en-1-yl)-7a-methyl-6-((Z)-2-(3-propylbenzo[d]thiazol-2(3H)-ylidene)ethylidene)benzofuran-2,7(6H,7aH)-dione (4.50)**



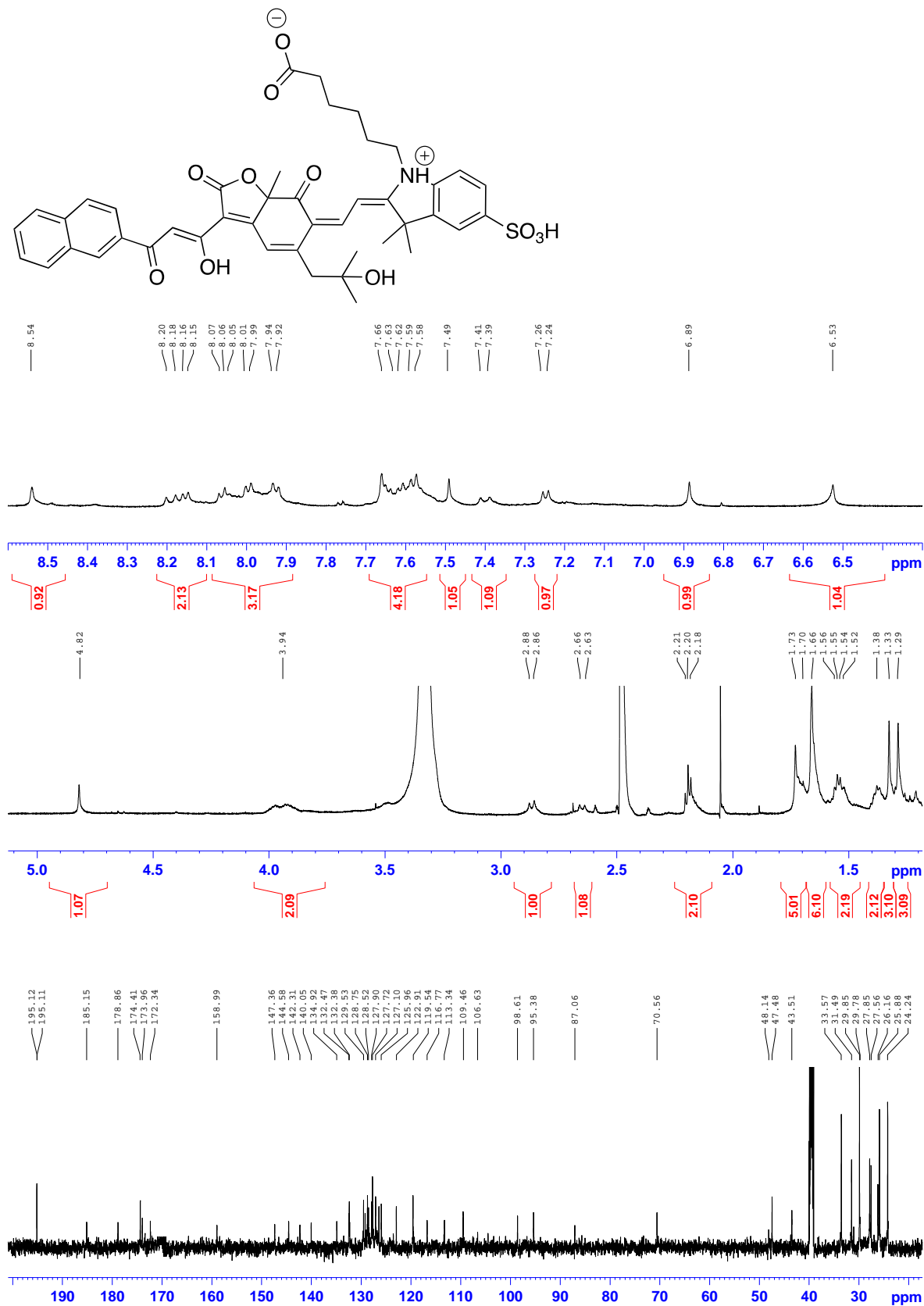
**3-((Z)-2-((Z)-2-(5-(2-hydroxy-2-methylpropyl)-3-((Z)-1-hydroxy-3-(naphthalen-2-yl)-3-oxoprop-1-en-1-yl)-7a-methyl-2,7-dioxo-7,7a-dihydrobenzofuran-6(2H)-ylidene)ethylidene)benzo[d]thiazol-3(2H)-yl)propane-1-sulfonic acid (4.51)**



**(*E*)-1-ethyl-2-((*Z*)-2-(5-(2-hydroxy-2-methylpropyl)-3-((*Z*)-1-hydroxy-3-(naphthalen-2-yl)-3-oxoprop-1-en-1-yl)-7a-methyl-2,7-dioxo-7,7a-dihydrobenzofuran-6(2*H*)-ylidene)ethylidene)-3,3-dimethylindoline-5-sulfonic acid (4.52)**

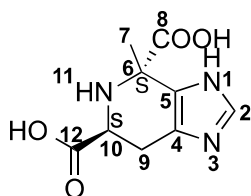


**6-((*E*)-2-((*Z*)-2-(5-(2-hydroxy-2-methylpropyl)-3-((*Z*)-1-hydroxy-3-(naphthalen-2-yl)-3-oxoprop-1-en-1-yl)-7a-methyl-2,7-dioxo-7,7a-dihydrobenzofuran-6(2*H*)-ylidene)ethylidene)-3,3-dimethyl-5-sulfoindolin-1-ium-1-yl)hexanoate (4.53)**



### 6.1.1. NMR Spectroscopic Data- 2D Correlation for Selected Compounds

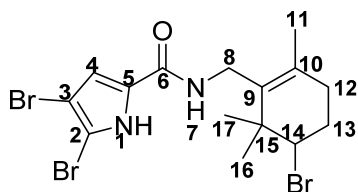
(4*S*,6*S*)-4-methyl-4,5,6,7-tetrahydro-3*H*-imidazo[4,5-*c*]pyridine-4,6-dicarboxylic acid (1.8)



#### NMR Spectroscopic Data-2D correlation (600 MHz, MeOD-*d*<sub>4</sub>, 598K)

Position	$\delta_c$ , Type	$\delta_H$ , Multiplicity	COSY	HMBC
1-NH	-	-	-	-
2	135.3, CH	8.63, s	-	4, 5
3-N	-	-	-	-
4	124.5, C	-	-	-
5	123.6, C	-	-	-
6	158.8, C	-	-	-
7	21.29, CH <sub>3</sub>	1.83, s	-	5, 6, 8
8	169.85, C	-	-	-
9	21.32, CH <sub>2</sub>	3.33/3.00, dd	9, 10	5, 10
10	53.9, CH	4.42, dd	9	4
11-NH	-	-	-	-
12	169.95, C	-	-	-

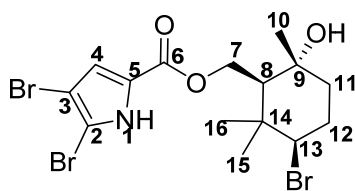
**4,5-dibromo-N-((5-bromo-2,6,6-trimethylcyclohex-1-en-1-yl)methyl)-1H-pyrrole-2-carboxamide (3.37d)**



**NMR Spectroscopic Data-2D correlation (600 MHz, CDCl<sub>3</sub>, 598K)**

Position	$\delta_c$ , Type	$\delta_H$ , Multiplicity	COSY	HMBC
1-NH	-	9.72, br s	-	-
2	105.3, C	-	-	-
3	99.9, C	-	-	-
4	111.6, CH	6.50, d	-	2, 5
5	126.0, C	-	-	-
6	158.8, C	-	-	-
7-NH	-	5.37, br t	8	-
8	38.0, CH <sub>2</sub>	4.00, d	7	6, 9, 10, 15
9	131.8, C	-	-	-
10	133.4, C	-	-	-
11	19.6, CH <sub>3</sub>	1.69, s	-	10, 9
12	29.6, CH <sub>2</sub>	2.23/2.16, m	13	9, 14
13	31.9, CH <sub>2</sub>	2.16, m	12, 14	10, 15
14	65.0, CH	4.21, m	13	9, 12, 16, 17
15	40.0, C	-	-	-
16	27.4, CH <sub>3</sub>	1.165, s	-	9, 15
17	25.0, CH <sub>3</sub>	1.17, s	-	9, 15

**((1S,3R,6R)-3-bromo-6-hydroxy-2,2,6-trimethylcyclohexyl)methyl 4,5-dibromo-1H-pyrrole-2-carboxylate (3.38d)**

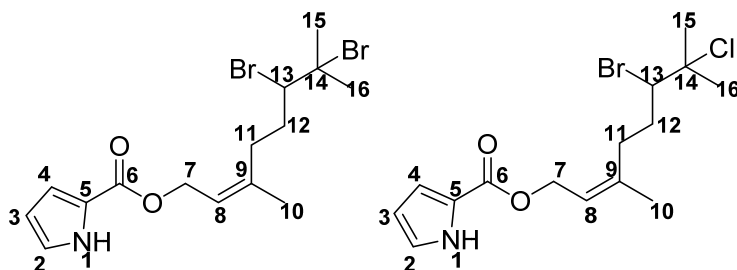


**NMR Spectroscopic Data-2D correlation (600 MHz, CDCl<sub>3</sub>, 598K)**

Position	$\delta_c$ , Type	$\delta_H$ , Multiplicity	COSY	HMBC	NOESY
1-NH	-	9.14, br s	-	-	-
2	100.9, C	-	-	-	-
3	107.2, C	-	-	-	-
4	117.7, CH	6.81, d	-	2, 5	-
5	124.0, C	-	-	-	-
6	159.3, C	-	-	-	-
7	62.9, CH <sub>2</sub>	4.61/4.49, dd	8	6, 8, 9, 14	8, 10, 15, 16
8	47.2, CH	1.85, t	7	7, 10, 14	7, 10, 11, 16
9	71.9, C	-	-	-	-
10	31.2, CH <sub>3</sub>	1.34, s	-	8, 9, 11	7, 8, 11
11a/11b	36.1, CH <sub>2</sub>	2.17/1.53, m	-	8, 9, 13	10, 11, 12
12a/12b	27.6, CH <sub>2</sub>	2.43/1.89, m	11, 13	9, 13, 14	11, 12, 13
13	69.6, CH	4.31, t	12	8, 11	12, 15, 16
14	38.7, C	-	13	-	-
15	23.1, CH <sub>3</sub>	1.25, s	-	8, 13, 14, 16	7, 13, 12a
16	32.3, CH <sub>3</sub>	1.17, s	-	8, 13, 14, 15	7, 13, 8



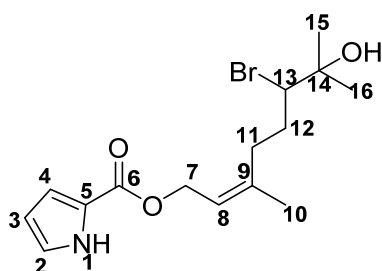
**(Z)-6,7-dibromo-3,7-dimethyloct-2-en-1-yl 1H-pyrrole-2-carboxylate (3.39a) and (Z)-6-bromo-7-chloro-3,7-dimethyloct-2-en-1-yl 1H-pyrrole-2-carboxylate (3.39b)**



**NMR Spectroscopic Data-2D correlation (600 MHz, CDCl<sub>3</sub>, 598K)**

Position	$\delta_c$ , Type	$\delta_H$ , Multiplicity	COSY	HMBC
1-NH	-	9.11, br s	-	-
2	122.6, CH	6.92, m	3	3
3	110.4, CH	6.24, m	2, 4	2, 4
4	115.3, CH	6.92, m	3	3
5	122.9, C	-	-	-
6	161.0, C	-	-	-
7	60.8 (60.7), CH <sub>2</sub>	4.80, m	8	6, 8, 9
8	121.3(121.3), CH	5.55, t	7, 10	10, 11
9	140.7(140.8), C	-	-	-
10	23.3 (23.3), CH <sub>3</sub>	1.80, s		8, 9, 11
11a, 11b	30.2, CH <sub>2</sub>	2.48/2.37, m	12	8, 10, 13
12a, 12b	34.0, CH <sub>2</sub>	2.58/1.90, m	11, 13	9, 14
13	65.6 (64.7), CH	4.12(3.98), dd	12, 15, 16	11, 14, 15, 16
14	68.7, C	-	-	-
15	35.4 (32.5), CH <sub>3</sub>	1.95(1.76), s	16	13, 14, 16
16	28.0 (26.9), CH <sub>3</sub>	1.78(1.64), s	15	13, 14, 15

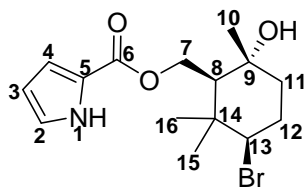
**(Z)-6-bromo-7-hydroxy-3,7-dimethyloct-2-en-1-yl 1H-pyrrole-2-carboxylate (3.39c)**



**NMR Spectroscopic Data-2D correlation (600 MHz, CDCl<sub>3</sub>, 598K)**

Position	$\delta_c$ , Type	$\delta_H$ , Multiplicity	COSY	HMBC
1-NH	-	9.12, br s	-	-
2	122.6, CH	6.92, m	3	3
3	110.5, CH	6.24, q	2, 4	2, 4
4	115.4, CH	6.92, m	3	3
5	122.7, C	-	-	-
6	160.6, C	-	-	-
7	60.8, CH <sub>2</sub>	4.79, m	8	6, 8, 9
8	121.1, CH	5.52, t	7, 10	10, 11
9	141.3, C	-	-	-
10	23.4, CH <sub>3</sub>	1.76, s		8, 9, 11
11a, 11b	30.9, CH <sub>2</sub>	2.38, m	12	8, 10, 13
12a, 12b	32.3, CH <sub>2</sub>	2.03/1.84, m	11, 13	9, 14
13	70.4, CH	3.96, dd	12, 15, 16	11, 14, 15, 16
14	72.6, C	-	-	-
15	26.0, CH <sub>3</sub>	1.32, s	16	13, 14, 16
16	26.5, CH <sub>3</sub>	1.33, s	15	13, 14, 15

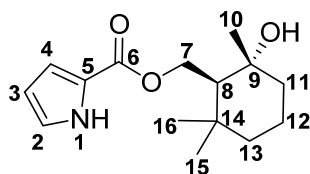
**((1S,3R,6R)-3-bromo-6-hydroxy-2,2,6-trimethylcyclohexyl)methyl 1H-pyrrole-2-carboxylate (3.39d)**



**NMR Spectroscopic Data-2D correlation (600 MHz, CDCl<sub>3</sub>, 598K)**

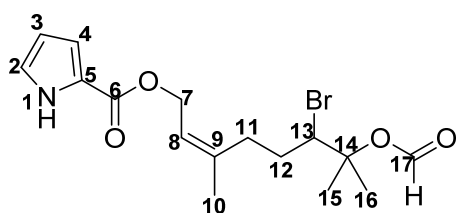
Position	$\delta_c$ , Type	$\delta_H$ , Multiplicity	COSY	HMBC
1-NH	-	9.14, br s	-	-
2	123.3, CH	6.95, m	3	4, 5
3	110.7, CH	6.25, m	2, 4	5
4	115.2, CH	6.85, m	3	2
5	118.7, C	-	-	-
6	160.9, C	-	-	-
7	62.2, CH <sub>2</sub>	4.54, dd	8	6, 8, 9, 14
8	47.0, CH	1.91, t	7	7, 10, 14
9	72.0, C	-	-	-
10	31.1, CH <sub>3</sub>	1.36, s	-	8, 9, 11
11a/11b	36.1, CH <sub>2</sub>	2.16/1.56, m	-	8, 9, 13
12a/12b	27.8, CH <sub>2</sub>	2.46/1.85, m	11, 13	9, 13, 14
13	70.0, CH	4.32, t	12	8, 11
14	38.8, C	-	13	-
15	23.3, CH <sub>3</sub>	1.29, s	-	8, 13, 14, 16
16	32.3, CH <sub>3</sub>	1.18, s	-	8, 13, 14, 15

**((1S,2R)-2-hydroxy-2,6,6-trimethylcyclohexyl)methyl 1H-pyrrole-2-carboxylate (3.41)**



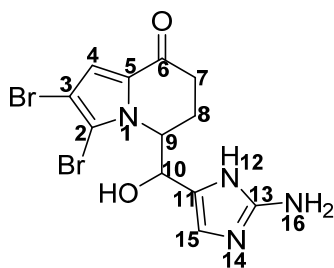
**NMR Spectroscopic Data-2D correlation (600 MHz, CDCl<sub>3</sub>, 598K)**

Position	$\delta_c$ , Type	$\delta_H$ , Multiplicity	COSY	HMBC	NOESY
1-NH	-	9.14, br s	-	-	2
2	123.0, CH	6.95, m	3	4, 5	1, 3
3	110.5, CH	6.24, m	2, 4	5	2, 4
4	115.0, CH	6.84, m	3	2	3, 16
5	122.9, C	-	-	-	-
6	161.0, C	-	-	-	-
7	62.6, CH <sub>2</sub>	4.54, dd	8	6, 8, 9, 14	8, 10, 15, 16
8	52.5, CH	1.39, m	7	10, 11, 16	10
9	72.1, C	-	-	-	-
10	31.3, CH <sub>3</sub>	1.29, s	-	8, 9, 11	8, 11
11b/11a	42.2, CH <sub>2</sub>	1.43/1.23, m	13	8, 9, 13	10, 11
12a/12b	18.2, CH <sub>2</sub>	1.81/1.41, m	12, 14	9, 13, 14	11, 12
13b/13a	41.5, CH <sub>2</sub>	1.66/1.40, m	13	8, 11	11, 12, 13
14	33.8, C	-	-	-	-
15	32.4, CH <sub>3</sub>	1.02, s	-	8, 13, 14, 15	7, 8, 13
16	22.3, CH <sub>3</sub>	1.05, s	-	8, 13, 14, 16	7, 12, 13

**(Z)-6-bromo-7-(formyloxy)-3,7-dimethyloct-2-en-1-yl 1H-pyrrole-2-carboxylate (3.42)****NMR Spectroscopic Data-2D correlation (600 MHz, CDCl<sub>3</sub>, 598K)**

Position	$\delta_c$ , Type	$\delta_H$ , Multiplicity	COSY	HMBC
1-NH	-	9.26	-	-
2	122.7, CH	6.92, m	3	3, 4
3	110.5, CH	6.22, m	2, 4	5
4	115.3, CH	6.91, m	3	2, 3
5	122.9, C	-	-	-
6	161.0, C	-	-	-
7	60.6, CH <sub>2</sub>	4.79, dd	8	6, 8, 9
8	121.2, CH	5.53, m	7	7, 10, 11
9	140.8 C	-	-	-
10	23.4, CH <sub>3</sub>	1.75, s	-	8, 9, 11
11	30.4, CH <sub>2</sub>	2.39, m	12	8, 9, 10, 12, 13
12	31.5, CH <sub>2</sub>	2.00, 1.80, m	11, 13	9, 11, 14
13	61.1, CH	4.41, d	12	11, 12, 14, 15, 16
14	84.4, C	-	-	-
15	24.6, CH <sub>3</sub>	1.60 s	-	13, 14, 16
16	23.1, CH <sub>3</sub>	1.60, s	-	13, 14, 15
17	160.0, CH	7.93, s	-	14

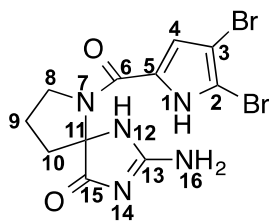
**4-((2-amino-1*H*-imidazol-4-yl)(hydroxy)methyl)-6,7-dibromo-3,4-dihydropyrrolo[1,2-*a*]pyrazin-1(2*H*)-one (3.45)**



**NMR Spectroscopic Data-2D correlation (600 MHz, CDCl<sub>3</sub>, 598K)**

Position	$\delta_c$ , Type	$\delta_H$ , Multiplicity	COSY	HMBC
1-N	-	-	-	-
2	104.9, C	-	-	-
3	97.3, C	-	-	-
4	112.6, CH	6.89, s	-	2, 5, 6
5	127.2, C	-	-	-
6	159.3, C	-	-	-
7-NH	-	8.03, t	-	6, 8
8	39.2, CH <sub>2</sub>	3.46/3.28, ddd	8, 9	6, 9, 10
9	81.3, CH	3.53, dt	8, 10	8, 10
10	76.9, CH	4.04, d	9	8, 9
11	128.7, C	-	-	-
12-N	-	-	-	-
13	149.7, C	-	-	-
14-N	-	-	-	-
15	113.7, CH	6.46, s	-	9, 10, 11, 13
16-NH <sub>2</sub>	-	5.26, br s	-	-

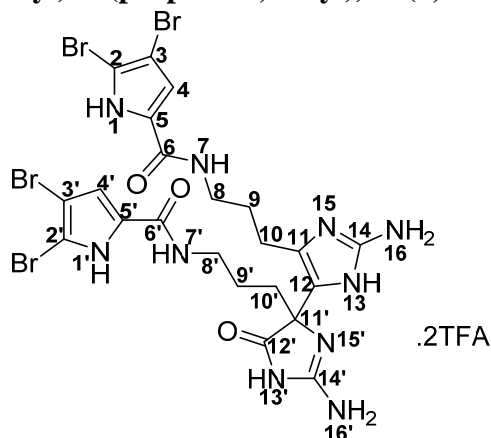
**2-amino-6-(4,5-dibromo-1*H*-pyrrole-2-carbonyl)-1,3,6-triazaspiro[4.4]non-2-en-4-one (3.43)**



**NMR Spectroscopic Data-2D correlation (600 MHz, MeOD-*d*<sub>4</sub>, 598K)**

Position	$\delta_c$ , Type	$\delta_H$ , Multiplicity	COSY	HMBC
1-NH	-	12.88, br s	4	2, 3, 4, 5
2	107.2, C	-	-	-
3	98.9, C	-	-	-
4	116.3, CH	6.96, s	1	2, 5, 6
5	125.7, C	-	-	-
6	158.2, C	-	-	-
7-N	-	-	-	-
8	48.7, CH <sub>2</sub>	3.88/3.80, q	9, 10	9, 10, 11
9	23.5, CH <sub>2</sub>	2.12, m	8, 10	10, 11
10	35.5, CH <sub>2</sub>	2.18, m	8, 9	8, 15
11	79.6, C	-	-	-
12-NH	-	10.28, br s	-	13, 15
13	157.5, C	-	-	-
14-N	-	-	-	-
15	173.3, C	-	-	10'
16-NH <sub>2</sub>	-	9.27, br s	-	-

**N,N'-((2,2'-diamino-5'-oxo-1',5'-dihydro-3H,4'H-[4,4'-biimidazole]-4',5-diyl)bis(propane-3,1-diyl))bis(4,5-dibromo-1H-pyrrole-2-carboxamide) (3.46)**



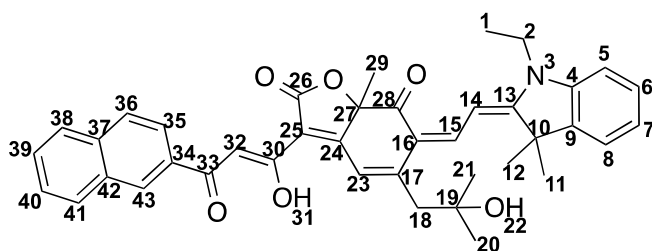
**NMR Spectroscopic Data-2D correlation (600 MHz, MeOD-*d*<sub>4</sub>, 598K)**

Position	$\delta_c$ , Type	$\delta_H$ , Multiplicity	COSY	HMBC
1-NH	-	-	-	-
1'-NH	209.8	-	-	-
2	107.2, C	-	-	-
2'	107.0, C	-	-	-
3	100.9, C	-	-	-
3'	100.8, C	-	-	-
4	115.2, CH	6.85, s	-	2, 5, 6
4'	115.1, CH	6.82, s	-	2', 5', 6'
5	129.4, C	-	-	-
5'	129.6, C	-	-	-
6	162.9, C	-	-	-
6'	162.8, C	-	-	-
7-NH	156.2	-	-	-
7'-NH	-	-	-	-
8	40.3, CH <sub>2</sub>	3.34, m	9	6, 9, 10
8'	40.5, CH <sub>2</sub>	3.37, m	9'	6', 9', 10'
9	31.5, CH <sub>2</sub>	1.82, q	8, 10	8, 10, 11
9'	25.7, CH <sub>2</sub>	1.56, br m	8', 10'	8', 10', 11'
10	23.4, CH <sub>2</sub>	2.63, m	9	8, 9, 11, 12
10'	35.4, CH <sub>2</sub>	2.15, br m	9'	8', 9', 11', 15, 12'
11	125.7, C	-	-	-
11'	67.6, C	-	-	-



12	121.4, C	-	-	-
12'	187.9, C	-	-	-
13-N	-	-	-	-
13'-NH	-	-	-	-
14	148.9, C	-	-	-
14'	148.9, C	-	-	-
15-NH	185.8	-	-	-
15'-N	-	-	-	-
16-NH <sub>2</sub>	-	-	-	-
16'-NH <sub>2</sub>	-	-	-	-

**(Z)-6-((E)-2-(1-ethyl-3,3-dimethylindolin-2-ylidene)ethylidene)-5-(2-hydroxy-2-methylpropyl)-3-((Z)-1-hydroxy-3-(naphthalen-2-yl)-3-oxoprop-1-en-1-yl)-7a-methylbenzofuran-2,7(6H,7aH)-dione (4.48)**



**NMR Spectroscopic Data-2D correlation (600 MHz, CDCl<sub>3</sub>, 598K)**

Position	$\delta_c$ , Type	$\delta_H$ , Multiplicity	COSY	HMBC
1	11.8, CH <sub>3</sub>	1.39, t	2	2
2	38.6, CH <sub>2</sub>	3.95, q	1	1, 4, 13
3	-	-	-	-
4	142.3, C	-	-	-
5	109.1, CH	6.95, d	6, 7, 8	7, 9
6	128.4, CH	7.32, t	5, 7, 8	4, 8
7	123.7, CH	7.13, t	5, 6, 8	5, 9
8	122.0, CH	7.30, d	5, 6, 7	4, 6
9	140.8, C	-	-	-
10	48.1, C	-	-	-
11	28.3, CH <sub>3</sub>	-	-	9, 10, 12, 13
12	28.5, CH <sub>3</sub>	-	-	9, 10, 11, 13
13	172.6, C	-	-	-

14	97.8, CH	7.54, d	15	10, 16
15	146.0, CH	8.11, d	14, 23	13, 17, 28
16	116.5, C	-	-	-
17	154.0, C	-	-	-
18	47.3, CH <sub>2</sub>	2.93/2.76, dd	20, 21, 23	16, 21, 22, 23
19	72.1, C	-	-	-
20	30.5, CH <sub>3</sub>	1.45, s	-	19, 18
21	31.2, CH <sub>3</sub>	1.46, s	-	19, 18
22	-	-	-	-
23	114.8, CH	7.03, s	15	16, 18, 27
24	171.1, C	-	-	-
25	110.0, C	-	-	-
26	169.6, C	-	-	-
27	87.3, C	-	-	-
28	195.4, C	-	-	-
29	29.5, CH <sub>3</sub>	1.83, s	-	24, 27, 28
30	176.9, C	-	-	-
31	-	-	-	-
32	96.6, CH	7.66, s	-	25, 34
33	188.2, C	-	-	-
34	133.4, C	-	-	-
35	123.7, CH	8.06, dd	36	37, 43
36	128.3, CH	7.89, d	35, 41	34, 42
37	135.4, C	-	-	-
38	127.7, CH	7.86, d	39, 40	40, 42
39	128.1, CH	7.57, m	38, 41	37, 41
40	126.7, CH	7.55, m	38, 41	38, 42
41	129.6, CH	7.98, d	36, 38, 39, 40	37, 39
42	132.8, C	-	-	-
43	128.8, CH	8.56, s	35, 36, 38, 41	-

---

## 6.2. UV-Vis Absorbance and Fluorescence Spectra of the Epicoconone-hemicyanine Hybrid Dyes.

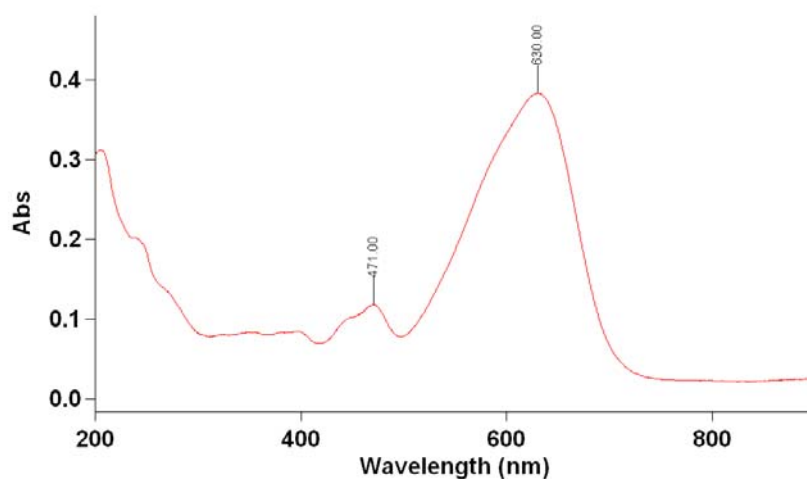
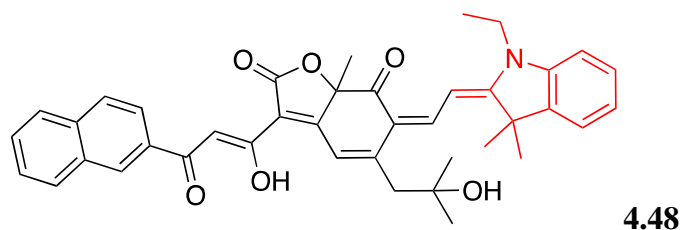


**Figure 6.2.1.** UV-Vis absorbance spectrum of **4.48**

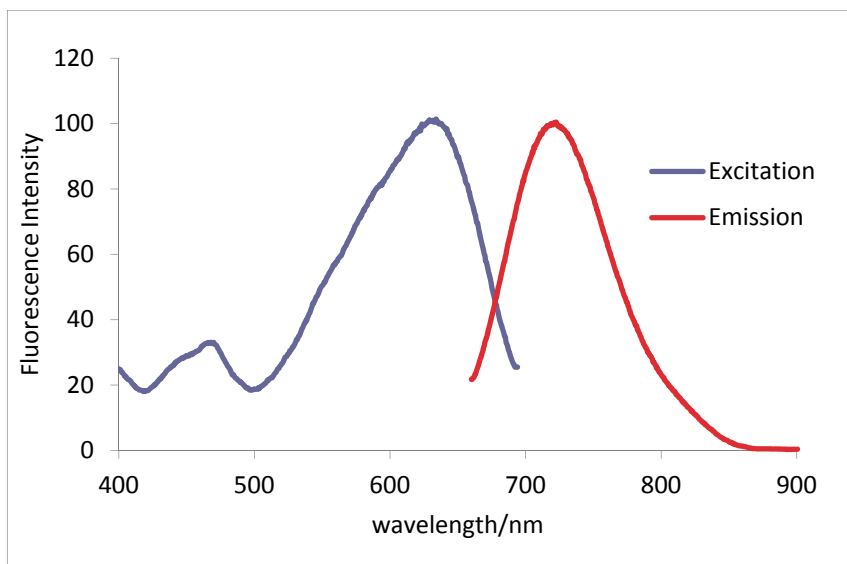


**Figure 6.2.2.** Fluorescence spectrum of **4.48** in ACN.

Extinction coefficient,  $\varepsilon = 12\,000\text{ M}^{-1}\text{cm}^{-1}$ ; Max  $\lambda_{\text{ex}} = 630\text{ nm}$ , Max  $\lambda_{\text{em}} = 715\text{ nm}$ ;  
Stokes' shift = 85 nm; Quantum yield = 0.056

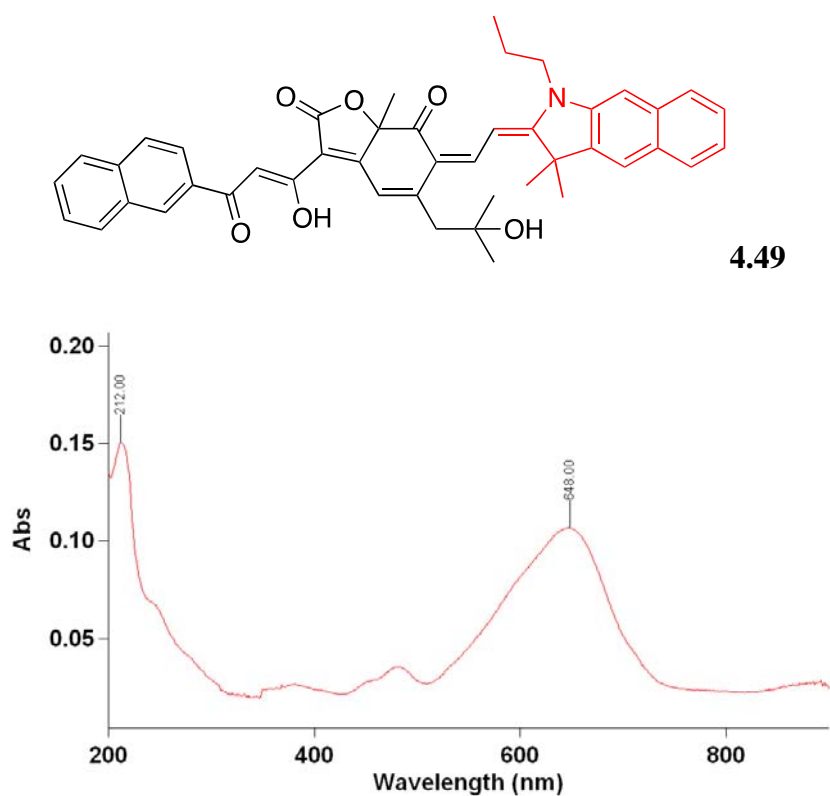


**Figure 6.2.3.** UV-Vis absorbance spectrum of **4.49**

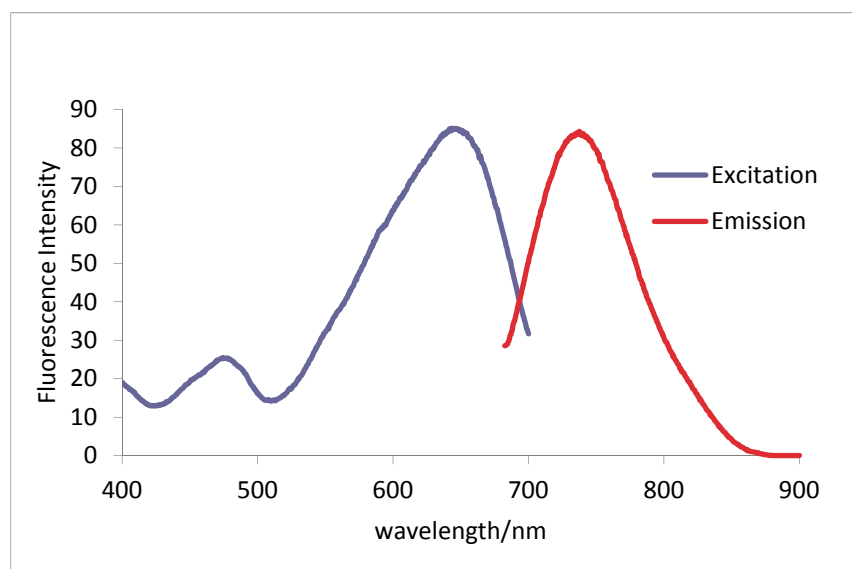


**Figure 6.2.4.** Fluorescence spectrum of **4.49** in ACN. (also as **Figure 4.15** in **Chapter 4**)

Extinction coefficient,  $\epsilon = 72\,000\text{ M}^{-1}\text{cm}^{-1}$ ; Max  $\lambda_{\text{ex}} = 650\text{ nm}$ , Max  $\lambda_{\text{em}} = 730\text{ nm}$ ;  
Stokes' shift = 80 nm; Quantum yield = 0.033

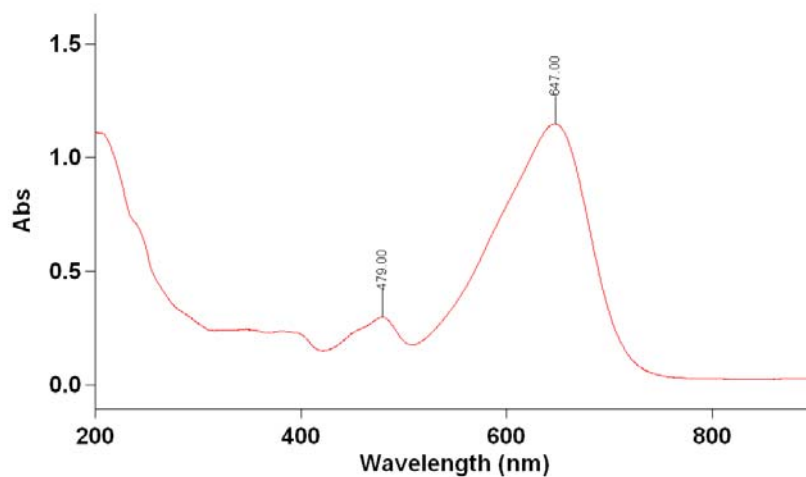
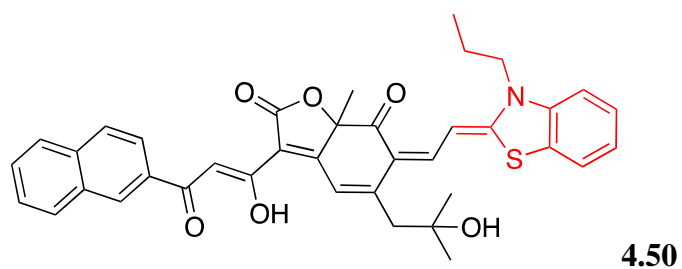


**Figure 6.2.5.** UV-Vis absorbance spectrum of **4.50**

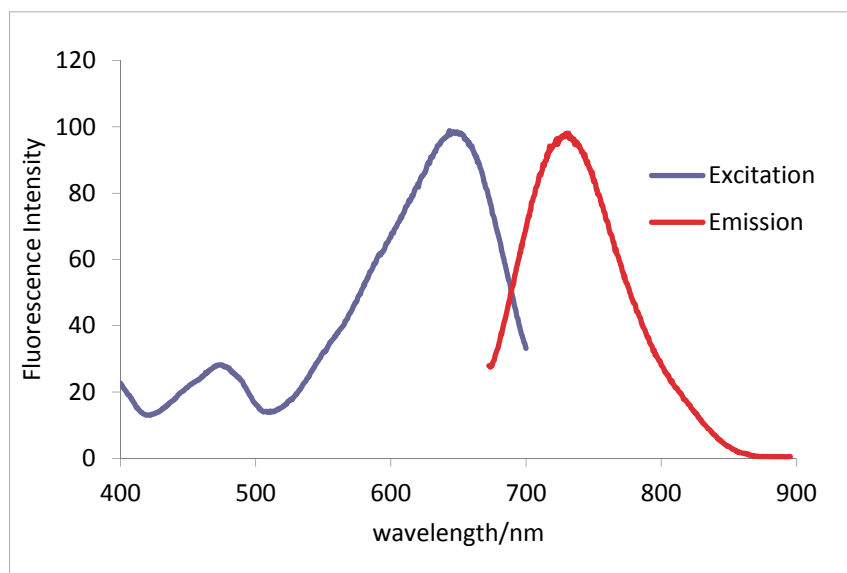


**Figure 6.2.6.** Fluorescence spectrum of **4.50** in ACN.

Extinction coefficient,  $\varepsilon = 37\,000\text{ M}^{-1}\text{cm}^{-1}$ ; Max  $\lambda_{\text{ex}} = 650\text{ nm}$ , Max  $\lambda_{\text{em}} = 725\text{ nm}$ ;  
Stokes' shift = 75 nm; Quantum yield = 0.033

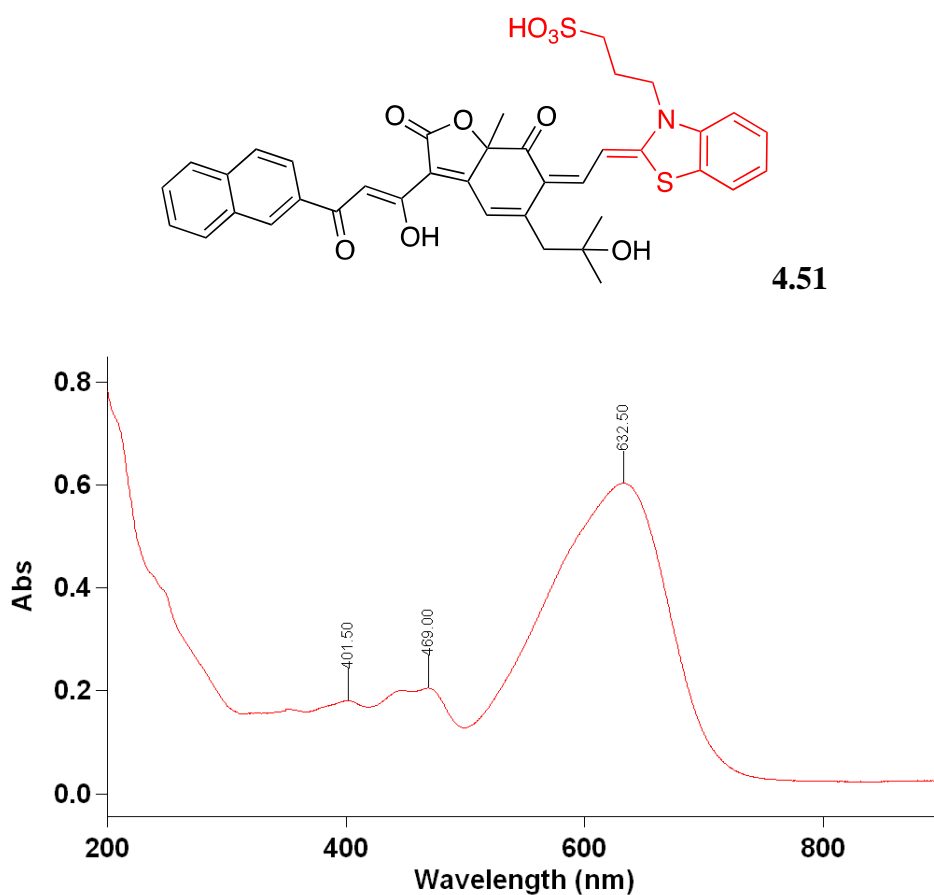


**Figure 6.2.7.** UV-Vis absorbance spectrum of **4.51**

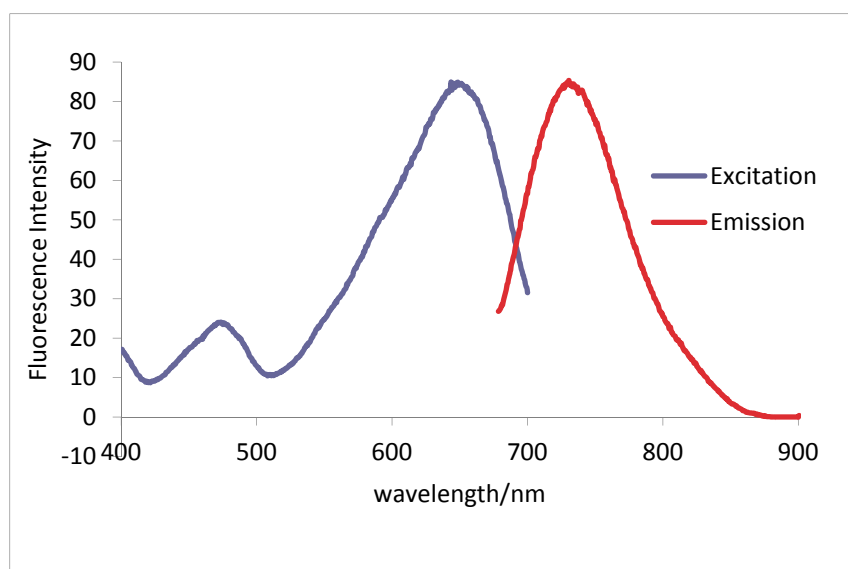


**Figure 6.2.8.** Fluorescence spectrum of **4.51** in ACN.

Extinction coefficient,  $\varepsilon = 71\,000\text{ M}^{-1}\text{cm}^{-1}$ ; Max  $\lambda_{\text{ex}} = 635\text{ nm}$ , Max  $\lambda_{\text{em}} = 725\text{ nm}$ ;  
Stokes' shift = 90 nm; Quantum yield = 0.028

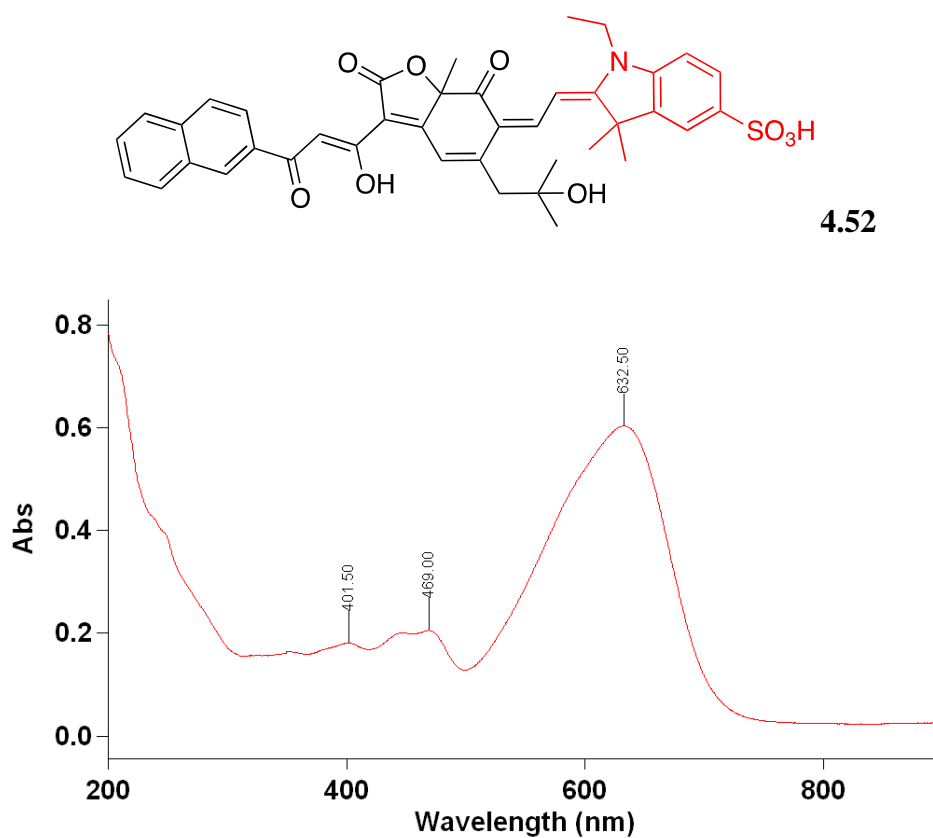


**Figure 6.2.9.** UV-Vis absorbance spectrum of **4.52**

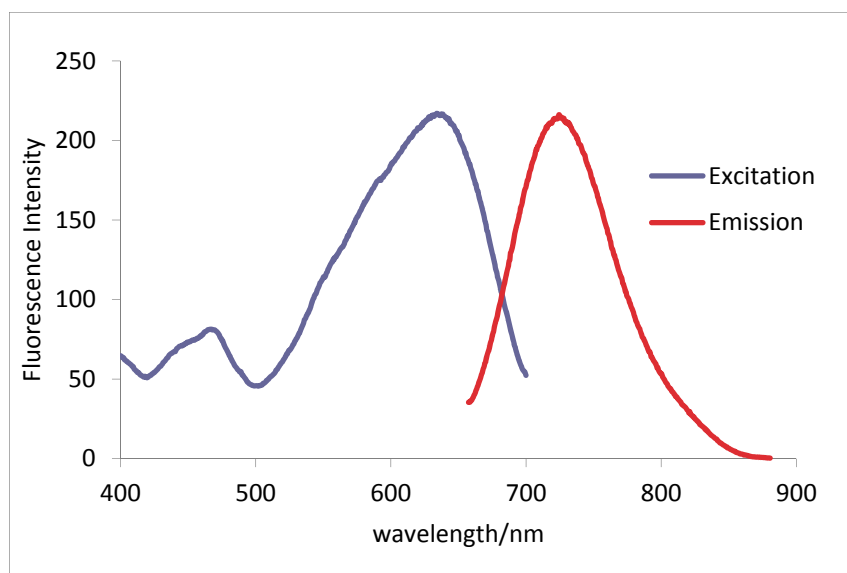


**Figure 6.2.10.** Fluorescence spectrum of **4.52** in ACN.

Extinction coefficient,  $\varepsilon = 41\,000\text{ M}^{-1}\text{cm}^{-1}$ ; Max  $\lambda_{\text{ex}} = 630\text{ nm}$ , Max  $\lambda_{\text{em}} = 720\text{ nm}$ ; Stokes' shift = 90 nm; Quantum yield = 0.066

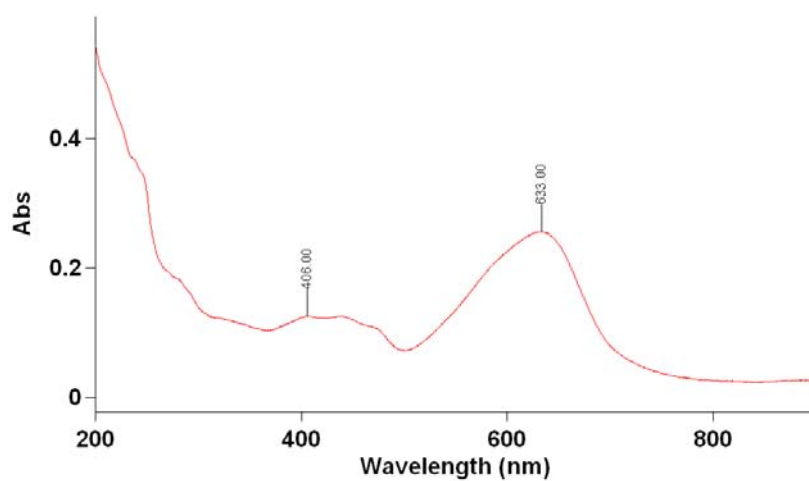
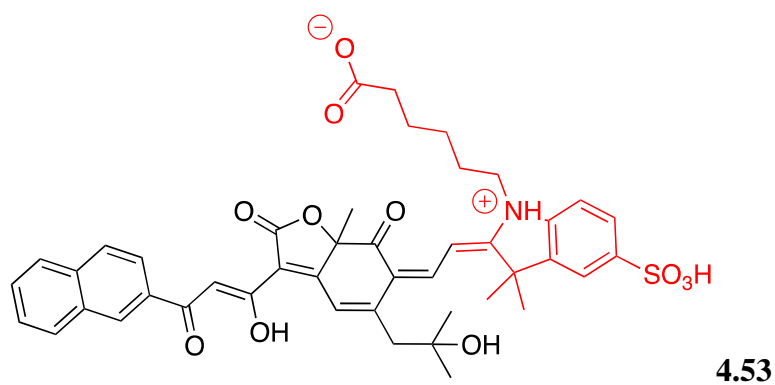


**Figure 6.2.11.** UV-Vis absorbance spectrum of **4.53**.

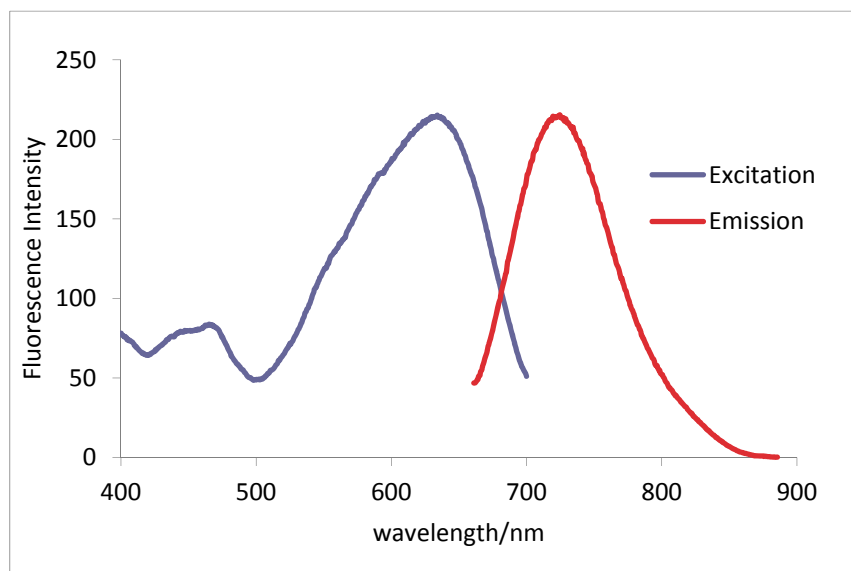


**Figure 6.2.12.** Fluorescence spectrum of **4.53** in ACN.

Extinction coefficient,  $\varepsilon = 19\,000\text{ M}^{-1}\text{cm}^{-1}$ ; Max  $\lambda_{\text{ex}} = 630\text{ nm}$ , Max  $\lambda_{\text{em}} = 720\text{ nm}$ ;  
Stokes' shift = 90 nm; Quantum yield = 0.058



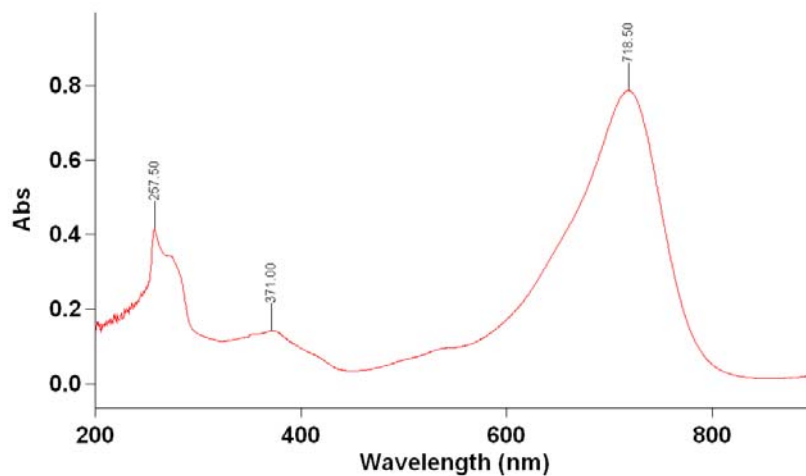
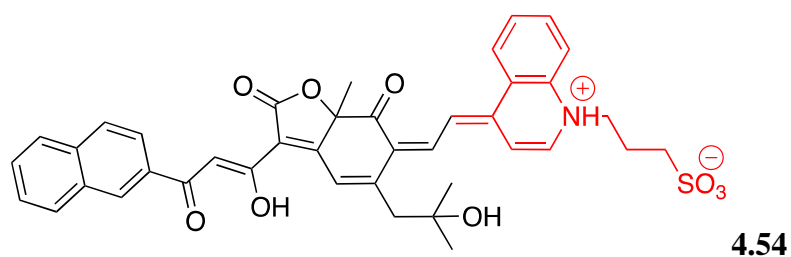


**Figure 6.2.11.** UV-Vis absorbance spectrum of **4.54**.

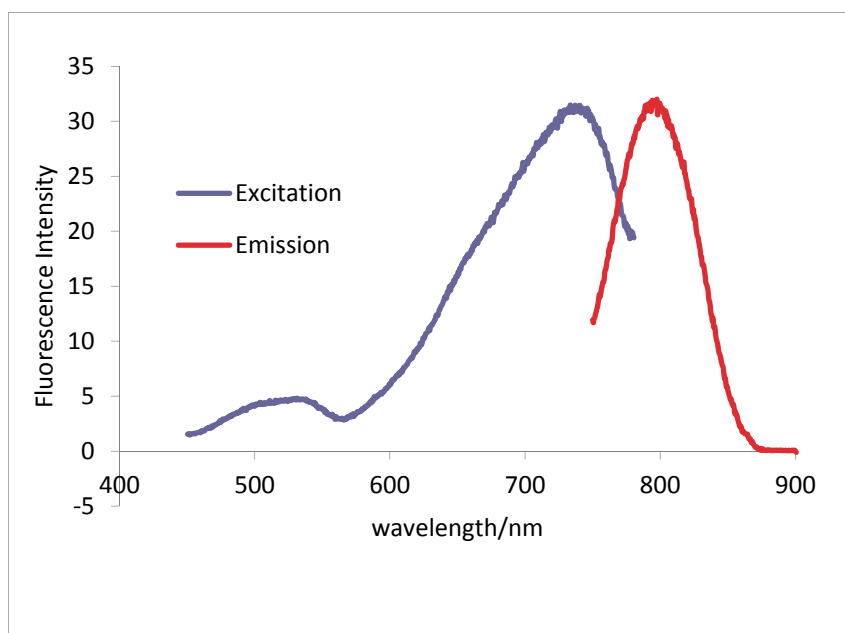


**Figure 6.2.14.** Fluorescence spectrum of **4.54** in DMSO.

Extinction coefficient,  $\varepsilon = 37\,000\text{ M}^{-1}\text{cm}^{-1}$ ; Max  $\lambda_{\text{ex}} = 720\text{ nm}$ , Max  $\lambda_{\text{em}} = 795\text{ nm}$ ;  
Stokes' shift = 75 nm; Quantum yield = 0.0027

### 6.3. Effect of pH on the UV-Vis Absorbance and Fluorescence of the Epicoconone-Hemicyanine Hybrid Dyes

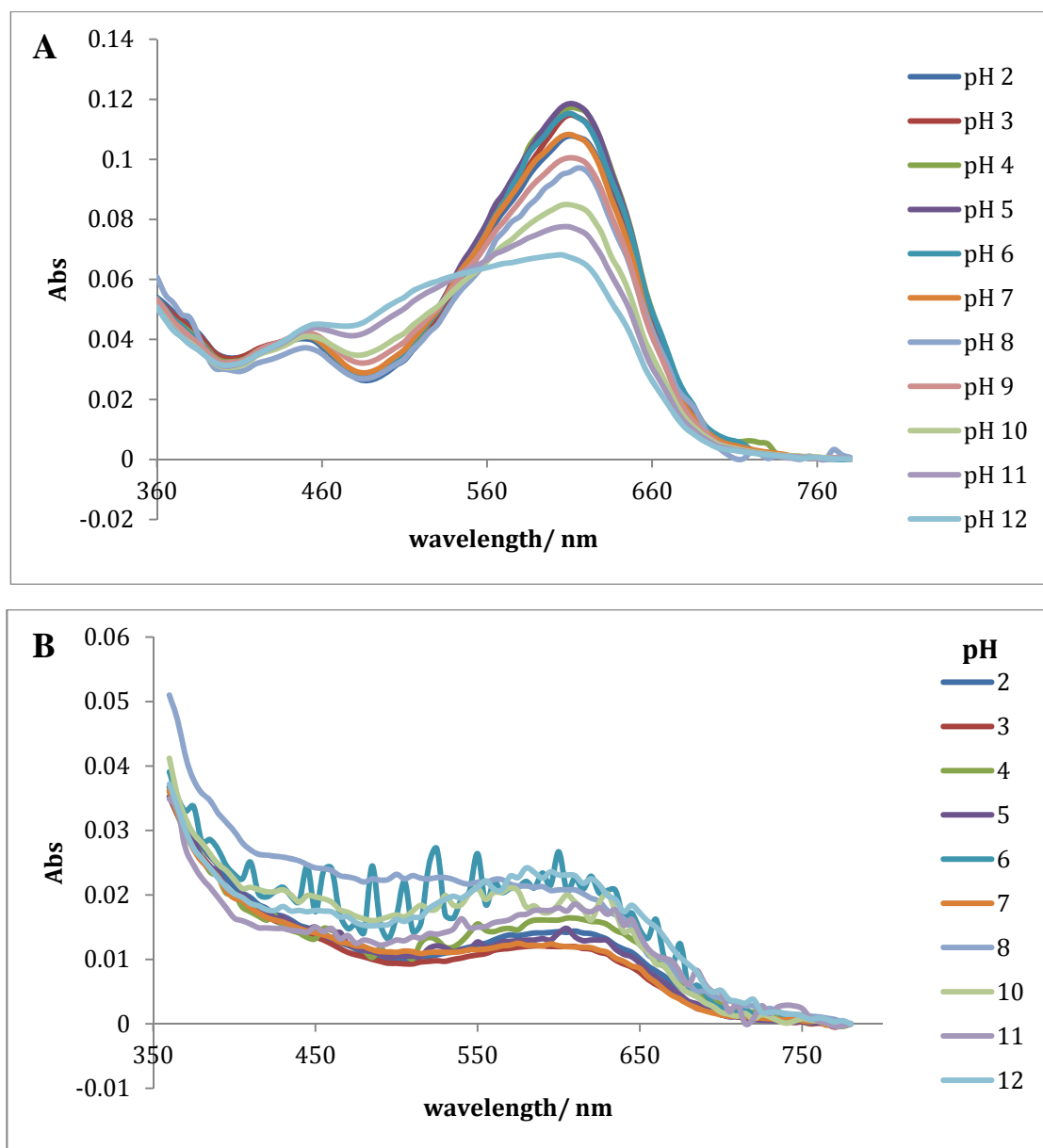


**Figure 6.3.1.** Absorbance spectrum of **4.48** measured at different pH **A.** initially and **B.** after 3 h.

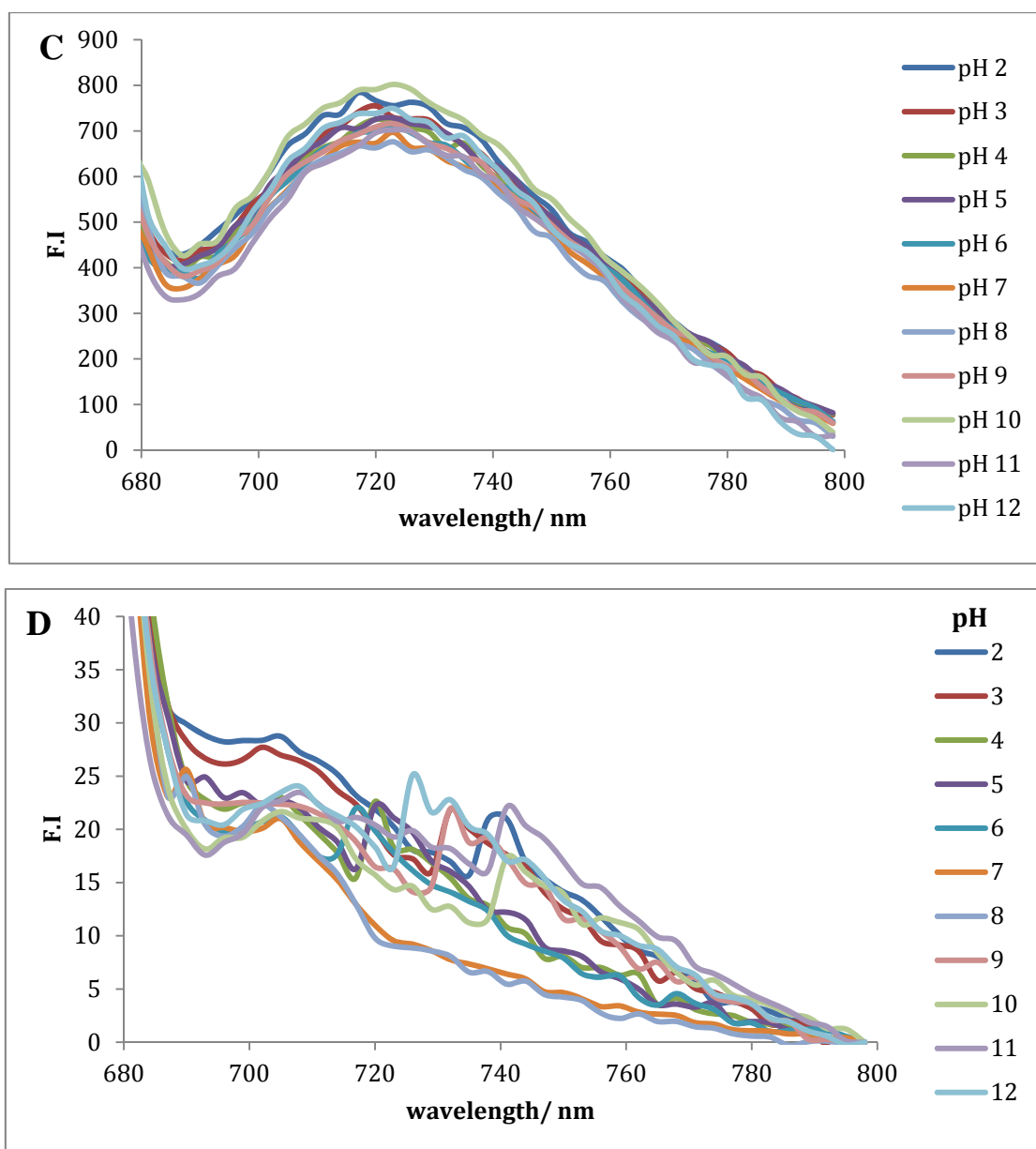


**Figure 6.3.1.** Emission fluorescence spectrum of **4.48** measured at different pH **C.** initially and **D.** after 3 h.

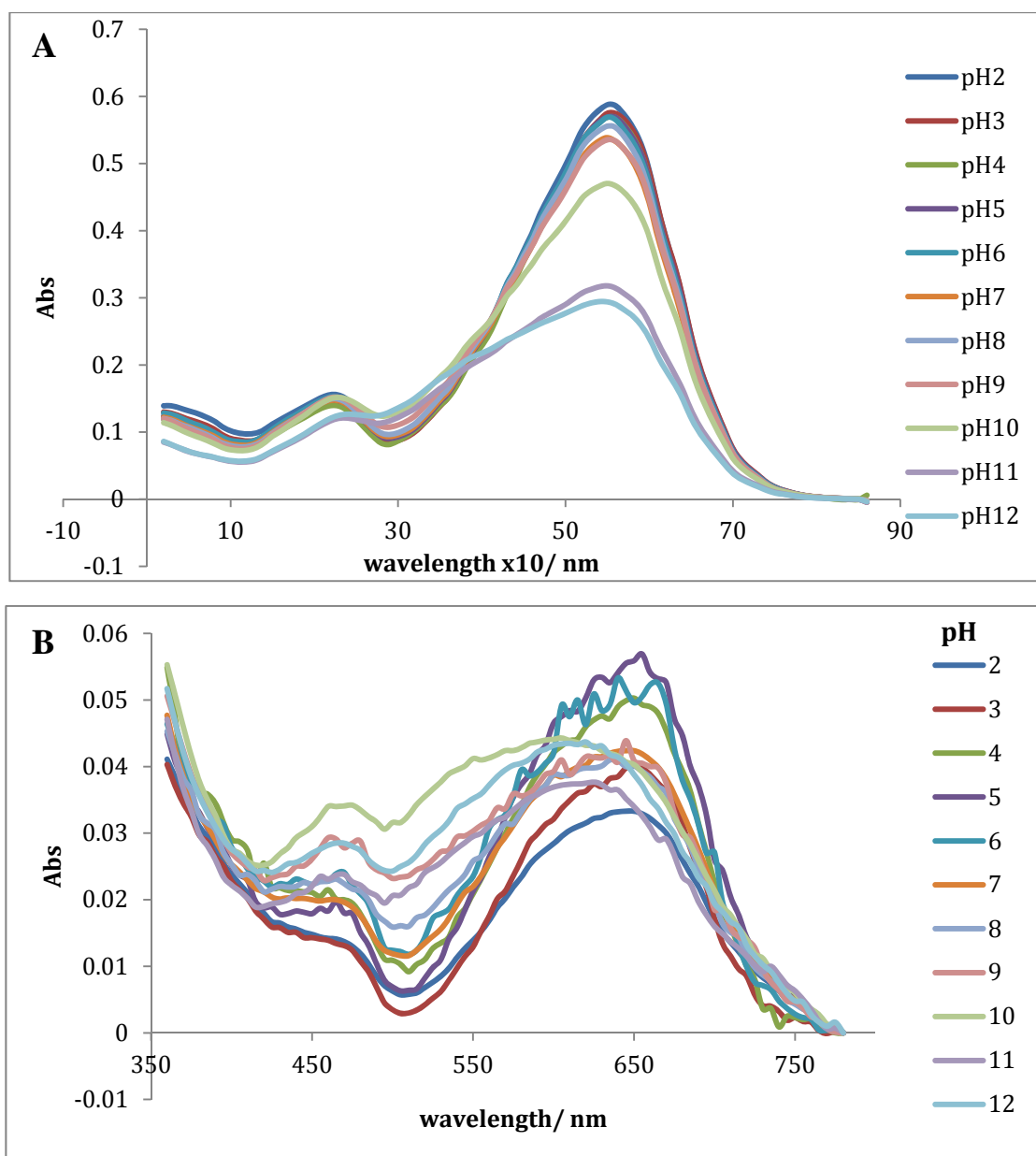


**Figure 6.3.2.** Absorbance spectrum of **4.49** measured at different pH **A.** initially and **B.** after 3 h.

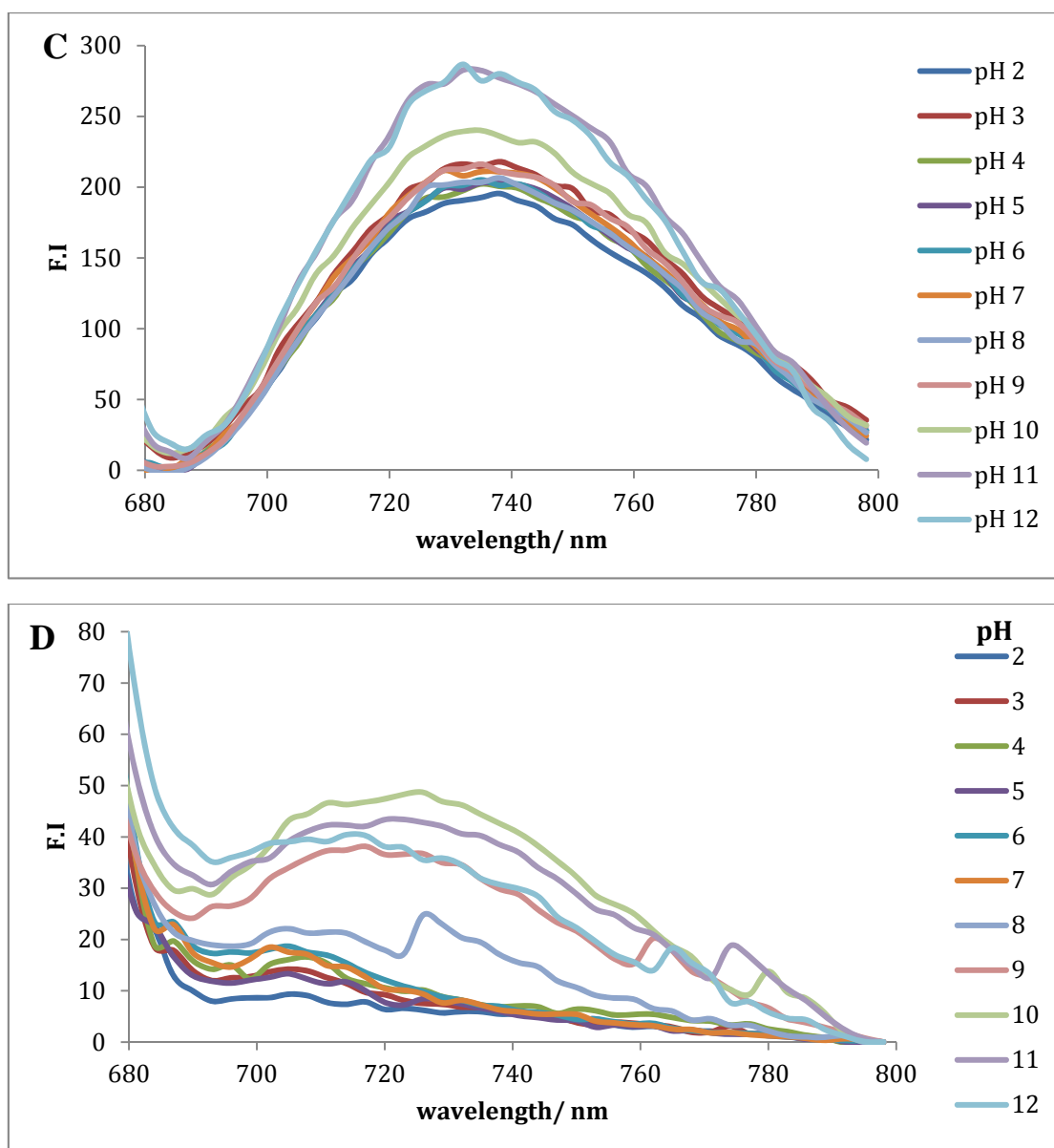


**Figure 6.3.2.** Emission fluorescence spectrum of **4.49** measured at different pH **C.** initially and **D.** after 3 h.

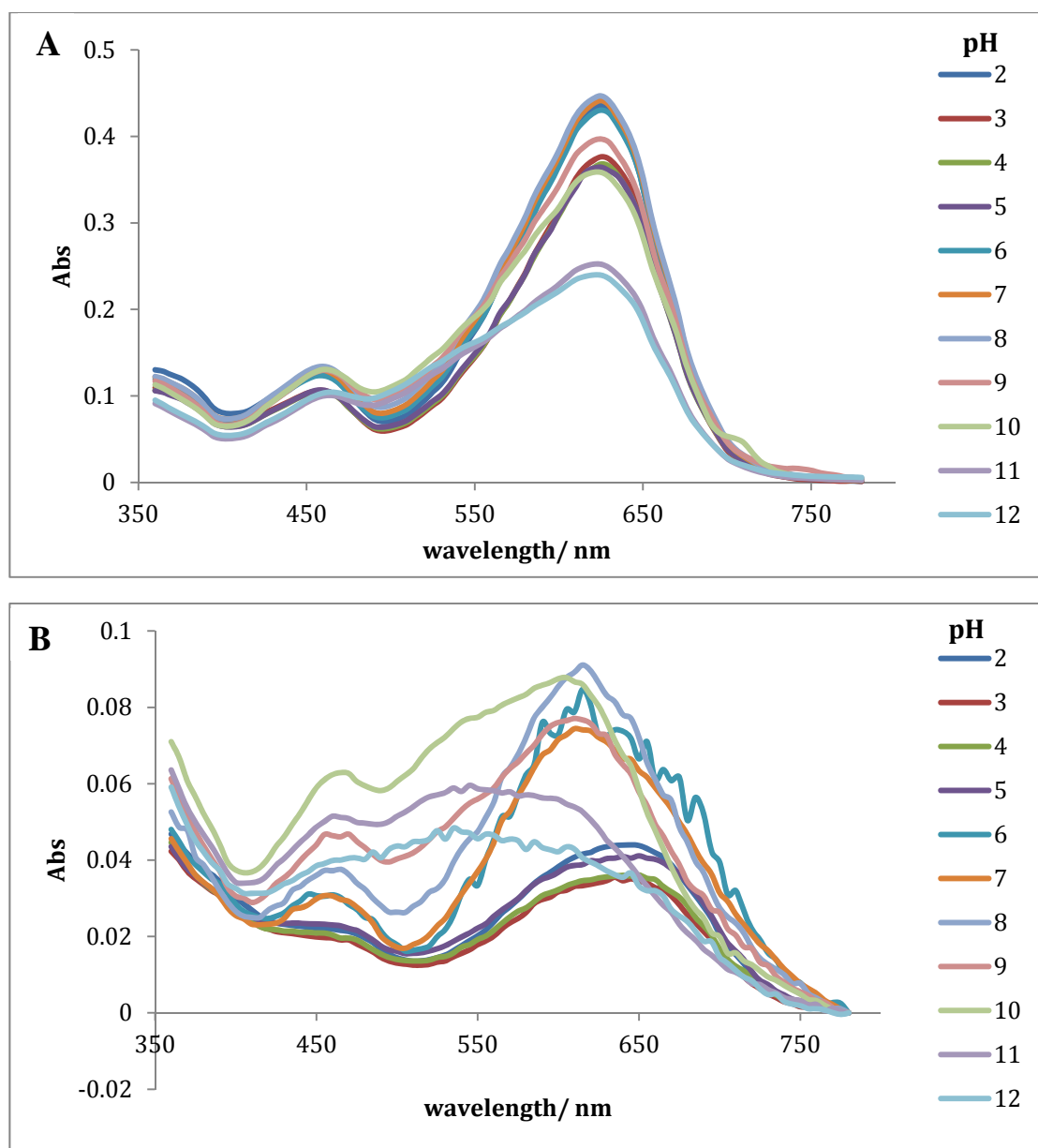


**Figure 6.3.3.** Absorbance spectrum of **4.50** measured at different pH **A.** initially and **B.** after 3 h.

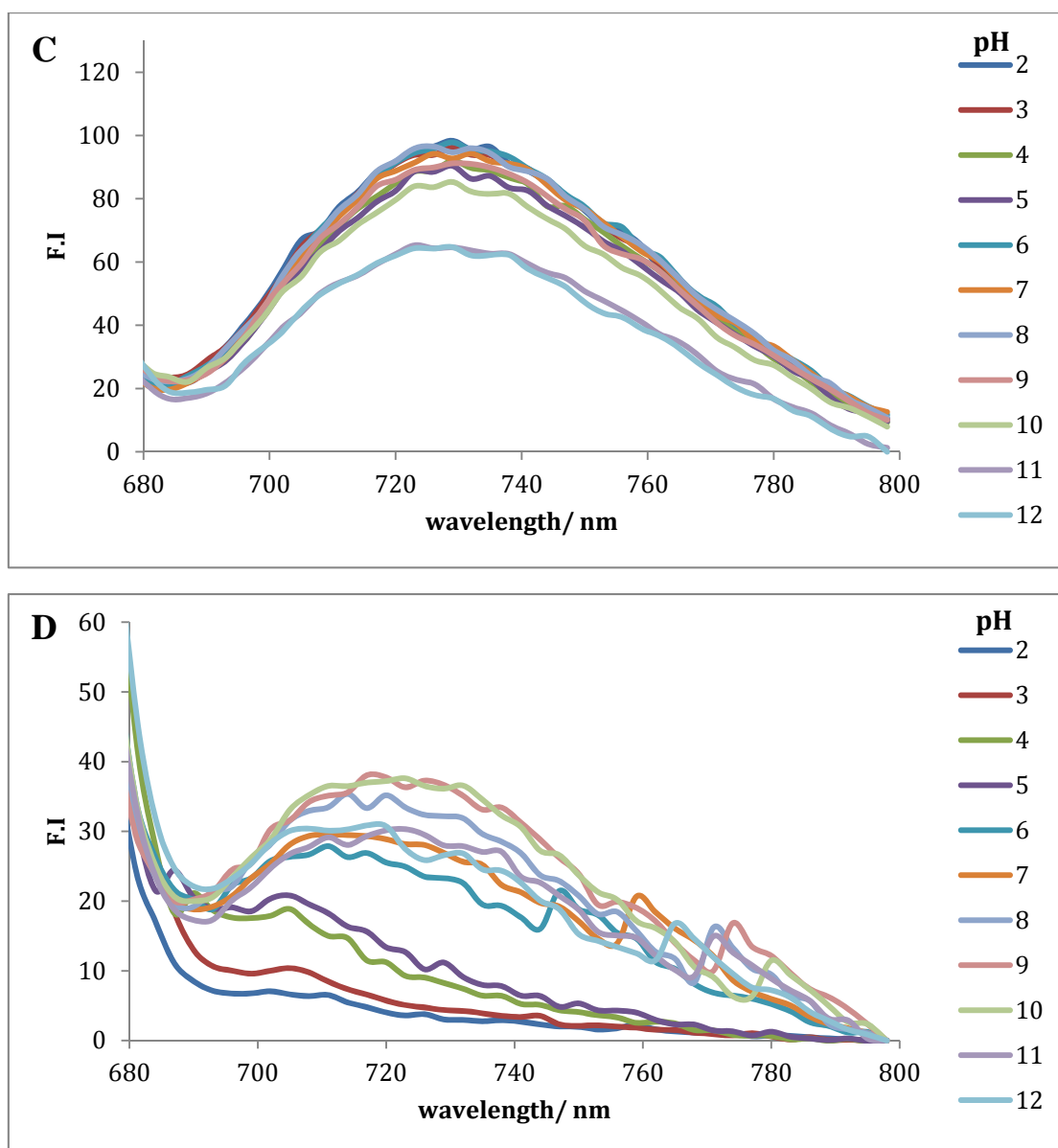


**Figure 6.3.3.** Emission fluorescence spectrum of **4.50** measured at different pH **C.** initially and **D.** after 3 h.

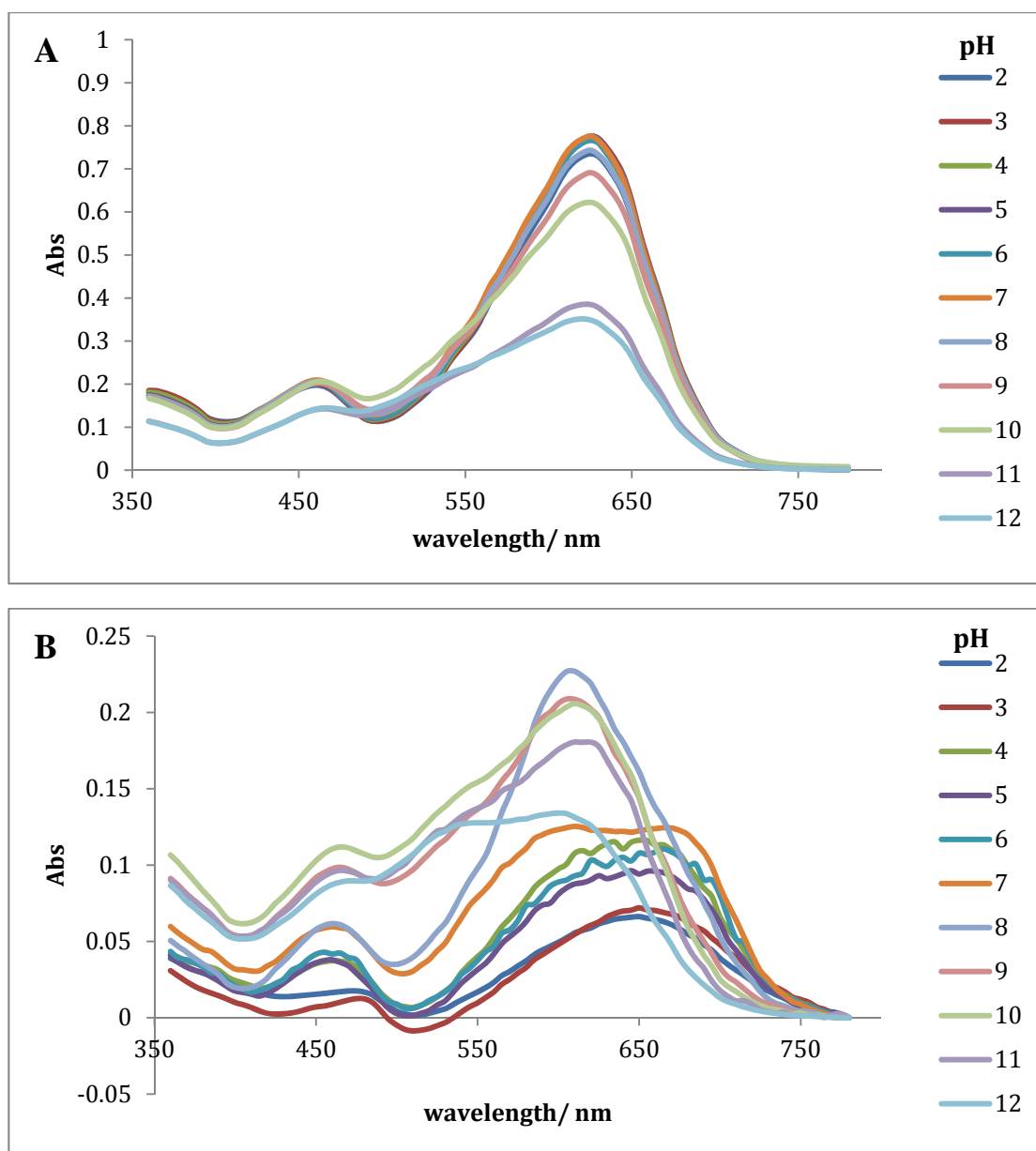


**Figure 6.3.4.** Absorbance spectrum of **4.51** measured at different pH **A.** initially and **B.** after 3 h.



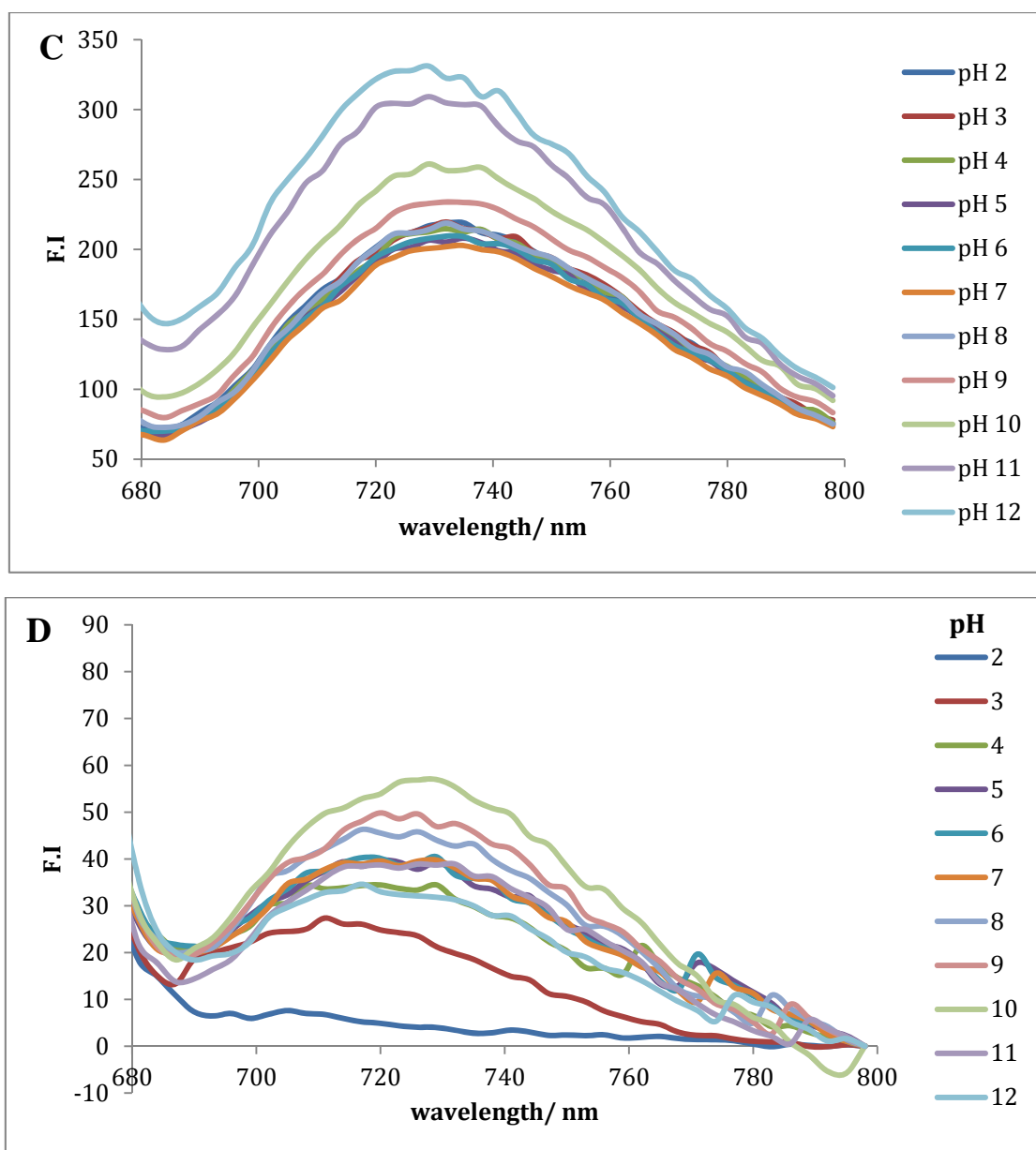


**Figure 6.3.4.** Emission fluorescence spectrum of **4.51** measured at different pH **C.** initially and **D.** after 3 h.

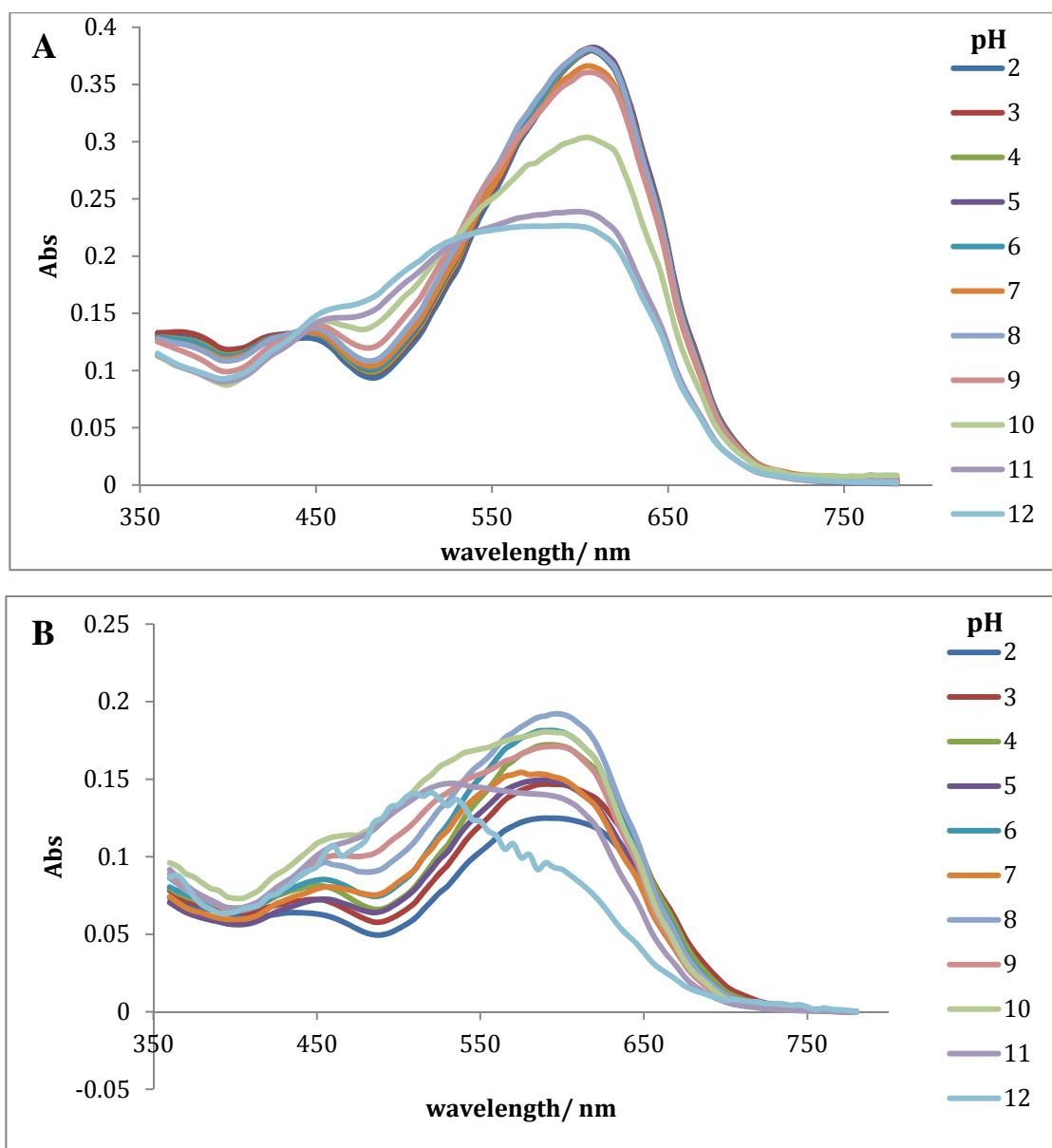


**Figure 6.3.5.** Absorbance spectrum of **4.52** measured at different pH **A.** initially and **B.** after 3 h.

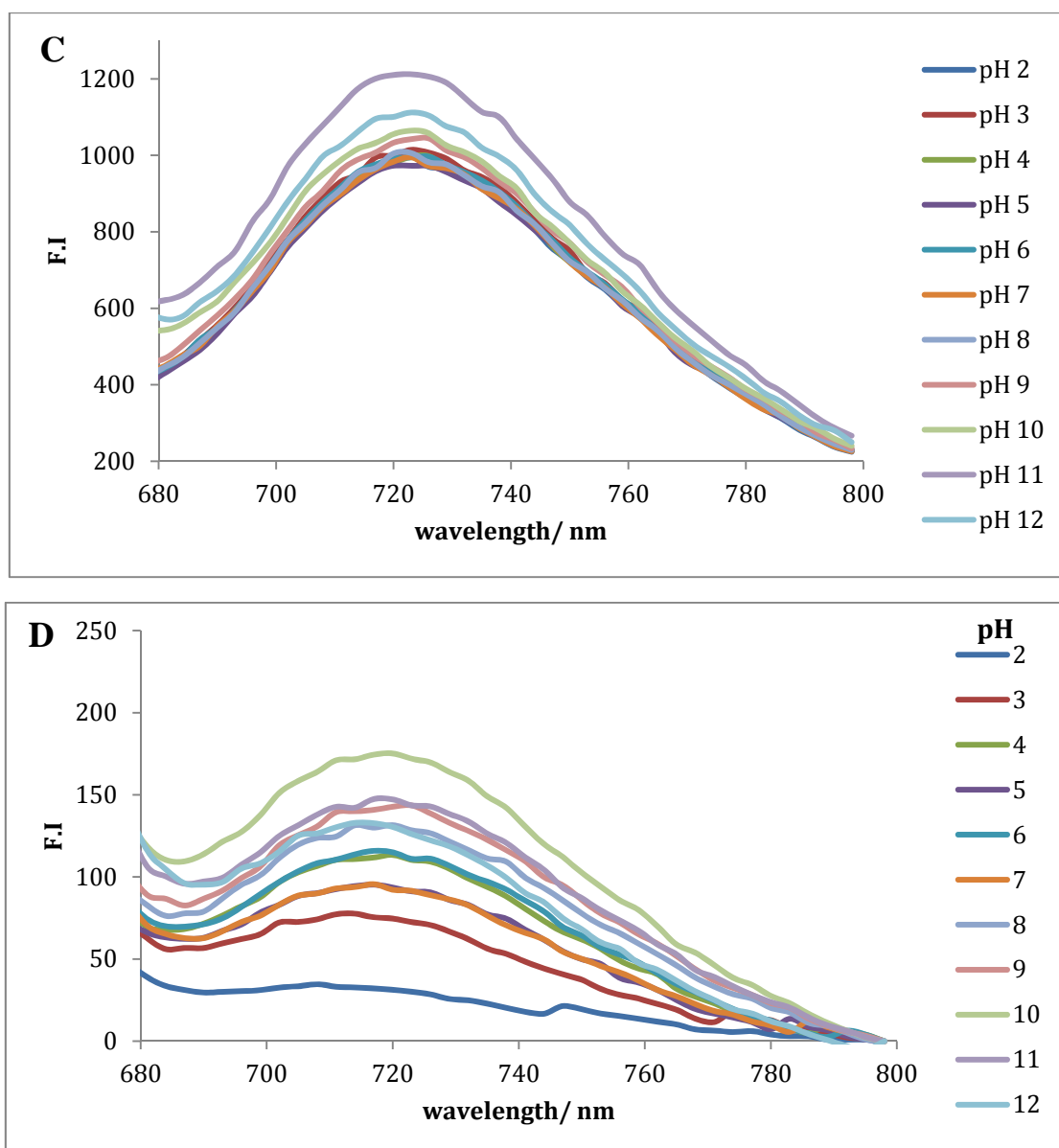


**Figure 6.3.5.** Emission fluorescence spectrum of 4.52 measured at different pH **C.** initially and **D.** after 3 h.

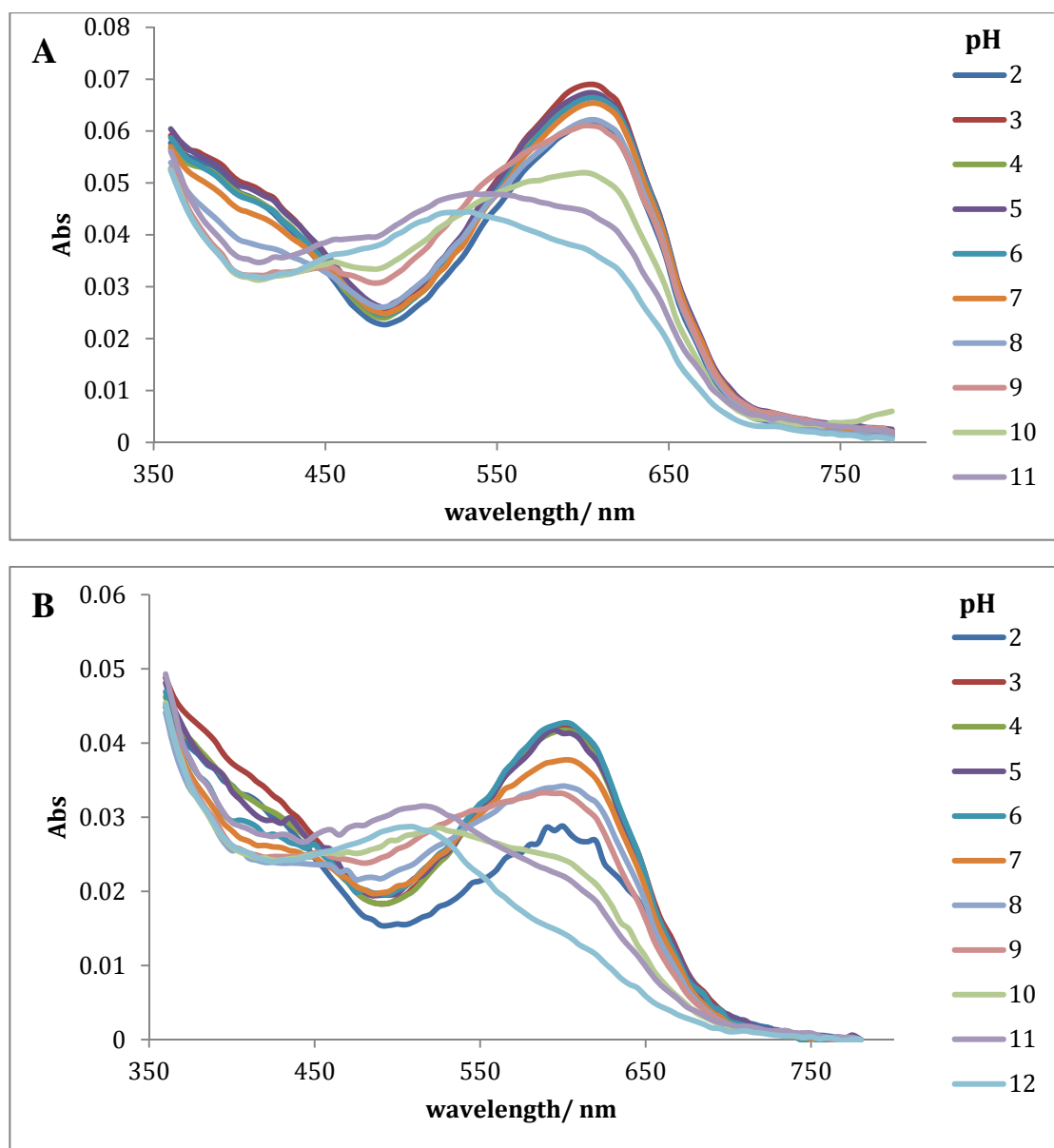


**Figure 6.3.6.** Absorbance spectrum of **4.53** measured at different pH **A.** initially and **B.** after 3 h.

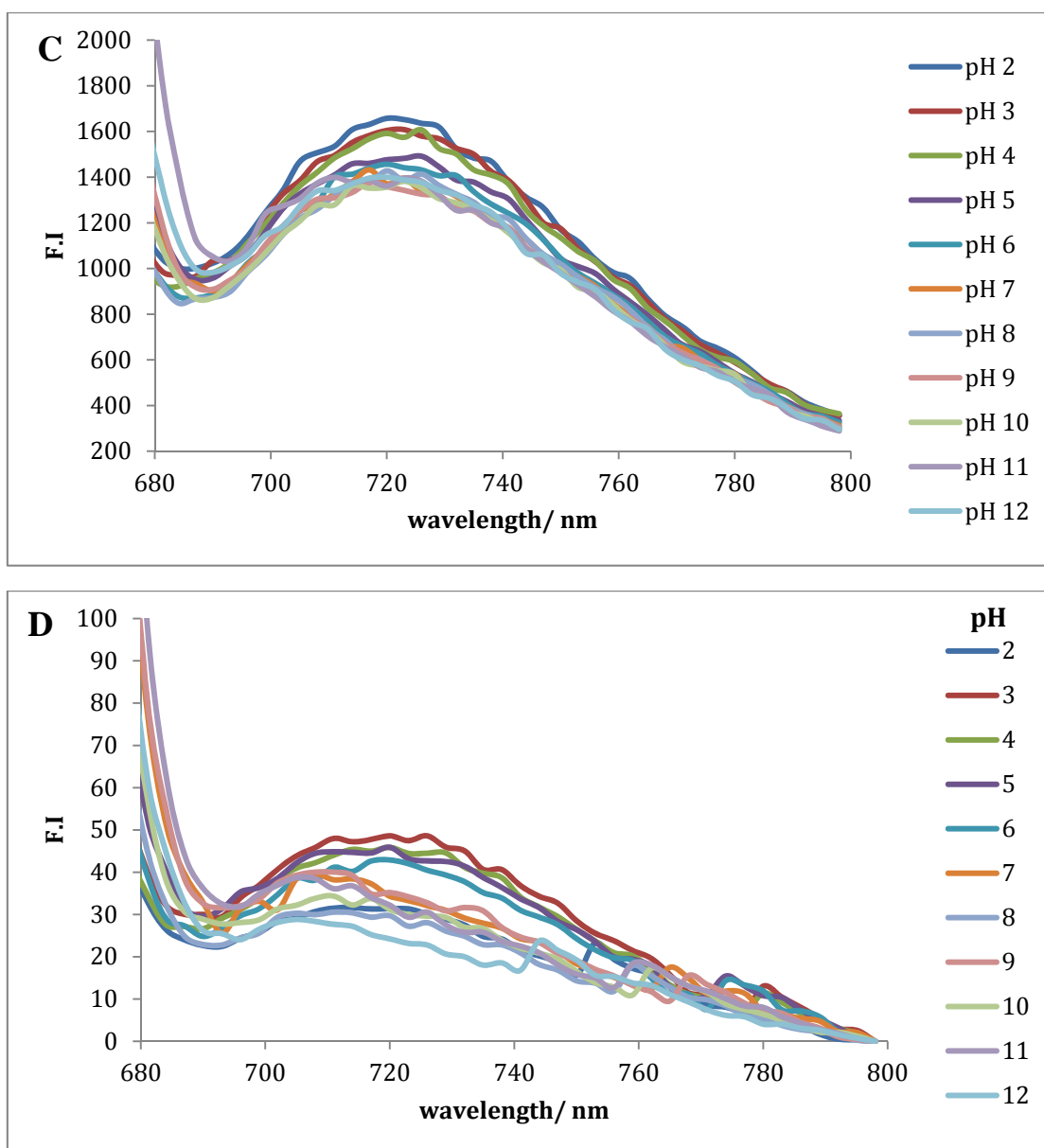


**Figure 6.3.6.** Emission fluorescence spectrum of 4.53 measured at different pH **C.** initially and **D.** after 3 h.

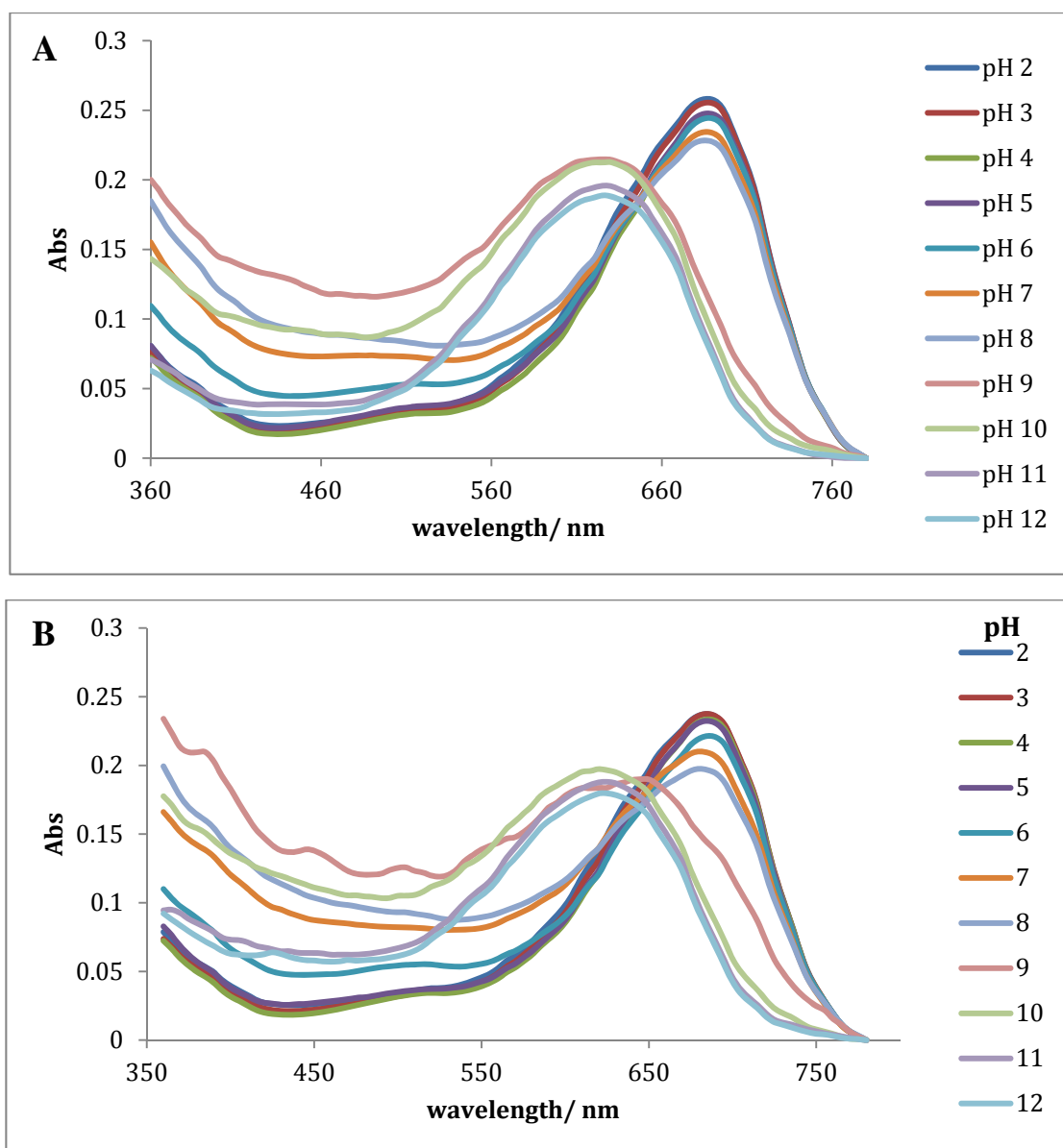


**Figure 6.3.7.** Absorbance spectrum of **4.54** measured at different pH **A.** initially and **B.** after 3 h.

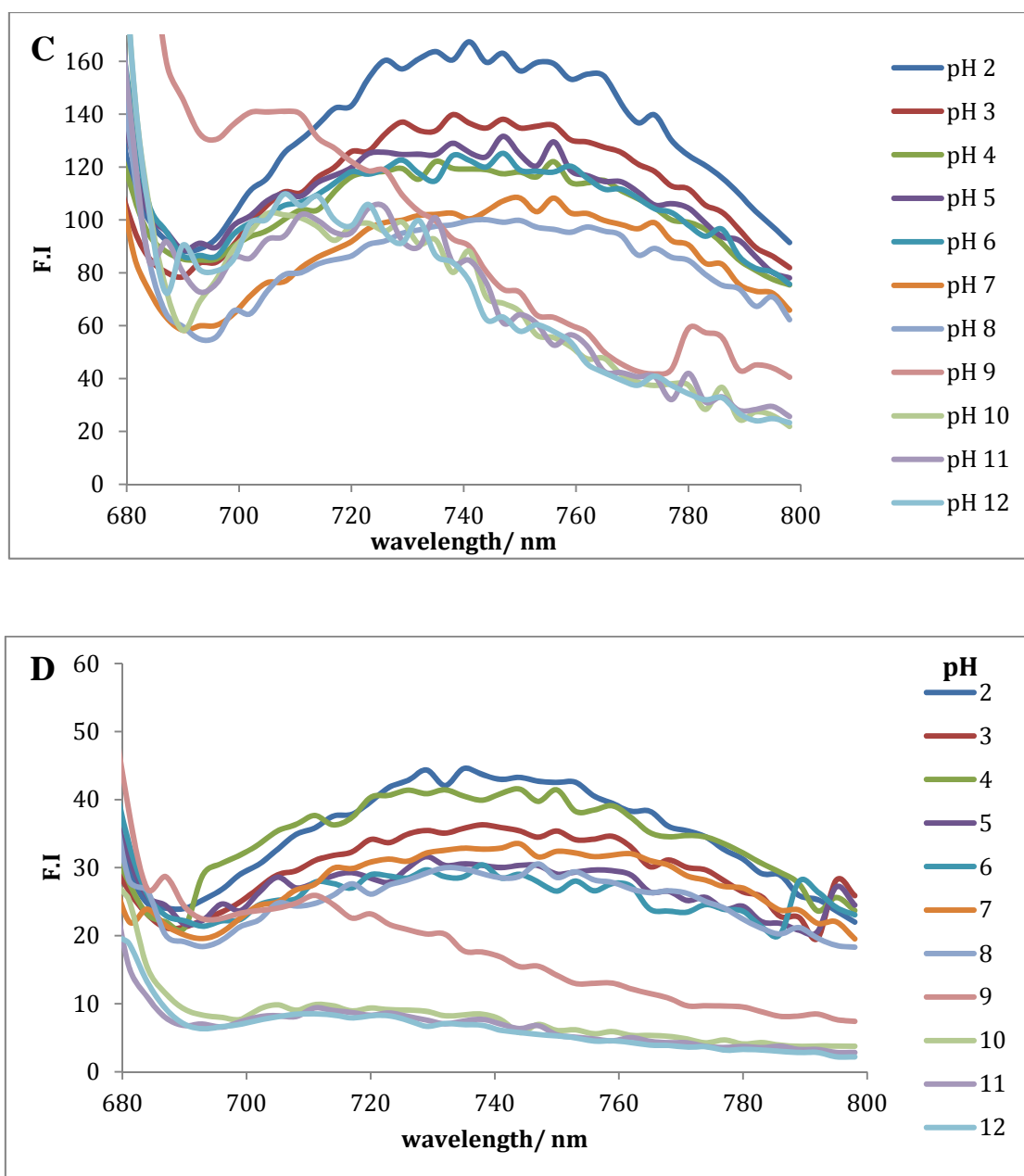


**Figure 6.3.7.** Emission fluorescence spectrum of **4.54** measured at different pH **C.** initially and **D.** after 3 h.

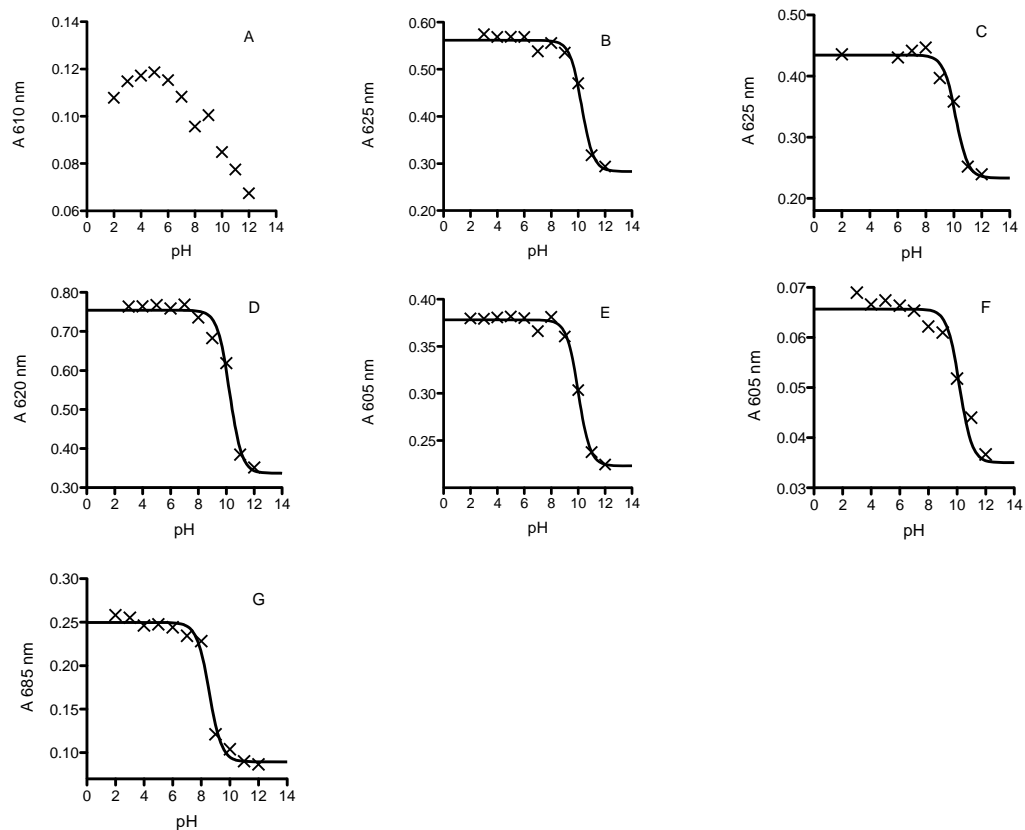


**Figure 6.3.8.** Absorbance vs pH plots for hybrid dyes fitted to sigmoidal pKa plot;  $Y = \frac{(\text{Bottom} \cdot 10^{(X - \text{pKa})} + \text{Top})}{(1 + 10^{(X - \text{pKa})})}$  4.48-4.54 (A-G).



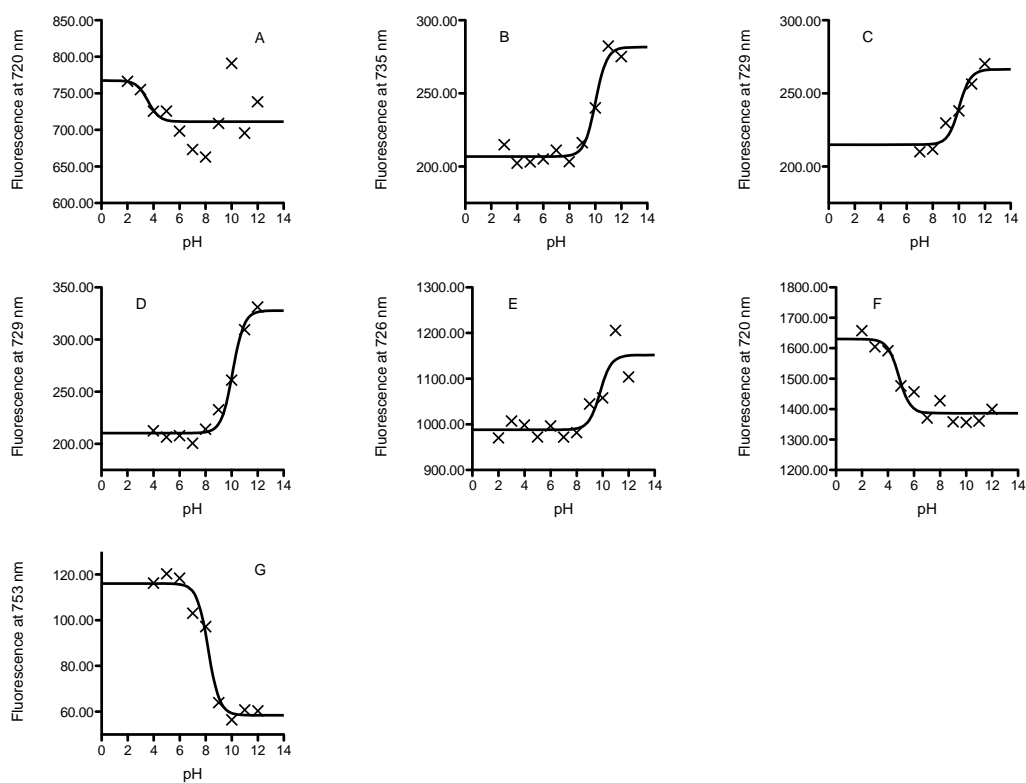


**Figure 6.3.9.** Corrected fluorescence vs pH plots for hybrid dyes fitted to sigmoidal pKa plot;  $Y = (\text{Bottom} \cdot 10^{(X - \text{pKa})} + \text{Top}) / (1 + 10^{(X - \text{pKa})})$  4.48-4.54 (A-G).

#### 6.4. Response of fluorescence of the Epicoconone-Hemicyanine Hybrid Dyes to SDS

Graph A is the fluorescence spectra of the hybrid dye at different concentrations of SDS, graph B is a plot of log of fluorescence intensity against log of SDS concentration and graph C is a plot of fluorescence intensity against log of viscosity of SDS micelles formed in water.

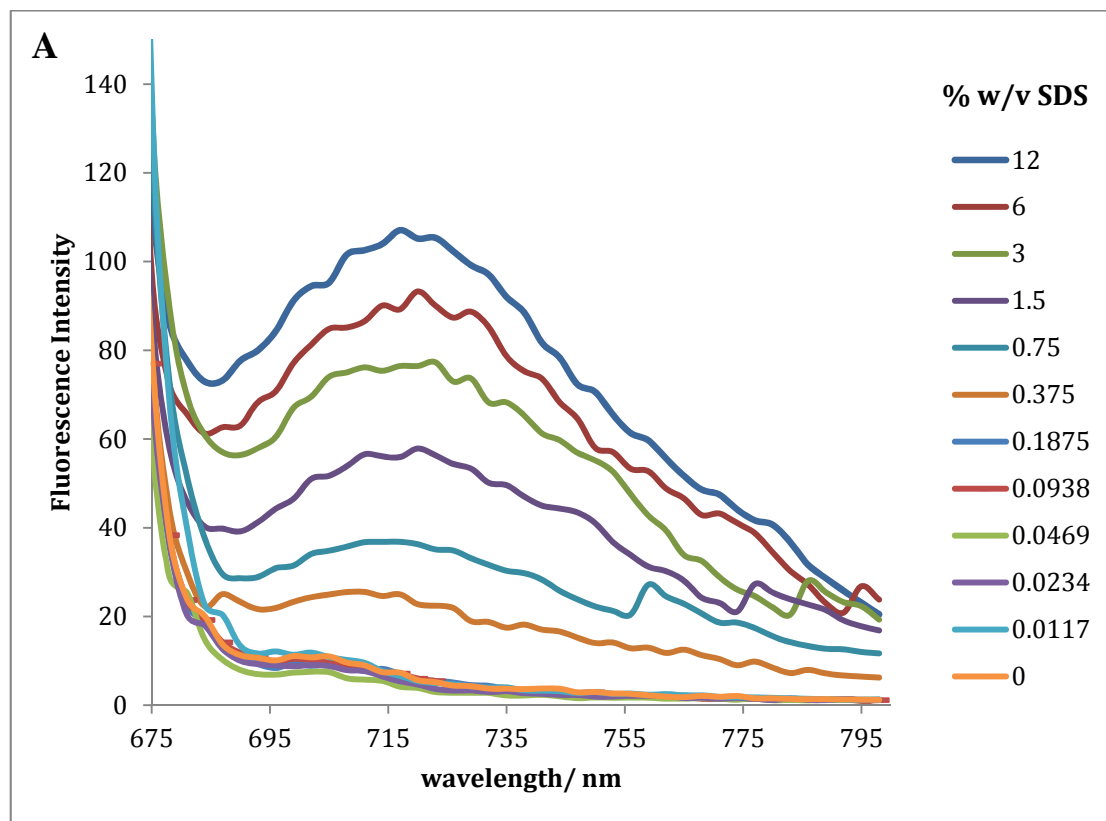


**Figure 6.4.1A.** Fluorescence spectrum of **4.48** measured at different [SDS] (% w/v).

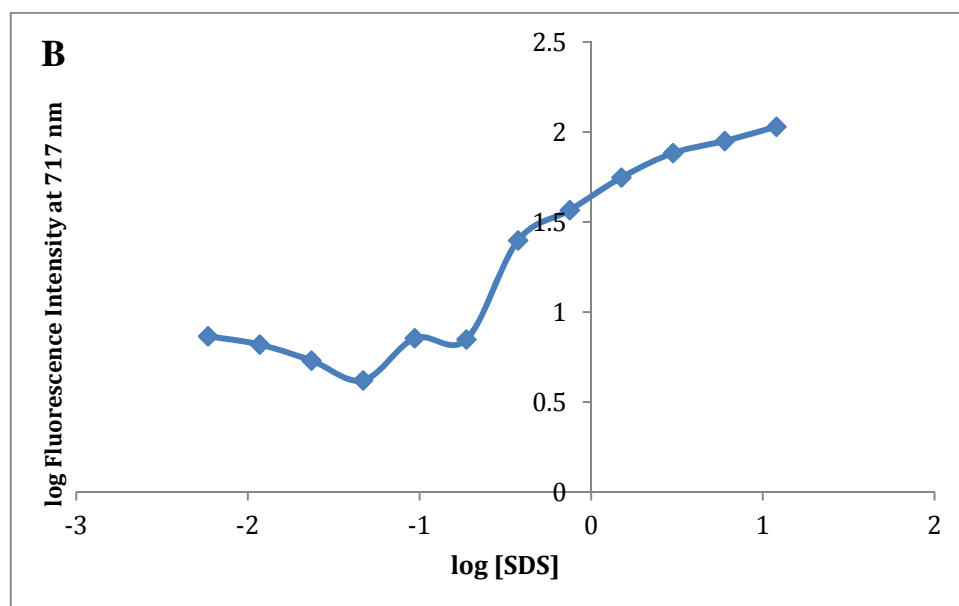


**Figure 6.4.1B.** log fluorescence intensity at max  $\lambda_{em}$  of 717 nm against log[SDS] of **4.48**.

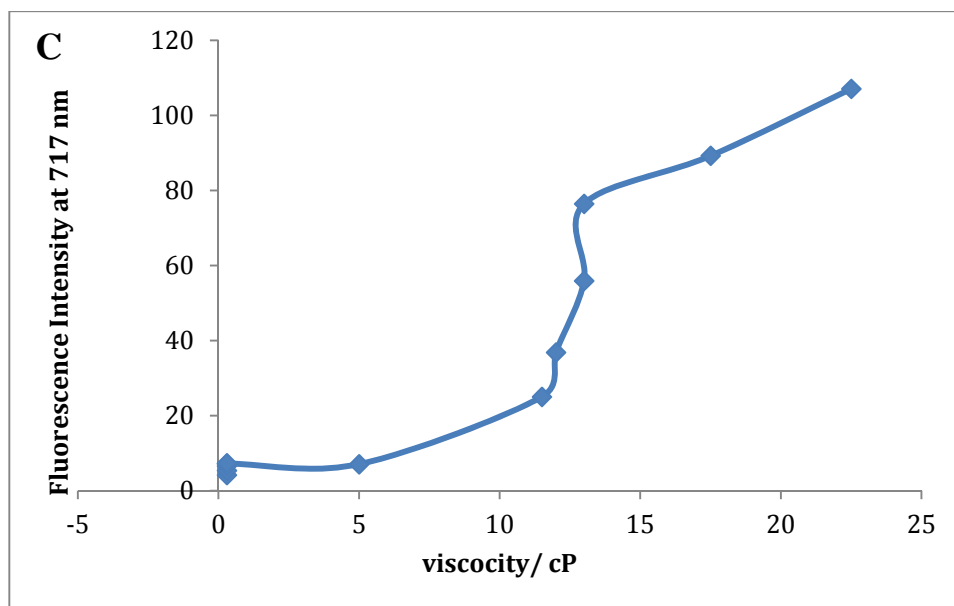


**Figure 6.4.1C.** Fluorescence intensity at max  $\lambda_{em}$  of 717 nm against viscosity/cP of **4.48**.

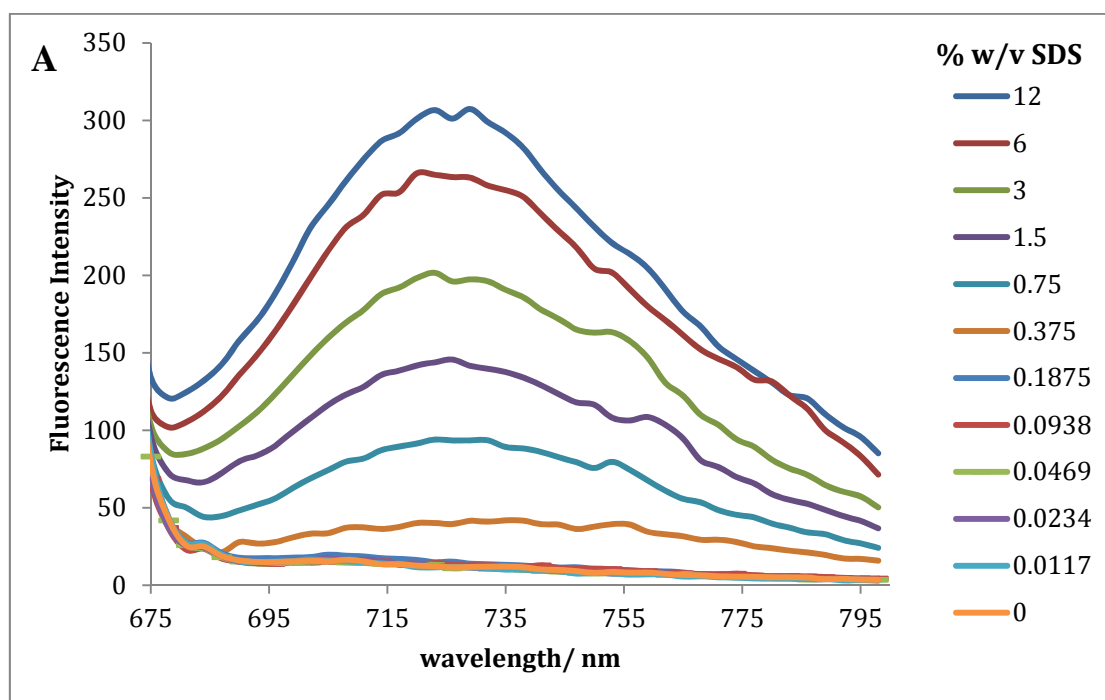


**Figure 6.4.2A.** Fluorescence spectrum of **4.49** measured at different [SDS] (% w/v).

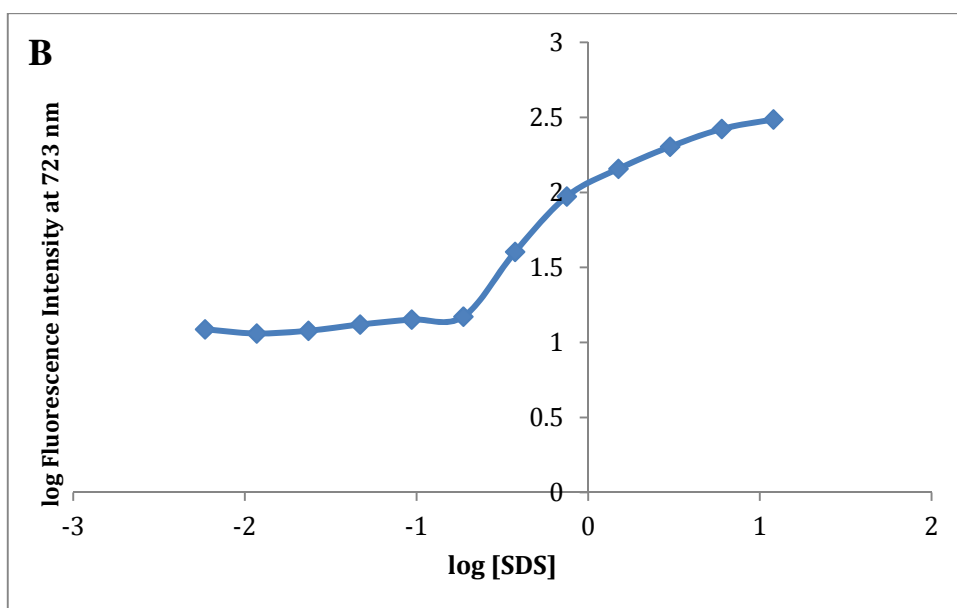


**Figure 6.4.2B.** log fluorescence intensity at max  $\lambda_{em}$  of 723 nm against log[SDS] of **4.49**.

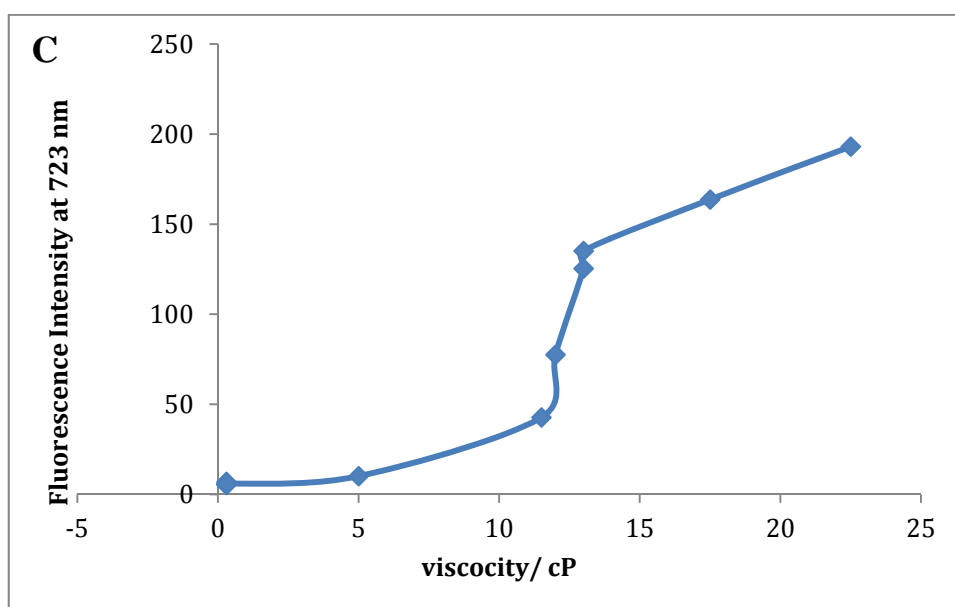


**Figure 6.4.2C.** Fluorescence intensity at max  $\lambda_{em}$  of 756 nm against viscosity/cP of **4.49**.

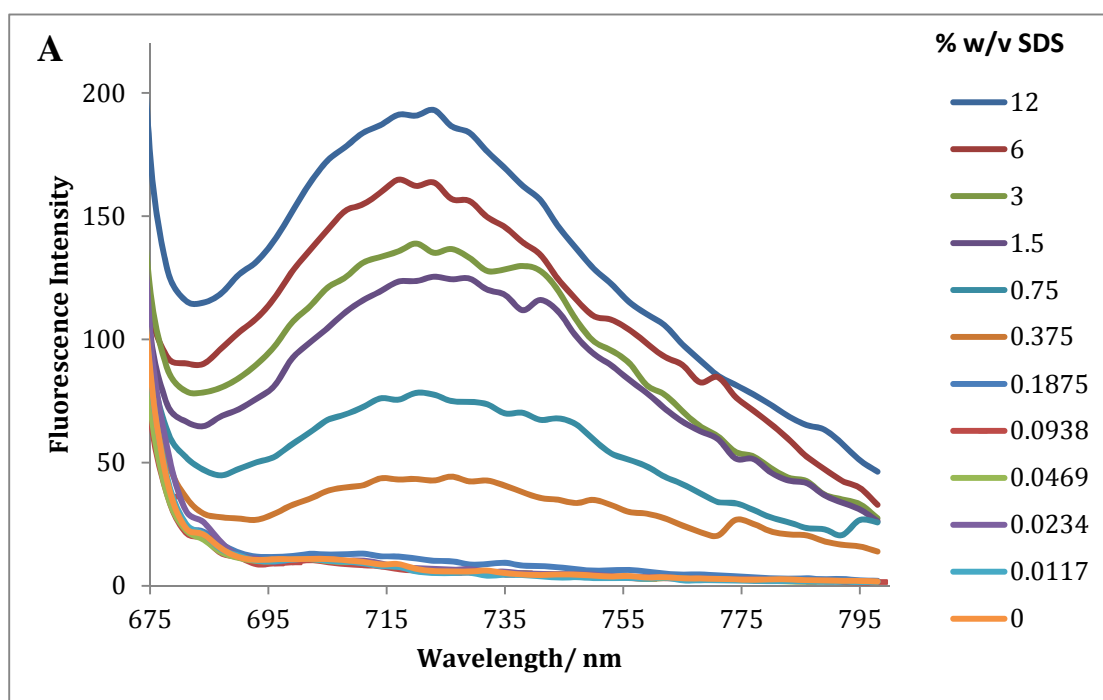


**Figure 6.4.3A.** Fluorescence spectrum of **4.50** measured at different [SDS] (% w/v).

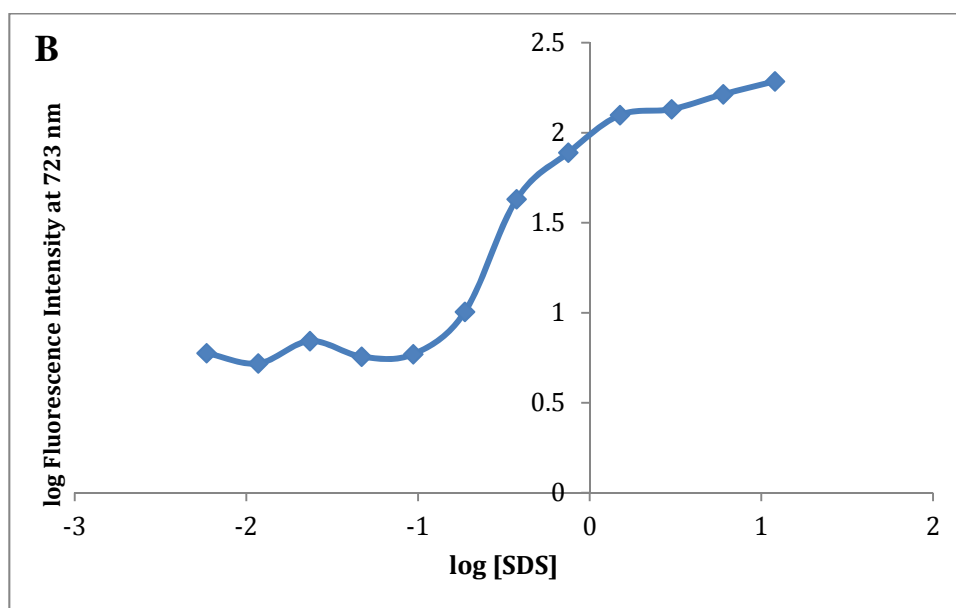


**Figure 6.4.3B.** log fluorescence intensity at max  $\lambda_{em}$  of 723 nm against log[SDS] of **4.50**.

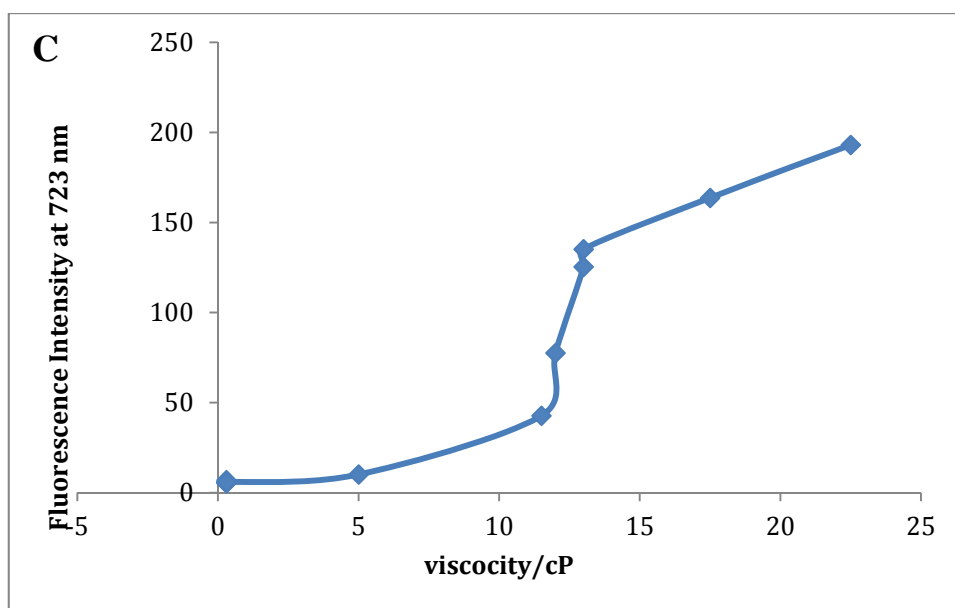


**Figure 6.4.3C.** Fluorescence intensity at max  $\lambda_{em}$  of 723 nm against viscosity/cP of **4.50**.

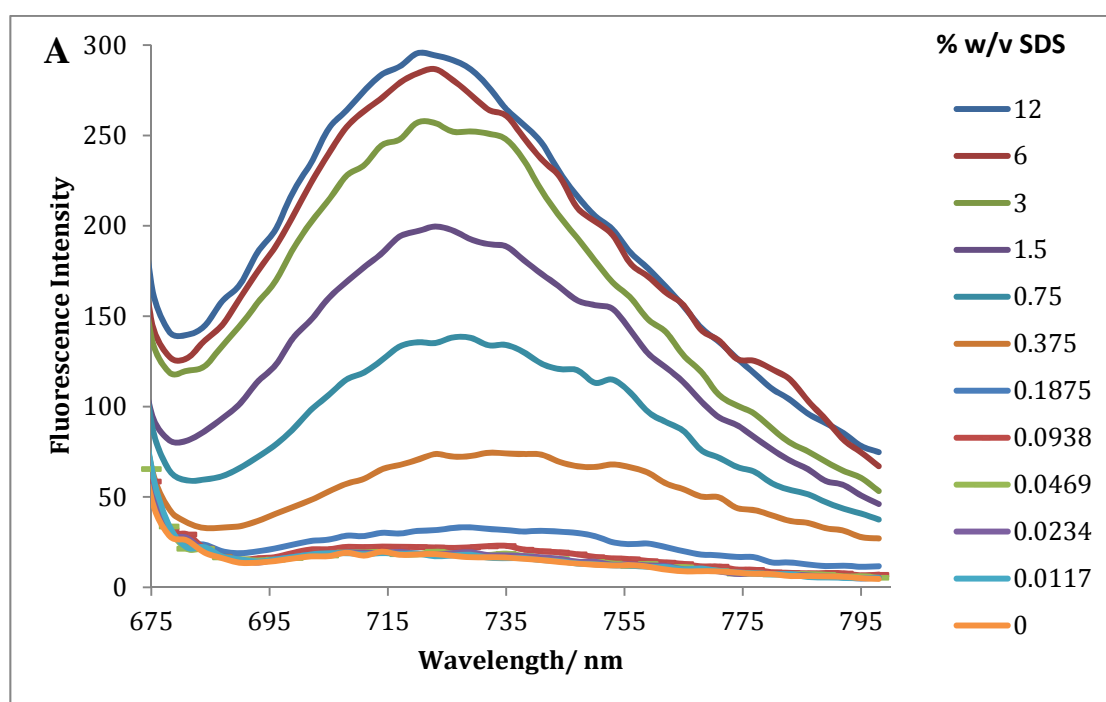


**Figure 6.4.4A.** Fluorescence spectrum of **4.51** measured at different [SDS] (% w/v).

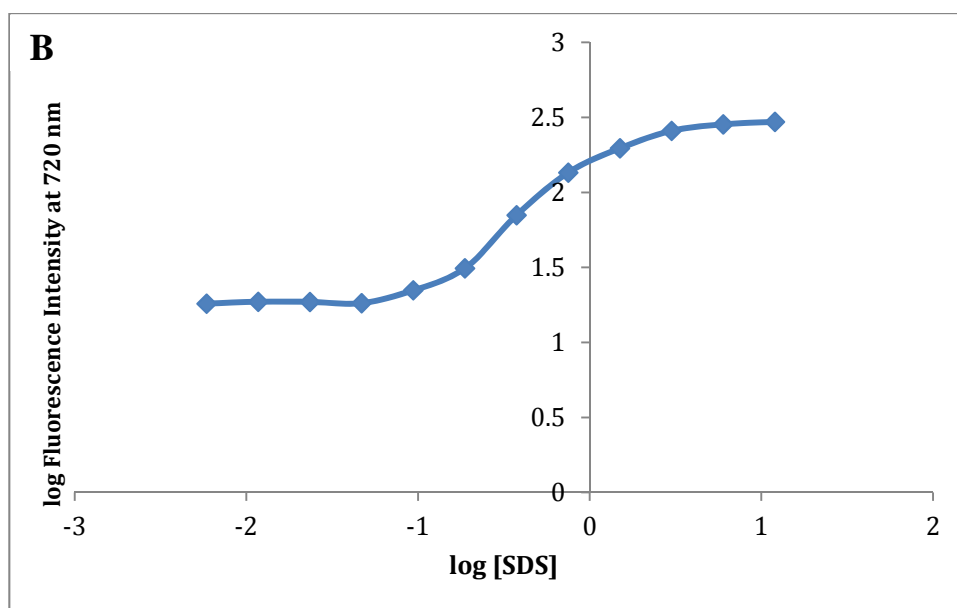


**Figure 6.4.4B.** log fluorescence intensity at max  $\lambda_{em}$  of 720 nm against log[SDS] of **4.51**.

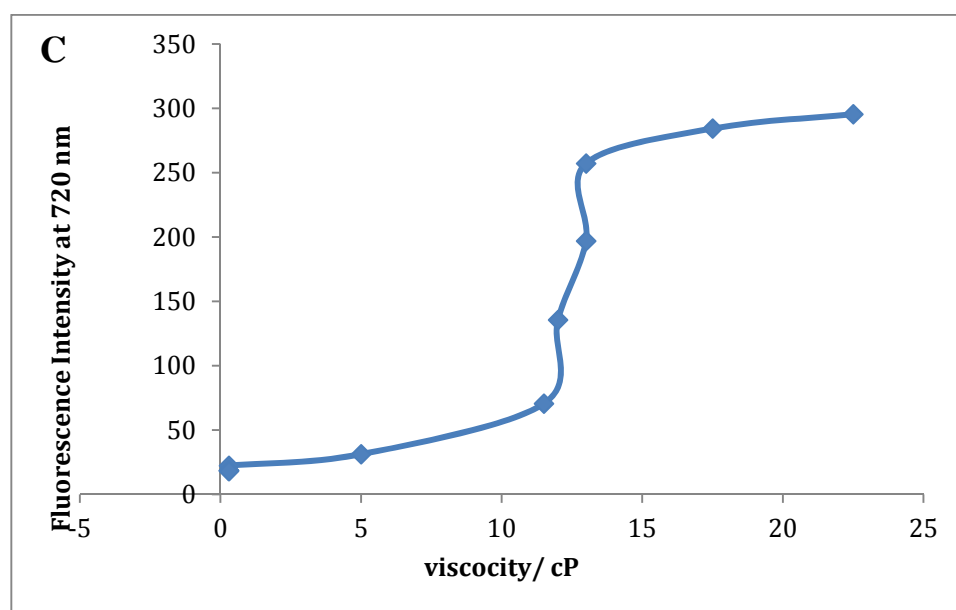


**Figure 6.4.4C.** Fluorescence intensity at max  $\lambda_{em}$  of 720 nm against viscosity/cP of **4.51**.

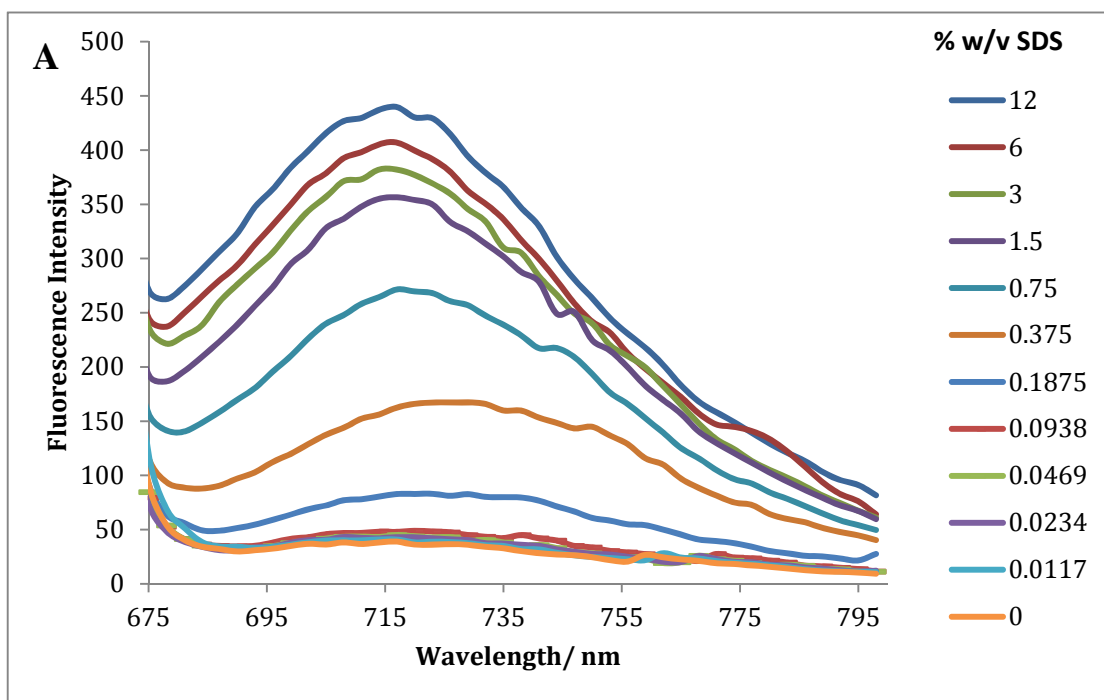


**Figure 6.4.5A.** Fluorescence spectrum of **4.52** measured at different [SDS] (% w/v).

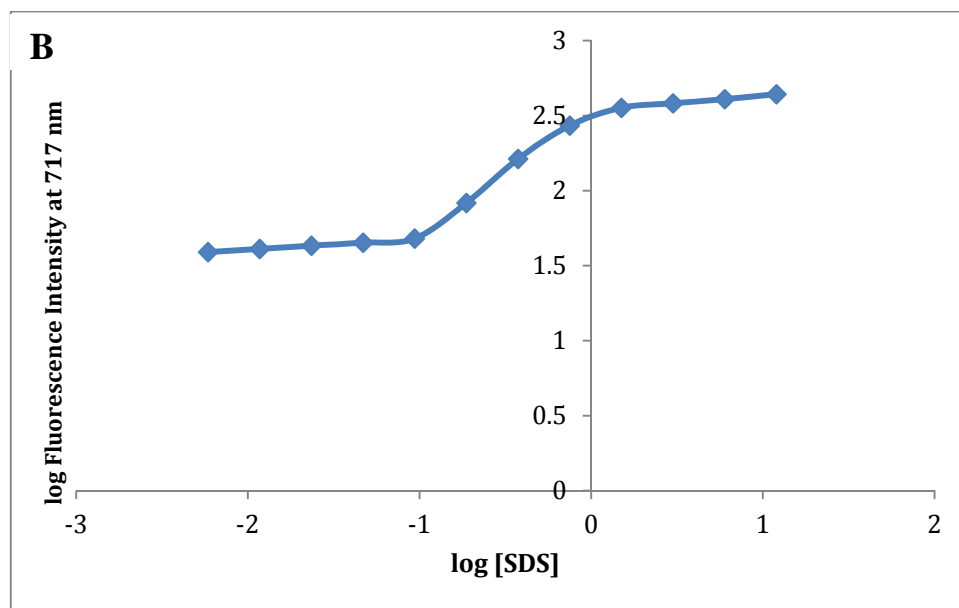


**Figure 6.4.5B.** log fluorescence intensity at max  $\lambda_{em}$  of 717 nm against log[SDS] of **4.52**.



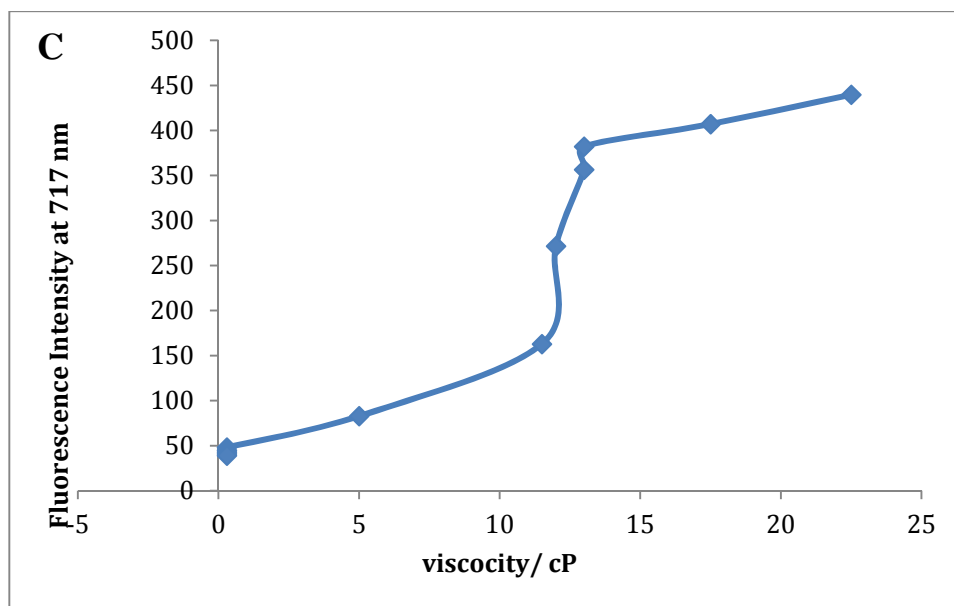


**Figure 6.4.5C.** Fluorescence intensity at max  $\lambda_{em}$  of 717 nm against viscosity/cP of **4.52**.

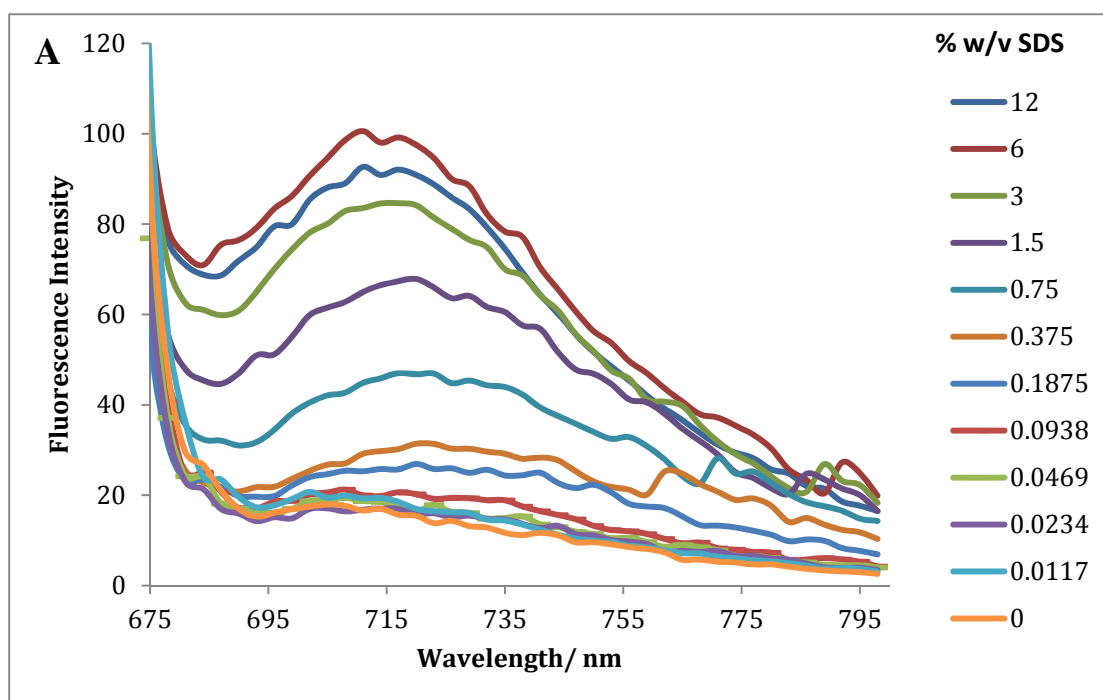


**Figure 6.4.6A.** Fluorescence spectrum of **4.53** measured at different [SDS].

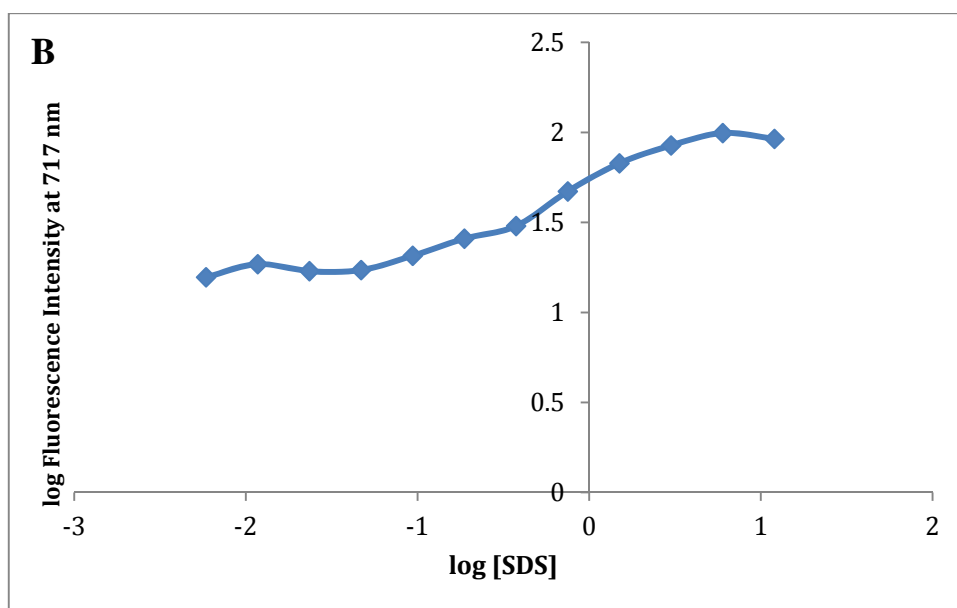


**Figure 6.4.6B.** log fluorescence intensity at max  $\lambda_{em}$  of 717 nm against log[SDS] of **4.53**.

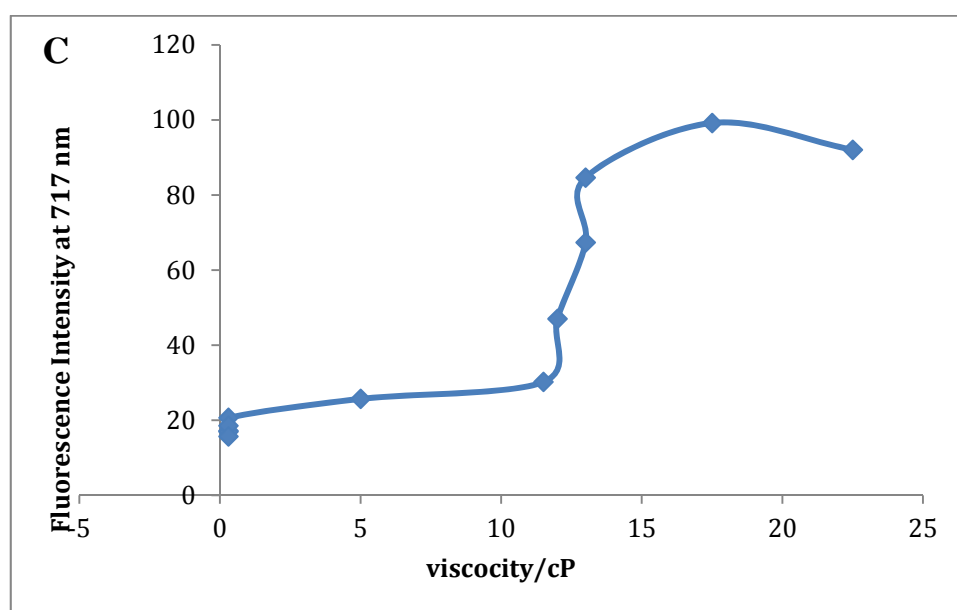


**Figure 6.4.6C.** Fluorescence intensity at max  $\lambda_{em}$  of 717 nm against viscosity/cP of **4.53**.

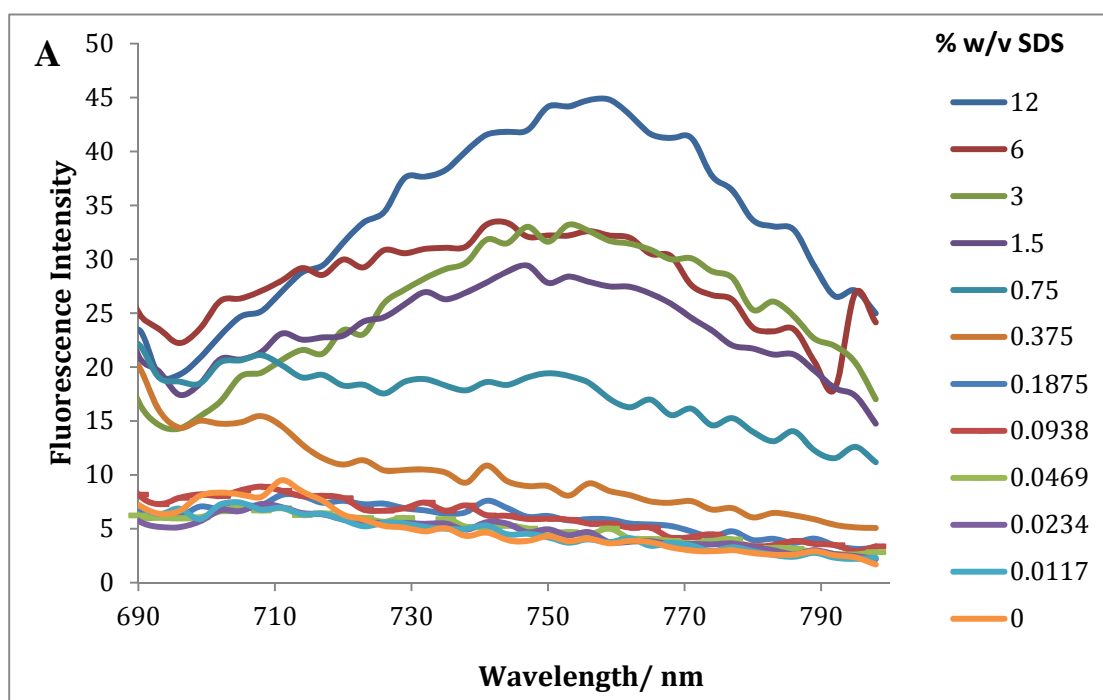


**Figure 6.4.7A.** Fluorescence spectrum of **4.54** measured at different [SDS].

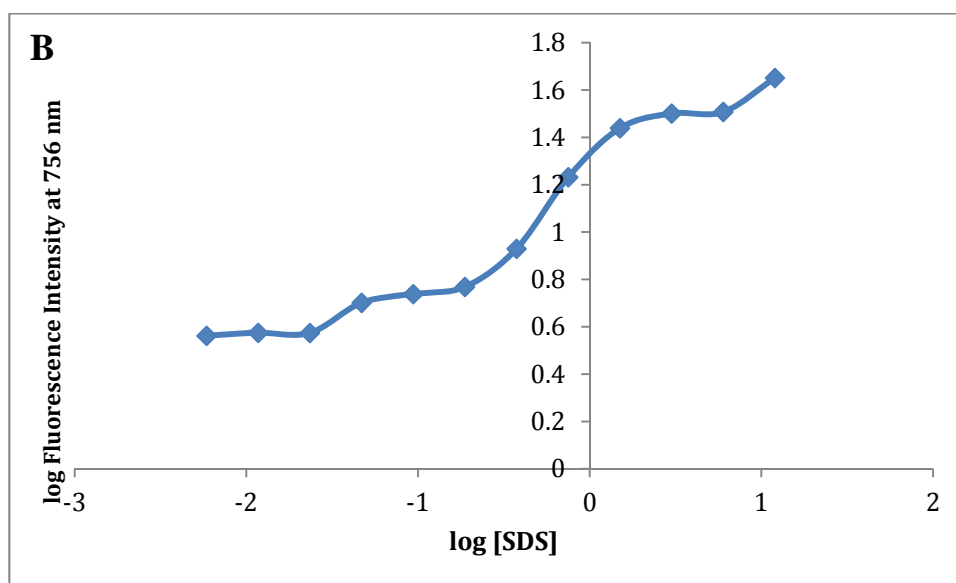


**Figure 6.4.7B.** log fluorescence intensity at max  $\lambda_{em}$  of 756 nm against log[SDS] of **4.54**.

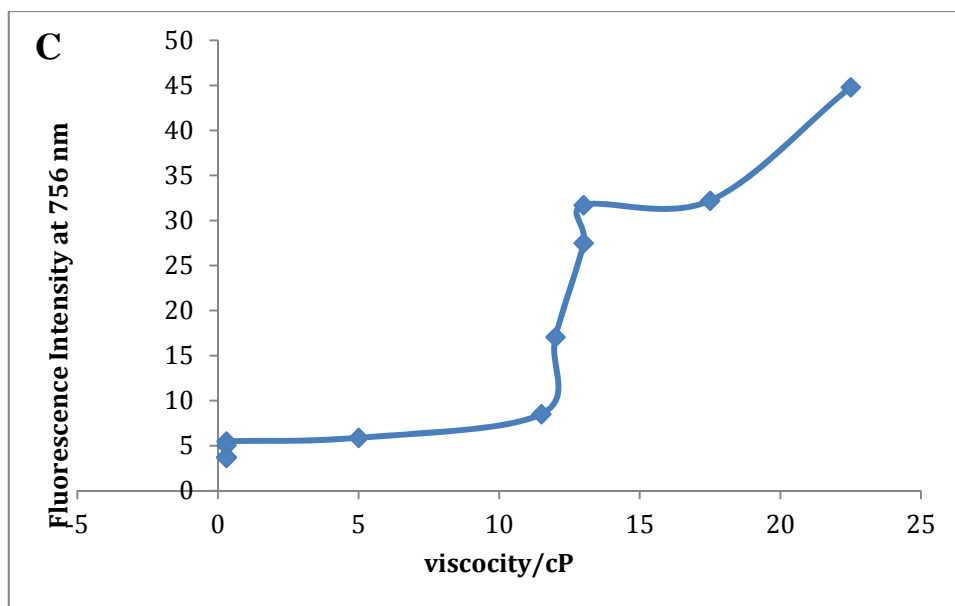


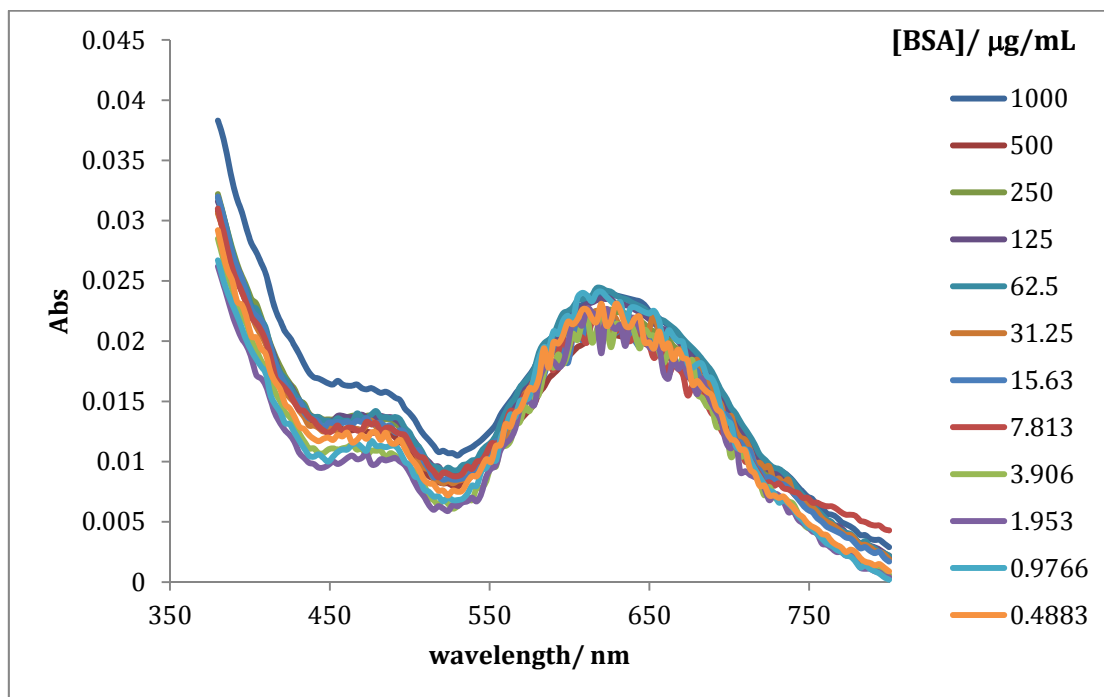
**Figure 6.4.7C.** Fluorescence intensity at max  $\lambda_{em}$  of 756 nm against viscosity/cP of **4.54**.

### 6.5. Response of the Epicocconone-Hemicyanine Hybrid Dyes to dsDNA

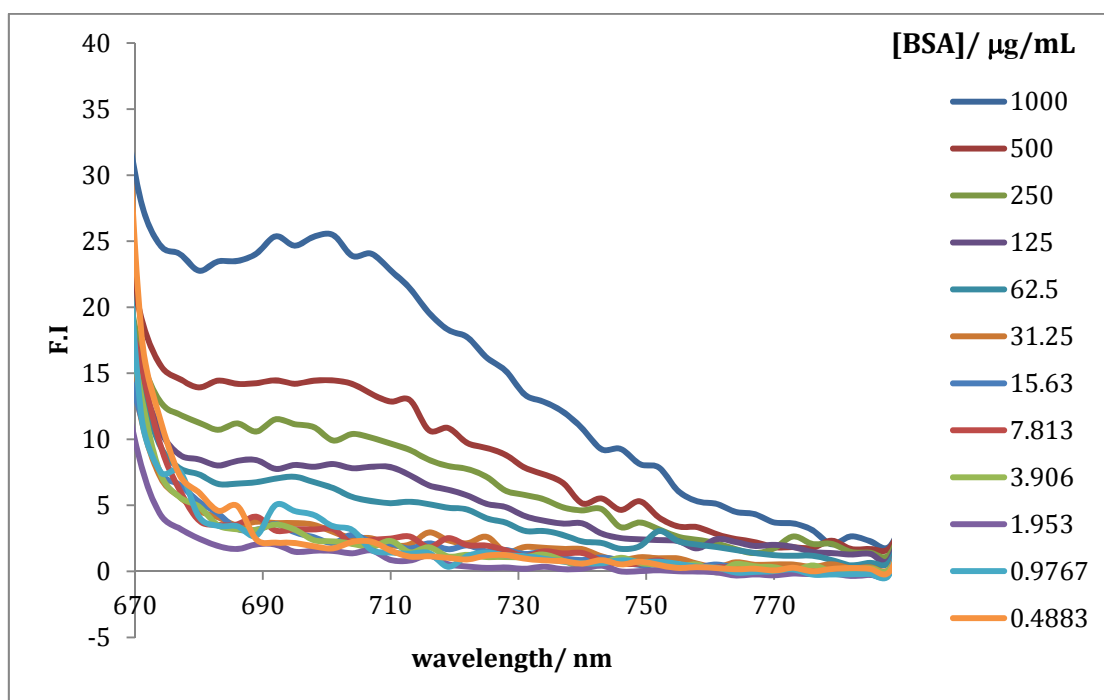
Fluorescence is quenched at all concentration of dsDNA and therefore no response to dsDNA was found.

### 6.6. Response of the Epicocconone-Hemicyanine Hybrid Dyes to BSA

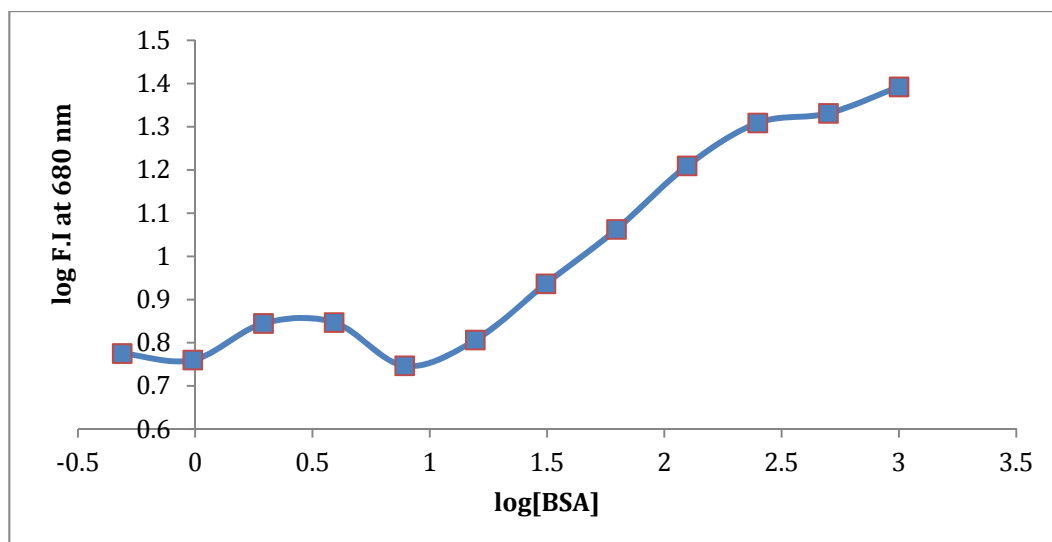
Graph A is the absorbance spectra of the hybrid dye at different concentrations of BSA ( $\mu\text{g/mL}$ ), graph B is the fluorescence emission spectra of the hybrid dye at different concentrations of BSA ( $\mu\text{g/mL}$ ) and graph C is a plot of log fluorescence intensity at max  $\lambda_{\text{em}}$  against log [BSA].



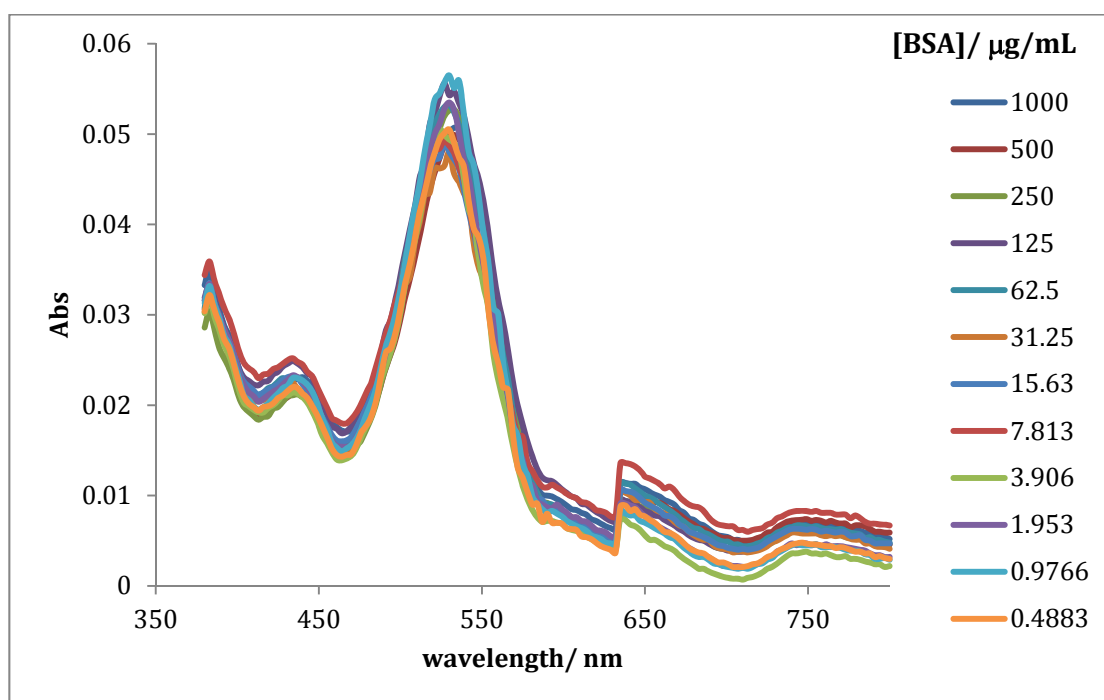
**Figure 6.6.1A.** Absorbance spectrum of **4.50** measured at different [BSA] ( $\mu\text{g/mL}$ ).



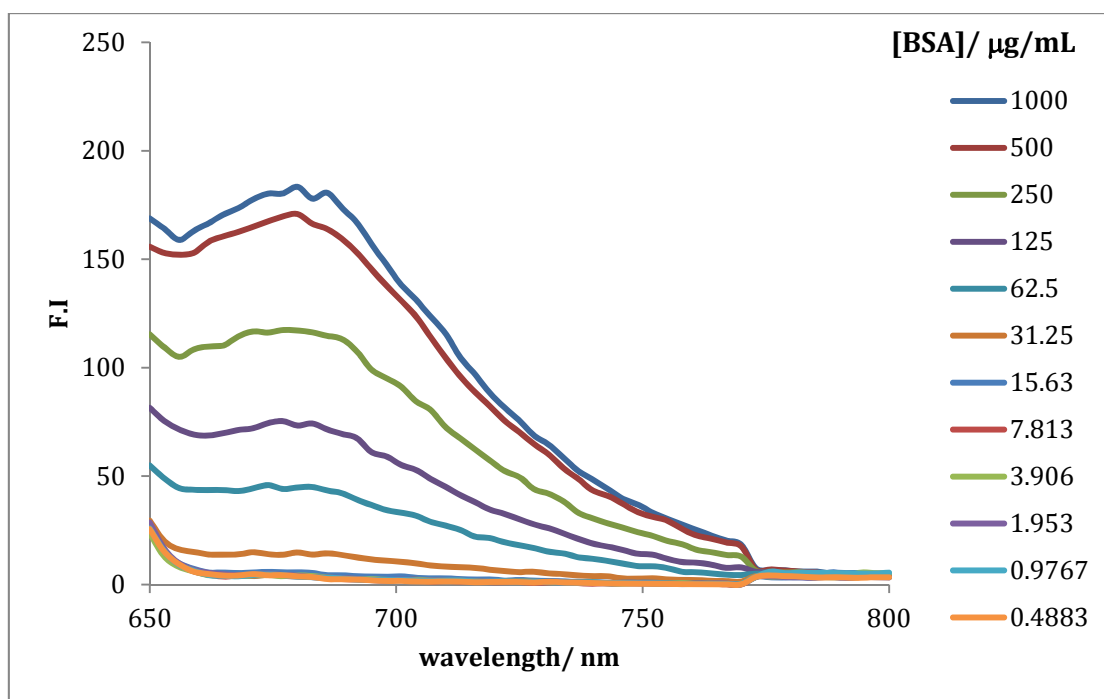
**Figure 6.6.1B.** Emission fluorescence spectrum of **4.50** measured at different [BSA] ( $\mu\text{g/mL}$ ).



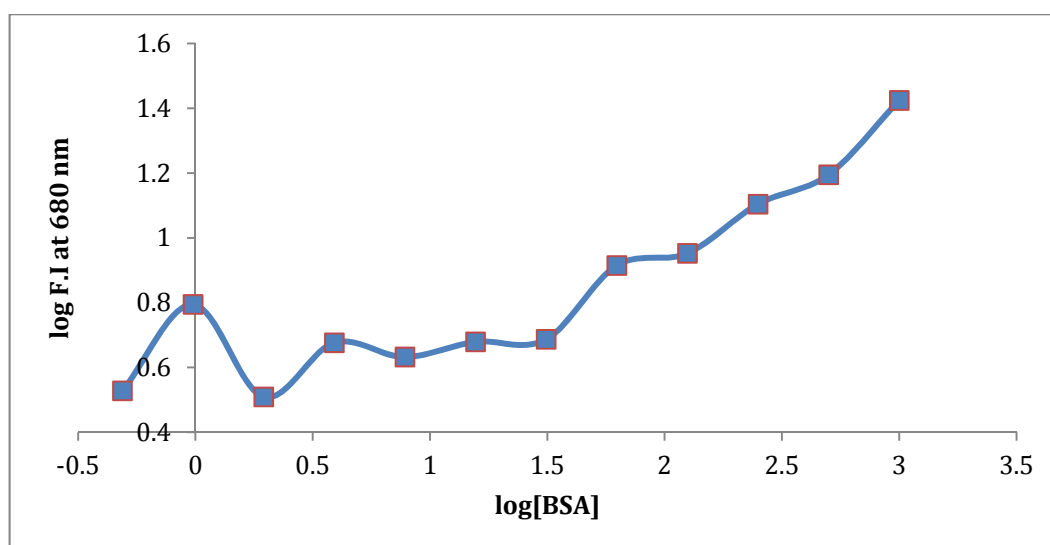
**Figure 6.6.1C.** log fluorescence intensity at max  $\lambda_{em}$  of 680 nm against log [BSA] of 4.50.



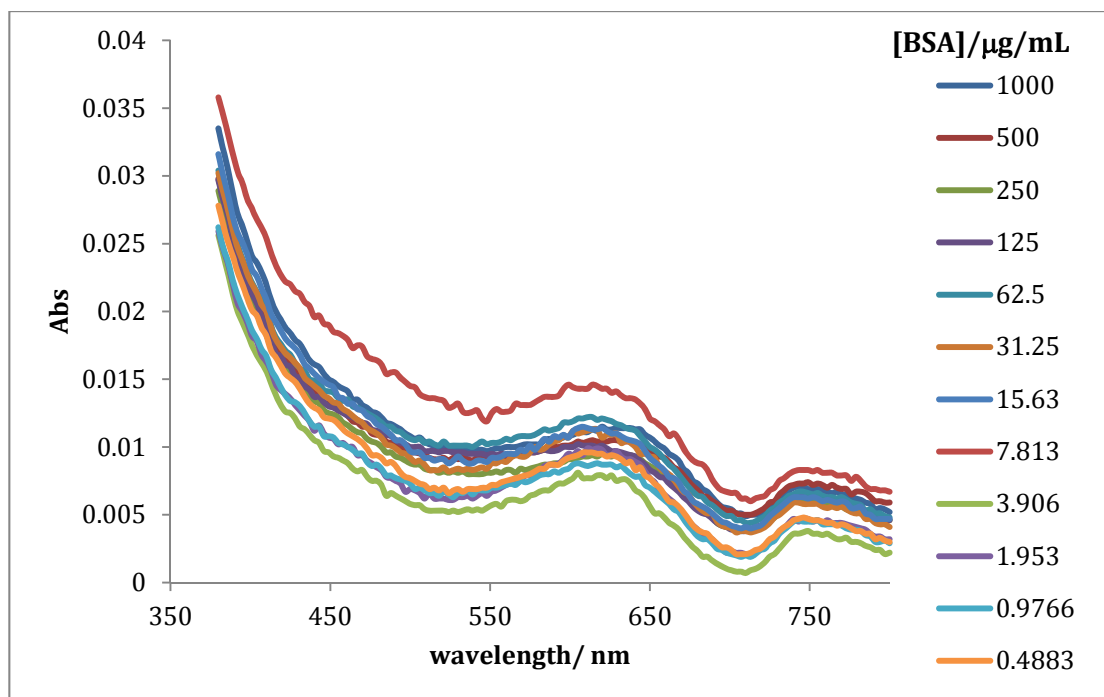
**Figure 6.6.2A.** Absorbance spectrum of 4.52 measured at different [BSA] ( $\mu\text{g/mL}$ ).



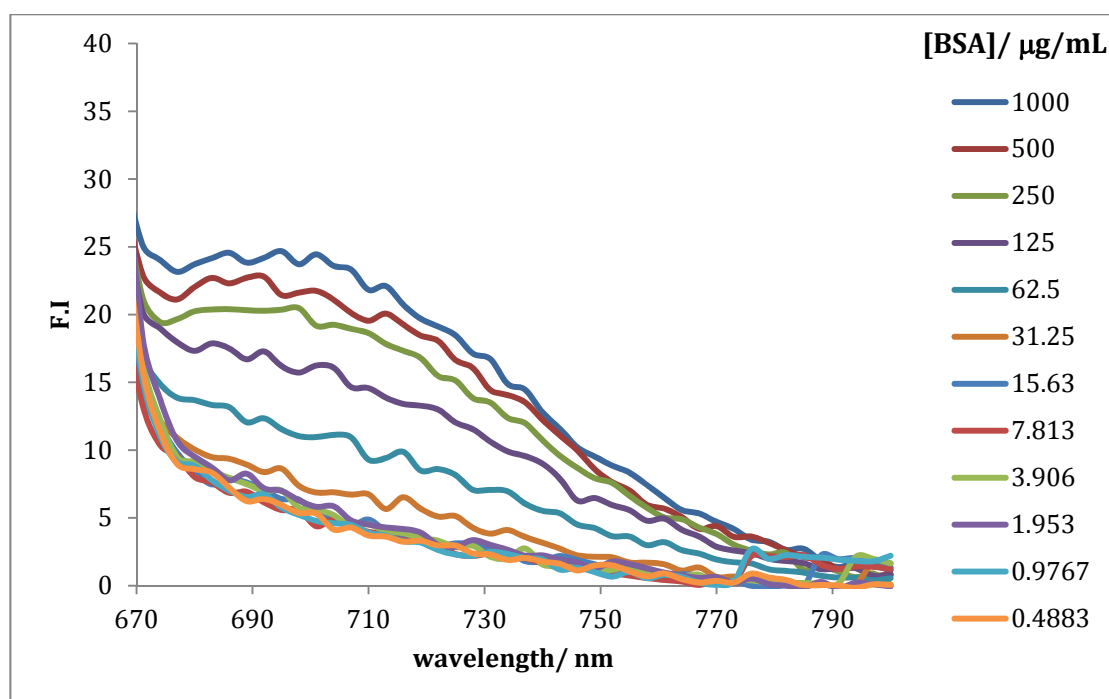
**Figure 6.6.2B** Emission fluorescence spectrum of **4.52** measured at different [BSA] ( $\mu\text{g/mL}$ ).



**Figure 6.6.2C.**  $\log$  fluorescence intensity at max  $\lambda_{\text{em}}$  of 680 nm against  $\log$  [BSA] of **4.52**.

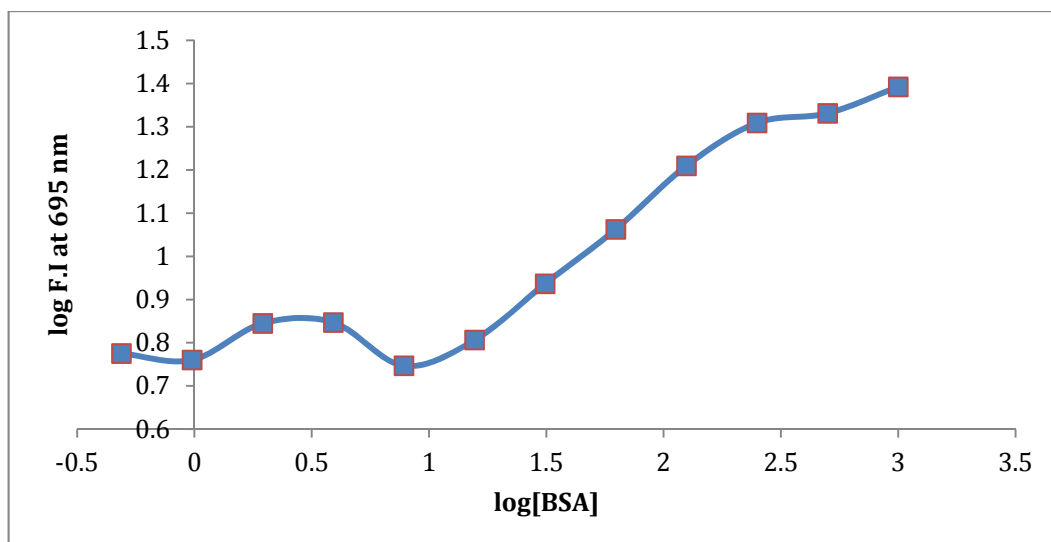


**Figure 6.6.3A.** Absorbance spectrum of **4.53** measured at different [BSA] ( $\mu\text{g/mL}$ ).



**Figure 6.6.3B** Emission fluorescence spectrum of **4.53** measured at different [BSA] ( $\mu\text{g/mL}$ ).

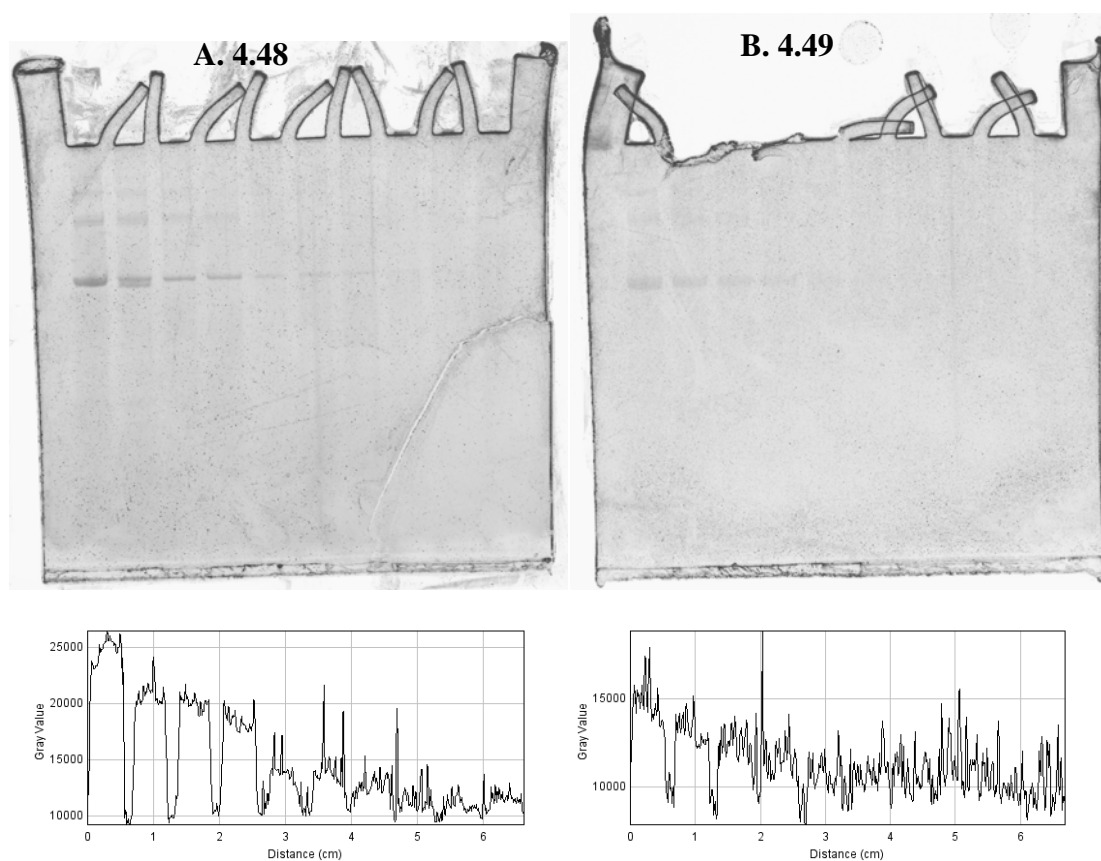


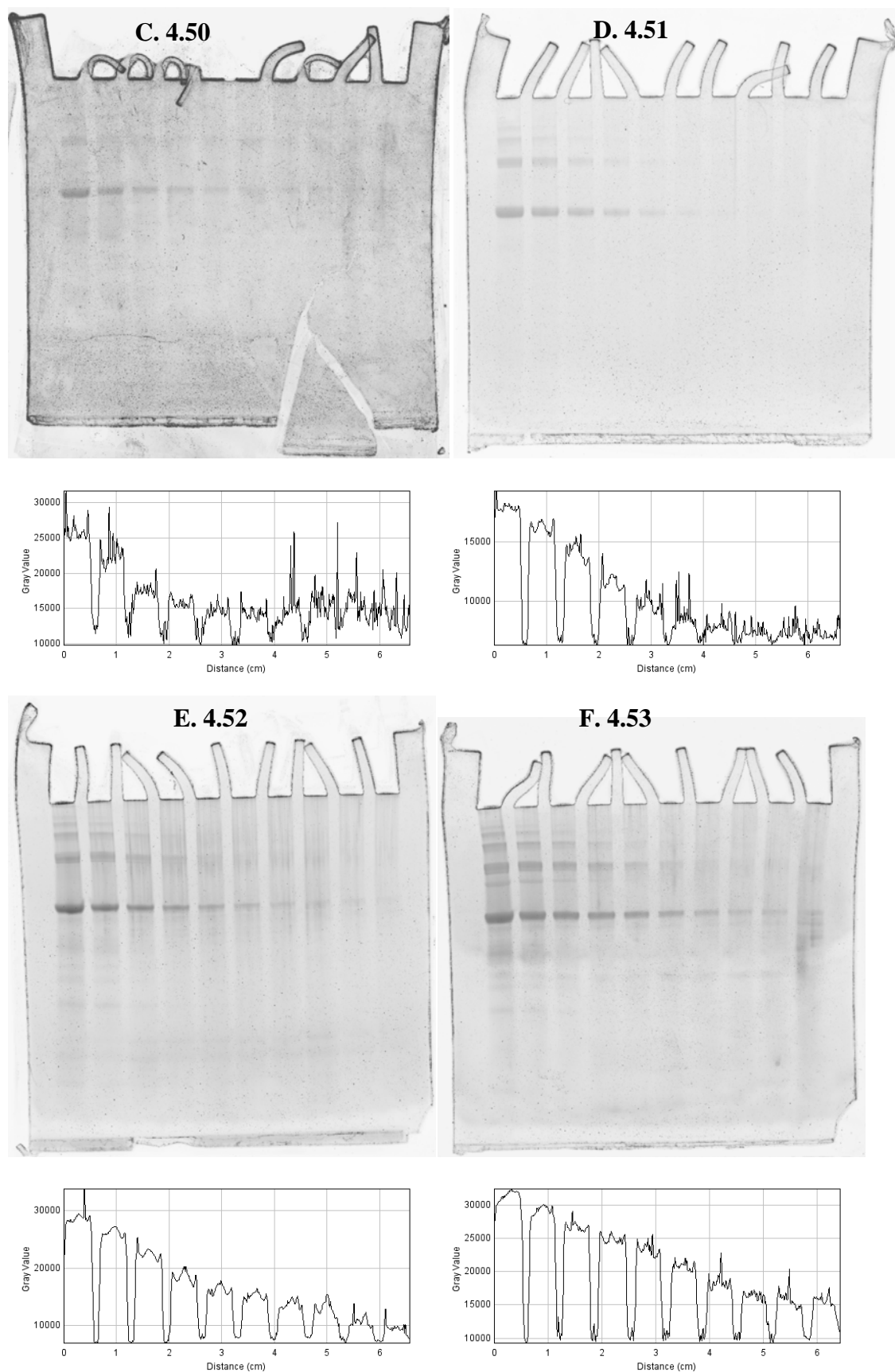


**Figure 6.6.3C.** log fluorescence intensity at max  $\lambda_{em}$  of 695 nm against log [BSA] of 4.53.

## 6.7. Protein Detection on Gel Electrophoresis

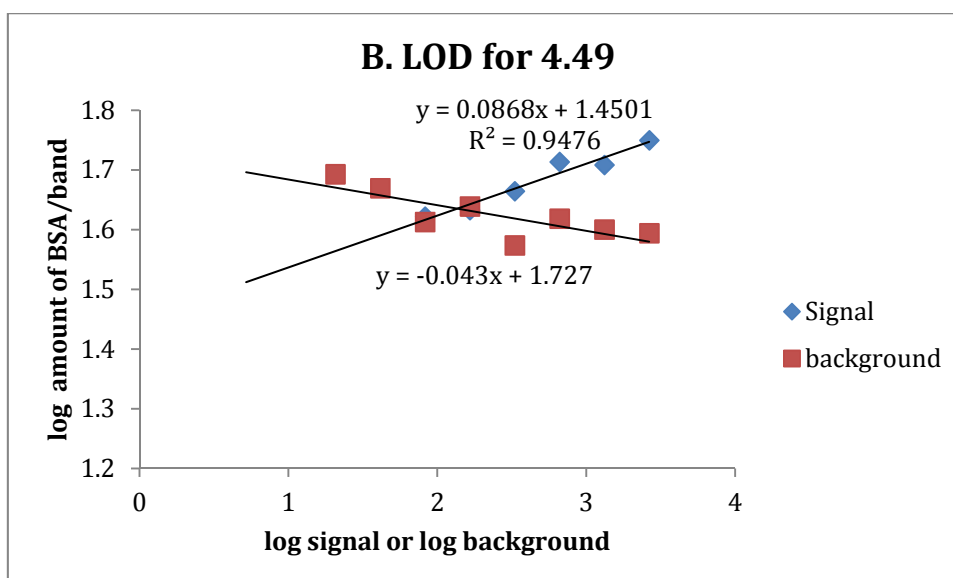
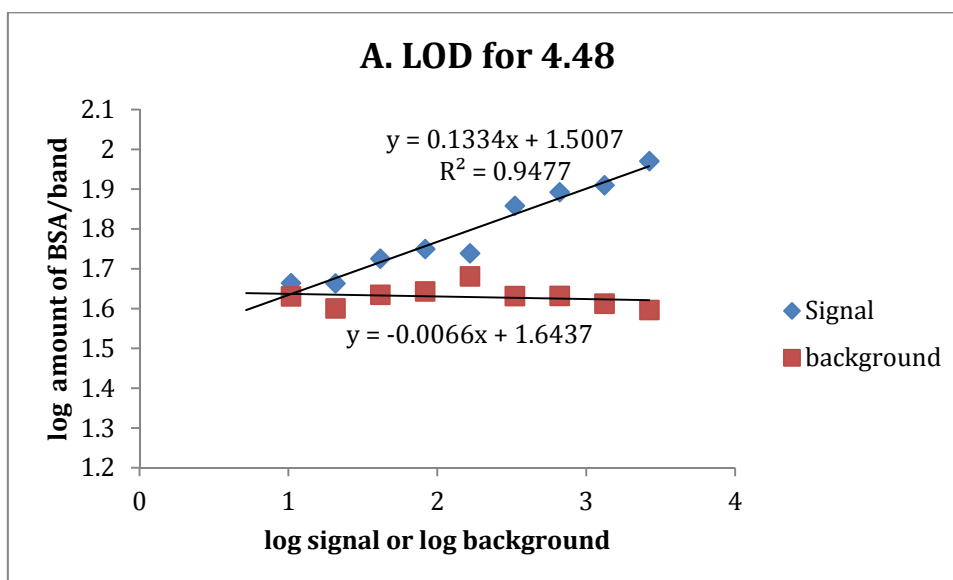
### 6.7.1. Typhoon Scans of Gels Stained with the Hybrid Dyes 4.48-4.53

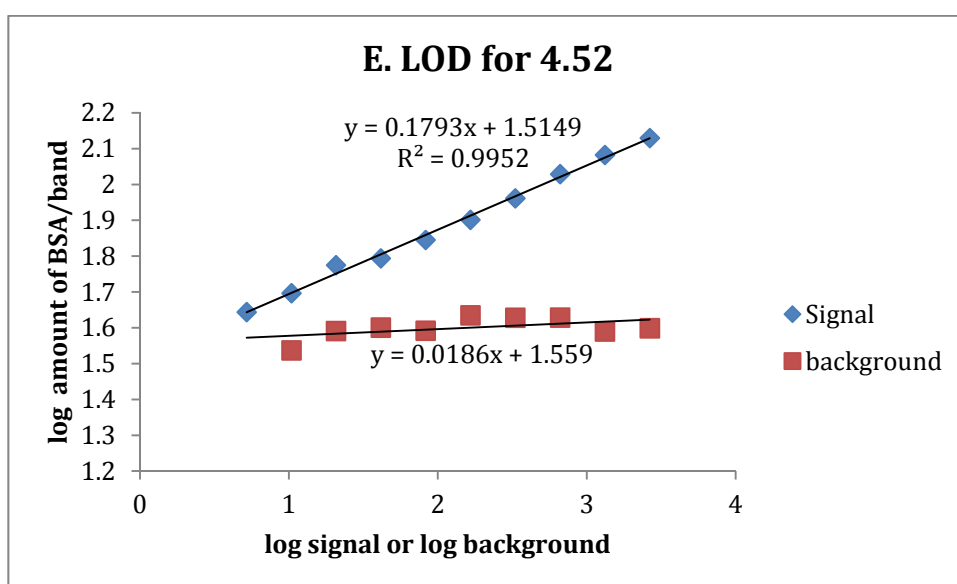
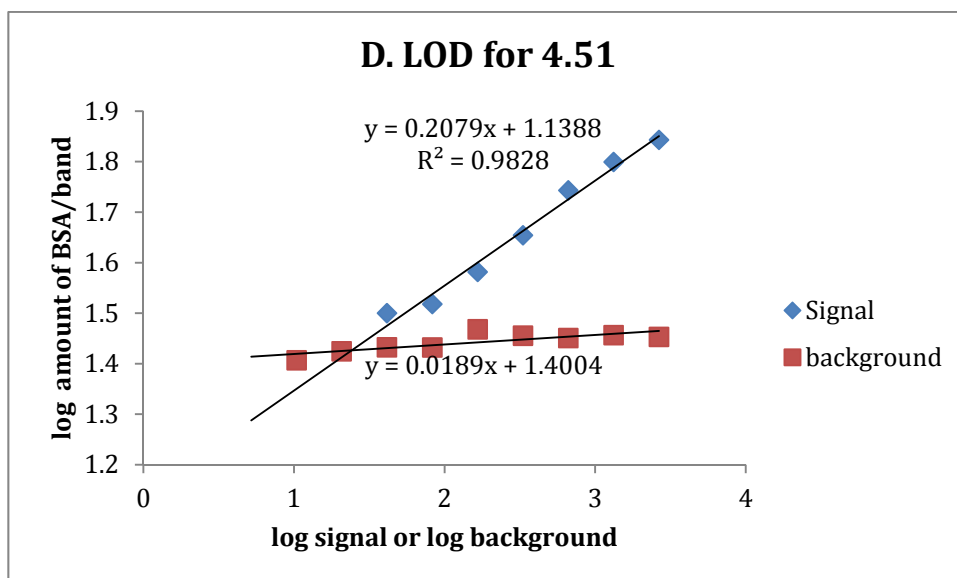
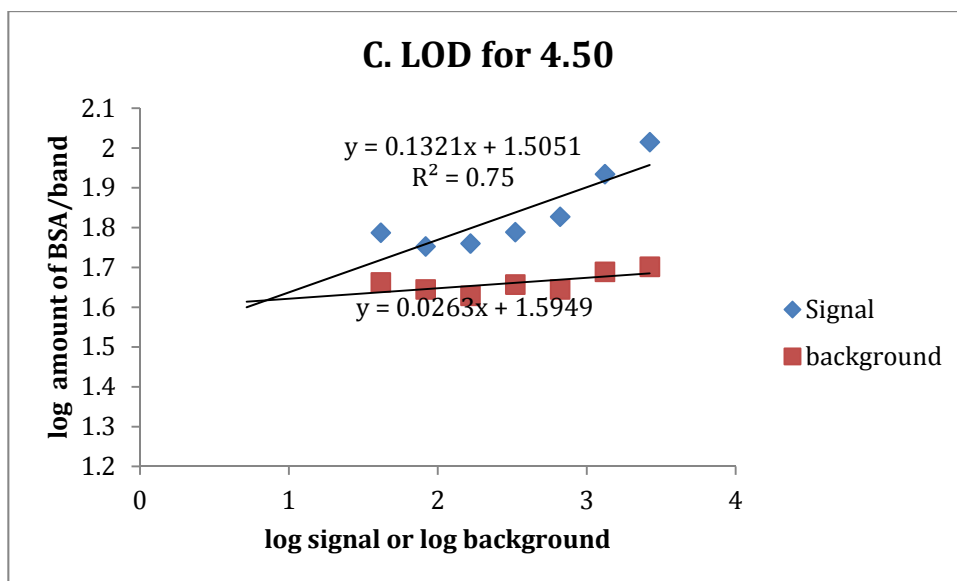




**Figure 6.7.1.** Serial dilution of BSA from 2.65  $\mu\text{g}$  to 5.2 ng/band and stained with 1  $\mu\text{g/mL}$  (50 mL) of hybrid dyes **A.-F. 4.48-4.53**. Typhoon scans of the gel stained with the epicocconone-hemicyanine hybrid dyes **A-F (4.48-4.53)**, along with a Plot Profile of the main protein band generated using ImageJ.

### 6.7.1. Determination of Limit of Detection of BSA Detected on Gel in ng of the Hybrid Dyes 4.48-4.53





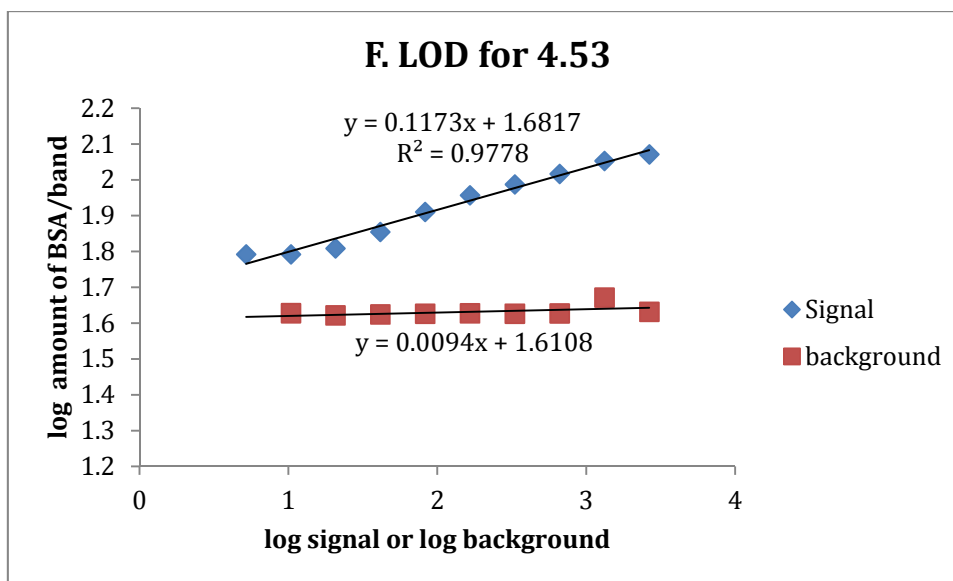


**Figure 6.7.2. A-F.** Determination of the limit of detection, LOD of the hybrid dyes **4.48-4.53** for BSA, was made by linear regression of background versus signal for BSA.

**Figure 6.7.2. A-F.** show the plots of log of amount of BSA/band vs. log of signal and log background. An average of the total grey values of the main protein band from the plot profile was taken as signal. Similarly, an average of the total grey value of an area in between bands was taken as background. The plot profiles were generated using ImageJ. The point of intersection of the two lines is where signal can no longer be differentiated from background and used here to define the LOD. The difference in slope of the signal (blue) and background (red) is an indication of contrast and the goodness of fit ( $R^2$ ), an indication of linearity of response.

## 6.8. Additional Live Cell Images with Hybrid dye 4.49

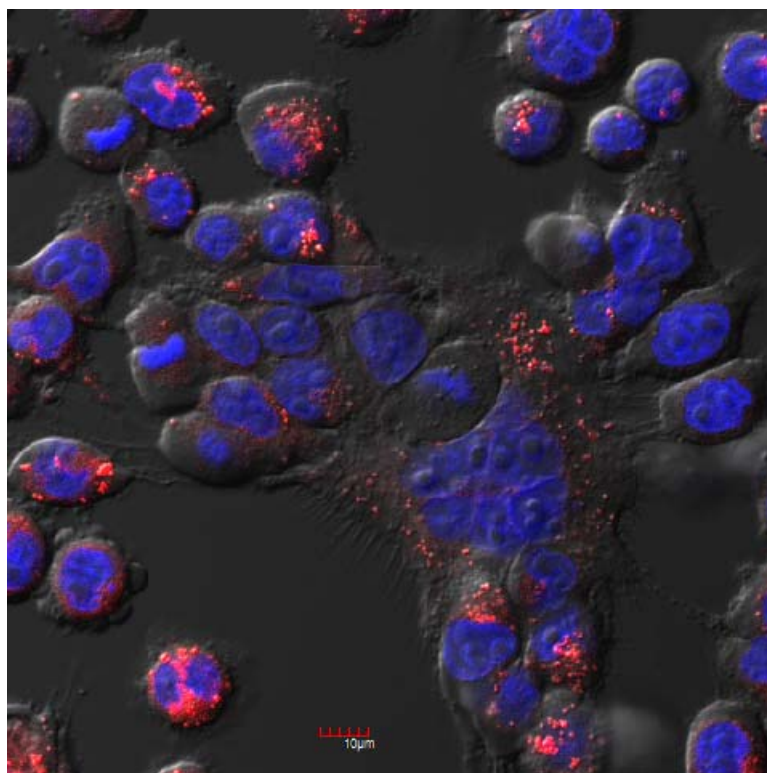


**Figure 6.8.1.** SW480 colon cancer cell stained with Hoechst (nucleus- blue) and the benzoindole hybrid dye 4.49 (red).

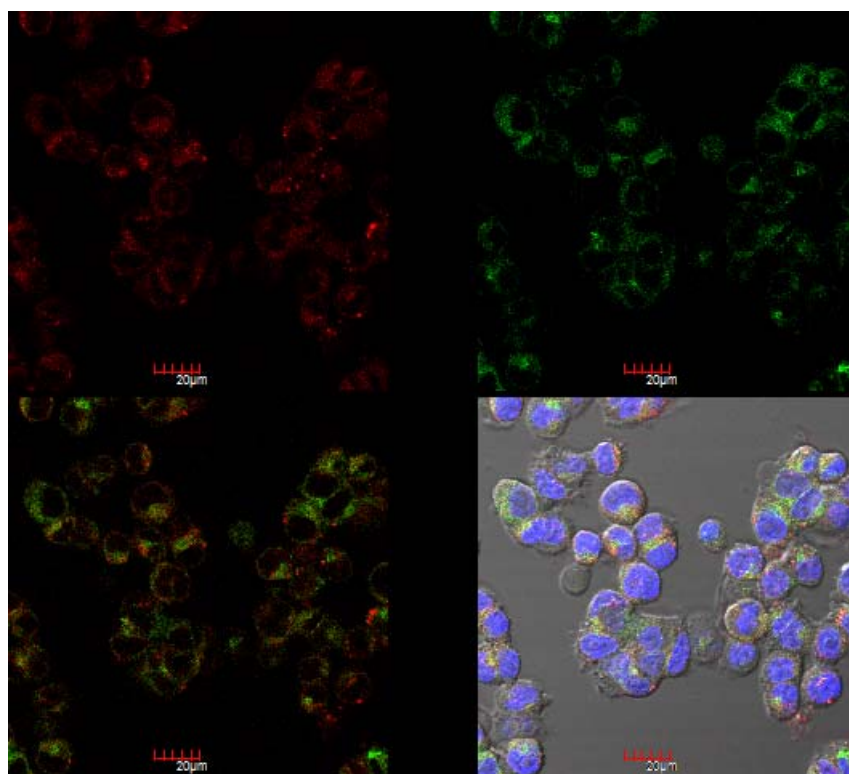


**Figure 6.8.2.** SW480 colon cancer cell stained with hybrid dye 4.49 (red), ER-tracker (ER- green) and Hoechst (nucleus- blue).

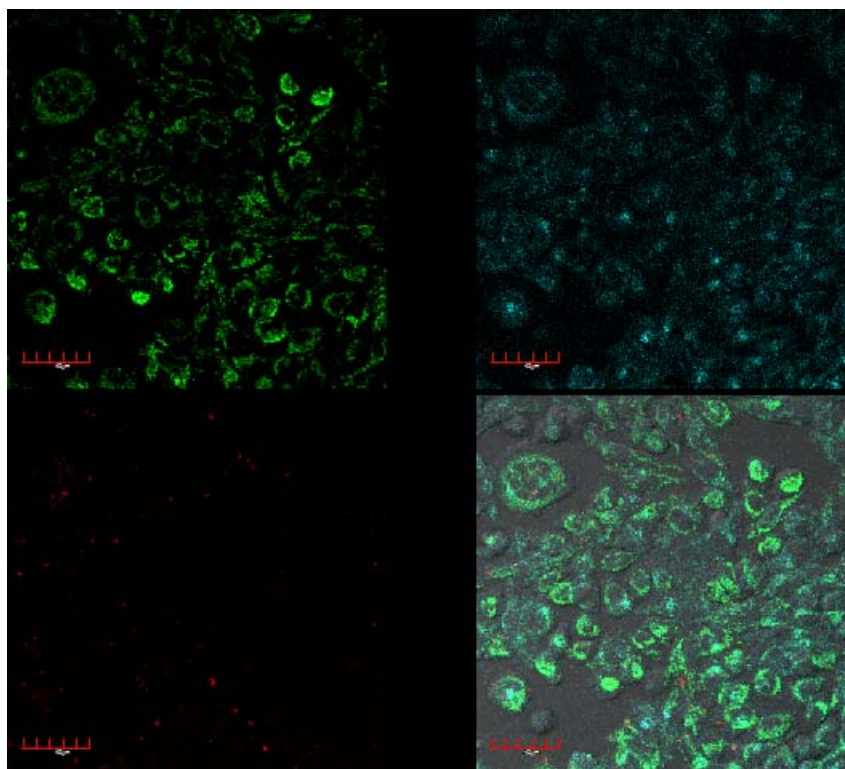


**Figure 6.8.3.** SW480 colon cancer cell stained with MitoTracker Red (mitochondria- green), LysoTracker Red (lysosomes- cyan) and hybrid dye **4.49** (red).

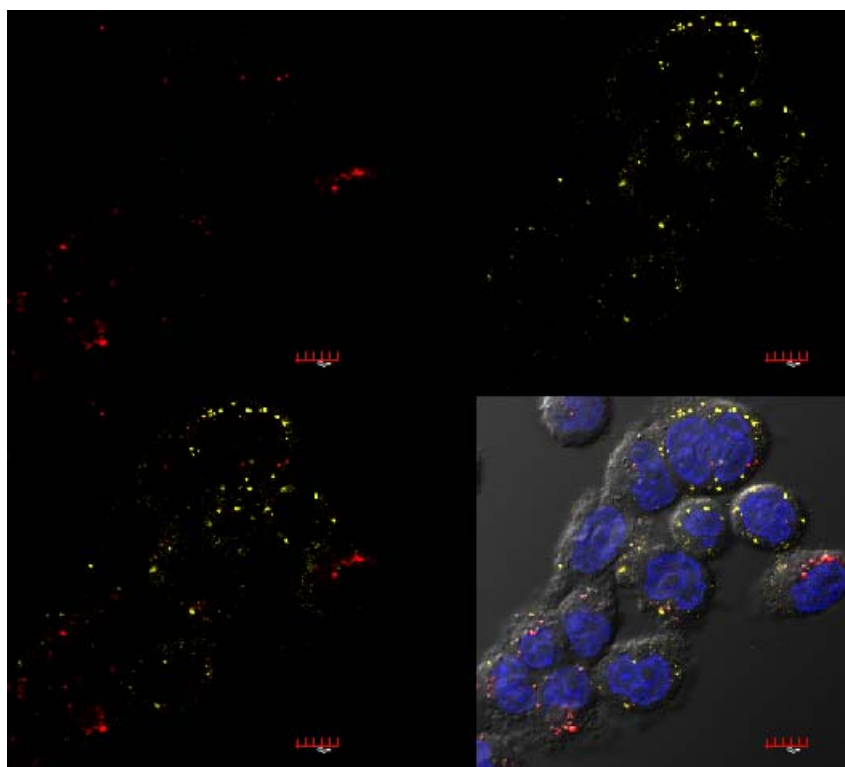


**Figure 6.8.4.** SW480 colon cancer cell stained with hybrid dye **4.49** (red), DiI (cytoplasmic vesicles- yellow) and Hoechst (nucleus- blue). Cells stained with both DiI and the hybrid dye, are low in numbers.



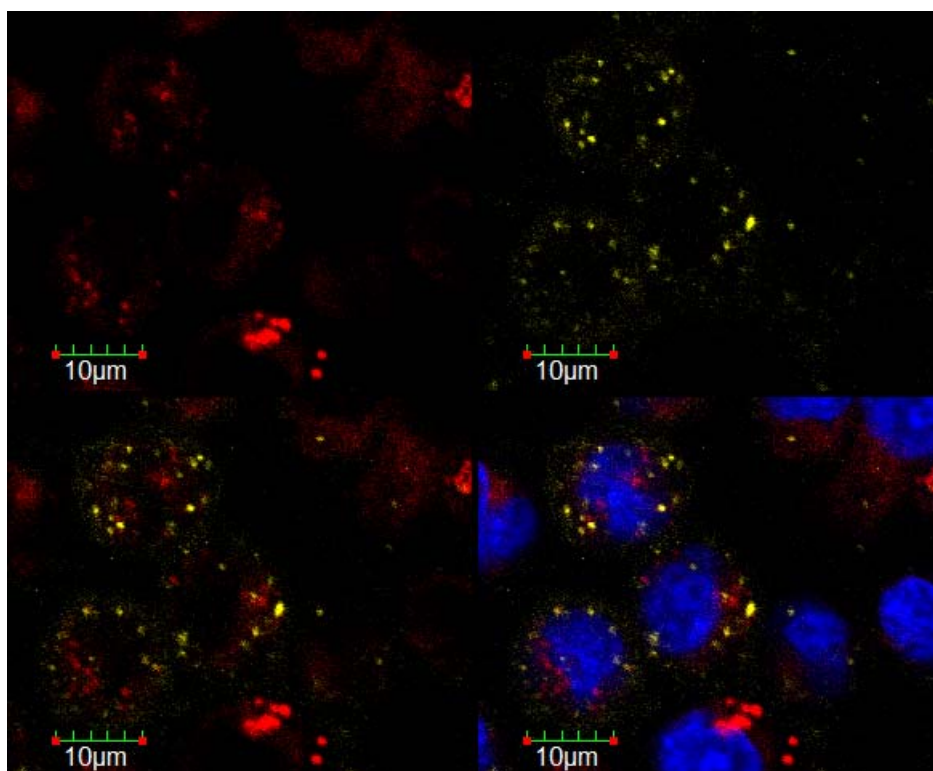


**Figure 6.8.5.** SW480 colon cancer cell stained with hybrid dye **4.49** (red), DiI (cytoplasmic vesicles-yellow) and Hoechst (nucleus- blue). Minimum to no co-localisation observed.